AD NUMBER: AD0390230
CLASSIFICATION CHANGES
TO: Unclassified
FROM: Confidential
LIMITATION CHANGES
TO: Approved for public release; distribution is unlimited.
FROM: Distribution authorized to U.S. Government agencies and their contractors; Adminstrative/Operational Use; 30 Apr 1968. Other requests for this document shall be referred to AFRPL (RPPR/STINFO), Edwards CA 93523.
AUTHORITY
C TO U GP-4, ST-A PER AFRPL ltr 16 Mar 1978

GENERAL DECLASSIFICATION SCHEDULE

IN ACCORDANCE WITH

DOD 5200.1-R & EXECUTIVE ORDER 11652

SECURITY MARKING

The classified or limited status of this report applies to each page, unless otherwise marked.
Separate page printouts MUST be marked accordingly.

THIS DOCUMENT CONTAINS INFORMATION AFFECTING THE NATIONAL DEFENSE OF THE UNITED STATES WITHIN THE MEANING OF THE ESPIONAGE LAWS, TITLE 18, U.S.C., SECTIONS 793 AND 794. THE TRANSMISSION OR THE REVELATION OF ITS CONTENTS IN ANY MANNER TO AN UNAUTHORIZED PERSON IS PROHIBITED BY LAW.

NOTICE: When government or other drawings, specifications or other data are used for any purpose other than in connection with a definitely related government procurement operation, the U. S. Government thereby incurs no responsibility, nor any obligation whatsoever; and the fact that the Government may have formulated, furnished, or in any way supplied the said drawings, specifications, or other data is not to be regarded by implication or otherwise as in any manner licensing the holder or any other person or corporation, or conveying any rights or permission to manufacture, use or sell any patented invention that may in any way be related thereto.

AFRPL-TR-68-60
Part I

(TITLE UNCLASSIFIED)
COMPOUND A/HYDRAZINE ENGINE DESIGN STUDY

Part I. Final Report

Clayton W. Williams, Werner P. Luscher, et al.

Propulsion Systems Division
Liquid Rocket Operations
Aerojet-General Corporation

TECHNICAL REPORT AFRPL-TR-68-60, PART I

30 April 1968

Air Force Rocket Propulsion Laboratory
Research and Technology Division
Air Force Systems Command
Edwards, California

3256

"When U.S. Government drawings, specifications, or other data are used for any purpose other than a definitely related Government procurement operation, the Government thereby incurs no responsibility nor any obligation whatsoever, and the fact that the Government may have formulated, furnished, or in any way supplied the said drawings, specifications, or other data, is not to be regarded by implication or otherwise, or in any manner licensing the holder or any other person or corporation, or conveying any rights or permission to manufacture, use, or sell any patented invention that may in any way be related thereto."

(TITLE UNCLASSIFIED)
COMPOUND A/HYDRAZINE ENGINE DESIGN STUDY

PART I. FINAL REPORT

Clayton W. Williams and Werner P. Luscher, et al.

AEROJET-GENERAL CORPORATION
A SUBSIDIARY OF THE GENERAL TIRE & RUBBER COMPANY

19488T

FOREWORD

This report summarizes the results of an analytical Compound A/Hydrazine Engine Design Study performed by the Aerojet-General Corporation, Liquid Rocket Operations, Sacramento, California, under Contract F04(611)-67-C-0092 for the Air Force Rocket Propulsion Laboratory (AFFTC), Edwards AFB, California. It encompasses the complete contractual period from 3 April 1967 through 9 November 1967. The Air Force Project Engineer was Mr. Edward C. Barth, RPREA.

The principal contributors to this project were:

Mr. Clayton W. Williams, Program Manager
Mr. Werner P. Luscher, Project Manager
Mr. C. Scott Henry, Systems Design Engineer
Mr. Clifford Paavola, Systems Performance Analysis
Mr. R. Verne Coats, Engine Weight Analysis
Messrs. Roy W. Michel and Stephen D. Mercer, Thermodynamics
Messrs. Jack D. Tuls and Leo D. Dean, Engine Performance Analysis
Mr. Ralph L. Sabiers, Turbopump Analysis
Mr. Don W. Culver, Thrust Chamber Design
Mr. Roger J. Roberts, Engine Control Design
Mr. Thomas E. Lavenda, Application Studies

This report contains classified information extracted from other classified documents which are identified with an asterisk in the Bibliography.

This report has been received and approved by the Air Force Propulsion Laboratory (AFTC).

Edward C. Barth, RPRA

ABSTRACT

The results of the Compound A/Hydrazine Engine Design Study, including the parametric engine information needed to perform mission analyses for evaluation of advanced engine design concepts, are reported in two parts. Part I includes parametric engine performance, weight, envelope, and capability for numerous engine concepts utilizing various fuels (N_2H_4, MMH, MHF-5, and .80 N_2H_4 + .20 NH_3) and different technologies for the feed system, propellant injection, and chamber cooling systems. These concepts encompass passive and active cooling methods, liquid and gaseous propellant injection, and pressure-fed as well as pump-fed systems of both the bleed cycle and the staged-combustion cycle. The applicability as well as comprehensiveness of the data is demonstrated by its use in three different missions specified by the Air Force. These include a synchronous orbit, trailer propulsion, and integrated propulsion for a re-entry vehicle. Payload or ideal velocity increment (ΔV) differences for various engine design concepts are shown. However, in view of the preliminary design concept approach as well as a lack of detailed engine design specifications, a number of basic assumptions were made in evolving the data within the scope of this program. Therefore, a description is provided for modifying the parametric data needed in a mission analysis to make it consistent with a different set of assumptions should new information subsequently become available. Part II is made up of six appendixes, which encompass a discussion of specific propellant characteristics, along with methods used in accomplishing performance, weight, and heat transfer calculations. In addition, those design methods for turbopumps and gas generators which are common to all engine concepts are discussed.

TABLE OF CONTENTS

TABLE OF CONTENTS (cont.)

TABLE OF CONTENTS (cont.)

TABLE OF CONTENTS (cont.)

TABLE OF CONTENTS (cont.)

TABLE OF CONTENTS (cont.)

TABLE OF CONTENTS (cont.)

TABLE OF CONTENTS (cont.)

TABLE OF CONTENTS (cont.)

TABLE OF CONTENTS (cont.)

TABLE OF CONTENTS (cont.)

TABLE OF CONTENTS (cont.)

TABLE OF CONTENTS (cont.)

LIST OF FIGURES

LIST OF FIGURES (cont.)

LIST OF FIGURES (cont.)

LIST OF FIGURES (cont.)

LIST OF FIGURES (cont.)

LIST OF FIGURES (cont.)

LIST OF FIGURES (cont.)

LIST OF FIGURES (cont.)

LIST OF FIGURES (cont.)

LIST OF FIGURES (cont.)

LIST OF FIGURES (cont.)

LIST OF FIGURES (cont.)

LIST OF FIGURES (cont.)

LIST OF FIGURES (cont.)

LIST OF TABLES

LIST OF TABLES (cont.)

LIST OF SYMBOLS USED IN THIS REPORT

Symbol	Description	Units
A_t	Thrust Chamber Throat Area	$in.^2$
cp	Heat Capacity	Btu/lb °F
D	Chamber Throat Diameter	in.
DE	Nozzle Discharge Diameter	in.
F	Thrust	lb
I_{sp}	Vacuum Specific Impulse	sec
L*	Characteristic Comustion Chamber Length	in.
MR	Mixture Ratio	--
N_t	Number of Regenerative Cooled Tubes	--
P_c	Thrust Chamber Pressure	psia
R	Gas Constant	ft/°F
R_{BO}	Burnout Heatflux Ratio	--
T_{wg}	Tube Wall Temperature Limit	°F
Tc	Combustion Chamber Flame Temperature	F
W	Weight	lb
WE	Engine Weight	
Wffc	Fuel Film Coolant Flow	lb/sec
Wofc	Oxidizer Film Coolant Flow	lb/sec
WP	Propellant Weight	lb
WPL	Payload	lb
ΔV	Velocity Increment	H/sec
ϵ	Nozzle Exit to Throat Area Ratio	--
∞	Ratio of Specific Heat	--

I. INTRODUCTION

This study was conducted for the purpose of providing design information for Compound A (CLF_5)/Hydrazine (N_2H_4) engines having potential application in the propulsion system for upper stages of launch vehicles, top stages, and maneuvering re-entry spacecraft. It was particularly intended that the design information evolved be useful in mission analyses of such propulsion systems.

Performance, weight, and size information was developed for CLF_5/N_2H_4, methyl hydrazine, and amine blend engines, which is readily usable in mission analyses. Practical design limits are identified, restricting evaluated engine concepts within the limits of feasibility. The practicability of the information as well as the limits is demonstrated by accomplishing three sample mission analyses utilizing several feasible engine concepts.

There are two secondary program objectives. One is to identify, from the design aspect, the critical components and areas of technology most seriously affecting the capabilities of Compound A engines. The other is to identify promising or probable cooling techniques and methods of chamber pressurization for several applications.

The following specified requirements governed the conduct of this study:

- CLF_5/N_2H_4 was selected as the base propellant combination, but the effect of alternative fuels upon engine design parameters also was investigated. These alternative fuels are MMH and MHF-5 as well as a mixture of hydrazine and ammonia (N_2H_4 + (80/20 by weight) NH_3), which is called the 80/20 blend.
- A maximum envelope diameter of 10 ft, but no limit on engine length.
- The investigation is restricted to deLaval nozzles (Rao Contour) with an area ratio of 150:1 maximum to 40:1 minimum.
- Specified fuels are not interchangeable for any engine concept, but the optimum engine configuration is defined for each propellant combination.
- Technology considered was that currently under development or anticipated by 1970 or 1971.
- All engine concepts to be capable of in-space restarts and investigated to the practical throttling range.

The Compound A/Hydrazine Engine Design Study was limited to engine data only and no over-all propulsion systems were defined for upper and top stages. The accuracy of the data provided within this scope is ± 10% for weight predictions as compared to a detailed final production unit design. This tolerance was confirmed through comparisons of component weights calculated against the equivalent weight of existing engines utilizing the same technology.

The engine performance calculated is estimated to be within ±1% of actual performance if the energy release losses are excluded. Accurate determination of the energy release losses requires detailed injector and chamber information, which is beyond the scope of this investigation.

The engine data generated are based upon a definition of an engine consisting of:

Injector	Thrust Chamber
Nozzle Extension	Turbopumps
Gas Generators	Engine Controls (excluding gimbal control)

The pump suction flange, the gimbal attachment pad, and the power supply J-box provide the interfaces between the engine and the propulsion system. The power and instrumentation harnesses were not considered part of the engine.

Considering the foregoing engine definition, all essential engine information is given to permit a complete mission analysis to be accomplished (excluding systems information, such as jettison weight or lift-off weight).

The requirements for a mission analysis as well as a flow chart of such an analysis are combined on Figure No. 1. It can be noted from this figure that the objectives of such an analysis are to provide an optimum engine design in relationship to payload or ΔV capability within the design limits of both the system and the engine as well as to specify the optimum combination of thrust level, chamber pressure, and nozzle expansion area ratio.

There are three areas of engine characteristics that must be considered for each engine design during mission analyses. These are:

- Design Characteristics

  Full thrust and throttled engine performance; engine wet weight; engine length; maximum engine diameter; and optimum engine mixture ratio.

- Design Constraints

  Propellant characteristic; engine design and technology limits; system requirement considerations; and mission requirement considerations.

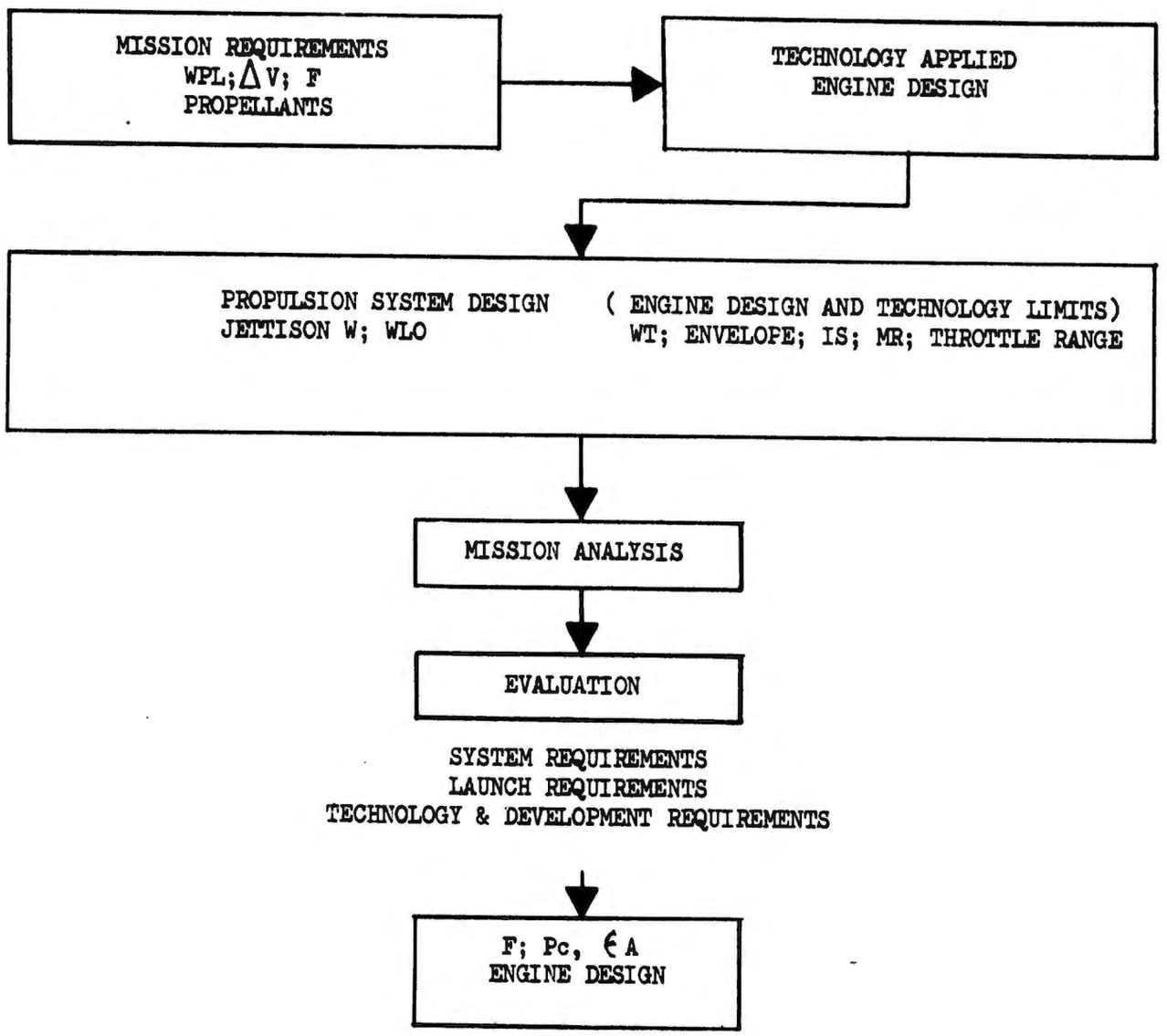

Figure 1. Mission Analysis, Information Requirements and Flow Chart

- Engine Design Variables

  Chamber pressure; design thrust level; nozzle expansion area ratio; and propellants.

It is the design constraints that are particularly emphasized because engines can rarely be made optimum within all of the design constraints. Wherever possible in this study, these design constraints have been presented as functions of the engine variables in a form applicable to computerized mission analysis. Table I is a summary of these design constraints oriented toward the requirements of mission analysis.

Sufficient flexibility of the design characteristics has been provided in this investigation to permit their modification as advanced technology is developed through 1970-1971. Whenever this necessitated that certain assumptions be made, these assumptions are identified along with a list of technology requirements.

The complete study effort was divided into two tasks, as follows:

- Task I

  Engine Point Design

  (Performance, weight, size, cooling requirement, stiffness requirement, material identification, and configuration)

  Parametric Expansion

  (Five engine concepts)

  Technology Comparison

  (Injection methods, cooling methods, cycle, and throttling methods)

- Task II

  Mission Analysis

  (Synchronous orbit, trailer propulsion system, and integrated propulsion system)

  Technology Requirement

  (Specifications)

TABLE I

DESIGN CONSTRAINTS SUMMARY

Propellant Characteristics	Design Limits	System Requirements	Mission Requirements
Theoretical Performance	Material	Tank Pressures	Mission Duration
Material Compatibility	Combustion Stability	NPSP	Burn Duration
Decomposition	Performance Degradation	MR Control (Including Density)	Restart
Gas Generator Characteristic	Cooling Limits	Heat Radiation	Environment
Cooling Capability	Burn Duration	Envelope	Throttling
Formation of Solids	Feed System Stiffness		Start and Shutdown
Properties			

A number of engine point designs were selected during Task I to provide the required engine design characteristics as a function of thrust, chamber pressure, and expansion area ratios. Then, selection of the point design engines was made to assure that the thrust and pressure levels of these engines were known to be within all of the design constraints. Also, they formed the basis for weight and envelope information. The majority of these engines, particularly those of variable thrust, were subsequently expanded over a given range of engine design variables. In each of these instances, the limits of feasibility and the practical design range are identified. Eight point design engines were investigated.

The intent of this analysis was to identify technologies and evaluate their effect upon engine performance, weight, and envelope rather than to evolve the design characteristics of an optimum engine configuration. Therefore, the parametric expansion of the point design engines was expanded by modifying technology concepts for each engine (i.e., injection method, cooling method, and thrust chamber material).

The engine performance and chamber weights are greatly dependent upon the combustion chamber length assumed for the various injection methods considered. For this analysis, the best estimate of an optimum L* was made, based upon available data. However, this information is rather limited for some injectors (e.g., HIPERTHIN); therefore, appropriate influence factors are presented in evaluating the effect of L*.

In addition, this report includes weight information for all pertinent components (i.e., injector, chamber, turbopumps, and controls) as functions of the design variables, thereby providing a capability for assessing the effects upon engine weight that replacing components with a different design concept would have.

The following range of engine design variables was specified for Task I:

Engine Feed System	Pressure-Fed	Pump-Fed
Cooling System	Passive	Passive and Active
Thrust (lb)	10K to 30K	25K to 70K
Chamber Pressure (psia)	100 to 300	300 to 1500
Throttling Range	1:1 to 10:1	1:1 to 10:1
Maximum Burn Duration (sec)	100 to 600	1500 to 3000*
Maximum Continuous Burn (sec)	100 to 300	100 to 300
Number of Restarts	0 to 30	0 to 30
Minimum Coast Period (sec)	300	300

*Including Refurbishment

A mission analysis was accomplished during Task II of this study to demonstrate the adequacy of the engine data developed during Task I. The missions were supplied by Headquarters, Air Force Flight Test Center, Edwards Air Force Base, California. These missions include: synchronous orbit mission; trailer propulsion system; and re-entry vehicle propulsion system.

The mission analysis includes a definition of payload and ΔV capability for the point design engine concept utilizing the fuel propellant considered to satisfy the mission and engine design requirements for each engine concept. The mission analysis culminated in specification of the maximum chamber pressure and expansion area ratio for each engine concept in the individually specified missions.

II. SUMMARY

A. CONCLUSIONS

(U) The following is a summary of conclusions pertinent to all aspects of this study.

1. Propellant Properties

a. Vapor Pressure

(C) All of the propellants studied are earth storable ones; however, a magnitude difference existed in the vapor pressure characteristics of CLF_5, MMH/MHF-5, and N_2H_4 propellants. The CLF_5 vapor pressure at 100°F is 80 psia. At these pressures, propellant tank wall thicknesses in excess of minimum gauge are required and the oxidizer tank weights for pump-fed systems are relatively heavy. Throttling of engines to chamber pressures below the CLF_5 vapor pressure are expected to result in two-phase flow at the injector face, which adversely affects performance.

(C) As a result of the high vapor pressure characteristics of CLF_5, it is necessary to reduce the oxidizer tank weight and turbopump weight for oxidizer boost pumps.

(C) It is recommended that propellant conditioning of the oxidizer be accomplished to reduce the vapor pressure, although this may not be compatible with Air Force launch requirements.

b. Freezing Point

(C) The baseline fuel (N_2H_4) has a 35°F freezing temperature, which is considered marginal for near-earth orbits achieved from an easterly launch, but it may be acceptable if tank and propellant line thermal insulations are provided.

c. Gas Generator Characteristics

(C) The bipropellant gas generator characteristics for CLF_5/N_2H_4 propellants result in very high gas temperatures even at the very low mixture ratios and are not considered compatible with the turbine temperature requirement. However, under proper decomposition conditions, N_2H_4 can be decomposed in a catalytic bed, which results in an acceptable gas temperature. The catalytic beds (CAT-PACK) are heavier than the gas generators, and it is estimated that, for each lb/sec of hydrazine through flow, 2 lb of CAT-PACK would be required for an 80% decomposition. This assumes Shell-405 as the catalyst. However, because of its current price and availability, Shell-405 is recommended as the igniter only, followed by a non-hypergolic catalyst. The ratio of Shell-405 to the non-hypergolic catalyst is dependent upon the response requirements as well as the degree of decomposition desired.

(C) To overcome the gas-generator difficulties with N_2H_4, a fuel-blend is recommended using a mixture of 80% N_2H_4 + 20% NH_3. This mixture results in acceptable turbine temperatures for CAT-PACK capability and reduces the freezing point to approximately 0°F. The vapor pressure characteristic is identical to CLF-5 but approximately 4 sec of specific impulse are sacrificed when compared to N_2H_4 fuel.

(C) MMH and MMF-5 are not considered suitable for CAT-PACK decomposition, but they yield acceptable turbine temperatures when used in a bi-propellant gas generator. These two fuels contain carbon which will form carbon deposits in the fuel-rich turbine as well as on the walls of the injector face and main chamber. This will affect turbine performance as well as chamber cooling characteristics.

(C) The oxidizer-rich gas generators leave for greater flexibility in regards to turbine temperature and in theory, they permit variation of turbine temperatures by shifting mixture ratio which is one possible method for engine throttling.

d. Propellant Decomposition

(C) The problems of the N_2H_4 exothermic mono-propellant decomposition are well known, which affects the restart capability of the engine for certain duty cycles. N_2H_4 vapors are considered to be particularly hazardous. NH_3 has a higher vapor pressure than N_2H_4; therefore, the 80/20 blend of these two propellants drastically decreases the pressure rise rate during decomposition because the vapors formed consist mostly of NH_3. The other fuels, MMH and MHF-5, decompose at a slower pressure rise rate than N_2H_4 and are more suitable for restart engine operation.

(C) The decomposition rate of CLF-5 has been established for temperatures up to 680°F but it is very low. Also, the endothermic reactions of CLF-5 decomposition was assumed to be ineffective in improving cooling capability.

e. Passivation

(C) CLF-5 is very reactive with most materials and requires passivation of all hardware contacting it. Fibrous graphite, which is considered non-reactive with CLF-5, may be an exception. Passivation techniques have been developed that are consistent with the practical operations of fluorine-constituted oxidizers. However, the possibility exists that any hardware failure could result in severe damage because of the exposure of non-passivated material to it.

2. Materials

a. Thrust Chamber

(C) The study revealed that the selection of thrust chamber material has a significant effect upon both the performance and weight of the engine system.

(C) For passively cooled engines, laminated chambers as well as radiation-cooled chambers were evaluated using fibrous graphite material. The results showed a substantial weight advantage for the radiation-cooled chambers. The performance level of both is largely dependent upon the chamber wall temperature limits, which establish the required coolant flow ratios.

(C) For the active cooling system, a comparison of nickel and fibrous graphite material indicates that relatively large weight and performance advantages exist if fibrous graphite material is used for transpiration-cooled chambers.

(C) If a nickel material is used, the permissible chamber wall temperature must be lower (1750°F) for oxidizer film-cooled or transpiration-cooled chamber walls than for fuel cooling (2000°F). This requirement increases the cooling performance losses for oxidizer-cooled chambers. For fibrous graphite material, the allowable wall temperature was assumed to be equal (based upon current experience) and makes fibrous graphite attractive for oxidizer-cooled chambers.

b. Injectors

(C) Throughout this study, nickel was used as the injector material regardless of injector type. This assumption is based upon actual experience with impinging orifice injectors, where "bellmouthing" of the fuel orifices occurred with aluminum and stainless steel injectors.

(C) For liquid/liquid injection, the platelet injector with its low energy release losses and short L* requirements appears very attractive for all chambers where either film or active cooling is necessary. However, the brazing of nickel platelets is not well developed and restricts this fabrication method to small diameters.

(C) The nickel material was selected again for injectors where both propellants are injected in the gaseous phase. However, this may not be necessary because it is expected that the "bellmouthing" of the fuel orifices will be reduced as compared to liquid injection.

c. Control Valves

(C) Based upon experience, the material selected for valve seals was phosphorous bronze sealing against an Inconel-718 housing. Throttle

control for fuel-rich turbine drives was obtained by using ring-gate pump valves, which combine mixture ratio control, throttle control, and shut-off sealing. For oxidizer-rich turbine drives, gas generator mixture ratio control was used for feed system throttling.

3. Performance

(C) The study results indicated that kinetic losses rapidly increase for chamber pressures below 500 psia to 600 psia. Therefore, the performance gains for low-pressure engines are quite moderate when compared with N_2O_4/A-50 propellants. At the higher chamber pressures of the pump-fed system, the performance gain, when compared to N_2O_4/A-50, is approximately 20 sec of specific impulse.

(C) The performance of systems utilizing gas/gas or liquid/gas injection appears most favorable because of a high energy release efficiency as well as the low coolant losses resulting from the short L* requirement.

(C) The study indicated that coolant losses have a significant effect upon the performance. A 1% coolant flow is approximately equivalent to 1 sec of specific impulse as compared with 1.8 sec for oxidizer cooling. Cooling requirements are approximately proportional to the chamber surface area; therefore, short chambers enhance performance capability. This indicates that gaseous injection of both propellants will result in the highest possible performance as a result of its very short L* requirement (less than 5-in.).

(C) The energy release losses were based upon experience with the various injector design concepts and no trade-off was made between energy release efficiency and potential chamber high frequency instability. This is of particular interest for low-pressure chambers operating with N_2H_4 fuel, where instabilities are more likely to be a comparative problem. For the impinging orifice type injectors of flat-face design, energy release efficiency has to be sacrificed somewhat to obtain stability, or acoustic chambers have to be used to suppress instability. At this time the trade-off effects upon performance are undefined.

4. Chamber Cooling Methods

a. Passive Cooling

(C) Passive cooling (i.e., ablative and radiation) are primarily considered for use in pressure-fed systems.

(C) The ablative chamber wall thickness requirements are extremely dependent upon burn-duration and duty cycle. It was concluded that these chambers are not suitable for prolonged throttled operation. In addition, they have a tendency to change thrust level with burn-duration as a result of throat ablation.

(C) The radiation-cooled chamber also is life-limited because of ablation characteristics with respect to chamber pressure level. At a chamber pressure of 100 psia, the ablation is approximately 6% in the throat area after a 600 sec burn duration. For short burn durations ($<$ 70 sec), fuel film cooling is not necessary. The cooling requirements at the lower chamber pressures are dependent upon the forward flange design.

(C) b. Active Cooling

The regneratively cooled engines were, by definition, existing technology engines. Therefore, the heat flux limit was assumed to be 16 BTUs/in.^{2} sec, which restricted these engines in application to certain thrust and chamber pressures as well as limited the range of throttling. In general, the maximum chamber pressure was approximately 700 psia to 800 psia, decreasing with thrust level. MHF-5 appeared to be the most promising fuel for regenerative cooling. The soot formation on the tube walls resulting from MMH and MHF-5 combustion was not considered in the definition of regenerative cooling limits.

(C) Even with these restrictions, regenerative cooling for fixed thrust operation is very competitive with transpiration-cooled chambers.

(C) The transpiration-cooled chambers have their application in engines with deep throttling requirements. Deep throttling (10:1 or greater) with liquid transpiration-cooled chambers is limited by the vapor pressure characteristic of the propellant (a very real limitation for CLF-5). Fuel cooling was considered in the gaseous phase only because of the mono-propellant characteristics of the fuel propellants. The coolant is decomposed N_2H_4 supplied by a CAT-PACK or gas generator tap-off for the carbon-containing fuels.

(C) Again, short L* appears highly desirable for these cooling methods to reduce both weight and coolant requirements. Fuel cooling with gas-gas injection appears to be a very attractive cycle and engine concept.

(C) It was concluded that transpiration cooling with graphite platelets is a very desirable chamber cooling method because of its excellent transient characteristics, lightweight, and low coolant requirement.

5. Throttling

It was concluded that the throttling capabilities of the engine concepts investigated largely depend upon the thrust chamber cooling concept. Regeneratively cooled chambers have a throttling limit which depends upon the heat flux capabilities of the design. It was further concluded that for the existing technology, regenerative cooling is not suitable for deep throttling.

Deep throttling requirements eliminate the pressure-fed engines and limit the engine concepts to the transpiration-cooled engines of high chamber pressure design.

(C) The ablative cooled chamber will permit deep throttling; however, the char characteristics of the chamber wall impose duration limits. It was concluded that CLF-5 could flash in the injector orifice as a result of the inherent low chamber pressure at deep throttling and adversely affect performance.

(C) The transpiration-cooled chambers are not limited within the specified 10:1 throttling range if the coolant is used in the gaseous phase.

(C) For liquid transpiration cooling, the section below the throat operates at very low pressure during throttling, which could cause the coolant to flash in the metering orifices and thereby reduce the local coolant flow. It is recommended that liquid transpiration-cooled chambers operate at high chamber pressures to protect the chamber throat during deep throttling operation. In particular, liquid transpiration cooling with CLF-5 is a problem because of its high vapor pressure characteristic.

6. Restart

(C) Special consideration must be given to the restart capability of the various design concepts because of the decomposition characteristics of the monopropellant fuels.

(C) The restart capability is dependent upon the engine hardware temperature at restart as well as the maximum hardware temperature during the coast period. These temperatures, in turn, depend upon the mission profile, the engine installation, and the engine design concept. The critical components affecting the heat soak-back are the turbine drive assembly in pump-fed systems as well as the injector assembly. It was concluded that decomposed gaseous injection can negate the injection problem. To reduce the turbine heat soak-back, it was concluded that an oxidizer-rich turbine drive is desirable because the fuel pump and bearings are removed from the outboard turbine and the turbine operates at the relatively low temperature of 1200°F.

(C) For actively-cooled systems, the heat soak-back coming from the injector face is not considered very critical; however, this depends upon the extent of injector face exposure to the flame zone.

(C) For passively cooled chambers, the injector heat soak-back is larger because of the relatively slow cooling rates of the very hot chamber surfaces. Lithium heat accumulators are recommended for use in these chambers.

(C) The actively cooled chambers are required to provide adequate cooling during the start transient. This is a particular problem with CLF-5 in transpiration-cooled chambers because vapor locking of the chamber could occur during restart as a result of the high vapor pressures. Similarly in regenerative-cooled chambers, the tubes must be pressurized prior to start to avoid the burn-through caused by vapor locking.

7. Mission Study

(C) The mission study indicated that most engine designs became optimum outside of their capability limits. This is particularly true of the passively cooled systems as well as the regeneratively cooled systems. Only the transpiration-cooled chambers satisfied all of the mission requirements. To calculate the payloads, the appropriate fuels were selected upon the basis of compatibility with the engine design and mission analysis. It appears that only the ARES type engine is suitable for use with N_2H_4 as the fuel because it operates with an oxidizer-rich turbine drive.

(C) For the synchronous orbit type of missions, the payload difference between the pressure-fed and pump-fed systems is considerable, but lessens as the ΔV requirement is reduced. The system capability is independent of the engine design if pump-fed systems are compared. Engine selections have to be based upon restart, throttling, reliability, cost, and technology requirements rather than payload capability.

B. TECHNOLOGY

(U) The level of technology assumed for the parametric analysis of this study effort was that which can be reasonably expected to be available by 1970-1971. The ensuing summary of the technology investigated includes only those concepts where design data or current development programs are in existence.

1. Cooling

(U) The following passive and active chamber cooling concepts were investigated:

Passive Chamber Cooling Systems	Active Chamber Cooling Systems
Radiation - Fuel Film Cooled	Regenerative (including fuel film)
Ablative - Fuel Film Cooled	Transpiration - Liquid Oxidizer Cooled
	Transpiration - Gas Fuel Cooled

(U) Other than the propellant injection method, the thrust chamber cooling method has the most pronounced effect upon engine performance and engine weight as well as upon design and operational limits. Figure No. 2 illustrates the chamber cooling concepts considered.

(U) Only the passive cooling systems (i.e., ablative-cooled chambers and radiation-cooled chambers) were considered for the pressure-fed engines and in these instances, fuel film cooling was utilized. Active cooling systems were eliminated for the pressure-fed systems because of the high tank pressures required. The nozzle extension of all passive cooled systems is radiation-cooled by a detachable columbium skirt.

For the active cooling systems, regenerative, transpiration, radiation, and ablative cooled chambers were considered.

Tube bundles only were considered for regenerative chambers. The use of thermal coatings or laminated chambers were excluded. The heat transfer analysis showed that only liquid fuel, particularly MHF-5, was the practical coolant with this method. This cooling method imposes severe restrictions on the useful range of thrust and chamber pressure as well as throttling capability.

Both liquid oxidizer and gaseous fuel cooling were considered for transpiration-cooled chambers; however, all of the fuels specified are mono-propellants which makes liquid fuel transpiration cooling impractical.

Analysis indicated that gaseous fuel transpiration cooling is dependent upon the gas generation characteristics of the specified fuels and its application is limited to those specialized fuels containing carbon depressing additives. In addition, gaseous fuel cooled chambers will operate at approximately mean material temperatures of 900°F to 1000°F, which aggravates the problem of heat soak-back.

The use of oxidizer-cooled chambers does not exclude any of the specified fuels and also results in lower operating temperatures of the chamber.

Transpiration-cooled chambers permit deep throttling and show few limitations in application within the scope of this study.

2. Injector

The following three different injection methods were included in the analysis:

Liquid/Liquid	Gaseous/Liquid	Gaseous/Gaseous
Conventional	Laminar (Platelets)	Platelets
Laminar (Platelets)		Conventional
Momentum Exchange		

Three different injector configurations were investigated for the liquid/liquid injection system. Conventional injectors and platelet (HIPERTHIN) injectors were considered in connection with fixed thrust engines. For the throttleable engines, the laminar flow HIPERTHIN and momentum exchange injectors were applied. Figure No. 3 illustrates these injector concepts.

The gas/liquid injection system was investigated for gaseous oxidizer and liquid fuel as well as for gaseous fuel and liquid oxidizer. The specific method used has a considerable effect upon the gas generator system.

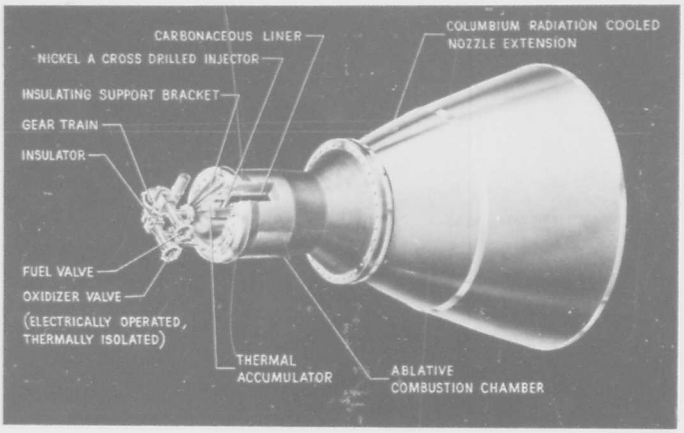

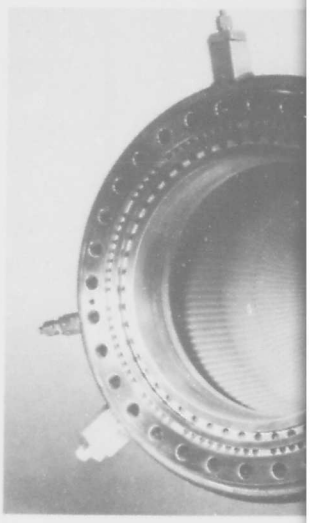

ABLATIVE

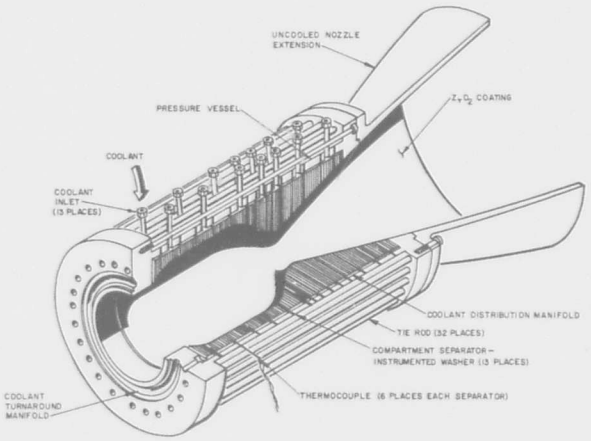

TRANSPIRE

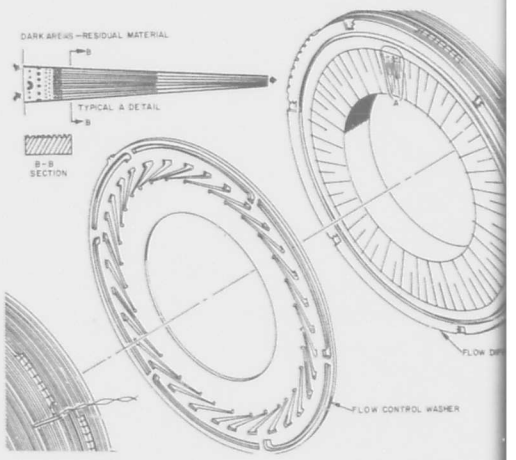

TRANSPIRE

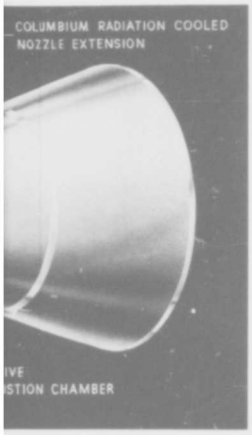

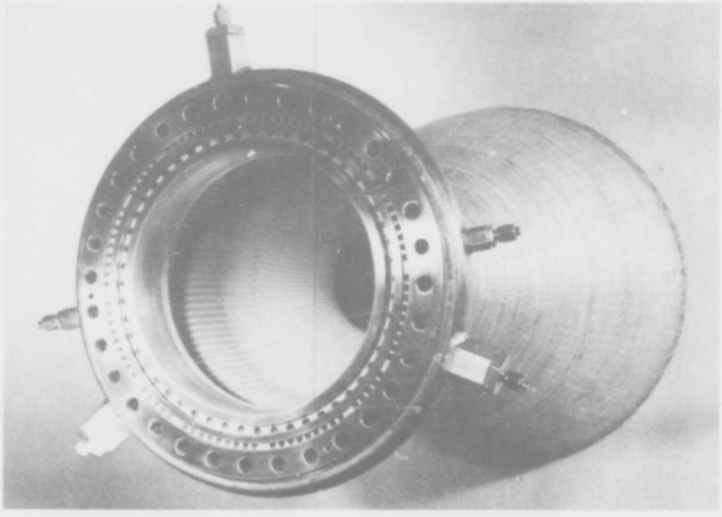

REGENERATIVE

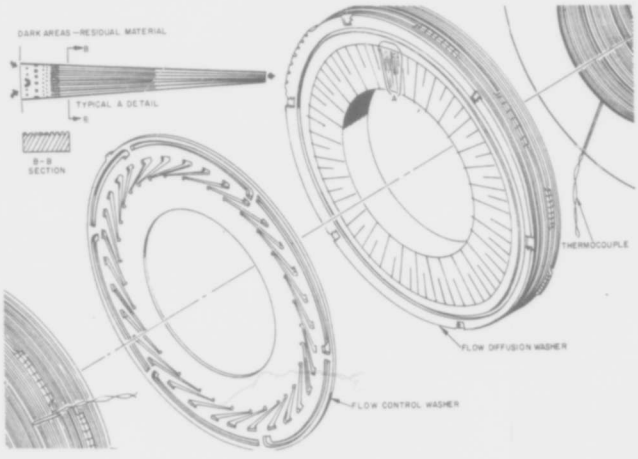

TRANSPIRE

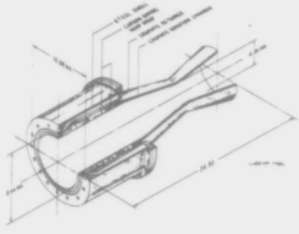

RADIATION

Figure 2. Thrust Chamber Types

2

The platelet type of injector, which has a laminar flow for the liquid phase, provides a deep throttling capability with this type of injection method.

Conventional injectors (tubelets) (see Figure No. 4) or a HIPERTHIN injector operating in the turbulent flow regime can be used in the gas/gas injection system. Both provide deep throttling capability because the stiffness of the injectors is maintained.

3. Turbine Drive and Gas Generator

The following cycles were considered for the turbine drive:

Bleed Cycles	Topping Cycles
Fuel-Rich Turbine	Fuel-Rich Turbine
	Oxidizer-Rich Turbine

Both turbine bleed cycles as well as staged-combustion cycles were considered for the pump-fed system. In all instances, the turbine bleed cycle, which is used for the liquid/liquid injection systems, has a two-stage, fuel-rich turbine drive and the turbine exhaust is introduced into the nozzle extension at the appropriate area ratio. Both fuel-rich and oxidizer-rich turbines were considered in connection with the staged-combustion cycle. The turbine drive gas for a liquid/gas injector is the same as gaseous propellant injected into the main combustion chamber in contrast with the gas/gas injector where a choice is possible.

The use of either a fuel-rich or an oxidizer-rich turbine directly affects the method of gas generation as well as the method of feed system throttling. Where fuel-rich gas generation is utilized, the method for accomplishing this is dependent upon the fuels considered. For N_2H_4, catalytic decomposition is required to obtain acceptable turbine temperatures whereas with the 80/20 blend, both Cat-Packs and bipropellant gas generators are feasible. When the carbon containing fuels (MMH and MHF-5) are considered, either bipropellant gas generators or thermal beds used in conjunction with a primary gas generator are feasible.

All of the pumps considered are of the centrifugal type.

4. Throttling

The following four methods for turbopump throttling were considered:

By-Pass Valve
Ring-Gate Valve
Gas Generator Mixture Ratio Control
Turbine Hot Gas Valve

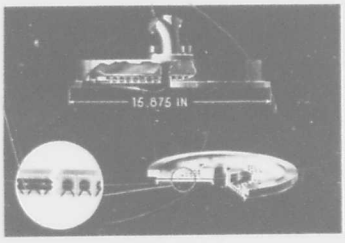

CONVENTIONAL (HSIP)

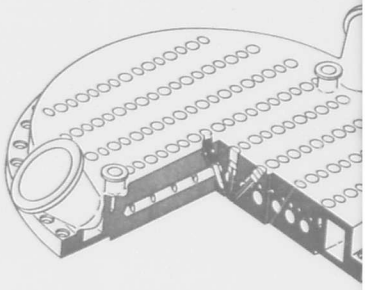

MOMENTUM EXCHANGE

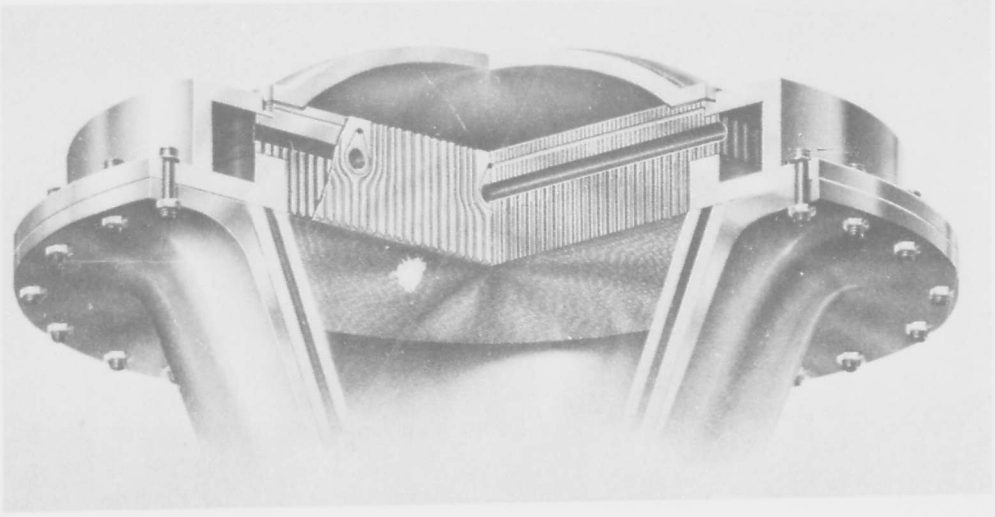

Patent Pending

AXIAL FLOW - HIPERTHIN

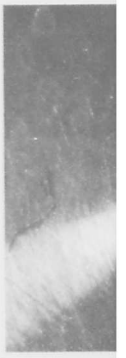

Patent Pend

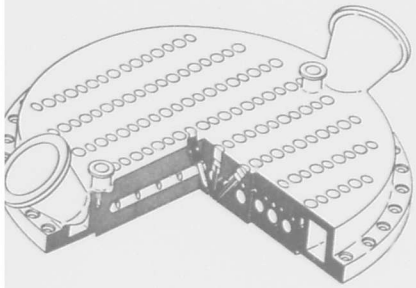

MOMENTUM EXCHANGE

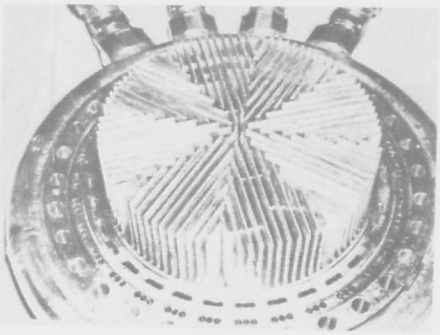

GAS/LIQUID (ARES)

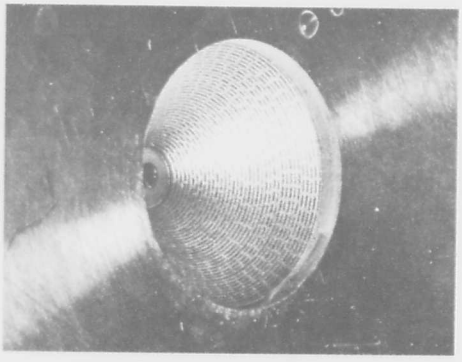

Patent Pending

RADIAL FLOW - HIPERTHIN

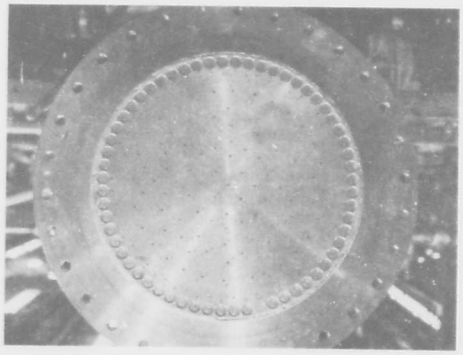

CONVENTIONAL (LF_2)

Figure 3. Injector Types (u)

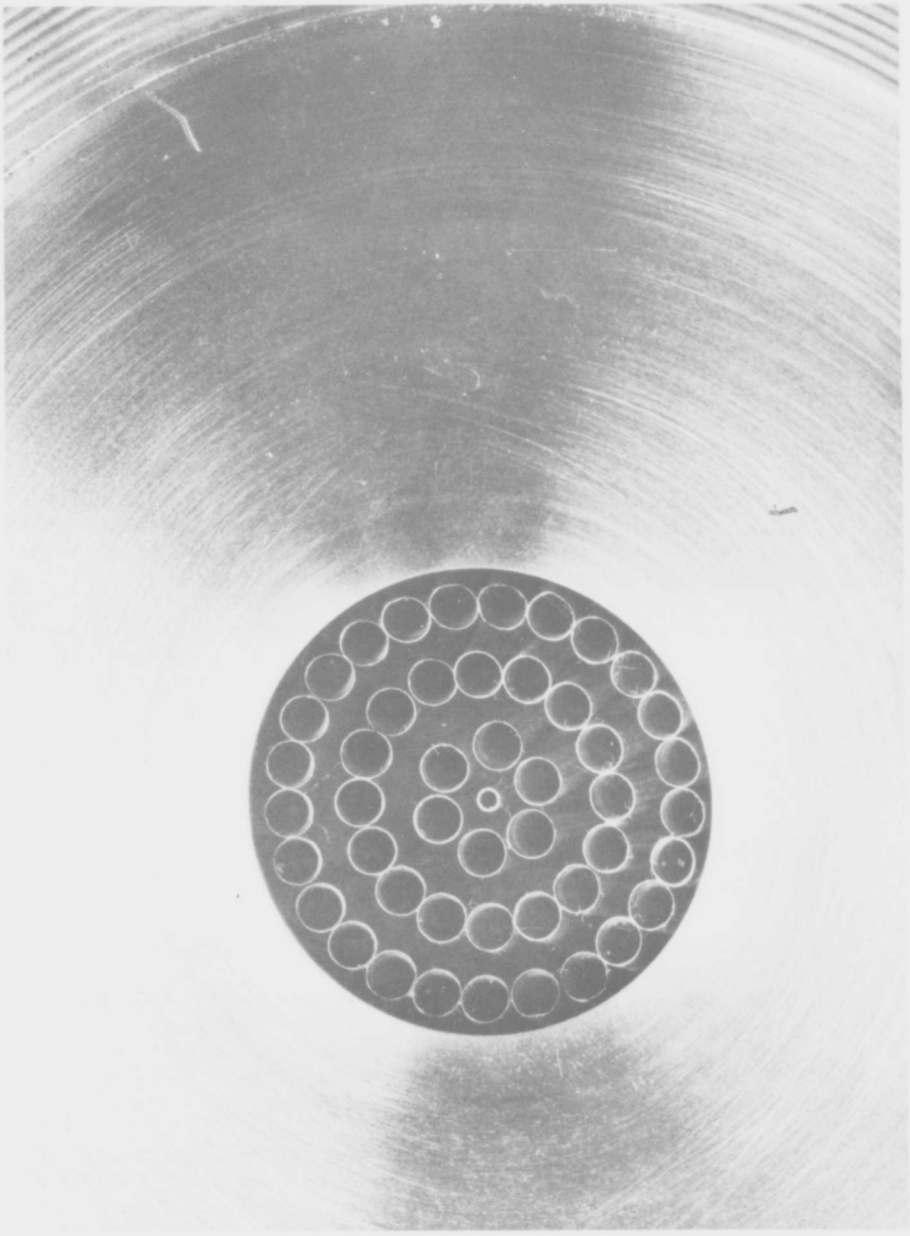

Figure 4. Aerojet-General Tubelet Injector

Where engines are pump-fed, it is necessary to assure that pumps do no surge or stall during deep throttling operation. Use of a pump by-pass valve offers the simplest system. Propellant flow is recirculated from pump discharge to pump suction, thereby maintaining the high pump flow coefficients. The use of this system has little effect upon engine weight, but it is not generally recommended where prolonged deep throttling is required because of the excessive heat input into the pumped fluids.

In staged-combustion cycles utilizing an oxidizer-rich turbine drive, throttling can be obtained by lowering the turbine temperature, which is accomplished by increasing the oxidizer-rich propellant gas generator mixture ratio. This throttling method is applied in the ARES-Mist engine concept and permits throttling with only a small change in pump flow coefficient. This variation in over-all engine mixture ratio during throttling is very small and has no significant effect upon propellant utilization. Where fuel-rich turbine drives are used, the turbine temperature reduction by means of altering the gas generator mixture ratio is not possible because of the bipropellant gas generator temperature characteristics of the specified fuels.

The third method of throttling technology applies to fuel-rich turbine drives and features variable geometry diffusers for both the fuel and oxidizer pumps (ring-gate valves). With this method, throttling is obtained at fixed gas generator mixture ratio and turbine temperatures.

Lastly, feed system throttling by means of a turbine by-pass is feasible, but it requires the use of a hot gas valve that operates at the gas generator temperature level. For a fuel-rich turbine drive, the operating temperature level depends upon the fuels considered. It is between 1400°F and 1600°F for bi-propellant gas generators while it is approximately 1200°F for a monopropellant gas generator. This method of throttling is applicable primarily where relatively cool turbine drive gases are available.

5. Thrust Chamber Assembly Material

The following thrust chamber materials were considered:

Material	Type of Cooling
Inconel	Regenerative
Nickel	Transpiration
Fibrous Graphite	Transpiration
Fibrous Graphite	Radiative
Graphite Phenolic	Ablative

The material assumed for the thrust chamber has a highly significant effect upon performance and engine weight because the permissible material temperature limits define the chamber cooling requirements to a large extent. Only Inconel tube bundles were considered for the regeneratively-cooled chambers. For the transpiration-cooled chambers, either nickel or

fibrous graphite platelets can be used. These fibrous graphite platelets have nearly double the temperature capability of nickel and are presumed to be compatible with CLF_5. Also, they appear to be the most promising new technology emerging from this investigation. Where engines were passively-cooled, fibrous graphite was selected for the radiation-cooled chamber. Fibrous graphite also was selected as the throat inserts of the ablative-cooled engines and graphite phenolic as the back-up material in the same application.

III. APPLICATION OF TECHNOLOGIES

It was necessary that the technologies considered for this study be integrated and applied to engine concepts because of the primary objective of the effort to provide information for evaluating technology by means of mission analysis.

The general approach used was to define eight point design engines representing both pump-fed and pressure-fed engines as well as passive and active cooling systems. Then, all of the information required for a mission analysis was generated for these base engine concepts (engine point designs) using a specific line of technology. These engine point designs were subsequently used to evaluate the effect of each technology by systematically substituting each method within a given area of technology. For example, all injection methods were compared using one base engine concept. The same was true for all active cooling methods. Then, performance and weight effects were determined and presented in a form suitable for use in mission analysis.

A. ENGINE TECHNOLOGY CONCEPTS

Several carefully selected engine concepts were defined during Task I. They represented all of the technologies considered for both pressure-fed and pump-fed systems and became the basis for the required parametric engine characteristic data. The pertinent engine point design data as well as design characteristics are summarized on Table II.

Point Design Engines I and II represent the pressure-fed engines. A chamber pressure of 100 psia was assumed for both of these engines and reflects the recommended approximate chamber pressure for avoiding significant combustion stability problems. A 10K thrust level was assumed in both cases.

Point Design Engine I incorporates a HIPERTHIN injector with a liquid/liquid injection system. The thrust chamber assembly consists of a radiation-cooled fibrous graphite chamber with a detachable columbium nozzle extension. This configuration permits deep throttling and is not limited by burn duration.

Point Design Engine II is a fixed thrust engine utilizing a conventional liquid/liquid injection system. It has an ablative thrust chamber of phenolic graphite with a fibrous graphite throat insert as well as an attachable columbium nozzle extension.

The remaining engines are all pump-fed. Engines III and IV represent the passively-cooled engines while Engines V through IX represent the active cooled systems.

Engine III (30K thrust and 600 Pc) features a fuel-rich turbine bleed cycle with a conventional liquid/liquid injection system for fixed thrust application. The thrust chamber concept is identical to Engine I, except that the turbine exhaust manifold located at the columbium skirt attachment area

TABLE II

ENGINE POINT DESIGN DEFINITION

Point Design	F	Pc	Feed System	Cycle Category	TCA Inj	Inj Type	Throat Cooling	Nozzle Cooling	Throttling
I	10K	100	Press	--	Liq/Liq	HYPERTHIN	Rad	Rad	Throttleable
II	10K	100	Press	--	Liq/Liq	Convent	Abl	Abl/Rad	Fixed
III	30K	600	Pump	Bleed	Liq/Liq	Convent	Rad	Rad	Fixed
IV	30K	600	Pump	Bleed	Liq/Liq	MMX	Abl	Abl/Rad	Throttleable
V	25K	500	Pump	Bleed	Liq/Liq	Convent	LF/Regen	Reg/Rad	Fixed
VI					Eliminated				
VII	40K	1500	Pump	Staged	Gas/Liq	(Platelet)	LOX Transp	Graphite/ Colb/Rad	Throttleable
VIII	40K	1500	Pump	Staged	Gas/Gas	(Platelet)	GF Transp	Graphite/ Colb/Rad	Throttleable
IX	70K	1500	Pump	Bleed	Liq/Gas	(Tubes)	LOX Transp	Reg/Rad	Fixed

ratio. Engine IV is the sister engine but features a momentum exchange injector capable of 10:1 throttling. In this case, the thrust chamber assembly is an ablative chamber similar to Engine II in design.

(U) Engine V is a liquid fuel regeneratively-cooled engine. It represents the current or baseline technology. As such, it is designed as a fixed thrust engine with a liquid/liquid conventional injection system and is fed by a fuel-rich bleed turbine drive.

(U) Engine VII represents a staged-combustion engine utilizing a gaseous oxidizer/liquid fuel platelet injector. This engine configuration is very similar to the ARES engine, modified to obtain deep throttling. It features an oxidizer-rich turbine drive, fed by an oxidizer-rich bipropellant gas generator. The thrust chamber is liquid oxidizer transpiration-cooled followed by a fibrous graphite nozzle extension and an attachable columbium skirt. The engine is fully-throttleable 10:1. A chamber pressure of 1500 psia was selected. This approaches the upper limit for a 1200°F turbine inlet temperature, but is necessary because of difficulties in meeting the turbopump assembly power balance with oxidizer-rich turbine gases.

(U) Engine VI was originally intended to be the high pressure version (Pc = 2500 psia) of Engine VII, but was eliminated because of problems in meeting the turbopump assembly power balance.

(U) Engine VIII represents a gas/gas injection staged-combustion engine. The fuel-rich turbine drive gases are generated in a CAT-Pack, thermal-bed, or bipropellant gas generator depending upon the fuel specified. The thrust chamber is transpiration-cooled by gaseous fuel, followed by a gaseous fuel regeneratively-cooled nozzle extension and an attachable columbium skirt.

(U) Engine IX is a fixed thrust engine. It was an attempt to combine the bleed cycles with the staged-combustion cycle by injecting gaseous fuel and liquid oxidizer into the main chamber via a tubelet injector. A small part of the gaseous fuel flow is used to drive the bleed turbine. The chamber is transpiration-cooled by liquid oxidizer followed by a liquid oxidizer regeneratively-cooled nozzle extension and a columbium radiation-cooled skirt. However, this engine did not compare favorably with the other concepts and was subsequently eliminated.

(C) Table III is a summary of the thrust chamber and engine performance for CLF_5/N_2H_4 while Table IV summarizes this information for the CLF_5/MHF-5 propellant combination. The performance level in both tables was calculated in an identical manner using the methods described in Appendix II (Part II of this report). The cooling flow rates, which were calculated for each engine design point, also are included on the tables. Table IV is of particular interest because it shows the lowest performance numbers of all the specified propellant combinations.

TABLE III

BASELINE ENGINE PERFORMANCE SUMMARY (U)

Engine No.	CLF_5/N_2H_4 Thrust Level lb	CLF_5/N_2H_4 Chamber Pressure psia	Throat Cooling Method	Thrust Chamber Mixture Ratio O/F	Thrust Chamber Delivered Specific Impulse sec	Thrust Chamber % Theo I_s	Engine Mixture Ratio O/F	Engine Delivered Specific Impulse sec
I	10K	100	Radiative (FFC 0-3.4% Wt)	2.25/2.03	330/327.1	89/89	2.25/2.03	330/327.1
II	10K	100	Ablative (FFC 3.4% Wt)	2.04	325.4	88.7	2.04	325.4
III	30K	600	Radiative (FFC 7.7% Wt)	1.97	340.0	92.4	1.94	339.1
IV	30K	600	Ablative (FFC 7.0% Wt)	2.0	338.0	92.0	1.97	337.1
V	25K	500	Regen. (FFC 0.0% Wt)	2.50	346.0	92.5	2.45	345.1
VII	40K	1500	Transpire - Liq. Oxid. (5.5% Wt)	2.74	347.4*	92.1	2.74	347.4
VIII	40K	1500	Transpire - Gas Fuel (4% Wt)	2.25	357.8	96.1	2.25	357.8
IX	70K	1500	Transpire - Liq. Oxid. (7.1% Wt)	2.82	347.4**	92.5	2.69	344.5

Conditions:

CLF_5/N_2H_4

$\varepsilon = 150$

Vacuum

**ARES Tubelet Injector

*ARES HIPERTHIN Injector

TABLE IV

BASELINE ENGINE PERFORMANCE SUMMARY (U)

Engine No.	CLF_5/MHF-5 Thrust Level lb	CLF_5/MHF-5 Chamber Pressure psia	Throat Cooling Method	Thrust Chamber Mixture Ratio O/F	Thrust Chamber Delivered Specific Impulse sec	Thrust Chamber % Theo I_s	Engine Mixture Ratio O/F	Engine Delivered Specific Impulse sec
I	10K	100	Radiative (FFC 0-2.86% Wt)	2.0/1.86	322.7/ 319.3	89.4/ 89.0	2.0/1.86	322.7/319.3
II	10K	100	Ablative (FFC 2.86% Wt)	1.86	317.3	88.5	1.86	317.3
III	30K	600	Radiative (FFC 6.5% Wt)	1.84	331.7	92.2	1.81	330.8
IV	30K	600	Ablative (FFC 6% Wt)	1.88	329.6	91.4	1.85	328.7
V	25K	500	Regen	--	--	--	--	--
VII	40K	1500	Transpire - Liq. Oxid (5.1% Wt)	2.50	340.2*	92.5	2.50	340.2
VIII	40K	1500	Transpire - Gas Fuel (5.3% Wt)	1.98	349	96.2	1.98	349.2
IX	70K	1500	Transpire - Liq. Oxid (6.5% Wt)	2.60	341.6**	93.3	2.47	338.7

Conditions:

CLF_5/MHF-5

ε = 150

Vacuum

**ARES Tubelet Injector

*ARES HIPERTHIN Injector

VI - Eliminated

(C) The performance for the other specified fuels also was determined. This information is tabulated and compared on Table V, whereon the data are estimated based upon theoretical performance differences (i.e., the loss of performance from the base propellant is approximately 4 sec for the 80/20 blend, 6.5 sec for MMH, and 8 sec for MHF-5). It was found that the actual performance difference between the various fuels is approximately equal to the theoretical performance differences.

(U) As indicated on Table V, the engine performance levels of the pressure-fed engines is not much higher than could be achieved with the current earth storable propellants N_2O_4/A-50. This is partly attributable to the rapid increase of the kinetic losses for chamber pressures below 600 psia. The cooling requirements for Point Design Engines III and IV are large as can be seen from Table III. This could be reduced by one half if HIPERTHIN injectors had been incorporated. It also is estimated that an increase in performance of 7 sec of specific impulse could have been achieved.

(C) The highest performance of 358 sec was calculated for Engine VIII which features gas/gas injectors and gaseous fuel transpiration cooling. This results in a very short chamber and consequently, a small coolant flow requirement. The high level of performance was achieved by incorporating advanced technological techniques for almost every component.

(U) The performance numbers provided in this report are not specific because currently, little experience exists with the specified propellant combination or some of the more advanced concepts. This performance tolerance is both difficult to assess and will be different for each engine concept as well as the technology used.

(U) In view of the performance numbers not being specific, it was decided to investigate the effect of individual technology changes upon engine capabilities rather than to compare engine against engine. This significantly reduces the uncertainty and is in agreement with the basic study objective.

(U) As shown in the subsequent discussion, it is not possible to utilize the best performing propellant combinations for all engine concepts because of the significant differences in fuel characteristics. Selection depends largely upon the mission requirements and engine chamber cooling concepts.

B. PRINCIPAL ASSUMPTIONS

(U) Specific basic assumptions were necessary to provide realistic point design engines as well as technology variations within the scope of this study.

TABLE V

ENGINE PROPELLANT PERFORMANCE COMPARISON OXIDIZER - CLF_5 (U)

Engine Point Design	Specific Impulse (DEL) sec			
	N_2H_4	.80 N_2H_4 + .20 NH_3	MHF-5	MMH
I	327.1	323.6	319.3	321.8
II	325.4	321.9	317.3	319.8
III	339.1	336.4	330.8	333.9
IV	337.1	334.1	328.7	331.7
V	345.1	---	---	---
VII	347.4	343.2	340.2	342.2
VIII	357.8	354.9	349.2	351.9
IX	344.5	340.3	338.7	340.7

1. Performance

The following assumptions were made in connection with performance:

ERL Losses for Various Injection Methods were Based Upon Experience

L* Assumed for Various Injection Methods was in Agreement with ERL

MRD Losses Considered Coolant Flow Only (No Injector Flow Distribution Effects)

MR and Percentage of Coolant Flow was Constant During Throttling Mode

The most fundamental assumption in the analysis is the definition of ERL losses and L* requirements for all of the different injection methods and injector configurations. An ERL and L* relationship was assumed to preclude a detailed layout as well as evolvement of an optimum chamber-injector relationship. These assumptions were based upon experience and engineering judgment (see Figure No. 5).

The low ERL and very short 5-in. L* assigned to the gas/gas injection method is of particular interest. This assumption is based upon Aerojet-General Independent Research and Development investigations conducted with gaseous oxygen and gaseous hydrogen injection, wherein it was indicated that ERL leveled out after only 3.5 in. of L* (see Figure No. 6). However, a more accurate determination of the optimum L* is required for the specified propellants, particularly as regards the staged-combustion engine concept. To offset this lack of optimum L* information, provisions have been made to correct both weight and performance information for different characteristic lengths. The L* assumed for the different injector concepts used in this analysis are shown on Figure No. 5.

The performance data shown on Figure No. 6 as a function of combustion chamber characteristic length (L*) were obtained from an IR&D program (8709-40) completed in February 1967.(1) During this program, four gas/gas injector types (axial tubelet and radial tubelet) were built. They were tested at a chamber pressure of approximately 600 psia and a thrust level of approximately 700 lb with oxygen/hydrogen propellants. The gaseous propellants (approximately 1400°F) were supplied by two gas generators (fuel-rich and oxidizer-rich). Thrust and flow rate were measured. In addition, complete pressure and temperature surveys were accomplished. The performance shown on

(1) IR&D Program No. 8709-40, Low L* Gas/Gas Combustion Study, Completed February 1967.

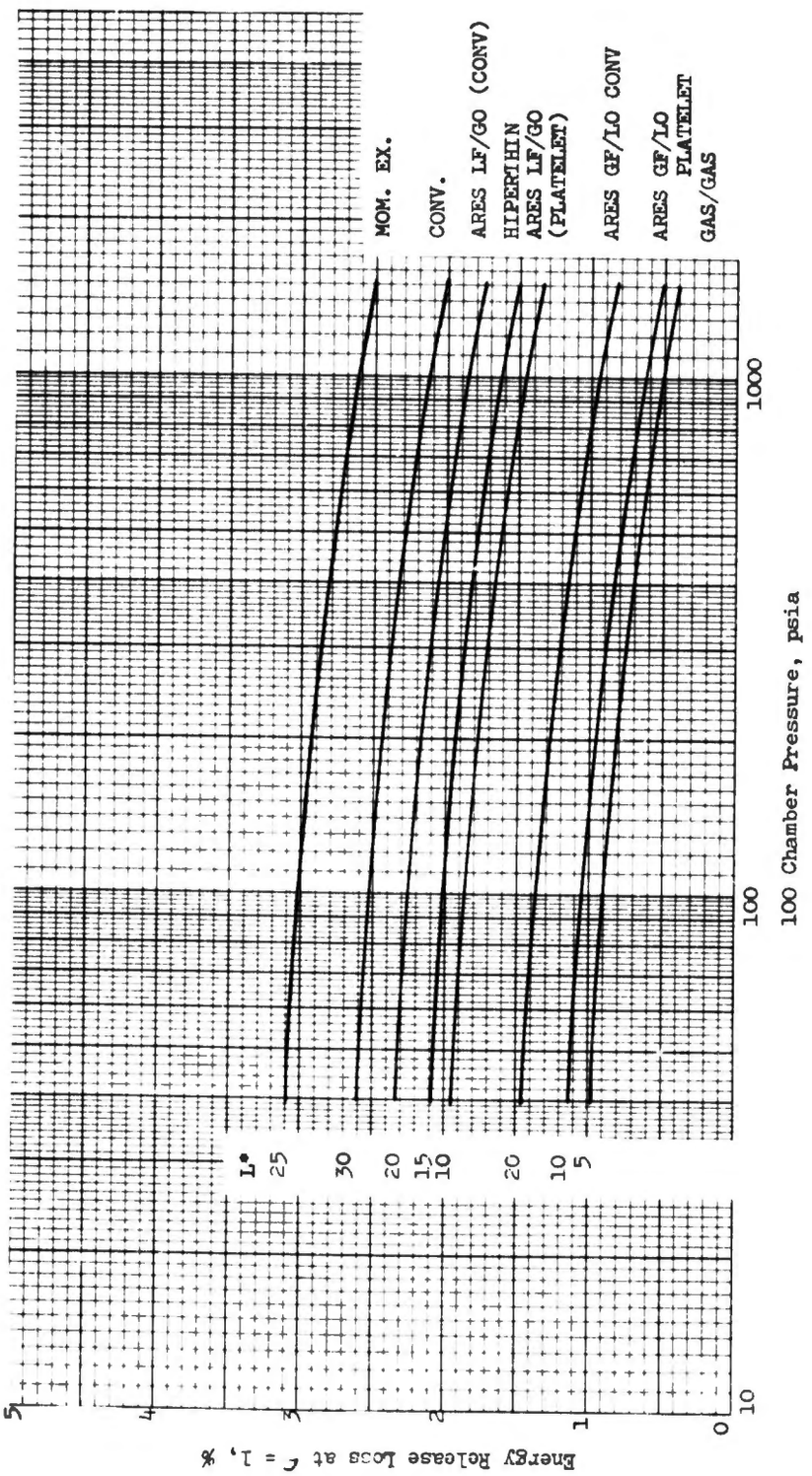

Figure 5. ClF_5/N_2H_4 Energy Release Loss-Injector Trade-Off

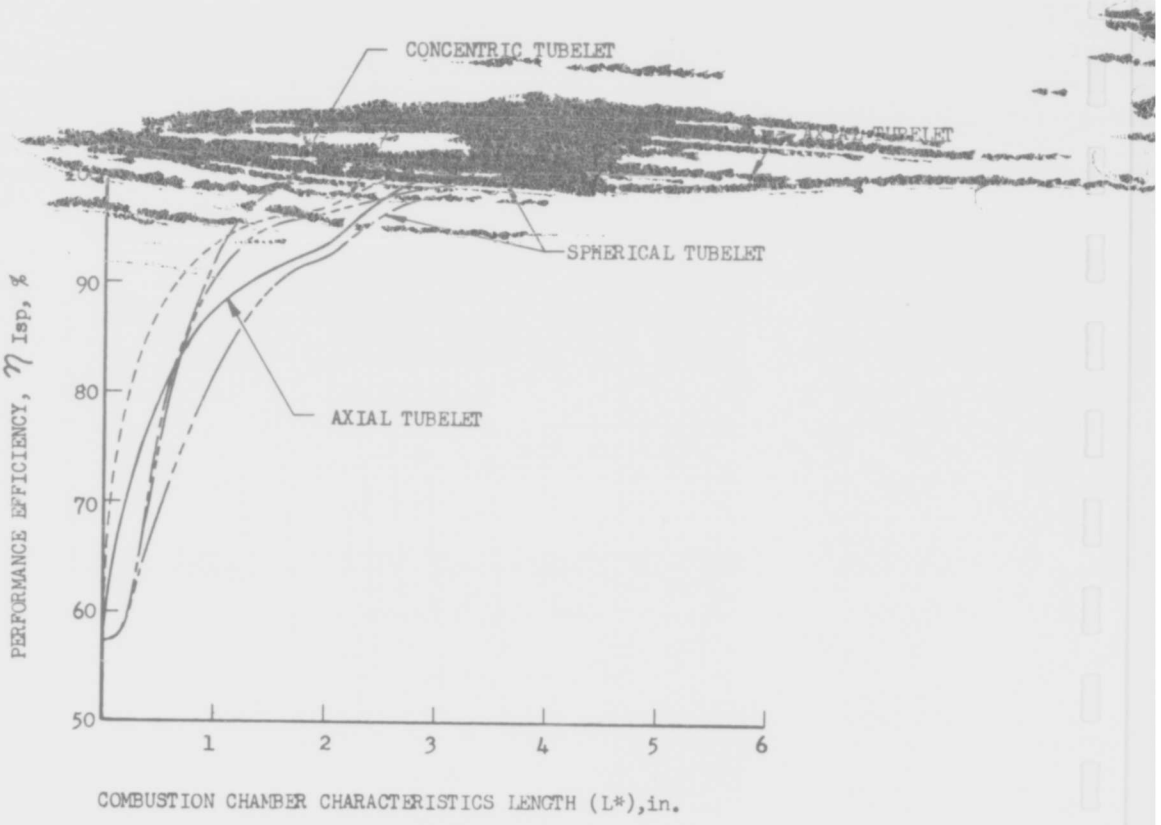

Figure 6. Characteristic Length (L*) for Gas/Gas Injection, O_2/H_2

Figure No. 6 was obtained by eliminating friction and heat transfer losses in the same manner as accomplished in the referenced IR&D Program.(2) The remaining loss in performance was attributed to combustion performance (ERL). The performance profile shown on Figure No. 6 is of even greater importance than absolute performance and was obtained similarly to the way this was done in IR&D Program 8709-40(3). The chamber length (L^*) associated with no further change in combustion performance represents the location at which combustion and mixing was [illegible] complete. Therefore, the combustion [illegible] lengths could be [illegible] to approximately 3 in.

[illegible] the method of performance analysis, it was further assumed that mixture distribution losses are caused only by film cooling and transpiration cooling requirements. In all cases, the core was assumed to have a constant mixture ratio distribution.

Appendix II (Part II of this report) provides a complete listing of basic assumptions for determining performance.

2. Chamber Cooling

The following assumptions were made in connection with chamber cooling:

Fuel Cooling has Zero Reaction with the Core

Fuel is Completely Decomposed

Liquid Oxidizer Partially Reacts with the Core (50% Performance Effectivity)

No Enhancement Resulting from the Decomposition of CLF_5

Cooling requirements for all of the cooling methods were determined by assuming that all of the injectors considered were non-streaking and operating stably. Therefore, the cooling requirements were based upon the chamber material capability, propellant cooling capability, and heat flux. Some uncertainty exists regarding the cooling capability of CLF_5 at elevated temperatures because the rate of the endothermic decomposition (enhancement) has not been determined. However, based upon available test data, the rate of reaction is extremely slow for temperatures as high as 750°F(4) and it was assumed that CLF_5 offers no benefit as a result of enhancement.

The coolant performance losses for fuel film-cooling and fuel transpiration-cooling were determined by assuming no reaction of the coolant

(2) Ibid.
(3) Ibid.
(4) Physical Chemical Characteristics of Hi-Energy Storable Propellants, Contract AF 04(611)-9380, Final Report R-6147, AFRPL-TR-65-125, May 1965.

flows with the core, which is already essentially fuel-rich. However, for the oxidizer transpiration coolant, it was assumed that 50% reaction with the core could be obtained (i.e., for each percentage of coolant flow, only .5% of performance is lost). The fuels considered have monopropellant characteristics; coolant losses are therefore, lower than for the oxidizer because of the available monopropellant specific impulse.

In determining the monopropellant fuel coolant flow requirements, it also was assumed that the fuel approaches the complete decomposition temperatures at the point of injection into the thrust chamber.

3. Material Capability

The following assumptions were made in connection with material capability:

Nickel in Liquid Oxidizer Cooling	1750°F
Nickel in Gaseous Fuel Cooling	2000°F
Fibrous Graphite Platelets in Oxidizer and Fuel Cooling	3500°F
Fibrous Graphite Nozzle Extensions	4500°F
Columbium Nozzle Extension	2200°F
Turbine Maximum Temperature in CLF_5-Rich Gases	1200°F
Turbine Maximum Temperature in Fuel-Rich Gases	1600°F

The material temperature capability for most of the critical components (i.e., thrust chamber assembly and turbine) is summarized in this section.

Different allowable maximum temperatures were assumed for material operating in an oxidizer-rich environment than was assumed for material in a fuel-rich environment.

In the case of nickel platelets with transpiration cooling, 2000°F was assumed for fuel cooling while 1750°F was assumed for liquid oxidizer cooling. An operating temperature of 3500°F was assumed for fibrous graphite platelets in both a fuel-rich and oxidizer-rich environment. A temperature of 4500°F was assumed for determining the attachment area ratio for fibrous graphite nozzle extensions.

The attachment area ratio of columbium nozzle extensions was determined by assuming a temperature capability of 2200°F, which is in agreement with current experience.

For turbine operation, it was assumed that for a fuel-rich turbine, a 1600°F inlet temperature is feasible, based upon experience. There is no available experience for oxidizer-rich turbine operation; therefore, it was assumed that a 1200°F inlet temperature for Udimet 700 blade material constitutes the maximum temperature limit.

4. Engine Cycle

The following assumptions were made in connection with the engine cycle:

Injector Stiffness Requirements Based upon Experience

Bleed Turbine Exhaust through Nozzle Extensions

Two-Stage Bleed Turbines

Staged-Combustion Turbines Are Single-Stage

Single Shaft Turbopump Assembly

Partial-Admittance, Hydraulic-Driven Boost Pumps

It was necessary to provide criteria for the minimum feed system and injector stiffness to permit a determination of turbopump discharge pressure requirements. The minimum ratio of $\Delta P/P_c$ is as follows:

	Gas Generator		Main Injector Type					
			Liquid-Liquid		Liquid Gas		Gas-Gas	
	Ox	Fuel	Ox	Fuel	Ox	Fuel	Ox	Fuel
$\frac{\Delta P \text{ (Over-all,)}}{P_c}$%	20	20	35	40	10	40	10	10
$\frac{\Delta P \text{ (Injector)}}{P_c}$%	10	15	15	20	10	20	10	10

Over-all % indicates the minimum stiffness requirement from the pump discharge to the injector face for both the gas generators and main injectors in bleed cycle engines. Staged-combustion engines utilize the over-all stiffness between the pump discharge and the gas generators as well as between the turbine discharge and the main chamber. "Injector" in the above tabulation includes the injector manifold as well as the orifice pressure drop.

In some instances, after a detailed injector analysis of each injection method and configuration was accomplished, the stiffness requirements were increased.

A number of assumptions were necessary when considering the pump-fed systems to limit the scope of this investigation. These assumptions follow.

All bleed turbines working at large pressure ratios were limited to two-stage configurations. In all cases, the bleed turbine exhaust was manifolded back into the thrust chamber nozzle extension to supply coolant gas (700°F) for the columbium nozzle extension. In turn, this reduced the nozzle extension attachment area ratio and resulted in an engine weight savings. All the turbines for staged-combustion cycles working at a small pressure ratio, were assumed to be single-stage turbines.

For both the bleed and the staged-combustion cycles, the turbopump assembly was assumed to be a single shaft design. This simplified control design although it necessitated advanced seal designs between the oxidizer and fuel circuits.

All controls were assumed to be electromechanically actuated or solenoid-actuated valves. Hydraulic and pneumatic actuating systems were not considered in this analysis. These controls include mixture ratio control, gas generator control, and the ring-gate valve, as applicable. Suction valves were not included in the weight information because they are considered part of the systems weight.

It was determined that oxidizer boost pumps are required for all pump-fed engines because of the CLF_5 vapor pressure characteristics. The boost pump weights are not included in the engine weight because suction pressure requirements can change from mission to mission. These weights are identified separately. It was assumed that all boost pumps are partial-admission, hydraulic turbine-driven inducers to obtain maximum installation flexibility.

IV. POINT DESIGN ENGINE DESCRIPTION

The ensuing discussion is a detailed description of the design concepts for each of the Engine Point Designs. This design effort was accomplished to obtain mechanically feasible concepts for each of the engines as well as their physical dimensions. In this way, a base was established, from which parametric weight and envelope information could be derived. Layouts of pertinent components (i.e., thrust chamber assembly, turbopumps, and engine control valve) were produced and integrated into an engine system. Weight factors were defined in this way and the integrated engine weight was compared with the sum of component weight. Subsequently, this data were applied to the parametric engine weight definition.

The cooling requirement for each engine was determined by heat transfer analysis for full thrust as well as throttled conditions. Also, the transition section between the chamber and nozzle extension cooling methods were defined. Then, the analysis was extended in a parametric expansion to define the cooling requirements for each engine concept.

The thrust chamber assembly, the heat transfer aspect, and the engine control concept are detailed for each Point Design Engine, along with a discussion of engine capability. Detailed performance weight, and heat transfer analyses are presented in Appendixes II, III, and IV, respectively, of this report (Part II). Appendix V is a description and discussion of the gas generator concepts while Appendix VI details turbopump design. Appendix I is an extensive discussion of the propellant characteristics.

A. PASSIVELY-COOLED ENGINE CONCEPTS

The passively-cooled engines include those with radiation-cooled and ablative-cooled thrust chambers. These cooling concepts offer the advantages of being able to accept all of the specified propellant combinations and their use results in a relatively simple system with high reliability.

The technology for Engines I through IV is quite similar. Therefore, they are discussed as a single group. Although only the Point Design Engines are detailed, a large number of other engine configurations are possible utilizing the same technology (see Table VI). The complete parametric data for seven out of a possible twelve configurations are subsequently presented in this report.

1. Pressure-Fed Engines

Engine Point Designs I and II are designed for identical thrust chamber pressure, thrust, and a nozzle expansion area ratio of 150:1. Both are intended for CLF_5/N_2H_4 propellants. This was done so as to obtain a direct comparison of weight and performance between radiative-cooled and ablative-cooled engines.

TABLE VI

PASSIVELY COOLED ENGINE TECHNOLOGY MATRIX

		Pressure Feed		Pump Feed Bleed Turbine Drive	
		Ablative TCA	Radiative TCA	Ablative TCA	Radiative TCA
Fixed Thrust Engines	Convent Injector Liq/Liq	Point Des. II P	P		Point Des. III P
Throttleable Engines	HYPERTHIN Injector Liq/Liq		Point Des. I P		
	Momentum Exchg. Liq/Liq		P	Point Des. IV P	- P

P = Parametric Data

Point Des. = Complete Layouts and Parametric Data

a. Point Design Engine No. I

This engine has a 10K thrust level, radiation-cooled thrust chamber assembly, and an expansion area ratio of 150:1 (see Figure No. 7). The exit diameter is 104 in. and the over-all length is 179.2 in. The Point Design performance was calculated using the methods described in Appendix II and this performance is summarized on Table VII along with the optimum engine mixture ratio. The flow and pressure schedule established is shown on Figure No. 8.

(1) Thrust Chamber Design

The thrust chamber is of the radiation-cooled variety. Auxiliary fuel film cooling is provided to reduce the thermal load at the throat section and injector flange if necessary. It is desirable to operate this chamber at as high an inner wall temperature as possible to minimize the cooling performance losses resulting from a minimal film coolant flow rate.

The combustion chamber is made from high density fibrous graphite followed by an attached columbium skirt (see Figure No. 9).

Graphites are almost the ideal material for use with halogen systems. They are chemically compatible, have a very high operational temperature of 4500°F or higher, and are easily fabricated. However, their mechanical strength and shock resistance has severely hampered their use for anything other than such items as nozzle inserts. Relatively recent developments have revealed a class of graphites that has high strengths (e.g., 30,000 psi tensile) and good shock resistance, both thermally and mechanically. This new class of graphites is termed Fibrous Graphite because it is composed of built-up graphite fibers (cloth or filaments), impregnated with pitch, carbonized, and graphitized in high temperature furnaces. The resulting structure is slightly porous, but it is nearly ideal for a free-standing, radiation-cooled thrust chamber. Such a chamber has been successfully tested by Aerojet-General at 100 psia. The calculated wall temperature at the throat was 4500°F and the chamber showed no erosion after several tests. The density of this material is less than that of most metals; therefore, lightweight, high performance thrustors are possible, at least in the low chamber pressure range. No film cooling is required for the throat because 4500°F is the steady-state operating temperature at full thrust without coolant. A small amount of cooling would still be required at the injector-chamber joint depending upon the burn duration.

It has been assumed that large diameter fibrous graphite shells are beyond the capabilities of existing graphitization furnaces. However, it is possible that at large area ratios, fibrous graphite nozzles would require carbonization only without graphitization. If this is possible, such nozzles could be used instead of the columbium nozzle extensions.

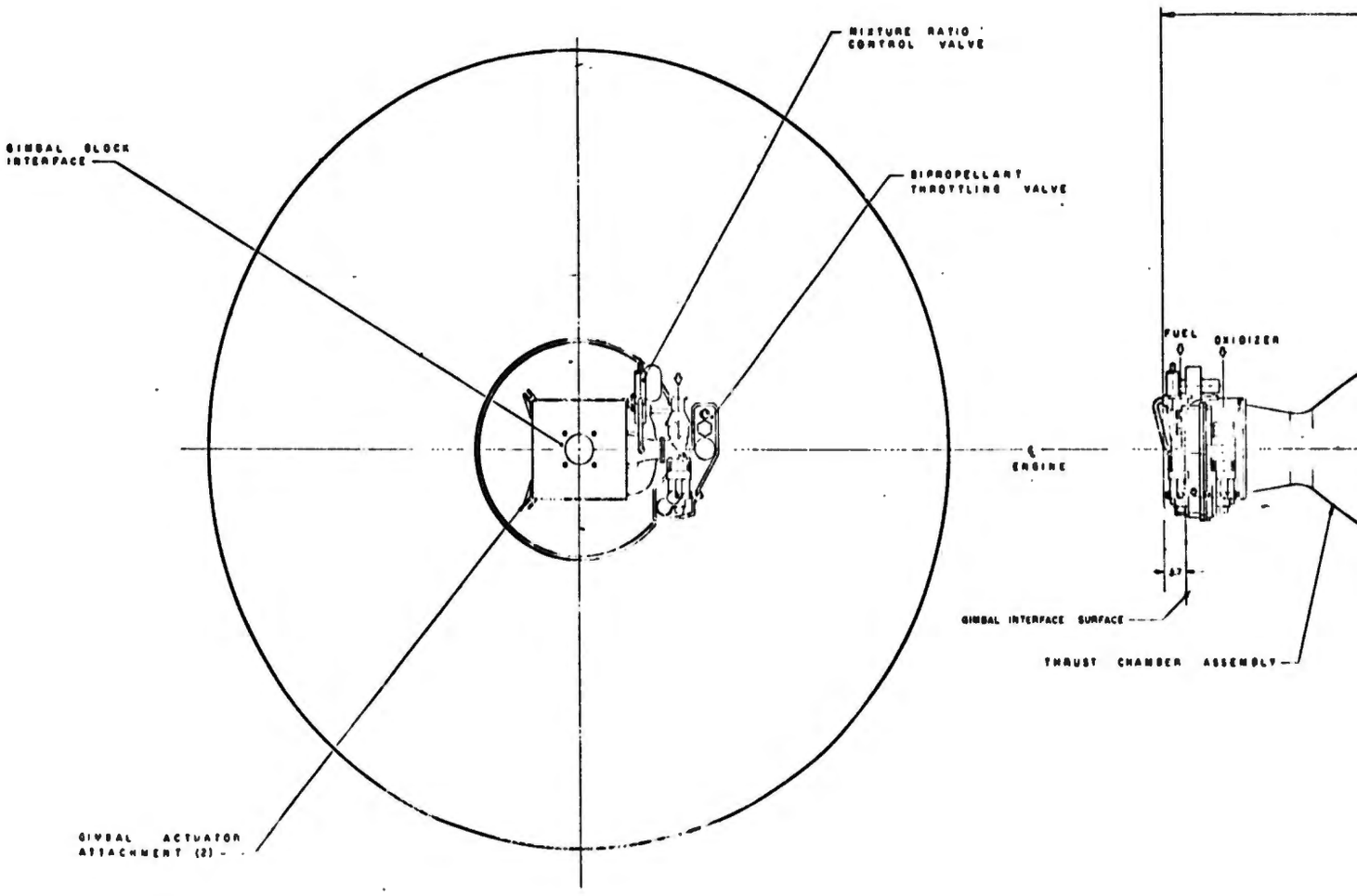
MIXTURE RATIO CONTROL VALVE
GIMBAL BLOCK INTERFACE
BIPROPELLANT THROTTLING VALVE
FUEL
OXIDIZER
ENGINE
GIMBAL INTERFACE SURFACE
THRUST CHAMBER ASSEMBLY
GIMBAL ACTUATOR ATTACHMENT (2)

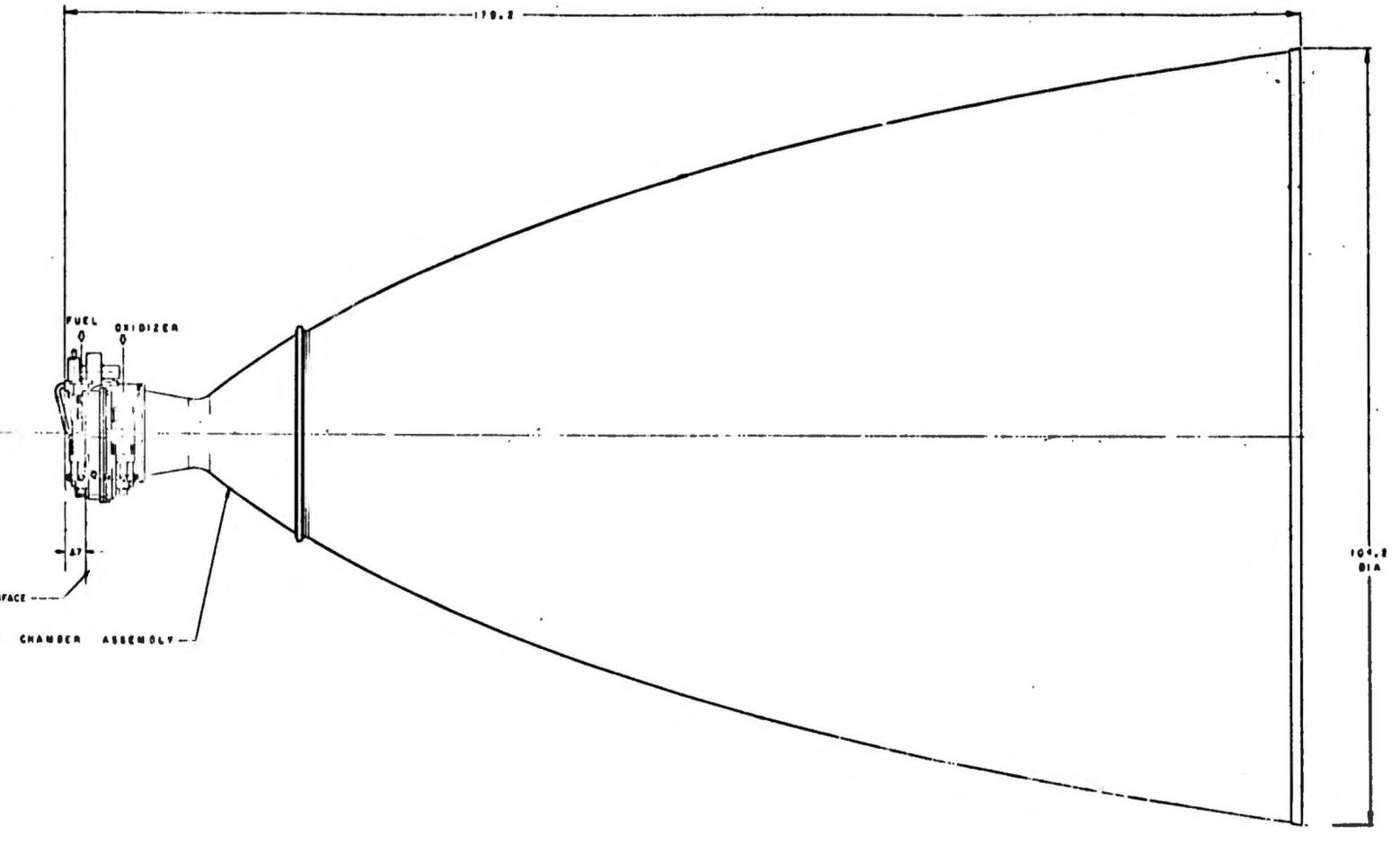

Figure 7. Point Design Engine No. I Assembly

TABLE VII

POINT DESIGN ENGINE NO. I (U)

Engine Configuration	
Pressure Fed	
Nickel HIPERTHIN Injector (Liquid-liquid laminar)	
Fibrous Graphite Chamber (to 10:1)	
Columbium Nozzle Extension (from 10:1 to 150:1)	
Performance	
Thrust	10,000 lb
Chamber Pressure	100 psia
Mixture Ratio	2.03
Delivered I_{sp}	327.1 sec
I_{sp} Efficiency	89.0

Design Specifications	
Dry Weight	531.4 lb
Wet Weight	544.5 lb
Length	179.2 in.
Diameter	104.2 in.
Throttling Range	(2 to 1)
Interface Pressure	
Oxidizer	150.0 psia
Fuel	150.0 psia
Fuel Film Coolant (% total flow - required to cool forward flange)	0-3.4%
Max Throat Wall Temperature	4500°F

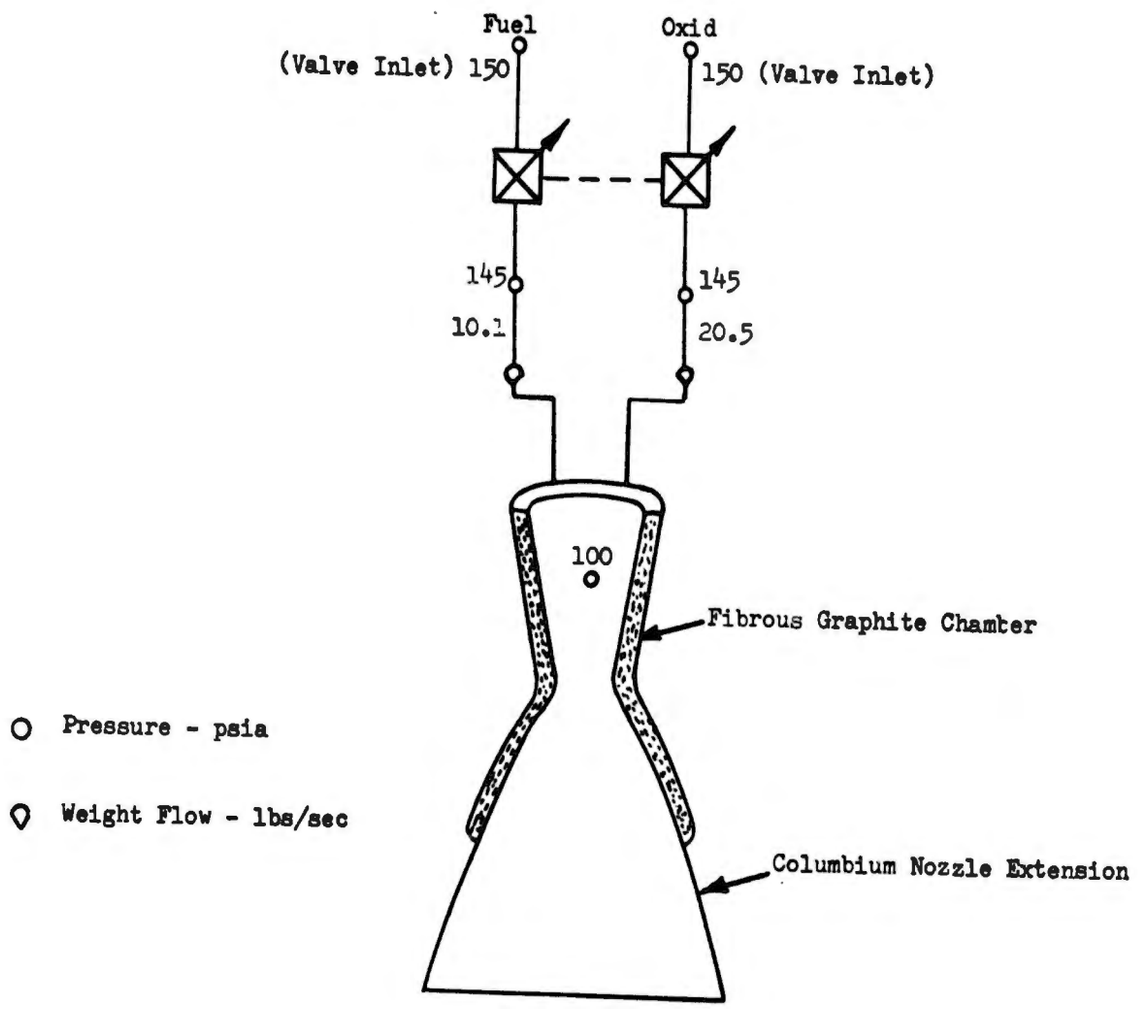

Figure 8. Engine Point Design I

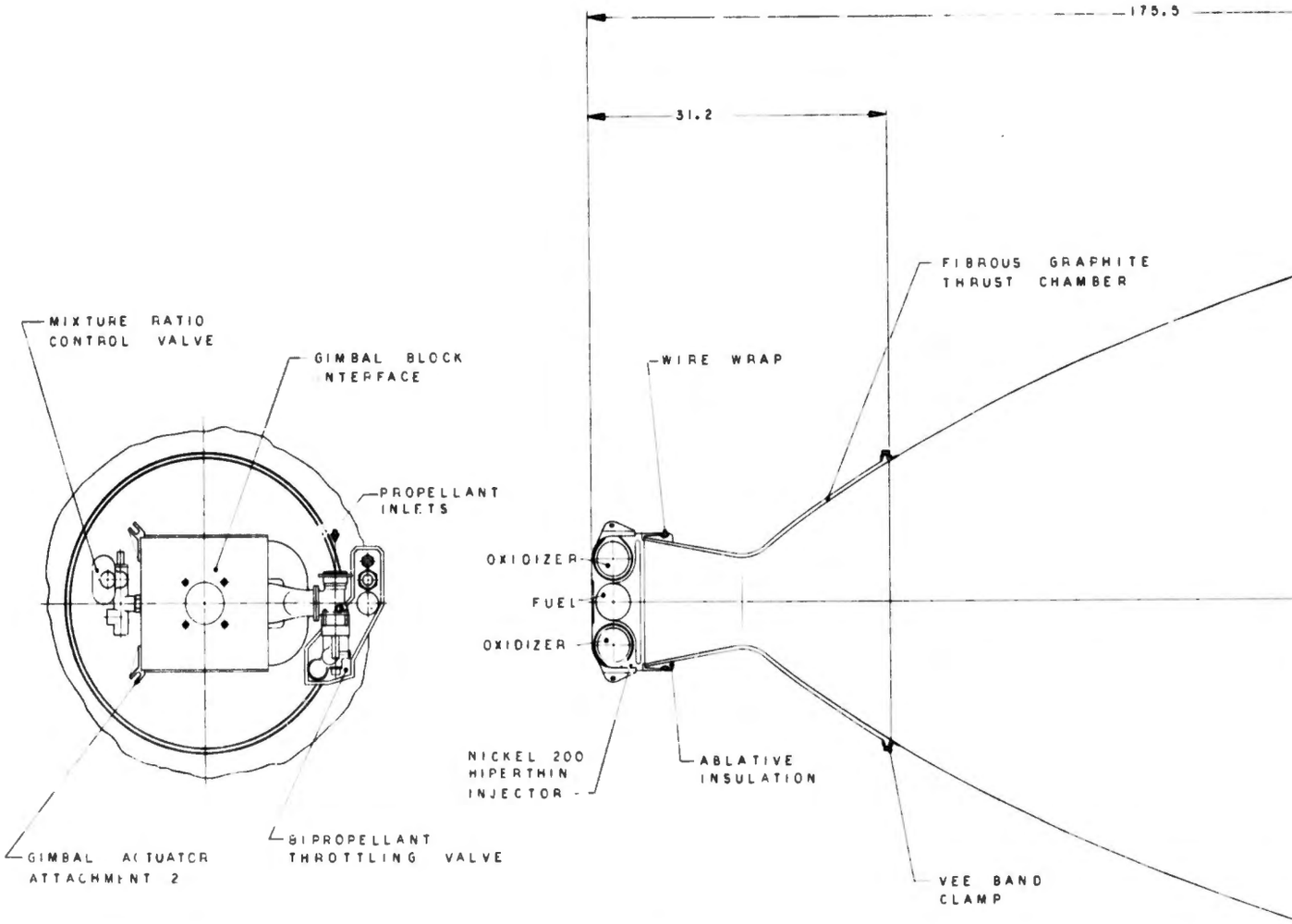

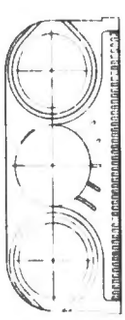

FUEL PLATELET TYPICAL

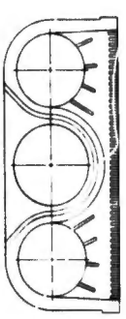

OXIDIZER PLATELET TYPICAL

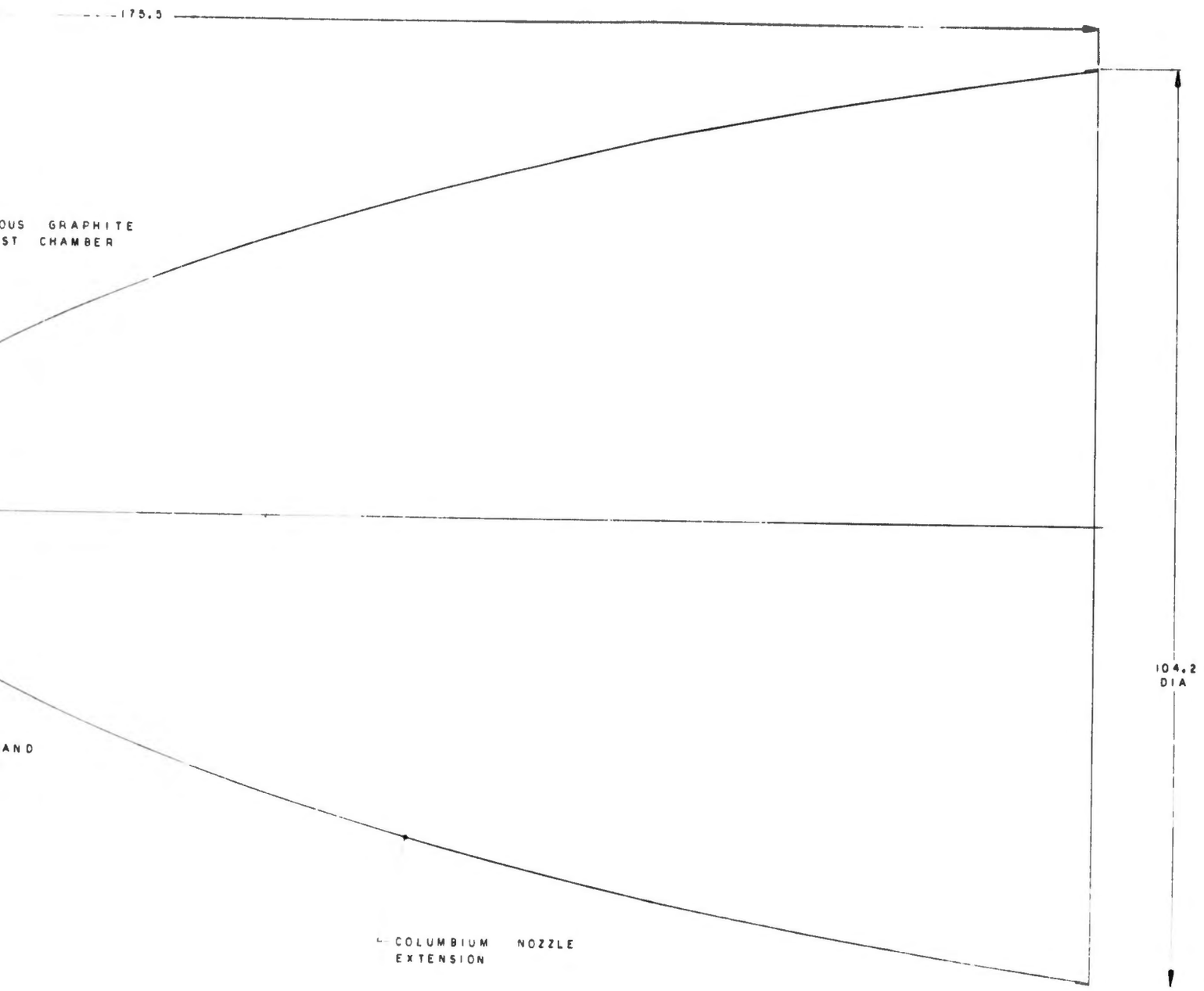

Figure 9. Thrust Chamber Assembly, Engine No. I

(2) Injector Selection

To obtain deep throttling, the HIPERTHIN injector concept was incorporated into Point Design Engine No. I, which characterized the laminar flow injector orifices. This is an Aerojet-General proprietary concept, which has been designated HIPERTHIN (High Performance Throttleable Injector) and is undergoing continuing development. It provides significant advantages over conventional injectors in the following four areas:

- Combustion Efficiency
- Throttleability
- Chamber Volume and Length Requirements
- Cooling Capability

Table VIII is a summary of Aerojet-General test experience with this concept. It also indicates that the concept is limited to relatively low thrust ranges.

It has other potential advantages in the areas of combustion stability and reliability; however, these have not been sufficiently demonstrated as yet. Currently, the concept appears to be applicable to virtually all of the propellant combinations, including liquid storables, cryogenics, and gaseous. The laminar flow injector selected requires no modification to the engine or pressurization system. The propellants are injected in laminar instead of turbulent flow; therefore, the relationship between pressure drop and flow rate is linear rather than logarithmic. As a result, injector "stiffness" (Pj/Pc) is automatically retained throughout the throttling range and no performance loss or feed system instability is anticipated. Laminar flow can be achieved only by using very small orifices if any significiant pressure drop per the unit length of the orifice is to be attained. The most convenient method for constructing such an injector is by stacking a set of thin, etched platelets. Small grooves are etched in one side of the metal plates and they become the feed and injection orifices (rectangular) when the plates are stacked and brazed together. The braze material is usually plated on one surface of the platelets so that only carefully controlled amounts of alloy are present. The area between the platelets is sealed to prevent internal leaks. Special care is taken so as not to plug the small etched grooves with the excess of braze alloy. This has been done successfully with CRES 347 platelets and copper or nickel alloys.

The "fine" resultant injection pattern provides good performance in small characteristics length chambers. It is possible to arrange the platelets so that only the alternate platelets flowing fuel will inject out to the thrust chamber wall. In this way, fuel film-cooling can be supplied concurrently to the chamber wall during throttling to preclude severe cooling and mixture ratio losses during deep throttling.

The thin platelets between injector propellant orifices are effectively transpiration-cooled by the injectants. Good injector face cooling is one of the significant assets of this platelet type injector, although it is probably essential because of the rapid energy release near

the injector face that these finely-divided hypergolic propellants produce. As with any injector, feed system stability is a mainly function of injector stiffness, or Pj/Pc for the platelet unit. Also, like any other injector, it can experience high-frequency combustion stability within the chamber. But, unlike many injectors, integral, self-cooled, injecting baffles can be electro-machined into the injector face. This has been done and was demonstrated to be very effective, even with short baffles, because the energy release zone is close to the injector face.

Testing has shown that CLF_5 is incompatible with 347 CRES injector platelet stacks although N_2O_4 has been successfully tested with this hardware. Therefore, Ni-200 platelet material was specified for this injector. This material appears to be the most compatible common metal for use with interhalogen oxidizers and is serviceable with liquid hydrazine. Ni-Oro braze alloy will be used to join the stack. Propellant feed lines will be of Ni-200 to handle the liquid oxidizer and also allow easy joining of the lines to the end plate of the injector.

(3) Thrust Chamber Geometry

The combustion chamber geometry is controlled by three parameters; characteristic length, contraction ratio, and over-all shape. These parameters are shown on Table IX. Figure No. 6 shows how the characteristic length is related to the injector design and propellant phases. Of particular significance is that for a given contraction angle in a conical chamber, the injector-to-throat dimension varies directly with the chamber characteristic length.

(4) Thrust Chamber, Nozzle Extension, and Injector Structure

The structural design of Thrust Chamber Assembly No. I is quite straight forward (Figure No. 7). Its chamber and skirt walls are sufficiently thick to withstand pressure-induced as well as thrust-induced hoop and axial loads. Additional thickness at the chamber throat section wall is required to allow for greater longitudinal loads in that region caused by gimbaling accelerations. The large nozzle imposes high loads in the small diameter throat area. All thrust loads are transferred to the gimbal block through the brazed injector platelet stack. This injector is sufficiently thick and strong enough to absorb these loads.

(5) Flange Structural Description

The thrust chamber forward flange is conventionally bolted and sealed to the injector, but the flange cannot be exposed to the high temperature chamber wall. Therefore, a thick ring of ablative insulation is used between the flange ring and the fibrous graphite wall. In this way, the conical chamber is retained, insulated and sealed. The aft flange utilizes a columbium clamp-ring to hold the columbium nozzle extension to the graphite

TABLE VIII

AEROJET-GENERAL HIPERTHIN TEST HISTORY

Propellants	Program	Type Injector*	P_c	Thrust	Tests	Duration (sec)	
						Cum	Max
GO_2/GH_2	Ace	Axial-Square-SH	495-1170	660-1680	3	5.5	2.2
	Advanced Injector (NASA)	Axial-Rectangular -SH	122-778	172-1599	8	9.2	1.3
CLF_3/MHF-5	Navy	Radial-Conical	300	300	1	.5	.5
		Axial-Round-SH	300-981	300-1156	4	3.2	1.0
N_2O_4/Alumizine	IR&D	Axial-Round-SH	508-850	111-196	3	3.0	1.0
N_2O_4/A-50 & MMH	ACS	Radial-Cylincrical	77-400	40-170	24	80	25.5
		Axial-Round-SH	83-95	42-59	8	315	264
	Beryllium	Axial-Round-SH	100	50	41	5553	1200
	Bimetallic-CC IR&D	Axial-Round-SH	100	100	5	737	500
	Long-Life Thrustor (NASA)	Axial-Round-SH	125	100	4	294	143
	Bimetallic-CC	Axial-Round-IMP	75	20	1	5	5
	Hiperthin-IR&D	Axial-Round-SH	100-1000	100-1000	27	54	8.2
		Axial-Square-SH	50-300	65-110	19	120	48
	Prcject K	Axial-Rectangular -IMP	500	50	45*	15	.5
	Ace	Axial-Square-SH	974	10,220	1	1.5	1.5
	PBPS-Axial	Axial-Round-SH	300-500	300-500	6	6	1
N_2O_4/N_2H_4	PBPS-Axial	Axial-Round-SH	500	500	3	3	1

* Short Pulse Tests
SH - Showerhead
IMP - Impinging

TABLE IX

THRUST CHAMBER ASSEMBLY NO. 1 DESIGN PARAMETERS

General	Injector	Chamber	Nozzle Extension
Thrust: 10K lb	Type: Axial HIPERTHIN	Shape: Conical	Attachment Area Ratio: 10
Chamber Pressure: 100 psia	Propellant Phases: Liquid - Liquid	Material: Fibrous Graphite	Cooling Mode: Radiation
Nozzle Area Ratio: 150	Thrust per Element: 0.20 lb per Doublet	Contraction Ratio: 2	Material: Coated Columbium
Throttleability: Good	Type Element: Laminar Showerhead	Cooling Mode: Radiation with Fuel Film Cooling	
	$\Delta P_{inj}/P_c$: 0.45	Characteristic Length: 15 in.	
Duration: Unlimited	Material: Ni-200		
	Film Cooling: 3.4% Fuel	Throat Dia: 8.50 in.	

chamber. This clamp-ring is a lightweight attachment and permits simple flange configurations. It is important that this joint be flexible (i.e., capable of deflecting when acted upon by differential thermal expansion and/or gimbaling-induced loads). The thin columbium flange acts as a "plastic hinge," because the modulus of the material is lowered by the elevated operating temperature. The thin columbium clamp-ring is intended to act in much the same way while effecting a seal against low pressure leakage through the joint. The graphite flange, which is less flexible, is considerably stronger and thicker than the columbium.

(6) Film Cooling Requirements

Point Design Engine No. I is a radiation-cooled, throttleable engine with a full thrust of 10K and a chamber pressure of 100 psia. A fibrous graphite wall (.35-in. thick) does not require any film cooling to operate at the full thrust maximum design temperature of 4500°F. However, fuel film cooling may be required to protect the chamber flange (maximum allowable temperature is 500°F) and prevent heat soak-back to the injector. The fuel film cooling flow rate was calculated so that the film coolant is a saturated vapor at the downstream edge of the flange. This flow rate is 3.4% of the total propellant flow. This cooling requirement assumes a burn duration in excess of 70 sec. For short burn durations, it appears that the forward flange cooling could be deleted for a 10K, 100 psia engine.

(7) Controls System Description

The pressure-fed engine system configuration of Point Design Engine No. I requires variable positioning of the thrust chamber valve for propellant flow control in response to an engine thrust or vehicle acceleration input value (see Figure No. 10). This valve will be electrically-operated in accordance with the basic criteria established at the outset of this study program. A poppet-type valve design utilizing an all-metal shut-off seal configuration will be used. The oxidizer and fuel valves will be mechanically-linked for reliable phasing during engine starting and shutdown transient operations. The all-metal, electrically-actuated bipropellant valve recently developed for the Transtage application (5) has been selected as the basic design for this pressure-fed engine system. This valve design, shown on Figure No. 11, would require a modification of the actuator to provide modulated control in addition to "on-off" operation. The mixture ratio fuel system bypass valve is shown on Figure No. 12.

The engine is started by supplying an opening signal to the bipropellant thrust chamber valve assembly which admits the hypergolic propellants to the thrust chamber. The opening time of the thrust chamber valves is controlled to 0.4 sec. Engine thrust can then be varied by applying appropriate input signals to the servo control network for the bipropellant thrust chamber valves. The electric servo actuator will then position the

(5) Contract AF(04)695-197

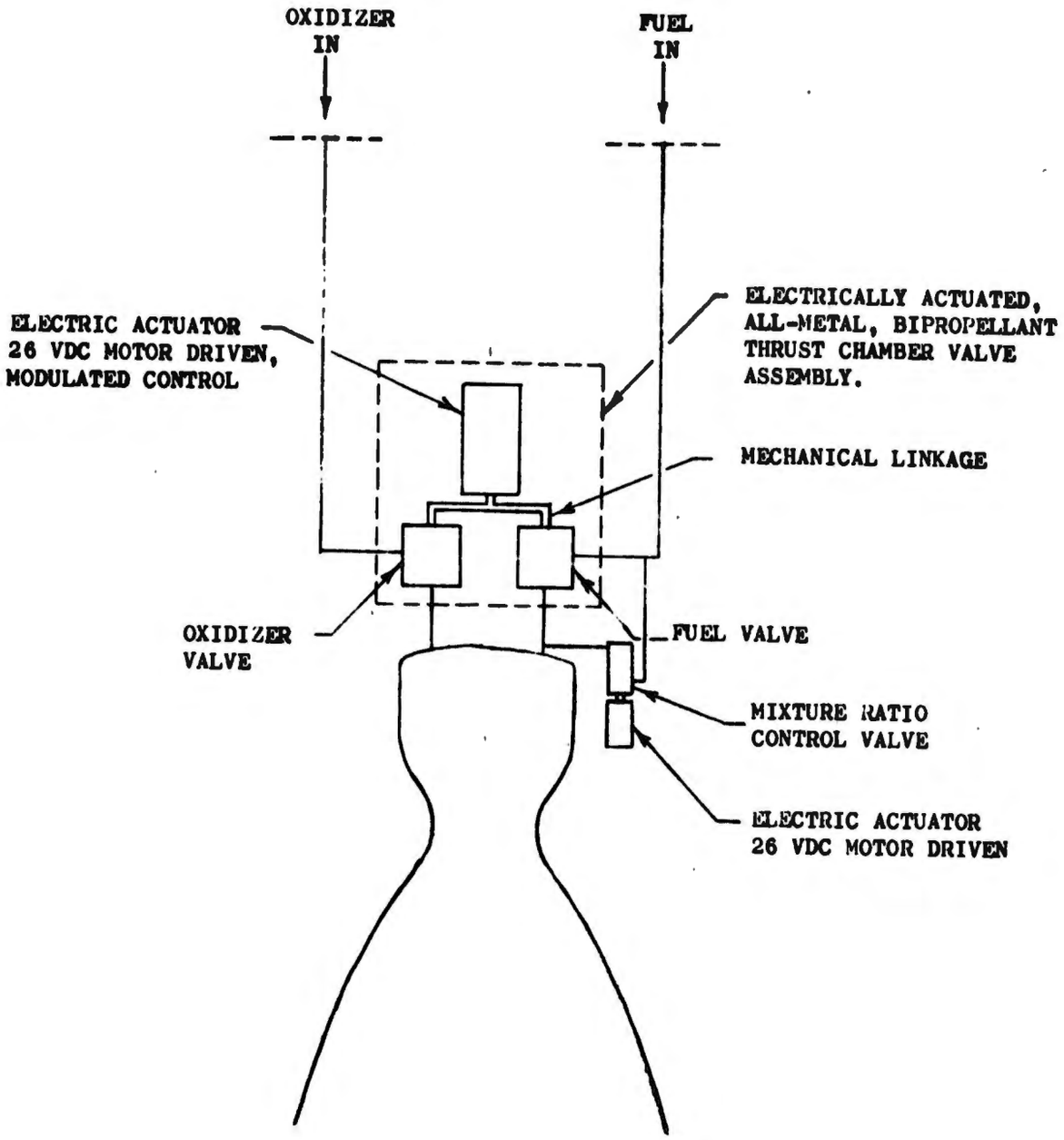

Figure 10. Controls Schematic, Point Design Engine No. I

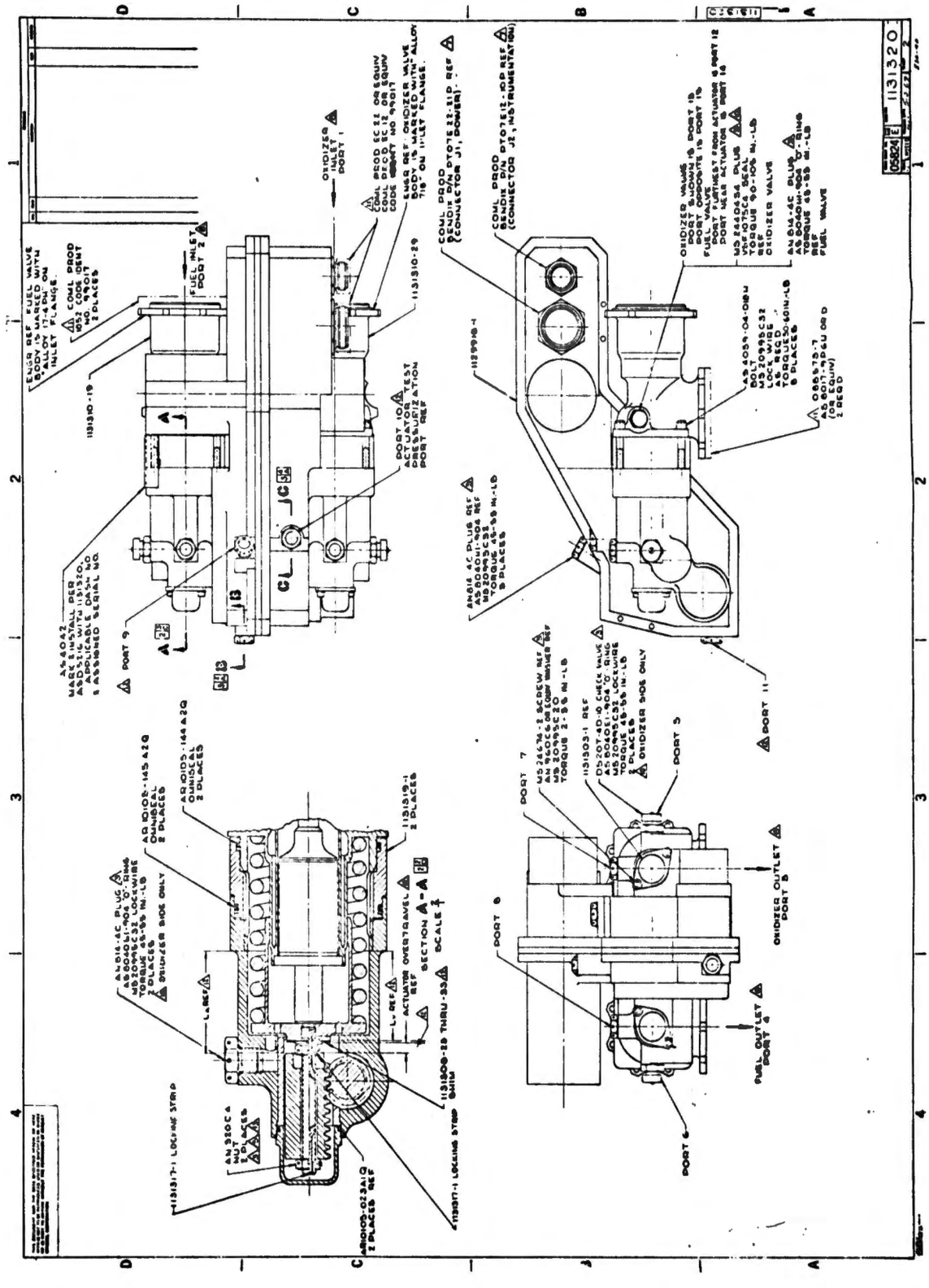

Figure 11. Control Valve, Point Design Engine No. I

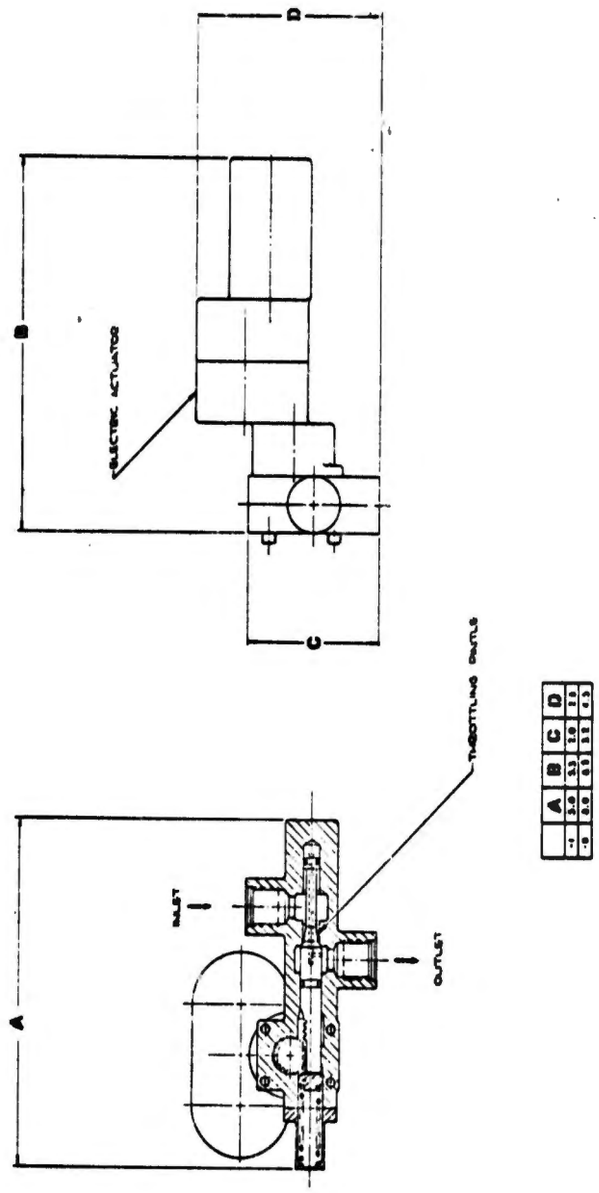

Figure 12. Fuel Valve, Mixture Ratio Control

thrust chamber valves to a value corresponding to the input signal. The poppets of the fuel and oxidizer valves will be appropriately contoured to control engine mixture ratio during excursions from minimum thrust to maximum engine thrust. In the event that adequate control of engine mixture ratio cannot be achieved solely through the contouring of thrust chamber valve poppets, the mixture ratio fuel bypass valve around the fuel thrust chamber valve is included to provide a broader control capability. This additional valve will provide a capability to compensate for appreciable variations in oxidizer tank pressures which could occur because of the vapor pressure variation of Compound A over the range of operating temperatures.

It has been assumed that both valves of the bipropellant thrust chamber valve assembly will be of all-metal valve design similar to the Transtage valve. The bodies used for each of the valves will be made from a suitable stainless steel alloy. The all-metal poppet shut-off seal would be made of phosphor bronze material. The mixture ratio valve will have a 6061 aluminum body and a 17-4 PH pintle. Again, the valve opening time for the bipropellant flow control valve is assumed to be 0.4 sec and the closing time is 0.3 sec; these opening and closing times are the same as those of the Transtage electrically-actuated bipropellant valve. Equivalent times are assumed for the mixture ratio fuel bypass valve.

Operating power requirements for the electrically-actuated bipropellant thrust chamber valve are established using the 0.4 sec opening time. These operating power requirements represent the average power necessary to open the bipropellant thrust chamber valves at the system inlet pressures; power levels for valve closing are significantly less because of pressure differential forces across the poppets in the closing direction. The mixture ratio fuel bypass valve is a balanced design and therefore requires a minimum of actuation power.

Information pertinent to the control system valve and actuators as well as the associated controls are presented on Table X. The weights for the various components are divided into those which apply to the valves, valve actuators, and the control harness, transducers, and amplifiers. From this table, it can be seen that the dry weight of the bipropellant thrust chamber valve assembly is 20.5 lb and the dry weight of the mixture ratio fuel bypass valve is 3.5 lb. The remainder of the controls, consisting of the harness, transducers and amplifiers, weighs a total of 9.0 lb. The total controls system weight, dry and wet, is 33.0 lb and 34.3 lb, respectively.

(8) Point Design Engine Performance

The performance of Point Design Engine No. I for CLF_5/N_2H_4 was computed utilizing the procedures outlined in Appendix II (Part II of this report). Plots of this information are provided on Figures No. 13 and No. 14. As indicated on Figure No. 13, the performance was evaluated for various fuel film cooling rates. This was done to determine the

TABLE X

SUMMARY OF VALVE AND ACTUATOR CHARACTERISTICS

Engine	Type	Valve Flow Rate, lb/sec	ΔP, psi	Line Size, in.	Valve Wt, lb	Actuator Hp	Actuator Wt, lb	Linkage (W_{FCV}) Wt, lb	Harness, Transducers and Amplifiers Wt, lb	Total Control wt, lb Dry	Total Control wt, lb Wet
II	Bipropellant FCV - Oxid.	20.68	7.5	1 7/8	*7.0	.3	7	N/A	5.0	23.5	24.8
	Fuel	9.85	7.5	1 1/4	**4.5			N/A			
I	Bipropellant FCV - Oxid.	20.53	7.5	1 7/8	*7.0	.3	9	N/A	9.0	33.0	34.3
	Fuel	9.77	7.5	1 1/4	**4.5			N/A			
	MR Control Valve - Fuel	1.0	7.5	1/4	***1.5	.02	2	N/A			
VIII	Ring-Gate Valves - Oxid.	78.4	-	-	-	.133	6	6.3	9.0	29.3	29.3
	Fuel	35.6	-	-	-	.053	4				
	Ox. Rich. G.G. MR Valve - Fuel	2.75	1080	1/4	***1.5	.02	2.5	N/A			
IV	Ring-Gate Valve - Fuel	32.7	-	-	-	.044	3.8	4.3			
	Oxid.	58.08	-	-	-	.024	3				
	Main Mom. Exch. Valve - Oxid.	52.3	50	1 5/8	*6.0			N/A			
	Fuel	26.9	50	1 3/8	**5.0	.4	10	N/A	11.0	45.6	46.8
	Fuel Film Coolant Valve - Fuel	2.4	50	1/2	***2.0			N/A			

* Add 12.5% to obtain wet weight.
** Add 8.5% to obtain wet weight.
*** Add 1.0% to obtain wet weight.

N/A-Not Applicable

TABLE X (cont.)

Engine		Valve				Actuator		Linkage (RGV)	Harness, Transducers and Amplifiers	Total Control wt, lb	
	Type	Flow Rate, lb/sec	ΔP,psi	Line Size, in.	Wt,lb	Hp	Wt,lb	Wt,lb	Wt,lb	Dry	Wet
IX	Ring-Gate-Fuel	57.3	-	-	-	.124	5.5	6.5	6	16	16
	Valves-Oxid.	141.8	-	-	-						
VII	Ring-Gate-Fuel	30.2	-	-	-	.187	7.5	7	9	28	28
	Valves-Oxid.	84.5	-	-	-	.09	4.5				
V	Ring-Gate-Fuel	28.56	-	-	-	.094	4.5	6	6	16.5	16.5
	Valves-Oxid.	48	-	-	-						
III	Ring-Gate-Fuel	32.50	-	-	-	.044	3.8	5	6	14	14
	Valves-Oxid.	57.74	-	-	-						

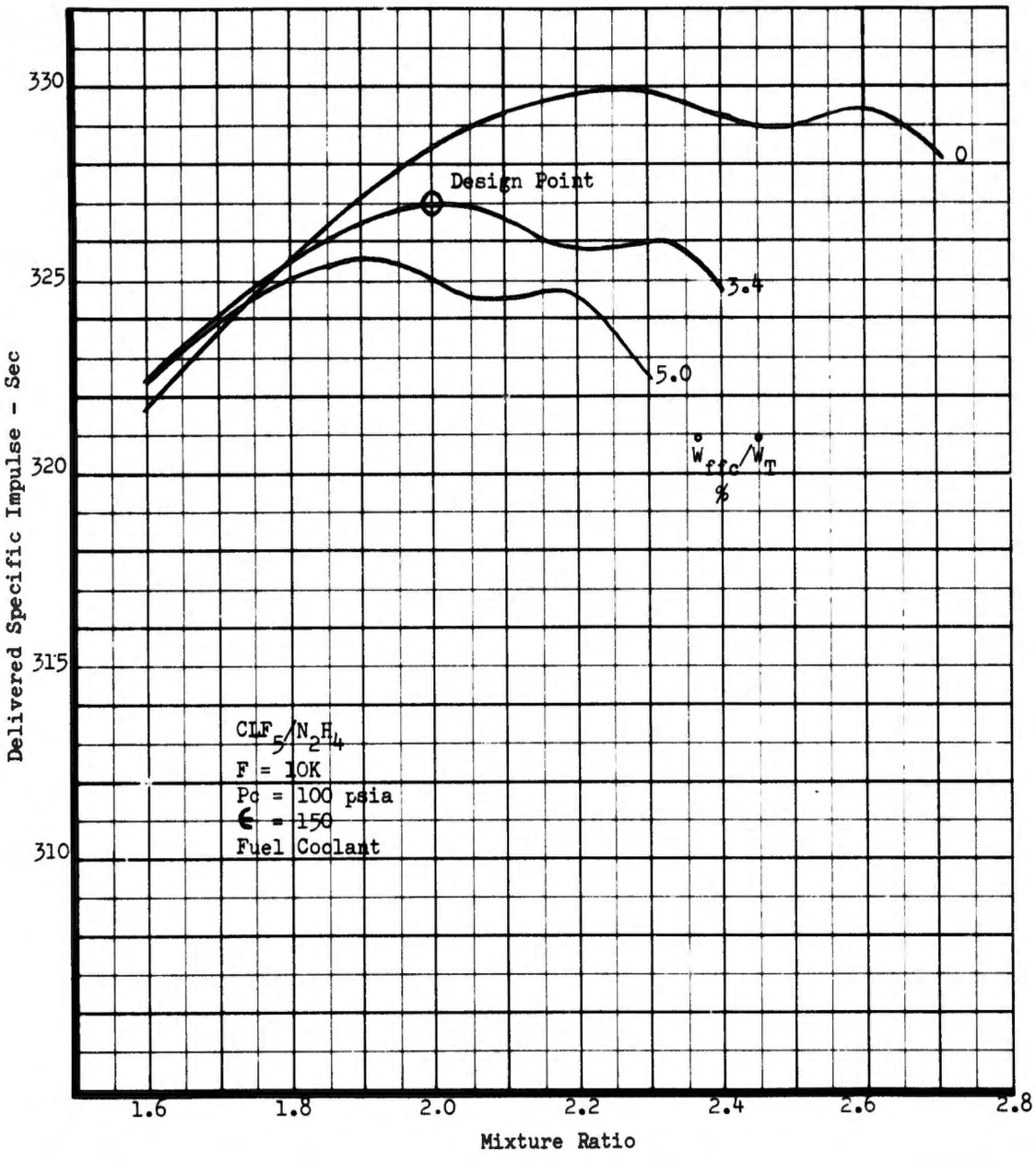

Figure 13. Point Design Engine No. I, Performance/Mixture Ratio-Coolant Flow Trade-Off (CLF_5/N_2H_4) (u)

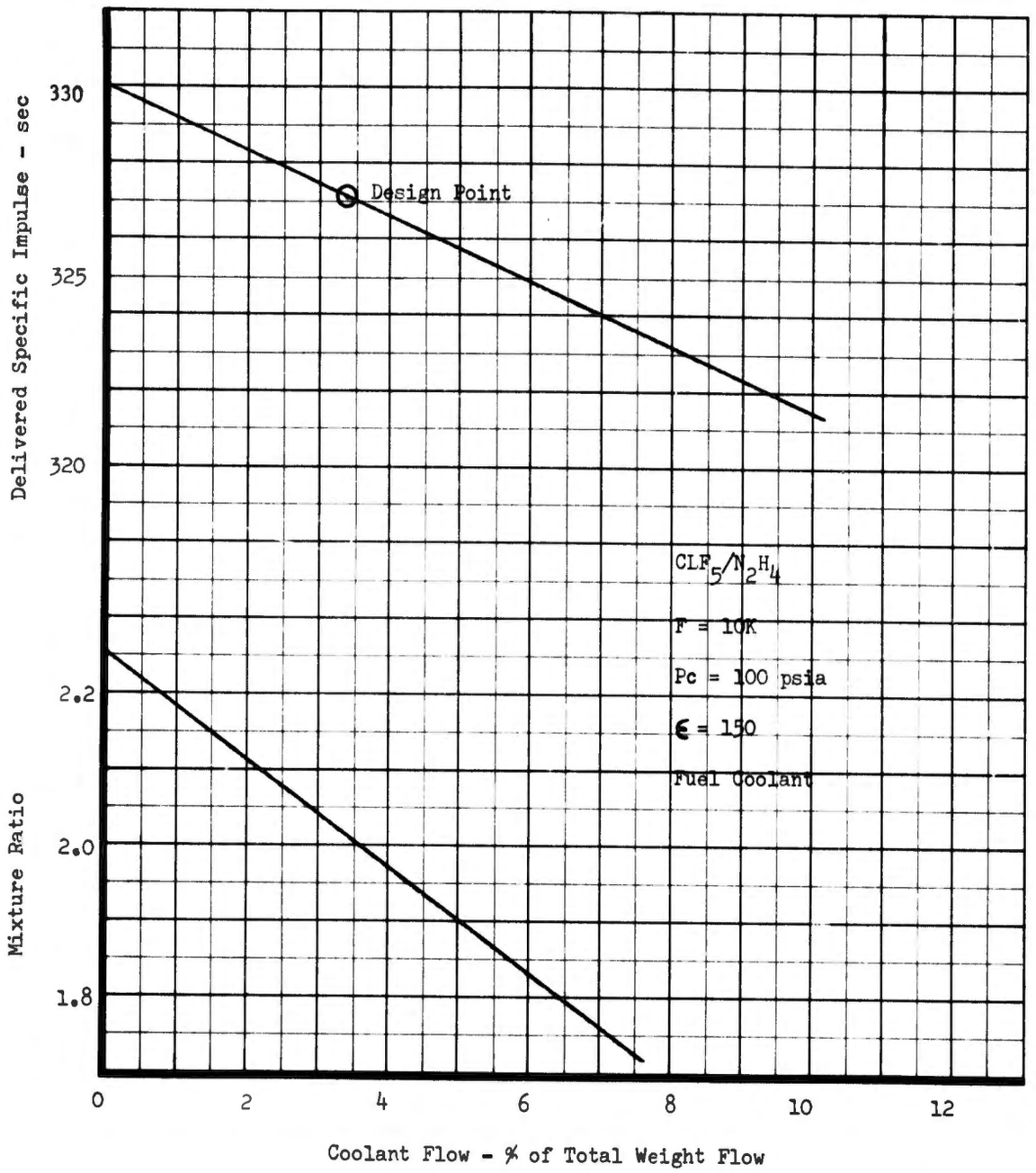

Figure 14. Point Design Engine No. I, Performance/Coolant Flow Interaction (CLF_5/N_2H_4) (u)

sensitivity factor of fuel film cooling upon engine performance as well as to determine the optimum engine mixture ratio as a function of coolant flows. The delivered vacuum specific impulse is shown on Figure No. 14 for various coolant flows and related optimum mixture ratios.

(U) The significance of this relationship is that for each percentage point of coolant, approximately 1 sec of specific impulse is lost.

(U) The performance plots for the CLF_5/MHF-5 propellant combination are shown on Figures No. 15 and No. 16.

(9) Engine Capabilities and Limits

(U) The following considerations must be included in the mission analysis to evaluate the capability of an engine:

- Throttling Capability
- Burn Duration Effects
- Installation
- Restart and Transients
- Launch Capability
- Propellant Compatibility
- Stability Criteria

(a) Throttling Capability

(U) Although the HIPERTHIN injector concept provides the opportunity for throttling to very low limits, the physical properties of CLF_5 are such that the throttling of low-pressure engines is not straightforward.

(C) The vapor pressure of CLF_5 is high (see Appendix I) and throttling below the vapor pressure within the requirement is quite possible but depends upon the propellant temperature and chamber pressure. If flashing in the injector occurs, it is speculated that mixture ratio distribution losses may increase rapidly. However, no stability problems are expected because partial vaporization can increase the injector stiffness and stability. If no control provisions are made, the engine is expected to go off-mixture ratio. Performance predictions are not attempted herein beyond the point where the chamber pressure equals the vapor pressure of CLF_5.

(C) The effects of the CLF_5 vapor pressure characteristics also should be considered during the start transient. If starting is required at a very low thrust level following a long duration coast, wherein the oxidizer experiences solar heat input and inert gas recovery, the engine can operate off of the optimum mixture ratio for a considerably long period of time. It is recommended that a mixture ratio control be included on throttleable pressure-fed engines to avoid excessive residual propellant.

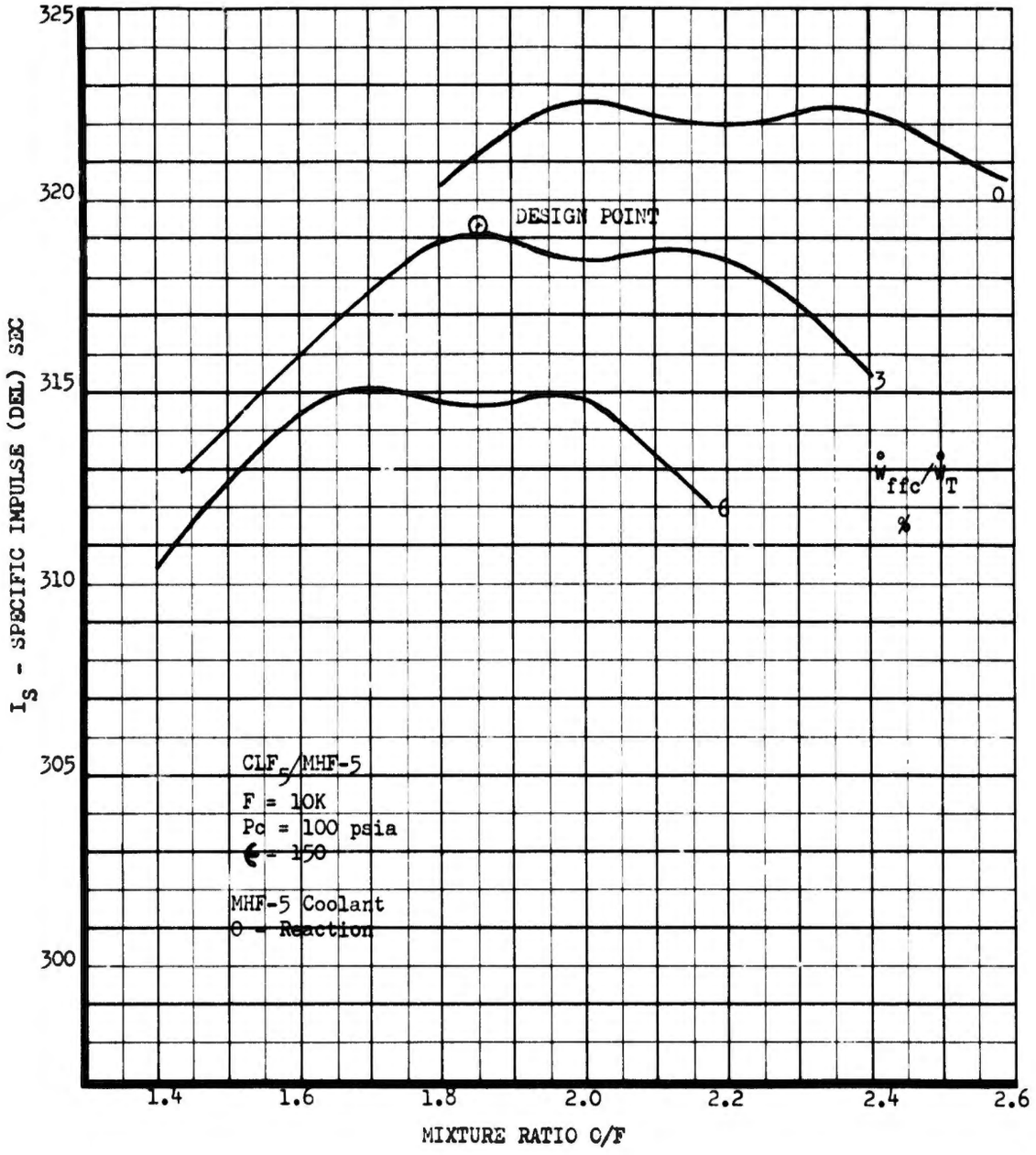

Figure 15. Point Design Engine No. I, Performance/Mixture Ratio-Coolant Flow Trade-Off (CLF_5/MHF-5) (u)

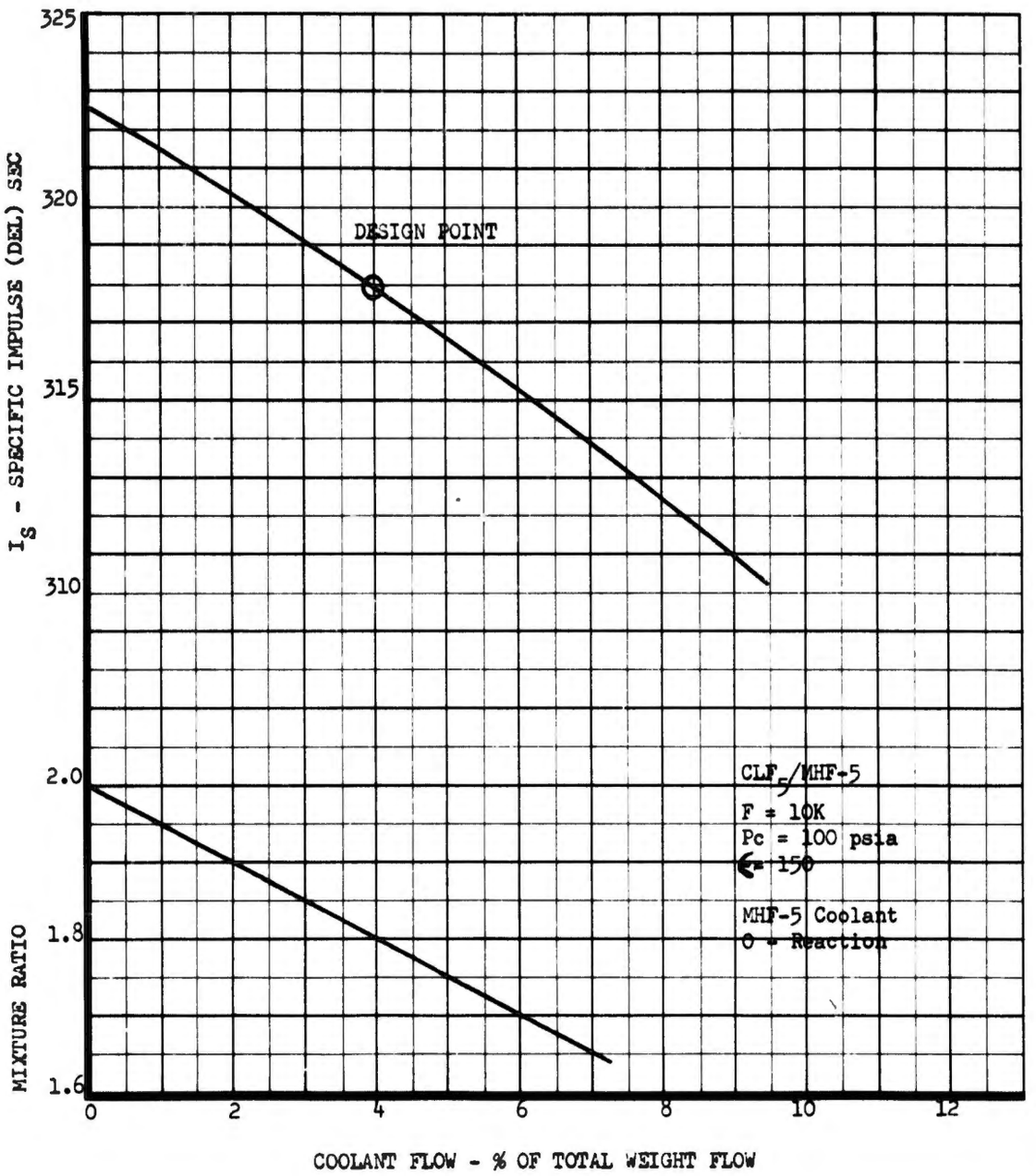

Figure 16. Point Design Engine No. I, Performance/Coolant Flow Interaction (CLF_5/MHF-5) (u)

(b) Burn Duration Effects

(C) For burn durations below 70 sec, it is estimated that no forward flange cooling is required; therefore, film cooling for the specified thrust level and chamber pressure is completely eliminated. However, for longer burn durations, 3.4% film cooling is required. Very little change in performance is anticipated as the result of burn duration. Recent test data at similar thrust and chamber pressure demonstrated that the throat radius increased only .035-in. after 235 sec of burn duration.

(c) Installation

(C) This type of chamber cooling is not suitable for a buried installation and will require a radiation heat shield. Again, the problem of heat radiation is connected with the burn duration. An overhead gimbal system is required.

(d) Mission Capability

(U) Pressure-fed engines have a very good response characteristic (i.e., very small start and shutdown transient impulse) and are preferred for application where exact, predictable timing is vital. The combination of fibrous graphite and the HIPERTHIN injector hold promise for providing a simple, deep throttling pressure-fed engine free of burn duration limitations.

(U) The radiation-cooled chamber has a low heat storage capacity; therefore, it is expected that an excellent restart capability can be obtained. This is particularly true with the HIPERTHIN injector, which has almost its entire surface area cooled.

(U) A further consideration for mission analysis is the relatively large gaseous residuals of CLF_5 for unconditioned propellant.

(U) The propellant tank pressure requirements at the engine interface are $\Delta \frac{P}{P} = .50$ for the HIPERTHIN injector which includes the control valve resistance. This results in a propellant interface pressure of 150 psia.

(e) Launch Pad Hold Capability

(C) Current launch procedure requires tank pressures to be less than 25 psia during checkout procedures on the pad. This would require that the CLF_5 temperature not exceed 35°F which coincides with the freezing temperature of N_2H_4. If such a requirement is enforced, thermal insulation of propellant tanks has to be considered as well as propellant being loaded in a pre-conditioned state.

(f) Propellant Compatibility

(U) This engine design concept can accept any of the specified fuel propellants. The only consideration here is the magnitude of the heat soak-back, which depends upon the firing sequence during the mission. For practical missions and radiation heat shielding, it is assumed that even N_2H_4 is acceptable for this design concept.

(g) Chamber Pressure Limitations

(C) Because of the extremely heavy weight of the tanks and inert pressurization system for large ΔV missions, the pressure fed-engines have a tendency to become optimum at very low chamber pressures. It is difficult to design stable injectors of high performance at these lower chamber pressures. Therefore, a minimum chamber pressure of 100 psia is considered mandatory for fixed thrust and most certainly, for throttlable engines.

b. Point Design Engine No. II

(U) This engine is designed as a fixed thrust engine with a conventional injector. It has a 10K thrust level and operates at 100 psia chamber pressure. Point Design Engine No. II is shown on Figure No. 17 for a nozzle extension area ratio of 150:1. This results in a maximum diameter of 104.7 in. and an over-all length of 193 in. Figure No. 18 is a schematic of the engine while pertinent data are summarized on Table XI.

(1) Thrust Chamber Design

(U) The materials selected for use in the thrust chamber are shown on Figure No. 19[6] Previous studies suggested that the degree of erosion at the throat would be greater than allowable for practical application of this thrust chamber. Therefore, fibrous graphite was selected as a throat insert to provide hardness.

(U) Fibrous graphite offers a relatively erosion resistant surface capable of operating at a relatively high temperature (4500°F). Graphite phenolic provides compatibility with the products of combustion upstream as well as downstream of the throat insert. Silica is used because of its excellent insulation and charring characteristics. However, silica melts at approximately 3200°F and it is necessary to adjust the graphite phenolic thickness so that the silica-graphite interface does not exceed 3000°F. The glass over-wrap results in another temperature limitation and the maximum allowable glass temperature has been restricted to 650°F to assure the maintenance of its structural integrity.

(U) The chamber for this engine was designed for 600 sec of continuous burn duration. The necessary layer and total wall thickness were defined to satisfy this requirement. The following is a summary of the ablative liner design for this engine.

(6) Based upon the chamber design in Contract F04611-67-C-0003 (Develop and Demonstrate Ablative Thrust Chamber Using LF_2/N_2H_4 Blend Propellants)

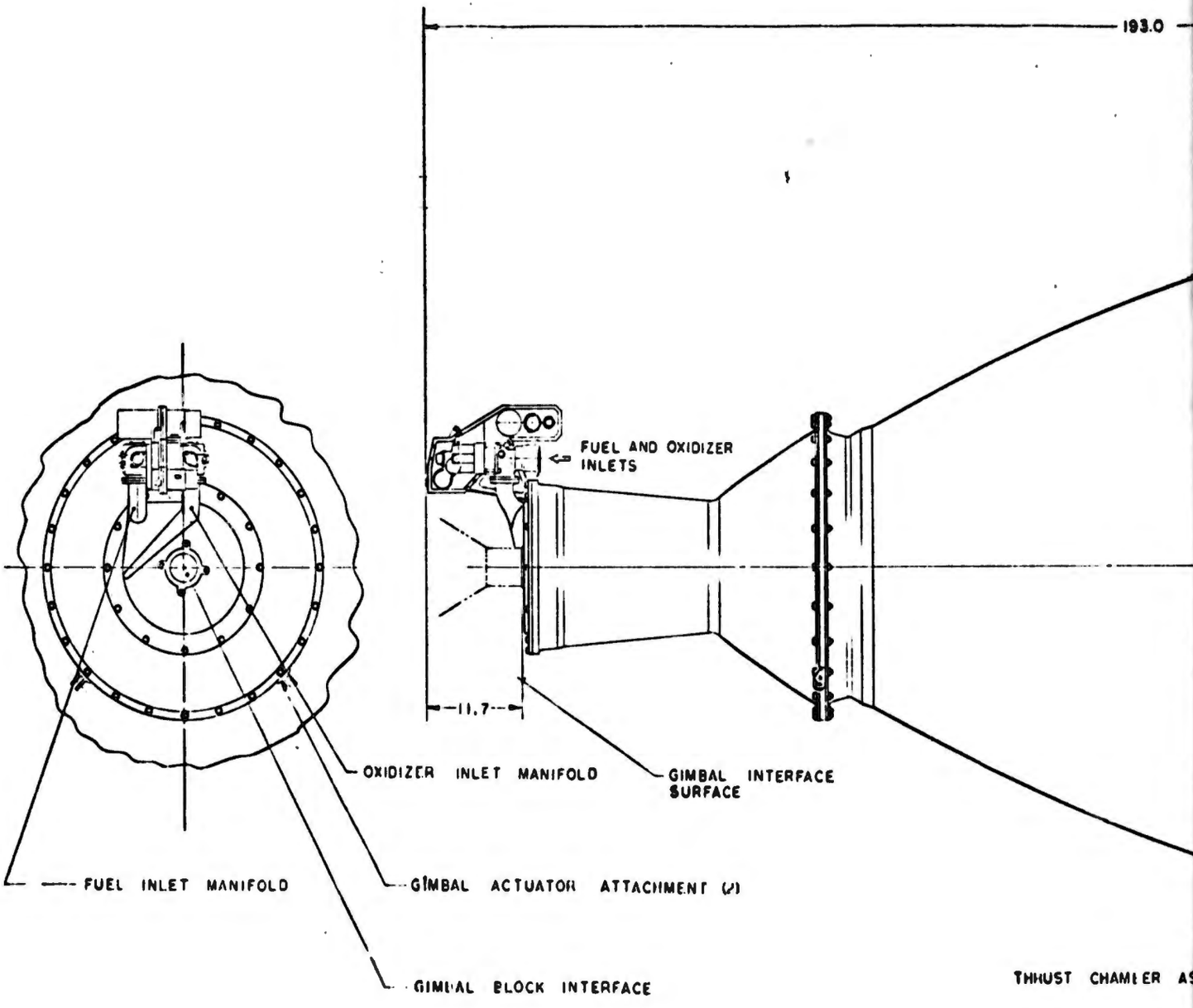
193.0
FUEL AND OXIDIZER INLETS
11.7
OXIDIZER INLET MANIFOLD
GIMBAL INTERFACE SURFACE
FUEL INLET MANIFOLD
GIMBAL ACTUATOR ATTACHMENT (2)
GIMBAL BLOCK INTERFACE
THRUST CHAMBER AS

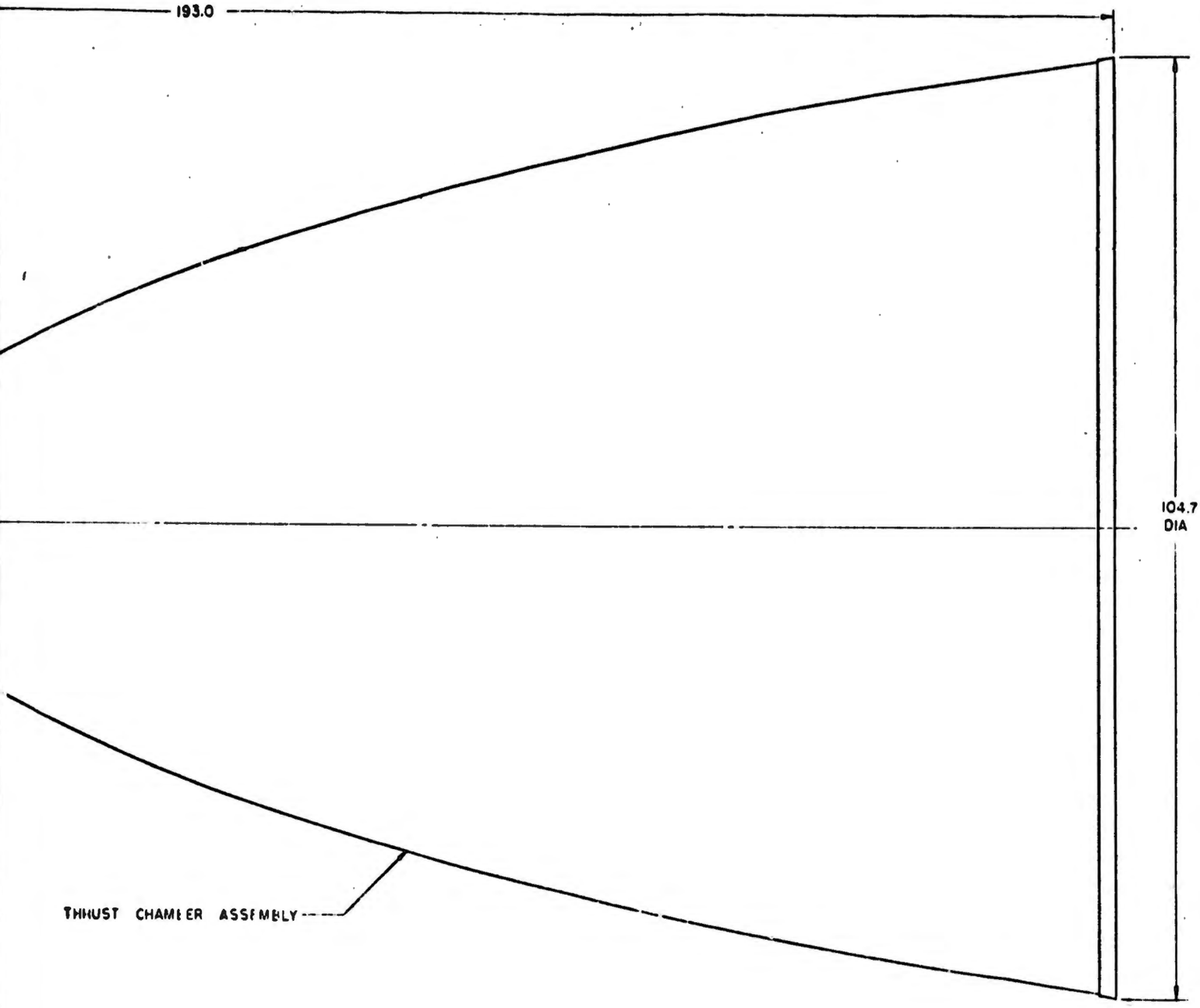

Figure 17. Point Design Engine No. II Assembly

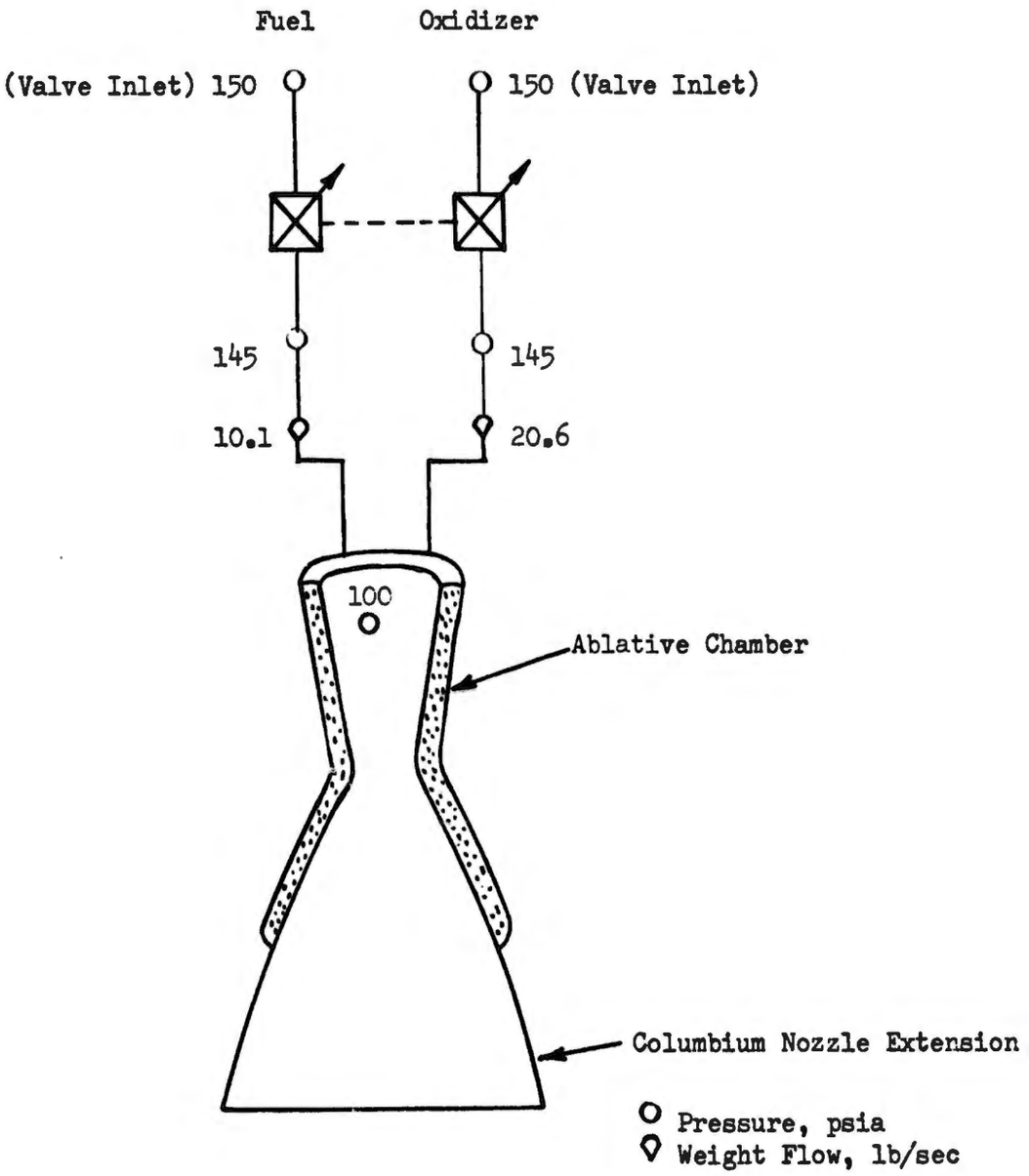

Figure 18. Engine Point Design II

TABLE XI

POINT DESIGN ENGINE II (U)

Engine Configuration	
Pressure Fed	
Nickel Conventional Injector (Liquid-liquid)	
Ablative Chamber (to 10:1)	
Columbium Nozzle Extension (from 10:1 to 150:1)	

Performance	
Thrust	10,000 lb
Chamber Pressure	100 psia
Mixture Ratio	2.04
Delivered I_{sp}	325.4 sec
I_{sp} efficiency	88.7

Design Specifications	
Dry Weight	766 lb
Wet Weight	770 lb
Length	193 in.
Diameter	105 in.
Fixed Thrust	-
Interface Pressure	
Oxidizer	150.0 psia
Fuel	150.0 psia
Fuel Film Coolant (% total flow - required to cool throat	3.4

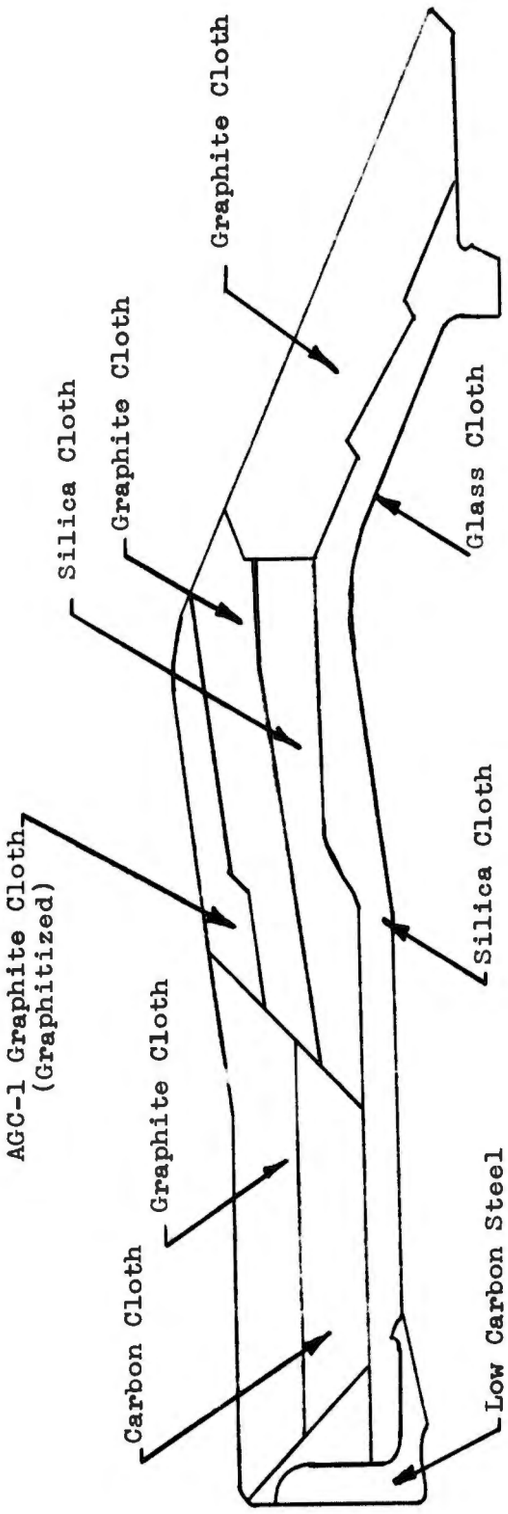

Figure 19. Ablative Thrust Chamber with Throat Insert, Final Design

Liner Cross-Section at Throat	Temperature Limits, °F	Required Thicknesses in.	Total Char Depth at end of 600 sec
Fibrous Graphite	4500	0.4	
Graphite Phenolic (FM-5064)	3000	1.5	
Silica-Phenolic (FM-5067)		0.6	
Glass Overwrap	650	0.125	
	Total	2.625 in.	2.2 in.

It is necessary to provide film cooling from the injector to satisfy the 4500°F fibrous graphite design.

As shown on Figure No. 20, the thrust and gimbaling loads are transferred to the gimbal block through the single-piece injector body, which is hollowed, rigid, and lightweight. The injector flange, which is welded to the injector body and fuel manifolding, is bolted to the chamber flange. Axial loads are transmitted to this flange from the ablative chamber wall through "fingers" that are integral with the chamber flange and are wrapped into the chamber wall with glass cloth and roving. The glass roving, cloth, and phenolic extend the entire length of the chamber and form the structural part of that component. The columbium nozzle extension is bolted to the silica phenolic-glass cloth aft flange, which is current practice with ablative thrust chamber assemblies. This columbium extension is sufficiently thick to prevent its buckling during gimbaling maneuvers. In addition, it is stiffened at its aft end.

(2) Injector Selection

The injector design concept for Point Design Engine No. II is identical to that used for Point Design Engine No. V. The injector body and inlet manifolds are to be made from Ni 200 material, which is expected to be compatible with the oxidizer. Also, it is expected that this material will resist "bell mouthing" of the fuel orifices, which is a phenomenon wherein fuel orifices are gradually enlarged from the injector face back into the fuel manifolds.

Table XII is a summary of injector and chamber design parameters.

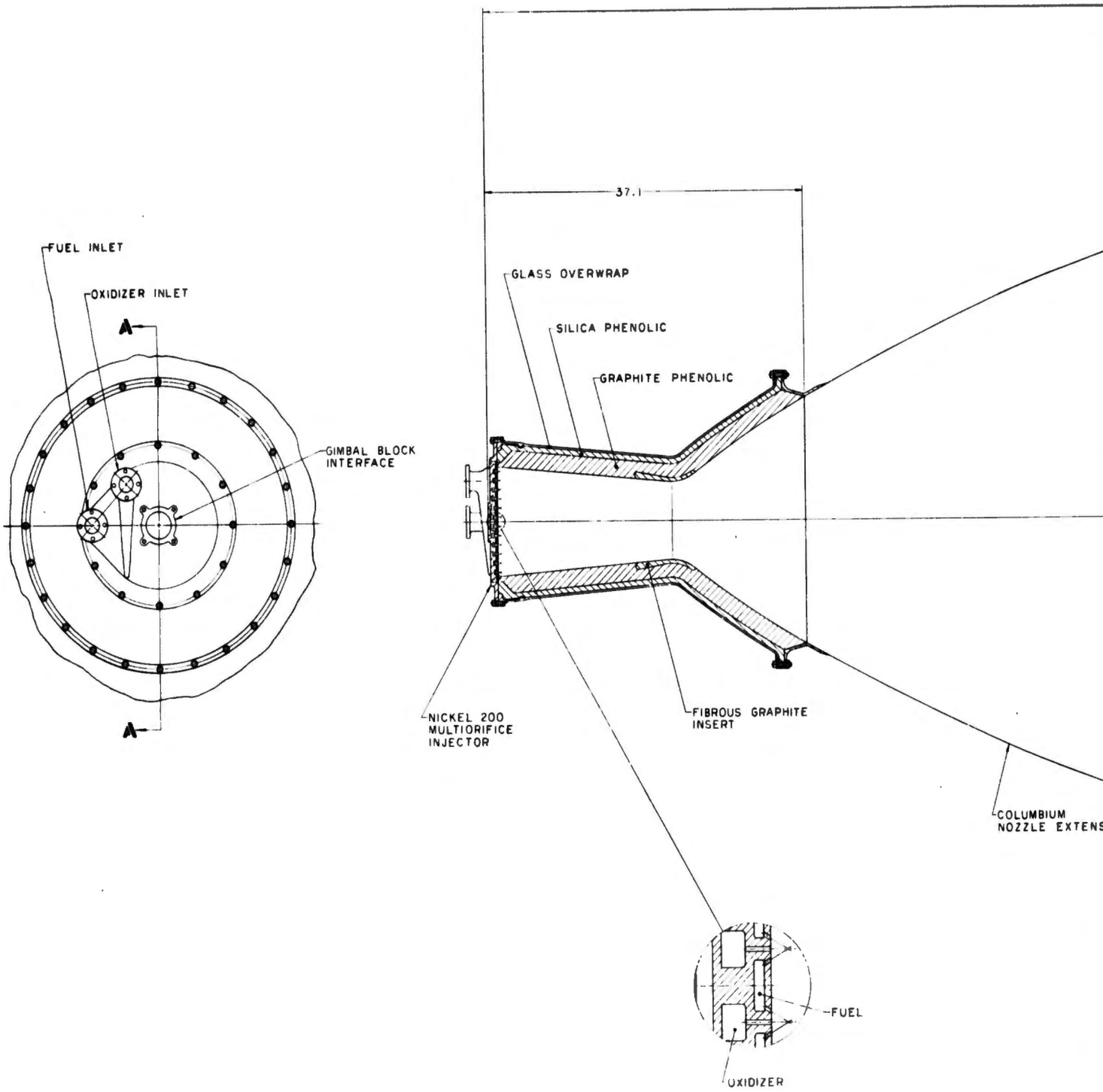
FUEL INLET
OXIDIZER INLET
A
A
GIMBAL BLOCK INTERFACE
37.1
GLASS OVERWRAP
SILICA PHENOLIC
GRAPHITE PHENOLIC
NICKEL 200 MULTIORIFICE INJECTOR
FIBROUS GRAPHITE INSERT
COLUMBIUM NOZZLE EXTENS
FUEL
OXIDIZER

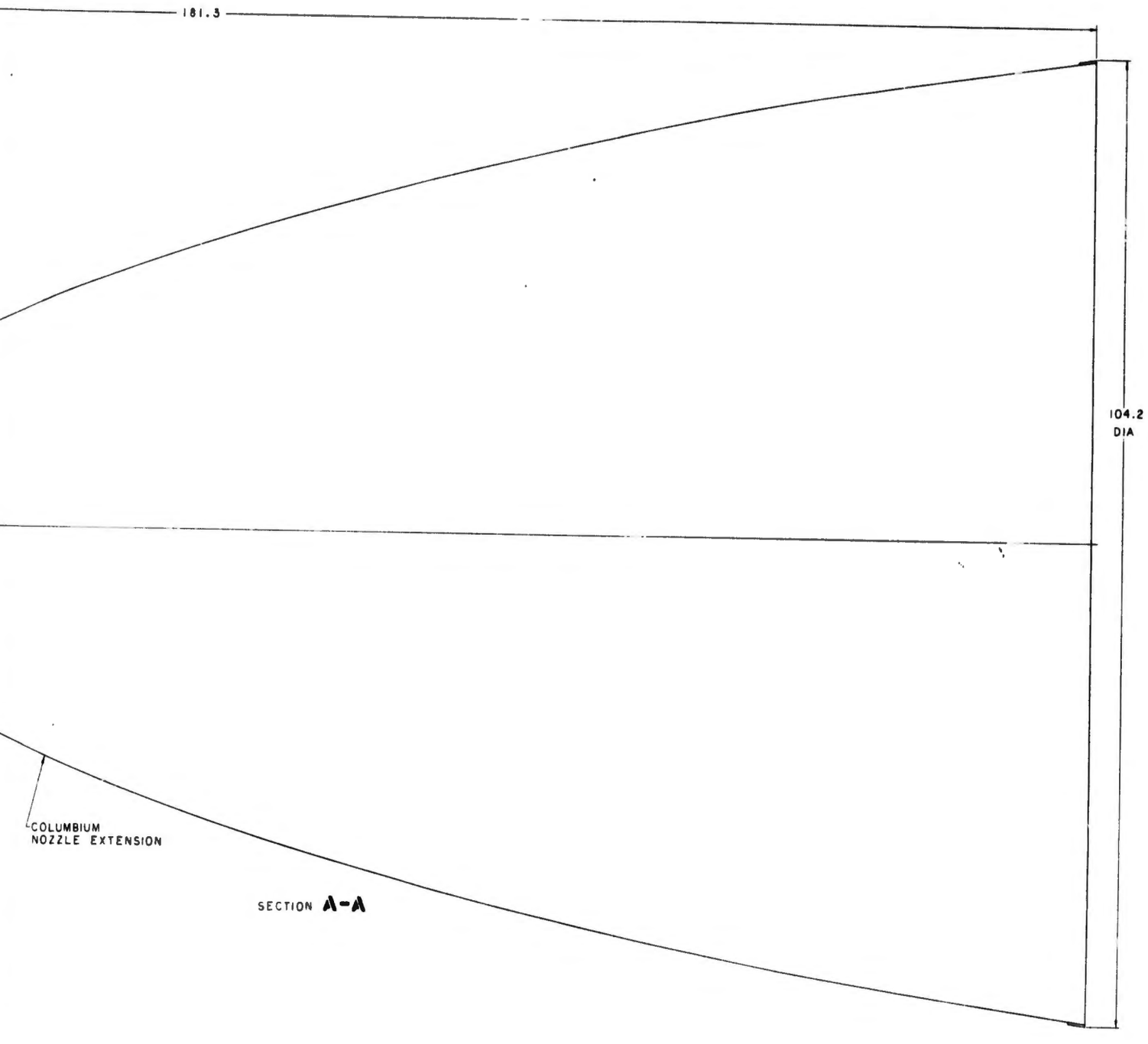

Figure 20. Thrust Chamber Assembly, Engine No. II

TABLE XII

THRUST CHAMBER ASSEMBLY NO. 2 DESIGN PARAMETERS

General	Injector	Chamber	Nozzle Extension
Thrust: 10K lb	Type: Conventional Flat Face, Cross Drilled	Shape: Conical	Attachment Area Ratio: 10
Chamber Pressure: 100 psia	Propellant Phases: Liquid - Liquid	Material: Ablative, Graphite & Silica Phenolics	Cooling Mode: Radiation
Nozzle Area Ratio: 150	Thrust per Element: 100 lb	Contraction Ratio: 2	Material: Coated Columbium
Throttleability: Fixed Thrust	Type Element, F-O-F Inline Triplet	Cooling Mode: Ablative with Fuel Film Cooling	Exit Diameter: 105.2 in.
Duration: 600 sec	$\Delta P_{inj}/P_C$: .45	Characteristic Length: 30 in.	
	Material: Ni-200	Throat Dia: 8.50 in.	
	Film Cooling: 3.4% Fuel of Total		

(3) Controls System Description

The pressure-fed engine system configuration of Point Design Engine No. II requires an "on-off" thrust chamber valve propellant flow control as shown schematically on Figure No. 21. This valve will be electrically-operated in accordance with the criteria established at the outset of this study. A poppet-type valve design utilizing an all-metal shut-off seal configuration will be used. The oxidizer and fuel valves will be mechanically-linked for reliable phasing during engine starting and shutdown transient operation. The all-metal, electrically-actuated, bipropellant valve recently designed for the Transtage application has been selected as the basic design to be used in the pressure-fed engine system of Engine II. This valve design was shown on Figure No. 11.

The data required to establish the weight of the electrically-actuated, bipropellant valve assembly for fixed thrust, pressure-fed engines (Engine No. II) are shown on Figure No. 22 which is a plot of valve assembly weight in relationship to engine thrust over a thrust range of 10K to 30K. A range of valve inlet pressures from 100 to 500 psia was selected to encompass a range of chamber pressures from 100 to 300 psia. Several basic assumptions were made in establishing the curves on Figure No. 22. The data shown are applicable only to engines utilizing Compound A/N_2H_4 propellants at a mixture ratio (O/F) of 2.1 and the specific impulse listed in the applicable specifications for this system. Valve weight is a function of valve size, and valve size for a given flow rate is a function of pressure drop; therefore, it was assumed that valve pressure drop for this engine system will equal 5% of the valve inlet pressure values. Weight values obtained using Figure No. 22 will apply to the entire valve assembly (both valves) excluding the electrical actuator. The relationships of weight to horsepower for the electrical actuator is plotted on Figure No. 23. Valve assembly weight for a given thrust is essentially the same over the entire range of valve inlet pressures (100 psia to 500 psia). Valve line size becomes smaller at the higher inlet pressures because pressure drop increases as a fixed percentage (5%) of valve inlet pressure. However, operating horsepower and actuator weight increases in a manner which keeps weight of the over-all valve assembly essentially constant. For this reason, the data can be presented by the single curve shown.

It has been assumed that both valves will be of all-metal design similar to that of the Transtage valve. The bodies used for each of the valves will be made from a suitable stainless steel alloy. Other assumptions used as a basis for establishing the parametric data shown on Figure No. 22 are valve operating times of 0.4 sec for opening and 0.3 sec for closing. These operating times are the same as those of the Transtage electrically-actuated bipropellant valve.

Operating power requirements for the electrically-operated bipropellant thrust chamber valve over the range of thrust values and valve inlet pressures for the pressure-fed engines being considered are shown on Figure No. 24. These operating power requirements

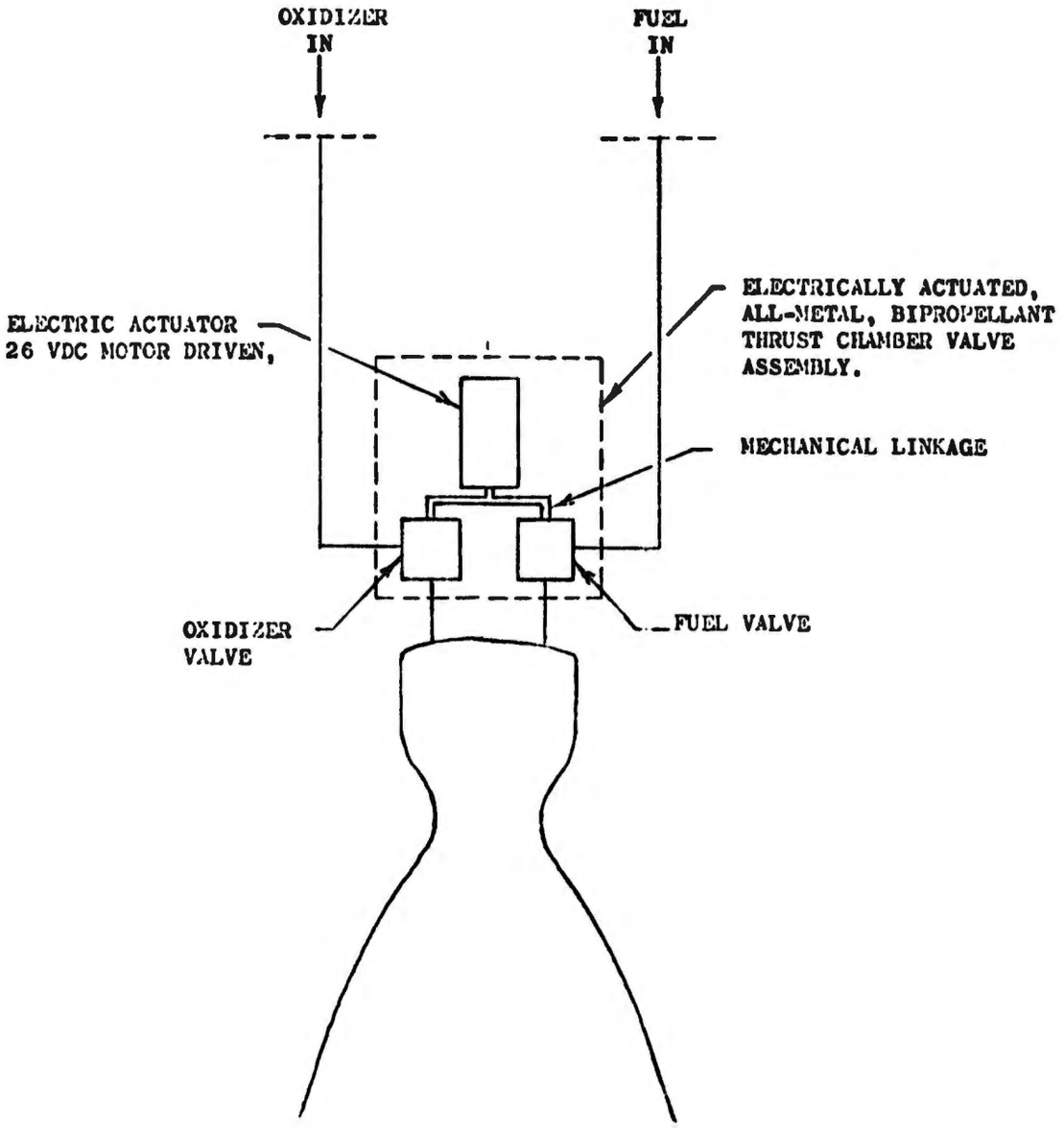

Figure 21. Controls Schematic, Point Design Engine No. II

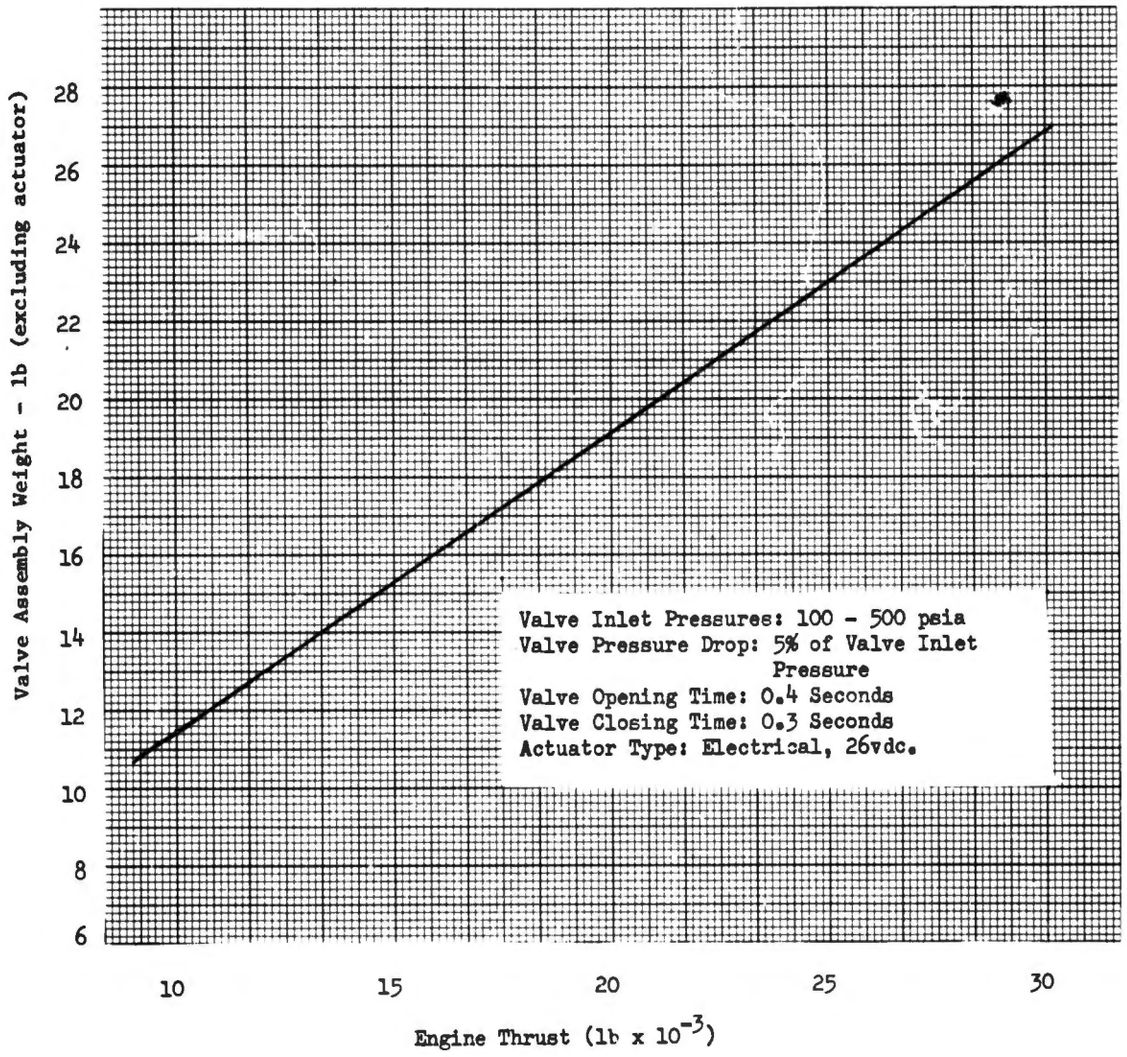

Figure 22. Valve Assembly Weight vs Engine Thrust, Point Design Engine No. II, Pressure-Fed, Fixed Thrust

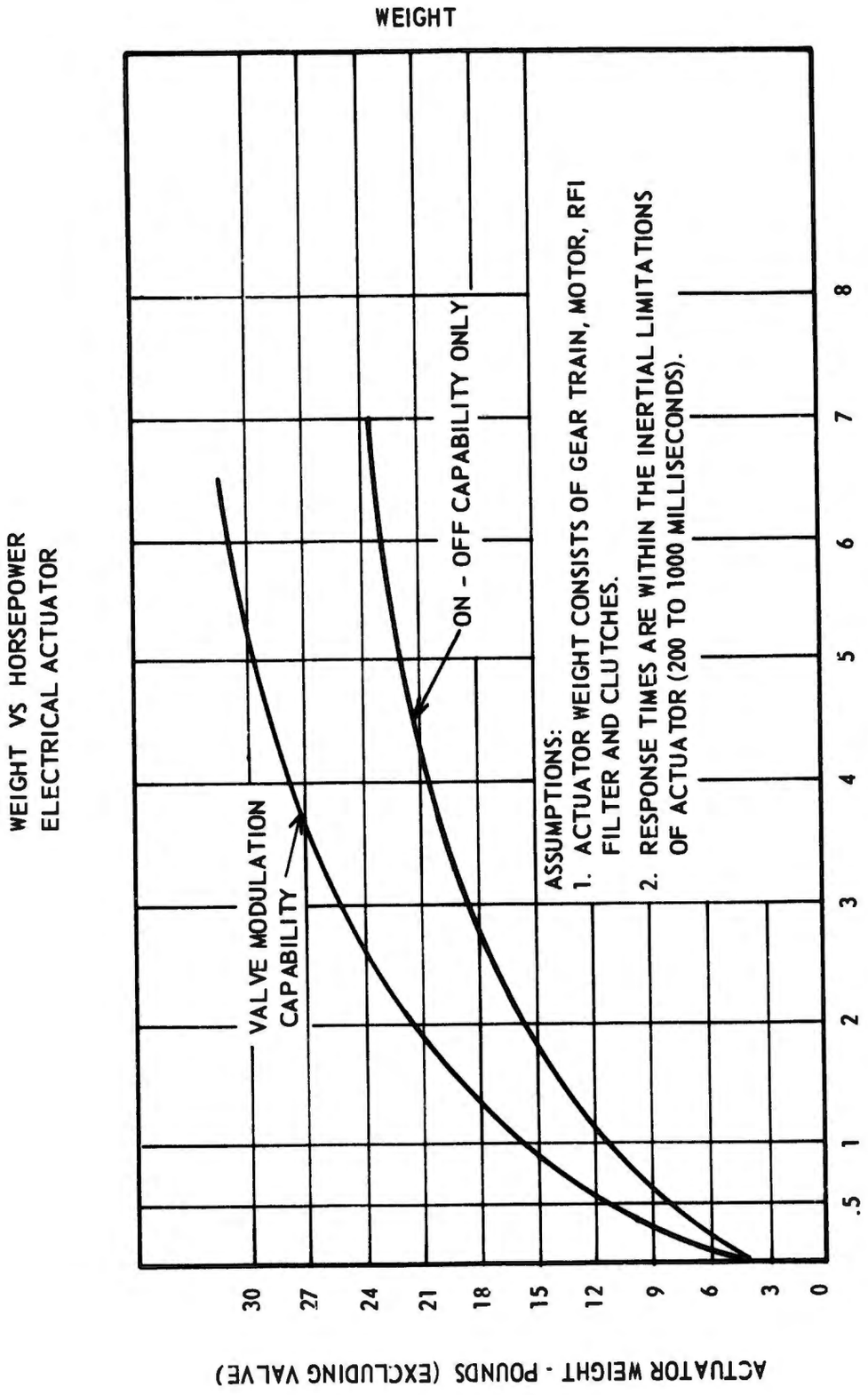

Figure 23. Weight vs Horsepower, Electrical Actuator

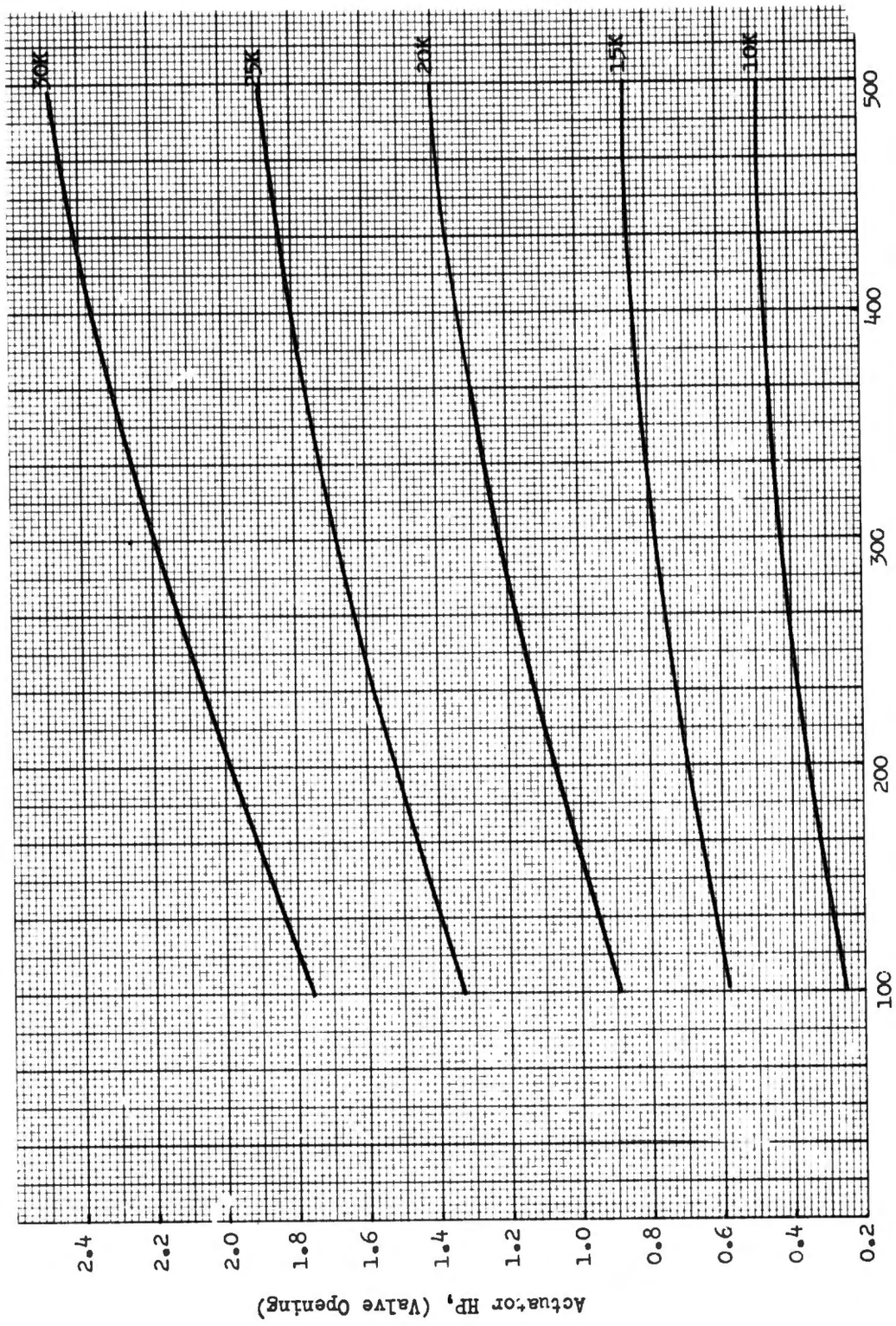

Figure 24. Electric Actuator Power vs Valve Inlet Pressure, Bi-Propellant Thrust Chamber Valve Assembly (Valve Opening Time - 0.4 sec)

represent the average power necessary to open the bipropellant thrust chamber valves. Power levels for valve closing are significantly less because of pressure differential forces across the poppets in the closing direction. A valve opening time of 0.4 sec was assumed in calculating the data shown on Figure No. 24.

(4) Point Design Engine Performance

(U) The performance of Point Design Engine No. II was computed utilizing the procedures outlined in Appendix II (Part II of this report). Plots of this information for the CLF_5/N_2H_4 propellant combination are shown on Figures No. 25 and No. 26 while these same data for CLF_5/MHF-5 are shown on Figures No. 27 and No. 28. Performance is presented as a function of cooling requirements in all four figures, which indicates the same coolant performance sensitivity effect as was found for Point Design Engine No. I. However, the performance of this engine is slightly lower than Engine No. I because of the ERL increase experienced with the conventional injector as compared with the HIPERTHIN injector.

(5) Engine Capabilities and Limits

(U) The Engine II mission considerations are simpler than for Engine I because of its fixed thrust design.

(a) Burn Duration Effects

(C) This engine is extremely sensitive to burn duration which affects mission analysis. As indicated, the wall thickness is determined as a direct function of burn duration, which affects the engine weight. This relationship is subsequently detailed as part of the Point Design Engine No. IV discussion. The burn duration also affects the decrease in chamber throat area, which establishes an absolute limit for the acceptable burn duration. A limit criterion is presented under the Technology Limits discussion. It is based upon recent test data for the CLF_3/MHF-3 propellant combination (7). These data were extrapolated for the specified thrust and chamber pressure limits. Further information pertinent to CLF_5 and the specified fuels is needed.

(C) The burn duration also directly affects the heat stored in the ablative chamber after shutdown. This heat is partially dissipated by radiation into space and partially by conduction into the injector and injector feed lines. The relatively large amount of heat soak-back has an adverse effect upon the restart capability of ablative-cooled engines.

(b) Installation

(C) Theoretically, this engine is suitable for buried installation; however, such an installation aggravates the heat

(7) Naval Test Station Report 6C-5148

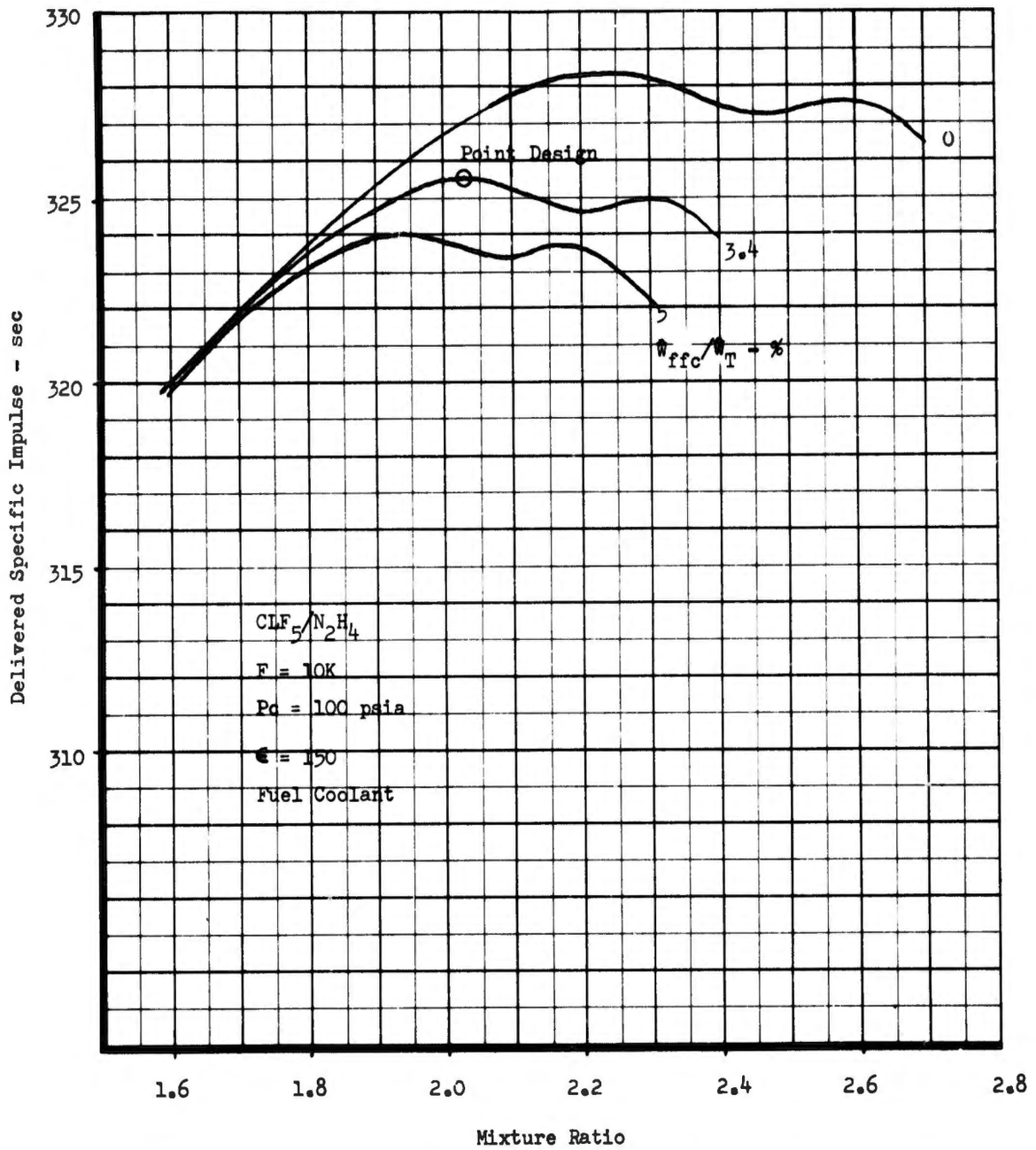

Figure 25. Point Design Engine No. II, Performance/Mixture Ratio-Coolant Flow Trade-Off (CLF_5/N_2H_4) (u)

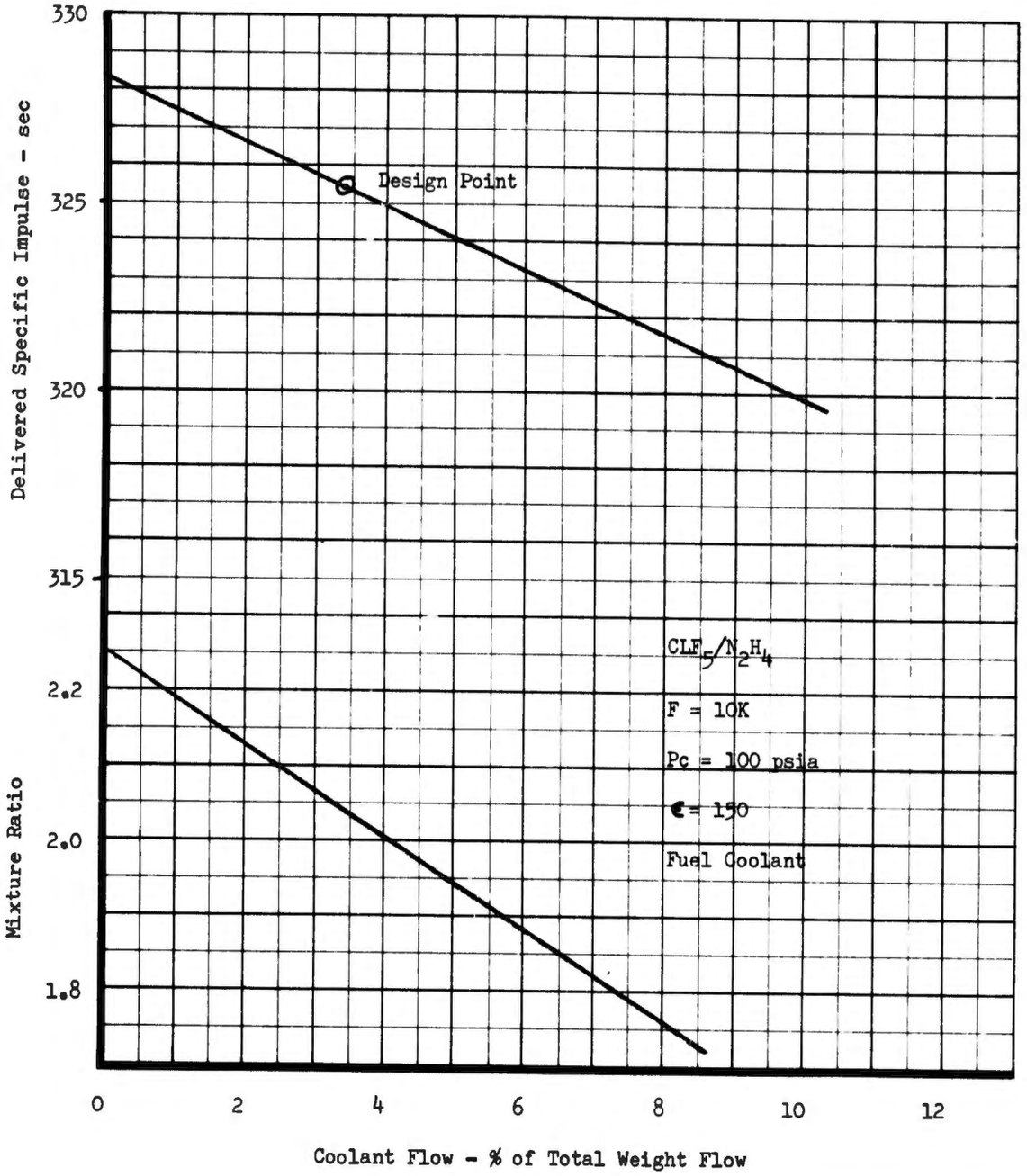

Figure 26. Point Design Engine No. II, Performance/Coolant Flow Interaction (CLF_5/N_2H_4) (u)

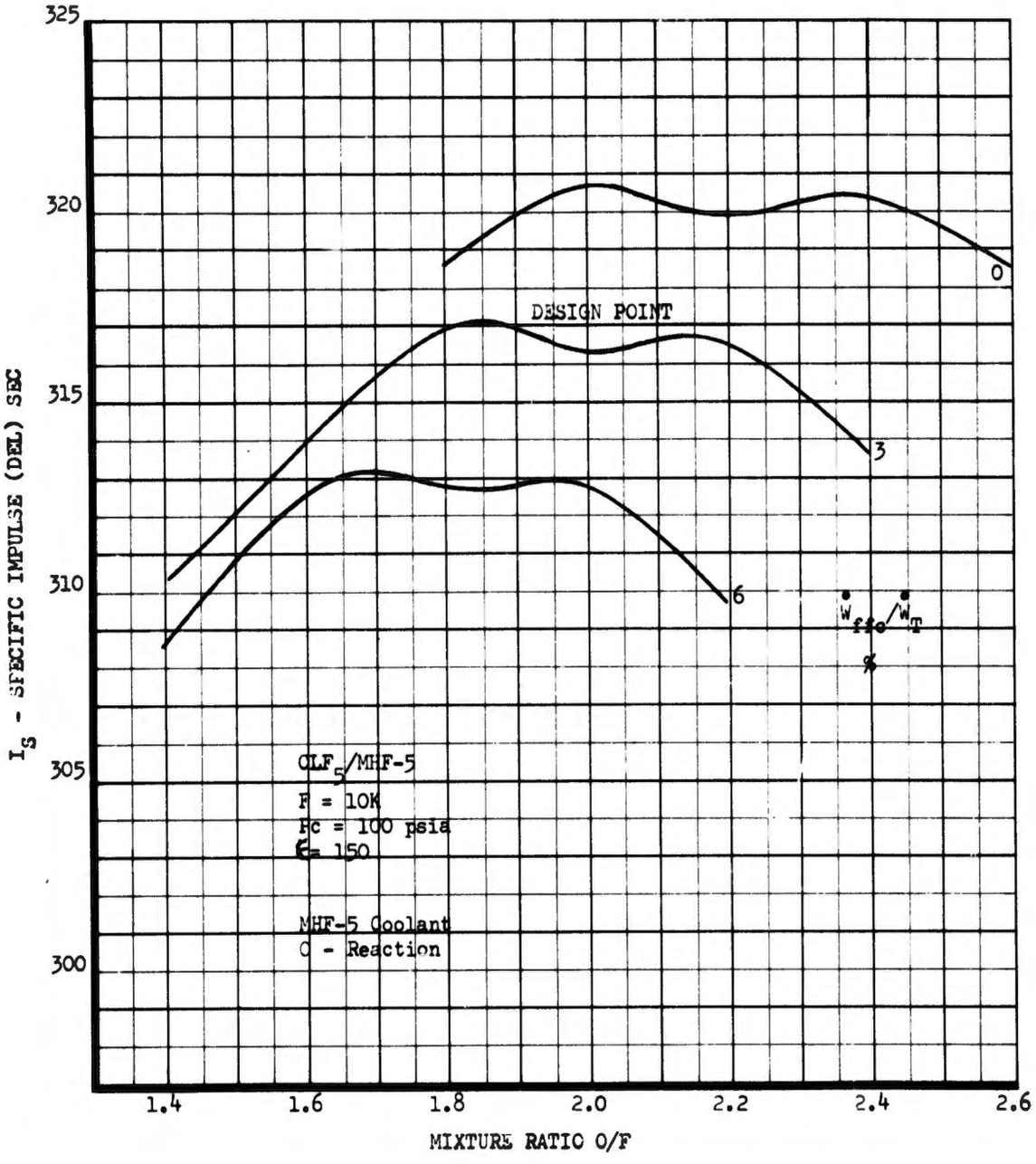

Figure 27. Point Design Engine No. II, Performance/Mixture Ratio-Coolant Flow Trade-Off (CLF_5/MHF-5) (u)

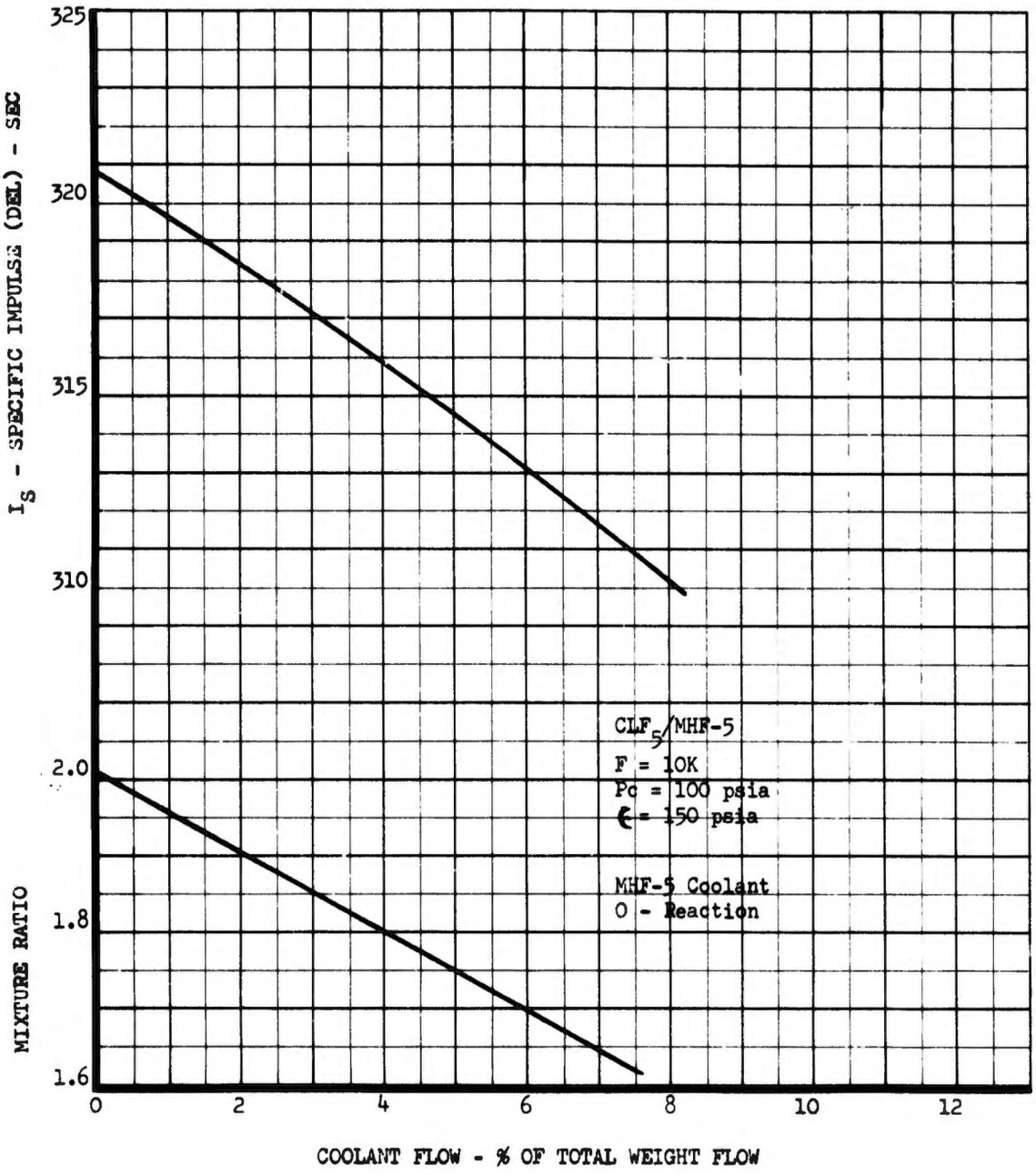

Figure 28. Point Design Engine No. II, Performance/Coolant Flow Interaction (CLF_5/MHF-5) (u)

soak-back problem because the chamber and injector are prevented from radiating into space. These heat soak-back effects require careful evaluation.

(c) Mission Capability

(C) The transient characteristics of this engine are the same as for Engine No. I except that valve timing at restart may be affected by the heat soak-back. The valve control solenoid temperature or the motor temperature would have a direct effect upon valve speed. The actual temperature at restart of any component is not only a function of burn duration, but also of the coast duration preceding the restart. To eliminate this mission sensitivity, the use of heat sinks on the backside of the injectors has been considered because they would restrict the maximum injector temperature to approximately 350°F (8).

(C) In an exposed installation, the solar heat input also has an effect upon the radiation heat dissipation. The extent of this effect depends upon the attitude of the vehicle in relationship to the sun.

(C) It is recommended that heat sink compounds be used for restartable ablative cooled engines to obtain greater mission flexibility as well as to eliminate all of these mission effects upon the engine capability.

(d) Propellant Compatibility

(C) In view of the heat soak-back problem associated with ablative chambers, the use of N_2H_4 propellant is not recommended where long burn durations are required. All of the other specified fuels are usable. However, the 80/20 blend may make the face cooling of conventional injectors difficult because of its high vapor pressure characteristics.

2. Pump-Fed, Passively Cooled Systems

(U) Point Design Engines No. III and No. IV are basically pump-fed versions of Point Design Engines No. I and No. II. All of these engines use liquid/liquid injection systems with bleed turbine drive. The restriction to a bleed turbine cycle is an arbitrary one and has the objective of obtaining simple engine concepts for liquid/liquid injection methods.

a. Point Design Engine No. III

(U) This engine is conceived as a fixed thrust engine with a conventional liquid/liquid injection system. It is designed for a chamber pressure of 600 psia and a thrust level of 30K. The configuration shown on Figure No. 29 is for an expansion area ratio of 150:1 which results in a

(8) Contract F04611-67-C-0003

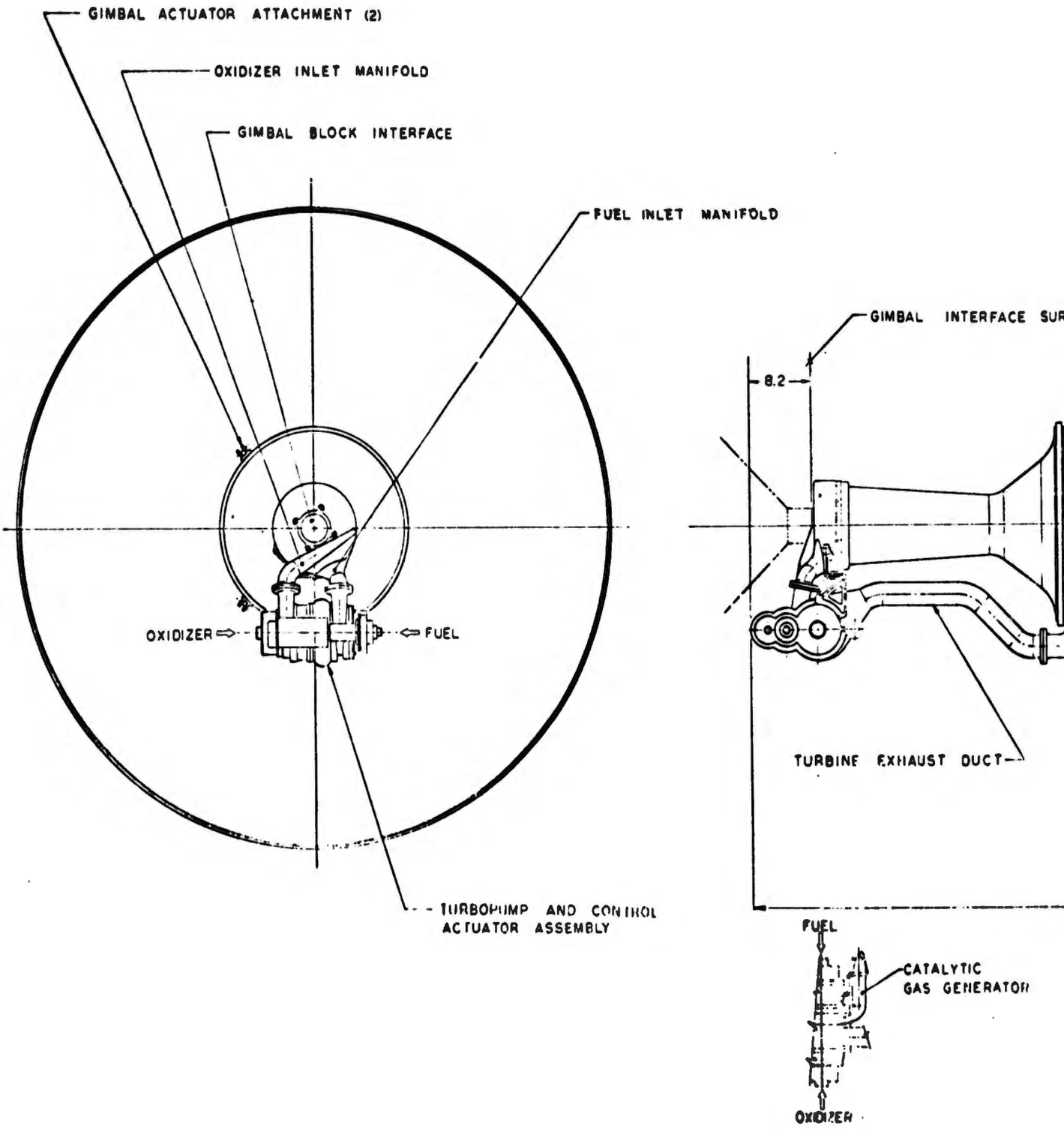
GIMBAL ACTUATOR ATTACHMENT (2)
OXIDIZER INLET MANIFOLD
GIMBAL BLOCK INTERFACE
FUEL INLET MANIFOLD
OXIDIZER
FUEL
TURBOPUMP AND CONTROL ACTUATOR ASSEMBLY
GIMBAL INTERFACE SUR
8.2
TURBINE EXHAUST DUCT
FUEL
CATALYTIC GAS GENERATOR
OXIDIZER

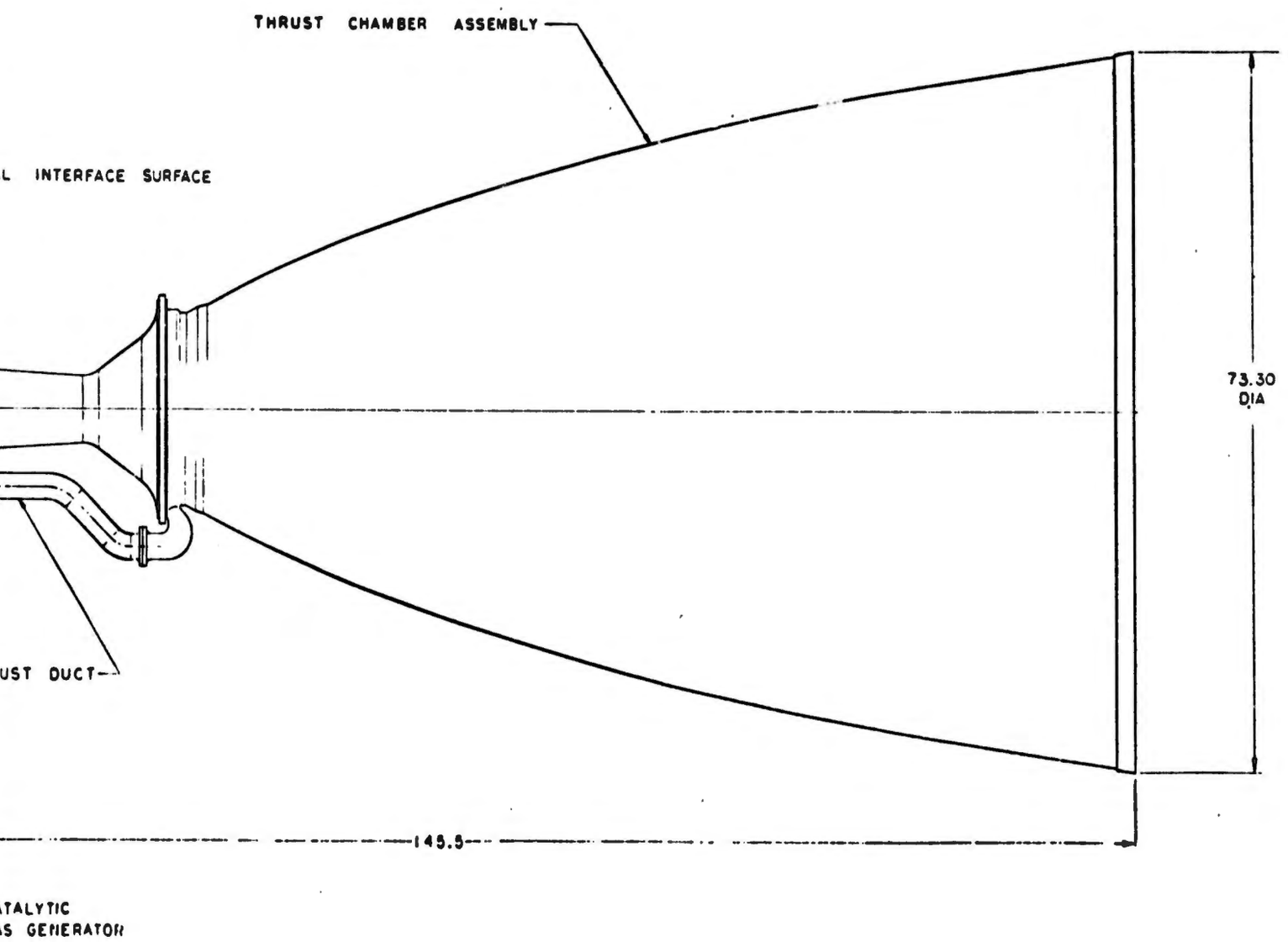

Figure 29. Point Design Engine No. III Assembly

maximum engine diameter of 73.3-in. and an over-all length of 145.5-in. Figure No. 30 is an engine schematic, which includes the flow and pressure schedules. Table XIII is a summary of pertinent engine data.

(1) Thrust Chamber Design

The pertinent thrust chamber design parameters are summarized on Table XIV. A detailed description of the thrust chamber geometry is presented as part of the Point Design Engine No. V discussion.

Thrust and gimbaling loads are transferred to the gimbal block through the single piece injector body. This member is hollowed, rigid, and lightweight. The fuel manifolding acts as an injector flange and is welded to the injector body. This manifold contains integral "fingers" as shown on Figure No. 31. The fibrous graphite chamber wall is sufficiently thick and strong to withstand all pressure, thrust, and gimbaling induced hoop and axial loads. The wall is made thicker at the small diameter throat region to accomplish this. The aft flange utilizes a columbium clamp-ring to hold the columbium nozzle extension to the graphite chamber. This clamp-ring is a lightweight attachment and it permits simple flange configurations. It is important that the chamber/nozzle extension interface joint be flexible (i.e., capable of deflecting when acted upon by differential thermal expansion and/or gimbaling-induced loads). The columbium nozzle flange acts as a "plastic hinge," because the modulus of the material is low at its elevated operating temperature. The clamp-ring, which is of similar material and thickness, is expected to act in much the same way while effecting a seal against low pressure leakage from the joint.

A flow rate of 7.7% is required for this chamber to maintain a wall temperature of 4500°F.

Injector and chamber materials selection criteria as well as the materials used in thrust chamber assembly No. 3 are the same as those used for thrust chamber assembly No. 1. Ni-200 was selected for the injector and its manifolding because this material is expected to be compatible with the oxidizer. Also, it is expected to resist fuel orifice "bellmouthing," which is a phenomenon wherein the fuel orifices are gradually enlarged from the injector face back into the fuel manifolds. Fibrous graphite and columbium were selected for the radiation-cooled thrust chamber and nozzle extension, respectively. The turbine exhaust bleed manifolding and injector also are of columbium as is the material between the chamber forward wall and the injector flange "fingers."

(2) Turbopump Configuration

In the bleed cycle, the turbopump has a significant effect upon engine weight and a relatively minor effect upon engine performance. Appendix VI (Part II of this report) includes a description of the turbopump design concept and the weight of bleed turbine turbopumps is further discussed in Appendix III.

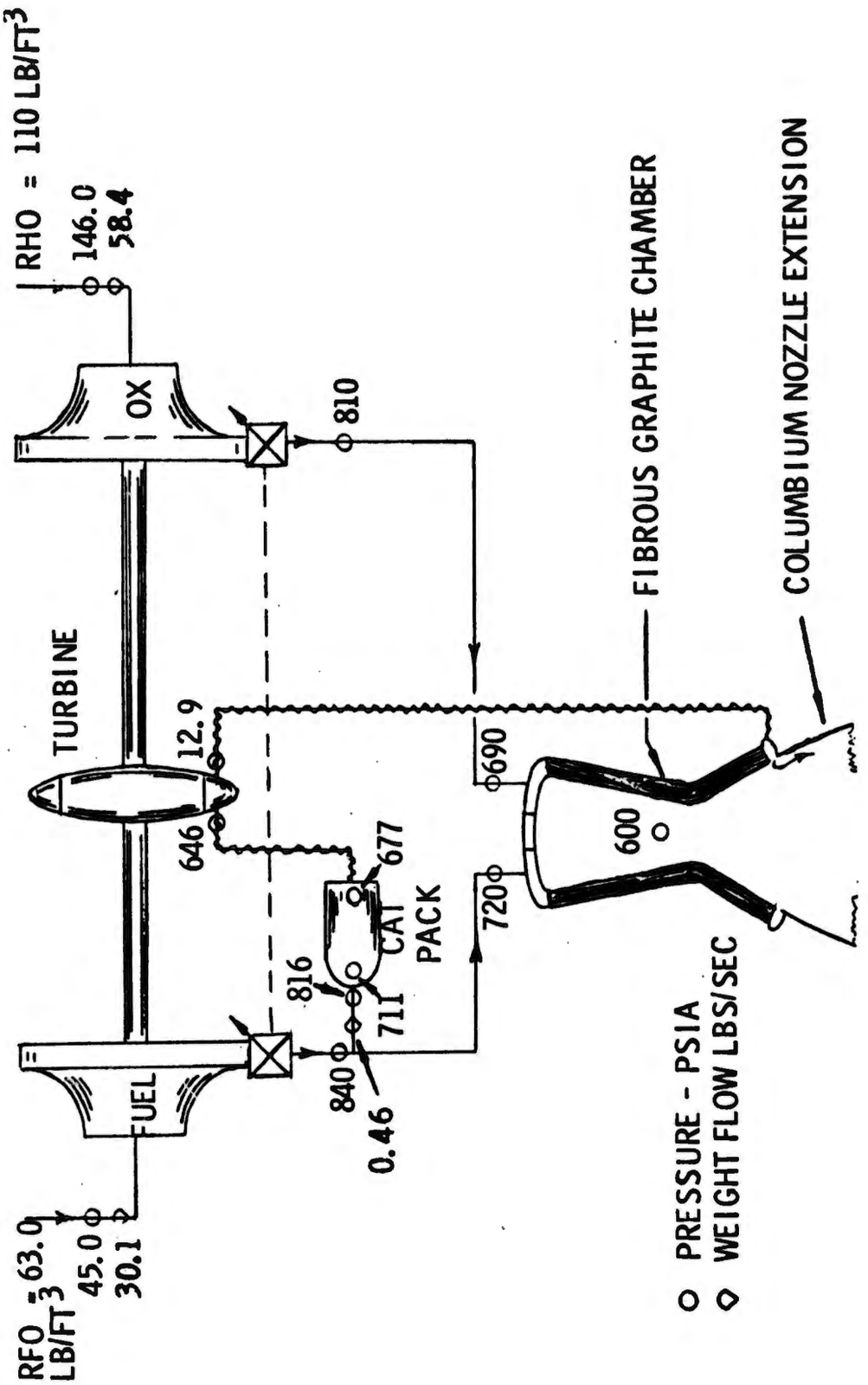

Figure 30. Engine Point Design III

TABLE XIII

POINT DESIGN ENGINE III (U)

Engine Configuration	Performance	
Pump Fed- Bleed Cycle	Thrust	30,000 lb
Single Shaft Pump - with RGV	Chamber Pressure	600 psia
Conventional Injector (liquid/liquid)	Mixture Ratio	1.97
Fibrous Graphite Chamber (to 10:1)	Delivered Isp	340.9 sec
Columbium Nozzle Extension (from 10:1 to 150:1)	Isp Efficiency	92.4
	Design Specifications	
N_2H_4 Catalyst Pack (G.G.)	Dry Weight	302 lb
Turbine Exhaust Gas Injected into Nozzle at 10:1	Wet Weight	307 lb
	Length	145.5 in.
	Diameter	73.3 in.
	Fixed Thrust	
	Interface Pressure	
	Oxidizer	146.0 psia
	Fuel	45.0 psia
	Fuel Film Coolant (% Total Flow)	7.7%

TABLE XIV

THRUST CHAMBER ASSEMBLY NO. 3 DESIGN PARAMETERS

General	Injector	Chamber	Nozzle Extension
Thrust: 30K lb	Type: Conventional, Flat Face, Cross Drilled	Shape: Conical	Attachment Area Ratio: 5
Chamber Pressure: 600 psia	Propellant Phases: Liquid - Liquid	Material: Fibrous Graphite	Cooling Mode: Radiation with Turbine Exhaust Bleed Film Cooling
Nozzle Area Ratio: 150	Thrust per Element: 100 lb	Contraction Ratio: 2	Material: Coated Columbium
Throttleability: Fixed Thrust	Type Element: F-O-F Inline Triplet	Cooling Mode: Radiation with Fuel Film Cooling	
Duration: Unlimited	$\Delta P_{inj}/P_c$: 0.20 (0.45 proposed)	Characteristic Length: 30 in.	
	Material: Ni-200	Throat dia: 6.00 in.	
	Film Cooling: 7.7%		

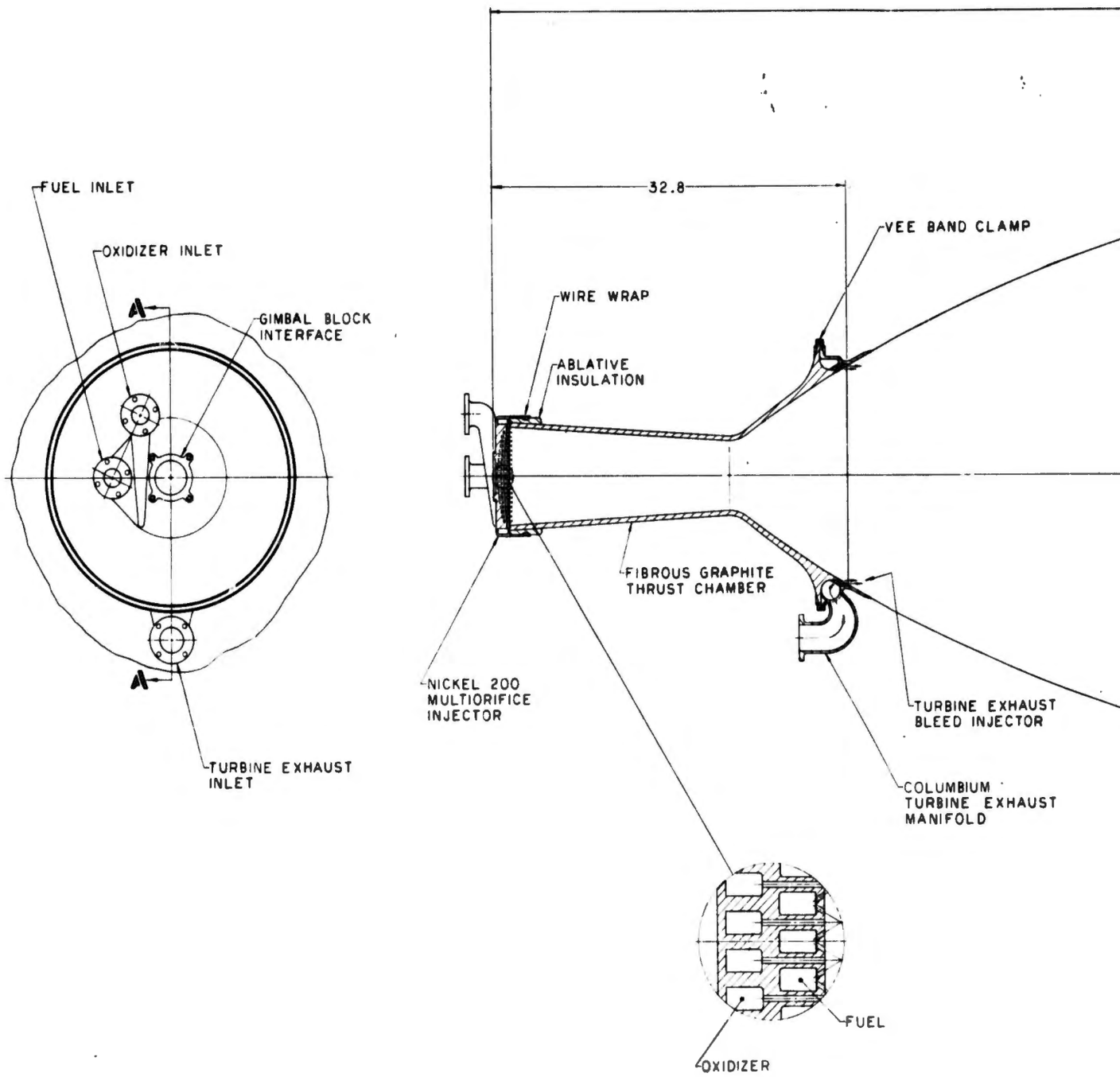
FUEL INLET
OXIDIZER INLET
GIMBAL BLOCK INTERFACE
A
A
TURBINE EXHAUST INLET
32.8
VEE BAND CLAMP
WIRE WRAP
ABLATIVE INSULATION
FIBROUS GRAPHITE THRUST CHAMBER
NICKEL 200 MULTIORIFICE INJECTOR
TURBINE EXHAUST BLEED INJECTOR
COLUMBIUM TURBINE EXHAUST MANIFOLD
FUEL
OXIDIZER

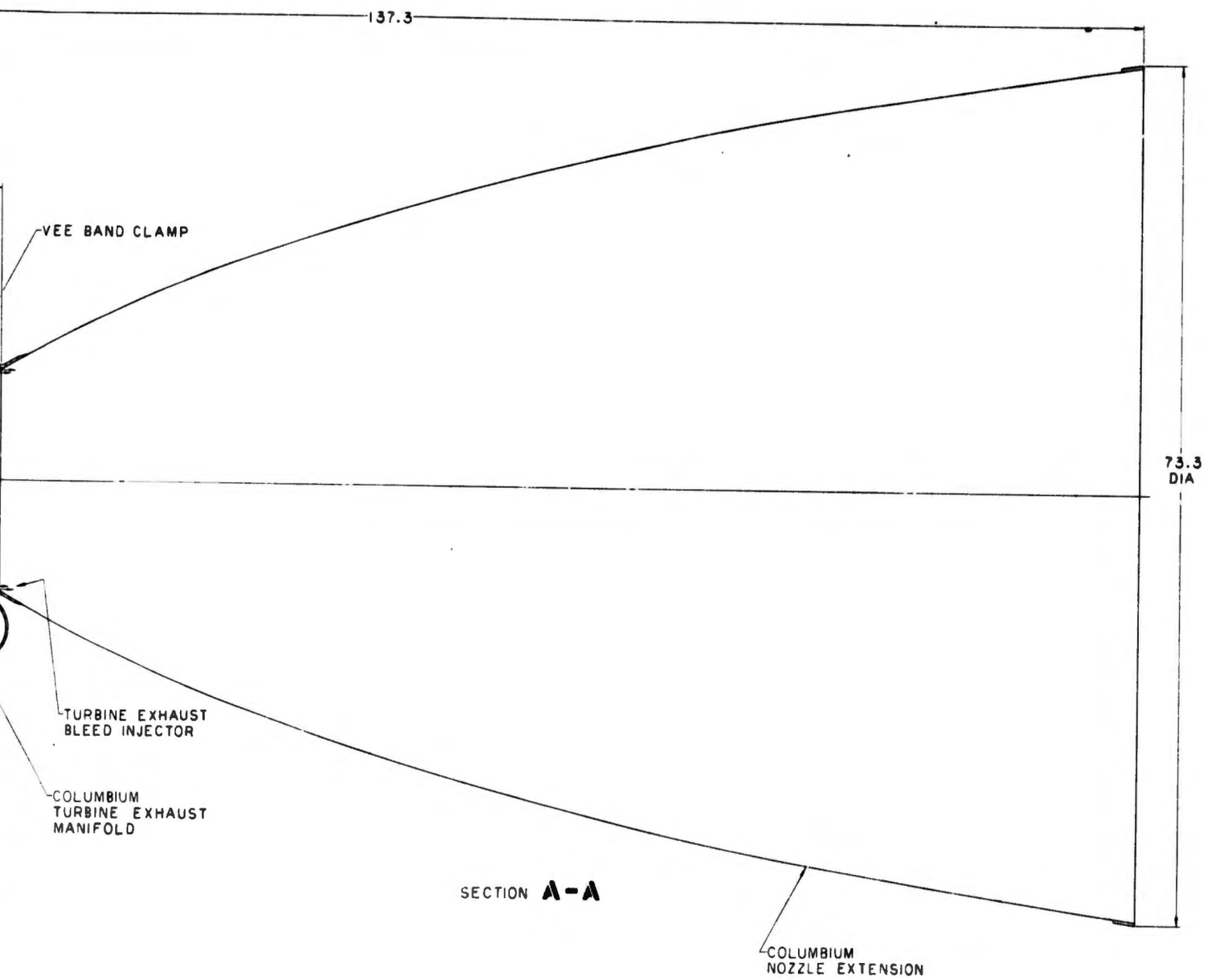

UEL

Figure 31. Thrust Chamber Assembly, Engine No. III

(3) Engine Performance

Plots of Point Design Engine No. III performance are shown on Figure No. 32 for the propellant combination CLF_5/N_2H_4. The optimum mixture ratio performance for these propellants is shown on Figure No. 33. Similar performance information for CLF_5/MHF-5 propellants is provided on Figures No. 34 and No. 35. A large loss in performance is characteristic of this type of engine. It results from the significant amount of fuel film cooling required at the higher chamber pressures of pump-fed engines. The performance of these passively-cooled engines could be significantly improved by using an injector configuration which requires a short L* or by applying the gaseous injector systems.

(4) Controls System Description

An "on-off" propellant flow control is needed for Point Design Engine No. III because it is of a fixed thrust design. A turbopump ring-gate valve with a single, electrically-operated actuator is used in accordance with the criteria established at the outset of the study. The individual fuel and oxidizer valves of the ring-gate valve system will be mechanically-linked for reliable operation during engine start and shutdown transient conditions. Figure No. 36 shows the ring-gate linkage and actuator system.

The detail operation of this ring-gate valve system operates identically to that described for Point Design Engine No. VIII except that the electrical actuator, which is connected directly to the valve combination, is designed for "on-off" operation rather than "throttling" and permits a simplied electrical control circuitry to be used. The electric motor assembly (complete with clutch, brake, and gear train) is almost identical in design to that used for the Transtage electrically-actuated valve. Envelope size and weight will vary slightly depending upon the actual power requirements. The relationship between actuator weight and horsepower is shown by the "on-off" capability curve plotted on Figure No. 37. The parametric study leading to the plots of Figure No. 37 considered valve operating times of 0.4 sec opening and 0.3 sec closing, which are the same as those of the Transtage electrically-actuated bipropellant valve.

(5) Engine Capabilities and Limits

(a) Burn Duration Effects

Pump-fed engines have a considerably higher chamber heat flux than pressure-fed engines of the same thrust level because of the increased chamber pressure. The burn duration limits for fibrous graphite radiation cooled chambers have not as yet been established for pressure levels of pump-fed engines. It is recommended that the same burn duration limit as for the ablative chambers with a fibrous graphite throat insert be used.

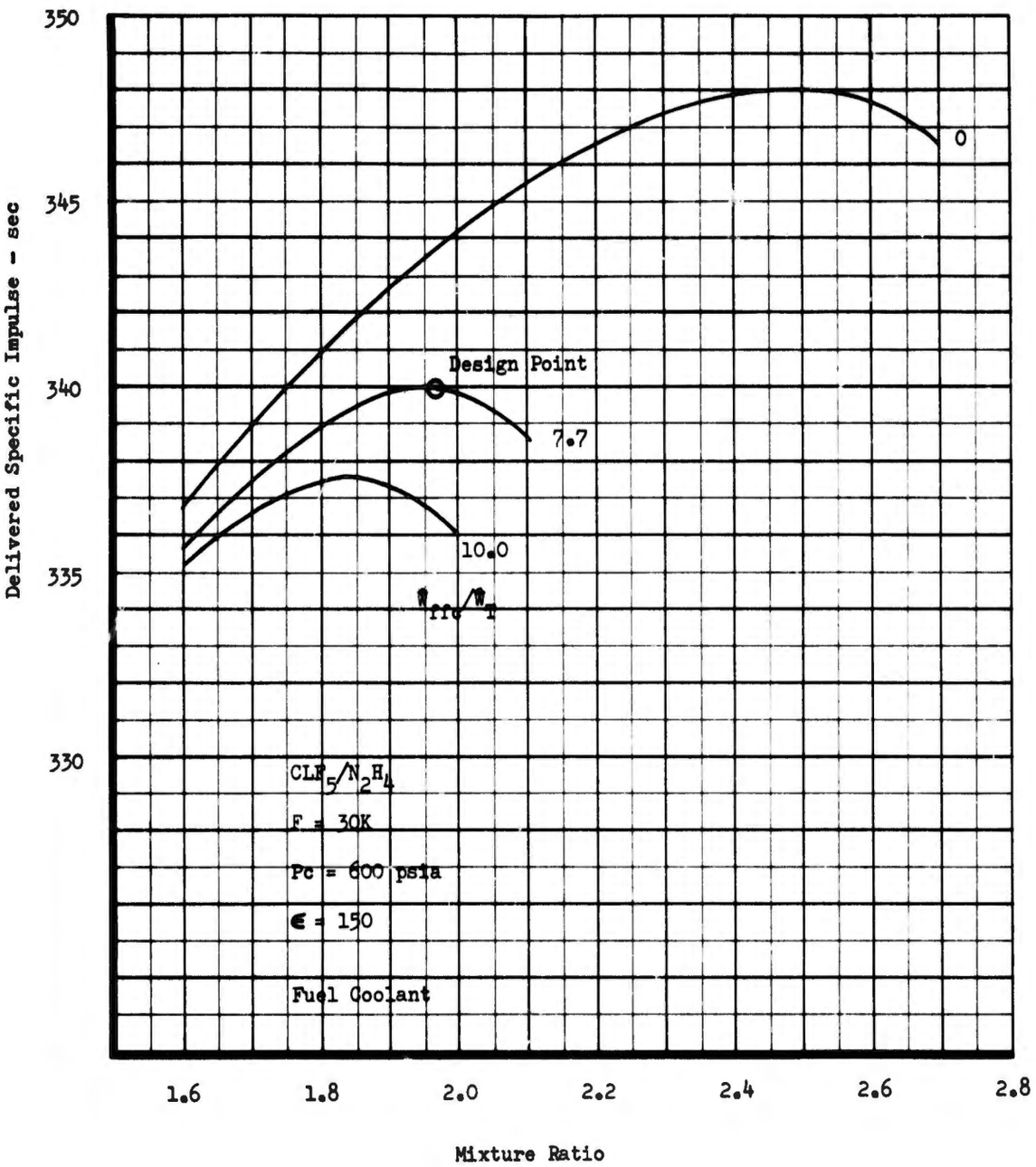

Figure 32. Point Design Engine No. III, Performance/Mixture Ratio-Coolant Flow Trade-Off (CLF_5/N_2H_4) (u)

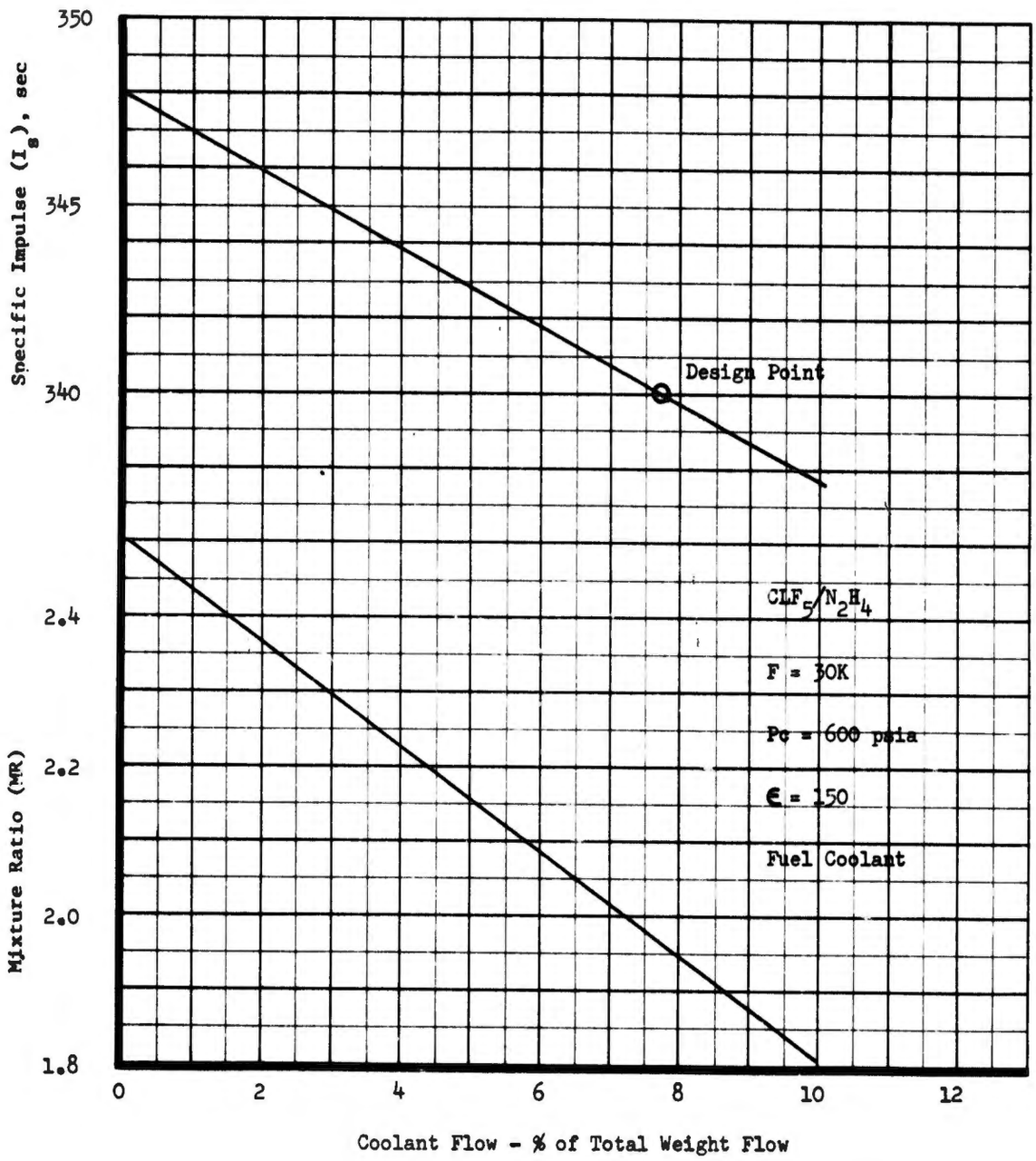

Figure 33. Point Design Engine No. III, Performance/Coolant Flow Interaction (CLF_5/N_2H_4) (u)

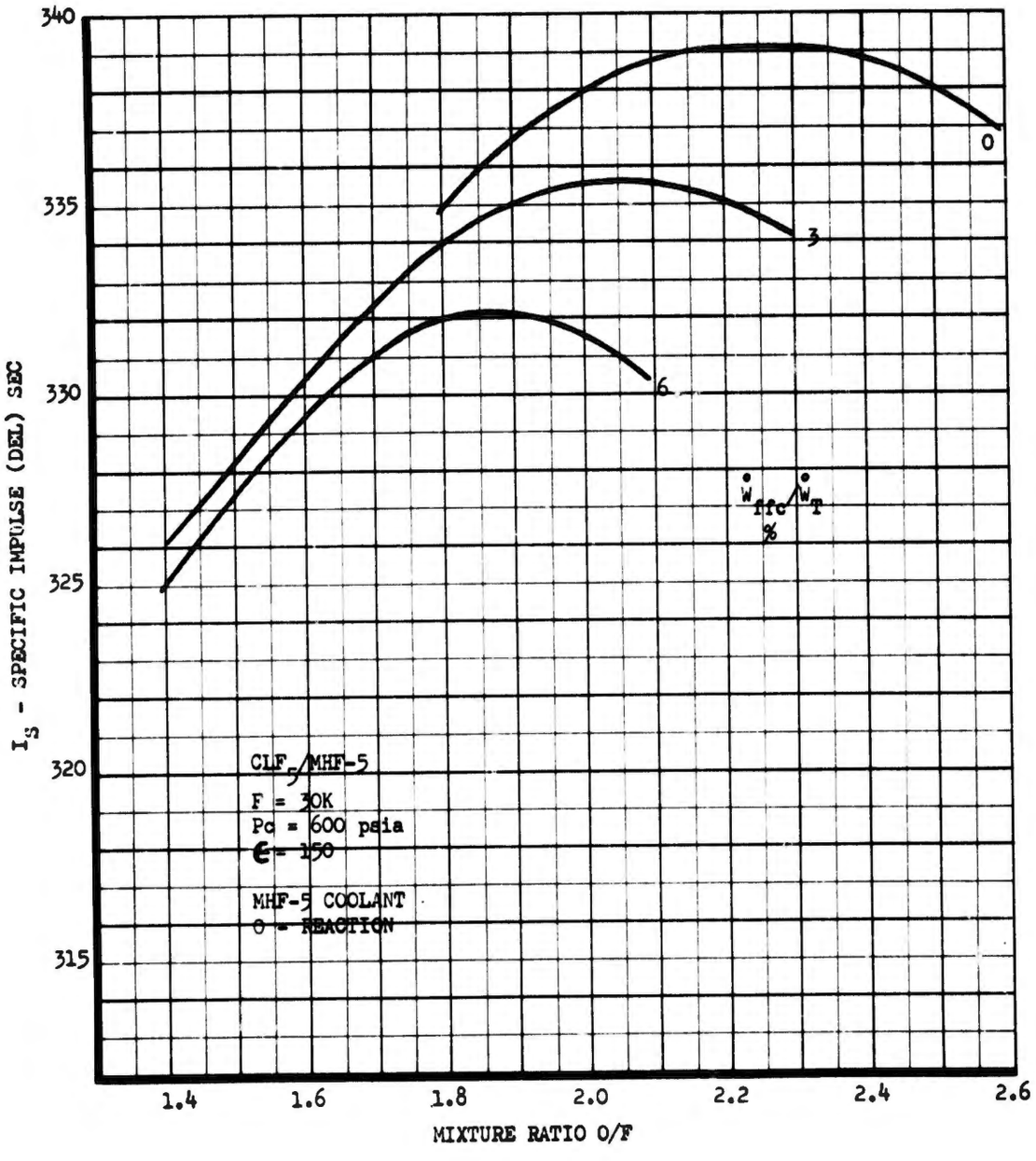

Figure 34. Point Design Engine No. III, Performance/Mixture Ratio-Coolant Flow Trade-Off (CLF_5/MHF-5) (u)

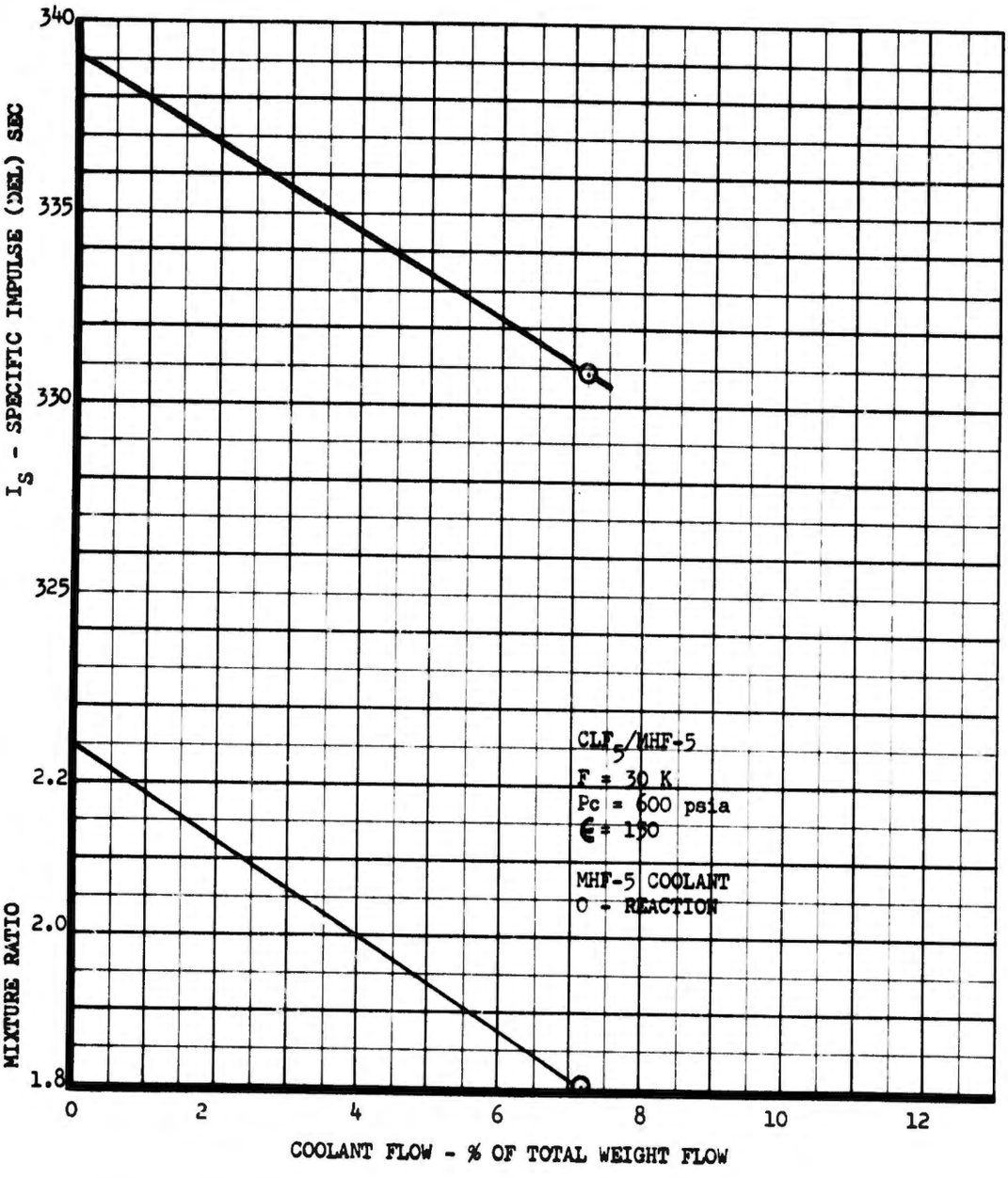

Figure 35. Point Design Engine No. III, Performance/Coolant Flow Interaction (CLF_5/MHF-5) (u)

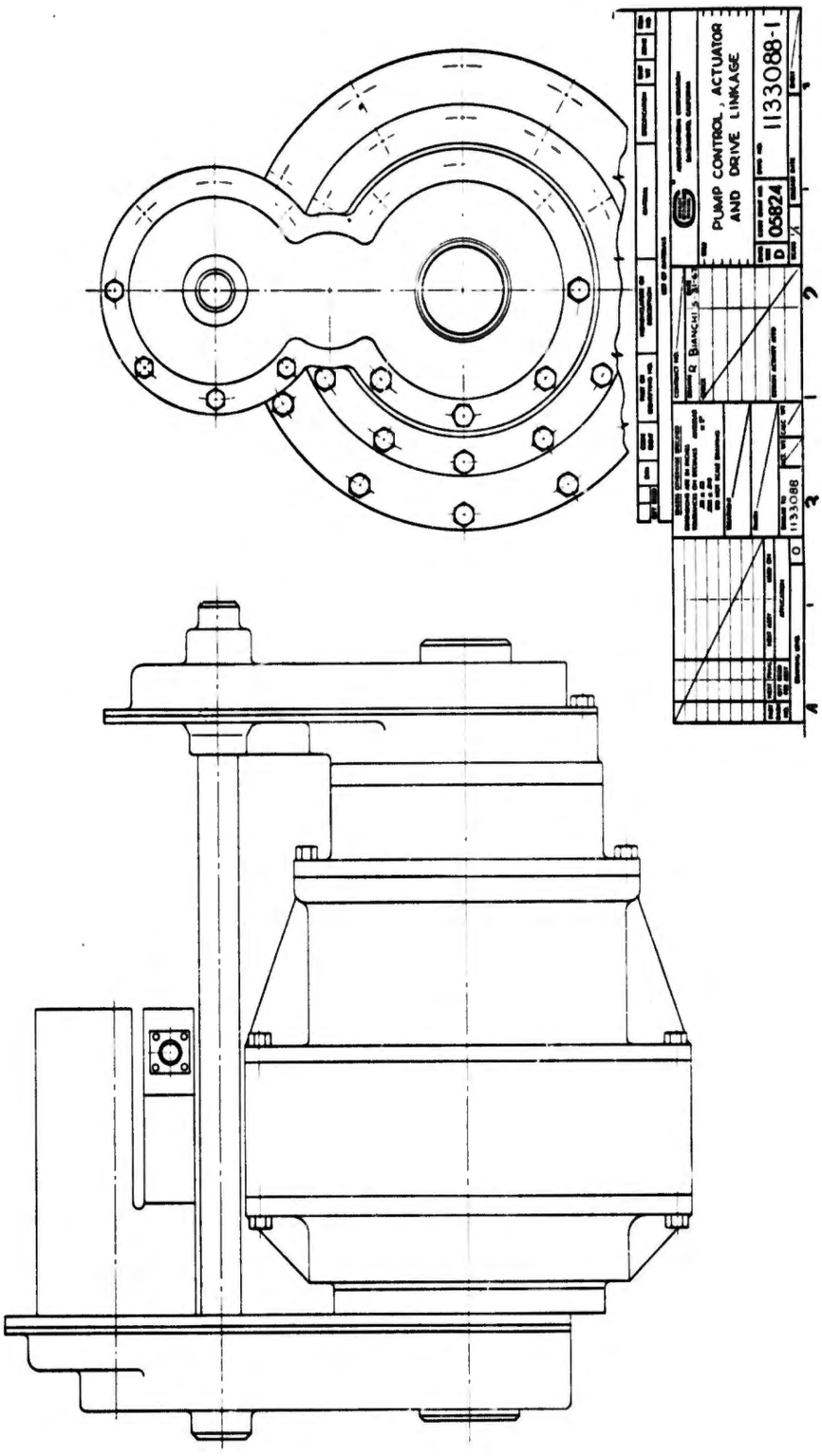

Figure 36. Pump Control, Actuator and Drive Linkage

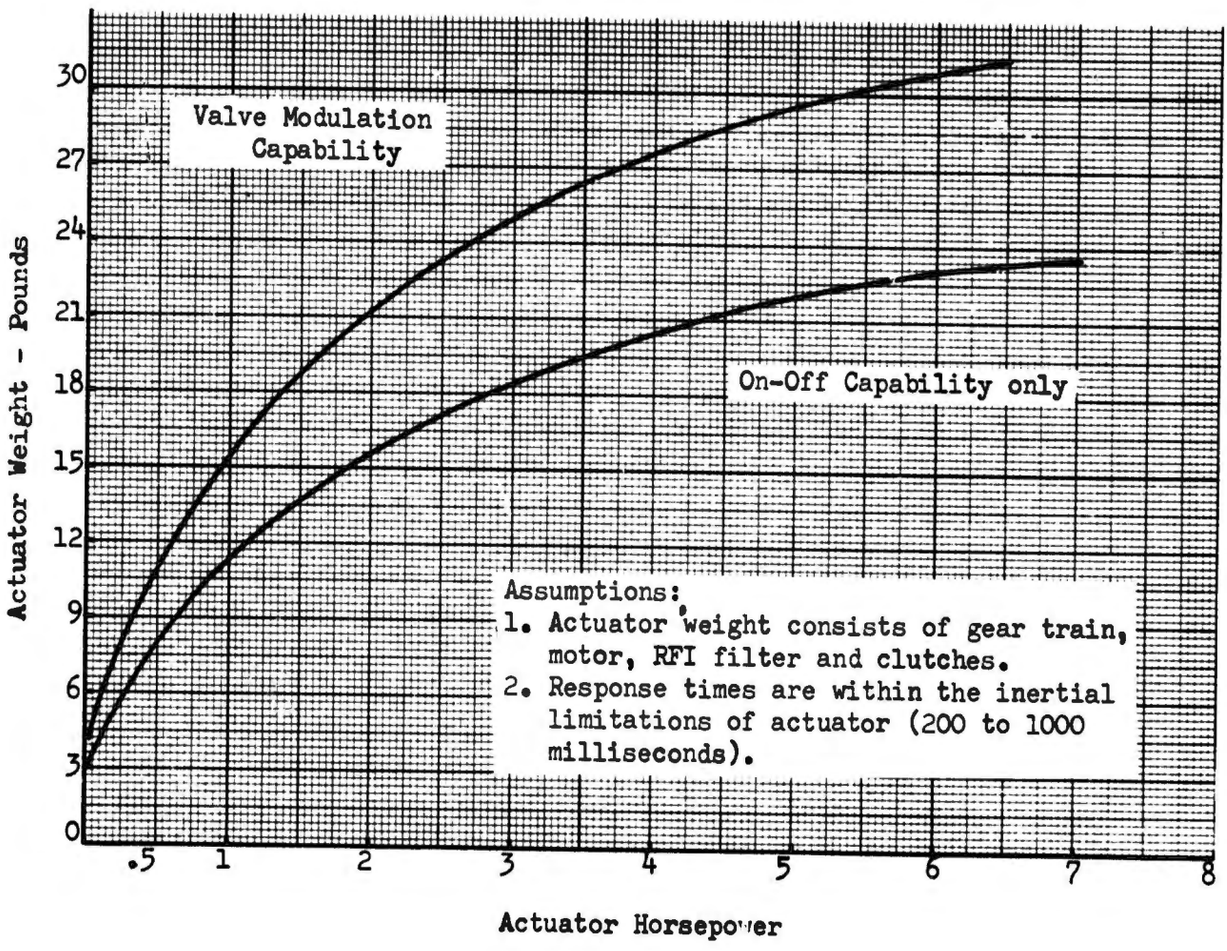

Figure 37. Weight vs Horsepower, Electrical Actuator

(b) Installation

(U) Installation problems are identical to those described for Point Design Engine No. I.

(c) Mission Capability

(C) The start transient of this engine is considerably slower than that of the pressure-fed engines if it is started by means of tank head. An improved start transient can be achieved by using rechargeable pressure bottles which are not included in the engine weight. CAT-Pack gas generators are very suitable to pressure bottle starts because they require only small amounts of fuel.

(U) The heat soak-back of the turbine must be considered when assessing the restart capability of this engine concept. The critical components are the injector, the fuel pump, and the suction lines. It is assumed that the fuel and the oxidizer pump represent sufficient heat-sink capability to absorb sufficient turbine heat soak-back so as not to generate a critical situation.

(d) Propellant Compatibility

(C) Engine design considerations do not exclude any of the specified fuels. However, if the restart requirements are severe, N_2H_4 should not be considered as a fuel, because of the danger of detonation at restart.

b. Point Design Engine No. IV

(U) This engine is throttleable and utilizes a momentum exchange liquid/liquid injection system, which is fed by a fuel-rich bleed turbine-driven turbopump assembly. It has an ablative-cooled thrust chamber with a columbium skirt nozzle extension. The design thrust level is 30K and the chamber pressure 600 psia. For a nozzle expansion ratio of 150:1, as shown on Figure No. 38 the engine has a maximum diameter of 73.3 in. and an over-all engine length of 145.5 in.

(U) Pertinent performance, specification, and configuration information for this engine is summarized on Table XV.

(U) The effect of burn duration upon an ablative chamber was analyzed in detail and this information is presented as part of the Engine No. IV discussion. The effect of burn duration was assessed by evaluating two limiting cases of burn sequences. The results are applicable to pump-fed as well as pressure-fed engines because they are independent of thrust level and chamber pressure, depending only upon the wall temperature.

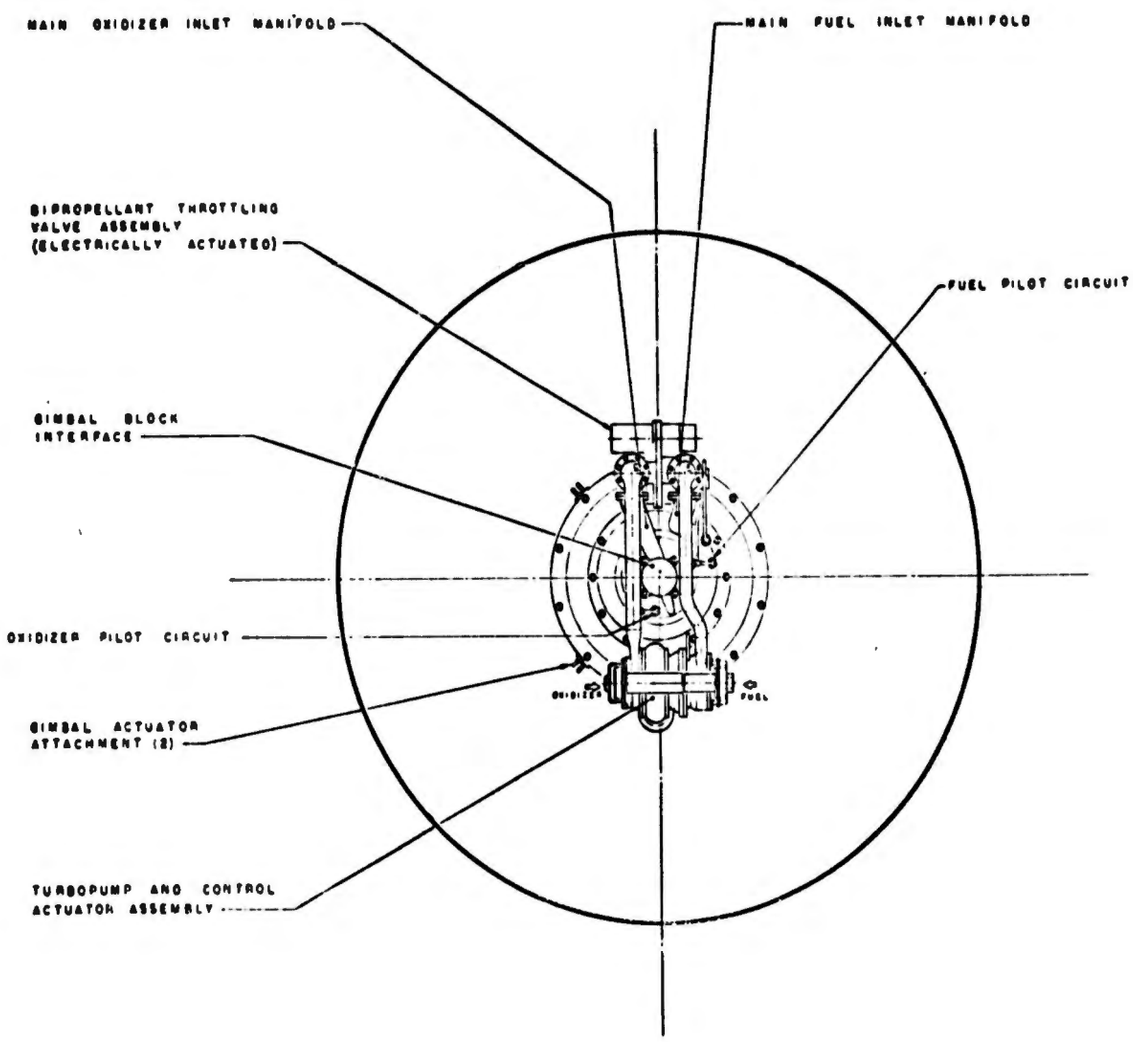
MAIN OXIDIZER INLET MANIFOLD
MAIN FUEL INLET MANIFOLD
BIPROPELLANT THROTTLING VALVE ASSEMBLY (ELECTRICALLY ACTUATED)
FUEL PILOT CIRCUIT
GIMBAL BLOCK INTERFACE
OXIDIZER PILOT CIRCUIT
GIMBAL ACTUATOR ATTACHMENT (2)
TURBOPUMP AND CONTROL ACTUATOR ASSEMBLY
OXIDIZER
FUEL

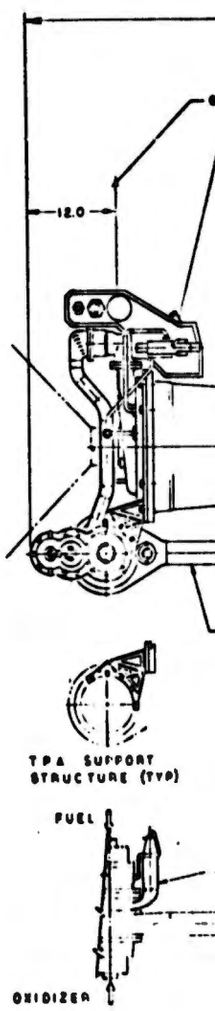
12.0
TPA SUPPORT STRUCTURE (TYP)
FUEL
OXIDIZER

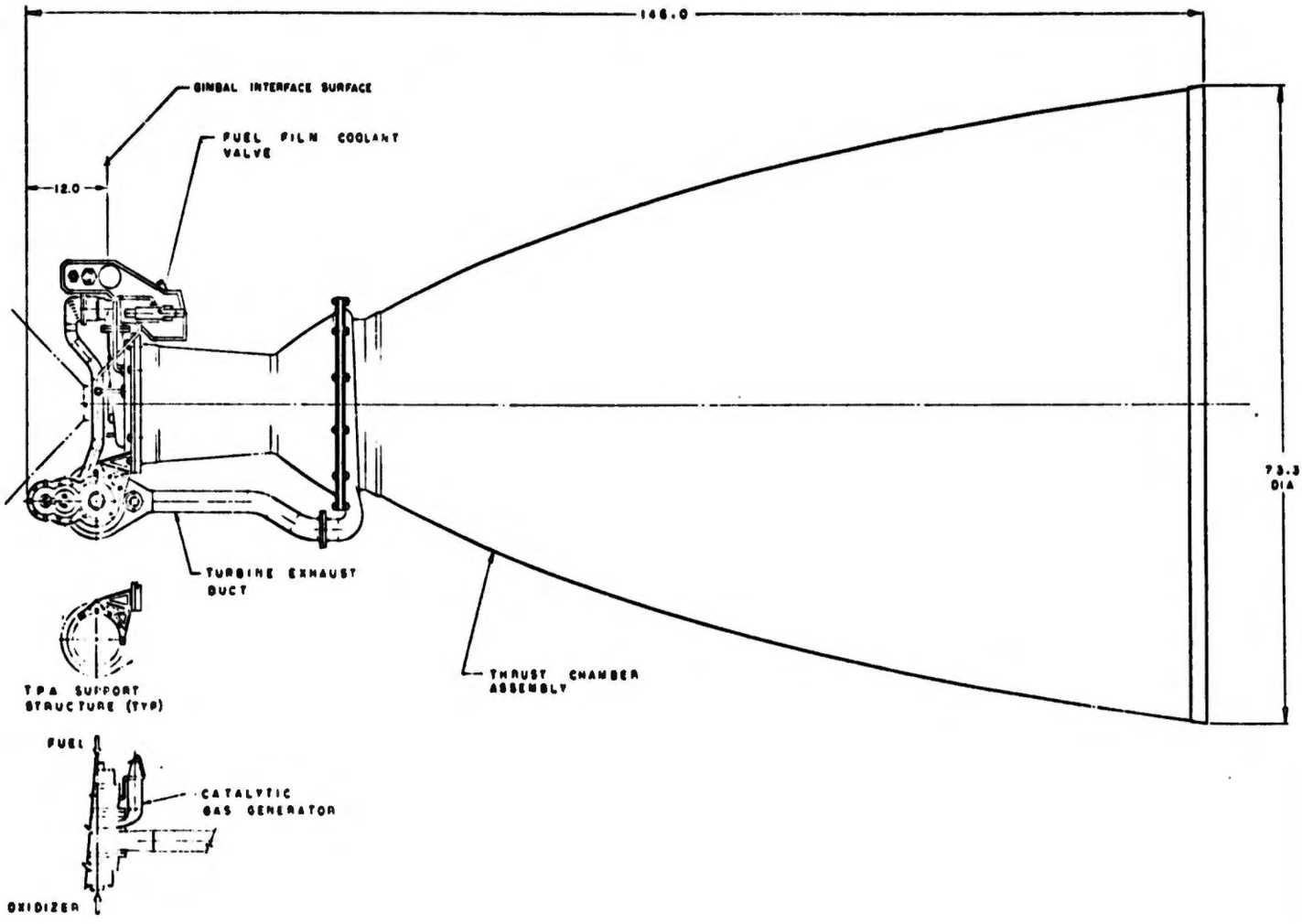

Figure 38. Point Design Engine No. IV Assembly

TABLE XV

POINT DESIGN ENGINE NO. IV (U)

Engine Configuration	Performance	
Pump Fed - Bleed Cycle	Thrust	30,000 lb
Single Shaft Pump - with RGV	Chamber Pressure	600 psia
Momentum Exchange Injector (liquid/liquid)	Mixture Ratio	2.0
Ablative Chamber (to 10:1)	Delivered I_{sp}	337.1 sec
Columbium Nozzle Extension (from 10:1 to 150:1)	I_{sp} Efficiency	92.0
N_2H_4 Catalyst Pack (G.G.)	**Design Specifications**	
Turbine Exhuast Gas Injected into Nozzle at 10:1	Dry Weight	513.4 lb
	Wet Weight	525.8 lb
	Length	146.0 in.
	Diameter	73.3 in.
	Throttling Range	(10 to 1)
	Interface Pressure	
	Oxidizer	45.0 psia
	Fuel	146.0 psia
	Fuel Film Coolant (% Total Flow Required to Cool Throat)	7.0%

(1) Injector Description

Figure No. 39 is an engine schematic showing the different circuits required for a deep throttleable momentum exchange injector, including the flow and pressure schedules for full thrust conditions.

Figure No. 40 shows the thrust chamber assembly and an enlarged cross-section of a portion of the injector. This injector contains five separate hydraulic circuits, but is monolithic in structure so that no inter-manifold leaks can be caused by poor welds. There are two fuel systems; a high pressure, pilot circuit, and a lower, variable pressure main circuit. The two oxidizer systems are similar. The fuel film cooling system makes up a fifth circuit, which is controlled separately to avoid excessive performance losses resulting from over-cooling during throttled operation. The basic concept of the momentum exchange element is to allow a small high velocity stream to mix with a larger low velocity one of the same propellant to provide a stream with a fairly high velocity core. Then, the low velocity stream can be throttled back without causing any significant decrease in the resultant injected stream velocity. Ten to one throttling is expected to be achieved with this engine as follows:

- At full thrust, all circuits are at full pressure, which results in maximum flow rates.

- For throttling to 25% thrust, the main fuel and oxidizer valves will be closed to decrease the flow rates rate and pressures in the main circuits while the pilot circuits continue at full pressure.

- For throttling from 25% of thrust to 10% of thrust, the pump ring-gate valves will be closed to decrease the pressures and flows in all circuits.

Note that the injector face shown on Figure No. 40 is regeneratively-cooled by the main fuel flow. During throttled operation, the fuel velocity is less, but so is the heat flux to the injector face. The internal injector propellant manifolds will be formed by a combination of gun-drilling and electrical discharge machinery. The purpose of the momentum exchange element itself is to maintain injection velocity during throttling so that good impingements and droplet break-up can be maintained. Also, it assures that feed system induced combustion stability does not appear. A comparison of the resultant injection velocity is shown on Table XVI for full thrust, 25% thrust, and 10% thrust.

(2) Combustion Chamber Geometry

The conical combustion chamber of thrust chamber assembly No. 4 has a contraction ratio of 2.0 and a characteristic length of 25 in. These parameters were determined based upon the performance

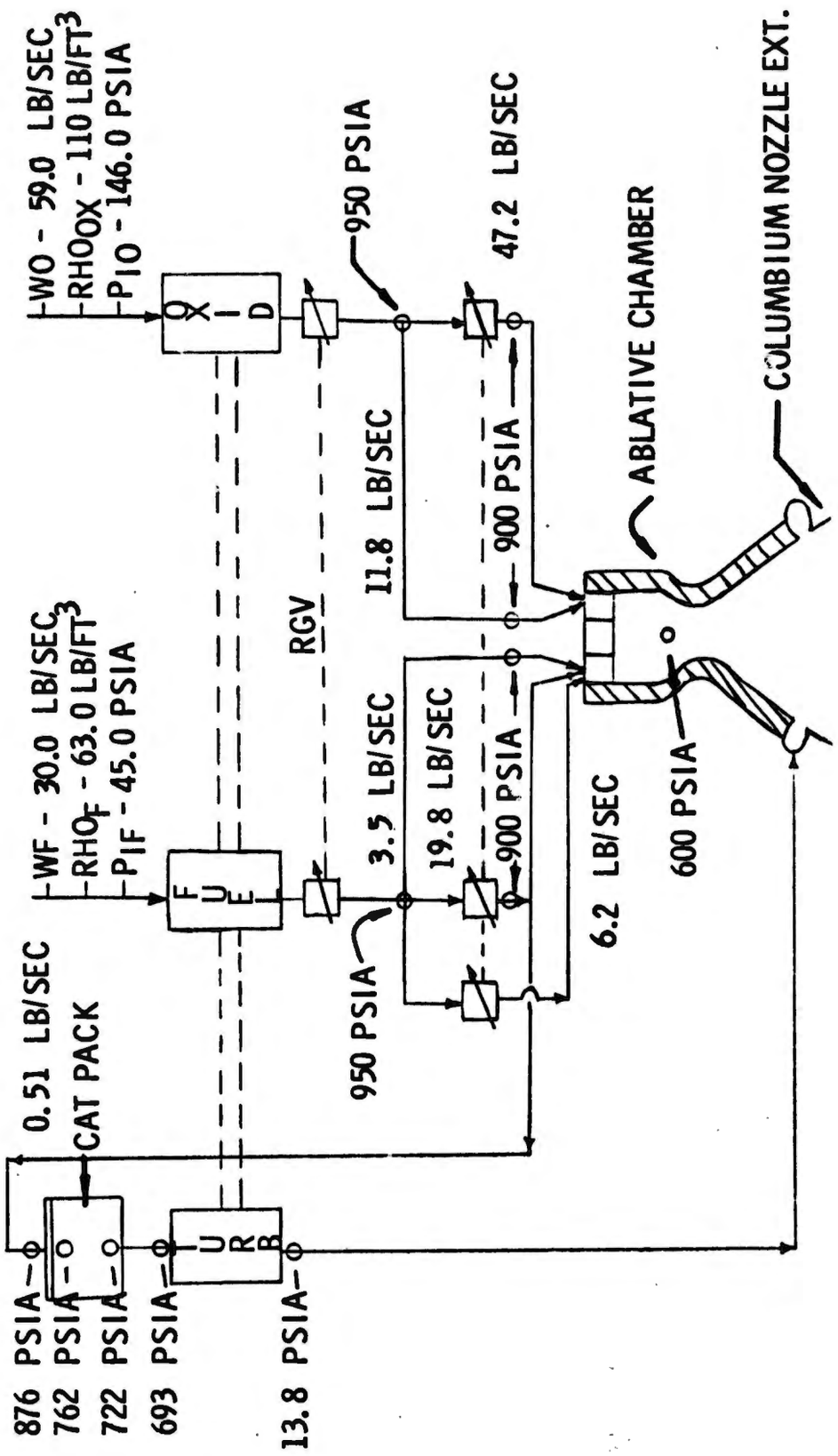

Figure 39. Point Design Engine No. IV Schematic

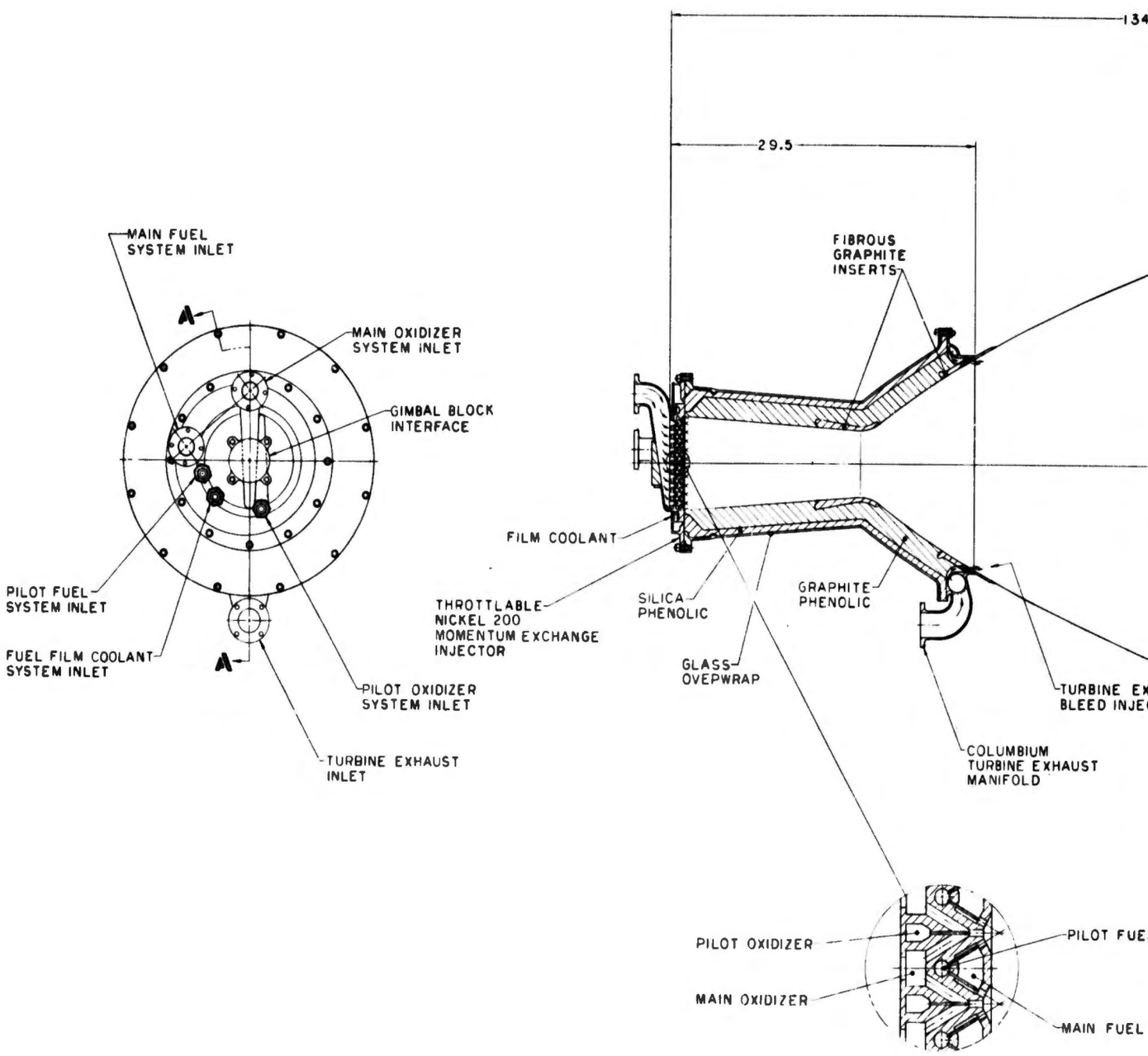
MAIN FUEL SYSTEM INLET
MAIN OXIDIZER SYSTEM INLET
GIMBAL BLOCK INTERFACE
PILOT FUEL SYSTEM INLET
FUEL FILM COOLANT SYSTEM INLET
PILOT OXIDIZER SYSTEM INLET
TURBINE EXHAUST INLET
A
A
134
29.5
FIBROUS GRAPHITE INSERTS
FILM COOLANT
THROTTLABLE NICKEL 200 MOMENTUM EXCHANGE INJECTOR
SILICA PHENOLIC
GRAPHITE PHENOLIC
GLASS OVEPWRAP
TURBINE EX
BLEED INJE
COLUMBIUM TURBINE EXHAUST MANIFOLD
PILOT OXIDIZER
MAIN OXIDIZER
PILOT FUE
MAIN FUEL

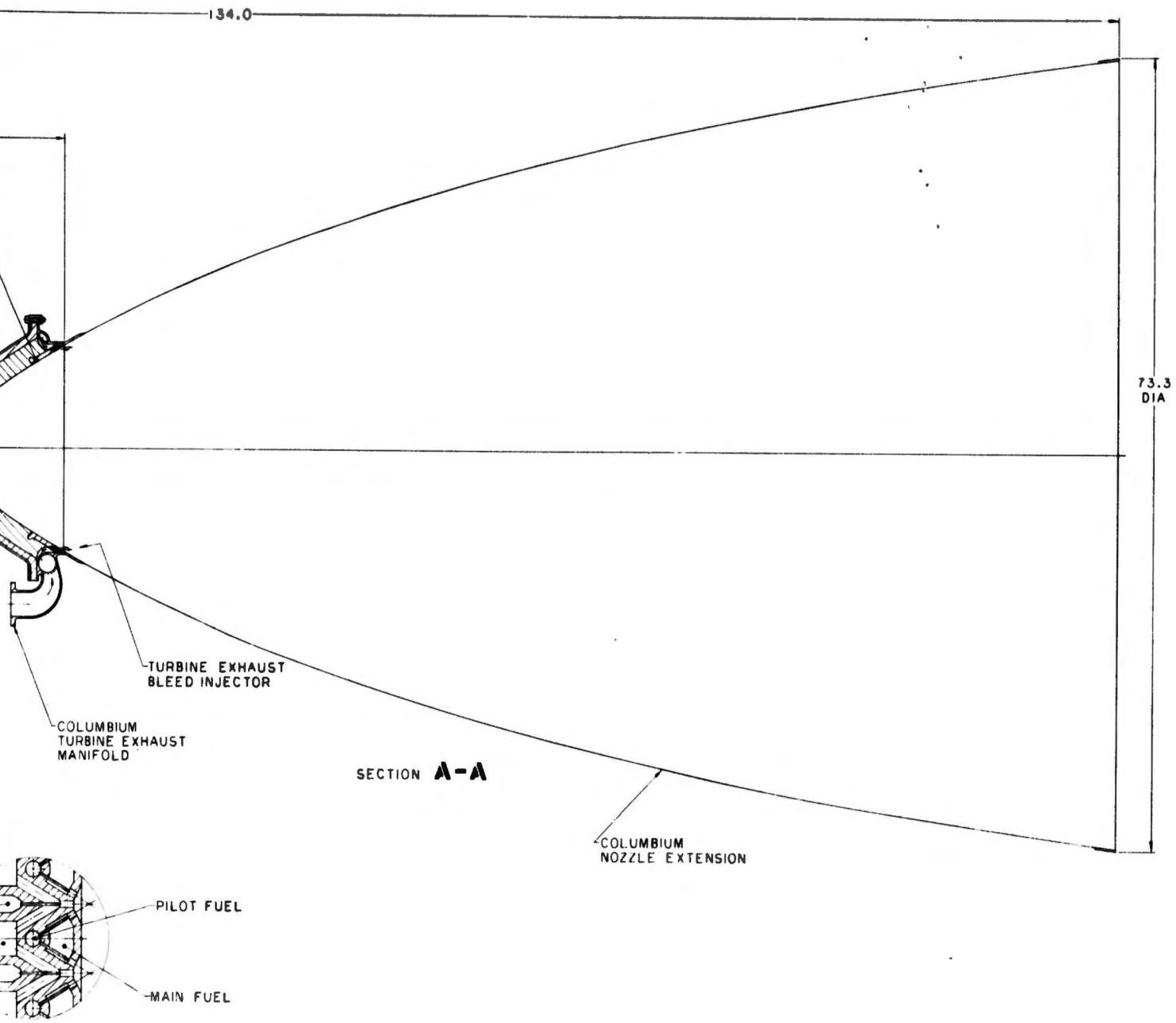

Figure 40. Thrust Chamber Assembly, Engine No. IV

TABLE XVI

COMPARISON OF INJECTION VELOCITIES, ENGINE NO. IV

Summary of Flows and Velocities Through Momentum Exchange Injector During Throttling

	Full Thrust		25% Thrust		10% Thrust	
	Oxid	Fuel	Oxid	Fuel	Oxid	Fuel
Main Flow Rate (M), lb/sec	46.19	27.27	3.82	3.22	1.53	1.28
Pilot Flow Rate (P), lb/sec	11.55	4.81	10.1	4.38	4.28	1.76
Total Flow Rate (M + P), lb/sec	58.08	32.08	14.52	7.60	5.82	3.04
% Main Flow Rate (M/(M + P))	80.0	85.0	26.3	42.4	26.3	42.1
% Pilot Flow Rate (P/(M + P))	20.0	15.0	73.7	57.6	73.7	57.9
Main Inj Velocity, ft/sec	142.0	200.0	11.5	25.5	4.6	10.1
Pilot Inj. Velocity, ft/sec	142.0	200.0	131.0	179.0	52.5	72.0
Resultant Velocity, ft/sec	142.0	200.0	99.0	136.0	40.0	46.0

NOTE: Analysis assumed: 1. Constant 5% fuel film coolant, constant I_{sp}.
2. No additional fuel film coolant circuit.

considerations shown on Table XVII. Small contraction ratios yield high gas to liquid velocity ratios, which results in droplet break-up and more complete combustion within a given size chamber. The chamber length is a direct trade-off between weight and performance.

(3) Structural Design Description

Thrust and gimbaling loads are transferred to the gimbal block through the single-piece injector body, which is rather thick and cored-out to make it both lightweight and rigid. The injector flange is bolted to the chamber flange, which is, in turn, fastened to the chamber wall. Fingers on the chamber flange lock over the silica phenolic portion of the forward chamber wall. These fingers are wrapped in place by glass cloth and glass roving which form the longitudinal and hoop structures, respectively, of the thrust chamber wall. The columbium nozzle extension is bolted to the silica phenolic-glass cloth aft flange similarly to what is now done with ablative thrust chamber assemblies. The aft flange bolts to a turbine exhaust bleed manifold, which distributes turbine exhaust gases to an axial flow injector at the forward end of the columbium nozzle extension.

Turbine exhaust gases are injected into the nozzle to allow the columbium skirt to be used at a smaller area ratio than would otherwise be possible. Turbine exhaust gases are cool (700°F) as compared to the thrust chamber assembly exhaust gases and act as film coolant for the forward portion of the nozzle extension. Injection into the main nozzle also eliminates the need for a second nozzle, and supporting structure for the long feed line running the length of the engine. However, performance loss can be incurred, if the entrance of the turbine exhaust gases causes a shock wave to form in the supersonic nozzle. These gases must be bled-in at a small angle to the wall, at a relatively low velocity, and quite uniformly. A fine injector can be constructed by wrapping a long strip of columbium around the nozzle diameter and skewing the coil to fit the nozzle contour. Axial injection of gases would result if the strip had small etched grooves across its width. The coil can be tack-welded together and to the columbium nozzle extension. The assembled arrangement is shown on Figure No. 40.

(4) Materials Selection

As with other thrust chamber injectors, Ni-200 has been selected for the injector material of thrust chamber assembly No. 4. Compatibility with the propellants and their reaction products is the primary factor involved in this selection as will be subsequently detailed in the discussion of thrust chamber assembly No. 8. From the materials aspect, the most interesting portion of thrust chamber assembly No. 4 is the chamber itself. It is of ablative design and must withstand 600 sec at 600 psia chamber pressure. Silica phenolic, which is a good insulator, is the material used in most ablative chambers, but it is not compatible with halogen oxidizers. Carbon phenolic has been tested with ClF_3 and was severely eroded by oxidizer-rich

TABLE XVII

THRUST CHAMBER ASSEMBLY NO. 4 DESIGN PARAMETERS

General	Injector	Chamber	Nozzle Extension
Thrust: 30K lb	Type: Momentum Exchange	Shape: Conical	Attachment Area Ratio: 5
Chamber Pressure Max: 600 psia	Propellant Phases: Liquid - Liquid	Material: Ablative, Graphite and Silica Phenolics	Cooling Mode: Radiation with turbine exhaust bleed film cooling
Nozzle Area Ratio: 150	Thrust per Element: 375 lb	Contraction Ratio: 2	Material: Coated Columbium
Throttleability: 10/1	Type Element: F-O-F Inline Triplet of Co-axial Momentum Exchange Elements	Cooling Mode: Ablative, with Fuel Film Cooling	
Duration: 600 sec	$\Delta P_{inj}/P_c$ (max): 0.50 Material: Ni-200	Characteristic Length: 25 in.	
	Film Cooling: 7.0% Fuel	Throat Dia: 6.00 in.	

gases. Graphite phenolic is highly compatible with the propellants, but its insulative properties are poorer than the other materials. Also, the graphite phenolic will probably be unable to maintain dimensional integrity at the throat because of the high chamber pressure. Therefore, the graphite phenolic inner shell will be wrapped around a fibrous graphite throat insert and then covered with silica phenolic insulation. Glass cloth, roving, and resin will form a structural over-wrap for the chamber, similarly to what is now done for the Apollo and Transtage engines. An additional fibrous graphite insert is added to the exit end of the ablative chamber so that the turbine exhaust bleed injector can be firmly retained. Figure No. 38 shows thrust chamber assembly No. 4 with its columbium turbine exhaust manifold, aft chamber flange, wrapped platelet injector, and nozzle extension. Also shown is the Inconel injector/chamber flange with its fingers wrapped into the chamber wall under the glass to form a seal and a mechanical lock between the flange ring and chamber.

(5) Thrust Chamber Wall Thickness Requirements

Thickness requirements are herein specified for each of three continuous firing duty cycles (100 sec, 300 sec and 600 sec). In all three cases, the fibrous graphite thickness was held constant to provide protection from throat erosion. The graphite and silica phenolic thicknesses were then adjusted to satisfy the 3000°F interface and 650°F exterior temperature design limits.

The following table is a summary of the liner thickness requirements at the throat for each of the three thrust chamber assemblies:

Engine No. IV Line Thickness Requirements (Full Thrust)

	Material Thickness, in.		
Liner Cross-Section	100 sec TCA	300 sec TCA	600 sec TCA
Fibrous Graphite	0.4	0.4	0.4
Graphite Phenolic (FM-5064)	0.4	0.95	1.5
Silica Phenolic (FM-5067)	0.2	0.30	0.60
Glass Overwrap	0.125	0.125	0.125
Total	1.125	1.775	2.625

To maintain the gas side surface temperature at 4500°F in the throat, 7% of the total propellant flow will have to be used as fuel film coolant. (9)

Ablative chambers are unique because the size or weight of the thrust chamber is dependent upon the desired firing duration and duty cycle. Thus, the optimum chamber design cannot be specified until

(9) The throat temperature assumption of 4500°F is based upon thermal data from Contract F04611-67-C-0003.

the required duty cycle or mission is known. Conversely, for a given chamber design, many duty cycles exist, through which, the design will operate satisfactorily.

The following three types of missions were analyzed. In one instance, the required change in liner thicknesses to accomplish a given mission is determined. In the other instance, the capabilities of a given design are determined.

(a) Impulse Throttling

In the impulse throttling mission, 80% of the available propellant is expended at full thrust and the remaining propellant is expended at 10% of full thrust. Thus, the duty cycle for thy engine carrying 600 sec of propellant would be 480 sec at full thrust at 1200 sec at 10% thrust.

Three liner designs were analyzed for this mission. These liners were designed for 100 sec, 300 sec, and 600 sec of continuous firing. The liners were analyzed for missions of 480/1200 sec, 240/600 sec, and 80/200 sec, respectively. In these studies, the silica phenolic thickness was varied so that the extension temperature reached the design limit of 650°F at the end of the mission.

Figure No. 41 shows the results of the study in terms of the total liner thickness required for both the continuous, the 90/10, and the 80/20 impulse mission. From the plot, it can be seen that an increase of approximately 40% in total thickness is required for a given design if the propellant is expended in the 90/10 sec mode rather than in a continuous firing.

(b) Infinite Capability Duty Cycles

In this duty cycle analysis, the 600 sec thrust chamber assembly (continuous fire) was subjected to both a 100 sec and a 300 sec initial firing. Then, it was determined which combination of fire and soak times can be applied to the chamber so that the char front is not moved. In this way, the chamber can be cycled indefinitely. Two distinct limiting cases exist, namely, the minimum and maximum fire times.

The minimum fire time actually corresponds to a minimum soak time subsequent to the initial 100 sec or 300 sec burn. This soak time is the time required for the char front to become stationary. During this time, no firings are possible because the char front would continue to move.

The maximum fire time is the longest possible firing of the chamber after it has chilled down to ambient (assumed to be 70°F) by radiating to space.

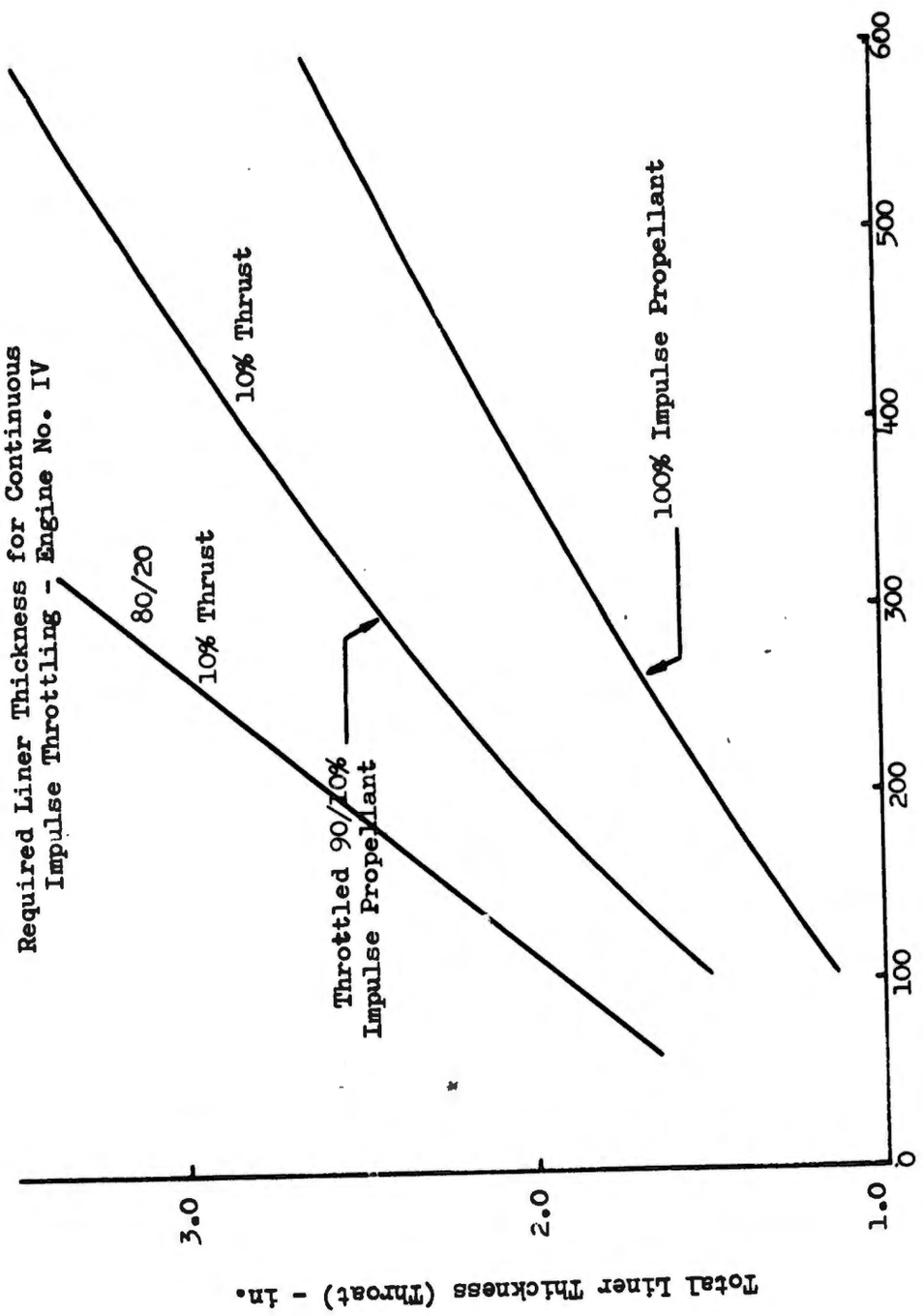

Figure 41. Required Liner Thickness for Continuous Impulse Throttling, Engine No. IV

Figure No. 42 shows the results of the analysis for the 100 sec and 300 sec initial burns. Theoretically, a chamber can be cycled indefinitely through any combination of fire and coast times specified by these curves.

(c) Critical Restart Duty Cycles

In the critical restart duty cycle analysis, the 600 sec (continuous fire) thrust chamber assembly is subjected to a 300 sec initial burn and subsequent burns of from 25 sec to 100 sec each. All the subsequent firings are initiated at that point in time when the chamber wall exterior reaches its peak value as a result of the previous firing. Thus, the purpose of this analysis is to determine the life (total possible duration) of the chamber and what fraction of the total available propellant can be expended without altering the liner design.

To provide a degree of flexibility in the analysis, two limiting factors have been considered. The first is the 650°F extension design temperature limit, which appears reasonable because chamber structural integrity would be a problem above this temperature. The second limiting factor is the time required to char through the ablative liner, which is a measure of the capability of the chamber with a relatively small change in insulation (silica phenolic) thickness.

Figure No. 43 shows the total life (fire and coast) of the chamber in terms of the restart fire times as well as both the exterior temperature and charring limits. The total allowable firing time in terms of the same parameters is shown on Figure No. 44. It is interesting to note that even taking the char limit case, the chamber cannot expend the available propellant (60 sec) by increasing the liner thickness.

(6) Controls System Description

The pump-fed variable thrust engine system configuration of Engine No. IV (shown on Figure No. 45) is a hybrid control system utilizing both turbopump ring-gate valve control and a separate bipropellant momentum exchange throttling valve assembly. The ring-gate valve system and the separate bipropellant momentum exchange valve will be electrically-operated in accordance with the criteria established at the outset of the study. A poppet-type, all-metal bipropellant valve design will be used for the momentum exchange control valve. The poppets of this valve assembly will contain small through-flow passages to permit a relatively small amount of propellant flow when the valve is in the shut-off or closed position; therefore, the shut-off seal performance of this valve will not be critical. The all-metal, electrically-actuated bipropellant valve recently designed for the Transtage application has been selected as a basis for the all-metal bipropellant momentum exchange valve design. This valve is shown on Figure No. 46. The oxidizer and fuel valves of this assembly will be mechanically-linked for reliable phasing during throttling and engine transient conditions. The ring-gate linkage and actuator system is shown on Figure No. 47.

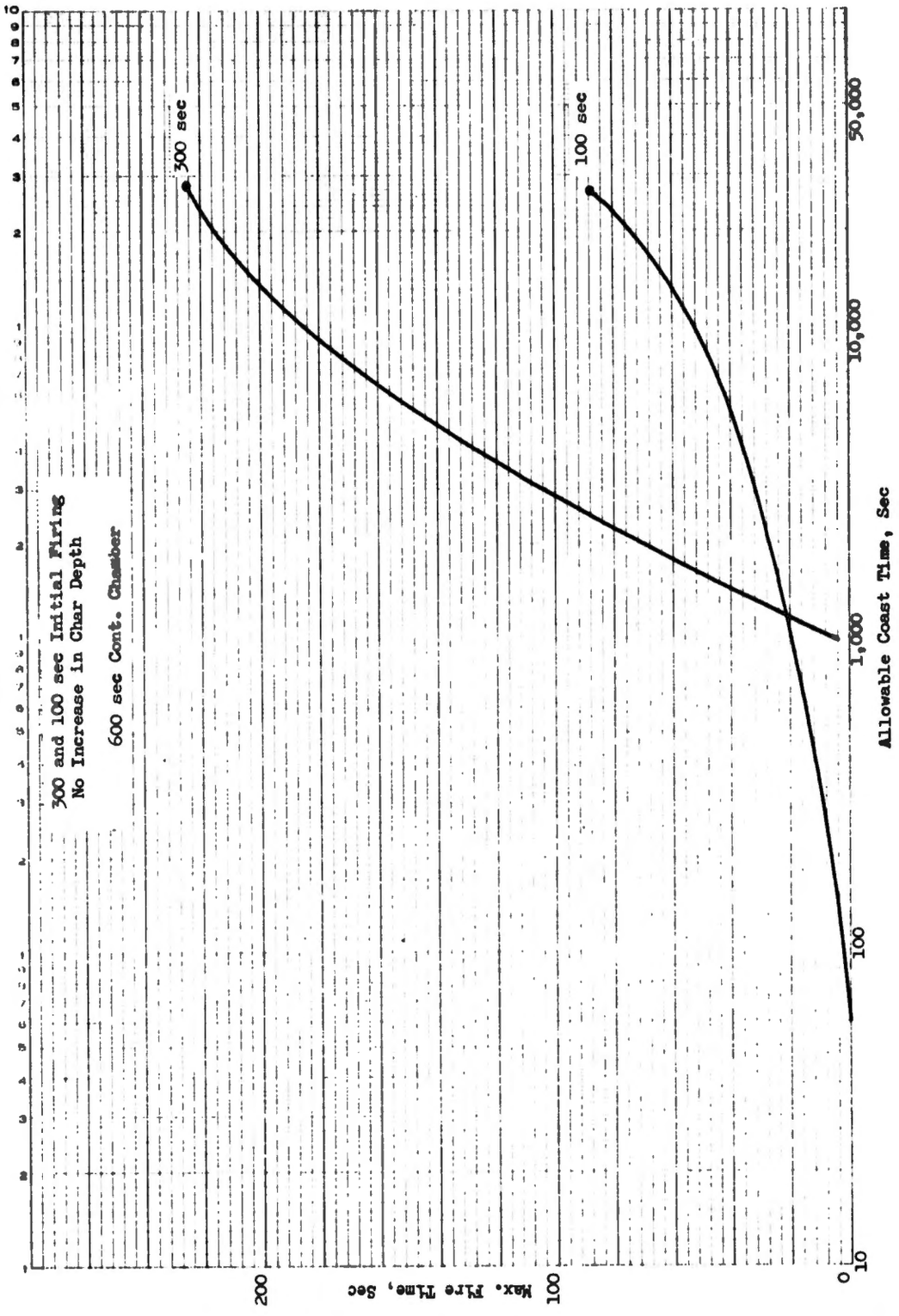

Figure 42. Engine No. IV Infinite Capability Duty Cycle

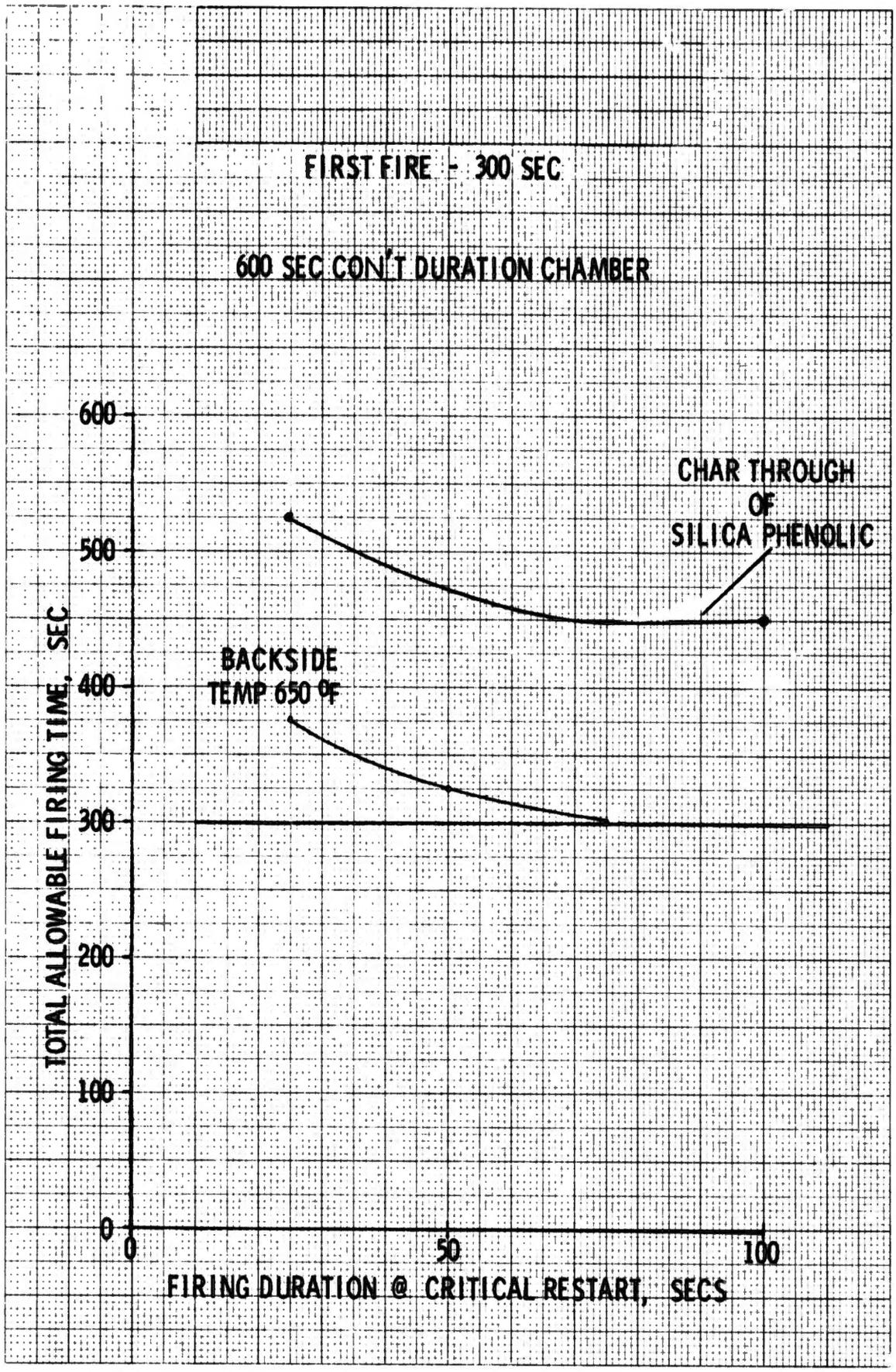

Figure 43. Engine No. IV Mission Analysis, Critical Restart Duty Cycle, Total Life of Chamber

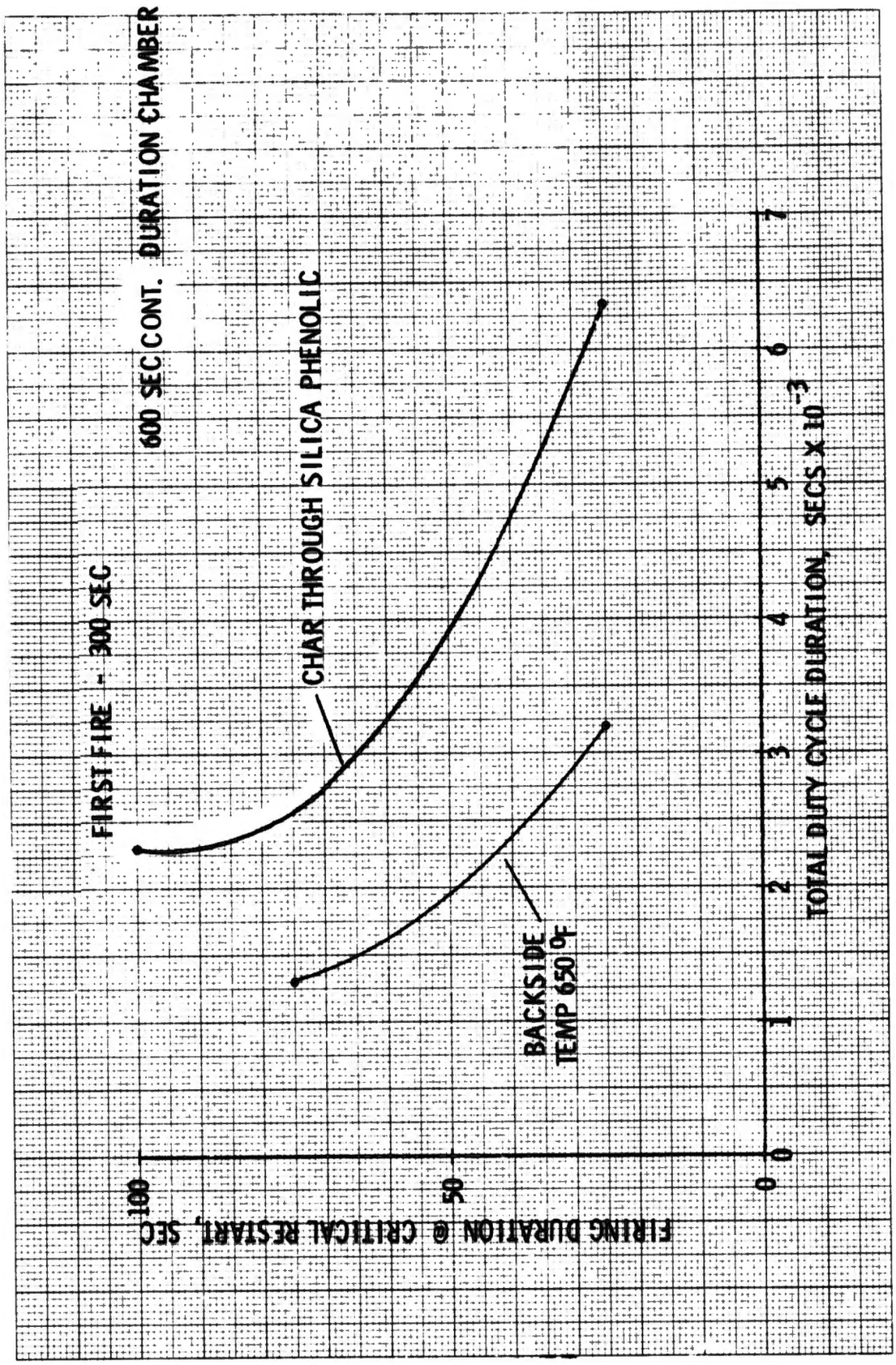

Figure 44. Engine No. IV Mission Analysis, Critical Restart Duty Cycle, Total Allowable Firing Time

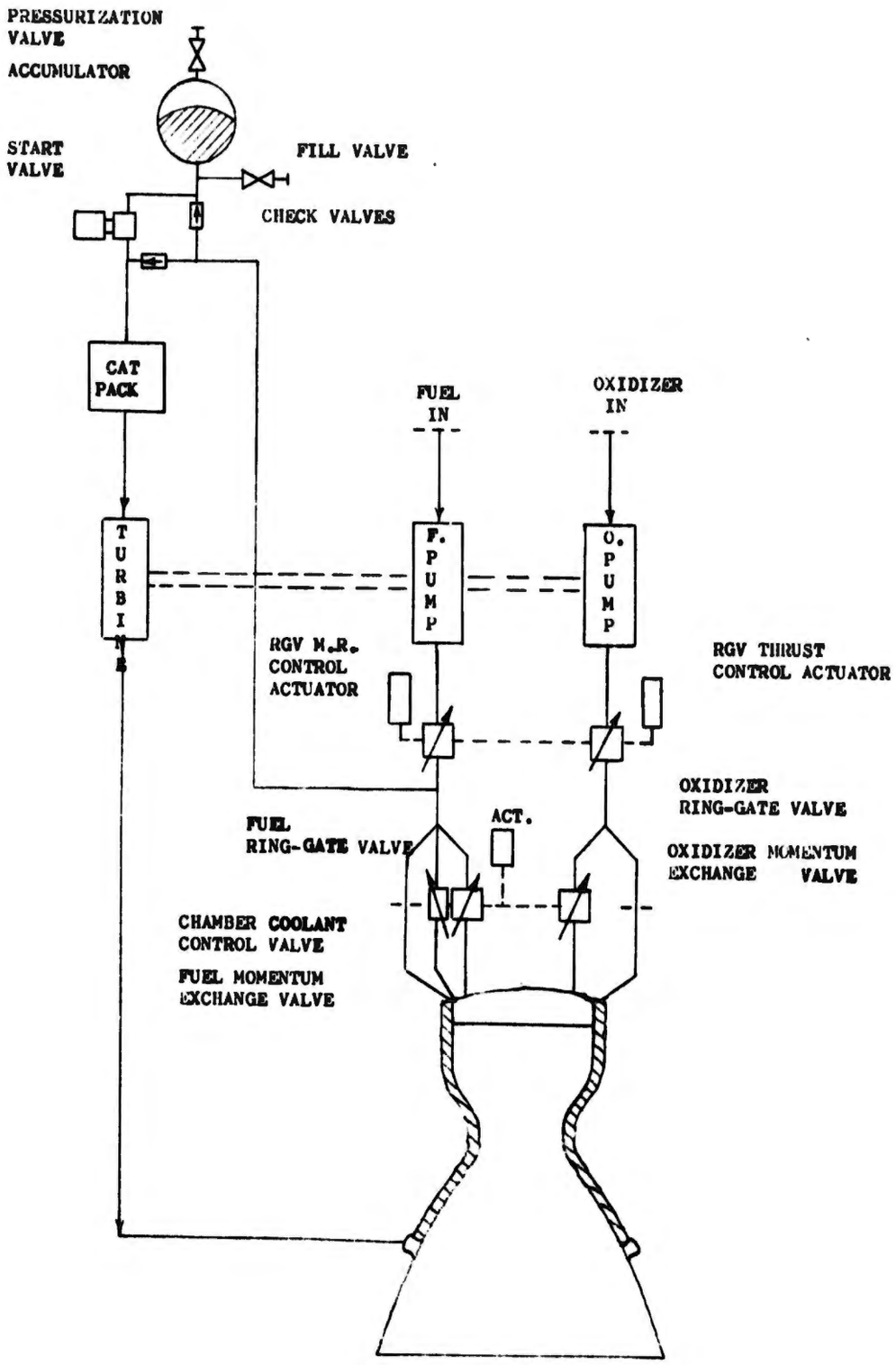

Figure 45. Controls Schematic, Point Design Engine No. IV

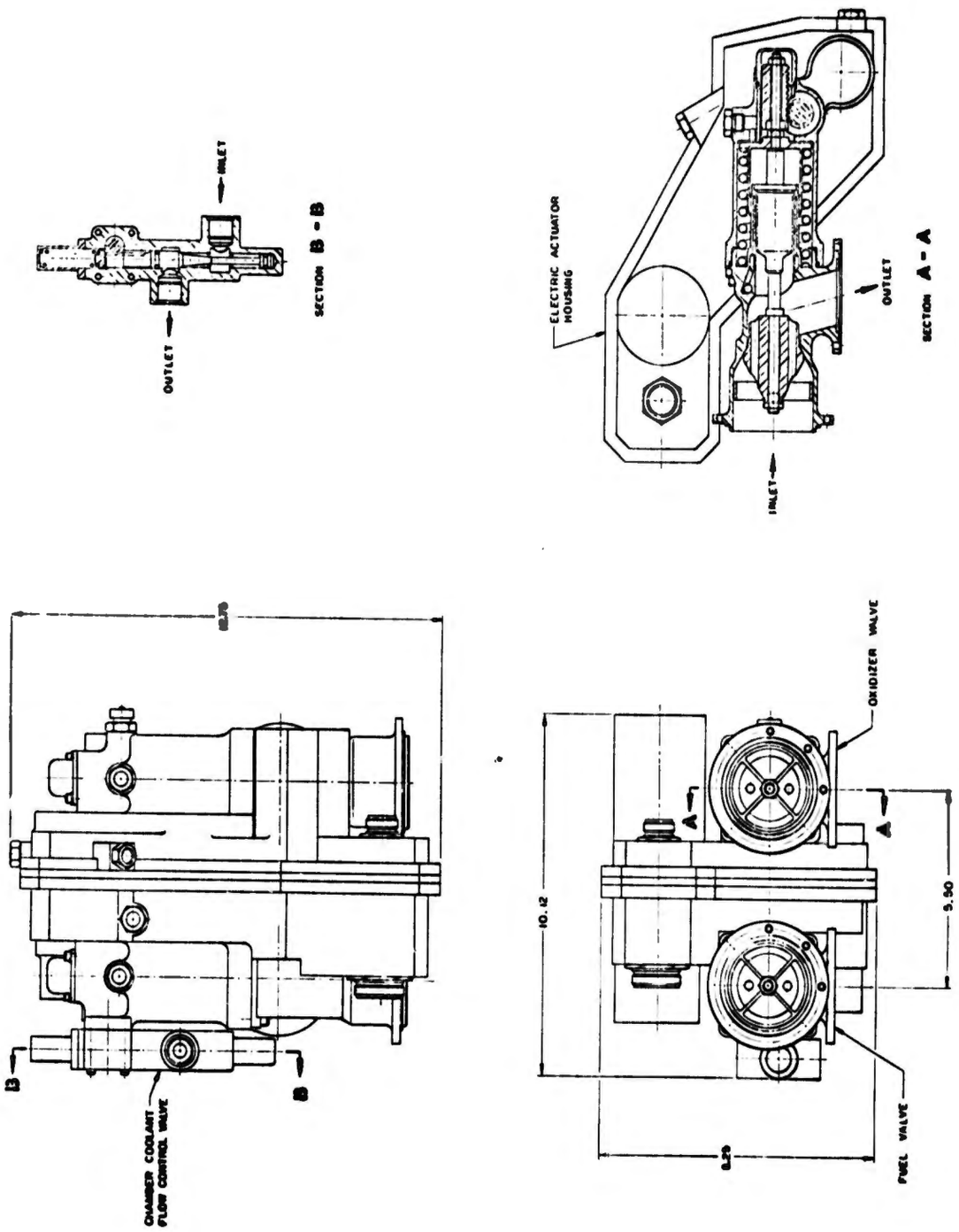

Figure 46. Throttling Valves, Bi-Propellant, Electrically-Actuated

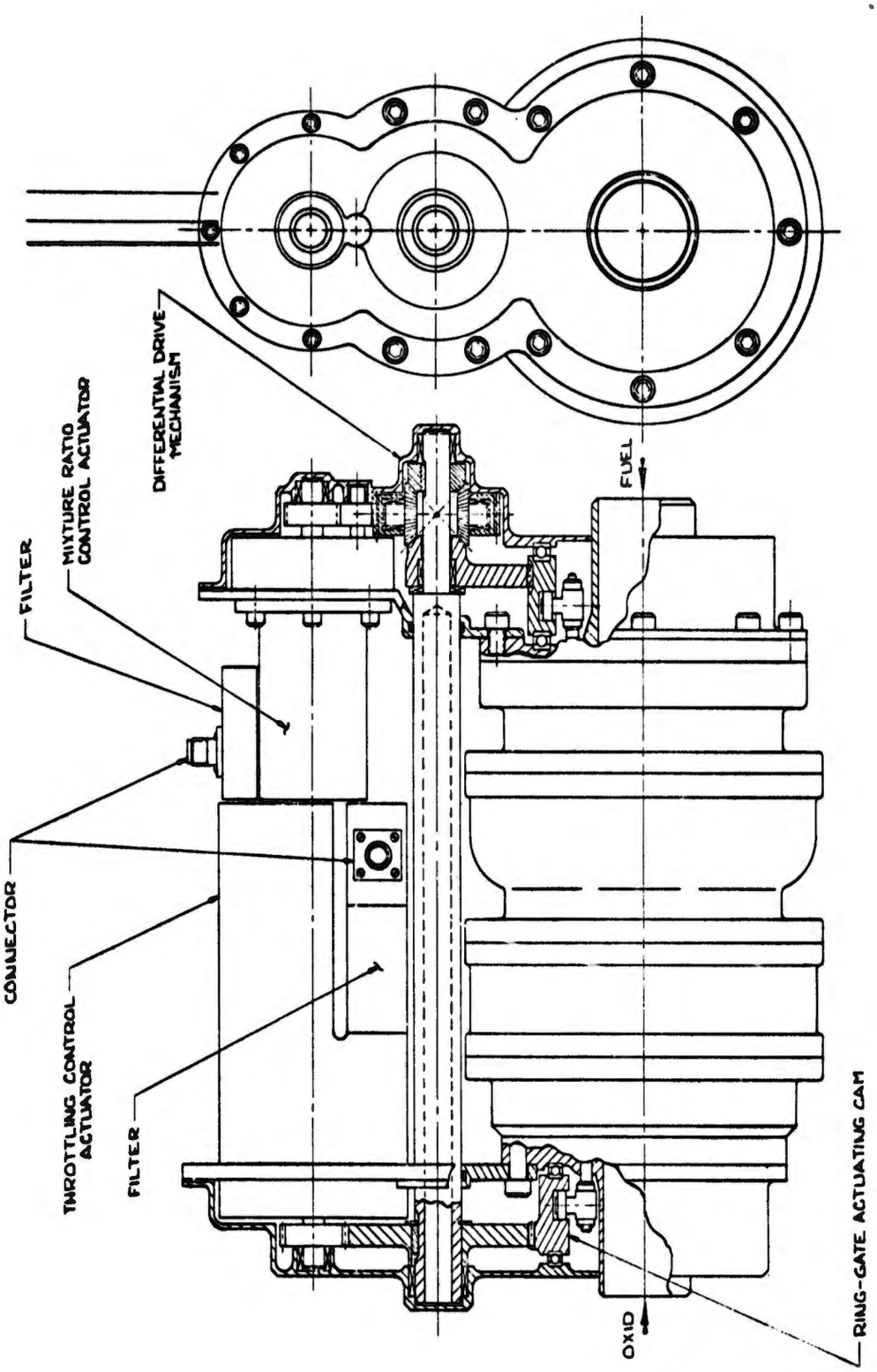

Figure 47. Pump Control, Actuator and Drive Linkage

This engine is capable of an over-all throttling range from 100% to 10% of rated thrust. Throttling control from 100% to 25% is achieved by operating the momentum exchange throttling valves from the wide-open position to the minimum area condition. During this time, the ring-gate valves of the turbopump system are maintained in a full-open (100%) position. At the 25% thrust point, approximately 8% of the propellant flow is channeled through the momentum exchange throttling valves with the remainder of the fuel and oxidizer flow being directed through the momentum exchange pilot flow circuits. A small percentage of the fuel flow is simultaneously controlled by the chamber coolant flow control valve which is mechanically linked to, and driven directly by, the main momentum exchange valves. As the momentum exchange valves are opened from the closed position to the 100% open position to increase thrust from 25% to 100% of rated value, a proportionately greater amount of the propellant flows through the momentum exchange valves than is channeled through the pilot flow circuits. Throttling operation from 25% to 10% of rated thrust is achieved with the momentum exchange valves in the closed (minimum flow) position. The throttling of propellant flow in this range is provided by the ring-gate turbopump valve system. Mixture ratio in the regime of 10% to 25% of rated thrust is provided by independent operation of the fuel ring-gate valve relative to the oxidizer ring-gate valve. Only single-stage pumps were considered to minimize the necessary ring-gate valve controls. A separate mixture ratio control actuator is included in the ring-gate valve actuation system for this purpose. Control of mixture ratio during engine operation in the range of 25% to 100% of rated thrust is achieved by the use of appropriately contoured pintles in the momentum exchange bipropellant valve assembly with a trimming capability provided by independent operation of the fuel ring-gate valve. Control parameters to be used in controlling engine mixture ratio with the combined ring-gate valve and momentum exchange valve system would be selected upon completion of appropriate systems analyses.

The material selected for the bodies of the momentum exchange throttling valves is a suitable stainless steel alloy. Operational assumptions used in determining valve actuator horsepower requirements include valve operating times 0.4 sec for opening and 0.3 sec for closing. These operating times correspond to the design conditions of the Transtage electrically-actuated bipropellant valve. The chamber coolant control valve is driven directly by the actuating shaft of momentum exchange throttling valves.

A rechargeable accumulator start system is included in the engine system as shown on the schematic of Figure No. 45. A 1/4-in. solenoid-operated start valve could be used in conjunction with 1/4-in. check valves. Capacity of the accumulator would be established through engine start transient analyses. Weight of the over-all start system, which is expected to be small relative to total weight of the over-all engine, is not included in the control system weight summary presented in Appendix C (Part II of this report).

(7) Turbopump Configuration

The turbopump for this engine is identical to the one for Point Design Engine No. III differing only in the ring-gate valve control and actuation system.

(8) Performance

(U) The thrust chamber assembly performance was calculated using the procedures detailed in Appendix II for three different fuel film cooling requirements. The results of this analysis for the propellant combination CLF_5/N_2H_4 are shown on Figure No. 48 with specific impulse as a function of thrust chamber assembly mixture ratio. The performance of optimum mixture ratios at various coolant flows for the same propellants is shown on Figure No. 49. Similar information for the CLF_5/MHF-5 propellant combination is provided on Figures No. 50 and No. 51.

(U) The performance losses resulting from film cooling are quite considerable. They can be improved by using other injector concepts, such as the HIPERTHIN injector, which improves both L* and the connected coolant losses as well as ERL.

(9) Engine Capabilities and Limits

(U) The capability of this engine is very similar to that of Point Design Engine No. III except for the burn duration capability and the installation, which is similar to Engine No. II.

(a) Burn Duration Effects

(U) From the analysis conducted it appears obvious that the throttling capability of ablative engines is very limited because of the sensitivity of the chamber of burn duration. Its practical application has to be limited to small impulse throttling and the firing sequence must be watched closely.

(U) For the mission analysis of ablative engines, it is necessary that the engine weight be interated in connection with total burn duration and wall thickness requirement.

(b) Propellant Compatibility

(C) Heat soak-back and injector face cooling problems appear to make the N_2H_4 and 80/20 blend undesirable if prolonged throttling is required. The formation of free carbon with MMH and MHF-5 are of no consequences in the design and operation of bleed turbine engines.

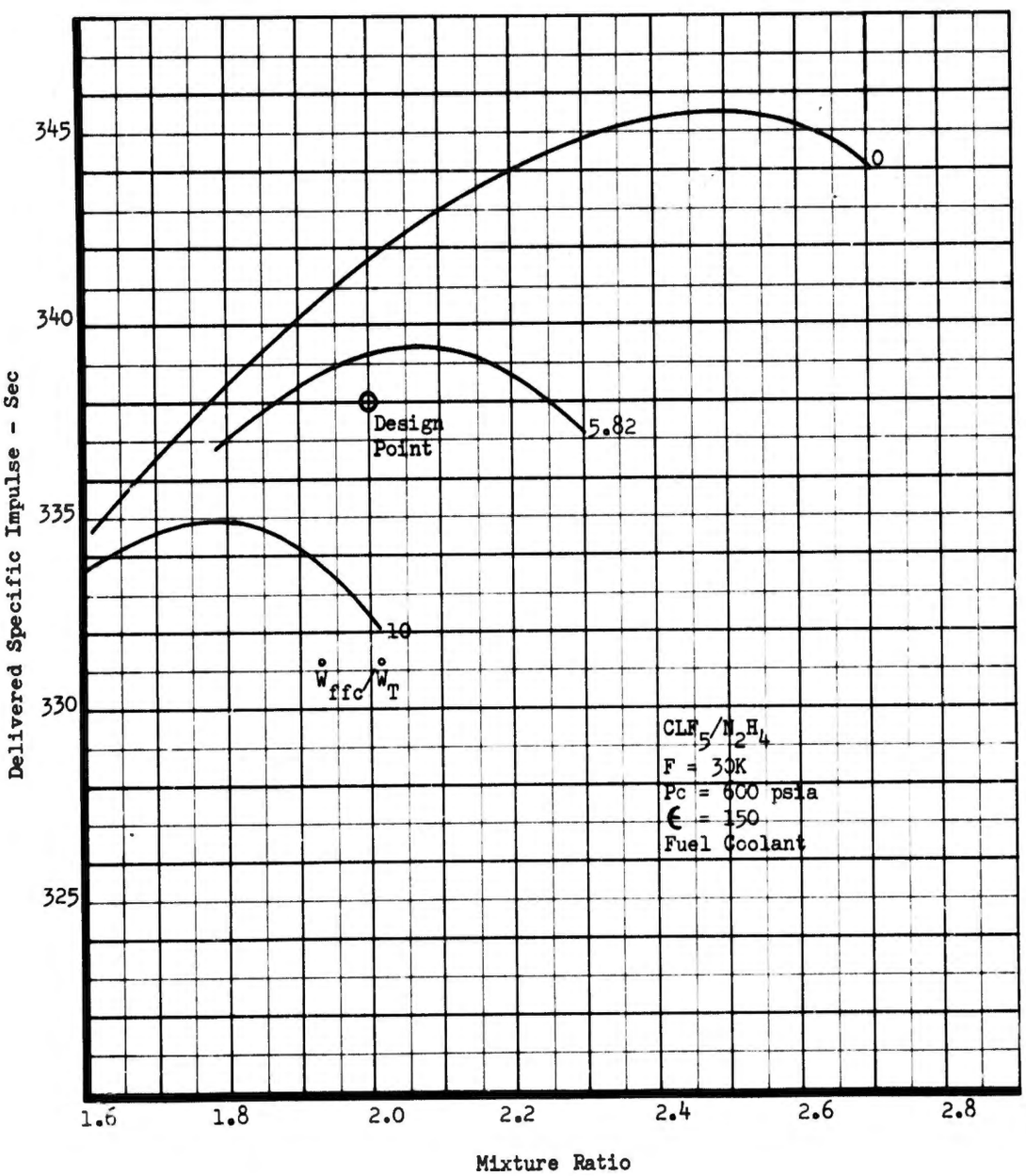

Figure 48. Point Design Engine No. IV, Performance/Mixture Ratio-Coolant Flow Trade-Off (CLF_5/N_2H_4) (u)

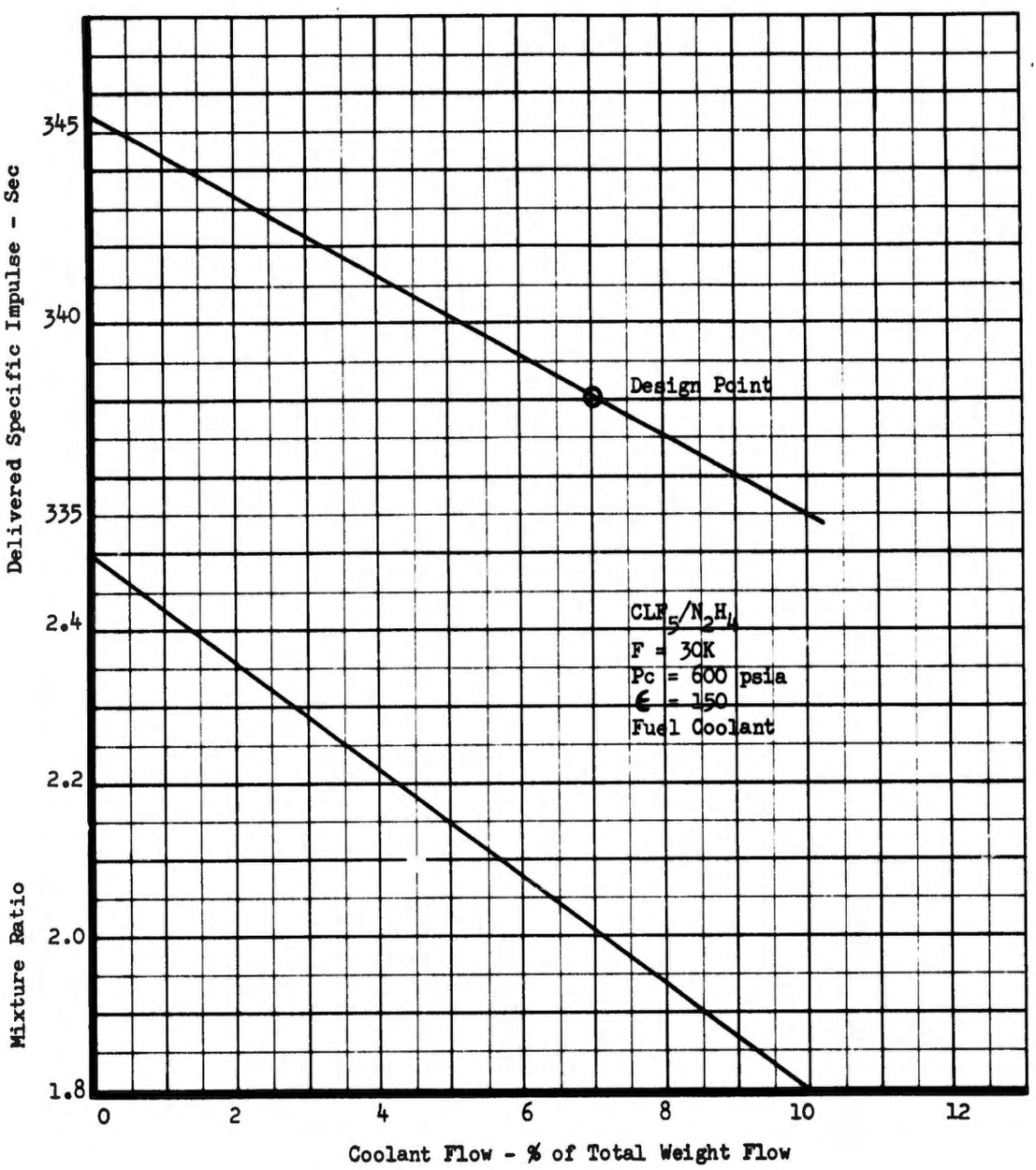

Figure 49. Point Design Engine No. V, Performance/Coolant Flow Interaction (CLF_5/N_2H_4) (u)

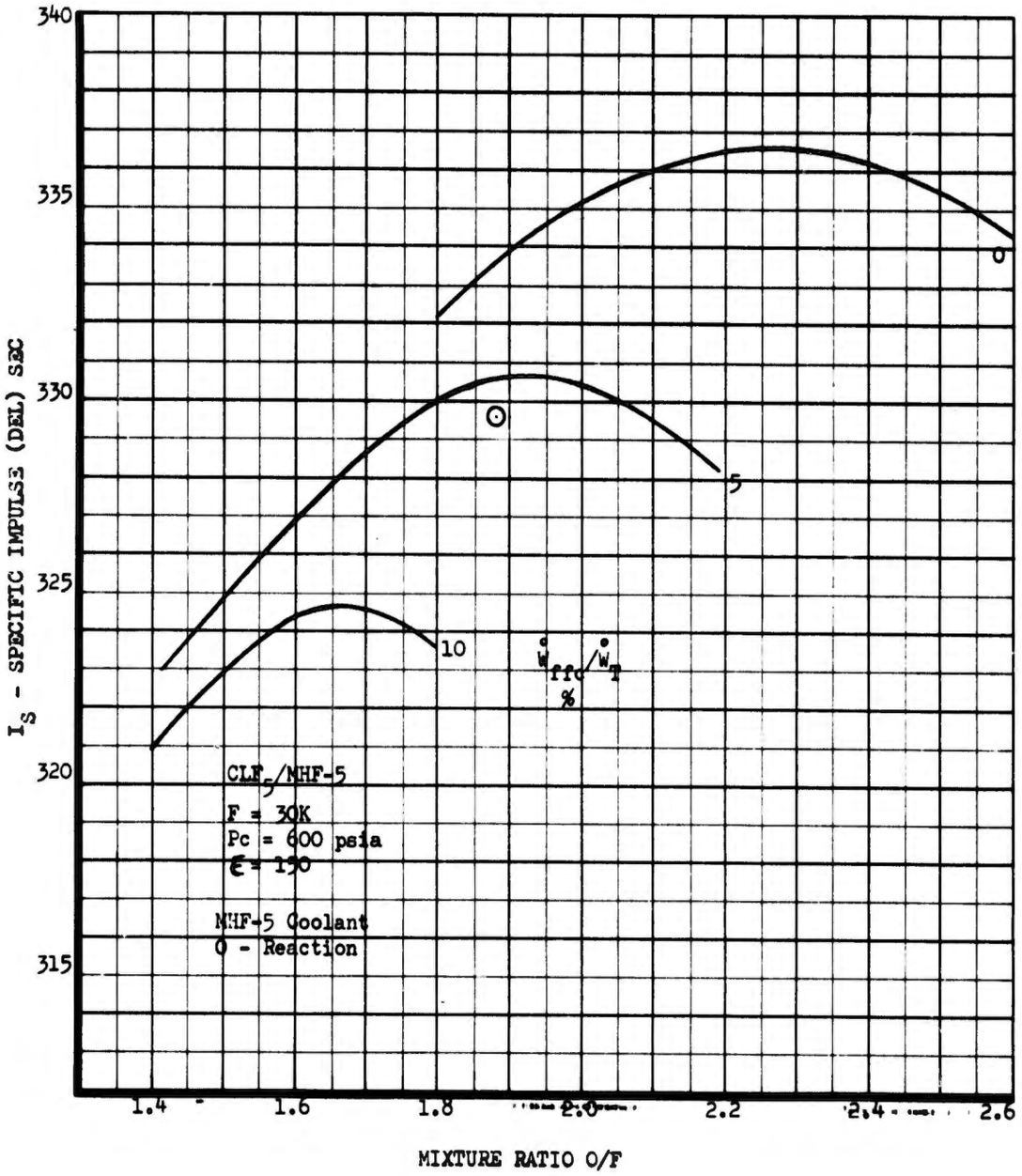

Figure 50. Point Design Engine No. IV, Performance/Mixture Ratio-Coolant Flow Trade-Off (CLF_5/MHF-5) (u)

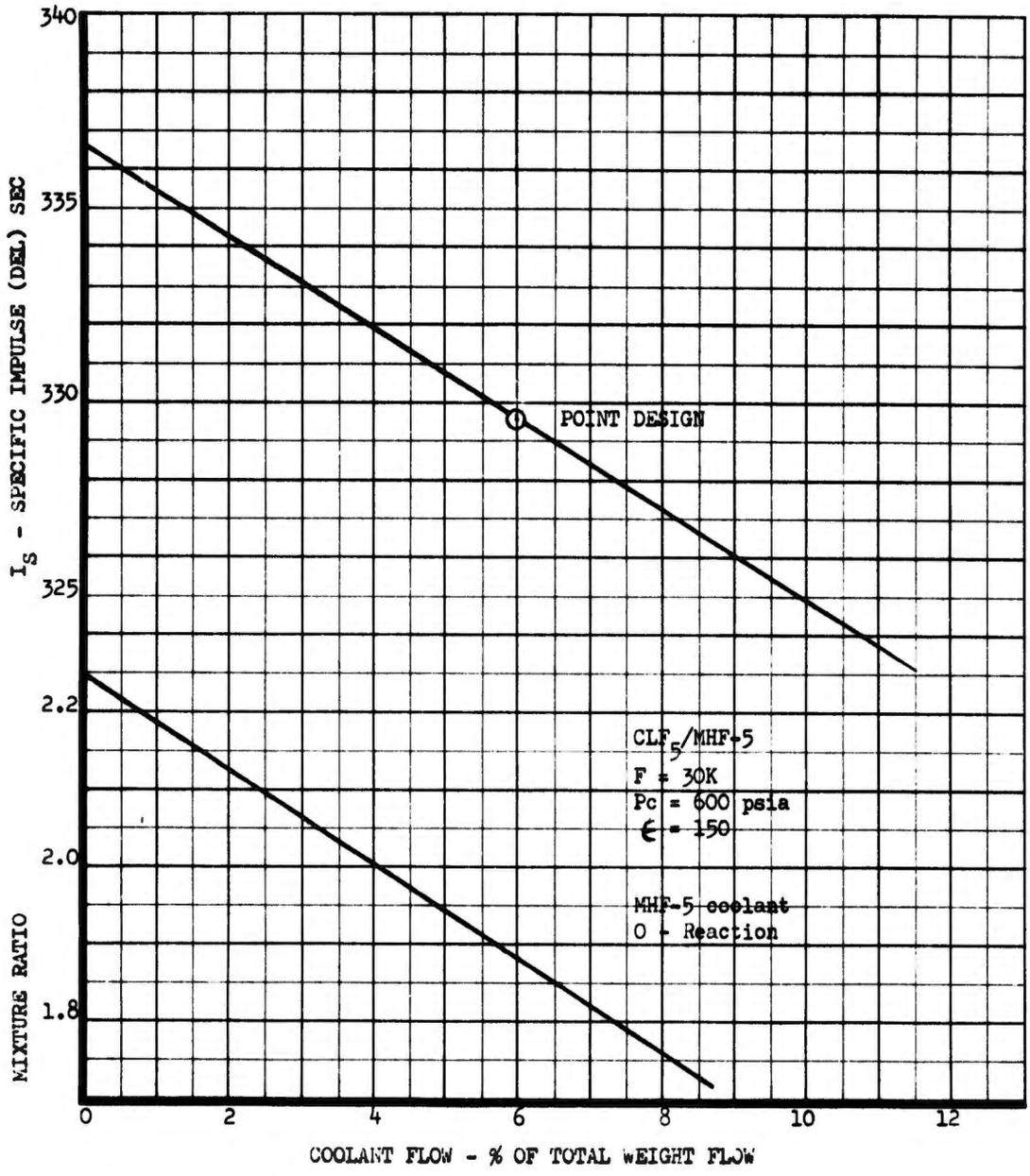

Figure 51. Point Design Engine No. IV, Performance/Coolant Flow Interaction (CLF_5/MHF-5) (u)

B. ACTIVELY-COOLED ENGINES

The actively-cooled engines (i.e., regenerative and transpiration concepts) are evaluated for pump-fed engine systems in the ensuring discussion.

1. Regeneratively Cooled Engines

Only Point Design Engine No. V is representative of those engines using liquid fuel regenerative cooling. It is considered the baseline engine utilizing current technology.

a. Point Design Engine No. V

This is a fixed thrust engine with a conventional liquid/liquid injection system. It has a 25K thrust level, a 500 psia chamber pressure, and a nozzle extension area ratio of 150:1. This results in a maximum engine diameter of 73.8-in. and an over-all engine length of 142.0-in. Point Design Engine No. V assembly is shown on Figure No. 52. Pertinent data is summarized on Table XVIII.

This engine is designed with a bleed cycle identical to that of Point Design Engines No. III and No. IV. The flow schematic and pressure schedule for Engine No. V are shown on Figure No. 53.

(1) Combustion Chamber Design

This chamber has a characteristic length of 30-in. and a contraction ratio of 2. Pertinent chamber design parameters are shown on Table XIX.

Thrust chamber assembly No. 5 is a regeneratively-cooled tube bundle unit. It is a double-pass design, which minimizes coolant manifolding and feed line requirements while doubling the coolant velocity within the tubes. This higher velocity increases the allowable heat transfer coefficient to the coolant from the hot tube inner wall. The only other active cooling system in the thrust chamber assembly is the film cooling benefit received by the columbium nozzle extension from the turbine exhaust bleed injector located at the chamber/nozzle extension interface. Turbine exhaust gases, which are considerably cooler than the thrust chamber assembly exhaust, are bled through the thrust chamber assembly wall into the supersonic nozzle boundary layer as shown on Figure No. 54. The cooling effect derived from this gas film allows the columbium nozzle extension to operate at a lower area ratio than would otherwise be possible.

The design limits for the regeneratively-cooled chamber design are:

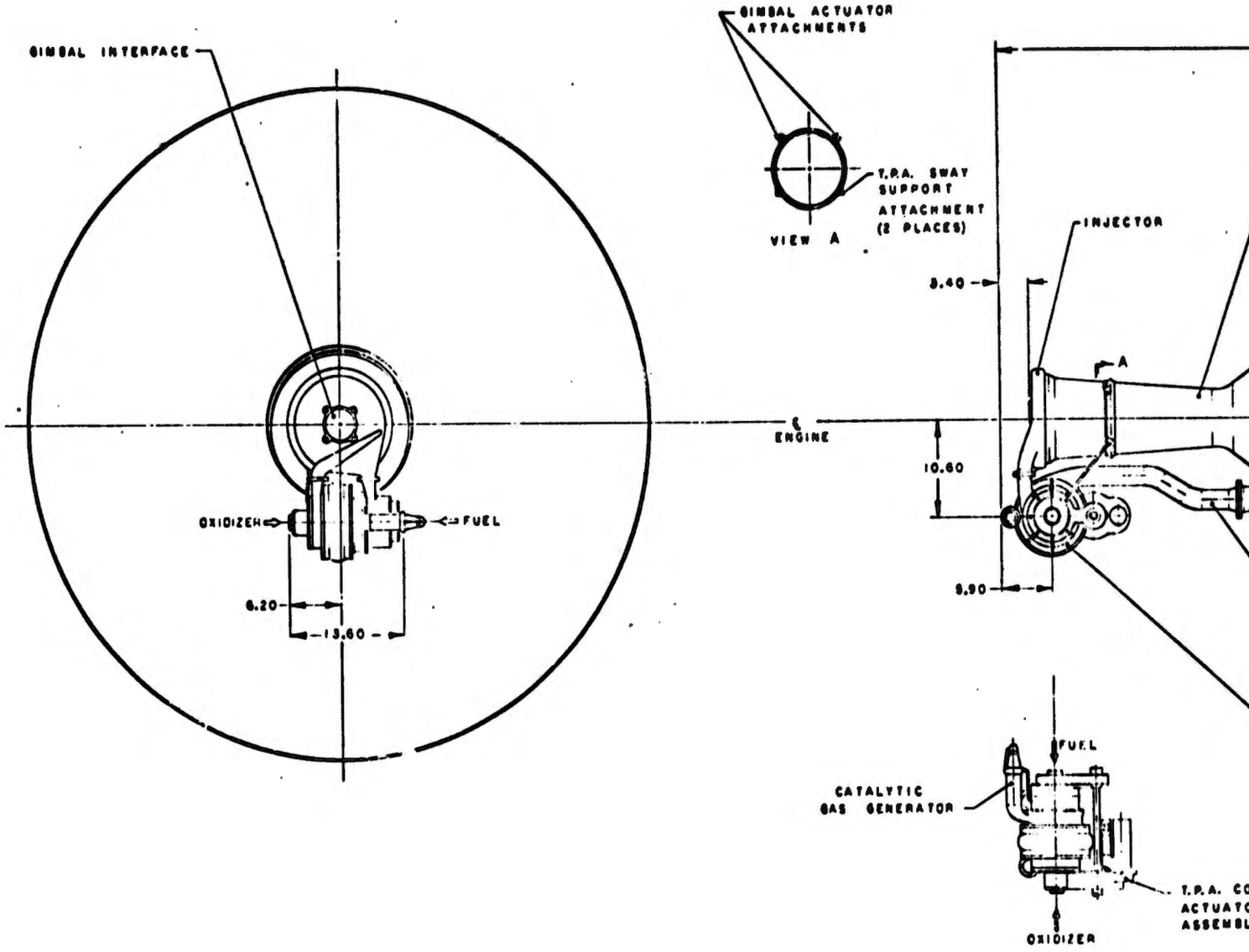
GIMBAL INTERFACE
GIMBAL ACTUATOR ATTACHMENTS
T.P.A. SWAY SUPPORT ATTACHMENT (2 PLACES)
VIEW A
INJECTOR
8.40
A
℄ ENGINE
10.60
9.90
OXIDIZER
FUEL
6.20
13.60
FUEL
CATALYTIC GAS GENERATOR
OXIDIZER

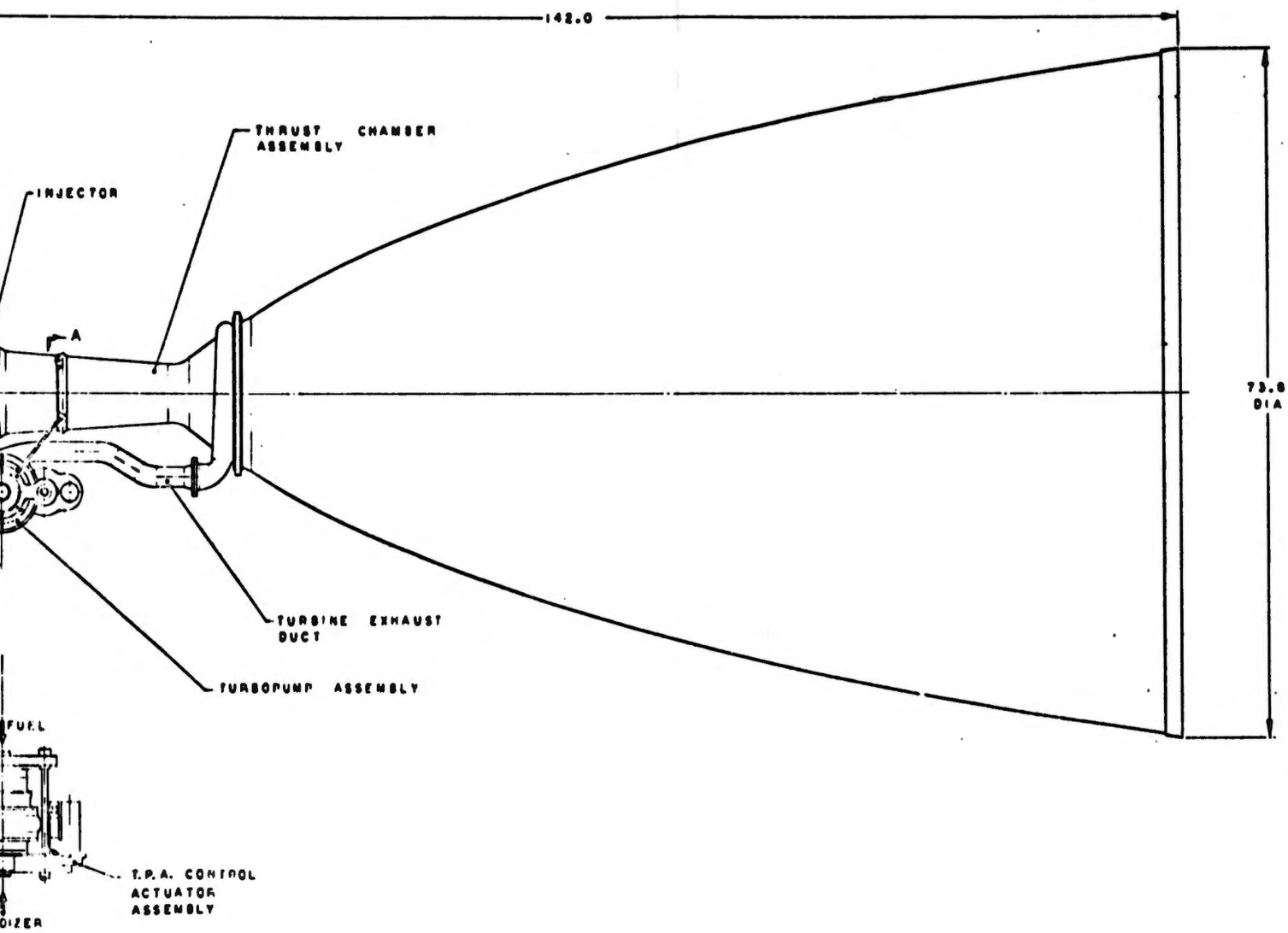

Figure 52. Point Design Engine No. V Assembly

TABLE XVIII

POINT DESIGN ENGINE NO. V (U)

Engine Configuration	Performance	
Pump Fed - Fixed Thrust	Thrust (Vac) lb	25,000
N_2H_4 Cat Pack Bleed Turbine Drive	Chamber Pressure, psia	500
Conventional Injector (L/L)	Mixture Ratio, O/F	2.5
Chamber & Nozzle Regen Cooled (LF)	Specific Impulse (Del) sec	345.1
Rad Cooled Nozzle Extension	% Theoretical I_s (S.E.)	92.5
Single Shaft Turbopump	Nozzle Area Ratio	150
Ring Gate Valve	Suction Pressure, psia	
	Oxidizer	146
	Fuel	45
Turbine Exhaust Gas Dump into T.C. Nozzle	Flow Rate, lb/sec	
	Oxidizer	51.4
	Fuel	21.1
	Film Coolant Flow % of Total Weight Flow	0
	Engine Weight	
	Dry	320 lb
	Wet	326 lb

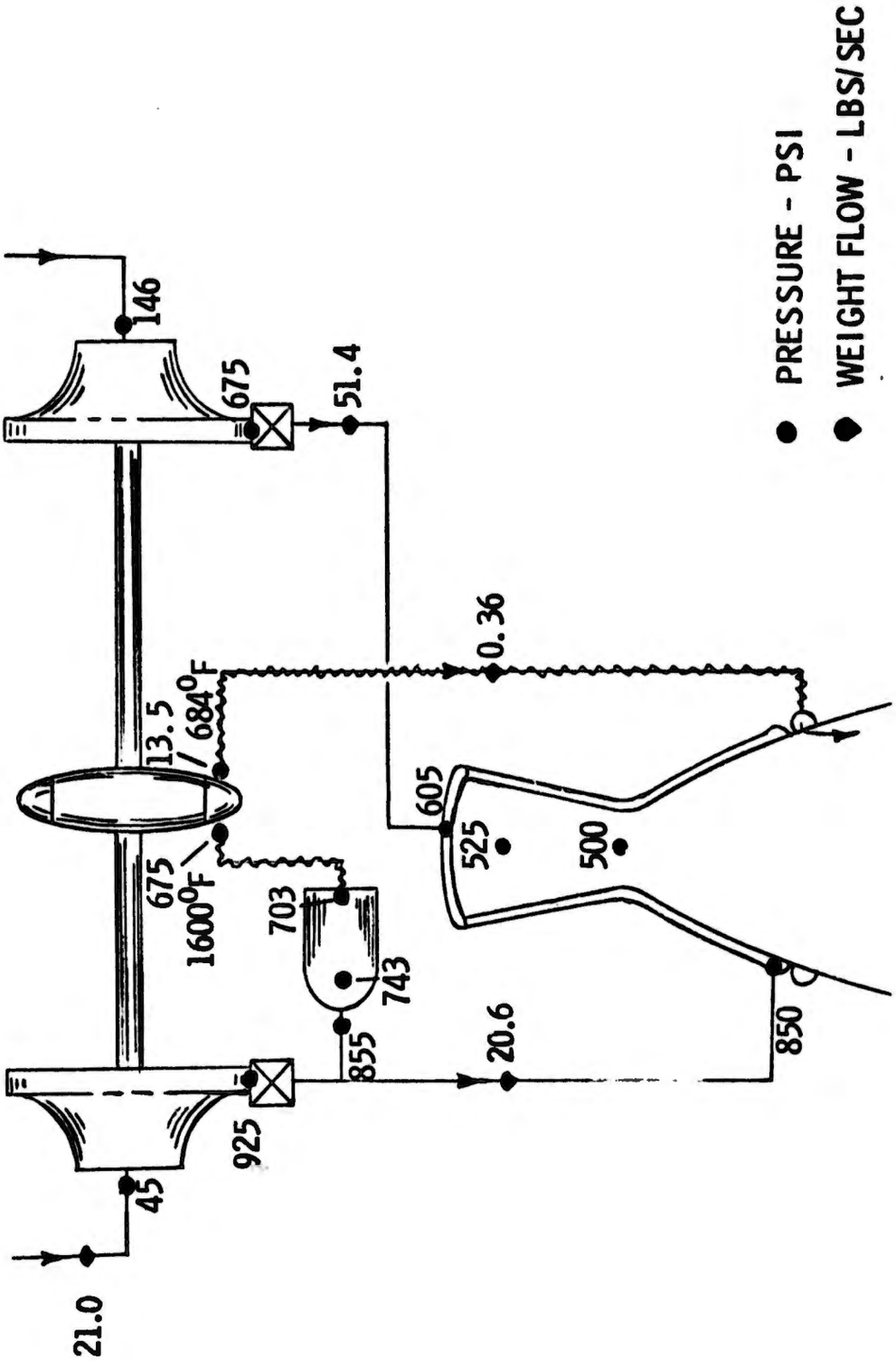

Figure 53. Flow Schematic and Pressure Schedule, Point Design Engine No. V

TABLE XIX

THRUST CHAMBER ASSEMBLY NO. 5 DESIGN PARAMETERS

General	Injector	Chamber	Nozzle Extension
Thrust: 25K lb	Type: Conventional, flat face, cross drilled	Shape: Conical	Attachment Area Ratio: 5.2
Chamber Pressure: 500 psia		Material: Inconel tubes	Cooling Mode: radiation
Nozzle Area Ratio: 150	Propellant Phases: Liquid - Liquid	Contraction Ratio: 2	Material: Coated Columbium
Throttleability: Fixed thrust	Thrust Per Element: 100 lb	Cooling Mode: Regen with fuel film cooling	Exit Diameter: 73.3 in.
	Type Element: F-O-F Inline triplet		
	$\Delta P_{inj}/P_c$ = .20	Characteristic Length: 30 in.	
	Material: NI-200		
Duration: Unlimited	Film Cooling: Zero	Throat Dia: 6.00 in.	

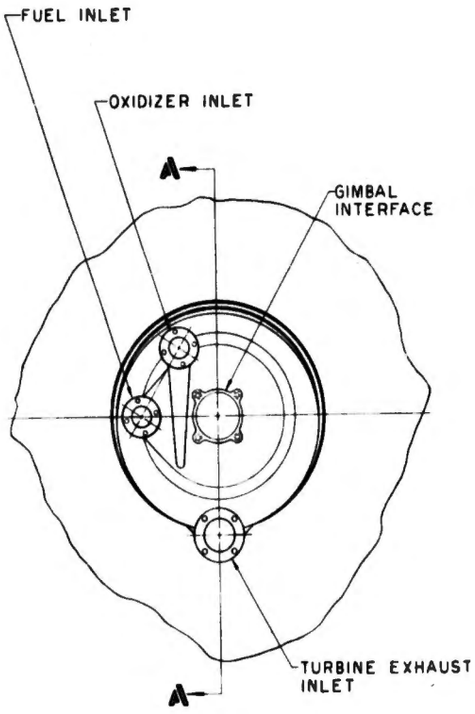
FUEL INLET
OXIDIZER INLET
A
GIMBAL INTERFACE
TURBINE EXHAUST INLET
A

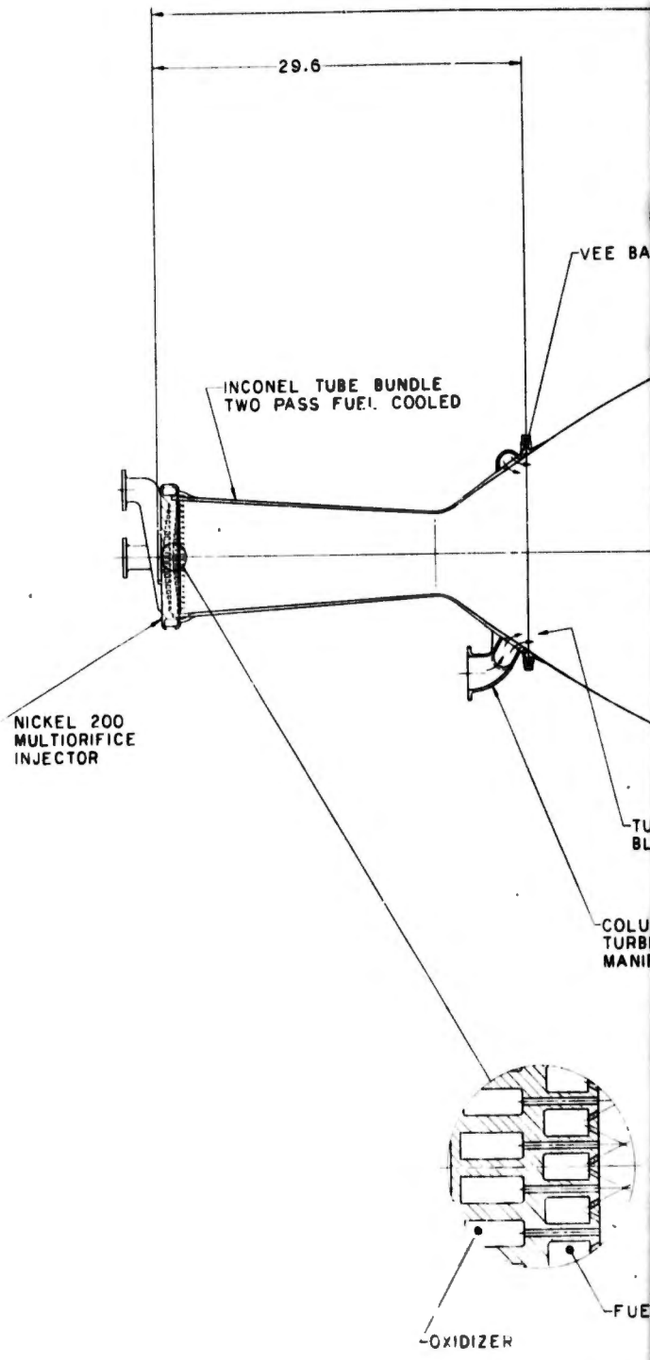
29.6
VEE BA
INCONEL TUBE BUNDLE TWO PASS FUEL COOLED
NICKEL 200 MULTIORIFICE INJECTOR
TU
BL
COLU
TURBI
MANI
FUE
OXIDIZER

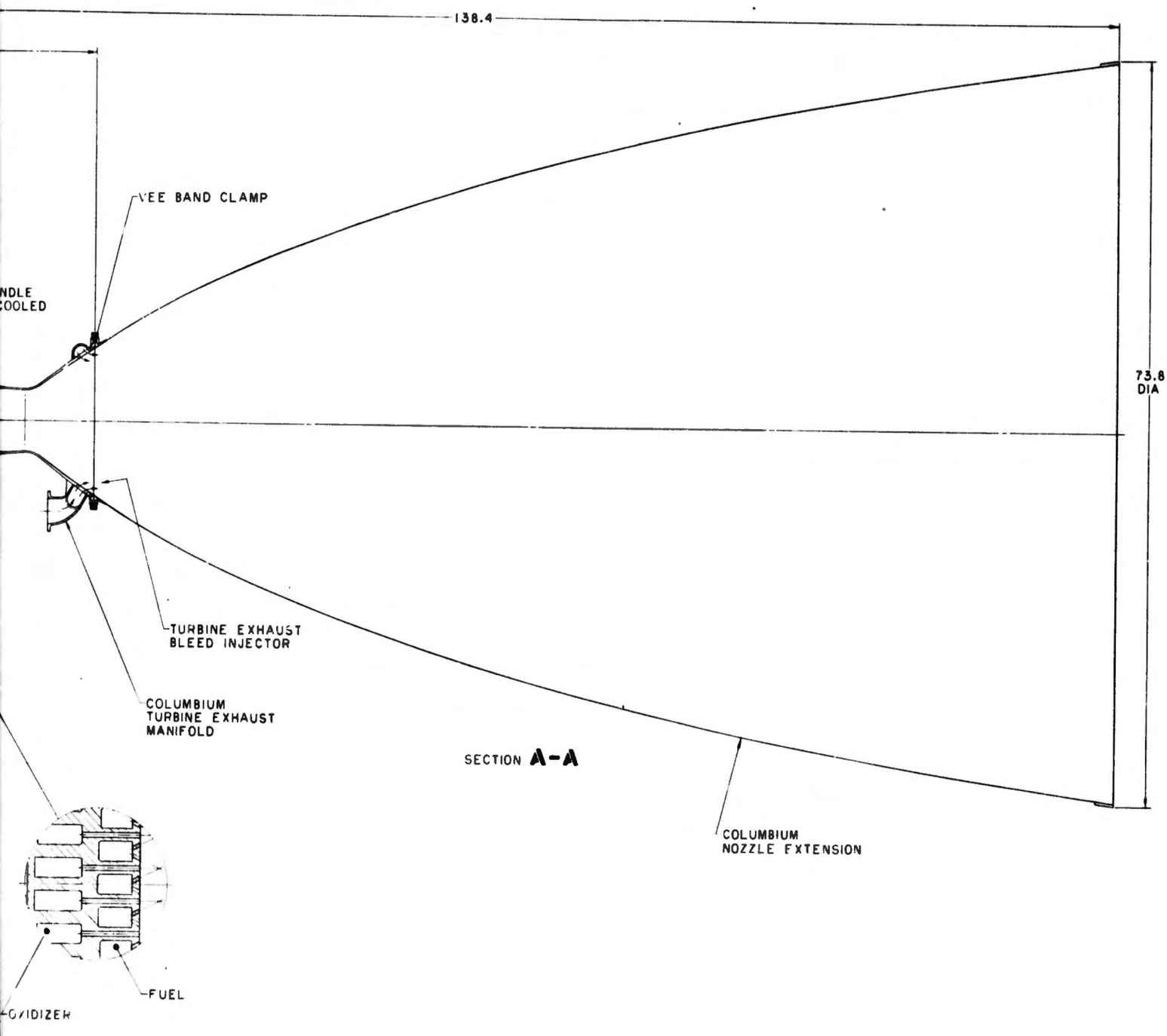

Figure 54. Thrust Chamber Assembly, Engine No. V

Maximum burnout heat flux ratio	0.8
Maximum tube wall temperature	1500°F
Minimum tube O.D.	0.20-in.
Tube wall thickness	0.015-in.

Inconel 625 was selected for the tube wall material. A minimum coolant pressure drop was assumed; therefore, all coolant tubes are round.

A minimum tube outer diameter of 0.120-in. in the throat regions requires 160 coolant tubes. In the course of the design analysis, the several alternative approaches discussed below were established.

Based upon 160 tubes, a bifurcation is required at area ratio 5 to maintain an adequate coolant velocity. At this point, it is possible to attach either a fibrous graphite radiation-cooled skirt or a turbine exhaust film-radiation-cooled skirt. If a bifurcation is made at A/At = 5, it is then possible to cool to A/At = 17, which is the attachment point for a coated columbium radiation-cooled skirt. No additional film cooling is required for full thrust operation.

For the selected design, the maximum cooled area ratio is 5. The following is a summary of the tube bundle design:

Number of coolant tubes	160
Maximum burnout heat flux ratio	0.8
Maximum tube wall temperature	1275°F
Coolant bulk temperature rise	356°F
Coolant tube static pressure drop	331 psi
Maximum heat flux	16 Btu/in.^{2}-sec

Figures No. 55 and No. 56 present the predicted tube wall temperature and heat flux profiles.

An analysis also was conducted to assess the applicability of coatings to the chamber design. Figure No. 57 shows the results of the parameter study, assuming no film cooling for the area ratio 5 chamber. For reference, once again the design limits are a R_{bo} of 0.8, and a maximum tube wall temperature of 1500°F. From the plot, a coating with a thermal

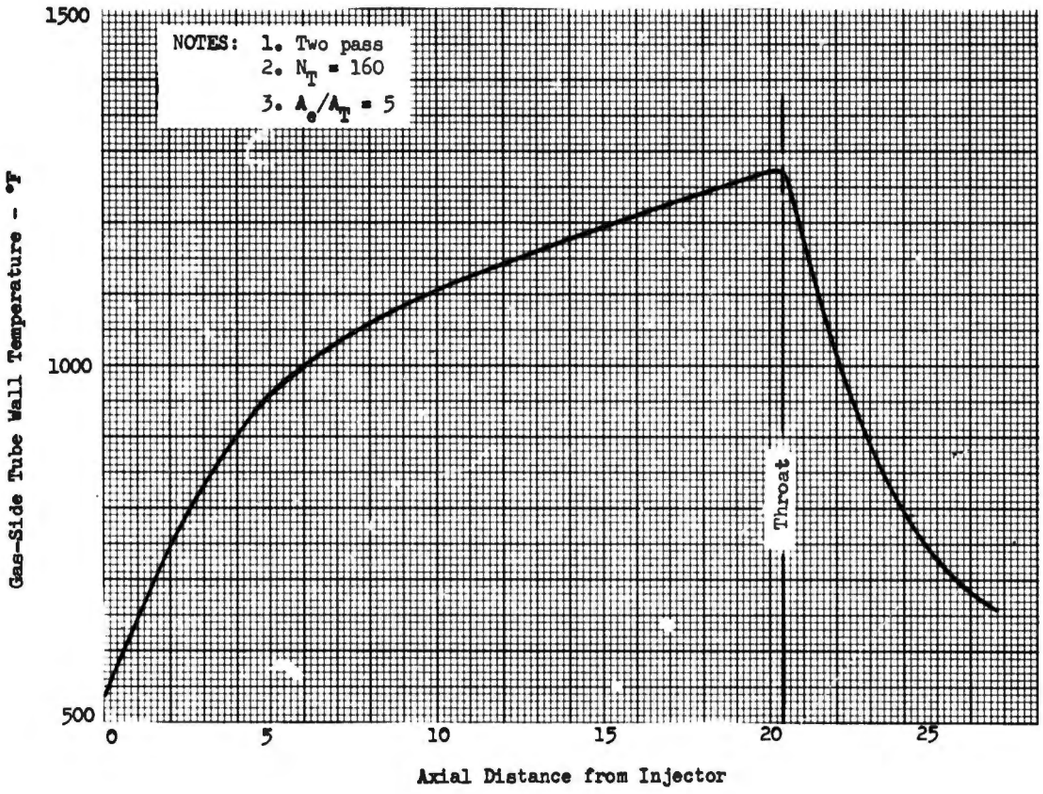

Figure 55. Engine No. V Tube Wall Temperature Profile Return Pass

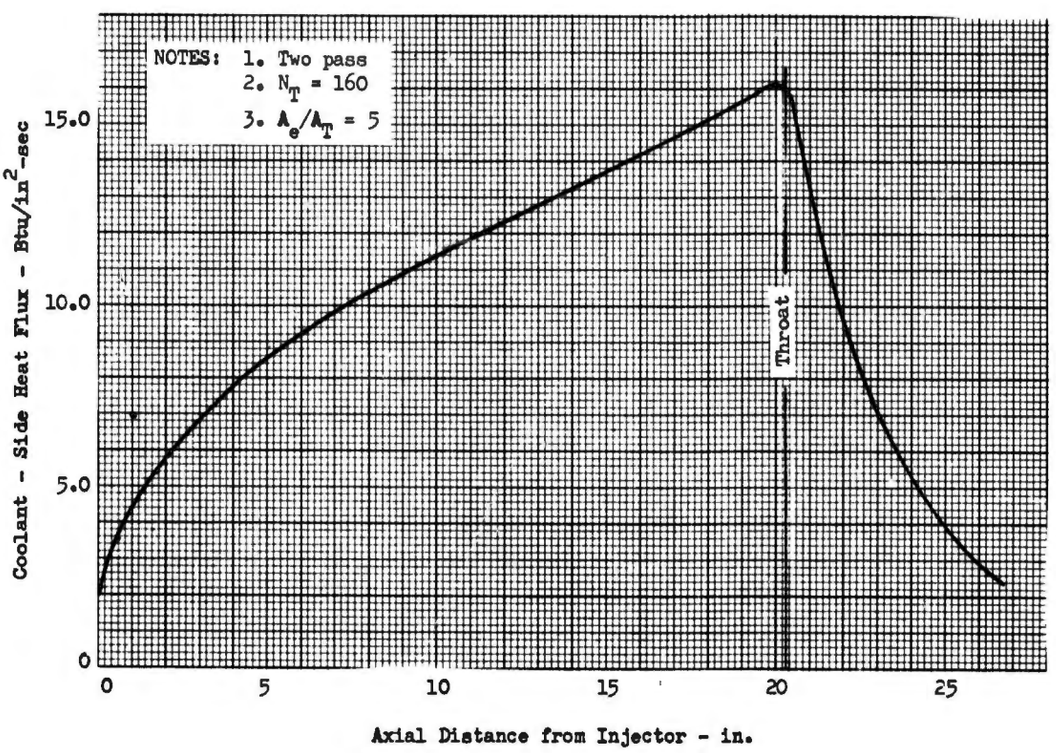

Figure 56. Engine No. V Heat Flux Profile Return Pass

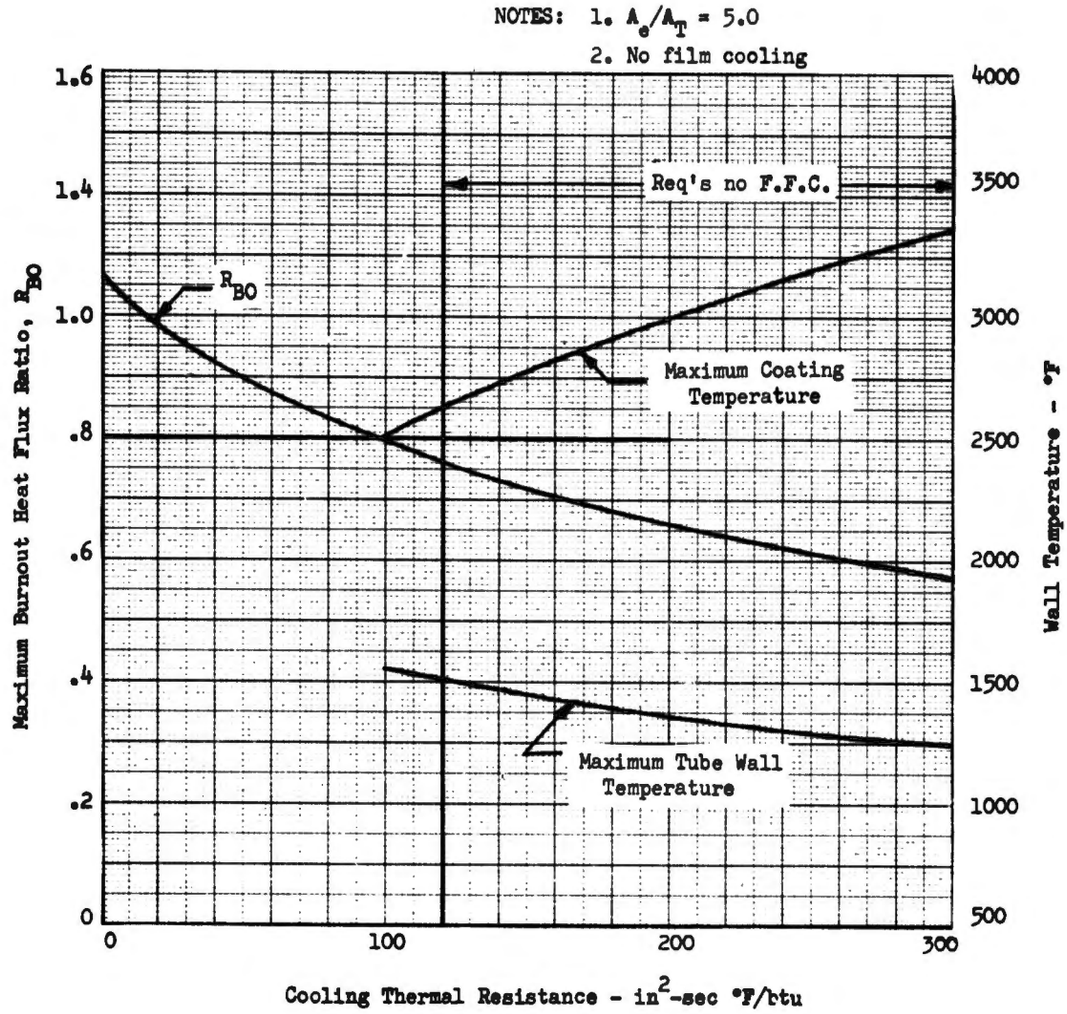

Figure 57. Engine No. V Coating Requirements

resistance of 120 $in.^2$-sec-/Btu is required. The resultant maximum coating temperature of 2600°F is within current technology for tungsten-zirconia thermal barriers.

(2) Materials Selection

The materials selection criteria and materials used in thrust chamber assembly No. 5 are similar to those used for thrust chamber assembly No. 8. Ni-200 was selected for the injector body and inlet manifolds. This material is expected to be compatible with the oxidizer and resists "bellmouthing" of the fuel orifices, a phenomenon wherein fuel orifices are gradually enlarged from the face back to the manifolds. Inconel 625 was selected for the regeneratively-cooled tube bundle chamber because it can withstand simultaneous exposure to the high temperature of the oxidizer as well as the large hoop stresses caused by the high pressure coolant within the tubes. Similarly, Inconel wire will be used as a chamber over-wrap to absorb the hoop stresses arising from the chamber pressure. Ni-Oro braze alloy will be used to seal the tube bundle against hot gas leaks through the wall. An Inconel turbine exhaust manifold attaches similarly to the chamber tubes near the nozzle extension interface. An Inconel coolant turn-around manifold and attachment flange for the columbium nozzle extension also are located at this interface.

(3) Injector Selection

Thrust chamber assembly No. 5 requires a light-weight, high performance, fixed thrust, liquid/liquid injector. This type of unit has a history of many years of development in the rocket engine industry, although not with these specific propellants.

The most recent development in "conventional" injectors is the "cross-drilled" design. Propellant distribution is accomplished for one propellant by using holes, which run the width (or one-half the width) of the injector. These holes, or manifolds, can be placed quite close to the injector face as well as close together to provide good face cooling. Usually, it is fuel that is passed through the cross-drilled holes because oxidizer is inferior as a coolant. The back side of the injector can be flooded selectively, if desired, with the other propellant, which is usually the oxidizer. This type of injector blank is monolithic and offers minimal leakage potential. It is usually lightweight and inexpensive to build. Any one of a great variety of injector patterns can be drilled into an injector body of this configuration. Also, development costs are minimal because unneeded orifices can be welded closed and others drilled, if desired.

Figure No. 54 shows such an injector with an F-O-F inline triplet injector pattern. The fuel passages have been electrically-discharged machined which permits the use of rectangular flow channels. These channels provide more even injector face cooling than do round holes. In addition, greater fuel flow area can be provided for a given channel width.

The oxidizer manifolds can be similarly formed; however, they are more commonly milled from the back side with cover(s) welded over them. The resulting injector is lightweight, leak-free, and very rigid. Cooled baffles can be welded to the injector face with only a few of the elements needing to be eliminated.

(4) Structural Design of Thrust Chamber Assembly

All thrust and gimbaling loads are carried to the gimbal block through the stiff injector body. The chamber tubes are brazed to the surrounding fuel manifold. Wire-wrap is used over the chamber tubes to contain the hoop loads caused by the chamber pressure developed during operation. A coolant turn-around is brazed to the tubes at the aft end of the chamber. It contains an integral attachment flange for the nozzle extension. The columbium extension attachment philosophy is based upon the "plastic hinge" concept. The turbine exhaust manifold will be brazed to the external walls of the chamber tubes.

(5) Controls System Description

The pump-fed engine configuration of Engine No. V is a fixed thrust design requiring an "on-off" thrust chamber propellant flow control identical to that for Engine No. III. This valve will be electrically-operated in accordance with the criteria established at the outset of the study. A poppet-type valve design utilizing an all-metal shutoff seal configuration will be used. The oxidizer and fuel valves will be mechanically-linked for reliable phasing during engine start and shutdown transient operation. The all-metal, electrically-actuated, bipropellant valve recently designed for the Transtage application has been selected as the basic design to be used in this engine.

Operating power requirements for the electrically-operated bipropellant thrust chamber valve over the range of thrust values and valve inlet pressures which are being considered for the pump fed engines are presented on Figure No. 58. These operating power requirements represent the average power necessary to open the bipropellant thrust chamber valves. Power levels for valve closing are significantly less because of pressure differential forces across the poppets in the closing direction. A valve opening time of 0.4 sec was assumed in calculating the data shown on Figure No. 58.

(6) Turbopump Configuration

The turbopump design concept is very similar to the one for Point Design Engine No. III and is detailed in Appendix VI (Part II of this report).

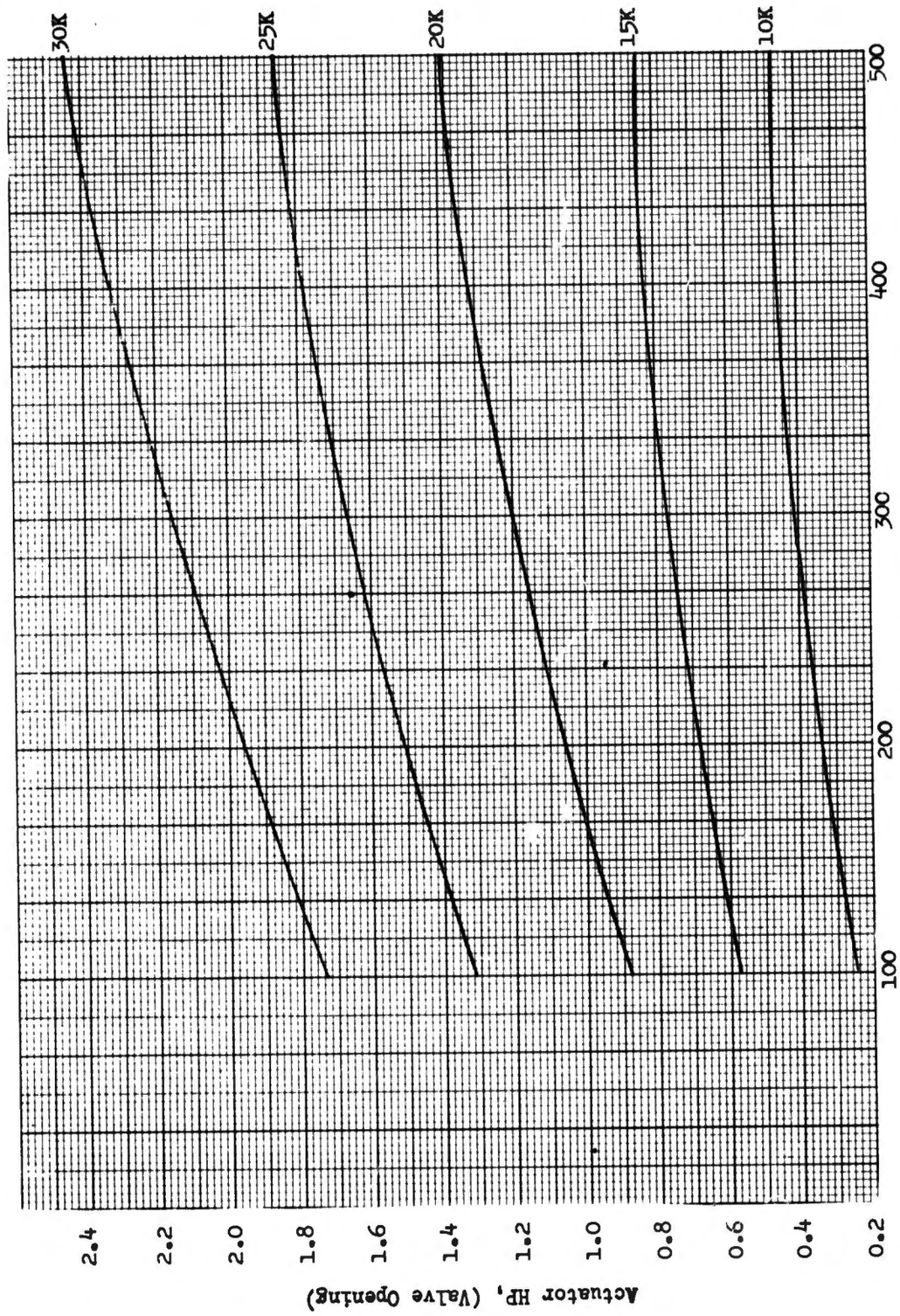

Figure 58. Electric Actuator Power vs Valve Inlet Pressure, Bi-Propellant Thrust Chamber Valve Assembly

(7) Engine Performance

(U) The thrust chamber assembly delivered vacuum specific impulse for Point Design Engine No. V is shown on Figure No. 59 for various percentages of fuel film cooling and as a function of optimum engine mixture ratio using the propellants CLF_5/N_2H_4. The performance for the optimum mixture ratio at various percentages of fuel film cooling using the same propellant combination is shown on Figure No. 60. Similar information for the propellant combination CLF_5/MHF-5 is presented on Figures No. 61 and No. 62. This latter combustion requires large amounts of film cooling (10%); therefore, it is not practical for use as a point design engine.

(U) Fuel film cooling is used to lower the burnout heat flux limit for certain thrust and chamber pressure combinations and will be subsequently discussed under Technology Limits. However, the gains in feasible range increases are very small for the large fuel film coolant flows required (i.e., the resultant performance loss). Therefore, regenerative chambers are competitive only where no fuel film coolant is required.

(8) Engine Capabilities and Limits

(U) This engine is severely limited in its over-all capability by the inherent limitations of the regeneratively-cooled chamber. This is particularly applicable as regards throttling capability and restarting.

(U) There is considerable experience in using hydrazine as a coolant in a regenerative system. Programs, such as HYFUS by the Bell Aerosystems Company and NOMAD by Rocketdyne, have successfully demonstrated that hydrazine, or a hydrazine blend, can be used in a regenerative system if the bulk temperature of the coolant is kept within acceptable limits. These methods include film cooling and/or refractory coating to the coolant tubes. Film cooling has some serious disadvantages, such as loss in performance, and is difficult to apply where it will be the most beneficial.

(C) Basically, this engine is designed as a fixed thrust engine although limited throttling is feasible. Limitations are the injector stability requirements, the burnout heat flux limit of the tube bundle, and the coolant bulk temperature rise. The regeneratively cooled systems are very sensitive as to which of the specified fuels is used. Only MHF-5 and N_2H_4 have burnout limits sufficiently low to be considered for practical regenerative coolant in the thrusts and chamber pressure levels considered. N_2H_4 has a very high pressure rise rate during its decomposition, which makes it a very dangerous fuel for regenerative cooling and precautions have to be taken to avoid flow stagnation. Wherever severe restart flexibility is required, the use of N_2H_4 as coolant should be avoided because of the danger of detonation in the tube bundle and injector as a result of heat soak-back. Restart and shutdown procedures must be defined to avoid detonation in the cooling tubes (see Section V,A,3,d). Therefore, only MHF-5 is considered as a practical fuel which meets all mission requirements except off-course deep throttling.

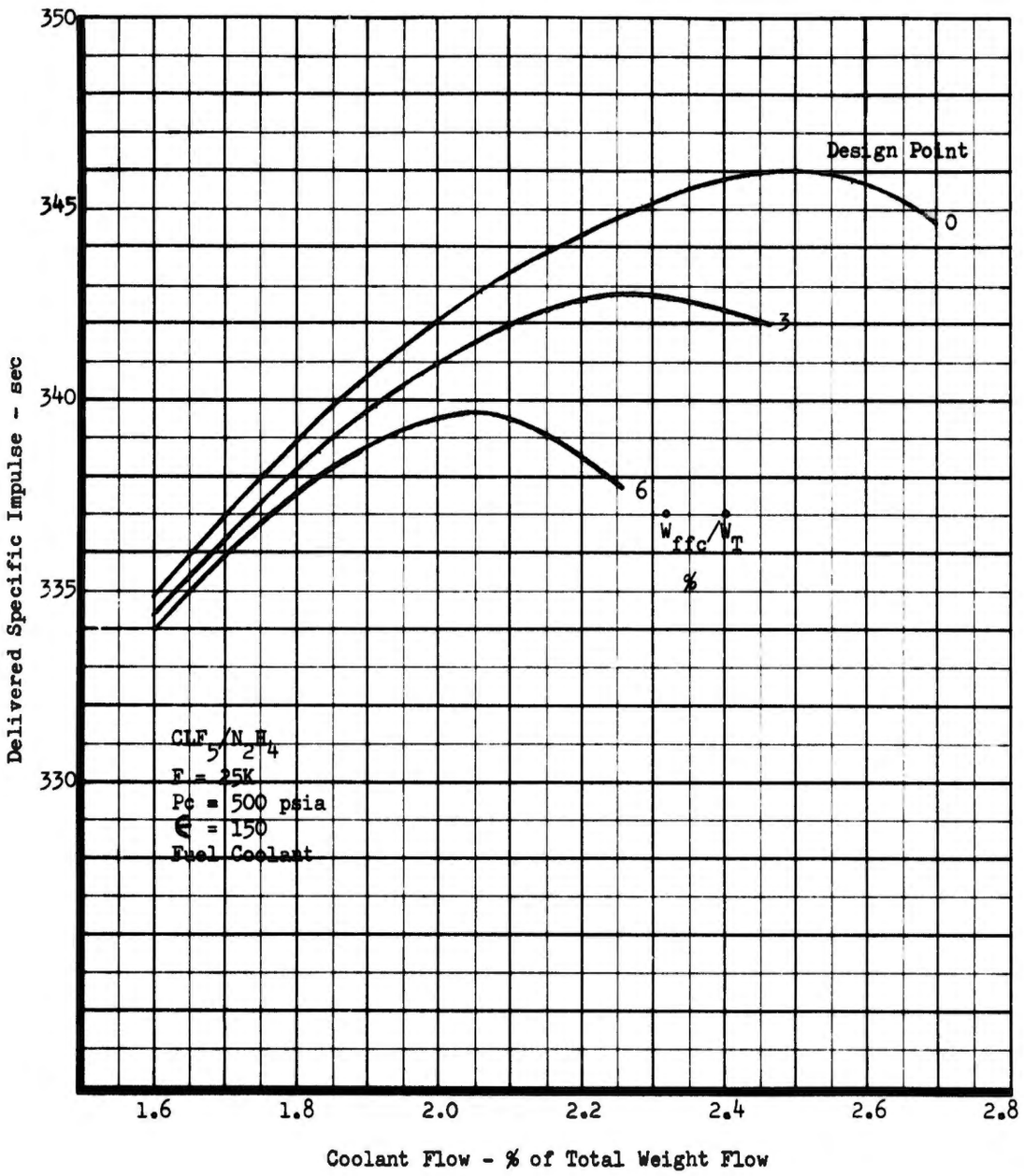

Figure 59. Point Design Engine No. V, Performance/Mixture Ratio-Coolant Flow Trade-Off (CLF_5/N_2H_4) (u)

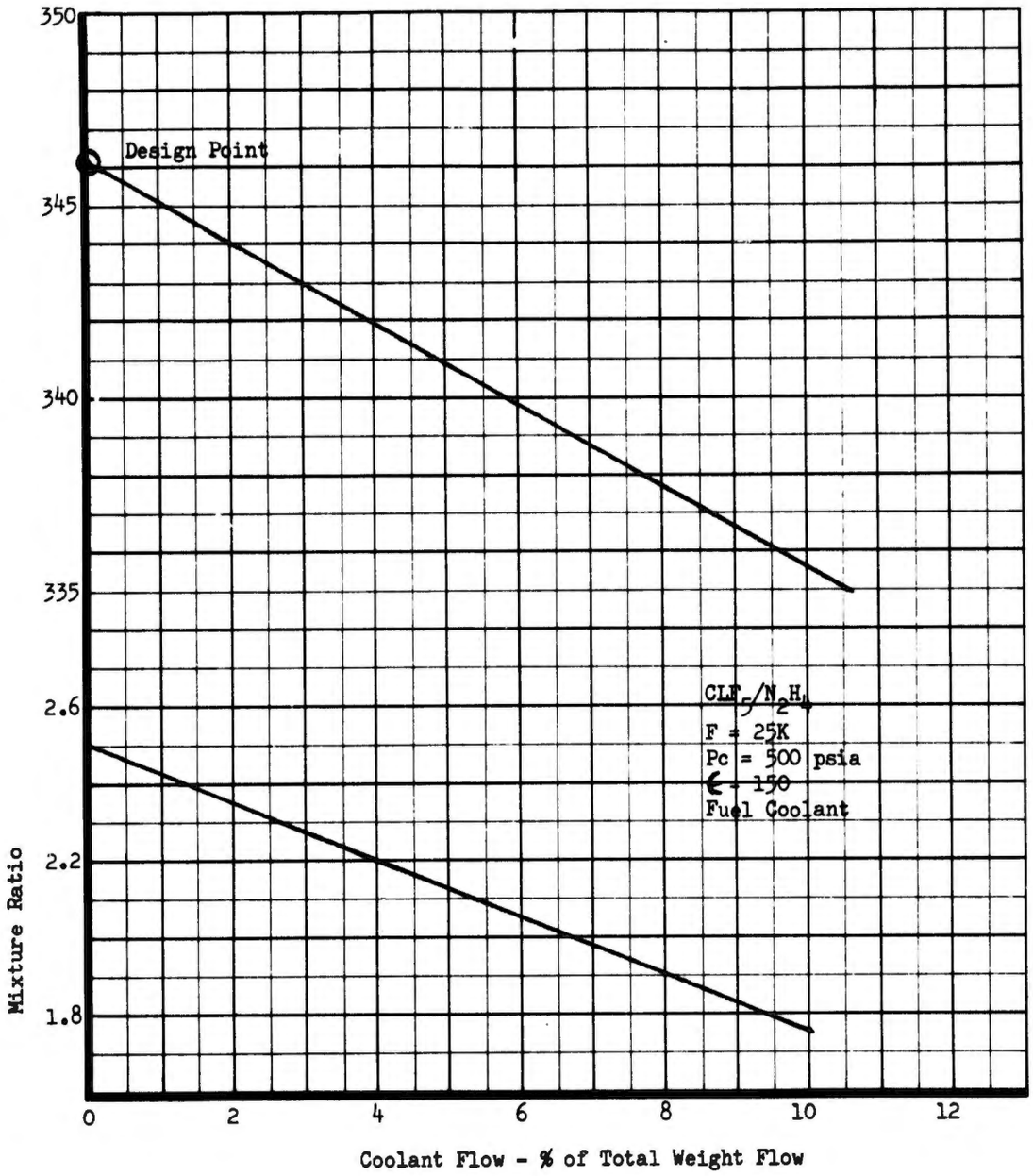

Figure 60. Point Design Engine No. V, Performance/Coolant Flow Interaction (CLF_5/N_2H_4) (u)

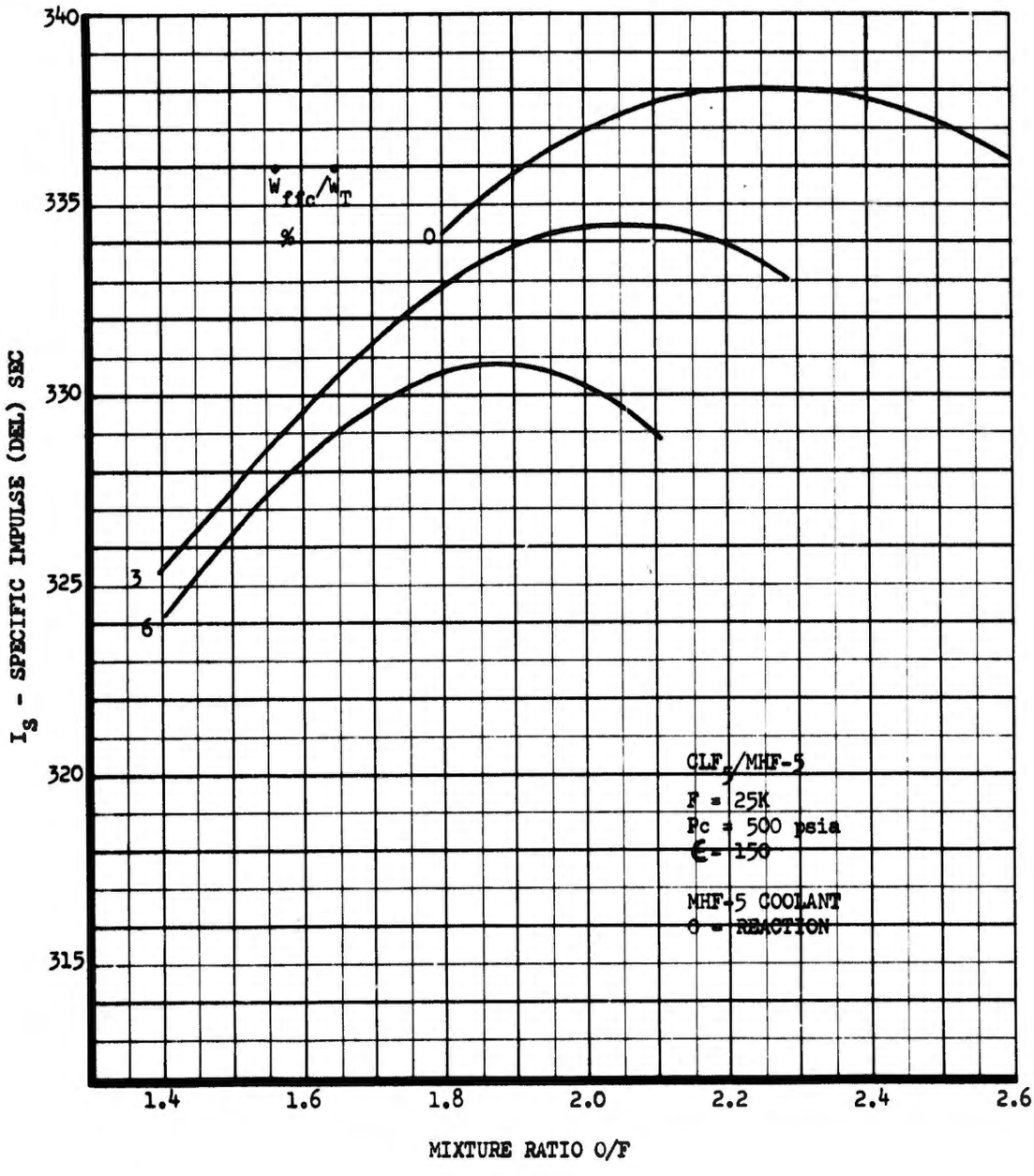

Figure 61. Point Design Engine No. V, Performance/Mixture Ratio-Coolant Flow Trade-Off (CLF_5/MHF-5) (u)

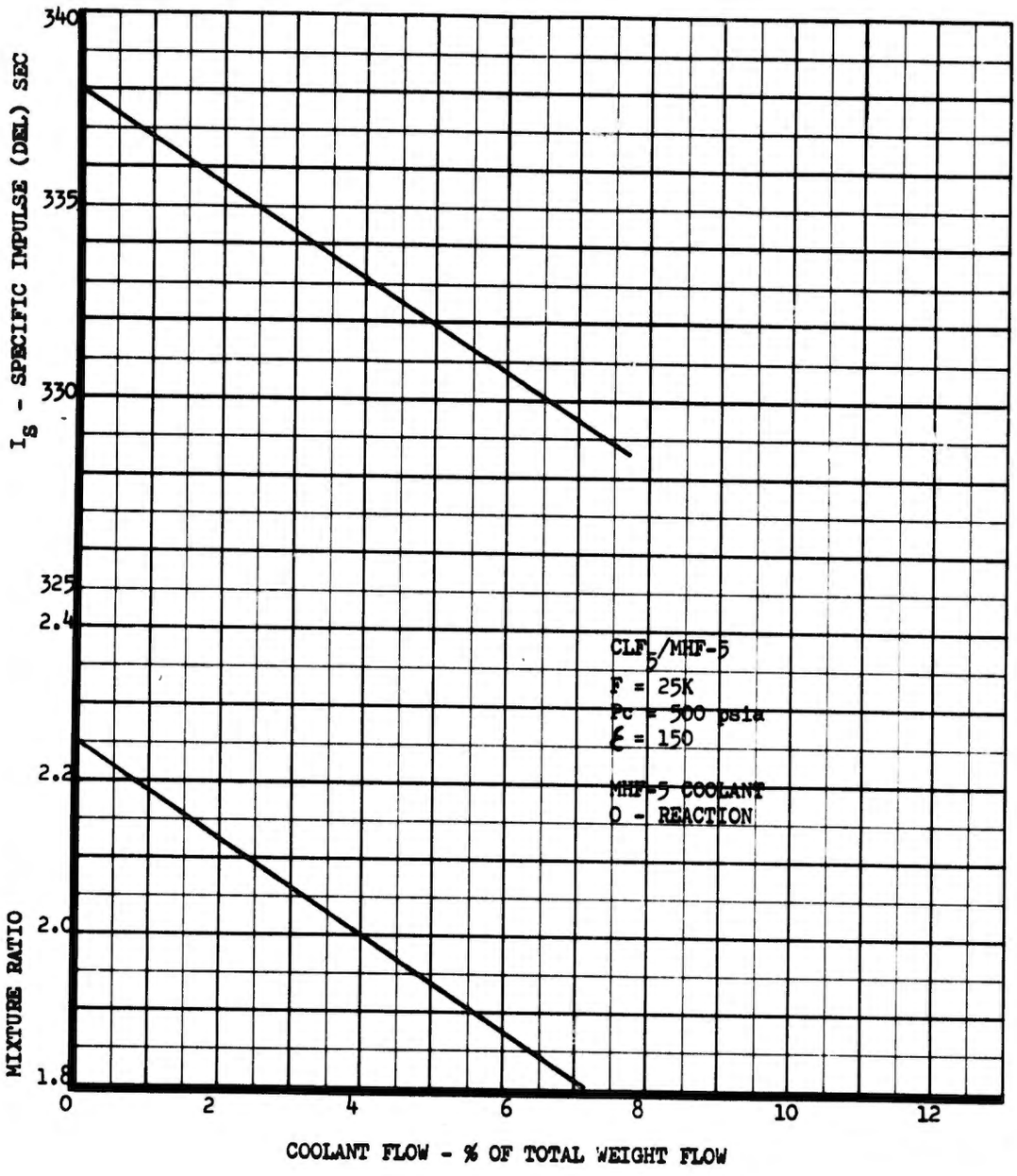

Figure 62. Point Design Engine No. V, Performance/Coolant Flow Interaction (CLF_5/MHF-5) (u)

More advanced injector concepts could reduce the L* requirement as compared to the conventional injector used. They would result in lower bulk temperature rise, which is desirable for reliability reasons in the rengenerative cooling systems using monopropellants.

2. Transpiration-Cooled Engines

In contrast to regenerative cooling, transpiration cooling has deep throttling capability. However, this new capability has a liability in the transpiration cooling losses, the magnitude of which depends upon the coolant selected. Transpiration cooling has no thrust or chamber pressure limit; therefore, it is feasible to design these concepts at much higher chamber pressures than the regeneratively-cooled chambers and the inherent coolant losses can be neutralized by smaller kinetic and ERL losses.

Coolant losses are minimized by using injector concepts with short characteristic lengths, which are obtained by means of the staged-combustion cycle. In this cycle, one or both of the propellants are injected in the gaseous state.

a. Point Design Engine No. VII

The Point Design Engine No. VII, which is shown on Figure No. 63, was designed for a thrust level of 40K and a chamber pressure of 1500 psia with an expansion area ratio of 150:1. This resulted in a maximum engine diameter of 53-in. and an over-all engine length of 102-in. Pertinent engine data is summarized on Table XX.

This engine, which is similar to the ARES design concept, is modified for deep throttling capability. The original engine cycle is shown on Figure No. 64. It consists of a thrust chamber assembly with gaseous oxidizer and liquid fuel injection. The thrust chamber was transpiration-cooled at the throat, followed by a liquid oxidizer regneratively-cooled nozzle extension and an attached columbium radiation-cooled skirt.

Heat transfer analysis revealed that the throttling requirement cannot be satisfied with the regenerative oxidizer-cooled nozzle extension and it was replaced by a fibrous graphite radiation-cooled section as shown in the modified engine schematic, Figure No. 65.

In the modified engine, the liquid oxidizer is split after pump discharge; a small amount is used for the transpiration throat cooling and the rest is injected into an oxidizer-rich, bipropellant gas generator, which supplies the drive gases for the turbine and is fed into the thrust chamber assembly through the main injector. The fuel is injected in the liquid state in both the gas generator and the main combustion chamber. In Figure No. 65, throttling is achieved by ring-gate valves, but this type of a cycle provides the opportunity for using the bipropellant gas generator

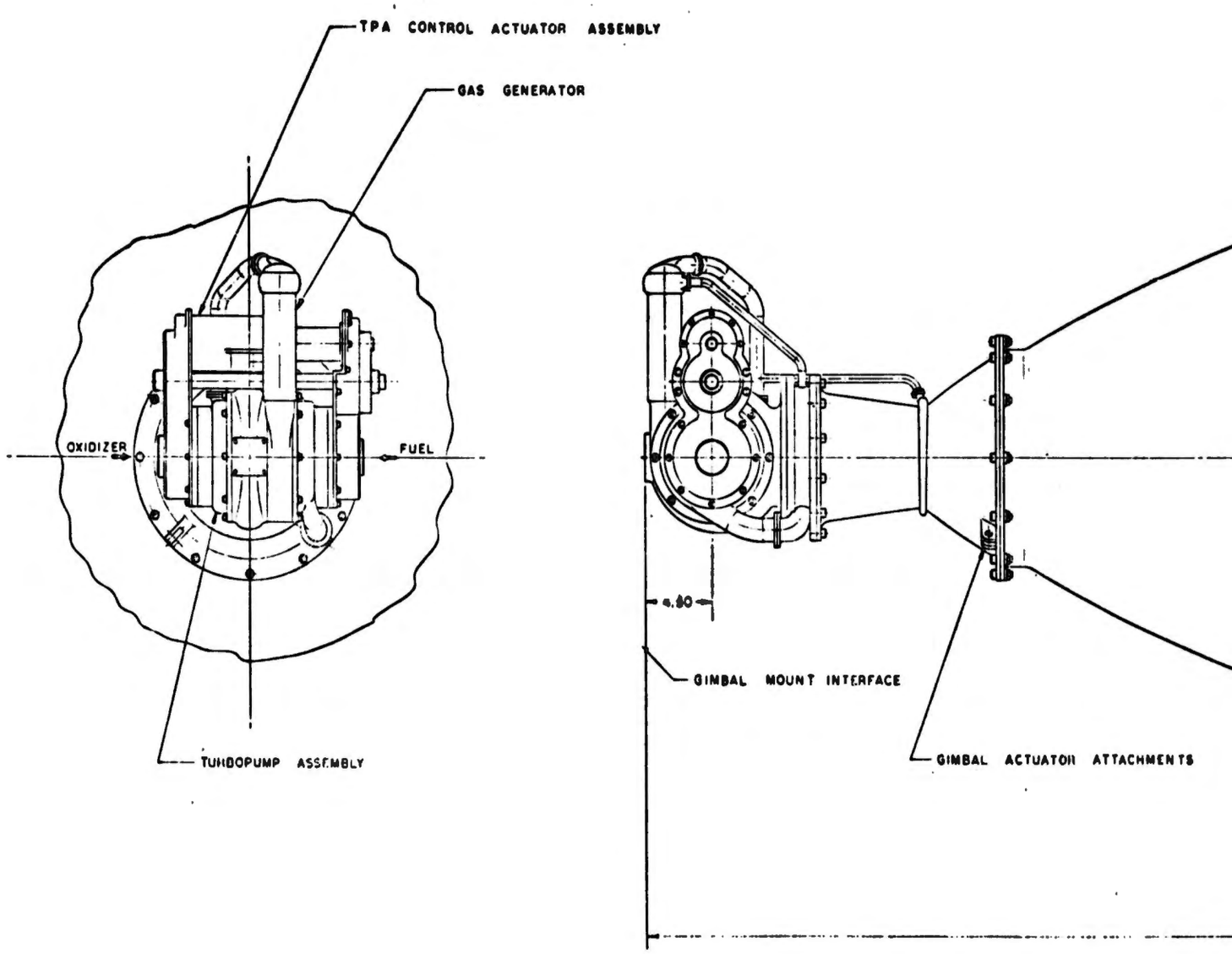
TPA CONTROL ACTUATOR ASSEMBLY
GAS GENERATOR
OXIDIZER
FUEL
TURBOPUMP ASSEMBLY
4.80
GIMBAL MOUNT INTERFACE
GIMBAL ACTUATOR ATTACHMENTS

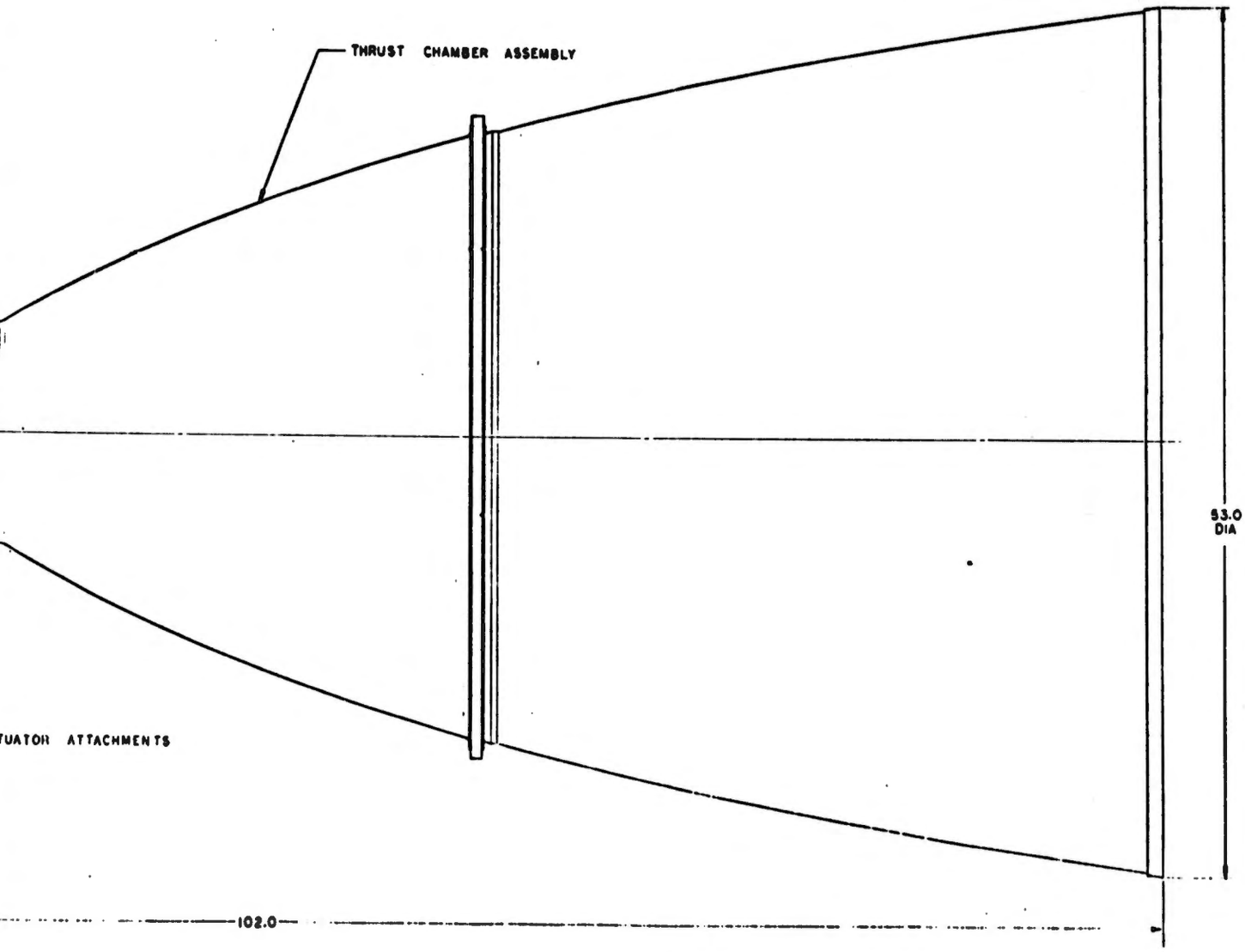

Figure 63. Point Design Engine No. VII Assembly

TABLE XX

POINT DESIGN ENGINE NO. VII (U)

Engine Configuration	Performance	
Pump Fed Throttleable	Thrust (Vac) lb	40,000
Staged Combustion Cycle - GO/LF	Chamber Pressure, psia	1,500
Oxidizer Rich Gases Turbine Drive Fluid	Mixture Ratio	2.74
ARES Type Injector	Specific Impulse (Del) sec	347.4
Transpiration Cooled Chamber Liquid Oxid.	% Theoretical I_s	92.1
Radiation Cooled Nozzle Extension	Nozzle Area Ratio	150
Single Shaft Turbopump	Suction Pressure, psia	
	Oxidizer	146
	Fuel	45
Ring Gate Valves	Flow Rate, lb/sec	
	Oxidizer	85.5
	Fuel	30.5
Nickel Construction	Dry Weight, lb	359
	Wet Weight, lb	367

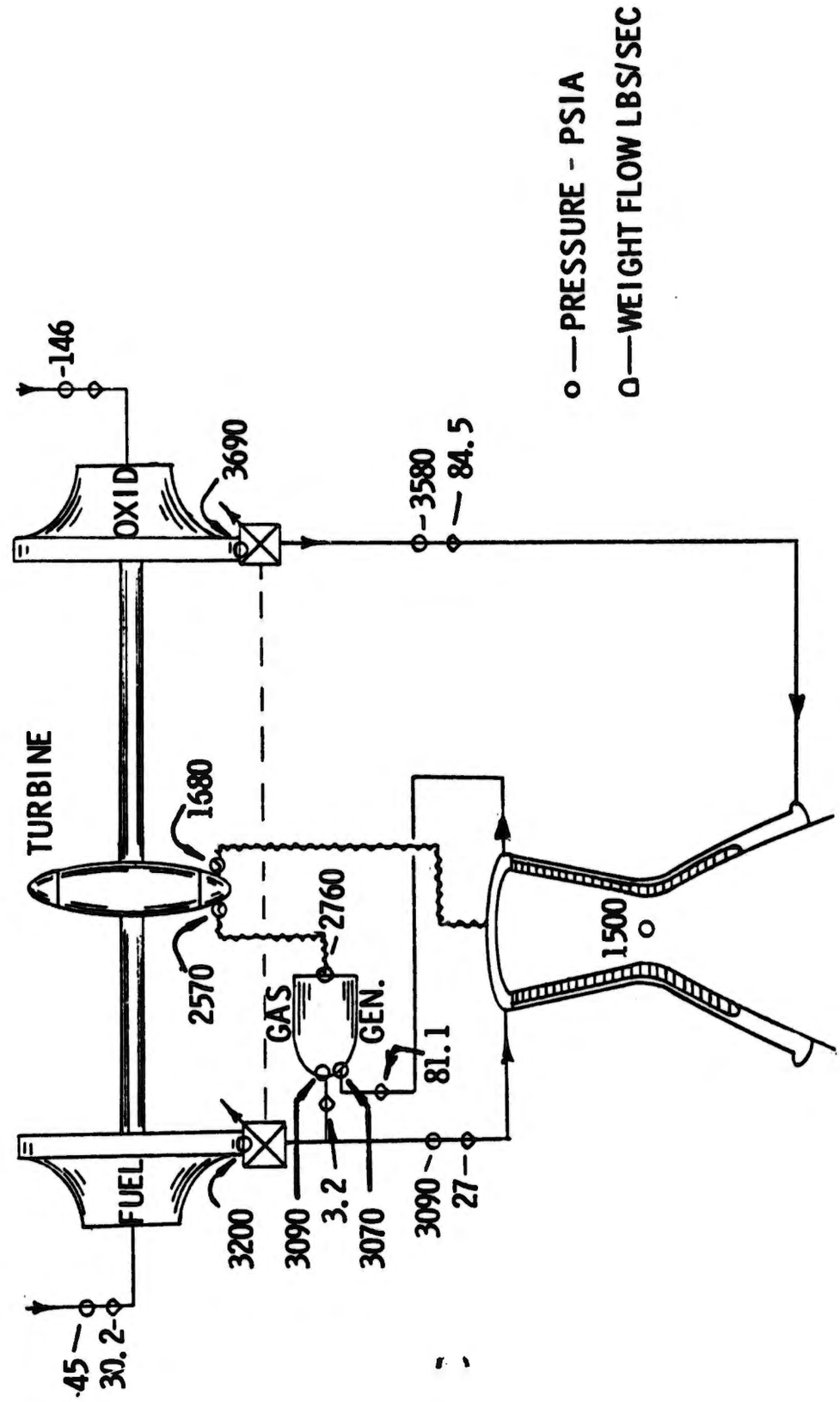

Figure 64. Point Design Engine No. VII Schematic (Original Cycle)

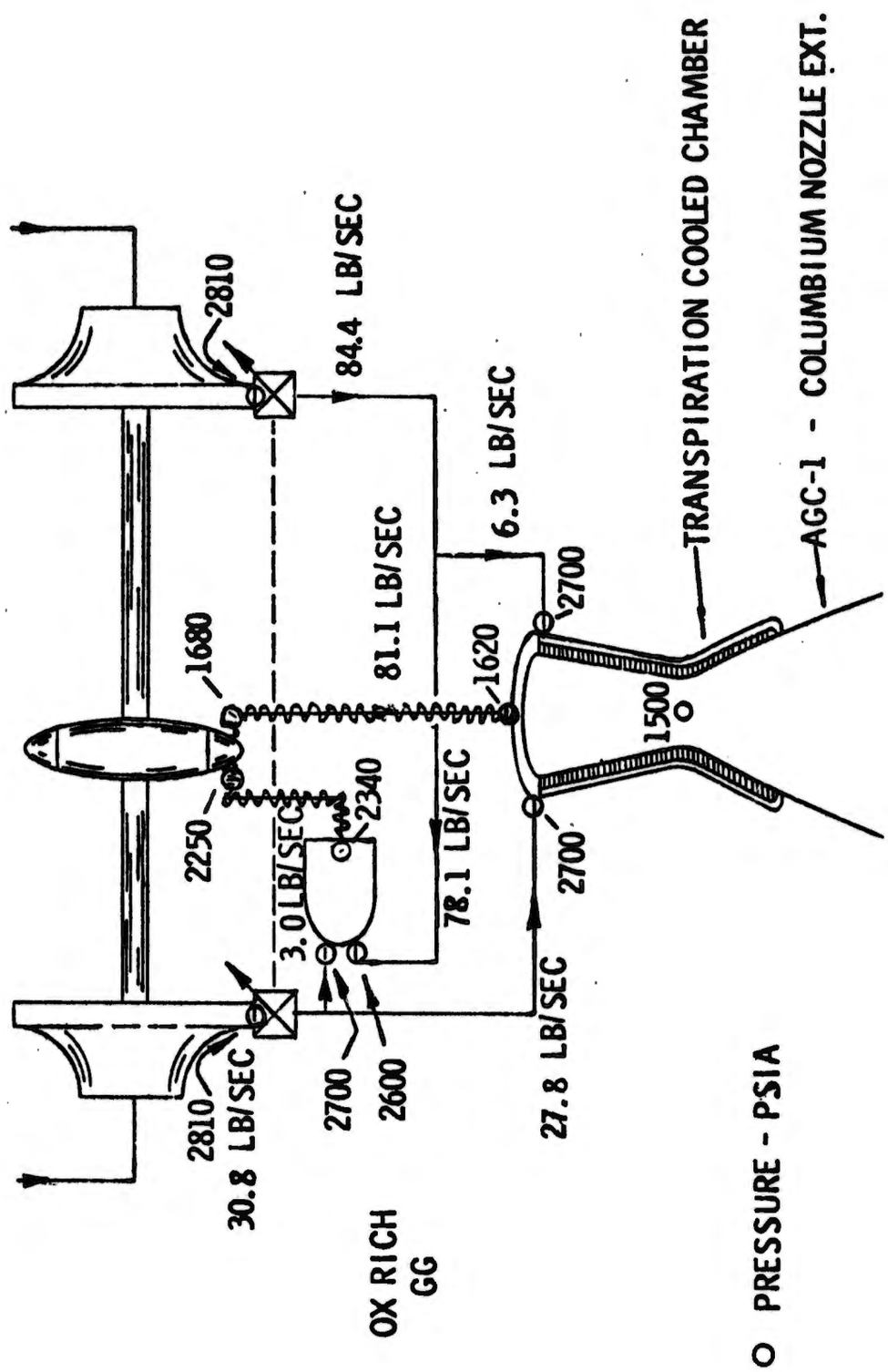

Figure 65. Flow Schematic and Pressure Schedule, Point Design Engine No. VII-4

mixture ratio for lowering the turbine temperature for throttling. It is not known whether the shifting of mixture ratio during throttling to greater values is feasible and thus constitutes an area of new technology. However, for the purpose of weight calculation, the ring-gate valve concept was used.

The flow and pressure schematic in Figure No. 65, is shown for an assumed turbine temperature of 1200°F. A literature search failed to uncover confirmation for this assumption. Therefore, this assumption is based purely upon engineering judgment. A power balance of the thrust pressure assembly was conducted for various turbine temperatures. The pump discharge requirement for various chamber pressures is shown on Figure No. 66. Results indicate that for oxidizer-rich turbine drive, certain chamber pressures cannot be met because of the power balance requirement; however, these chamber pressures are outside the scope of this analysis.

Table XXI shows the combustion chamber geometry parameters, including the characteristic chamber length of 20-in. In the case of an axial gas/liquid injector, the axial gas velocity is not zero at the injector face; therefore, chamber contraction ratio is a significant parameter because it determines the liquid droplet break-up near the injector resulting from the shear forces between the two propellant phases. The contraction ratio selected for this design is 2.0.

(1) Active Cooling System Description

Thrust chamber assembly No. 7 uses cooling modes; one active and one passive. The higher heat flux region (the chamber, throat, and forward section of the nozzle) is transpiration-cooled with liquid oxidizer so that the internal wall surface temperature remains below 1750°F. Figure No. 67 shows how this is accomplished. A liquid oxidizer inlet and manifold exist at the throat of the chamber. Axial coolant passages are formed between the chamber jacket and the cut-out exterior surface of the platelet stack. Liquid oxidizer is fed to each platelet orifice by this manifolding system as well as the system incorporated into each platelet etch pattern. A significant slot length is required to produce the proper pressure drop at the low flow rates demanded by this type of cooling. The passively-cooled nozzle extensions require no cooling systems. However, it is expected that the forward end of the fibrous graphite nozzle section may derive some film cooling benefit from the upstream coolant flow.

The required coolant flow rates were calculated assuming:

- no coolant carry-over from the adjacent plates
- no disassociation of the CLF_5 coolant
- nickel platelets with a maximum allowable wall temperature of 1750°F

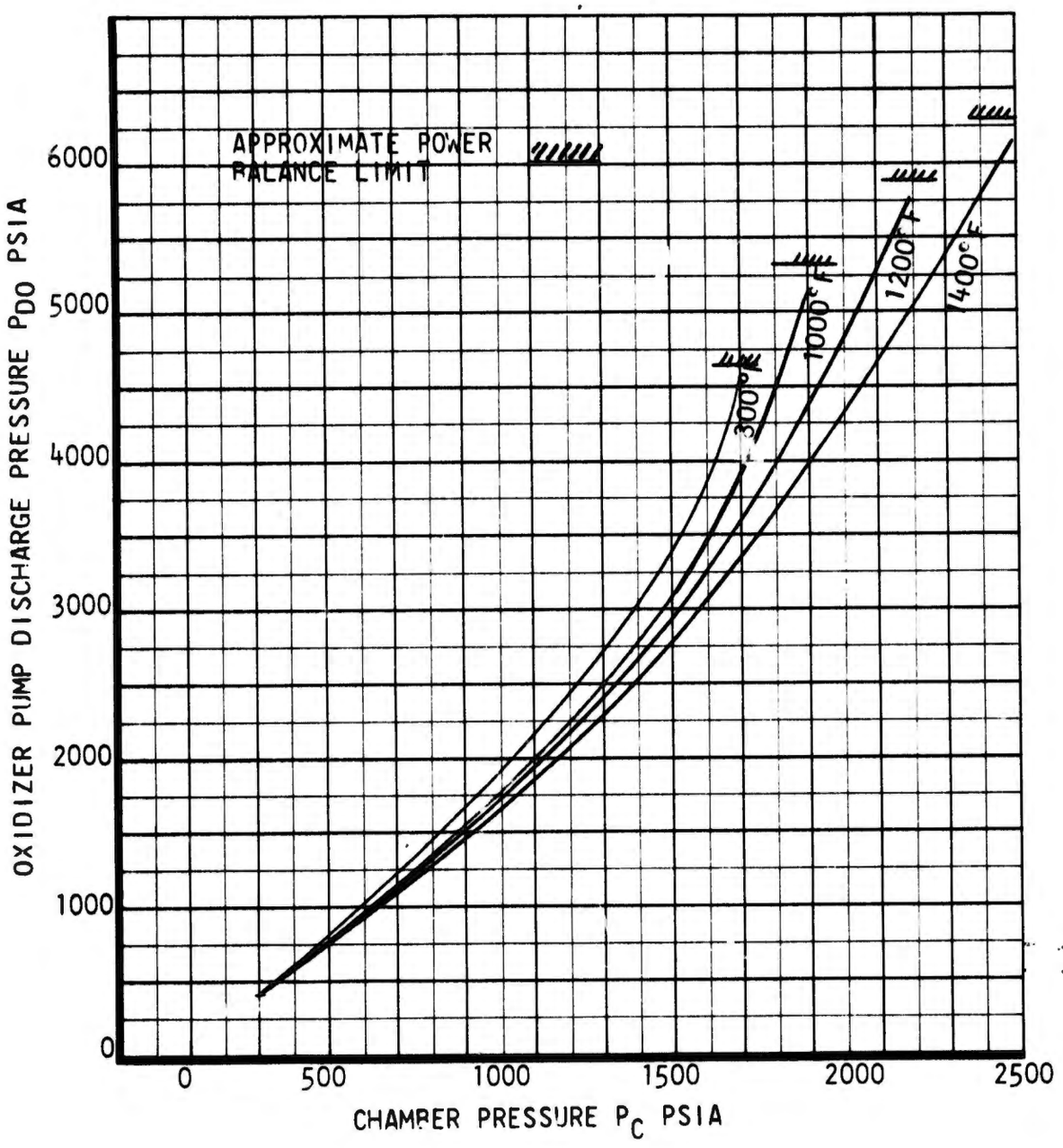

Figure 66. Oxidizer Pump Discharge Pressure vs Chamber Pressure, Engine No. VII

TABLE XXI

THRUST CHAMBER ASSEMBLY NO. 7 DESIGN PARAMETERS

General	Injector	Chamber	Nozzle Extension
Thrust: 40K lb	Type: Gas-Liquid Platelet	Shape: Conical	Attachment Area Ratio: 4
Chamber Pressure: 1500 psia	Propellant Phases: Fuel - Liquid Oxid - Gas	Material: NI-200 Platelet Stack	Cooling Mode: Radiation
Nozzle Area Ratio: 150		Contraction Ratio: 2	
Throttleability: 10/1	Thrust Per Element: Very Small	Cooling Mode: Transpire 8.8% Liquid Oxidizer	Material: Coated Columbium
Duration: Unlimited	Type Element: Laminar Fuel Showerhead		Exit Diameter: 53.0 in.
	$\Delta P_{inj}/P_c$ (Fuel, Max): 1.06	Characteristic Length: 10 in.	
	Film Cooling: None	Throat Dia: 4.30 in.	

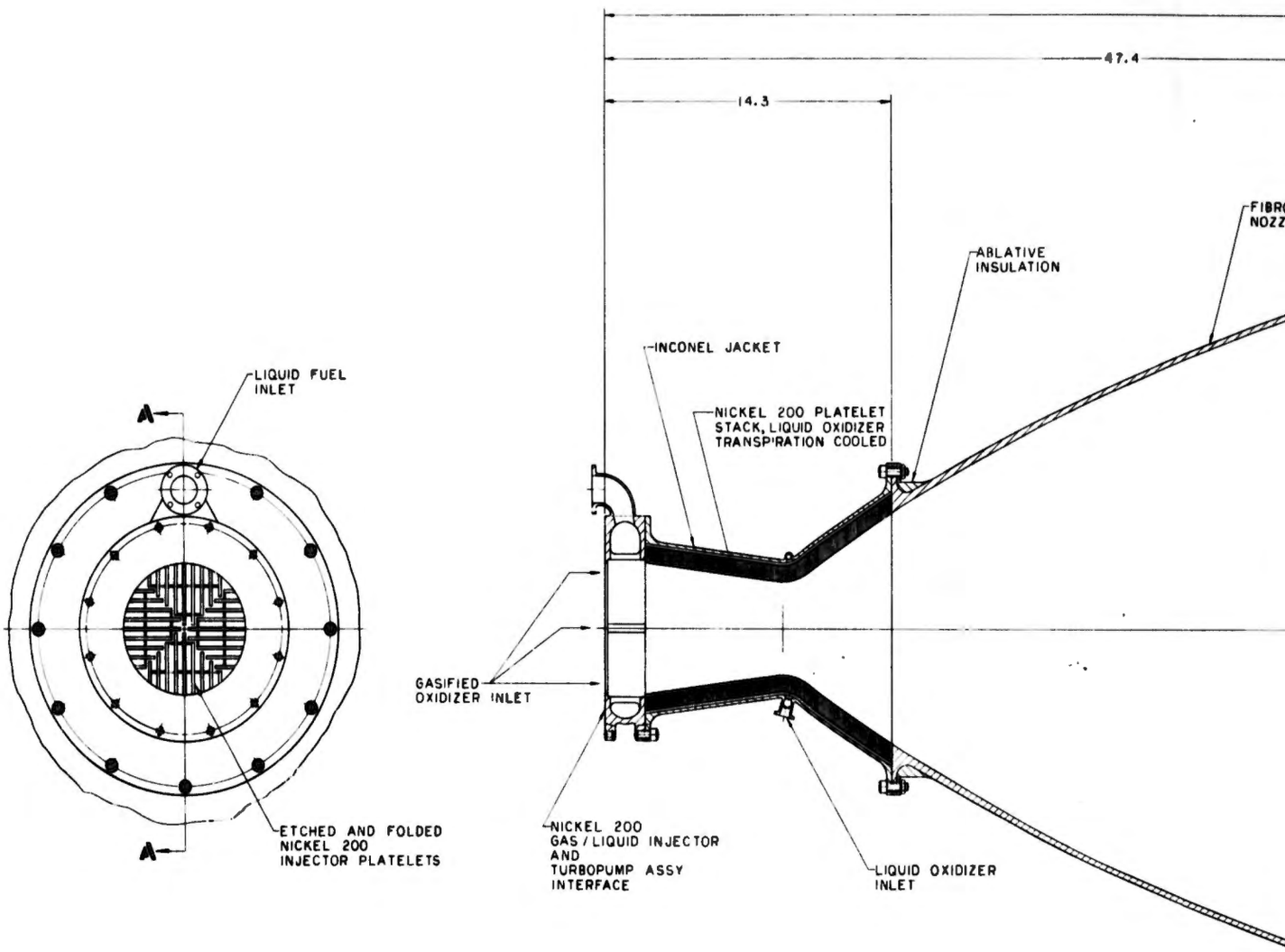
47.4
14.3
FIBR
NOZZ
ABLATIVE
INSULATION
INCONEL JACKET
NICKEL 200 PLATELET
STACK, LIQUID OXIDIZER
TRANSPIRATION COOLED
LIQUID FUEL
INLET
A
A
GASIFIED
OXIDIZER INLET
ETCHED AND FOLDED
NICKEL 200
INJECTOR PLATELETS
NICKEL 200
GAS / LIQUID INJECTOR
AND
TURBOPUMP ASSY
INTERFACE
LIQUID OXIDIZER
INLET

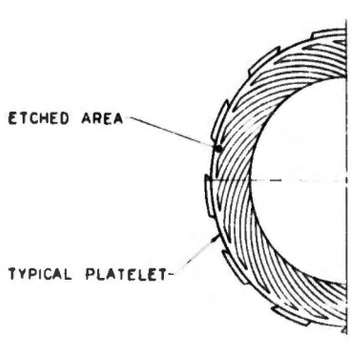
ETCHED AREA
TYPICAL PLATELET

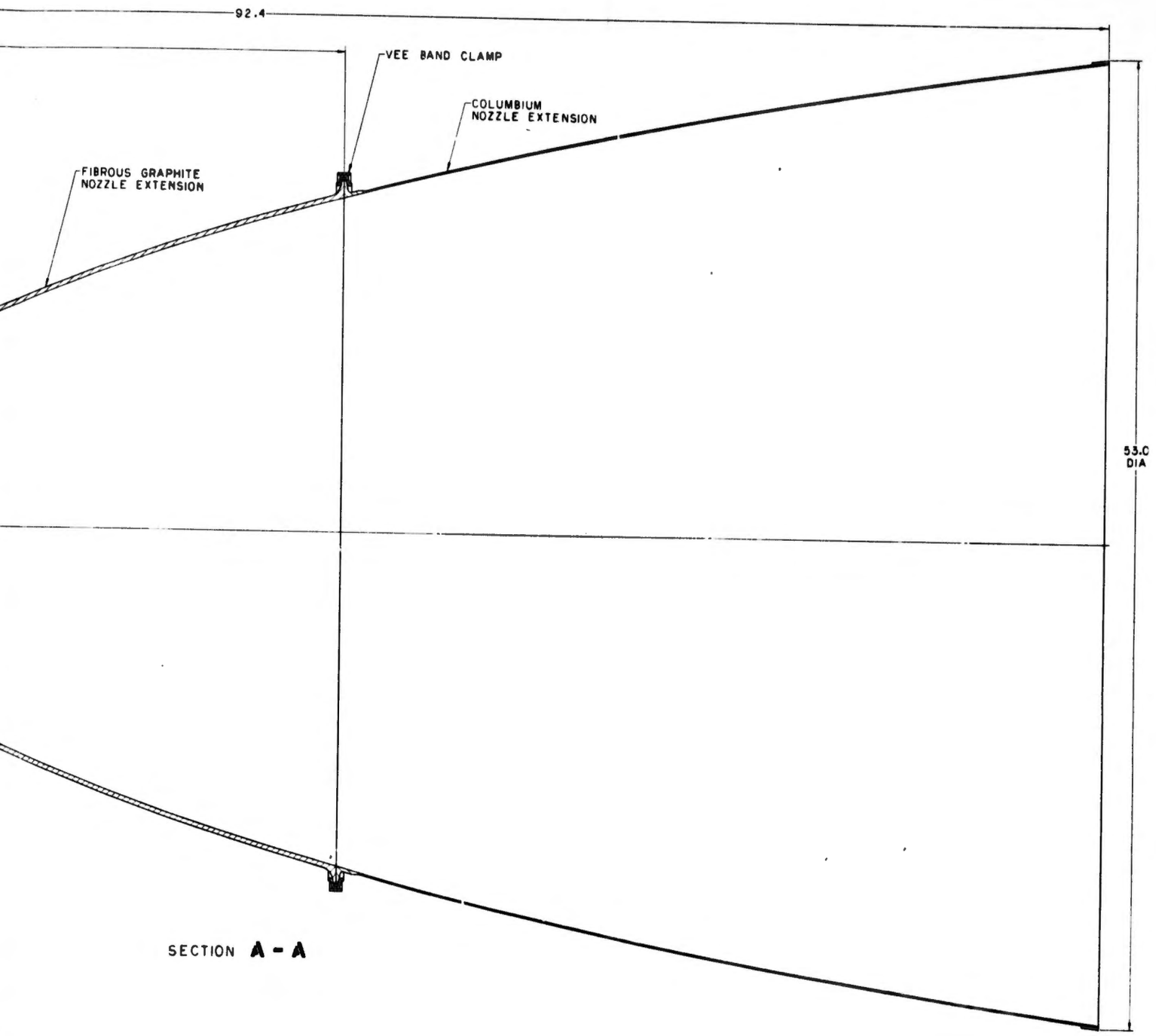

Figure 67. Thrust Chamber Assembly, Engine No. VII

Figure No. 68 shows the results of this analysis in terms of the total coolant weight flow required as a function of the transpiration-cooled section maximum area ratio.

The maximum transpiration area ratio assumed is such that a fibrous graphite radiation-cooled chamber can be attached without any film cooling requirement, which would excessively penalize engine performance. Using this assumption, the transition area ratio was 12:1, which results in an over-all transpiration cooling requirement of 5.5% of the total propellant flow rate.

(2) Injector Selection

The injector of thrust chamber assembly No. 7 is to be deeply throttleable, utilizing gasified oxidizer and liquid fuel as propellants. Throttling with gas injection presents no problems; however, when liquid propellants are used, special care must be taken to assure stable operation with good performance during throttled operation. The injector consists of "blades" protruding into the duct between the thrust pressure assembly and the thrust chamber assembly. These blades inject liquid fuel into the oxidizer-rich gas stream issuing from the turbine. Figure No. 67 shows the thrust chamber assembly with its gas/liquid injector. To be throttleable, the fuel system terminates with laminar flow injector orifices incorporated into the "blade" design. The fuel injection blades are etched platelets containing feed manifold and injection orifices, which are folded and brazed together at the resulting interface. The blade is positioned in the thrust chamber assembly with the fold facing upstream and the opposite edge containing the fold-formed orifices are downstream. Many such blades are used and they are fed by the annular injector manifold to form a virtual injector face. The platelets are well-cooled by the injectants they carry, and are not exposed to any great heat. The gasified oxidizer is cool (1200°F) and only the injecting edge of the platelets is exposed to the combustion front. Fuel injection blades make natural baffles if they are extended into the combustion front. Where high-frequency combustion instability is experienced, it can be suppressed using this method or by contouring the injection density to "starve" the favored mode.

(3) Materials Selection

The materials selection criteria as well as the materials used in thrust chamber assembly No. 7 are similar to those of thrust chamber assembly No. 8. A detailed discussion of the pertinent factors is presented as part of the Engine No. VIII section. Ni-200 was selected for injector and chamber platelets as well as for the injector body and manifolding. Inconel 625 was selected for the jacket around the thrust chamber platelet stack. The two nozzle extensions shows are radiation-cooled; the forward one, which runs at very high wall temperature, is made of fibrous graphite. The aft extension and its clamp-ring are made of columbium.

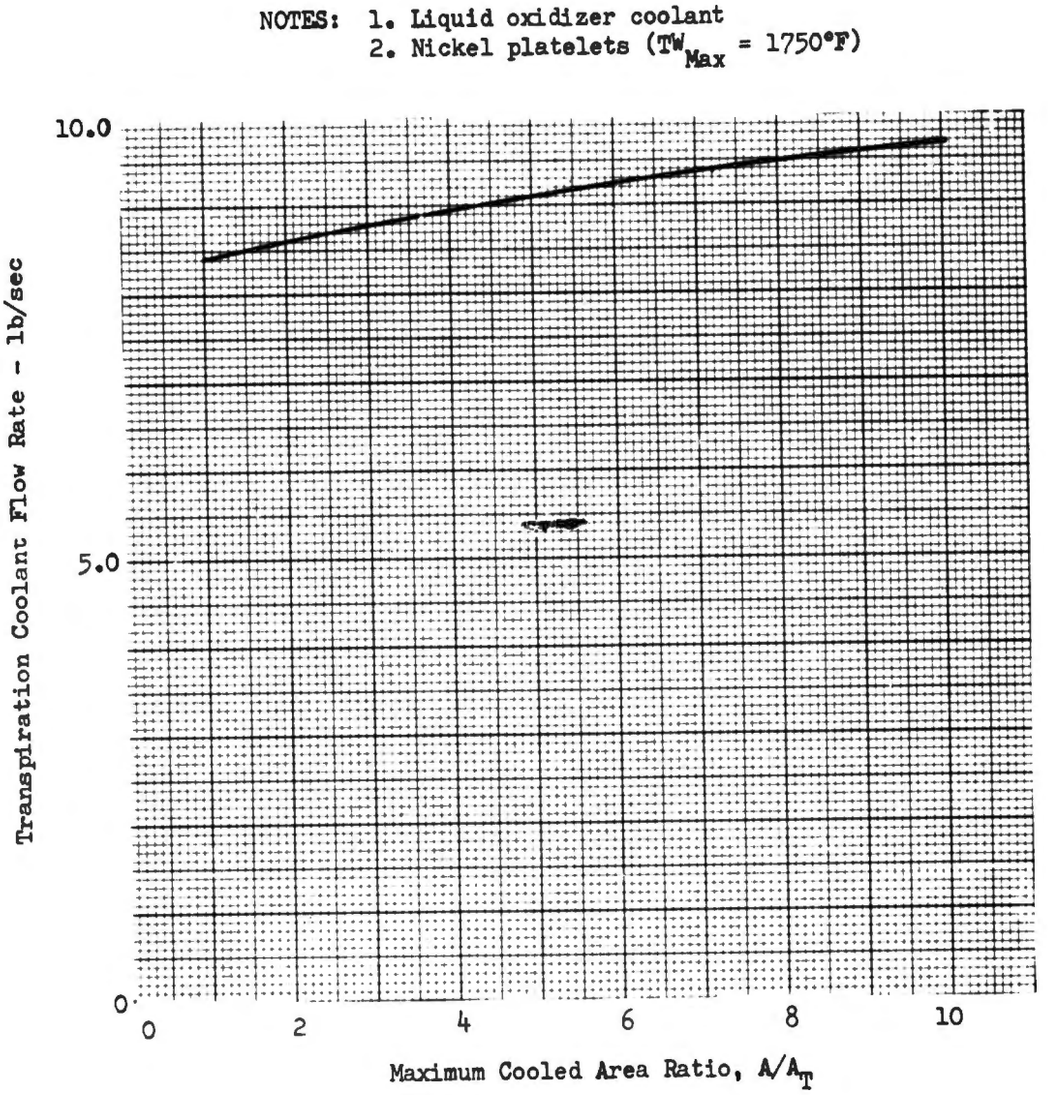

Figure 68. Engine No. VII Transpiration-Cooled Section

All thrust and gimbaling loads are carried to the thrust pressure assembly through the heavy-walled liquid fuel injector manifold. The chamber platelet stack jacket is attached to this same member by a bolt circle, as shown on Figure No. 67. The chamber jacket is constructed of higher strength material than are the platelets themselves. It withstands the high hoop and axial loads applied to thy chamber wall by the high chamber pressure without greatly increasing the thrust chamber assembly weight. Also, it provides an attachment flange at the chamber/nozzle extension interface, where the two rigid members are bolted together. The fibrous graphite nozzle extension is made sufficiently thick to absorb gimbaling-induced loads applied to it by the large columbium nozzle extension.

(4) Turbopump Configuration

The single-stage turbine which formed the basis for weight determination is described in Appendix VI (Part II of this report) as part of the detailed turbopump design discussion, including the staged-combustion cycle, provided therein.

(5) Controls System Description

The basic control elements for Engine No. VII are the oxidizer and fuel ring-gate combination shut-off and throttling valves which are integral with the turbopump assembly. The system includes two electrically-operated actuators. One opens and closes the ring-gate valves and the other controls the mixture ratio over the designed throttling range by varying the relative position of the fuel valve relative to the oxidizer valve. The actuation is accomplished electrically in accordance with the criteria established at the outset of this study.

The oxidizer and fuel ring-gate valves are mechanically-linked for reliable phasing, both during throttling and mixture ratio control operations. Each of the two separate electro-mechanical actuators for engine thrust and mixture ratio control are powered by 26 volt dc electric motors. The ring-gate throttling valves of the fuel and oxidizer turbopumps are opened by applying power to the motor and "opening" clutch of the throttling control actuator. The position of the actuator output drive shaft and the valves can be modulated within the range of 0 to 100% of full travel for variable thrust control by alternate application of electrical power to the two (opening and closing) magnetic powder clutches. This effects a modulating control of valve position corresponding to the input signal from the control programmer. The throttling valves are closed by applying electrical power to the "closing" clutch. The separate electrical actuator for mixture ratio control will operate similarly to maintain engine mixture ratio by controlling the fuel ring-gate valve independently of the oxidizer valve.

The use of an electrical actuator offers the advantage of high reliability in a space environment by eliminating any requirement for hydraulic or pneumatic actuating fluid which could possibly deplete itself through leakage. The electrical actuators will provide positive control of valve positions in response to input signals. An additional and significant advantage of the electrical actuation system is the inherent cleanliness and ease of operation afforded during engine system checkout operations because only electrical power need be supplied to operate the control valves.

The electric motors in the actuators would be similar in design to the 26 volt dc, compound wound, uni-directional motor used in the Apollo Service Module propulsion thrust vector control system developed by Aerojet-General. It will be capable of continuous operation in space vacuum for a considerably longer duration than any anticipated duty cycle and will be energized only to position the ring-gate throttle valve during engine firing. If a combined operating period longer than 20 min should become a requirement and brush life becomes a problem with the dc motor, it may be necessary to consider a two-phase or three-phase ac motor which would perform satisfactorily.

The primary control elements in the electro-mechanical servo actuator will be two magnetic particle clutches. The clutches will be of the same basic design as the clutches being used in the Apollo electrical gimbal actuators. These clutches are relatively simple in construction and consist of an input member, magnetic powder, low inertia drive disc, and output shaft assembly, plus the end fittings and associated bearings required for mounting as well as for sealing the entrapped powder. When control power is supplied to the coil, magnetic field action in the gap makes the powder a relatively solid mass, thereby coupling the output member to the input member. This type of clutch can be operated in the slip condition with negligible wear upon the metallic surfaces in the clutching space. The motor drive shaft is geared to the clutch output shafts so that the inputs rotate in opposite directions. The clutch output shafts are similarly geared to the actuator output shaft. A small quiescent current is supplied to the both clutches for balancing. The direction of actuator (and ring-gate valve) movement depends upon which of the two clutches is engaged and because the clutches are balanced with both carrying a small current, actuator and valve positioning response is fast. Control will be proportional and actuator/valve velocity feedback can be included if this degree of position accuracy is desired. Valve/actuator position transducers will be included in both the thrust control and mixture ratio control actuators.

Detailed mechanical functioning of the valve and actuator assembly as well as the electrical control network are discussed as part of the Engine No. VIII section.

(6) Engine Performance

Point Design Engine No. VII performance was calculated using the methods described in Appendix II. The result, assuming no

reaction of the coolant with the core, is shown on Figure No. 69 for the propellant combination CLF_5/N_2H_4. Based upon experience with oxidizer-cooled transpiration chambers, it is assumed that 50% of the coolant reacts with the core. The resulting thrust chamber assembly and engine performance are shown on Figure No. 70 for the optimum mixture ratios as a function of cooling flow requirements for the propellant combination CLF_5/N_2H_4. Also included is the extreme hypothetical performance level if all coolant reacted with the core along with the cooling requirements for nickel and graphite platelets.

(U) Figures No. 71 and No. 72 provide similar information for the propellant combination CLF_5/MHF-5.

(7) Engine Capabilities and Limits

(U) This engine is unique in that it uses liquid oxidizer as the coolant. CLF_5 has a high vapor pressure (see Appendix I), which affects engine capability, design, and operational limits.

(a) Burn Duration

(U) The radiation-cooled fibrous graphite nozzle extension may be the critical component limiting the burn duration; however, very little experience is currently available to provide useful criteria for mission analysis purposes.

(b) Throttling Capability

(C) The transpiration section of this engine is extended beyond the throat to an area ratio of 12, where the static pressure is reduced to 0.75% of the nominal chamber pressure. This results in a full thrust static pressure of 11.3 psia, which is below the vapor pressure of the nominal propellant temperature of 75°F. Therefore, partial flashing of the oxidizer in the transpiration cooling metering passages occurs which is an important consideration in this design.

(C) During throttling, the low pressure region grows back to the smaller area ratios and can even reach the throat for deep throttling. At the throat, the static pressure is approximately 54.6% of the nominal chamber pressure. For 10:1 throttling the minimum chamber pressure would be equal to 110 psia, at which pressure the liquid coolant at the throat starts to flash and reduce throat coolant flow. No data exist to indicate whether this phenomena constitutes a practical throttling limit and what pressure is considered to be the minimum feasible level.

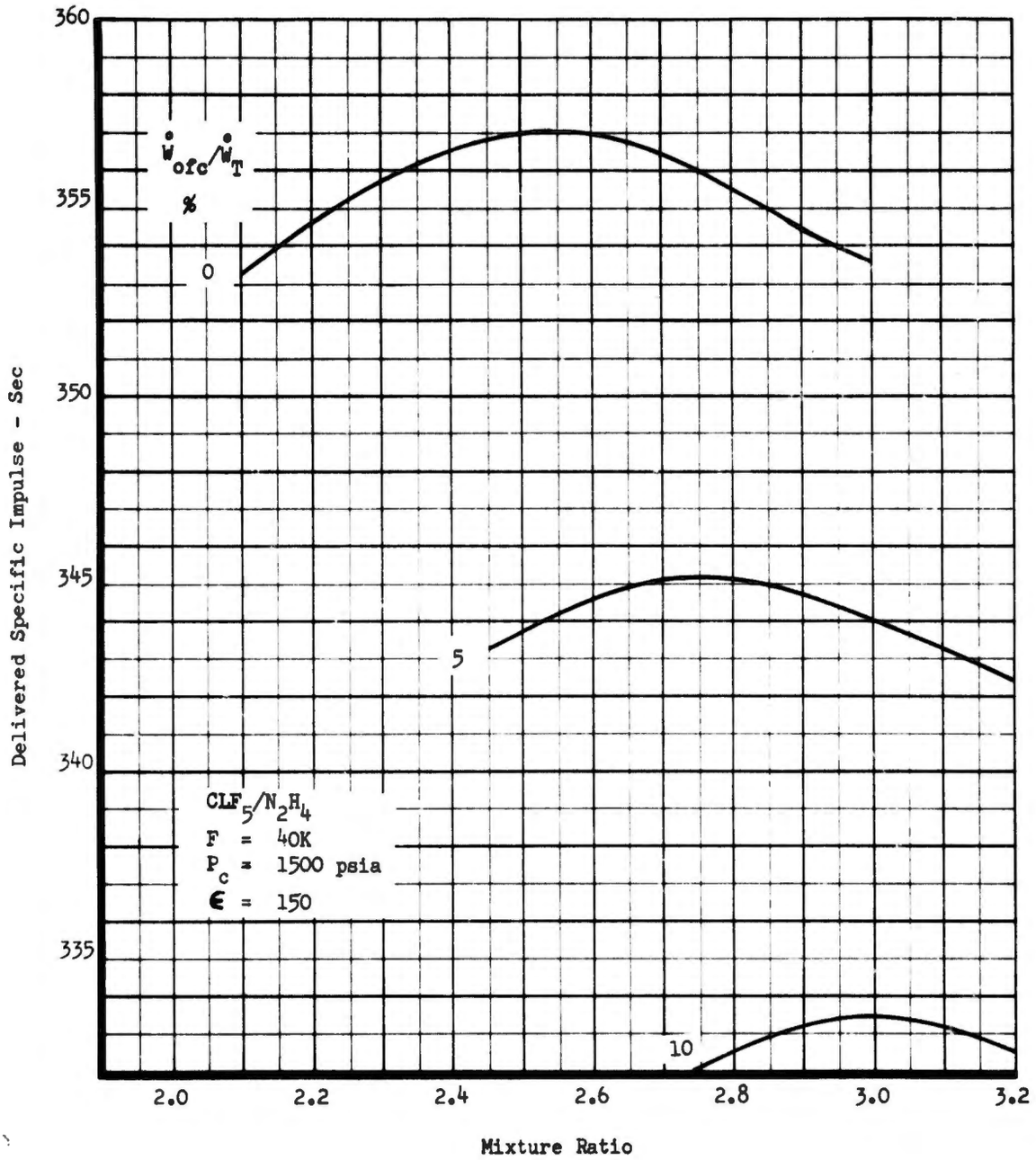

Figure 69. Point Design Engine No. VII, Performance/Mixture Ratio-Coolant Flow Trade-Off (CLF_5/N_2H_4)

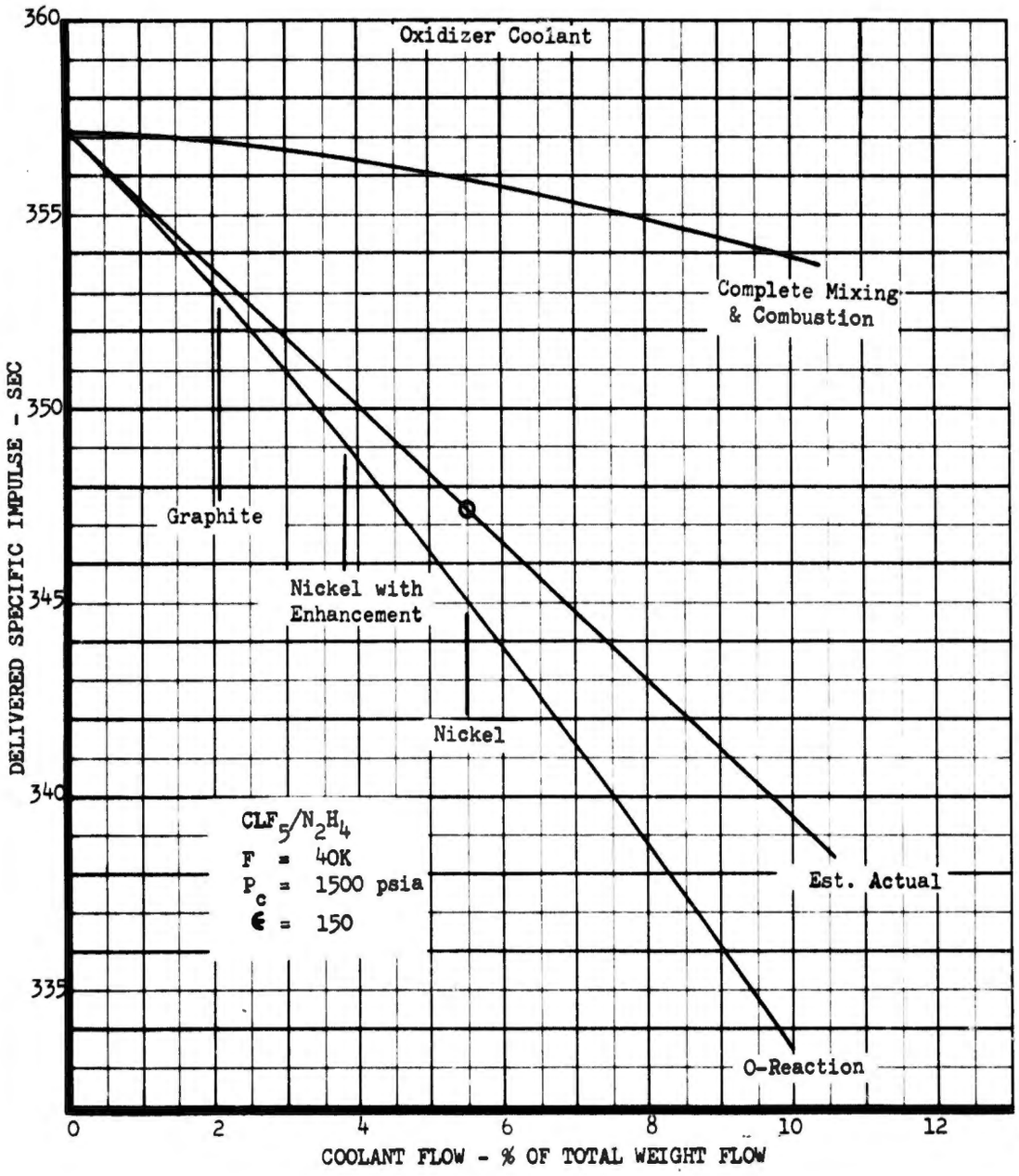

Figure 70. Point Design Engine No. VII, Performance/Coolant Flow Interaction (CLF_5/N_2H_4)

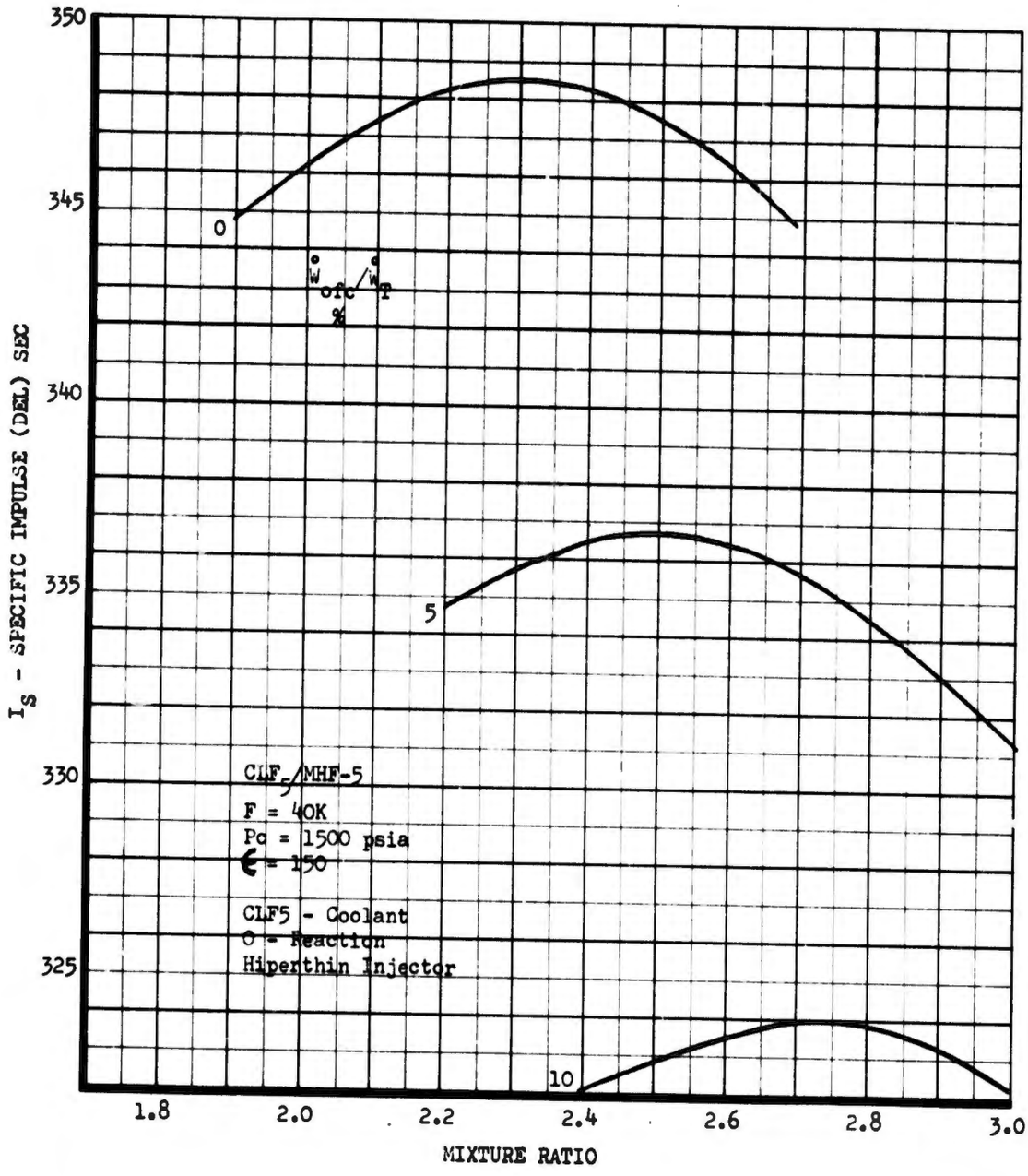

Figure 71. Point Design Engine No. VII, Performance/Mixture Ratio-Coolant Flow Trade-Off (CLF_5/MHF-5) (u)

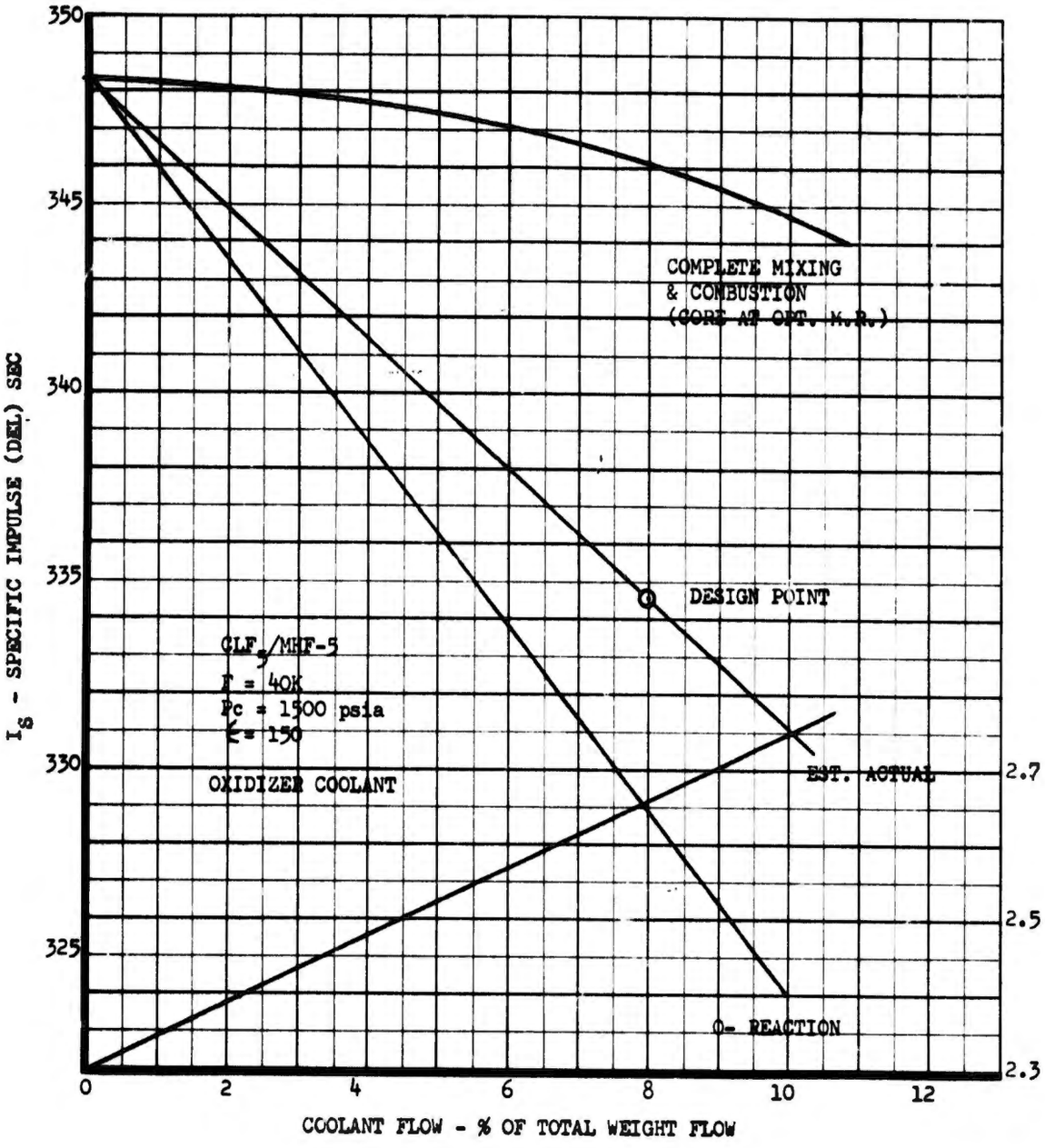

Figure 72. Point Design Engine No. VII, Performance/Coolant Flow Interaction (CLF_5/MHF-5) (u)

(c) Start Transient

(C) The high vapor pressure of CLF_5 will affect the fill time of the coolant manifold during the start transient. This fill time is very sensitive to propellant temperature and requires considerable oxidizer lead. As long as the chamber pressure is near vacuum, flashing of the coolant in the metering passages will occur and this will drastically reduce the cooling flow during the start transient. In the staged-combustion cycle, it is feasible to pre-pressurize the chamber with the gas generator gases if the design chamber pressures are sufficiently high. However, the start transient cooling of the convex section remains problematical.

(d) Mission Capability

(U) The engine is adaptable to accommodate any of the specified fuels. It operates coolly, does not store large amounts of heat, and little heat soak-back is experienced because of the liquid oxidizer-cooled chamber.

(U) The heat soak-back caused by the turbopump is minimized by the low turbine temperature and the feasibility of cooling the turbine disc with liquid oxidizer. Turbine cooling in a fuel-rich turbine is not feasible because of the monopropellant characteristic of the fuel. The only critical components for restart with N_2H_4 are the bipropellant gas generator and the main injector. Rapid cooling transients of the main injector can be expected permitting rapid engine restart even with N_2H_4 because of the cold chamber and the main injector design. No surface temperature problem is expected because of the little surface area exposed to the flame front.

(C) The chamber is cooled with liquid oxidizer and requires extensive passivation to obtain compatibility. It appears undesirable to operate a thrust chamber assembly for long durations in CLF_5 because small cracks, which are caused by vibration or temperature transients, can result in engine failure. However, a number of highly successful tests have been conducted with this concept and they seem to indicate that passivation and design methods have progressed to a level where liquid oxidizer transpiration cooling appears feasible.

b. Point Design Engine No. VIII

This engine is designed for the same 40K thrust level and 1500 psia chamber pressure as Engine No. VII. The design is shown on Figure No. 73 for a nozzle expansion area ratio of 150:1, which results in a maximum engine diameter of 53 in. and an over-all engine length of 83 in. Pertinent engine information is summarized on Table XXII.

Point Design Engine No. VIII represents a new design concept for fully throttleable engines. An injection system is used where both propellants are in the gaseous state and gaseous fuel is used as coolant for the transpiration-cooled throat.

Figure No. 74 is a schematic of this engine. It includes the pressure schedule and flow schematic for full thrust conditions. In this figure, practically all of the fuel is decomposed in a CAT-Pack and used in the fuel-rich drive turbine before entering the main injector. A small part of the liquid fuel is used in the oxidizer-rich gas generator. The oxidizer is first introduced into a bipropellant gas generator before injection into the main chamber. The thrust chamber, which is cooled by turbine exhaust gases at 1355°F, consists of a transpiration-cooled throat, a regeneratively-cooled nozzle extension and an attachable radiation-cooled columbium skirt, as shown on Figure No. 75. In an alternative version, the regeneratively-cooled nozzle extension was replaced by a radiation-cooled fibrous graphite nozzle extension in order to reduce the engine weight and increase the throttling capability. A weight saving was desirable because the ducting for all of the fuel propellant down into the regenerative section and that returning into the injector required that the platelet width be of large dimension to accommodate all the flow. By eliminating the regenerative section, the width of these platelets could be reduced considerably.

(1) Thrust Chamber Design

Thrust chamber injectors flowing gaseous propellants are intrinsically throttleable. A summary of the design parameters is shown on Table XXIII. Propellant weight flow rate per unit injection area is a function of the propellant inlet pressure, temperature, and molecular weight, as well as the injection Mach number. The Mach number is mainly dependent upon the pressure ratio across the injector. If the injector is supplied with gases of constant molecular weight and temperature, the inlet pressure and pressure ratio to the chamber control propellant flow rates. The thrust chamber throat area controls the pressure ratio across the injector by fixing the chamber pressure for any given propellant flow rate. If propellant inlet pressure is decreased, the reduced weight flow will cause chamber pressure to drop linearly, so that the pressure ratio across the injector is constant. The Mach number, and therefore, injection velocity is unchanged, as is the stability parameter $\Delta P_{inj}/P_c$. Therefore, thrust chamber throttling with gaseous propellants can be easily achieved without loss of injection velocity or combustion stability

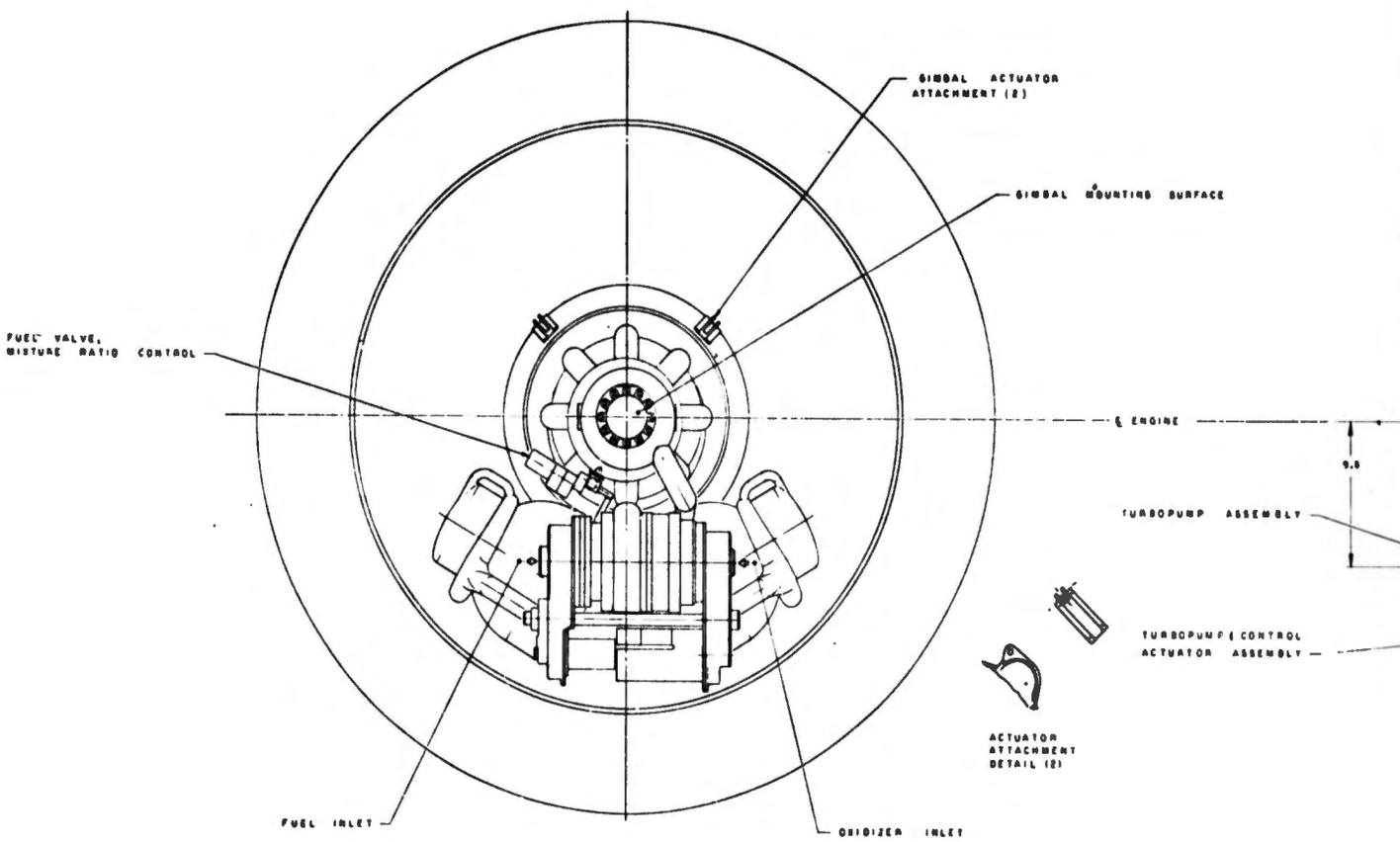
GIMBAL ACTUATOR ATTACHMENT (2)
GIMBAL MOUNTING SURFACE
FUEL VALVE, MIXTURE RATIO CONTROL
℄ ENGINE
9.8
TURBOPUMP ASSEMBLY
TURBOPUMP ℄ CONTROL ACTUATOR ASSEMBLY
ACTUATOR ATTACHMENT DETAIL (2)
FUEL INLET
OXIDIZER INLET

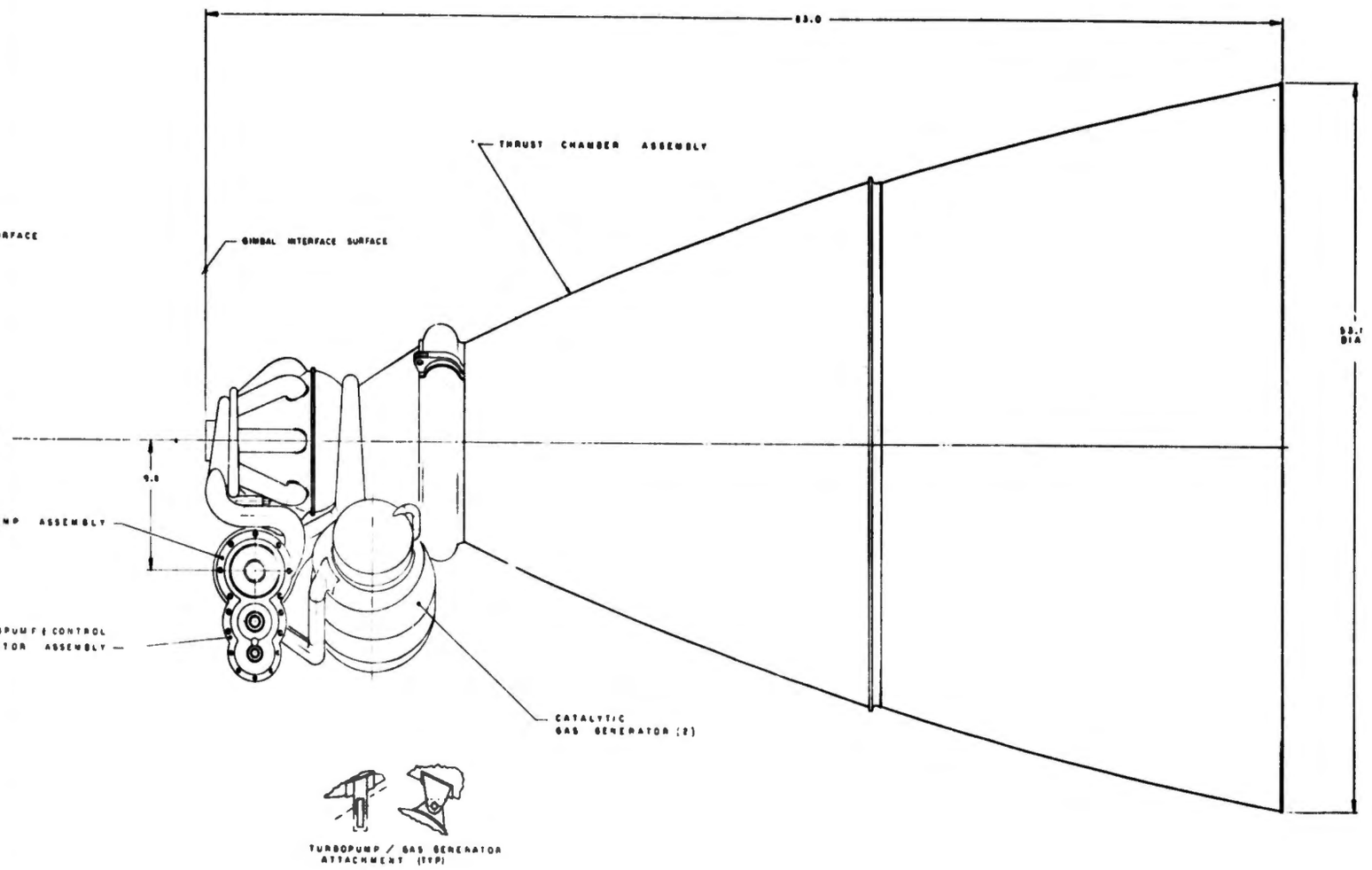

Figure 73. Point Design Engine No. VIII Assembly

TABLE XXII

POINT DESIGN ENGINE NO. VIII (U)

Engine Configuration	Performance	
Pump Fed	Thrust (Vac) lb	40,000
Staged Combustion - GO/GF	Chamber Pressure, psia	1,500
Throttleable	Mixture Ratio	2.25
HIPERTHIN Injector	Specific Impulse (Del) sec	357.8
Transpiration Cooled Chamber	% Theoretical I_s	96.1
Regen + Rad Cooled Nozzle Extension	Nozzle Area Ratio	150
N_2H_4 CAT-Pack Turbine Drive	Suction Pressure, psia	
Single Shaft Turbopump	Oxidizer	146
Ring-Gate Valve Flow Control	Fuel	45
	Flow Rate, lb/sec	
	Oxidizer	77.1
	Fuel	33.8
	Dry Weight	533.0
	Wet Weight	542.0

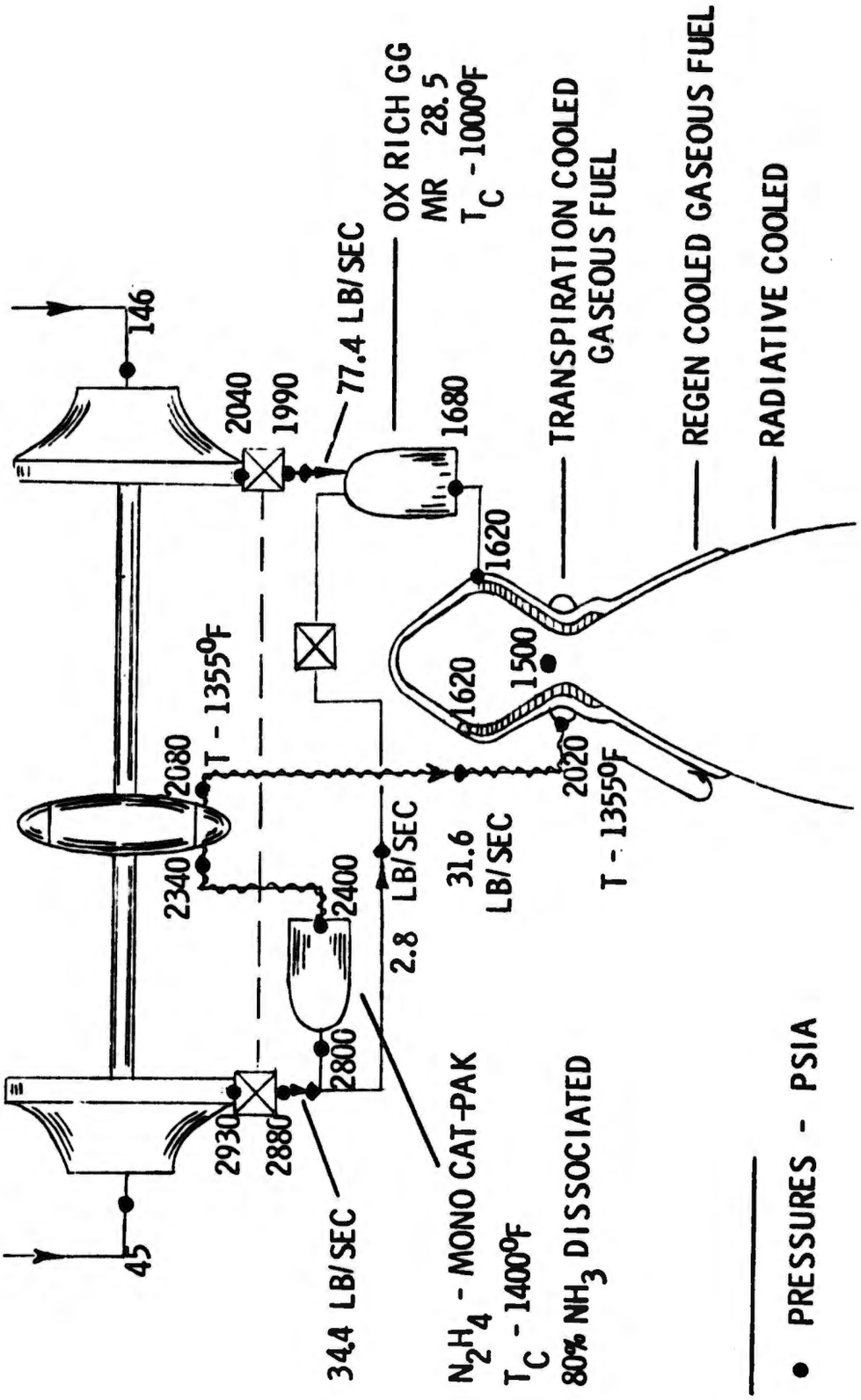

Figure 74. Flow Schematic and Pressure Schedule, Point Design Engine No. VIII

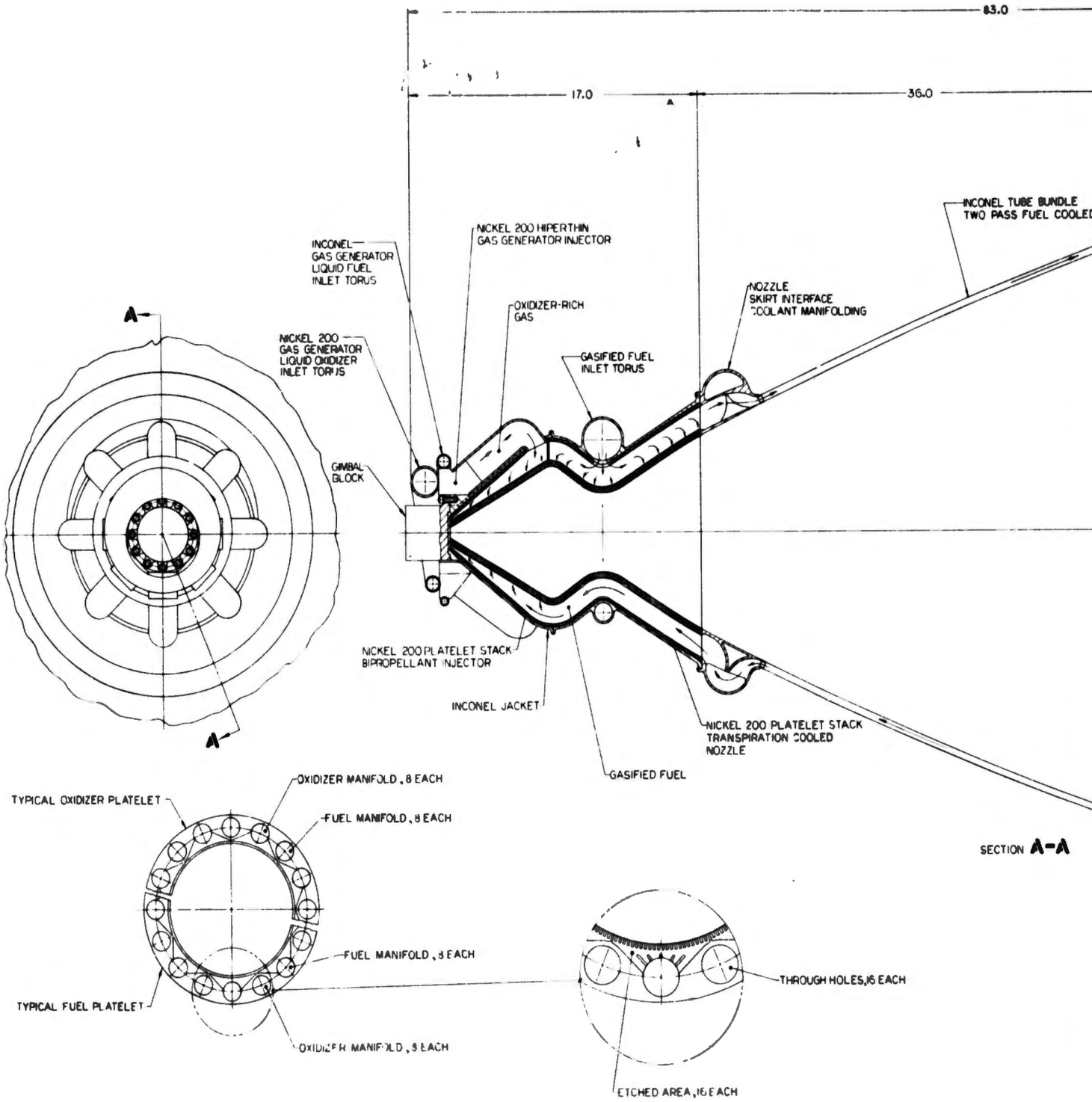
83.0
17.0
36.0
INCONEL TUBE BUNDLE
TWO PASS FUEL COOLED
NICKEL 200 HIPERTHIN
GAS GENERATOR INJECTOR
INCONEL
GAS GENERATOR
LIQUID FUEL
INLET TORUS
OXIDIZER-RICH
GAS
NOZZLE
SKIRT INTERFACE
COOLANT MANIFOLDING
NICKEL 200
GAS GENERATOR
LIQUID OXIDIZER
INLET TORUS
GASIFIED FUEL
INLET TORUS
A
A
GIMBAL
BLOCK
NICKEL 200 PLATELET STACK
BIPROPELLANT INJECTOR
INCONEL JACKET
NICKEL 200 PLATELET STACK
TRANSPIRATION COOLED
NOZZLE
GASIFIED FUEL
SECTION A-A
TYPICAL OXIDIZER PLATELET
OXIDIZER MANIFOLD, 8 EACH
FUEL MANIFOLD, 8 EACH
FUEL MANIFOLD, 8 EACH
TYPICAL FUEL PLATELET
OXIDIZER MANIFOLD, 8 EACH
THROUGH HOLES, 16 EACH
ETCHED AREA, 16 EACH

1

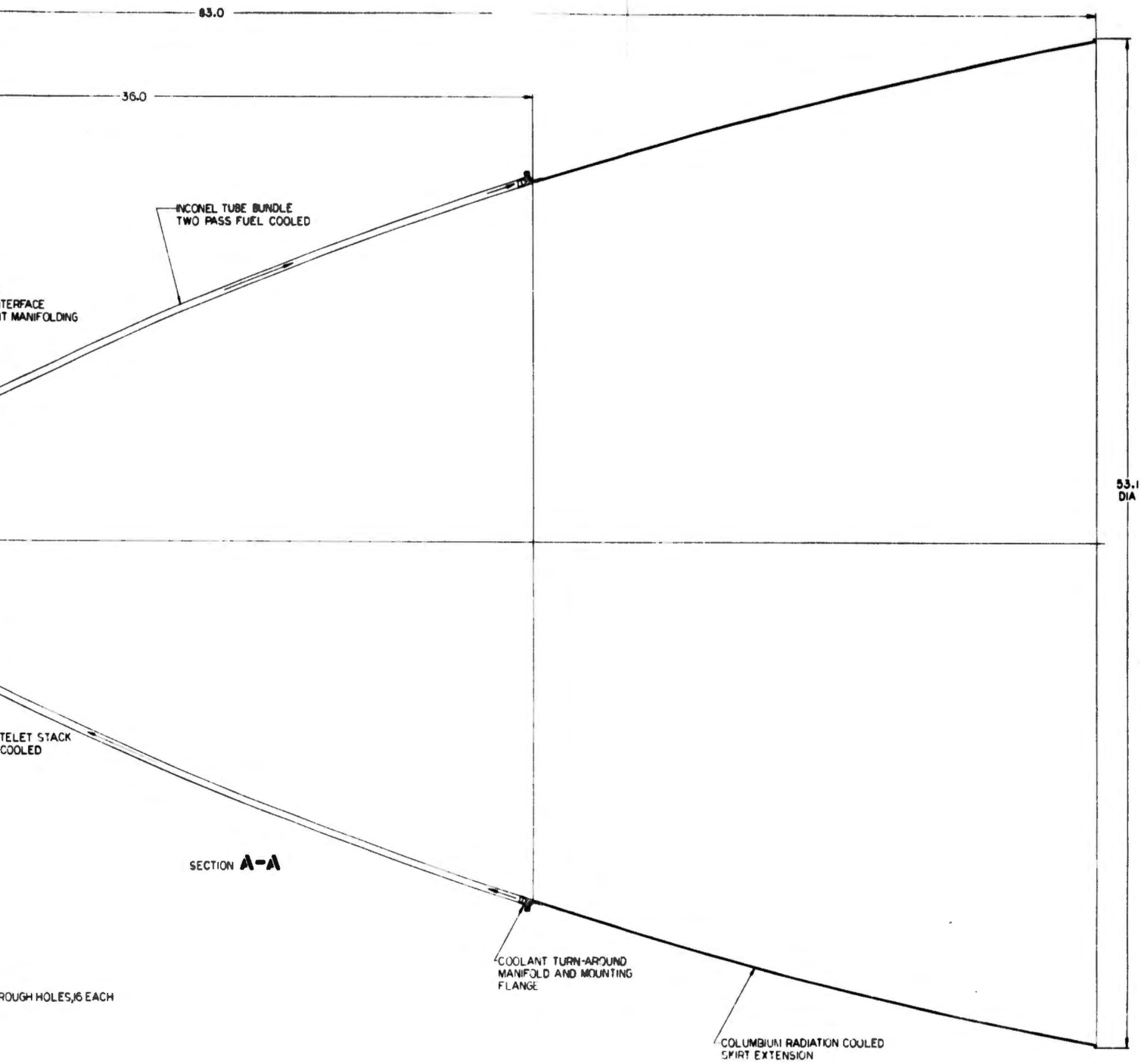

Figure 75. Thrust Chamber Assembly, Engine No. VIII

TABLE XXIII

THRUST CHAMBER ASSEMBLY NO. 8 DESIGN PARAMETERS

General	Injector	Chamber	Nozzle Extension
Thrust: 40K lb	Type: Radial Platelet	Shape: Double Conical	Attachment Area Ratio: 6
Chamber Pressure: 1500 psia	Propellant Phases: Gas-Gas	Material: Ni-200 Platelet Stack	Cooling Mode: Gaseous Fuel Regen
Nozzle Area Ratio: 150	Thrust per Element Very Small	Contraction Ratio: 2.8	Material: Inconel Tubes
Throttleability: 10/1 (or greater)	Type Element: Radial Showerhead	Cooling Mode: Gaseous Fuel Transpire, 4%	Attachment Area Ratio: 80
Length: 83.0 in.	$\Delta P_{inj}/P_c$ (max): .13	Characteristic Length: 11.5 in.	Cooling Mode: Rad
Duration: Unlimited	Material: Ni-200	Throat dia: 4.30 in.	Material: Coated Columbium
	Film Cooling: None		Exit dia: 53.0 in.

because of the automatic change of propellant density with inlet pressure and flow rates. Thus, throttleability is not a consideration in selecting a gas-gas thrust chamber assembly injector design.

It is always desirable to handle high density fluids because hardware size and weight can be minimized for any fixed flow velocity and flow rate. The density of a given gas can be increased only by increasing pressure or decreasing temperature. The primary objective of the thrust chamber is to increase the enthalpy of the propellants at low Mach number; therefore, cooling the inlet gases is not an efficient method for effecting density increases. As a result, high pressure systems are particularly desirable for gas-gas engines. However, high chamber pressures result in high heat fluxes to exposed interior surfaces. Thus, an important design consideration is injector face cooling because this includes the injector face. Naturally, a design which transfers heat from the face directly to the injected gases is desirable because it accomplishes two objectives simultaneously (e.g., face cooling and propellant heating). If no propellant is injected locally off mixture ratio, no mixture ratio performance loss will be suffered. It is desirable to minimize film cooling flow rates.

While regenerative cooling techniques appear to satisfy all of the requirements, the conventional methods suffer from at least one drawback. A pressure loss is taken in series with the injector and this artificially increases required pump discharge pressures for a given thrust and chamber pressure. Also, there may be insufficient heat capacity in the propellants to cool the chamber, throat, and nozzle. A system which allows regenerative-type cooling to be accomplished without the expense of an extra resistance is the most desirable. Actually, a very "fine" injector pattern is required and if sufficiently small orifices can be placed in close proximity to each other, the injected propellant can cool the surrounding solid material by conduction-convection. Heat accepted at the injector face can be quickly conducted to the orifice wall and convectively carried away by the propellant if the conduction path length is short enough. Naturally, a high conductivity, high melting point material is desirable here because it maximizes the allowable distances involved.

The whole problem finally reduces itself to one of a mechanical method for producing very fine patterns, especially because injector performance increases with the reduction in size of locally high and low mixture ratio zones. Good control must be maintained over the size and location of injector orifices. These characteristics must remain constant over a wide temperature range. For these reasons, materials such as porous metallic alloys and compressed ribbon composites, are not useful as injection faces. A particularly controllable injector design incorporating all of these features utilizes metallic platelets with pre-etched flow channels that are stacked to form a porous wall. The platelets are furnace-brazed together, making a structural unit and eliminating internal leaks inside of the bipropellant injector.

It is possible to construct "radial flow" or "axial flow" platelet stack injectors. The former concept requires a set of thin, flat annular rings, which essentially form part of the chamber wall and allow radial propellant injection into the thrust chamber. The latter design utilizes a set of straight or slightly curved strip platelets set on edge at the forward end of the chamber to form a flat or curved injector face. It injects propellants axially toward the throat.

When dealing with gaseous propellants in a fine-patterned injector at high chamber pressures, several conditions arise which influence the selection of injector configuration. First, there is the physical size of the injector to consider. Low density, gaseous propellants require large flow areas when compared to liquid systems of comparable thrust levels. A high-thrust thrust chamber assembly will require a very large diameter injector if it is of the axial variety (not integrated with the thrust chamber itself). Using a radial injection scheme, it is possible to utilize a large portion of the chamber wall as an active injection surface, which offers many advantages. The entire thrust chamber can be made smaller. Injection area rather than chamber volume is needed for complete combustion and controls the size of the unit. This explains the 11.5-in. characteristic chamber length of thrust chamber assembly No. 8 when minimum L*'s of 5 in. are theoretically allowable. The injector itself, being well-cooled, makes an ideal chamber wall and the more area of a chamber devoted to active injector, the smaller the cooling losses will be for the entire unit. Of course, heat addition at high Mach number is thermodynamically inefficient; therefore, the injector cannot extend very far into the convergent nozzle without incurring performance losses. However, the same cooling method (transpiration) can be used in the high heat flux regions of the nozzle by extending the radial platelet stack beyond the throat and injecting only one propellant as coolant. This design is mechanically efficient because it minimizes injector/nozzle interface and attachment difficulties. After brazing, a monolithic injector/chamber/nozzle results. The platelet stack is terminated in the divergent nozzle at an area ratio, at which the heat flux is low enough for a lightweight cooling mode to be used.

A radial flow platelet injector should be conically shaped so that the forward end of the chamber will be of minimum size and easily coated with a small amount of propellant. In conjunction with the deLaval nozzle, this forms a "Double Conical" chamber shape as shown on Figure No. 75. Fortunately, this shape is nearly ideal from several standpoints. It prevents thermal choking of the combustion gases and propellant flow rate per unit injector area is constant, which makes more reaction products available near the nozzle inlet than at the head of the chamber. In a constant area duct (e.g., a cylindrical chamber) this would result in a continual increase in Mach number from the forward to the aft end of the chamber. In the worst case, the Mach number could reach unity and the flow would choke in the chamber, resulting in unsteady operation. Failing this, a large pressure gradient would exist along the chamber axis. This would cause higher injection velocities and flow densities near the nozzle than exist upstream. The result

would be performance losses resulting from uneven propellant distribution, small effective chamber length, and combustion of a large percentage of propellant at high Mach number when compared with a double-conical chamber of the same size. It is possible to attain constant combusted gas properties (e.g., constant Mach number, velocity, pressure, and temperature) over the full combustion chamber length by selecting the proper injector cone divergence angle. The pressure drop and flow rate across the platelets will be constant at all points, which allows a single platelet design to be used over the entire injector. Further, the over-all configuration more closely approximates a sphere than it does a conical chamber with a flat-faced injector. This is a desirable geometry because platelet stacks are relatively heavy per unit area. This design also eliminates the injector/chamber joint and seal.

Pre-warmed, hypergolic gaseous propellants are expected to react very quickly, especially when injected in a fine pattern. This explains the high injector performance anticipated with small characteristic chamber lengths. The presence of exothermic reactions so close to the injector face provides another reason for care in selecting a well-cooled injector design. The energy release is expected to be rather sudden at high chamber pressures, especially, and the shape of the combustion front will largely be determined by the injector face contour. Low-frequency, or feed system flow stability can be controlled by proper pressure scheduling and system design, but the high frequency, or combustion stability cannot. The latter problem is usually solved by controlling the energy release pattern and the internal chamber geometry. If the regions of high energy release in the chamber are improperly located, they can reinforce small pressure oscillations that normally respond to the natural acoustic modes within that chamber. A cylindrical chamber with a constant injection density, flat-faced injector would be a particularly poor geometric choice for thrust chamber assembly No. 8 because only a small amount of "combustion spreading" is expected over the chamber volume. By way of contrast, a coarse-patterned liquid injection system would not be nearly so sensitive to chamber/injector geometry. In the double conical chamber of thrust chamber assembly No. 8, it is expected that the energy release will occur near the chamber wall (injector face). The conical geometry should not allow any single modal frequency from becoming predominant because there is no single characteristic length (or, therefore, time) associated with the chamber in either the longitudinal or transverse directions. The combustion is spread over the irregularly-shaped chamber as a result of its being injected at all points of the chamber wall. If needed, the injection density can be made non-uniform by proper platelet flow channel design. Also, baffles can be electro-machined into the platelet stack so that they protrude into and along the full length of the chamber. They would be cooled by their active propellant injection and would further spread the combustion over the chamber volume while providing compartments within its internal contour.

The injector and chamber platelets themselves are annular discs formed from Ni-200 sheet that is approximately 0.020-in. thick. The injection orifices are produced by chemically-etching grooves that are

approximately 0.010 in. deep and 0.100 in. wide on one side of the plate. These grooves are evenly-spaced and radially-directed on the inside edge of the platelet and lead to one of eight feed manifolds formed by circular holes in the outer periphery of the annulus. In the built-up stack, these holes form large manifolds running longitudinally within the chamber wall. In the injector portion of the stack, alternate platelets feed fuel and oxidizer. Sixteen such manifolds are required. Eight fuel and eight oxidizer manifolds alternate around the chamber wall. In the fuel transpiration-cooled section of the chamber, the eight alternate manifolds do not carry oxidizer as they do in the injector. Rather, they serve as integral ducts to transfer gasified fuel from the regeneratively-cooled nozzle section to the injector. The fuel inlet torus is located at the minimum chamber diameter region of the throat and feeds into the eight manifolds which serve the transpiration cooling passages. These large manifolds transport the greater portion of fuel (98%) to the two-pass tube bundle, regeneratively-cooled nozzle extension. A manifold collects the fuel, passes it down and back through alternate skirt tubes, and redistributes it to the eight alternate manifolds in the platelet stack. The warmed fuel flows forward through these passages, which become the fuel manifolds in the injector section of the chamber. The oxidizer manifolds are then in line with the fuel inlet manifolds, but are separated at the interface by blank platelet(s). The cooler inlet fuel is available for throat cooling and requires less weight flow than would be needed if it were passed through the regenerative bundle first. The propellant flow rate per unit area required to cool the throat region is dependent upon the coolant inlet temperature, its specific heat, the desired inner wall temperature, as well as the platelet thickness and thermal conductivity. Thus, thin platelets and cool fuel minimize cooling losses. The trade-off between platelet cost and performance losses appears to be in the 0.010-in. to 0.030-in. thick region, but further work in this area is required.

The regeneratively-cooled tube bundle nozzle extension is of double-pass design for two reasons. It eliminates the need for external feed lines and collector manifolding at the large diameter end, having only a lightweight turn around manifold. The latter is integral with the interface flange, to which the radiation cooled nozzle extension is attached. The two-pass system allows twice the coolant velocity in the tubes than does a single-pass system. It permits the nozzle to be extended to a larger area ratio, where the fluid velocity would otherwise be too low to provide a sufficiently high heat transfer coefficient. In this way, the regenerative skirt can be extended to the area ratio, at which a radiation-cooled skirt can operate without film cooling. The reason for using the regenerative section in the nozzle is that it is lower in weight and cost per unit area than a transpiration-cooled skirt would be. Also, it adds to the enthalpy of the fuel without loss of propellant into undesirable areas of the thrust chamber. However, at lower nozzle area ratios, it cannot exist without film cooling, which makes the transpiration cooling mode more attractive for this purpose. At the opposite end of the nozzle, the passively cooled extension is used because of its lighter weight as well as the limited total heat capacity of the fuel.

(2) Structural Design of the Thrust Chamber Assembly

High pressure thrust chambers of medium to high thrust levels develop large hoop and axial loads in the chamber wall. Therefore, it is necessary, from the standpoint of weight alone, to use high strength materials for the load-carrying portion of the thrust chamber assembly. For this reason, a thin walled, high-strength jacket surrounds and supports the injector/chamber/nozzle platelet stack. Otherwise annular platelet thicknesses would be excessive because of the low yield strength of the Ni-200 material. The jacket also provides a convenient member for flanged joints at the thrust takeout and nozzle extension interfaces. The columbium nozzle extension is stiffened at the exit end to minimize the possibility of buckling and/or vibration-induced standing noncircular shapes.

(3) Materials Selection

Propellant compatibility was the main factor involved in the selection of materials for use in the thrust chamber of Engine No. VIII. In particular, compatibility of metals with liquid CLF_5, gaseous CLF_5 at 1000°F, and thrust chamber reaction products dictated material selections for the oxidizer manifold, the oxidizer-rich gas generator, and the thrust chamber. Fabrication and joining techniques within the scope of presently developing technology further limited the range of materials. For instance, non-metallics, such as graphites, were not selected for the point design despite their apparent chemical and thermal compatibilities with the system. However, the low density of these materials makes them appear attractive.

Several materials appear to be compatible with CLF_5 for durations of one hour at 160°F. These include Ni-200, Hastelloy X, Yellow Brass, Monel 400, Inconel 718, 17-7 PH, 15-7 PH, and 347 CRES. Therefore, these materials could be used in the liquid oxidizer system, which involves only the feed system to the oxidizer-rich gas generators. However, compatibility data are relatively scarce at higher temperatures for metals with CLF_5 or any interhalogen oxidizer. It is known, for instance, that 17-7 PH begins to react rapidly with CLF_3 at 1200°F to 1400°F. Generally, even when considering the fluorine compatibility data, it is safe to conclude that Ni-200 will probably display the best compatibility of any common metal with hot CLF_5 rich gases, such as the reaction products of the gas generator. Nickel "A" does not ignite in CLF_5 until 1800°F, for example, and the generator gases will be only 850°F. Although there could be tiny hot streaks in the reaction products, the oxidizer film cooling should keep them away from the wall. The injector platelets will have to handle this same fluid plus 1200°F hydrazine; therefore, Ni-200 is also specified for them. The Ni-Oro braze alloy used to prevent propellant leaks in the injector melts at ≈1800°F and should be sufficiently compatible with the propellants, considering the very small contact area of the partially-alloyed braze material with the oxidizer at platelet edges.

The regeneratively-cooled tubes comprising the first nozzle extension must withstand hot hydrazine and thrust chamber reaction

products, which contain little CL, or F, but much HF. Inconel 625 was selected because of its relatively high strength at 2000°F and its high Ni content. The regenerative tubes carry high pressure, high temperature gases in a low pressure environment; therefore, the individual tubes develop large hoop stresses. A high strength is essential at the 1800 to 2000°F operating temperature.

Columbium is selected for the radiation-cooled nozzle extension because it has been well proven on many engines. It also may prove to be compatible with the cooled, lower pressure exhaust products at large nozzle area ratios. However, if it is not, candidate coating materials are available. Pre-oxidized, aluminide diffusion coatings may be useful because a good bond is attained between the base material and the coating. Aluminum oxide is reported to be relatively immune to fluorine and can be used in H_2 up to 3200°F. Tungsten coatings may be useful, but there are differing opinions about this. In any case, its use would involve a substantial weight increase to the nozzle. The outside of the nozzle would carry one of the well-proven emissivity coatings.

The structural jacket around the thrust chamber must be of a fairly high strength, tough material. It should have a degree of tolerance to the propellants in the case of such considerations as small leaks. A high-strength Inconel, such as 718, is specified.

(4) Heat Transfer Analysis

The cooling requirement for the transpiration section and the throttling capability of the regeneratively-cooled section were analyzed. The basic assumptions used in the analysis of the transpiration-cooled section are identical to those discussed for Engine No. VII. In addition, it was assumed that the decomposed hydrazine gas would be available at 1355°F and that the nickel plates would be capable of operating at 2000°F in the presence of gaseous fuel.

The results of the cooling analysis for full thrust are shown on Figure No. 76 in terms of the total coolant flow required as a function of maximum cooled area ratio. An area ratio of six was selected as the transition area ratio between the regenerative section and the transpiration-cooled section. This results in a 4.3% coolant flow of the total propellant flow.

In analyzing the gas cooled tube bundle, it was assumed that decomposed hydrazine gas was available at 1355°F. A limit of 0.5 Mach number was assumed as being practical for the maximum gas velocity. A two-pass design was selected for the tube bundle to eliminate large manifolding at the exit plane. In addition, it was assumed there is no film cooling effectiveness in the skirt region derived from the carry-over of transpiration coolant flow from the transpiration-cooled section.

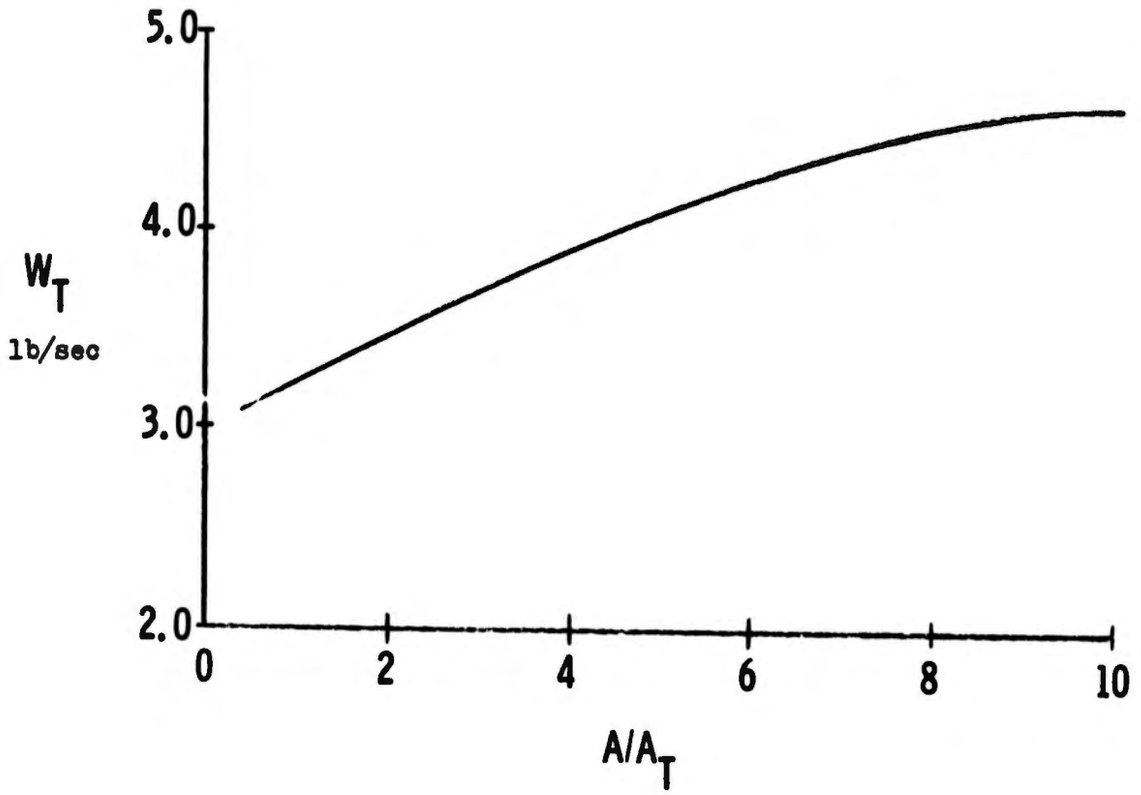

Figure 76. Total Transpiration Coolant Flow (Gaseous Fuel) vs Skirt Attachment Area Ratio, Engine No. VIII

In most applications of regeneratively-cooled tube bundles, the coolant is in the form of a liquid. Throttling with a liquid is limited because the heat transfer to the coolant decreases proportionally with pressure to the 0.8 power while the available coolant decreases directly with chamber pressure. However, in the case of Engine No. VIII, the coolant is a gas which is much more amenable to throttling. For a gas, the density decreases with pressure and increasing temperature; therefore; it is possible to maintain coolant velocity in the tubes as the engine is throttled.

A major difficulty in designing the gas-cooled skirt is that the tubes must be analyzed over the entire range of operating conditions to determine where the design limits are reached or exceeded. Originally, it was planned to extend the gas-cooled section to area ratio 80, the attachment point for an uncoated columbium chamber, but for the best possible tube design (in terms of geometry and number of tubes), it was found that the throttling limit of the design was only 4.4:1. The limiting factor being the tube wall temperature at the downstream end of the tube bundle. Coated columbium nozzle extensions were evaluated in another program.(10) Lunite 2(11) and Lunite 3(12) were found to be highly successful. If coated columbium is used for the radiation-cooled skirt, the attachment point is area ratio 50 and the gas-cooled tube bundle is capable of the required 10:1 throttling.

Figure No. 77 shows both designs in terms of the limiting parameter (maximum tube wall temperature) as a function of chamber pressure. Figure No. 78 shows the tube wall temperature profile for the 50:1 design at full thrust along with the upstream and downstream tube geometries. Note that the final design consists of 220 tubes with wall thicknesses varying between 0.015-in. and 0.035-in.

(5) Turbopump Configuration

The turbopump for Engine No. VIII is a single-stage turbine. The details of its design and the basis for the turbopump weight calculation are presented in Appendix VI (Part II of this report).

(6) Controls System Description

(a) General Requirements

The basic control elements for Engine No. VIII are the oxidizer and fuel ring-gate combination shut-off and throttling valve, which are integral with the turbopump assembly, and the gas generator mixture ratio control valve located in the fuel feed line leading to the gas generator assembly. These components are indicated on the control system schematic of Figure No. 79. Location of the ring-gate valves within the turbopump assembly eliminates the need for a collector manifold at the final stages of the pump to direct the discharge flows to the throttling valves. This integrated pump and valve assembly design assists in keeping over-all engine weight to a minimum because of the reduced wall thicknesses required for the relatively smaller diameters at the high system pressures which are being utilized. Additionally, the incorporation of primary throttling valve flow control at the discharge of

(10) Contract F04611-67-C-0003
(11) Lunite 2 is an aluminide diffusion coating from the VAC-HYD Processing Corp.
(12) Lunite 3 is a hafnium-tantalum diffusion coating from the VAC-HYD Processing Corp.

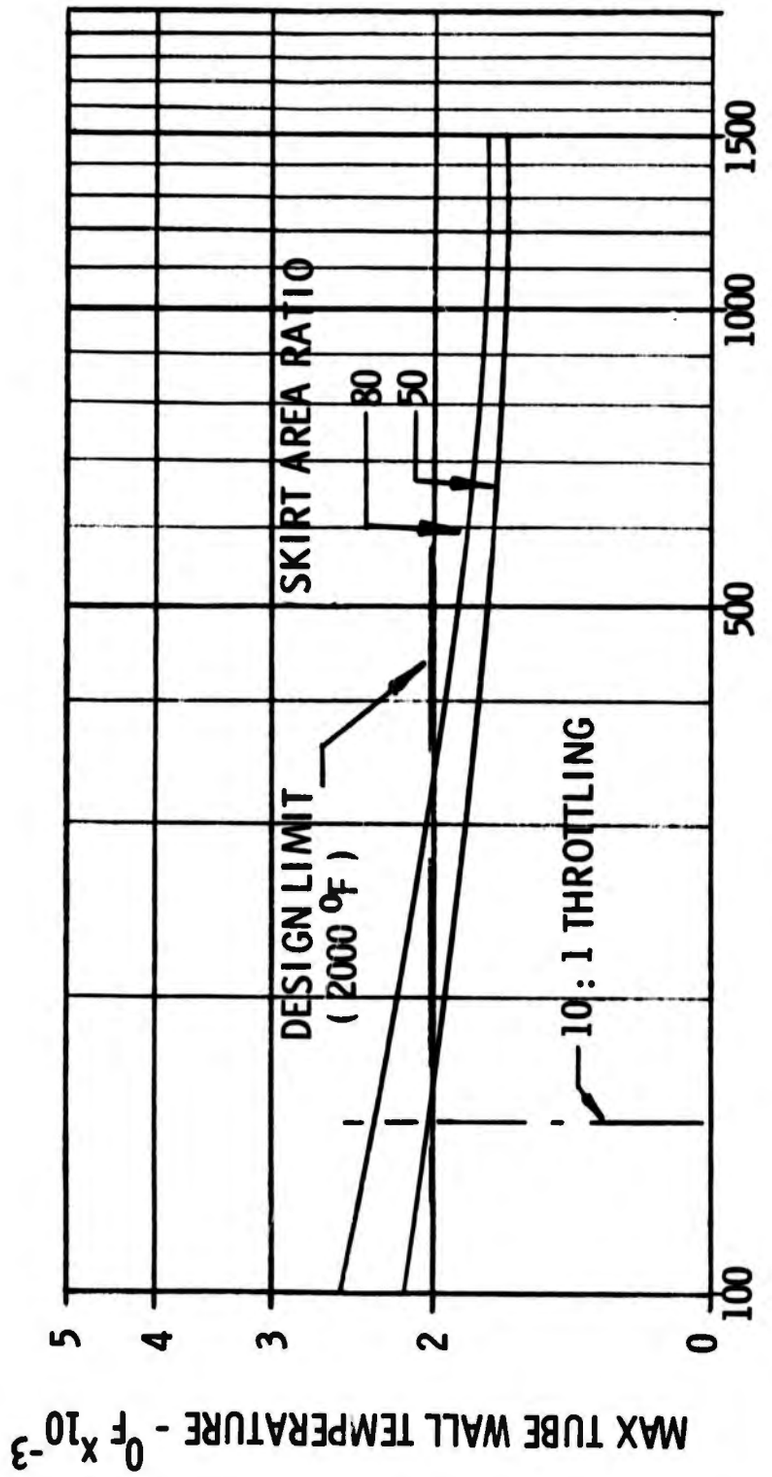

Figure 77. Engine No. VIII Gas-Cooled Skirt Throttling Limit

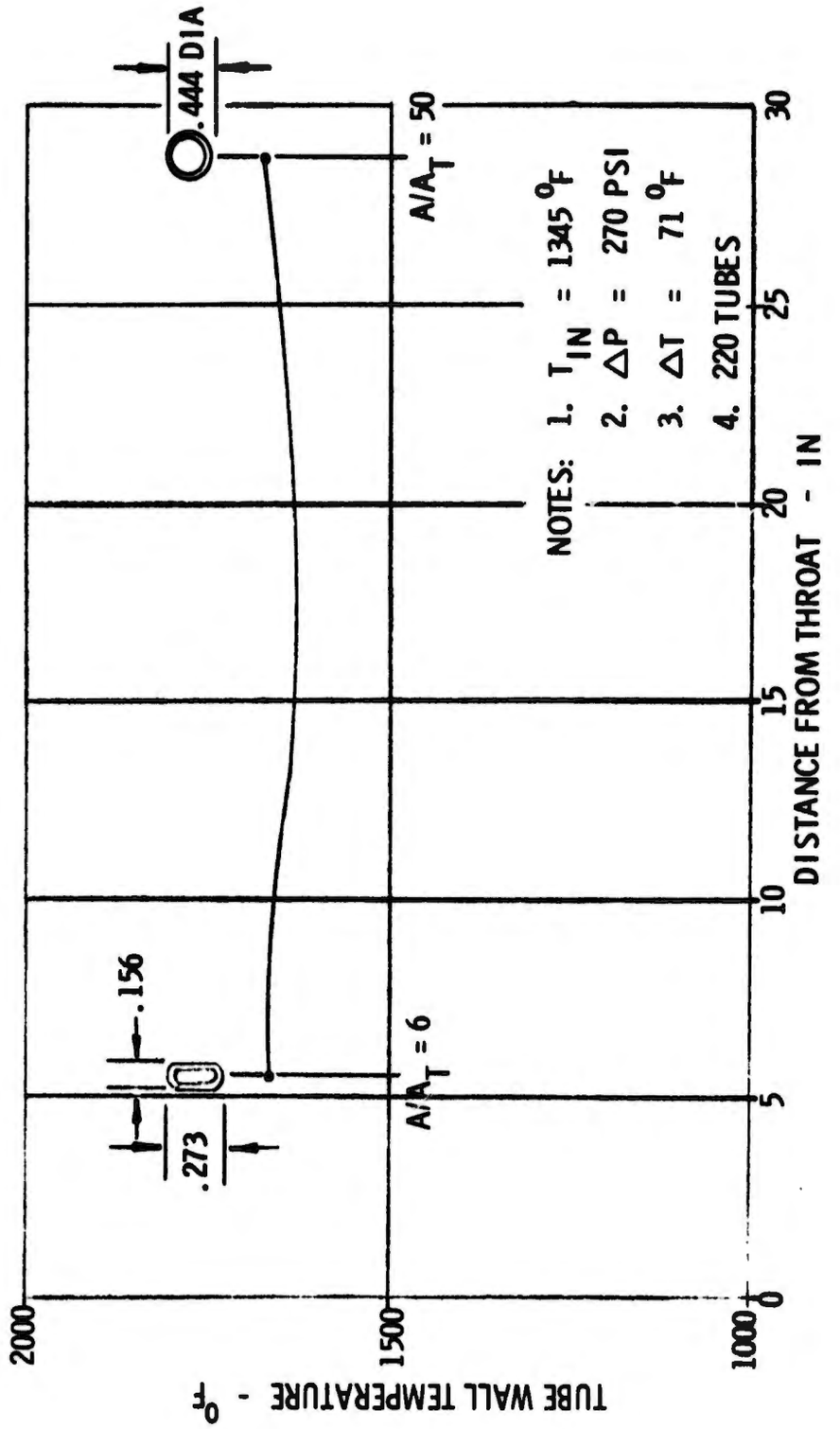

Figure 78. Gas-Cooled Skirt, Full Thrust, Engine No. VIII

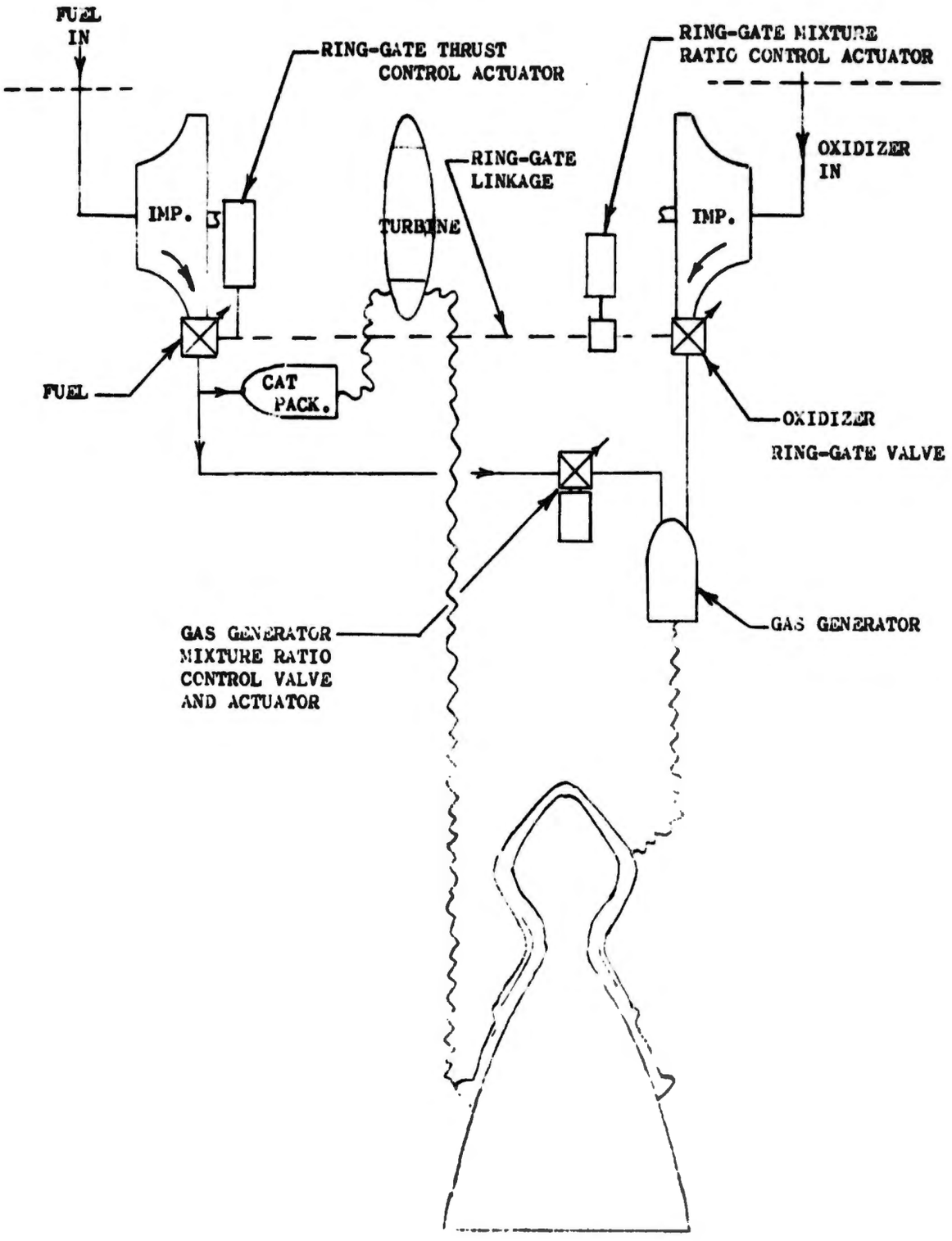

Figure 79. Control Schematic, Engine No. VIII

the pump impellers makes it possible to maintain pump operation outside of the stall regions during transient conditions. The oxidizer and fuel ring-gate valves will be mechanically-linked for reliable phasing during engine starting and shutdown transient operation as well as during throttling and mixture ratio control operations. The ring-gate valve system and the separate gas generator mixture ratio control valve will be electrically-operated in compliance with the criteria established at the outset of this study.

Potential system interactions between the throttling and mixture ratio control systems makes it necessary to include sufficient flexibility in the over-all control system so that response time and damping factors can be matched for system stability. This flexibility is obtained by incorporating proportional control in all of the control valve actuators (i.e., ring-gate valves and gas generator mixture ratio valve). Although an extensive investigation of engine system requirements could ultimately show that proportional control is not required for all actuators, it is assumed for the purposes of this study that this capability will be provided for maximum flexibility.

(b) Start and Shutdown Operations

A schematic representation of the main engine throttling and mixture ratio control elements is shown on Figure No. 80. The ring-gate valves, which are integral with the turbopump assembly, are instrumental in controlling the start and shutdown transient operation of the engine. The engine is started by opening the fuel ring-gate throttling valve to permit fuel under tank pressure head to flow through the turbopump assembly to the catalyst package. The resulting reaction of fuel with the catalyst bed generates hot gas which drives the turbopump assembly turbine to accelerate the turbopumps. After sufficient turbopump assembly speed is achieved (sensing parameters can be turbopump speed, or pump discharge pressure), the oxidizer ring-gate valve is opened to initiate flow of the oxidizer to the gas generator. After a sufficient oxidizer lead has been established in the gas generator as a function of elapsed time from valve opening, the gas generator mixture ratio control valve is opened to initiate flow of fuel to the gas generator. The engine now accelerates to a steady-state operating condition. This sequence is reversed for engine shutdown. To ensure proper time sequencing of the ring-gate valves and gas generator mixture ratio control valve during start and shutdown operation, a relay sequencing control panel will be included in the conditioning control elements of "C" shown on Figure No. 80.

(c) Engine Throttling

The callouts indicated in the ensuing discussion are shown on Figure No. 80.

Throttling control Actuator No. 1 is connected to the fuel and oxidizer ring-gate valves through shaft Linkage B and Differential D. As long as the output pinion gear of engine thrust control

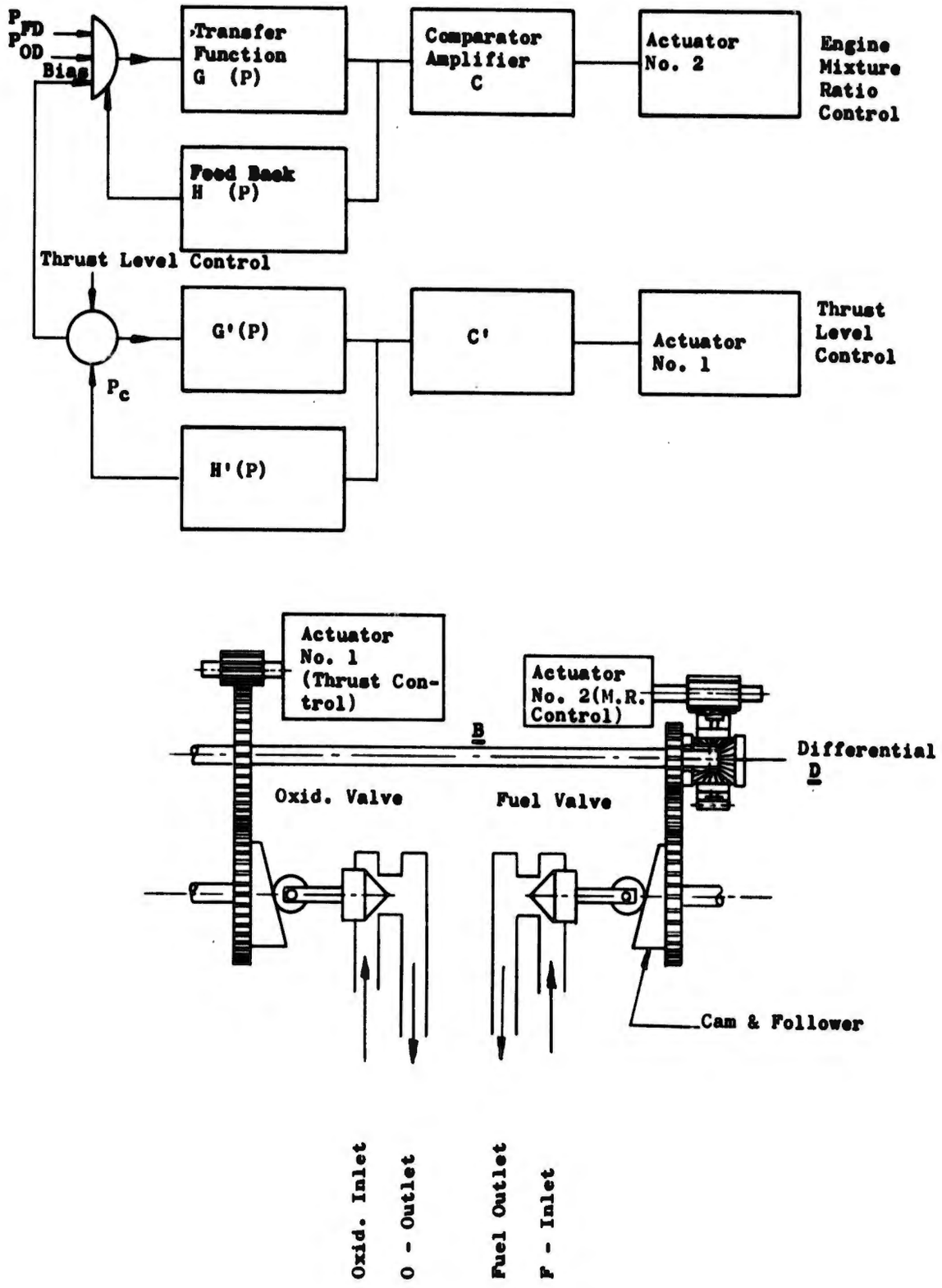

Figure 80. Engine Throttle and Mixture Ratio Control Schematic

Actuator No. 1 is free to rotate (i.e., its clutches are de-energized for zero output force), Actuator No. 2 acts only upon the fuel ring-gate valve. This permits the fuel valve to be opened first at engine start-up to accomplish the engine start transient operation described above. When sufficient fuel lead during starting is obtained, the motor and opening clutch of Actuator No. 1 are obtained, the motor and opening clutch of Actuator No. 1 are energized. This transmits power through mechanical Linkage B to open or close the oxidizer and fuel valves together as a function of control established by the control programmer.

(d) Mixture Ratio Control of Main Engine

Proper mixture ratio control will nominally be maintained during engine throttling by the simultaneous cam actuation of the linked ring-gate throttling valves; however, if environmental, catalytic, or other deviations in engine balance should affect mixture ratio, a relative change in the ratio between fuel and oxidizer system pressures at the injector inlet will be sensed by the pressure transducers (Pf_i and Po_i). Output signals from these transducers will be summed in the input to the mixture ratio control amplifier (Block G (P) on Figure No. 80). Control power will then be applied to the forward or reverse clutch of Actuator No. 2 to effect the proper phase displacement between oxidizer and fuel ring-gate throttling valves until the proper ratio of Pf_i to Po_i is obtained.

If different ratios of Pf_i to Po_i are required at different thrust levels, a biasing signal as a function of chamber pressure P_c can be used for compensation (see Figure No. 80).

(e) Mixture Ratio Control of Gas Generator

The gas generator mixture ratio control valve will maintain the proper ratio of gas generator fuel to oxidizer flow for controlling gas generator operating temperature. Engine line resistances are constant; therefore, it is possible that gas generator mixture ratio control will automatically be achieved with the control of main engine mixture ratio, thereby eliminating the need for a separate generator control. In any case, it is anticipated that the gas generator mixture ratio control valve would only be a device to provide trimming function to compensate for system interactions during main engine throttling excursions.

The control loop will consist of a temperature sensing transducer (or transducers) in the gas generator to signal through operational amplifiers any need for more or less fuel to maintain the desired temperature. Power will be applied to the electro-mechanical actuator of the gas generator mixture ratio control valve to open or close the valve as required for throttling.

(f) Control Network Function

Figure No. 81 is a simplified functional representation of the way that various control sensors are interconnected. These segments of the control system are discussed in relationship to the three basic control functions (i.e., main engine throttling, main engine mixture ratio control, and gas generator mixture ratio control).

1 Actuator No. 1 - Thrust Level Control

The bridge control circuit for thrust level control consists of:

Thrust Level Control Input
Chamber Pressure (P_c)
Adjustment Potentiometers (ADG)
Comparator and Amplifier
Bias Resistances

Thrust level control input can be programmed either as a direct thrust change (i.e., 50% to 70% thrust) or as controlled thrust to establish and maintain a desired rate of acceleration (i.e., from 5 g's to 10 g's at a maximum rate of 0.1 g sec/sec and to maintain 10 g's acceleration once achieved). For this type of control, acceleration (g's) would be used as the input parameter to the engine thrust control system. The rate of acceleration would be established by the vehicle guidance package which, in turn, signals the engine thrust control system for proper modulation of engine thrust.

Bridge configuration control is a simple means for interconnecting various control parameters to permit detection not only of individual magnitudes but also changes in parameter ratios as indicated by polarity change or direction change.

A way of changing engine thrust by means of varying input is represented on Figure No. 81 by a variable resistance. Chamber pressure is sensed by one or more strain gauge type pressure transducers. These transducers include temperature compensating and balancing circuitry. Because of the wide pressure ranges involved, it may be necessary to use double ranging techniques with two transducers to provide adequate control resolution. Sensors are available in the -65°F to 600°F temperature range. Adjustment potentiometers are included for balancing control.

The polarity and magnitude of the bridge being balanced is detected, compared, and amplified by a comparator and amplifier system to excite the proper respective magnetic clutch in the actuator control circuit.

It is conceivable that the ratio of chamber feed pressures corresponding to the desired mixture ratio could vary with engine

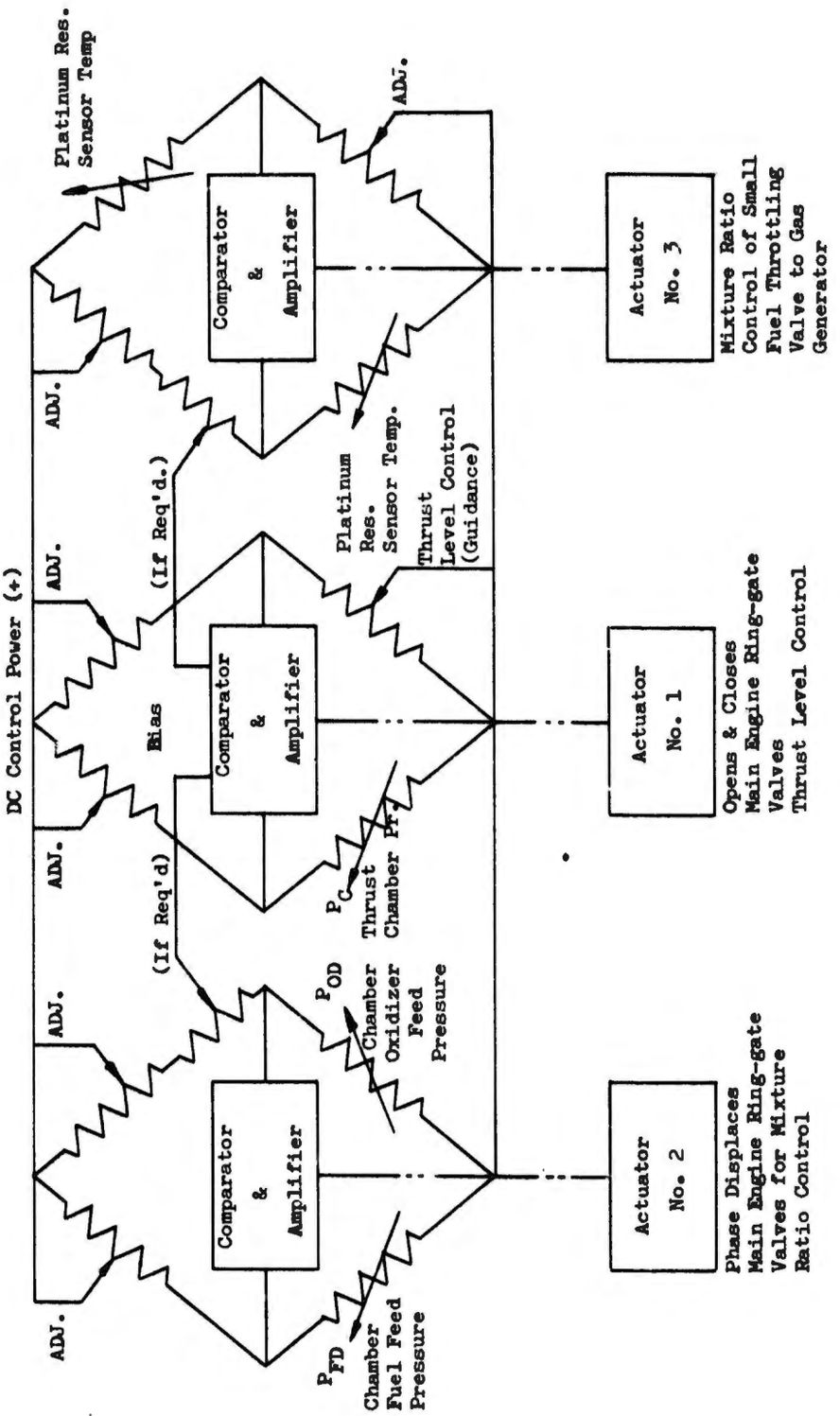

Figure 81. Thrust Level and Mixture Ratio Control (Elementary)

throttling and thrust variation. If necessary, bias values can be introduced into the electronic control network to compensate for this phenomenon.

A change in the Thrust Level Control will unbalance the potential between points C and D (see Figure No. 81). The comparator will sense the value and direction of the imbalance and signal the respective Actuator No. 1 clutch to close or open the main engine ring-gate throttling valves. The resulting variation in chamber pressure (P_c) will produce a change in transducer output value to match the imbalance and restore the bridge to a zero potential between terminals C and D.

2 Actuator No. 2 - Main Engine Mixture Ratio Control

The bridge circuit for this control consists of essentially the same circuit and types of sensors as used for Actuator No. 1 (see Figure No. 81).

Chamber inlet pressure transducers (Pf_1 and Po_1) measure pressure levels that will vary with engine thrust level. The amount and direction of such variation will cause a bridge imbalance between terminals A and B. The comparator will sense and amplify the difference of the two and will actuate the proper respective clutches in main engine mixture control Actuator No. 2 to rebalance the bridge.

3 Actuator No. 3 - Gas Generator Mixture Ratio Control

The bridge circuit for this control is essentially the same as described for Actuators No. 1 and No. 2 above; however, in this case temperature (rather than pressure) will be used for a control parameter. Temperature transducers will sense gas temperature in the oxidizer gas generator to provide the desired temperature control. Location of these transducers in the gas generator can be critical; therefore, more than one transducer is considere' necessary. Platinum temperature resistance sensors are indicated on Figure No. 81; however, thermocouples could be used by changing the bridge from resistance to potentiometric measurement.

Figure No. 81 is illustrative only of the elementary control concepts. The general use of potentiometric measurement might be advantageous. This would result in solid state control components being substituted for the bridge resistances.

Detailed analysis may indicate the advisability of simplifying actuator control by using servo motors, torque motors, or stepper motors; however, from the aspect of maximum control flexibility, all three actuators are assumed to contain two magnetic particle clutches rotating in opposite directions and are coupled to a common output spur gear.

(g) Component Description

The linear motion of the valve ring-gate for the fuel and oxidizer turbopumps is achieved by a slotted cam and drive bearing assembly. A drive bearing is attached to each of the six ring-gate extension rods extending from within the high pressure portion of each end (fuel and oxidizer) of the turbopump assembly. Each of these drive bearings rides with a cam slot in the valve actuating cam ring at six points, 60-degrees apart. The cam slots are contoured to provide the desired valve ring-gate opening and throttling characteristics for a given actuator input motion. The ring-gate member is restrained from rotating by bearing support afforded to the six ring-gate extension rods by the turbopump housing. Driving force is imparted to the cam ring by direct gearing to an externally-mounted actuation system.

A mechanical linkage will be provided in the engine assembly to connect the fuel pump throttling valve to the oxidizer pump throttling valve for positive and reliable phasing of valve operation during all transient, throttling, and mixture ratio control operations. This mechanical linkage system consists of a gear drive connected by a common rotating drive shaft to the fuel and oxidizer ring-gate valves. Actuation power for this system is provided by two separate, electromechanical, servo actuators external to the turbopump assembly and operating through self-contained planetary gear trains. The operation of the thrust control actuator will move both the fuel pump throttling valve and oxidizer pump throttling valve open or closed depending upon the direction of the force application. This control capability is used to open and close the primary pump throttling valves to achieve variable thrust control. The variation of mixture ratio is achieved by operating the separate mixture control actuator which results in a movement of the fuel pump throttling valve independent of the oxidizer pump throttling valve. The operation of this actuator in one direction or the other will then vary the mixture ratio alternately from slightly fuel-rich or oxidizer-rich conditions as they occur to maintain mixture ratio within the desired operating tolerances.

Each of the two separate electro-mechanical actuators for engine thrust and mixture ratio control are powered by 26 volt dc electric motors (see Figure No. 82). The ring-gate throttling valves of the fuel and oxidizer turbopumps are opened by applying power to the motor and "opening" clutch of the throttling control actuator. Position of the actuator output drive shaft (and valves) can be modulated within the range of 0 to 100% of full travel for variable thrust control by alternate application of electrical power to the two (opening and closing) magnetic powder clutches. This effects a modulating control of valve position corresponding to an input signal from the control programmer. The throttling valves are closed by applying electrical power to the "closing" clutch. The separate electrical actuator for mixture ratio control will operate similarly to maintain engine mixture ratio by controlling the fuel ring-gate valve independently of the oxidizer valve.

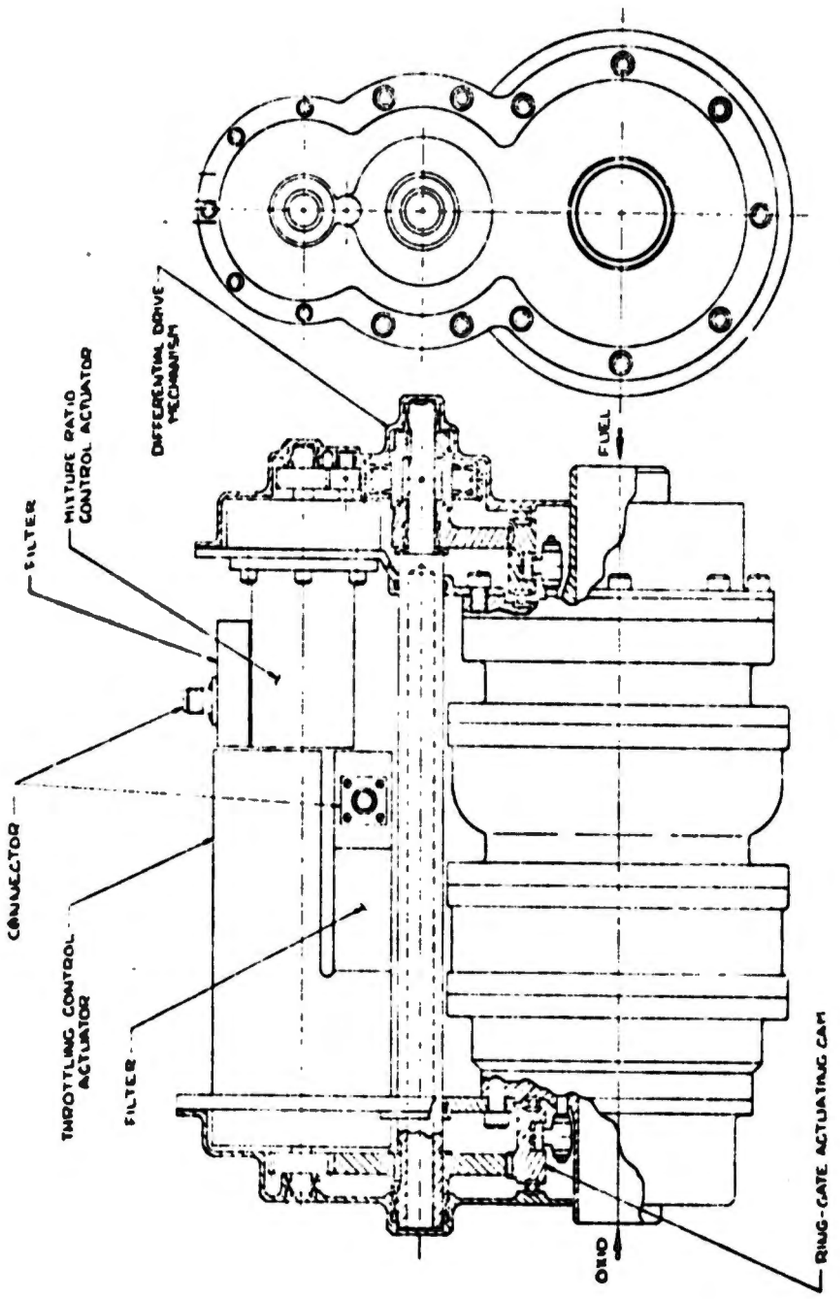

Figure 82. Pump Control, Actuator and Drive Linkage

The use of an electrical actuator offers the advantage of high reliability in a space environment by eliminating any requirement for hydraulic or pneumatic actuating fluid which could possibly deplete itself through leakage. The electrical actuators will provide positive control of valve positions in response to input signals. An additional and significant advantage of the electrical actuation system is the inherent cleanliness and ease of operation afforded during engine system checkout operations because only electrical power need be supplied to operate the control valves.

The electric motors in the actuators would be similar in design to the 26 volt dc, compound-wound, uni-directional motor used in the Apollo Service Module propulsion thrust vector control system developed by Aerojet-General. It will be capable of continuous operation in space vacuum for a considerably longer duration than any anticipated duty cycle and will be energized only to position the ring-gate throttling valves during engine firing. If a combined period longer than 20 minutes in hard vacuum becomes an operating requirement, brush life could conceivably become a problem with the dc motor. In this event, the selected motor design will be a two-phase or three-phase ac type. The thrust control actuator will require a motor rated at 0.13 horsepower, and the mixture ratio motor will be rates at 0.05 horsepower. These horsepower determinations are based upon valve excursion times of 0.6 sec (close-to-open and open-to-close).

The primary control elements in the electro-mechanical servo actuator will be two magnetic particle clutches. The clutches will be of the same basic design as clutches currently being used in the Apollo electrical gimbal actuators. These clutches are relatively simple in construction and consist of an input member, magnetic powder, low inertia drive disc and output shaft assembly as well as the associated bearings and end fittings required for mounting and sealing the entrapped powder. When control power is supplied to the coil, magnetic field action in the gap makes the powder a relatively solid mass, thereby coupling the output member to the input member. This type of clutch can be operated in the slip condition with negligible wear on the metallic surfaces in the clutching space. The motor drive shaft is geared to the clutch input shafts so that the inputs rotate in opposite directions. The clutch output shafts are similarly geared to the actuator output shaft. A small quiescent current is supplied to both clutches for balancing. The direction of actuator (and ring-gate valve) movement depends upon which of the two clutches is engaged and because the clutches are balanced with both carrying a small current, actuator and valve positioning response is fast. Control will be proportional and actuator/valve velocity feedback can be included if this degree of position accuracy is warranted. Valve/actuator position transducers will be included in both the thrust control and mixture ratio control actuators.

Alternative motor concepts can be entertained if digital power pulses could be obtained from the guidance package (i.e., stepper motors). This would eliminate the magnetic powder clutches but would introduce an over-all weight penalty.

The concept of using magnetic powder clutches is preferred because this approach has historically proven to give the greatest power density structure for electro-mechanical actuators used in conjunction with non-balanced valve configurations. All components selected are within current technological design practice.

Candidate seal designs for the ring-gate shut-off seal are shown on Figures No. 83, No. 84, and No. 85. These are all-metal designs to provide compatibility with Compound A. The toggle seal configuration shown on Figure No. 83 utilizes a flexible, circumferential beam (flange) member in the nose of the ring-gate to seal against the seat area which is integral with the turbopump housing. Deflection of the sealing flange effects a radial compressive load of high unit force with a minimum seating force applied to the ring-gate. Deflection of the sealing flange is confined to safe stress levels by an extension on the nose of the ring-gate which serves as an end position stop during ring-gate valve closure. The seat area of the fuel turbopump housing is tin-plated to provide a material which is relatively softer than the ring-gate for good sealing characteristics; the seat in the oxidizer turbopump will be plated with copper. These plating techniques also apply to the seats in the ring-gate designs subsequently described. An alternative shut-off design is the wedge seal shown on Figure No. 84. This configuration effects a sealing action by the contact of a conical sealing surface on the nose of the ring-gate with a mating seat area integral with the turbopump housing. A high unit loading would be achieved by providing a small included angle between the ring-gate taper and the mating seat surface to form a line contact.

A third alternative configuration for the shut-off seal is shown on Figure No. 85. In this design, a rounded nose in the ring-gate contacts the seat surface in the turbopump housing to form a line contact for sealing.

The ring-gate, actuating cam, drive gears, and associated linkage will be made of 17-4 PH because of the high strength and compatibility of this material. All surfaces subjected to high unit contact loading can be flame-hardened for maximum wear resistance if necessary; the surfaces would include the gear teeth and cam bearing surfaces.

The actuator designs described are identical in basic concept and operating principles to the electro-mechanical actuation system developed by Aerojet-General for the Apollo Service Propulsion System. The Apollo actuator uses a 1.5 hp 26 vdc motor in conjunction with magnetic particle clutches and a ball screw drive.

The ring-gate valve movable sleeve element is similar in concept to that of the sleeve-gate thrust chamber valve developed for the LO_2/LH_2 M-1 engine. The M-1 sleeve-gate valve effects a shut-off by forcing the nose of a sleeve element against a Kel-F seal retained in the

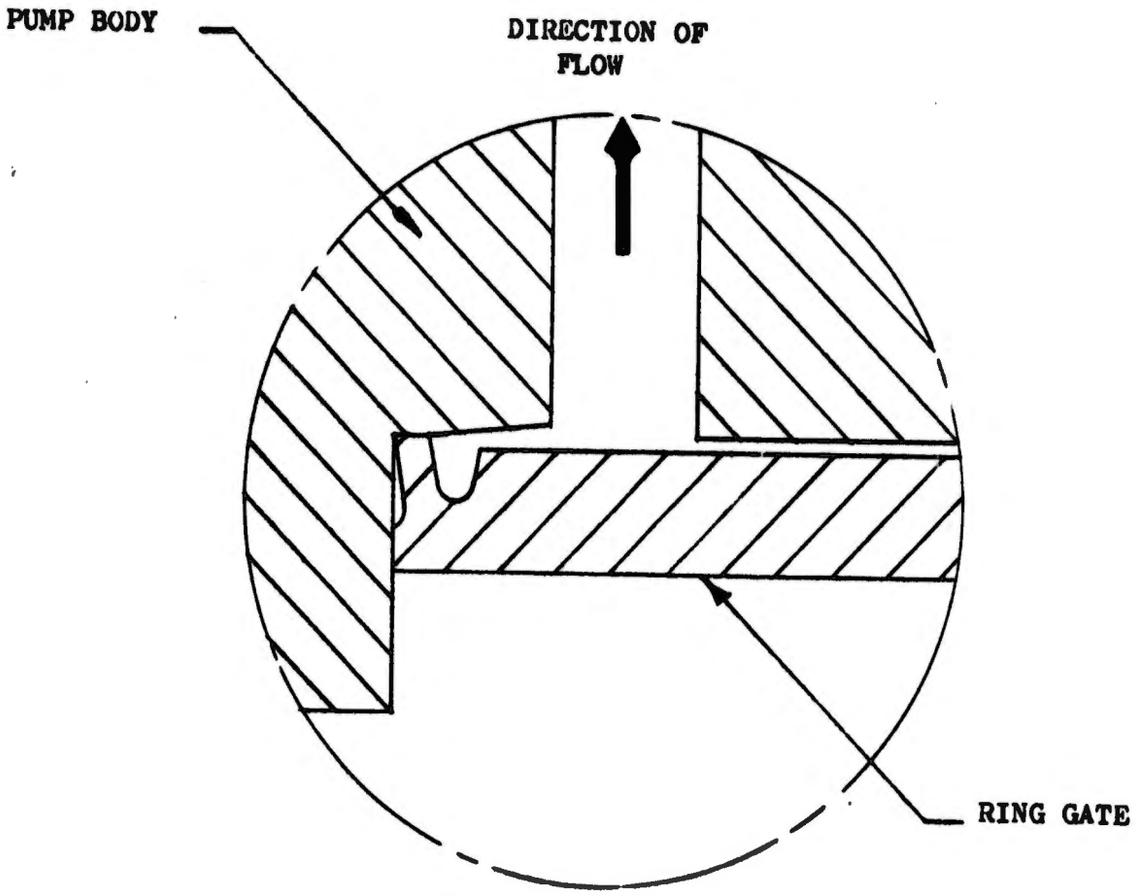

TOGGLE SEAL

APPROX. 10 X SIZE

Figure 83. Toggle Seal

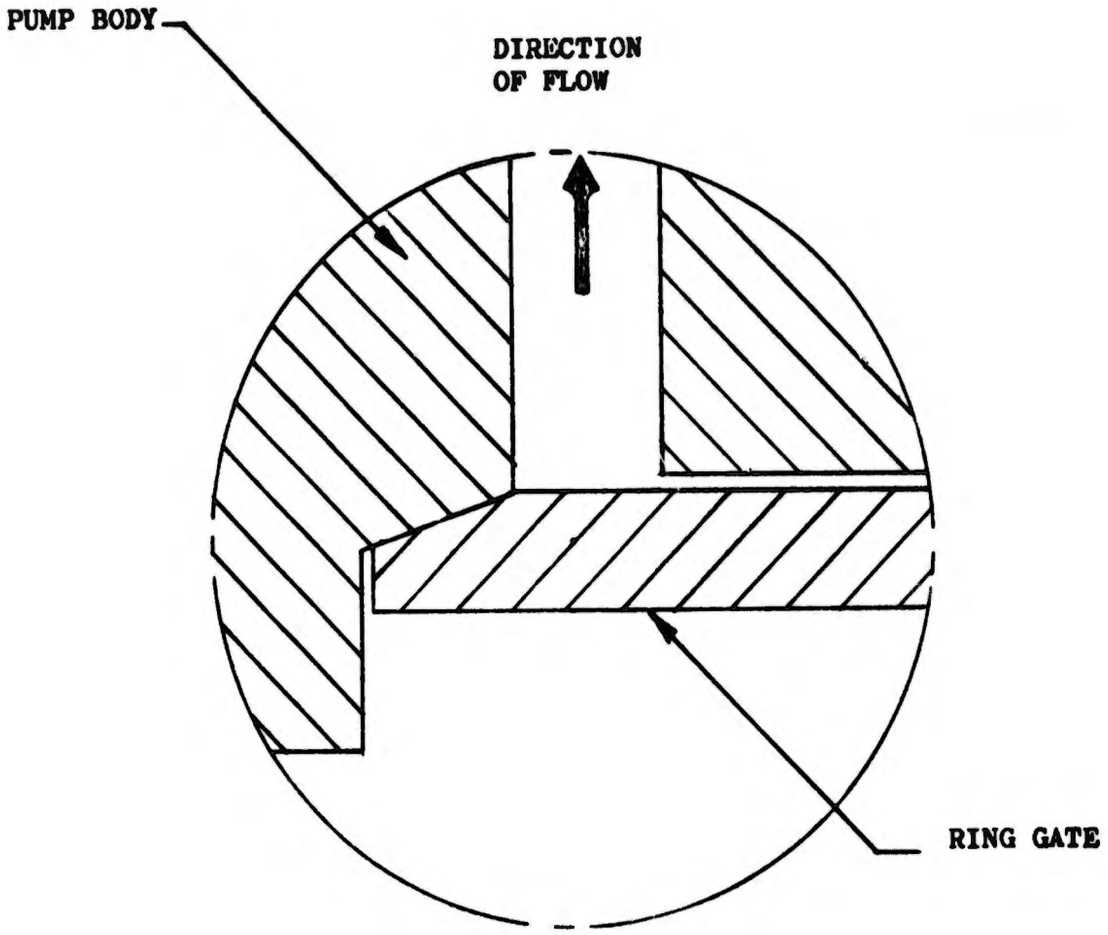

WEDGE SEAL

APPROX. 10 X SIZE

Figure 84. Wedge Seal

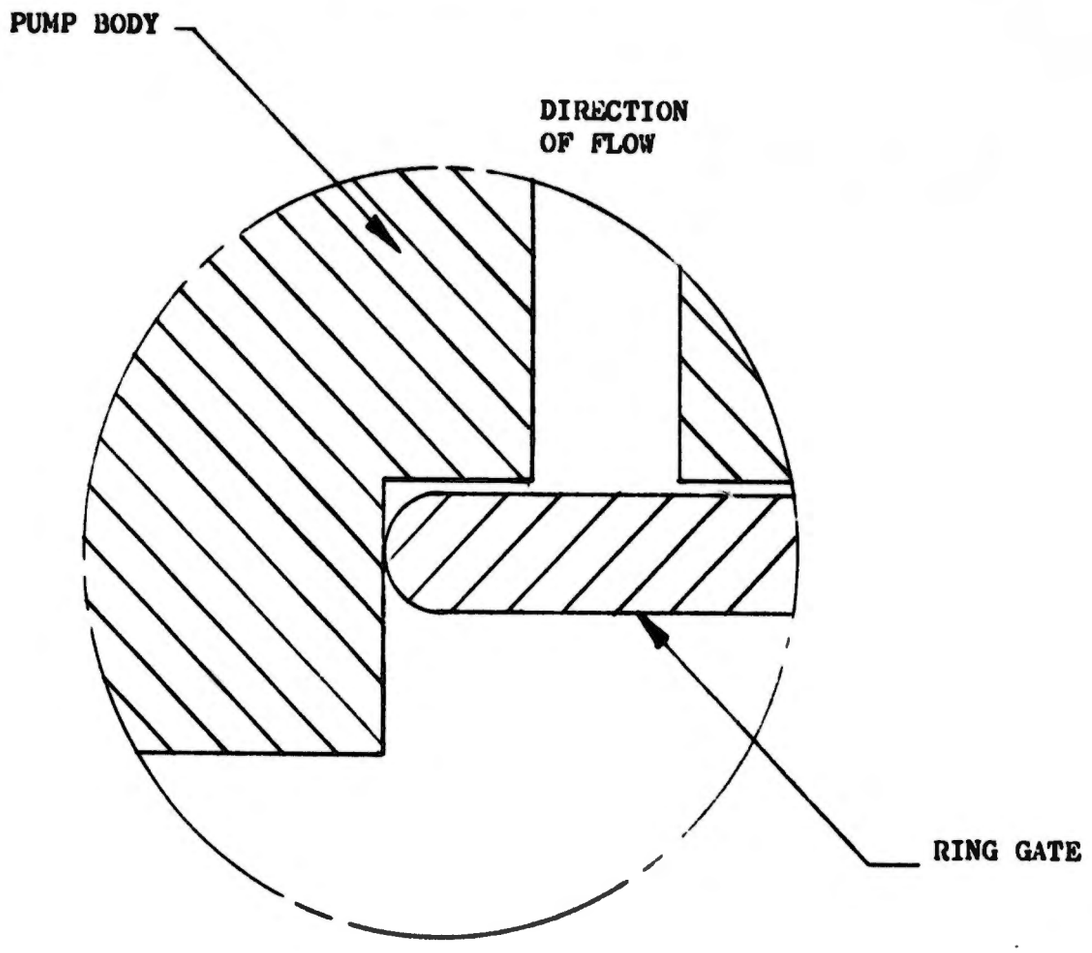

POPPET SEAL

APPROX. 10 X SIZE

Figure 85. Poppet Seal

valve body. Compatibility considerations with regard to the Compound A oxidizer precludes the use of non-metallics in the Compound A/N_2H_4 engine oxidizer ring-gate valve. For this reason, a copper plating of the seat area (in the pump housing) is selected. Although tin plating of the shut-off seat area in the fuel pump can be used, it would also be possible to use Teflon in the fuel system if the superior sealing characteristics of this material appear desirable.

The gas generator mixture ratio control valve was shown on Figure No. 11. This is a balanced poppet valve with a contoured pintle to provide the desired flow characteristics for various valve positions to maintain gas generator mixture ratio in response to temperature feedback signals.

(h) Weight Summary of Complete Control System

The weight summary tabulations presented below do not include the weight of the turbopump ring-gates as they are considered a part of the turbopump assembly. The ring-gate control system will interface with the turbopump assembly at the point where the ring-gate actuating rods extend from within the turbopump housing. The weight of the ring-gate valve, actuator, and linkage control system will include everything except the ring-gate elements. Weight values for the entire control system are tabulated as follows:

Item		Weight, lb
a.	PUMP CONTROL (Ring-Gate System)	
	Engine Mixture Ratio Control Actuator (Electrical)	4.0
	Engine Thrust Control Actuator (Electrical)	6.0
	Actuation Linkage (Mixture Ratio and Thrust Control)	6.3
b.	GAS GENERATOR MIXTURE RATIO CONTROL	
	Valve	1.5
	Actuator (Electrical)	2.0
c.	TRANSDUCERS, AMPLIFIERS, AND HARNESS	9.0
	TOTAL CONTROL SYSTEM WEIGHT	28.8

(7) Engine Performance

(U) The performance of Point Design Engine No. VIII was calculated utilizing the procedures delineated in Appendix II (Part II of this report). The engine and thrust chamber assembly performance is presented on Figure No. 86 for various mixture ratios and coolant flows using the propellant combination CLF_5/N_2H_4. This led to the optimum performance levels shown on Figure No. 87, which indicates performance levels for nickel as well as graphite platelets using the same propellant combination. Similar information for the propellant combination CLF_5/MHF-5 is shown on Figures No. 88 and No. 89.

(U) Engine No. VIII has the highest calculated performance of any of the eight engine concepts because of its short chamber length and the low ERL of the gas/gas injection system.

(8) Engine Capabilities and Limits

(a) Throttling Capability

(U) This engine concept can completely satisfy the 10:1 throttling requirement. The problem of propellant flashing at low chamber pressure does not occur because all propellants enter the thrust chamber in the gaseous phase. Fill times of the cooling and injector manifold are much shorter than in liquid systems and will result in decreased start and shutdown transients.

(b) Burn Duration

(U) As is the case for all the actively-cooled chambers, no inherent burn duration is assumed. However, for carbon-containing fuel, this engine may be duration limited as a result of clogging in the injector or coolant passages.

(c) Installation

(C) This chamber operates at an elevated skin temperature of 800°F to 1000°F depending upon the burn duration; therefore, it presents somewhat of a problem for buried installation. However, this is a problem that is quite similar to ablative cooled engines and it is expected that thermal insulation will be sufficient to protect the system from excessive heat inputs.

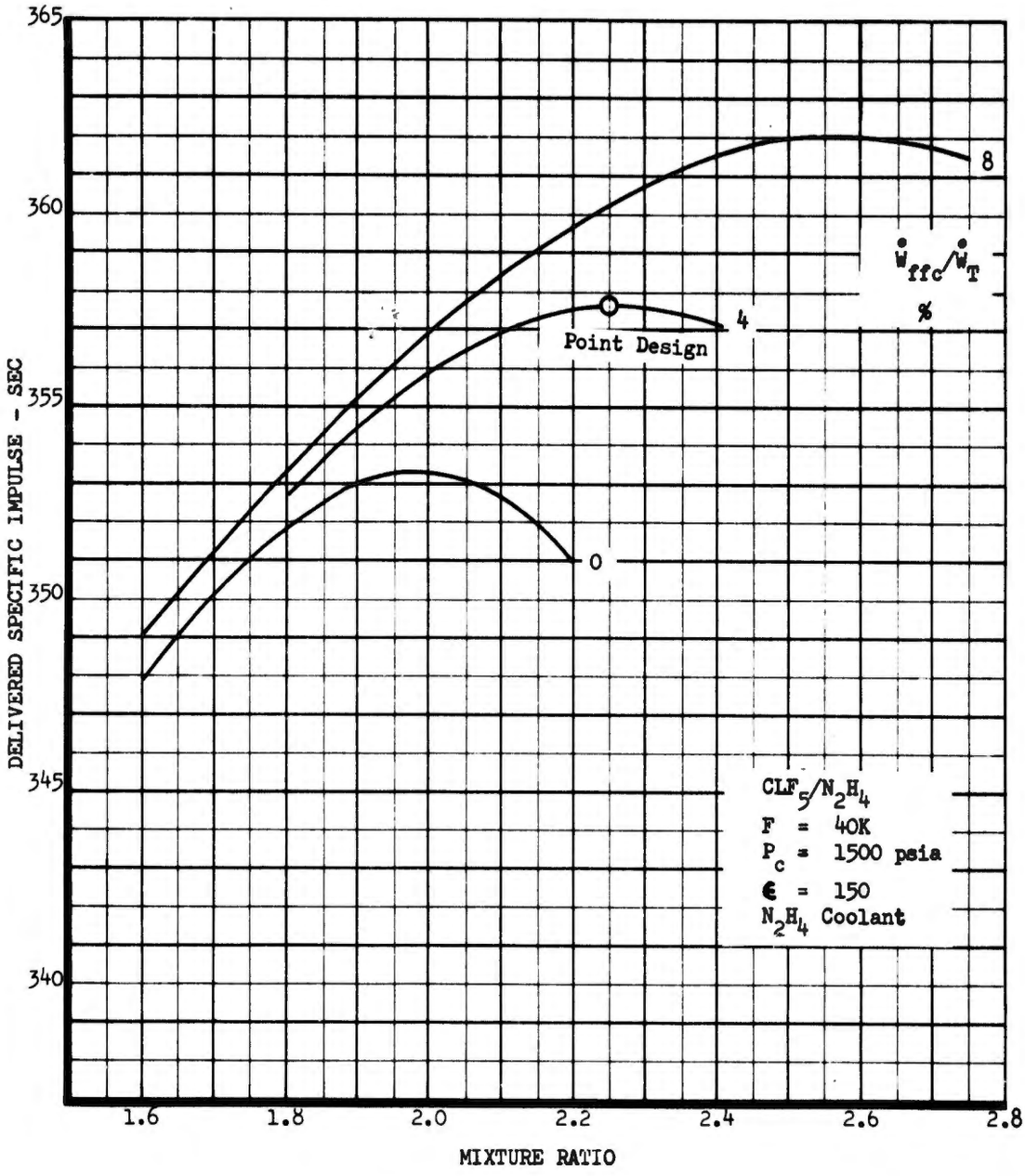

Figure 86. Point Design Engine No. VIII, Performance/Mixture Ratio-Coolant Trade-Off (CLF_5/N_2H_4) (u)

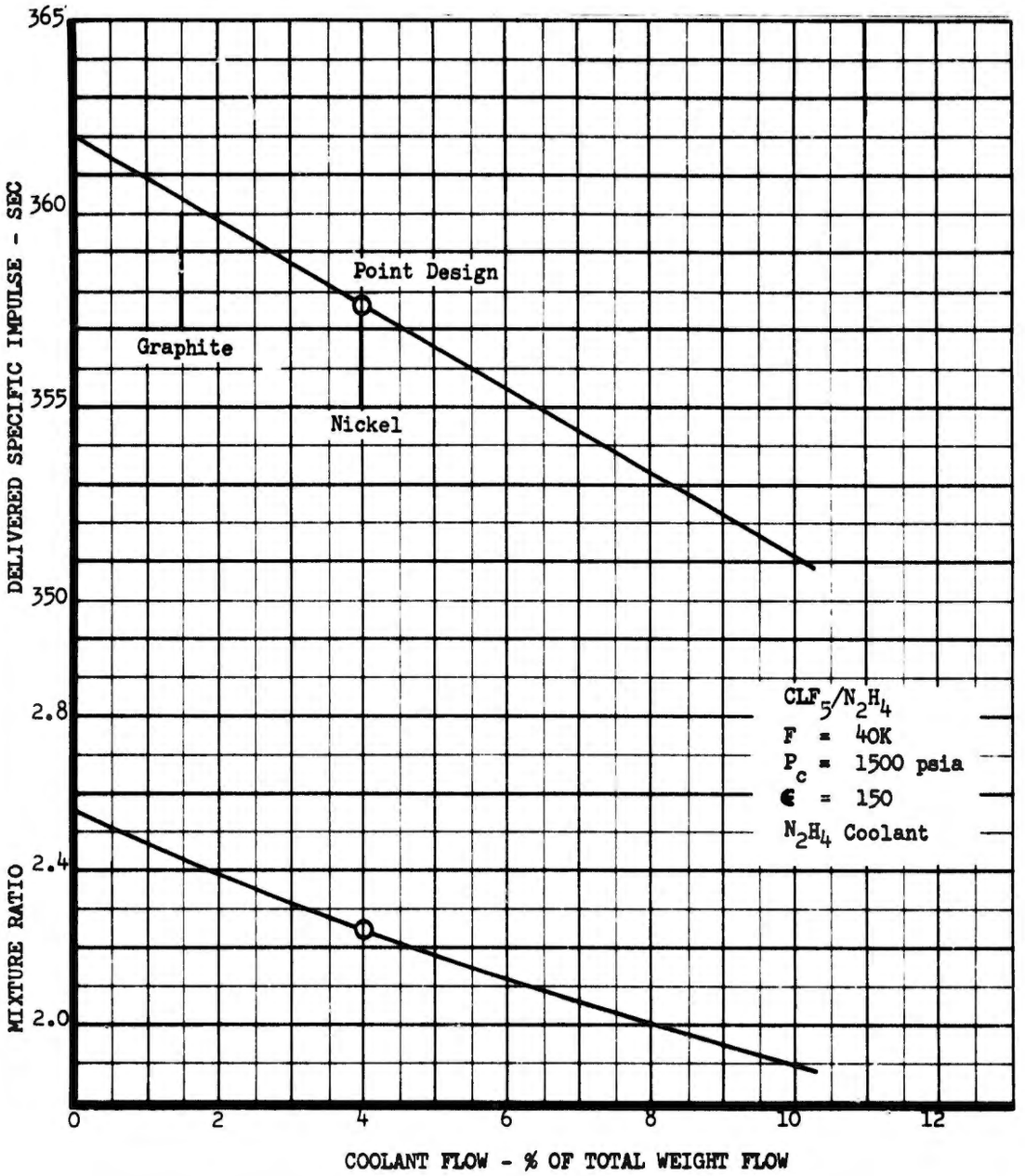

Figure 87. Point Design Engine No. VIII, Performance/Coolant Flow Interaction (CLF_5/N_2H_4) (u)

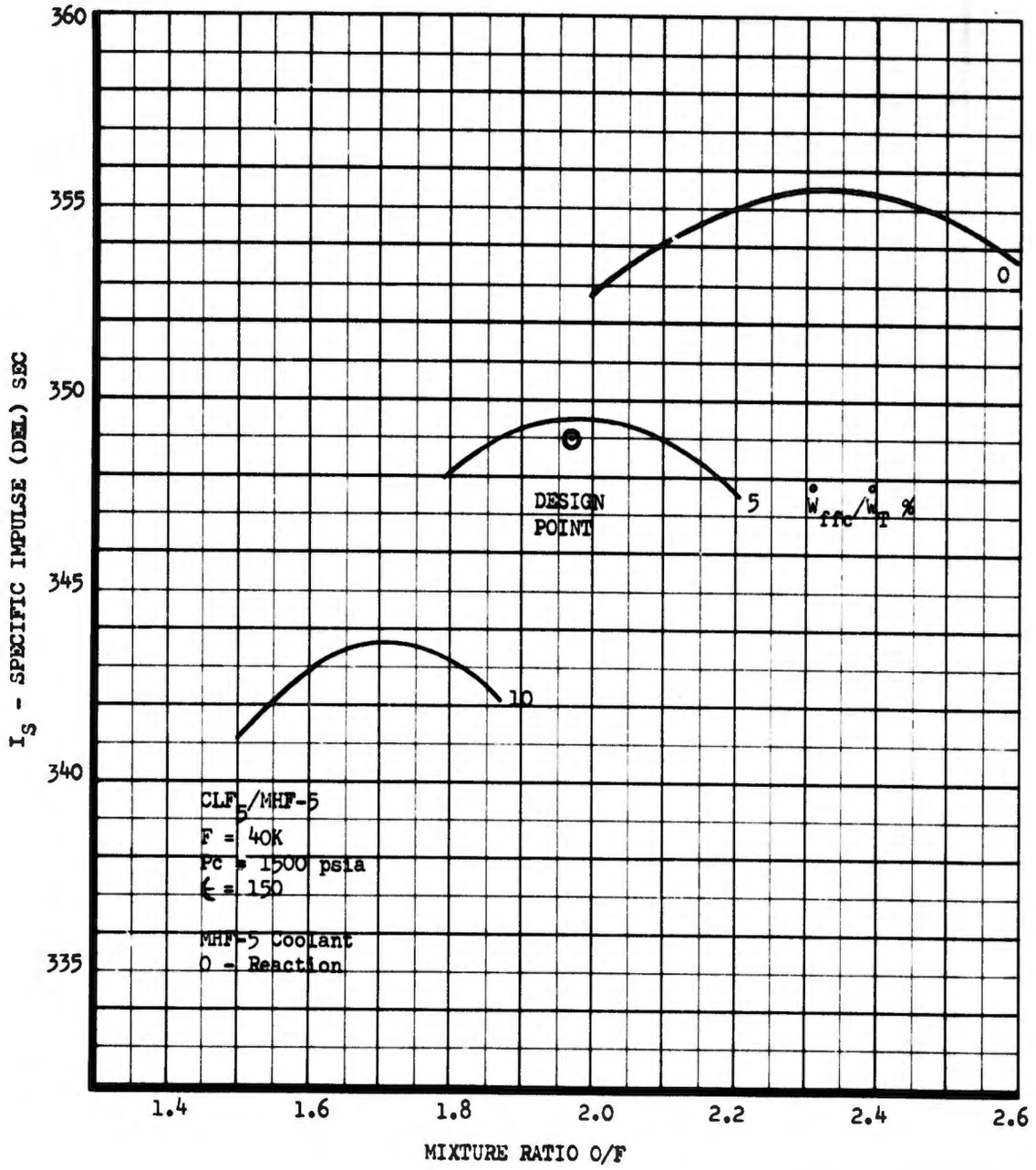

Figure 88. Point Design Engine No. VIII, Performance/Mixture Ratio-Coolant Flow Trade-Off (CLF_5/MHF-5) (u)

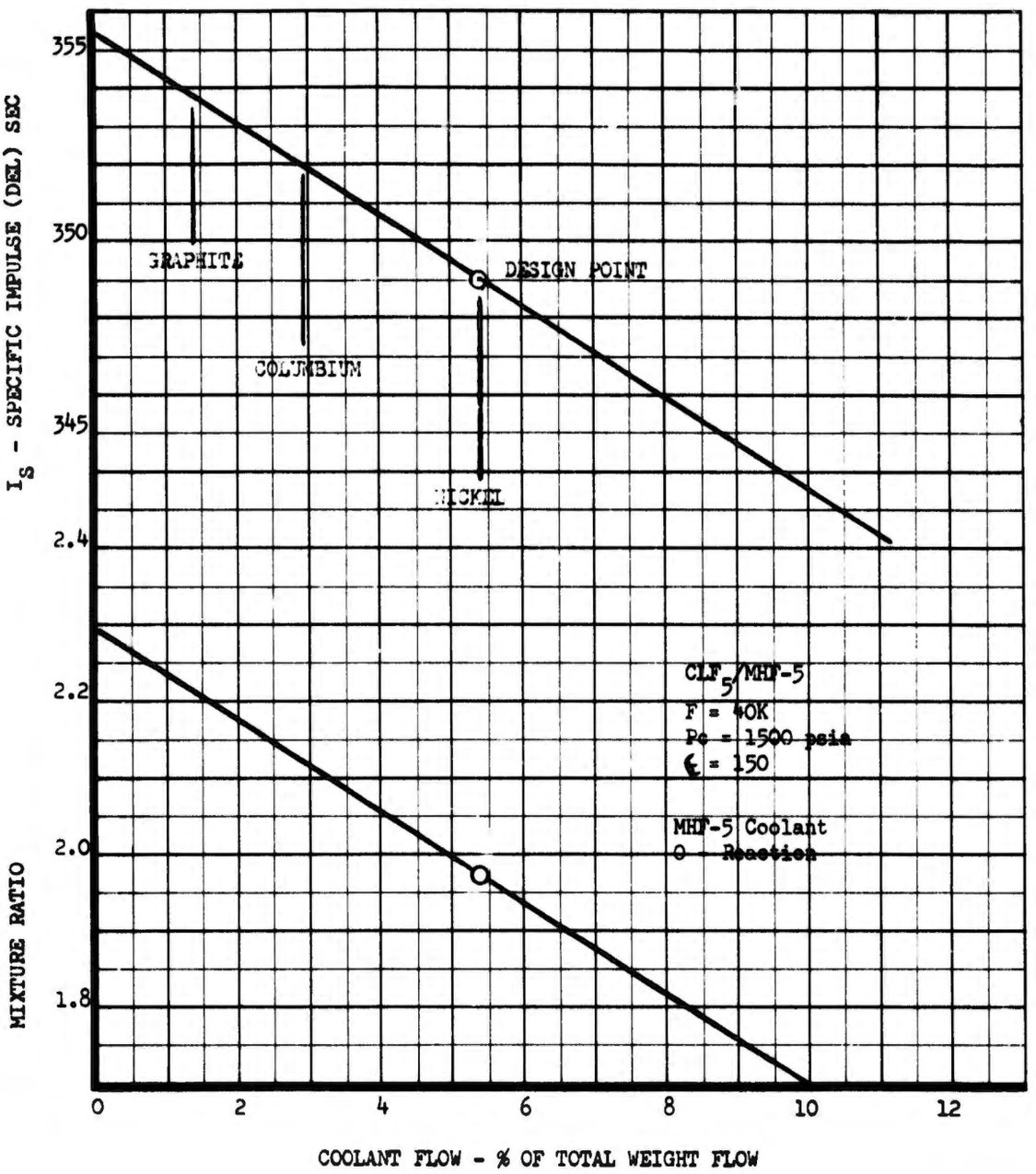

Figure 89. Point Design Engine No. VIII, Performance/Coolant Flow Interaction (CLF_5/MHF-5) (u)

(d) Mission Capability

(U) In this cycle, the fuel pump temperature transients after shutdown control the restart capability of the engine and the fuel pump is the only component exposed to liquid fuel. The pump thermal transient largely depends upon the installation because the stored engine heat has to be dissipated by radiation. To improve the restart capability, heat-sink material should be used at the inlet line of the CAT-Pack to prevent heat soak-back to the pump.

(U) Only the injector and chamber use decomposed hydrazine, which does not restrict the restart capability.

(e) Propellant Compatibility

(C) The gas-cooled engine concept feasibility largely depends upon the gas generator characteristic of the fuel propellant. N_2H_4 can be utilized only if catalytic decomposition is used because the bipropellant characteristic is not suitable (see Appendix I). For the 80/20 blend, both the CAT-Pack or the bipropellant gas generator are suitable. MMH and MHF-5 are very marginal. They have to be decomposed in a thermal bed to meet acceptable coolant temperature levels. These two propellants contain a certain amount of carbon which could present a clogging problem for long burn durations.

c. Point Design Engine No. IX

The thrust level of this engine is 70K at a chamber pressure of 1500 psia. It is shown on Figure No. 90 for a nozzle expansion ratio of 150:1. This results in an engine diameter of 70-in. and an over-all engine length of 135.9-in. The engine is a staged-combustion cycle with a fuel-rich bleed turbine drive and Figure No. 91 is a flow schematic and pressure schedule. Injection is achieved by a conventional tubelet-type injector for gaseous fuel and liquid oxidizer. Pertinent configuration and performance information is summarized on Table XXIV.

Engine No. IX is designed as a fixed thrust engine using a liquid oxidizer transpiration-cooled throat, liquid oxidizer regeneratively-cooled nozzle extension, and an attachable columbium radiation skirt. The performance of this engine is relatively low because its 20-in. characteristic length requires large amounts of oxidizer coolant. Gas generation is obtained by catalytic decomposition of the fuel for N_2H_4 or the 80/20 blend, which results in a very simple control system.

(1) Thrust Chamber Design

The materials selected for thrust chamber assembly No. 9 are similar to those for thrust chamber assembly No. 8. Ni-200 was selected for chamber platelets, injector manifolding, and blades. Inconel 625 was selected for the tubes comprising the regeneratively-cooled nozzle extension, the jacket around the chamber platelet stack, and for the manifolding at the interface between the tube bundle and the platelets. Columbium is used for the radiation-cooled nozzle extension as well as for its attachment flange which includes a turbine exhaust bleed injector and manifolding.

(a) Injector Selection

Thrust chamber No. 9 operates at fixed thrust with liquid oxidizer and gasified fuel. Gas/liquid injectors are still uncommon in the rocket engine industry and information regarding them is very limited. Figure No. 92 shows thrust chamber assembly No. 9 and includes the injector. The gasified fuel flows between the streamlined blades into the chamber. Liquid oxidizer passes around the injector wall, through the leading edge manifolds of the blades, and is injected through 19 tubes-per-blade. These tubes can contain swirling elements, or similar devices to provide fast break-up of the injected liquid. The gas/liquid velocity ratio is quite high and good performance has been indicated from the ARES unit. The injector is well-cooled because the gasified fuel is at a low temperature (1355°F) and the injector face area directly exposed to the combustion front is small. Further, the blades and tubes are cooled by the injected oxidizer. If high frequency combustion stability should become a problem, baffles can be added easily to the injector by extending a few of the blades into the chamber. Alternatively, providing high energy release per unit area near the center of the injector

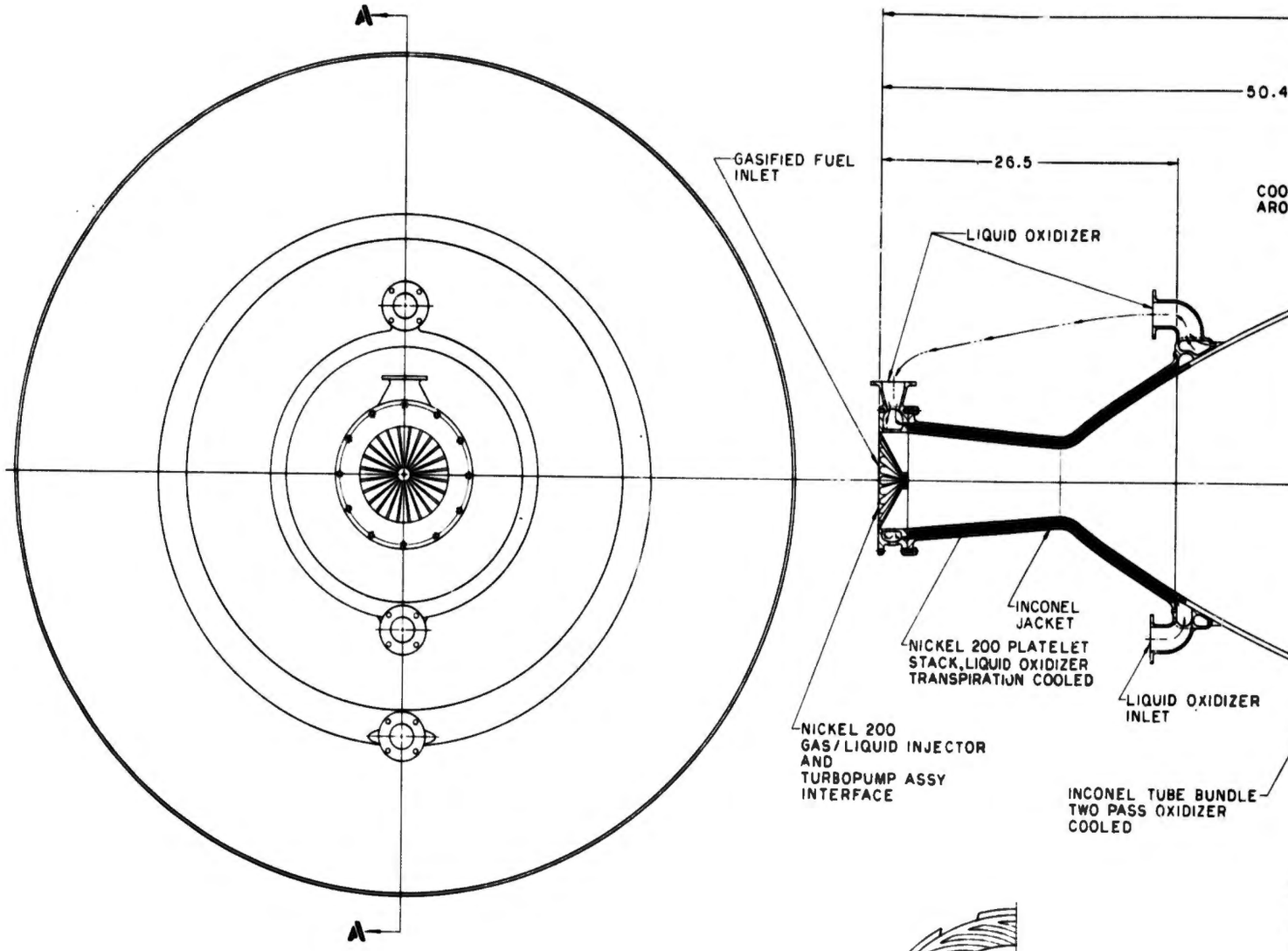
A
A
50.4
26.5
GASIFIED FUEL INLET
LIQUID OXIDIZER
INCONEL JACKET
NICKEL 200 PLATELET STACK, LIQUID OXIDIZER TRANSPIRATION COOLED
LIQUID OXIDIZER INLET
NICKEL 200 GAS/LIQUID INJECTOR AND TURBOPUMP ASSY INTERFACE
INCONEL TUBE BUNDLE TWO PASS OXIDIZER COOLED

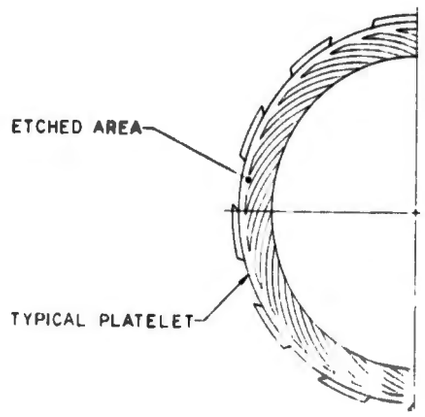
ETCHED AREA
TYPICAL PLATELET

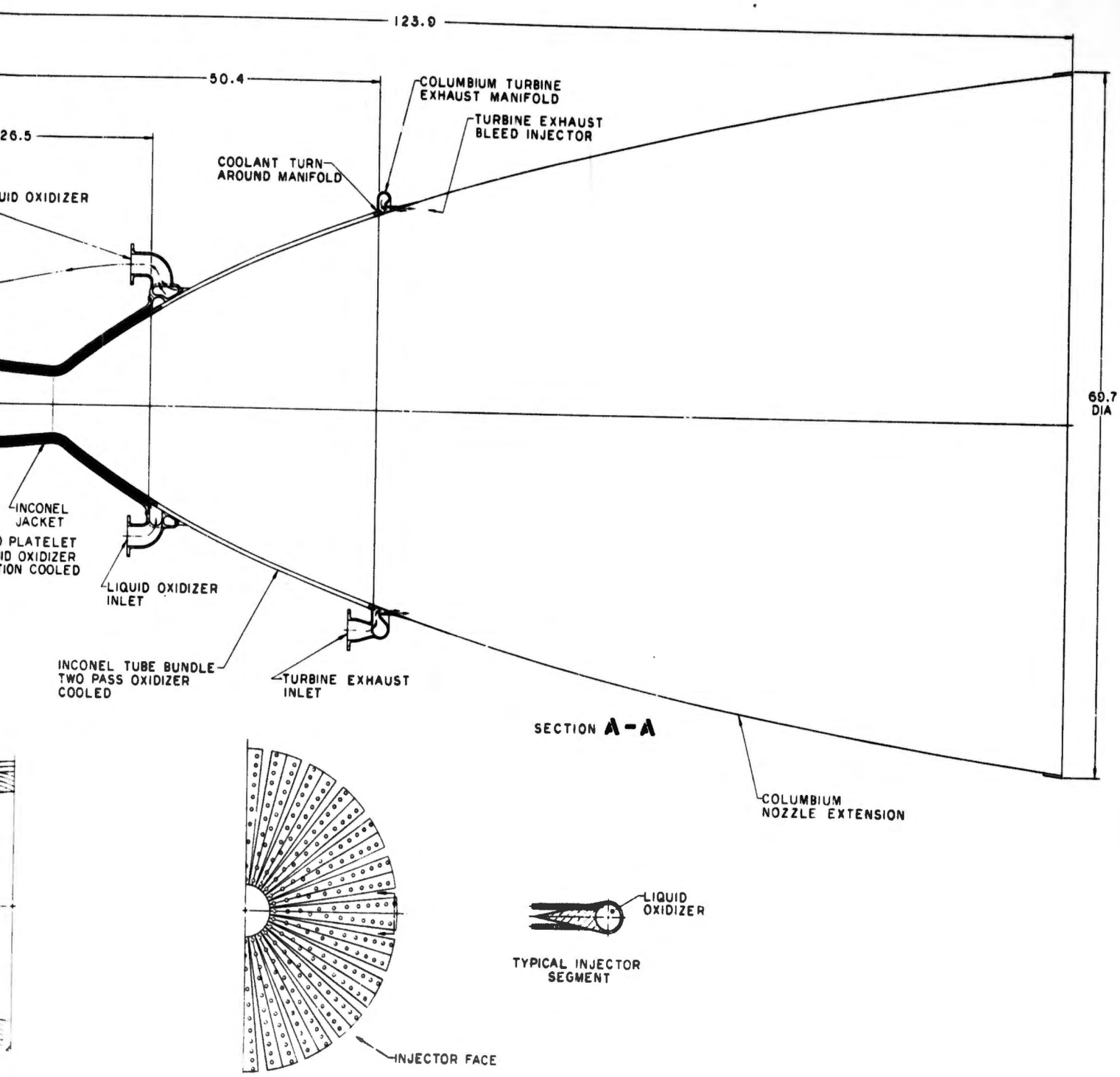

Figure 90. Point Design Engine No. IX Assembly

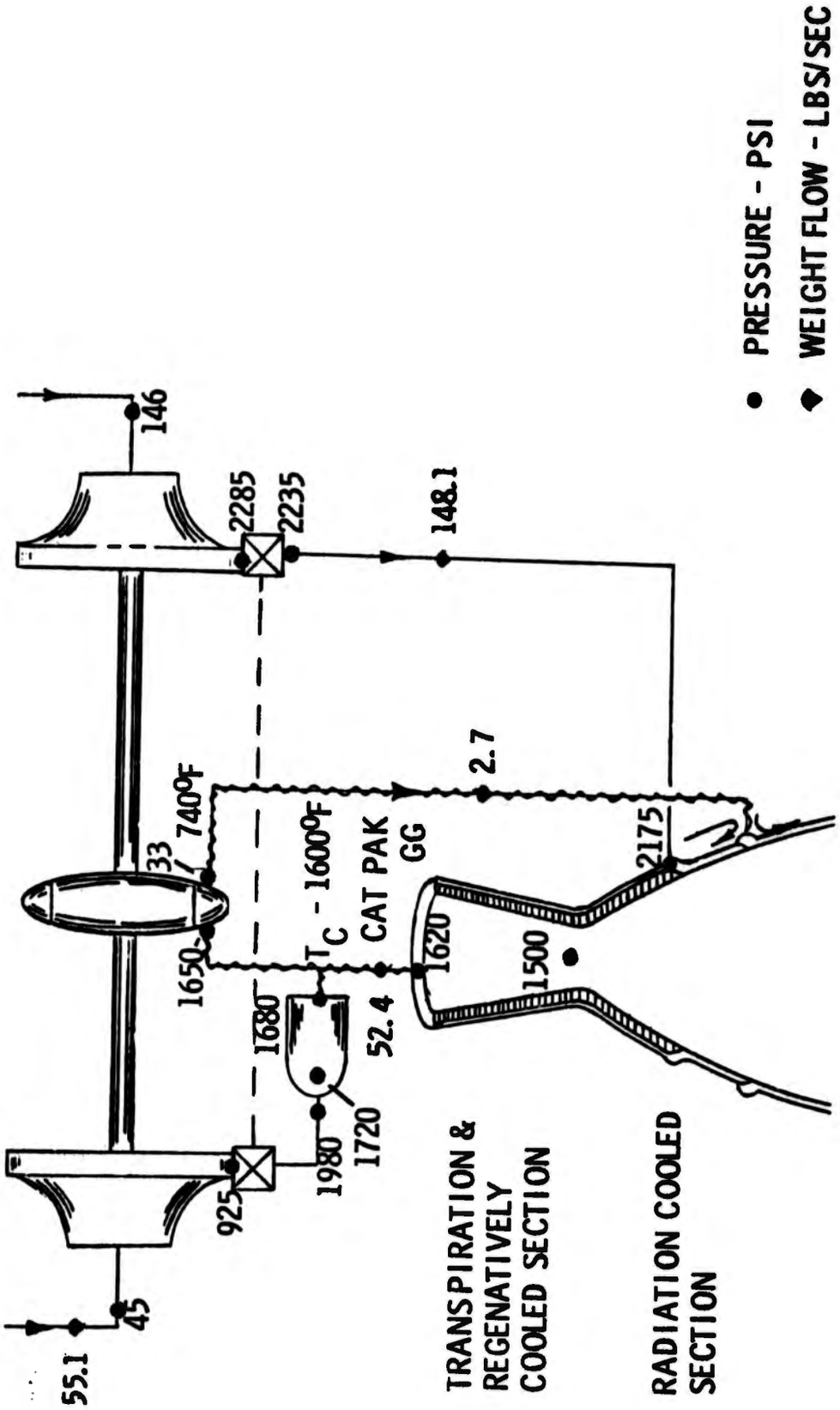

Figure 91. Flow Schematic and Pressure Schedule, Point Design Engine No. IX

TABLE XXIV

POINT DESIGN ENGINE NO. IX (U)

Engine Configuration	Performance	
Pump Fed-Fixed Thrust	Thrust (Vac) lb	70,000
N_2H_4 Cat Pack Bleed Turbine Drive	Chamber Pressure, psia	1,500
ARES Type - Injector	Mixture Ratio, O/F	2.85
Transpriation Cooled Chamber - LO	Specific Impulse (Del) Sec	344.5
Regen (LO) + Rad Cooled Nozzle Extension	% Theoretical I_s (S.E.)	92.5
Single Shaft Turbopump	Nozzle Area Ratio	150
Ring-Gate Valves	Suction Pressure, Psia	
	Oxidizer	146
Turbine Exhaust Gas Dump Extension to T.C.	Fuel	45
	Flow Rate, Lb/sec	
	Oxidizer	142.5
	Fuel	58.6
	Dry Weight	677 lb
	Wet Weight	730 lb

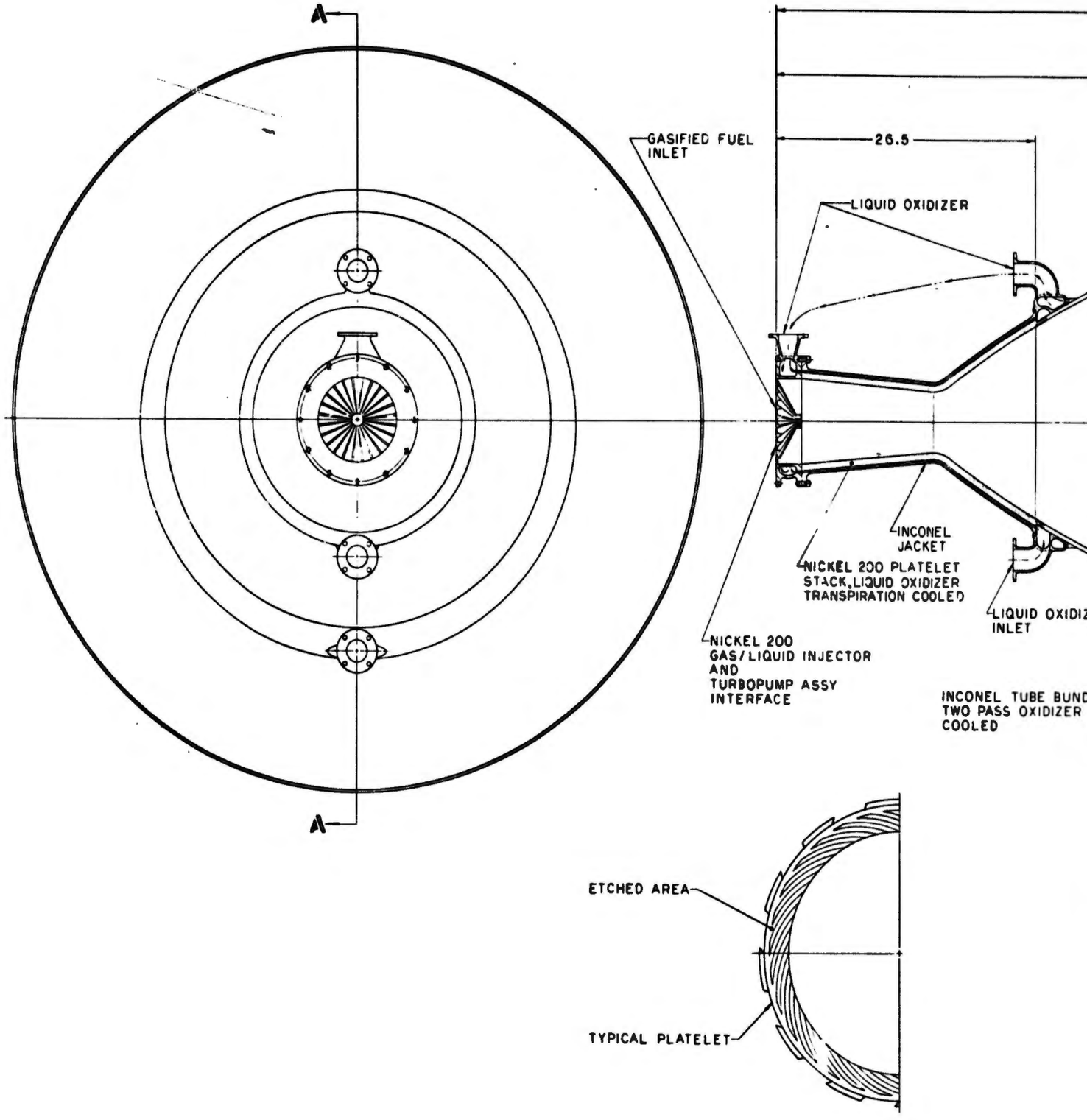
A
A
GASIFIED FUEL INLET
26.5
LIQUID OXIDIZER
INCONEL JACKET
NICKEL 200 PLATELET STACK, LIQUID OXIDIZER TRANSPIRATION COOLED
NICKEL 200 GAS/LIQUID INJECTOR AND TURBOPUMP ASSY INTERFACE
INCONEL TUBE BUND
TWO PASS OXIDIZER
COOLED

ETCHED AREA
TYPICAL PLATELET

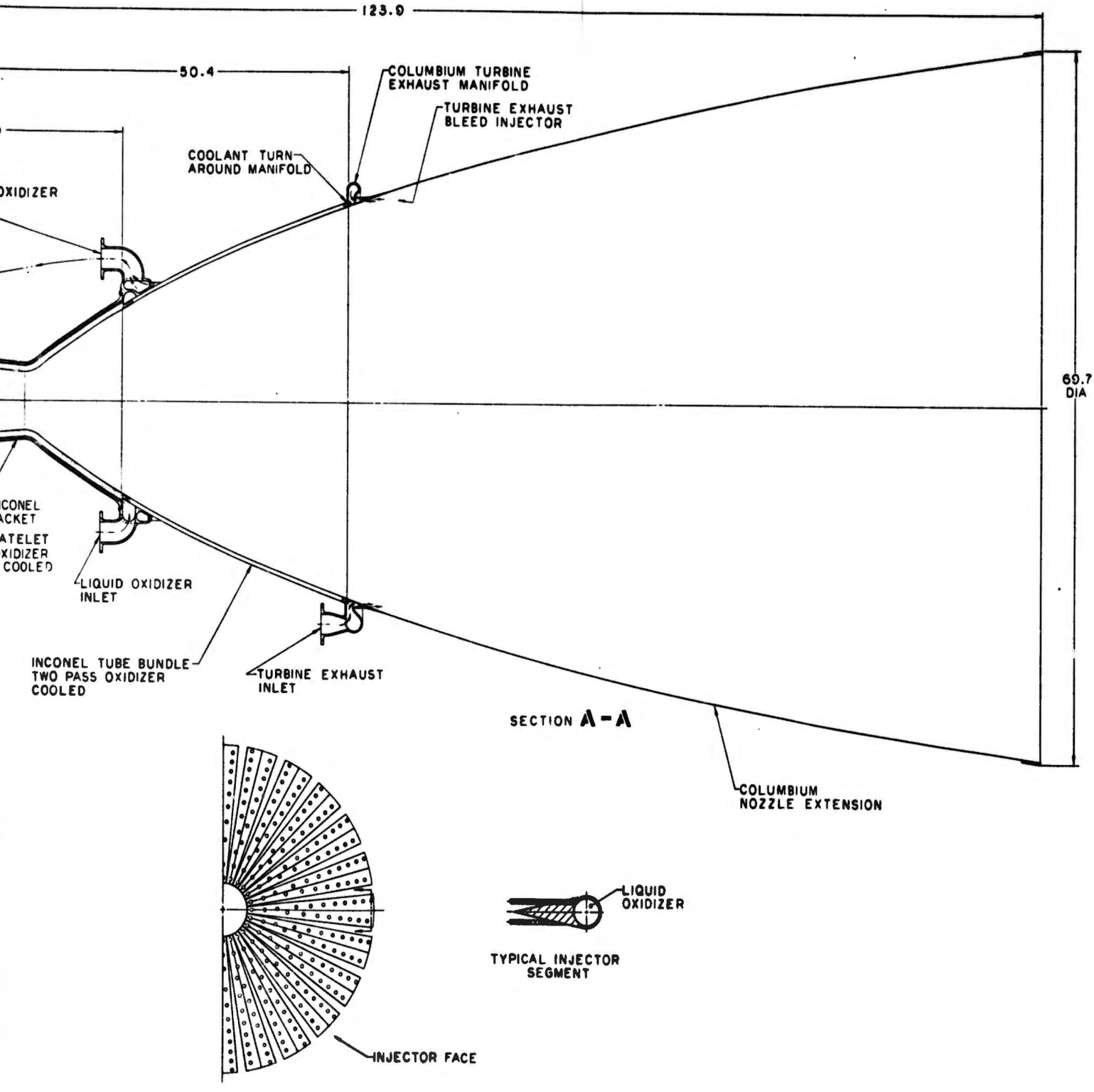

Figure 92. Thrust Chamber Assembly, Engine No. IX

should be simple which normally has the effect of eliminating troublesome tangential modes of combustion instability.

(b) Chamber Geometry

Many of the combustion chamber geometry parameters are shown on Table XXV, including the characteristic chamber length of 20-in. In the case of an axial gas/liquid injector, the axial gas velocity is not zero at the injector face. Chamber contraction ratio is a very important parameter because it determines the liquid droplet break-up resulting from shear forces between the two phases near the injector face. The contraction ratio selected is 2.0.

(c) Active Cooling System Description

Thrust chamber assembly No. 9 utilizes a combination of three cooling modes. The local heat flux determines the type at any specific location. The chamber, throat, and forward section of the supersonic nozzle is transpiration cooled with liquid oxidizer. Immediately aft of the chamber is a liquid oxidizer regeneratively-cooled tube bundle nozzle extension. Beyond that is a radiation-cooled nozzle extension whose forward portion is film-cooled by introducing turbine exhaust gases at the interface between the two nozzle extensions. Figure No. 92 shows the etched platelet design utilized for the chamber stack. Oxidizer flows axially along the chamber in the channels formed between the chamber jacket and the cutout sections on the exterior of the platelets. This oxidizer is fed to all injection slots of the platelets in the stack. The slots take the form of a spiral curve to maximize their length in a given annular thickness, or conversely, to minimize the chamber wall thickness for a given pressure drop across the transpiration slots. Coolant flow will be used to maintain a 1750°F internal chamber wall temperature.

The regenerative tube bundle is of two pass- design to double the coolant velocity as well as to minimize coolant manifold and feed line lengths and weight. The columbium nozzle extension may appear to begin prematurely at area ratio 10. However, its forward end is film-cooled by turbine exhaust gas injection. The design philosophy and execution of this exhaust injector is similar to that for thrust chamber assembly No. 4.

(d) Structural Design

All thrust and gimbaling loads are carried to the thrust pressure assembly through the heavy-walled liquid oxidizer injector manifold. The chamber platelet stack jacket is attached to this same member by a bolt circle as shown on Figure No. 92. The chamber jacket is constructed of higher strength material than are the platelets themselves. It withstands the large hoop and axial loads applied to the chamber wall by the high chamber pressure without greatly increasing thrust chamber assembly

TABLE XXV

THRUST CHAMBER ASSEMBLY NO. 9 DESIGN PARAMETERS

General	Injector	Chamber	Nozzle Extension
Thrust: 70K lb	Type: Gas-Liquid Axial Tubelet	Shape: Conical	Attachment Area Ratio: 10
Chamber Pressure: 1500 psia	Propellant Phases: Fuel - Gas Oxid - Liquid	Material: NI-200 Platelet Stack	Cooling Mode: Liquid Oxid Regen
Nozzle Area Ratio: 150	Thrust Per Element: 153:5 lb	Contraction Ratio: 2	Material: Inconel Tubes
Throttleability: Fixed Thrust	Type Element: Axial Showerhead	Cooling Mode: 7.3% Liquid Oxid. Transpire	Attachment Area Ratio: 46:1
Length: 123.9 in	P_{inj}/P_c(oxid): .25	Characteristic Length: 20 in	Coding Mode: Radiation with external turbine exhaust gas bleed
Duration: Unlimited	Material: NI-200	Throat: 5.67 in	Material: Coated Col.
	Weight: 41.8 lb Dry		Exit Dia: 69.5 in
	Film Cooling: None		

weight. It also provides an attachment flange at the chamber/tube bundle interface. The regenerative tubes are attached to an inlet/outlet manifold at the forward end and a turn-around manifold (integral with the turbine exhaust injector manifolding) at the other end.

(2) Heat Transfer Analysis

The transpiration cooling requirements of Point Design Engine No. IX (see Figure No. 93) are the same as for Engine VII; therefore, only the regeneratively-cooled section is discussed.

The following design limits for the heat transfer analysis were assumed:

- Burnout heat flux ratio = 0.8
- Maximum tube wall temperature = 1500°F
- Tube material = 347SS
- Minimum tube outside diameter (before forming) = 0.125-in.

In addition, only a two-pass design was considered. This means that the relatively heavy inlet and outlet manifolds are kept small because they are located at the minimum diameter of the tube bundle.

In the course of the design analysis, it was found that the limiting factor is the coolant bulk temperature rise and hence, burnout. The minimum feasible attachment area ratio for the regeneratively-cooled skirt is approximately 6.0. The cooling requirements are shown on Figure No. 94. If the skirt is extended to the allowable columbium skirt attachment point of 72, the resulting bulk temperature rise is excessive, resulting in predicted burnout. Two choices are equally possible for a satisfactory design of the regenerative skirt; namely, the transpiration-cooled section can be extended to a higher area ratio or the radiation-cooled skirt can be attached at a lower area ratio by using coated columbium. Both choices would reduce the regeneratively-cooled area and hence, the coolant temperature rise. The approach selected was to attach a Lunite 2 or Lunite 3 coated columbium skirt at area ratio 46 and to extend the regenerative skirt to the minimum possible area ratio.

The results of the analysis indicate that the maximum allowable burnout heat flux ratio and the minimum feasible tube size

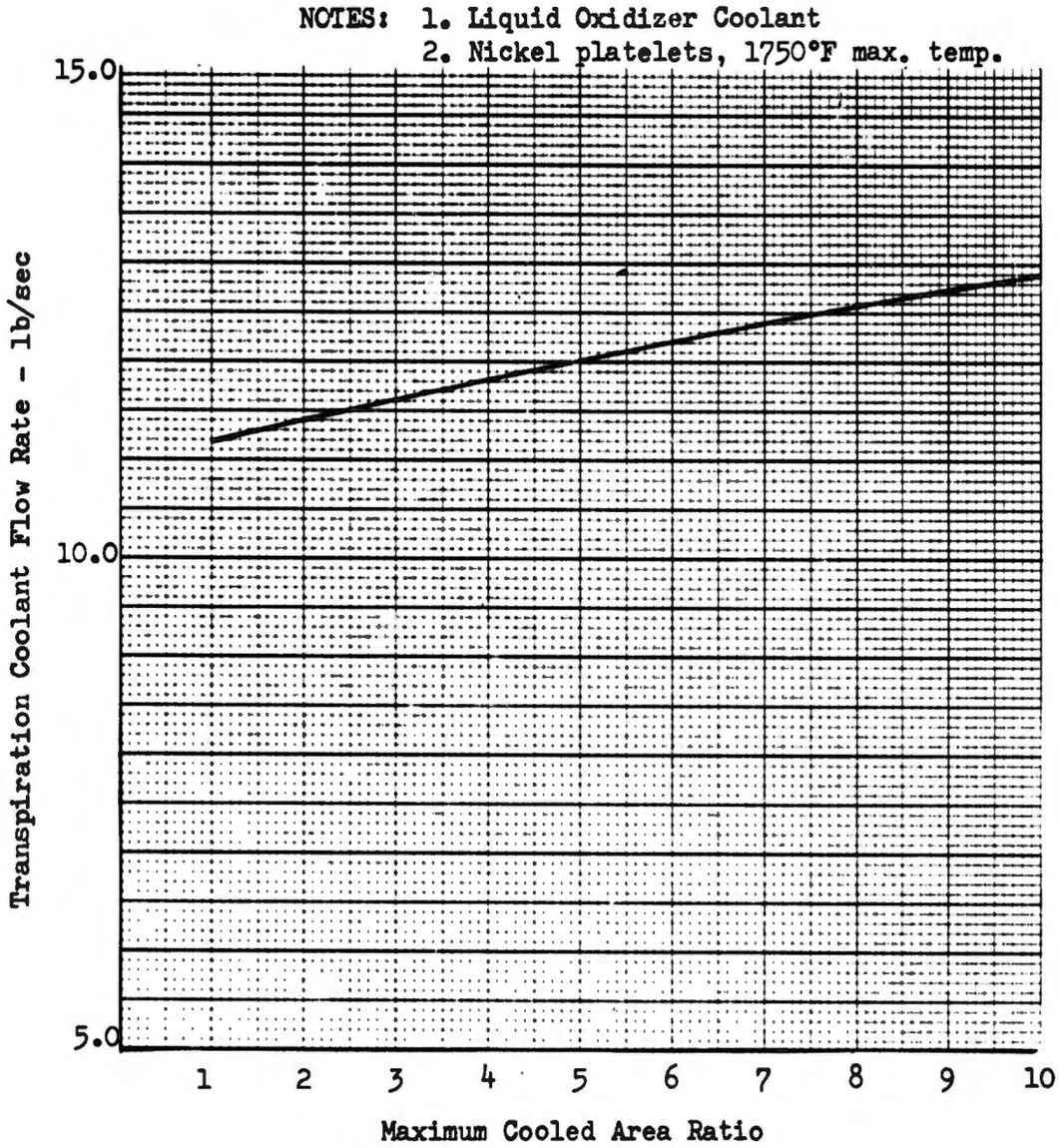

Figure 93. Engine No. IX Transpiration-Cooled Section

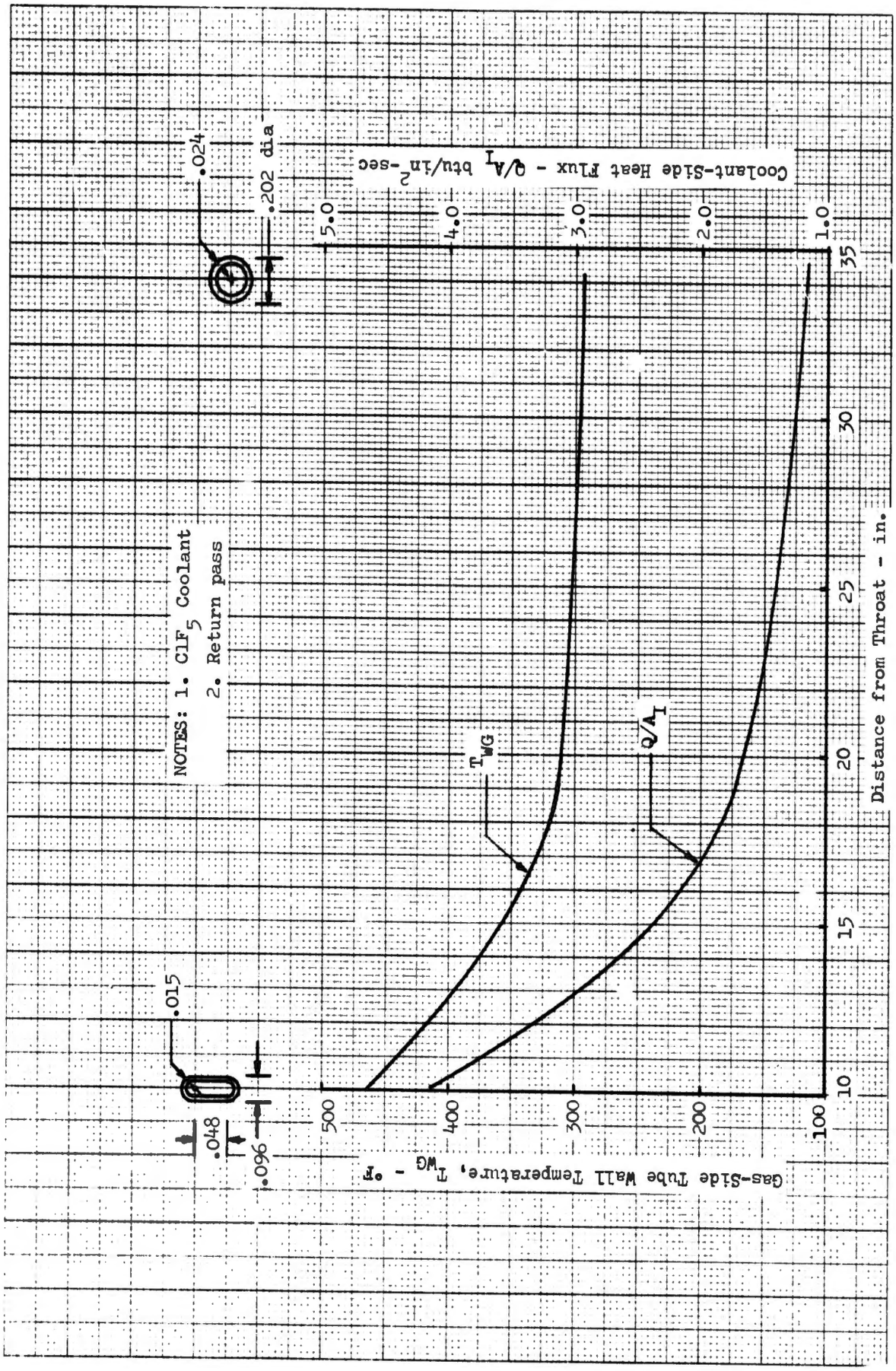

Figure 94. Engine No. IX Regeneratively-Cooled Skirt

occur almost simultaneously at an area ratio of 10. The following is a summary of this design:

- Number of coolant tubes	600
- Maximum burnout heat flux ratio	0.76
- Coolant temperature rise	67°F
- Maximum tube wall temperature	464°F
- Coolant tube static pressure loss	443 psi

Figure No. 94 shows the predicted tube wall temperatures and heat fluxes for the return pass. The coolant tube geometry at selected locations also is shown.

Coating could be applied to the tubes to reduce the coolant temperature rise and thereby extend the regeneratively-cooled area. However, the heat fluxes are so low in this area that the required coating thermal resistances would result in prohibitive coating thicknesses.

(3) Turbopump Configuration

Point Design Engine No. IX is designed for a bleed cycle; therefore, the turbine is a two-stage design. Although ring-gate valves are featured, they are used as on-off valves only because this is a fixed thrust engine. The turbopump weight for this engine was calculated based upon the information presented in Appendix VI (Part II of this report), wherein turbopump design is delineated.

(4) Controls System Description

The pump-fed engine system configuration of Engine No. IX is a fixed thrust design requiring a relatively simple "on-off" thrust chamber propellant flow control which is identical to that of Engine No. V. It utilizes a turbopump ring-gate valve system with a single, electrically-operated actuator. The decision to use an electrical actuator is in compliance with existing criteria established at the outset of this study. The individual fuel and oxidizer valves of the ring-gate valve system will be mechanically-linked for reliable operation during engine start and shutdown transient conditions.

The detailed operation of the ring-gate valve system is identical to that described for Engine No. VIII except that the electrical actuator, which is directly connected to the valve combination, is designed for "on-off" operation rather than "throttling." This difference permits use of simplified electrical control circuitry. The electric motor

assembly, complete with clutch, brake, and gear train, is similar to that used for the Transtage electrically-actuated valve. Envelope size and weight will change slightly depending upon the actual power requirements.

(5) Engine Performance

Point Design Engine No. IX performance was computed using the methods described in Appendix II (Part II of this report). Pertinent information is presented on Figures No. 95 and No. 96 for various mixture ratios, coolant flows, and percentage of reaction with the core using the propellant combination CLF_5/N_2H_4. Similar performance information for the propellant combination CLF_5/MHF-5 is presented on Figures No. 97 and No. 98.

(6) Engine Capabilities and Limits

The characteristics of this engine are very similar to that of Engine No. VII but it has a regenerative nozzle extension instead of the radiative skirt. Therefore, no critical burn duration limits are anticipated. The restart capabilities of this engine are very good because it combines a cool operating thrust chamber with injection of decomposed fuels.

The start transient problem of propellant flashing is identical to that of Engine No. VII.

(a) Mission Capability

In this cycle, the fuel pump temperature transients after shutdown control the restart capability of the engine and the pump is the only component exposed to liquid fuel. The pump thermal transient largely depends upon the installation because the stored engine heat must be dissipated by radiation. To improve the restart capability, heat-sink material should be used at the inlet line of the CAT-Pack to prevent heat soak-back to the pump.

The injector uses decomposed hydrazine, which does not affect the restart capability.

(b) Propellant Compatibility

This engine can accept any of the specified fuels because liquid oxidizer is used as the coolant. Carbon deposits in the tubelet injectors is not considered critical because the fuel is ducted outside of the tubes.

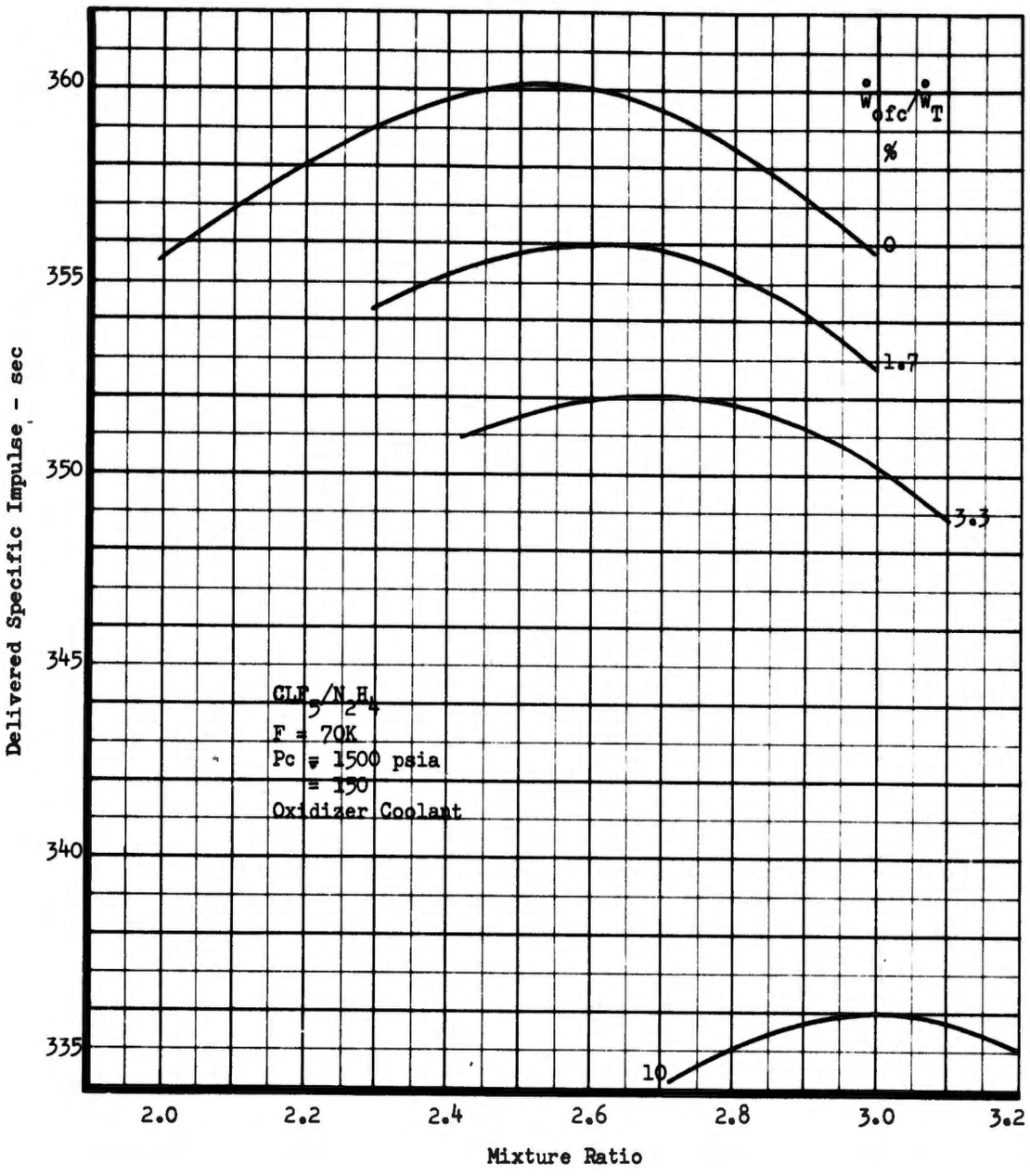

Figure 95. Point Design Engine No. IX, Performance/Mixture Ratio-Coolant Flow Trade-Off (CLF_5/N_2H_4) (u)

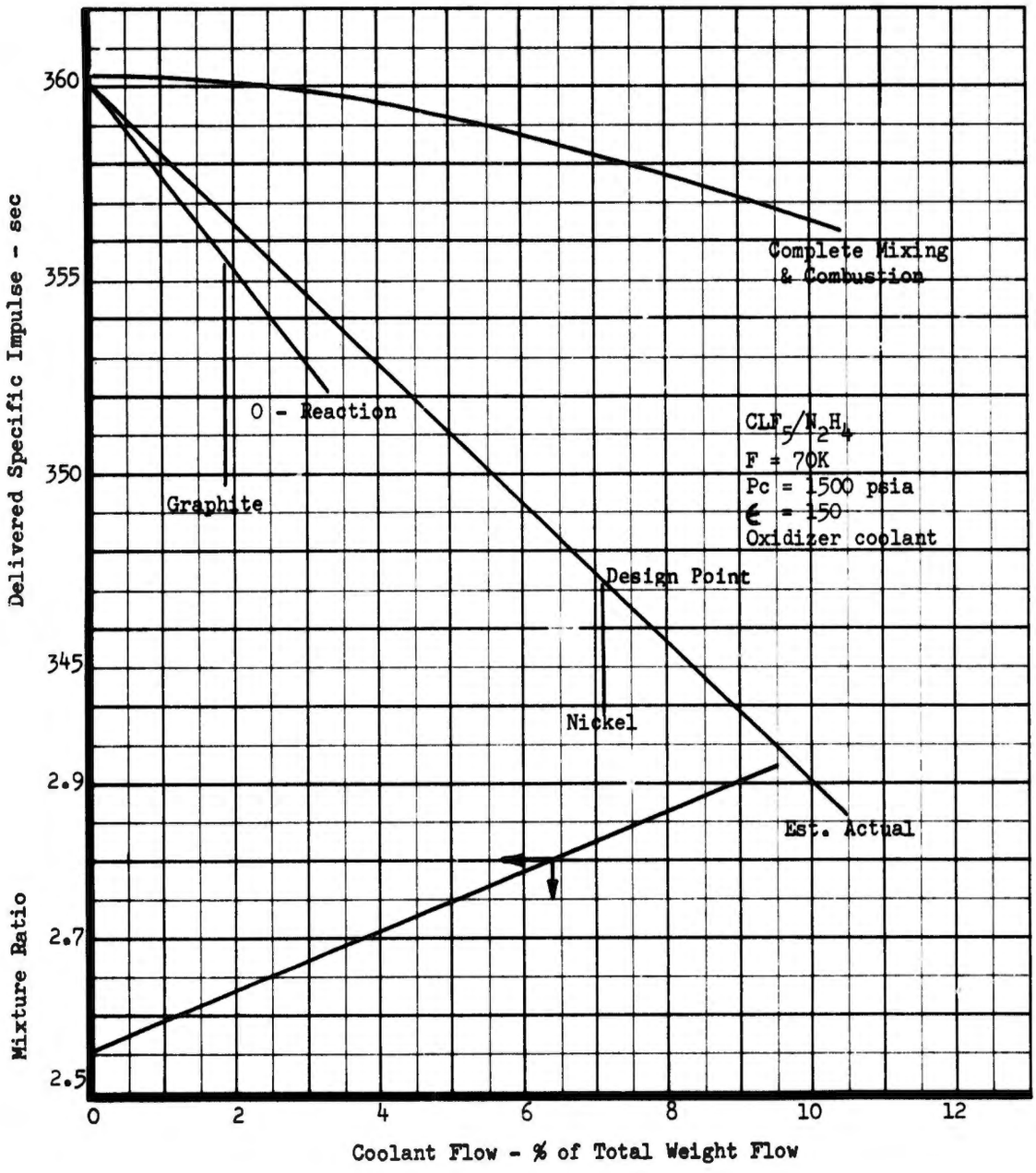

Figure 96. Point Design Engine No. IX, Performance/Coolant Flow Interaction (CLF_5/N_2H_4)

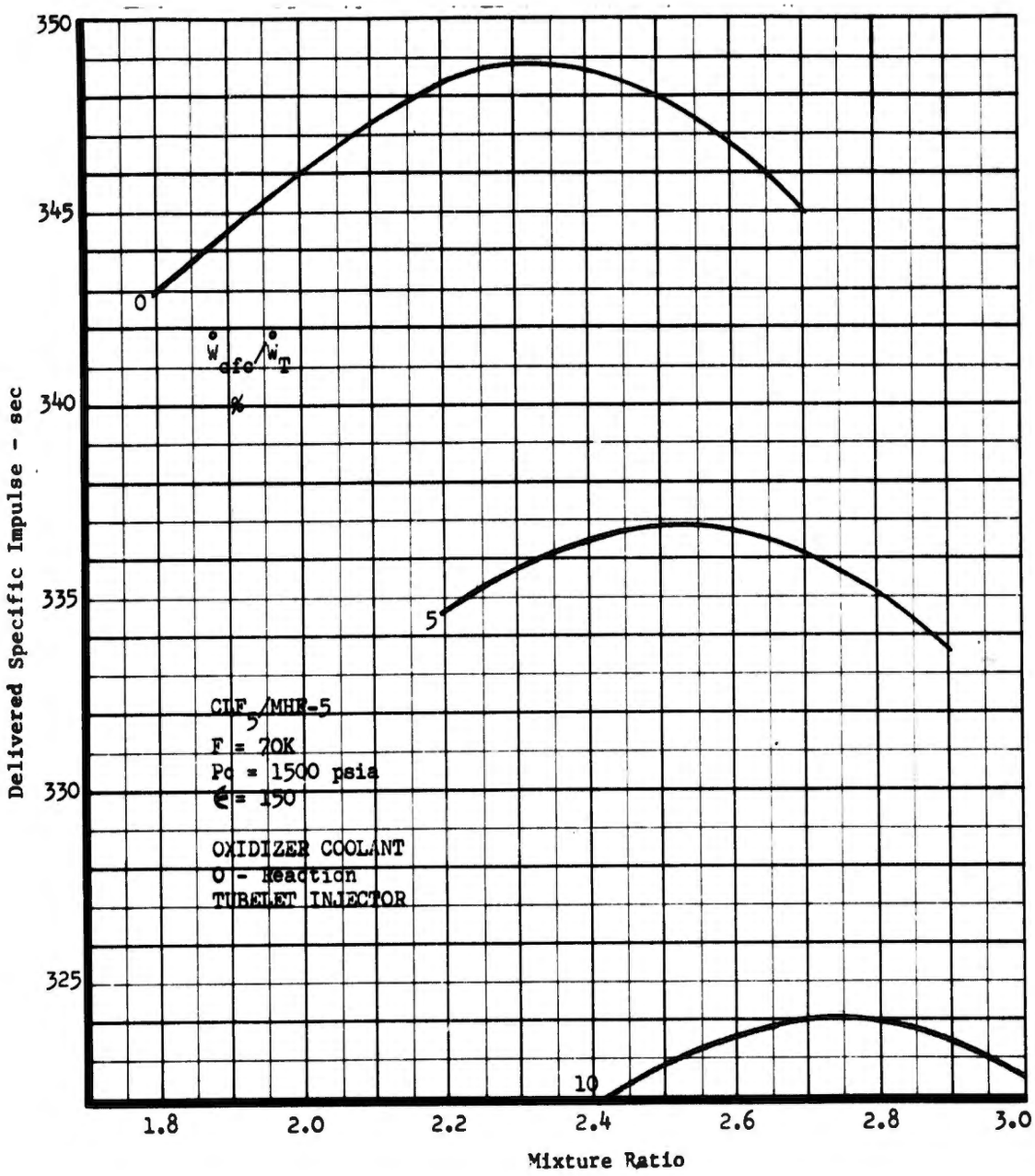

Figure 97. Point Design Engine No. IX, Performance/Mixture Ratio-Coolant Flow Trade-Off ($CLF_5/MHF-5$) (u)

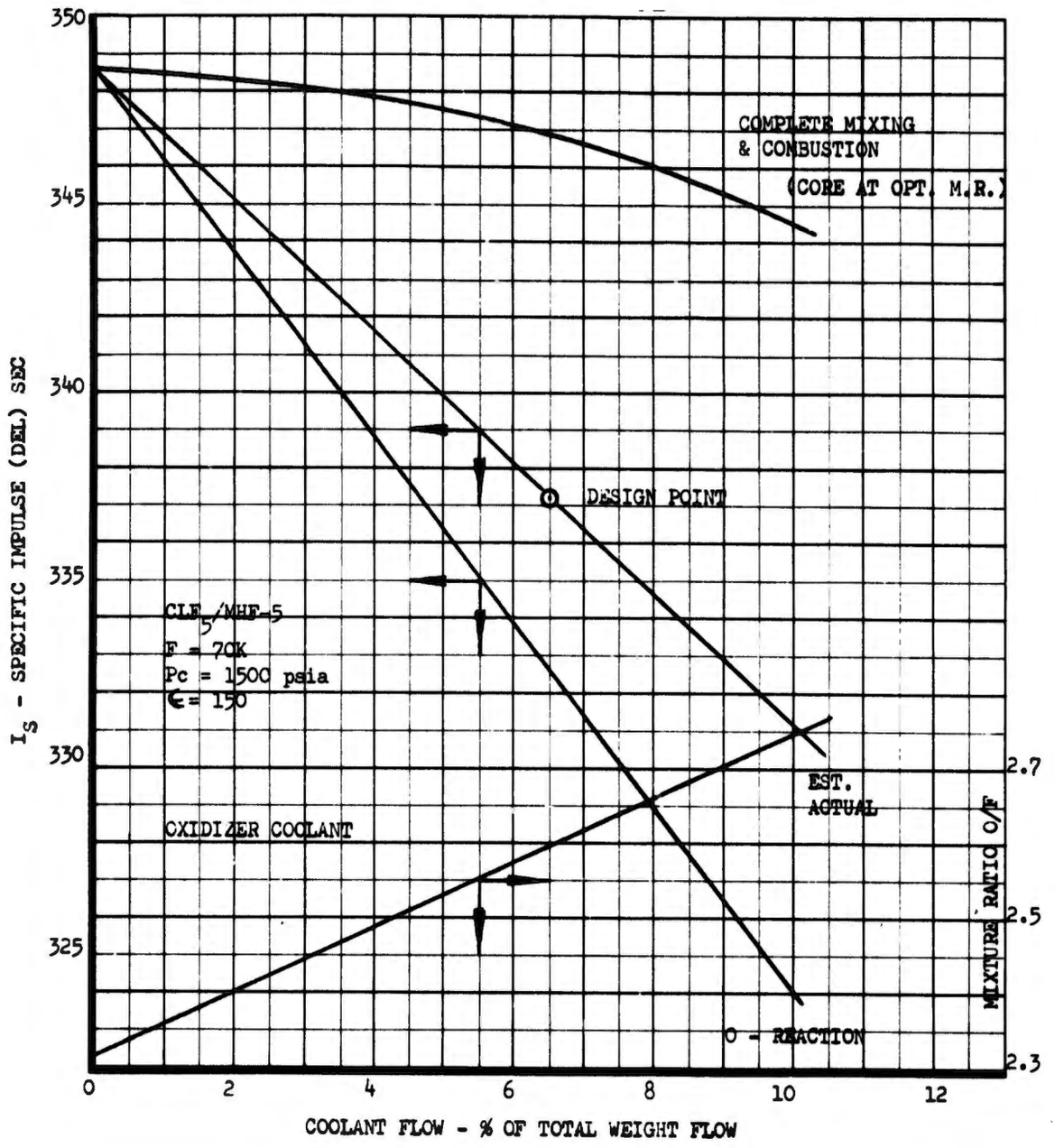

Figure 98. Point Design Engine No. IX, Performance/Coolant Flow Interaction (CLF_5/MHF-5) (u)

V. TECHNOLOGY LIMITS

(U) This section contains a summary of the practical design and operational limits pertinent for the mission analysis. It is based upon the Point Design Engine Study and is extended tc be useful for a parametric engine investigation.

(U) The discussion is divided into two parts. The first part concerns design limits for the engine which are constant and the second part discusses application limits which can differ from mission to mission.

A. ENGINE DESIGN LIMITS

(U) In this section, engine design limits are presented as functions of thrust level, chamber pressure, and specified propellants, which do not change with mission requirements.

1. Cooling Limits

(U) As indicated in the previous discussions, the coolant requirement has a significant affect upon the performance of an engine. The preferred cooling methods assure minimal losses in performance. Absolute limits exist for the cooling methods considered within the scope of this study. In addition, there are limits wherein any specific technology is superior to any other technology.

a. Absolute Limits for Regenerative Cooling

(U) The regeneratively-cooled engines are limited in application by the burnout heat flux and the gas side-wall temperature. These limits depend upon the coolant, the bulk temperature rise, and amount of film cooling.

(C) The indicated limits were ascertained for liquid N_2H_4 coolant and are presented on Figure No. 99 as a function of thrust and chamber pressure. The variation in these limits for zero and 5% film coolant as well as for three different L*'s are included. The results indicate that film cooling is not effective in lowering the heat flux limit or the gas-side tube wall temperature limit. A change in L*, which actually represents a change of chamber surface area, appears more effective. There data also indicate that a chamber pressure of 650 psia to 680 psia is the practical upper limit for engines above 30K thrust. For lower thrust levels, the upper chamber pressure limit decreases very rapidly.

(C) For a mission analysis using N_2H_4 as the fuel, only regenerative engines with limits above these should be considered. For thrust and chamber pressure combinations falling below the region of feasibility, other cooling methods (i.e., passive systems or transpiration cooling) should be considered.

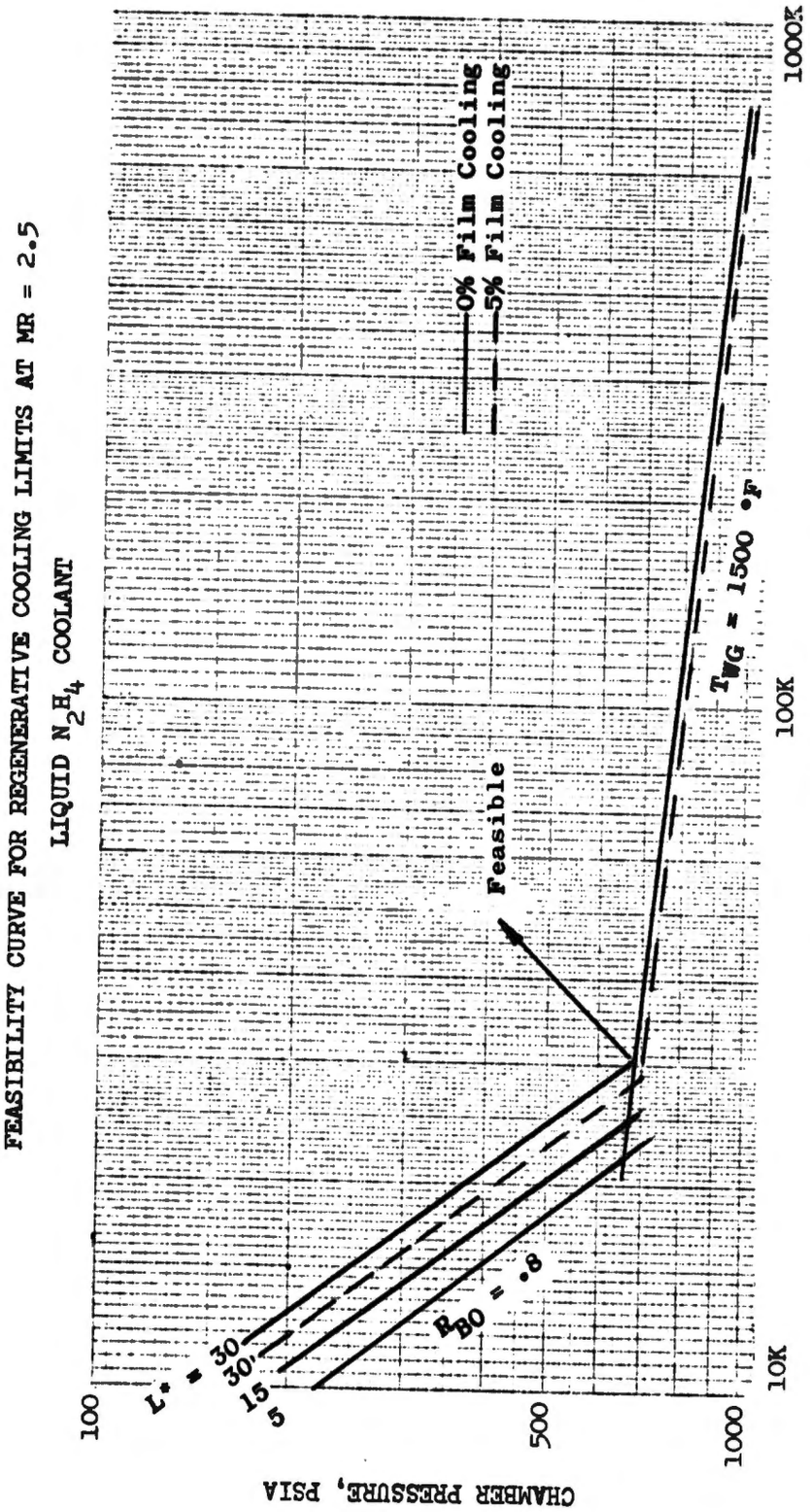

Figure 99. Feasibility Curve for Regenerative Cooling Limits at MR = 2.5, Liquid N_2H_4 Coolant (u)

(C) The burnout heat flux limit shown on Figure No. 99 also presents the practical limit, to which regenerative engines can be throttled. Therefore, the full thrust design point for throttleable regenerative-cooled engines should be removed sufficiently from the limit to satisfy the throttling requirement.

(C) For regeneratively cooled engines using N_2H_4 as coolant, it is very important to maintain the coolant bulk temperature rise to a minimum so as to reduce the danger of monopropellant detonations. Line of constant bulk temperature are shown on Figure No. 100 for a chamber with a characteristic length of 30-in. The bulk temperature rise is roughly proportional to L*. Injector designs, such as platelets or gaseous injection, with their short L* requirement considerably reduce the bulk temperature rise.

(C) The regenerative cooling limits for the other specified propellants also were analyzed. Only MHF-5, the limits for which are shown on Figure No. 101, appears to have a useful range of application.

(C) MMH has a very limited useful range within the specified thrust and chamber pressure range as shown on Figure No. 102

b. Absolute Limits for Ablative-Cooled Chambers

(U) As previously explained, the ablative chambers are very sensitive to burn duration, which affects the wall thickness requirement as well as the restart capability.

(U) A further characteristic of ablative chambers is the change of throat diameter with burn duration. This change is due to the result of the reaction of the chamber throat material with the combustion products. The magnitude of the throat diameter change is considered a function of the chamber heat flux. Therefore, it can be presented in terms of chamber pressure and thrust level. A chart of recommended upper burn duration limits is shown on Figure No. 103, based upon current experience.

(U) For the fibrous graphite radiation-cooled chambers the absolute burn duration is assumed to be identical as shown on Figure No. 103.

c. Absolute Limits for Transpiration-Cooled Chambers

(C) The liquid oxidizer transpiration-cooled chambers are limited in throttling range because of the high vapor pressure of CLF_5. The static pressure in the throat should not be lower than the CLF_5 vapor pressure. This restricts this engine to a minimum chamber pressure of 110 psia. Therefore, the 10:1 throttling requirement can only be satisfied for design chamber pressures larger than 1100 psia. This limit is somewhat arbitrary because no practical experience exists for the actual lower throttling limit of liquid oxidizer-cooled chambers.

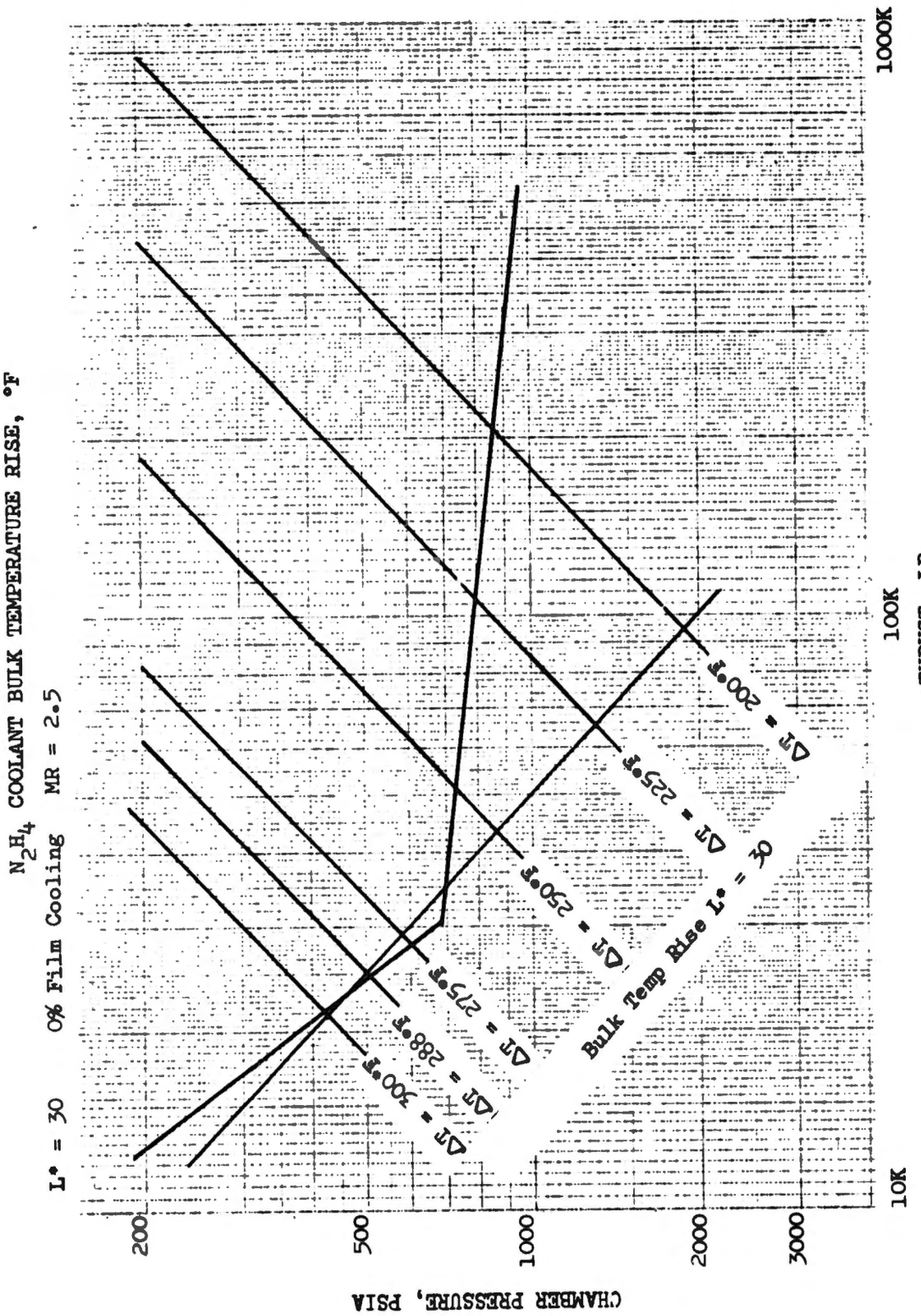

Figure 100. N_2H_4 Coolant Bulk Temperature Rise, °F (u)

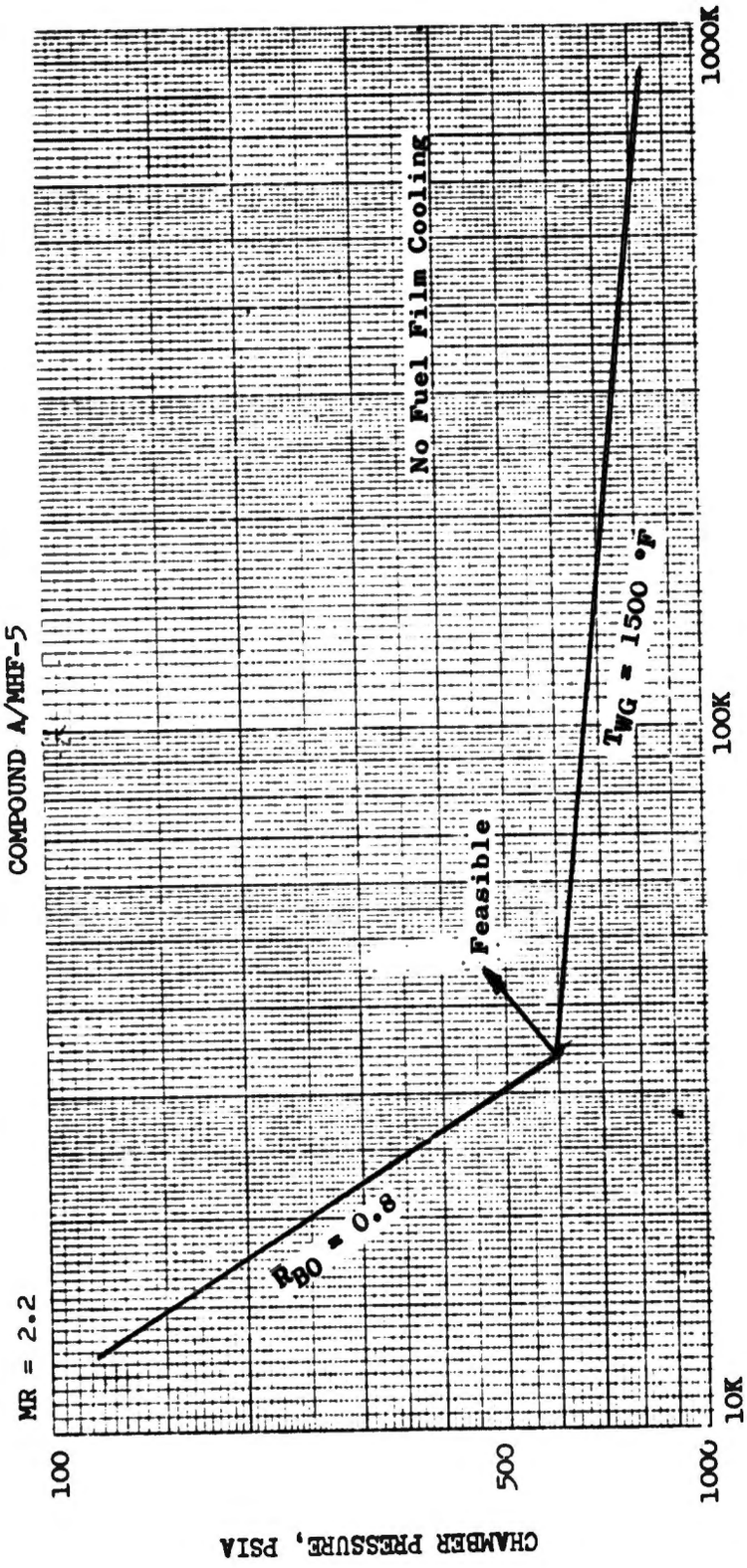

Figure 101. Feasibility Curve for Liquid MHF-5 Regenerative Cooling, Compound A/MHF-5 (u)

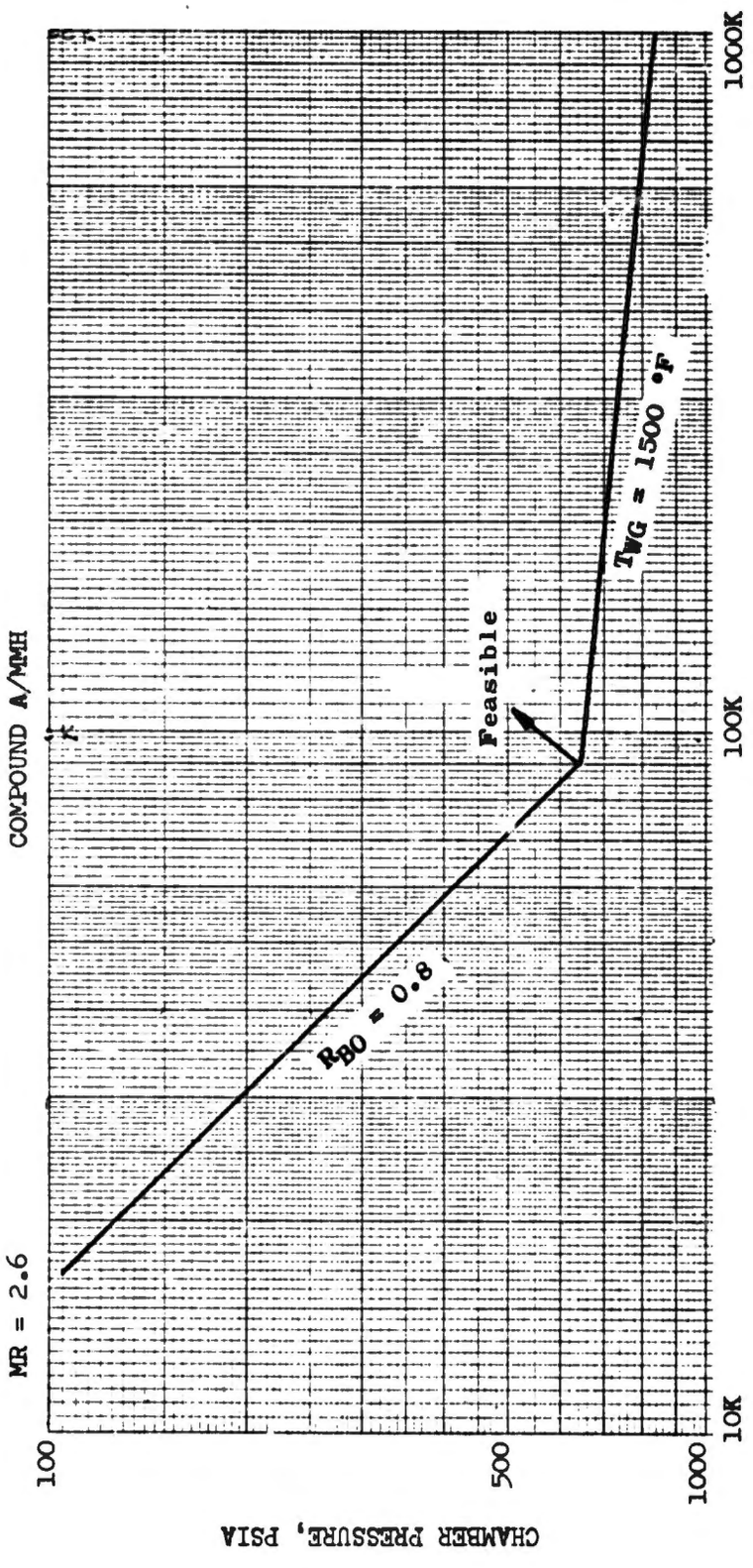

Figure 102. Feasibility Curve for Liquid MMH Regenerative Cooling, Compound A/MMH (u)

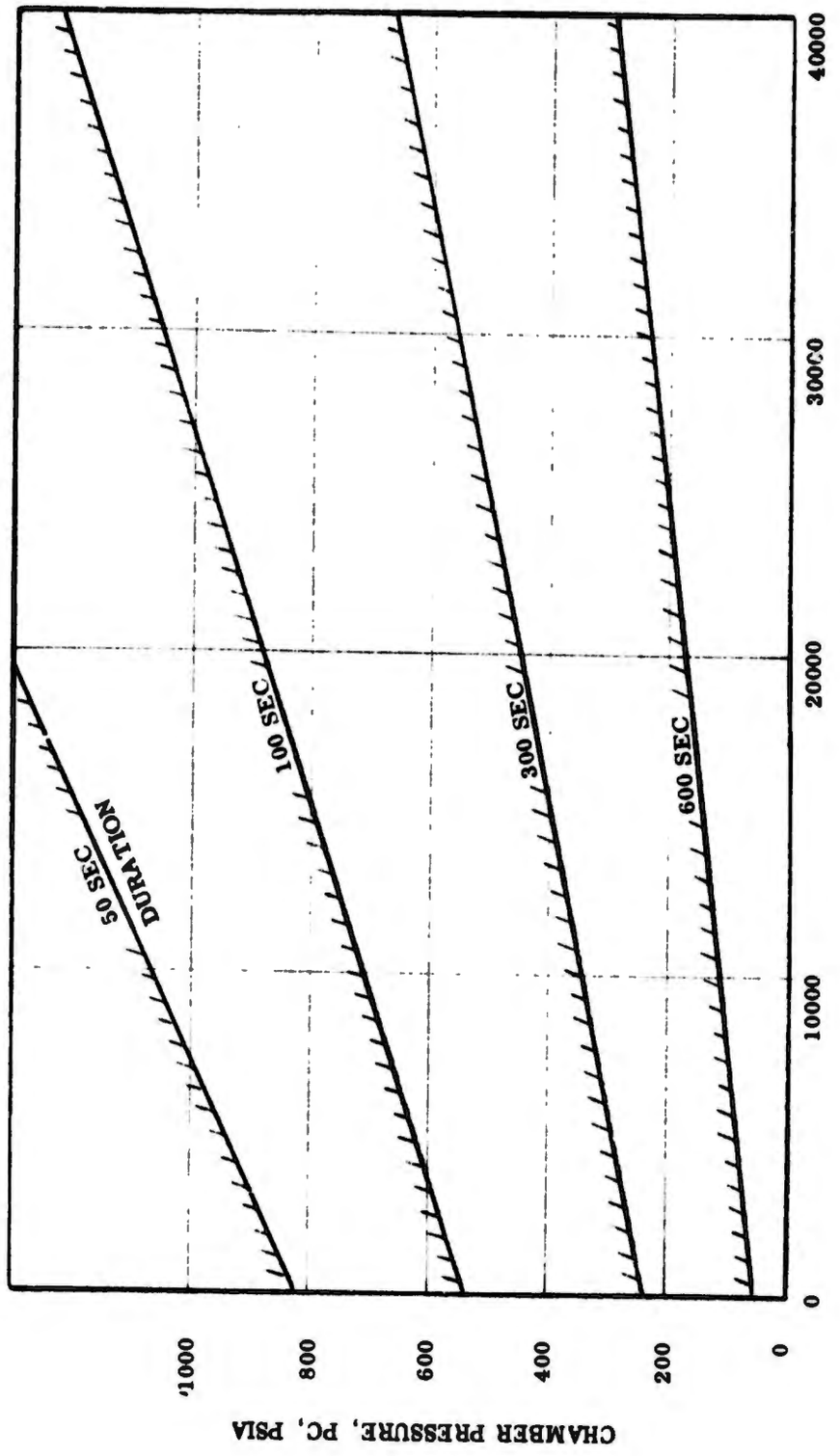

Figure 103. Limits of Chamber Pressure and Thrust for Various Durations - Point Design Engine No. IV (u)

(C) The gaseous fuel transpiration-cooled chambers are limited by the gas generation characteristic of the propellants. N_2H_4 and the 80/20 blend are most suitable for this type of cooling method. MHF-5 and MMH have very high propellant gas generator temperature (see Appendix I) and require a thermal bed for decomposition of the coolant flow to practical temperature levels. The carbon-containing fuels, such as MHF-5 and MMH, can be burn duration limited as a result of carbon deposits in the injector and cooling passages. However, no practical experience exists to permit definition of these limits.

2. Lower Limit of Chamber Pressure

(U) The lower limits of practical chamber pressures are determined by feed system stability requirements as well as injector limits.(13)

(U) In systems where CLF_5 is injected in the liquid state, the lower limit of practical chamber pressure is defined by the CLF_5 vapor pressure, which depends upon the propellant temperature.

(C) For normal, unconditioned oxidizer temperatures of 75°F to 80°F, the minimum chamber pressure is 55 psia to 60 psia for passive as well as regeneratively-cooled systems. It is 110 psia for liquid oxidizer transpiration-cooled systems. These are absolute limits for full thrust as well as throttled operating conditions. Where 80/20 blend is used, the identical limits apply for the fuel side because the vapor pressure of CLF_5 and the 80/20 blend are identical.

(C) To obtain a stable feed system, the feed system stiffness requirements shown on Figure No. 104 must be satisfied. Note that the stiffness requirement rapidly increases for chamber pressures lower than 100 psia to avoid low-frequency instabilities. For pressure fed engines, the criteria on Figure No. 104 also defines tank pressure requirements.

(U) Experience indicates that high-frequency instabilities have to be anticipated at chamber pressures below 100 psia for high-performing injectors and require special designs (i.e., injector baffles or acoustic liners). To avoid these problems, the following design recommendations are made.

(U) It is recommended that the minimum chamber pressure for fixed thrust engines be 100 psia. For throttleable engines, the minimum pressure corresponds with the critical vapor pressure, which, in most cases, will define the full thrust chamber pressure well above 100 psia. These limits are the subject of future technology programs and they are recommended only as guidelines for current mission analysis.

(13) The lowest chamber pressure considered in this analysis is 100 psia in accordance with the contractual work statement requirement.

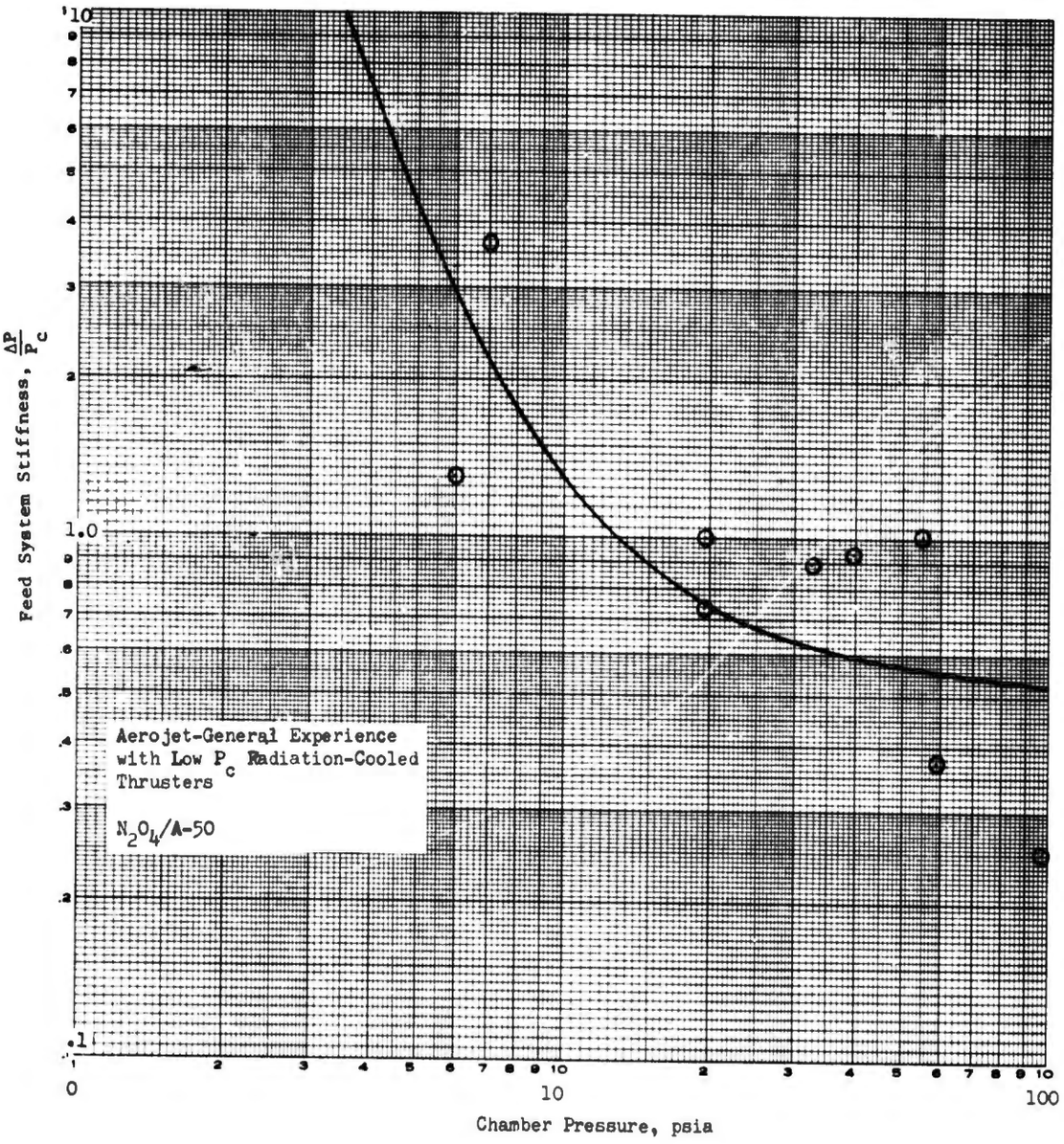

Figure 104. Aerojet-General Experience with Low P_c Radiation-Cooled Thrusters, N_2O_4/A-50

3. Mission Capability Limits

(U) Only those limits in technology which influence the mission requirement are discussed in this section.

a. Burn Duration

(U) Only the passively-cooled chambers are considered to be restricted by burn duration. All of the active systems are considered to have infinite burn durations.

(C) Ablative chambers are highly sensitive to burn duration. The wall thickness requirements of ablative chambers as a function of burn durations were presented in the preceding discussion (Section IV). These requirements indicate that prolonged and deep throttling extends the burn duration to such a level that the necessary chamber wall thickness becomes unrealistically thick. It should be noted that the wall thickness requirements that were shown on Figure No. 41 are for continuous burning. For intermittent burning, the wall thicknesses have to be increased further, but largely depend upon the firing sequence. Each mission requires a separate analysis.

(U) In conducting a mission analysis, an iteration process must be used because the ablative engine weight depends upon the firing duration sequence.

(U) For very short burning times, it may not be necessary to cool the radiation-cooled chamber wall with full film cooling and this would result in an increase in engine performance. It is estimated that these burning times would be a maximum of approximately 75 sec duration for thrusts larger than 10K and chamber pressures lower than 150 psia.

b. Throttling Limits

(U) Most of the engine concepts have extensive throttling limits as well as limits which are dependent upon burn duration requirements (i.e., ablative chamber and the gaseous fuel transpiration-cooled engines using carbon-contained fuels).

(U) Because of the limiting burn duration capability of the passively-cooled, pump-fed engines, only short throttling operation can be tolerated within the lower chamber pressure limit.

(U) The regenerative engines have a very limited throttling capability and are not capable of deep throttling within the design concept considered.

(U) Deep throttling requirements eliminate the pressure-fed engines and pretty much limit the engine concepts to the transpiration-cooled engines of high chamber pressure design.

c. Propellant Restrictions

(U) Basically, the passive-cooled engine designs using the bleed turbine cycle can operate using all of the specified fuels. However, a particular propellant may be better suited to meet a specific restart requirement depending upon the mission.

(C) While the regeneratively-cooled engine is almost completely restricted to the use of MHF-5, N_2H_4 can be used in some missions where restart requirements permit this, providing that the bulk temperature rise is kept to a minimum by selecting injectors requiring a short L*.

(C) The liquid oxidizer transpiration-cooled chamber is suitable for use with all fuels, but again, if the restart requirements are severe, N_2H_4 is not recommended because of the danger of detonation in the injector during restart.

(C) For the gaseous fuel-cooled engines, the N_2H_4 and 80/20 blend are the best suited propellants. This type of engine could use MMH and MHF-5 propellant if additives, such as NH_3 or N_2H_4 are used. These additives form methane (CH_4) with the carbon, which eliminates the carbon deposition problem.

(U) For the purpose of mission analysis, it is essential that engine design, propellant, and mission requirements be examined to assure that only feasible concepts are compared.

d. Restart

(U) The restart requirement has the most decisive affect upon propellant selection for the various design concepts.

(C) All of the four specified fuels are monopropellant which makes them susceptible to detonation if they became overheated (i.e., vaporize). N_2H_4 is the most dangerous because of its highly rapid pressure rise rate during decomposition. All of the other fuels have pressure rise rates that are magnitudes lower (see Appendix I).

(U) The restart capability is determined by the hardware temperature at restart; particularly by the hardware exposed to non-decomposed fuels.

(C) The injector face and manifold are most critical in the pressure-fed engines. The injector heat soak-back and cooling rate between shutdown and start dictates the restart capability. This restart capability is dependent upon burn duration and attitude during the coast period.

(U) Whenever a thrust chamber is shut down following a firing of extended duration, a quantity of entrapped heat flows or is radiated to the cooler adjacent areas. The injector is relatively cool at shutdown because of

the propellant flow through it. This also is true for the wall of a regeneratively-cooled or liquid transpiration-cooled combustion chamber.

Thrust chambers which rely on radiative, ablative, or hot gas transpiration cooling operate with a hot internal wall. The entrapped heat is dissipated into the adjacent areas upon shutdown. The radiation-cooled unit cools rapidly by radiation from its outer surface although the injector also is subjected to radiative and conductive heat loads. Essentially, the ablative unit has an insulated outer wall, which results in a still hotter internal surface and much of the heat is dissipated to the injector because of the limited view factor through the throat. This thermal load can result in the temperature at the face of the injector as well as the adjacent structure being raised to a point where the fuel will detonate on the next restart or where damage will be sustained as a result of melting or thermal distortion.

An ablative fluorine thrust chamber assembly is currently under development at Aerojet-General.(14) This includes the investigation of the feasibility of a thermal accumulator, which consists of a quantity of phase-changing material located on the injector to absorb heat during the period following thrust chamber shutdown. The quantity of material is selected to provide sufficient capacitance to prevent the injector from exceeding 350°F. Also, the phase-changing material takes advantage of the latent heat of fusion to minimize the mass required.

The effect of heat-sink technology upon engine restart capability has not been determined as yet.

Without heat-sinks to absorb the heat soak-back, it is estimated that 1-1/2 to 2-1/2 hours should elapse before pressure-fed engine restart could be safely attempted using N_2H_4 fuel. Based upon heat transfer analysis, the most critical time is estimated to be 10 to 30 minutes.

Pump-fed engines have two heat-soak-back problems; one attributable to the thrust chamber assembly and the other to the turbine drive and gas generator.

After shutdown the heat soak-back from the turbine is absorbed by the fuel and oxidizer pump. Therefore, it is advantageous to locate the fuel pump as far as possible from the drive turbine. This can be done readily for oxidizer-rich, gas-driven turbines.

With the single-stage turbines used in the staged-combustion cycle, the heat-sink capabilities of the two pumps are usually more than adequate to maintain the fuel pump temperature below critical. Therefore, the primary and secondary injectors remain the critical components.

---

(14) Contract F04611-67-C-0003

(C) The liquid fuel regeneratively cooled engines have a particular restart problem. As a result of the long transients connected with a tankhead start, tube cooling is not sufficient during the transient to prevent tube burnout. Therefore, it is desirable to pressurize the tube bundle prior to light-off by using a cartridge start system or rechargeable pressure bottle as well as a downstream valve. For multiple-restart capability, rechargeable pressure bottles are necessary because only a limited number of restarts can be accomplished using start cartridges.

(U) At shutdown, the cooling tubes flow has to be maintained to remove the tube heat soak-back. Usually, the down coast inertia of the pump is used to recirculate fuel through the tubes back into the tank. This increases the fuel tankhead load to an extent that depends upon the number of shutdowns.

(U) The main injector remains the critical component for regenerative engines but should demonstrate a better restart capability than the ablative engine because of the cool chamber. It is estimated that a flat-faced injector should be capable of restart after one hour of coast following a reasonably long burn duration. A platelet injector would improve this considerably.

(U) The restart capability of a two-stage bleed turbine has not been analyzed. It may require additional heat-sink to improve its capability.

(U) For the liquid oxidizer, transpiration-cooled chamber, a similar problem exists. In this cooling method, the chamber has to be pressurized prior to light-off to obtain liquid flow in the chamber cooling manifolds. In the staged-combustion cycle, this is accomplished with the oxidizer-rich primary gas generator. The restart capability of this engine also is determined by the primary and secondary injector temperature transient.

(U) The critical component of the gaseous fuel-cooled chamber is the CAT-Pack injector and feed line which should be kept as short as possible to use the pumps as heat-sinks. For short coast durations (approximately one hour) following a long burn duration, N_2H_4 should not be considered for this engine concept and the 80/20 blend should be used.

e. Envelope Limitations and Installation

(U) The mission requirement limits the available engine envelope. In this analysis, a 10 ft diameter was the limiting factor. However, only the larger area ratio of the pressure-fed engines was diameter limited.

(U) As previously discussed, the engine installation has an affect upon the restart capability because it determines the heat radiation rate and thus, the engine temperature transients.

Conversely, engine heat input into the system is not desirable because of structural reason. Therefore, hot-running engines, such as those required for re-entry vehicles, are not desirable for buried installations (i.e., radiation-cooled and gaseous fuel-cooled engines). Thus, heat-shielding weight penalties should be considered in a mission analysis.

f. Reusability

The reusability of engine hardware must be viewed in context with flight application as well as engine development.

Passive-cooled systems are not considered reusable in terms of flight application because of material consumption and the reaction of the chamber liners with the combustion products. Therefore, reusability is primarily restricted to the actively-cooled concepts. In terms of flight application, this reusability is equal to re-entry capability and requires special design considerations (i.e., jettisonable nozzle extension and propellant tank ventilation capability).

The reusability of engines is significant in the reduction of engine development costs. While the passively-cooled engines are reusable, they are restricted by the total burn duration, after which they no longer are of any value, which results in high development costs. The transpiration-cooled engine is very well-suited for development purposes because of its capability for being re-machined.

g. Start Impulse

Pressure-fed engines deliver very short and repeatable start impulses; therefore, they are suited for clustering. The starting transient from fire-switch to full thrust is approximately 0.3 sec to 0.4 sec. The start transients for pump-fed engines utilizing tankhead are generally in excess of0.4 sec duration depending upon the type of cycle and cooling method.

Start impulse should be kept minimal to simplify staging of the upper stage. For an intercept mission, tankhead start, with its long transient, is not acceptable because it is the equivalent of an additional ΔV requirement and pressure bottle start previously described in the discussion of Engine No. VIII. However, Engine No. VIII is expected to result in the shortest start transient of all the pump-fed engines because of its gas/gas feed and cooling system which hardens immediately.

B. COMPARISON OF THRUST CHAMBER THROAT COOLING LOSSES

During the analysis of the cooling requirements for the various methods of throat cooling, it became obvious that each cooling method has a thrust and chamber pressure region, wherein it can outperform any other cooling method as regards coolant losses. In this section, these regions are presented for the ablative, regenerative, and transpiration-cooled chambers. Comparison is made strictly on a coolant loss basis. Over-all performance or

capabilities (i.e., throttling or restart) are not considered. However, to assure a valid comparison based upon this approach, those areas common to the engines compared were ascertained.

1. Liquid/Liquid Injection Systems

This first comparison deals with liquid/liquid injection systems only and compares the effect of characteristic chamber length upon the cooling requirements. The comparison includes fuel film-cooled ablative chambers, liquid fuel regenerative chambers, and transpiration chambers using fibrous graphite platelets cooled by gaseous fuel or liquid oxidizer. In all cases, N_2H_4 is used as the fuel.

To clarify the comparison, the following tabulation is presented to identify the variation in the transpiration-cooled chamber:

	LIQUID OXIDIZER, TRANSPIRATION-COOLED	GASEOUS FUEL, TRANSPIRATION-COOLED	
L* = 30-in. All Chambers	Graphite Transpiration Throat Material (see Figure No. 105)	Graphite Transpiration Throat Material (see Figure No. 107)	
L* = 15-in. All Chambers	Graphite Transpiration Throat Material (see Figure No. 106)	Graphite Transpiration Throat Material (see Figure No.108)	Nickel Transpiration Throat Material (see Figure No. 109)

The comparison of the ablative and regeneratively-cooled chamber with a liquid oxidizer transpiration-cooled chamber is done for two characteristic lengths of 30-in. (Figure No. 105) and 15-in. (Figure No. 106). The results indicate that the regeneratively-cooled chamber has a relatively large region of performance superiority within the scope of thrust and chamber pressures investigated. Also, that L* has little effect upon boundaries. The ablative and transpiration-cooled chamber divides the remaining region nearly equally, restricting the transpiration-cooled engines to the higher chamber pressures. The film-cooling and transpiration-cooling requirement, W_c/W_t, is nearly proportional to the L* to yield increased performance for the shorter L* chambers. The boundary between the fuel film-cooled ablative and the oxidizer-cooled transpiration chamber includes a sensitivity factor for each coolant as regards performance. Therefore, the indicated boundaries identify equal losses.

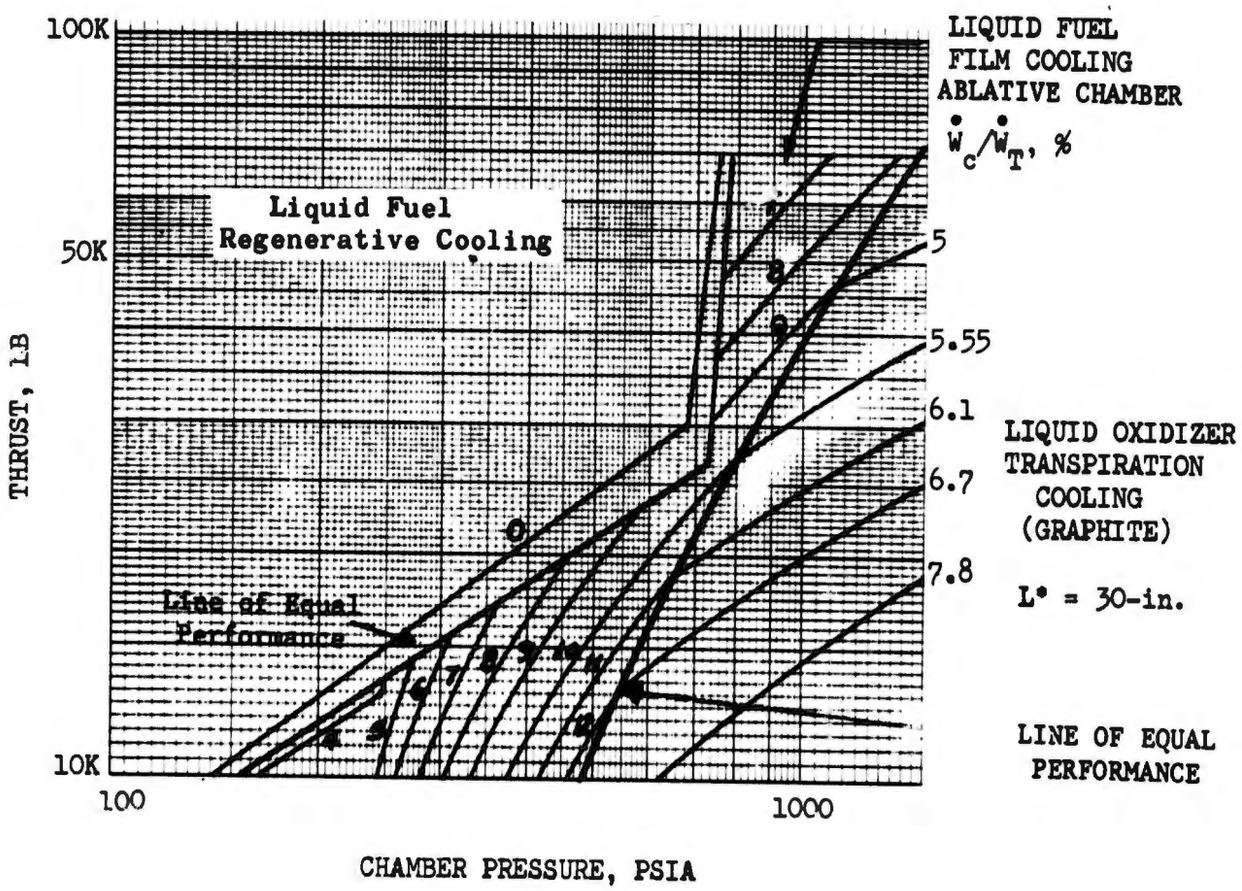

Figure 105. Operating Regimes of Various Cooling Methods, CLF_5/N_2H_4 (L* = 30 in.) (Liquid Oxidizer)

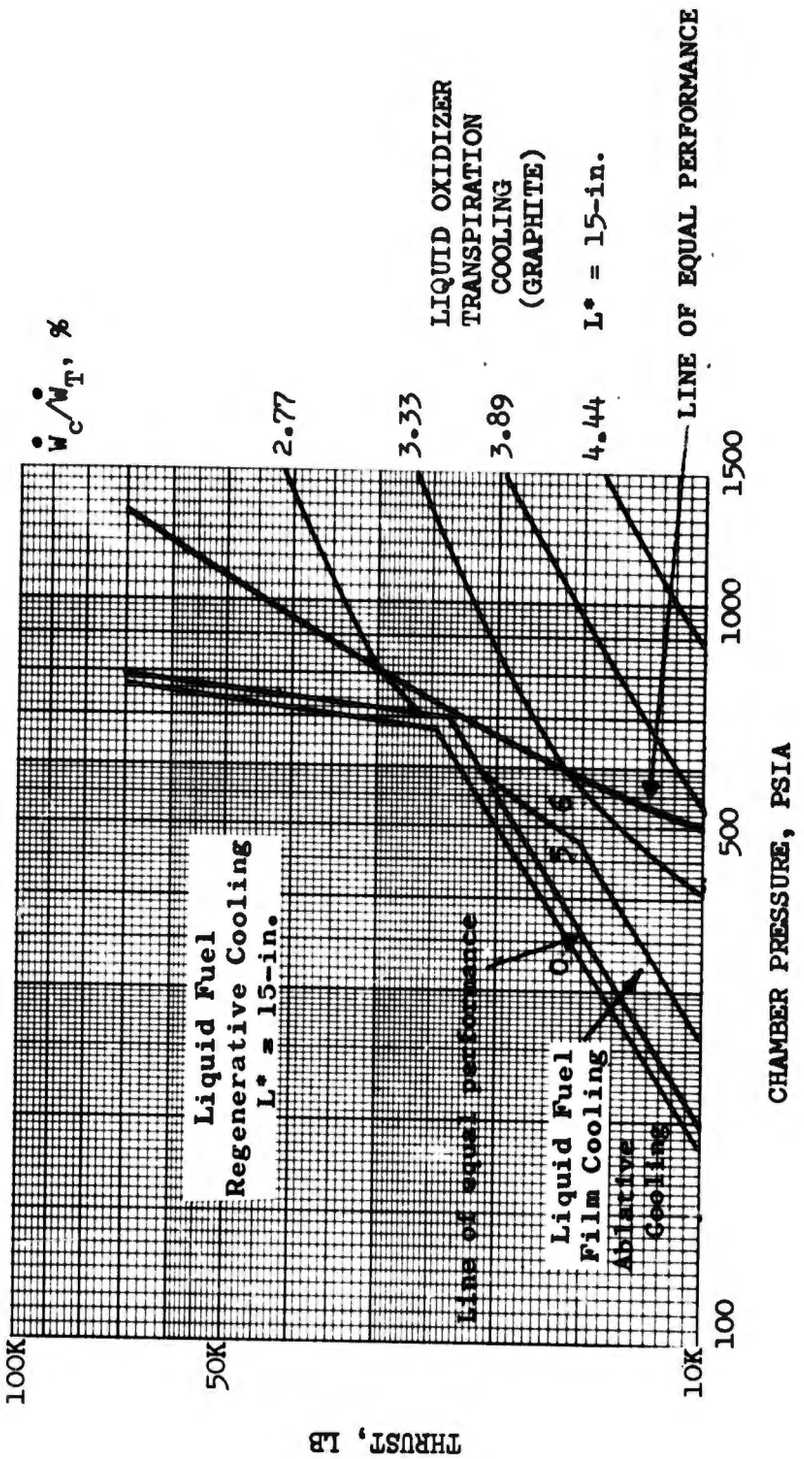

Figure 106. Operating Regimes of Various Cooling Methods, CLF_5/N_2H_4 (L* = 15 in.) (Liquid Oxidizer)

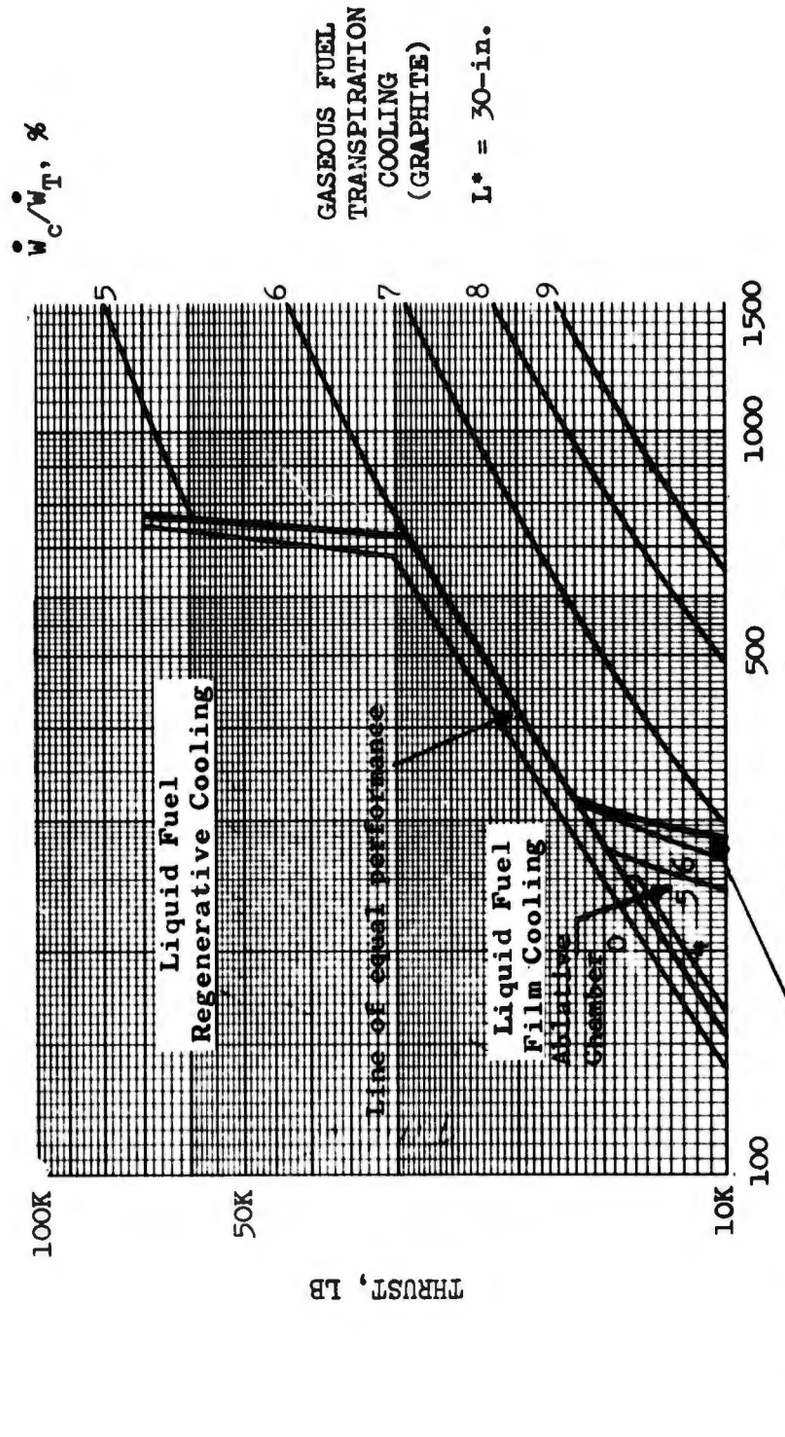

Figure 107. Operating Regimes of Various Cooling Methods, CLF_5/N_2H_4 (L* = 30 in.) (Gaseous Fuel)

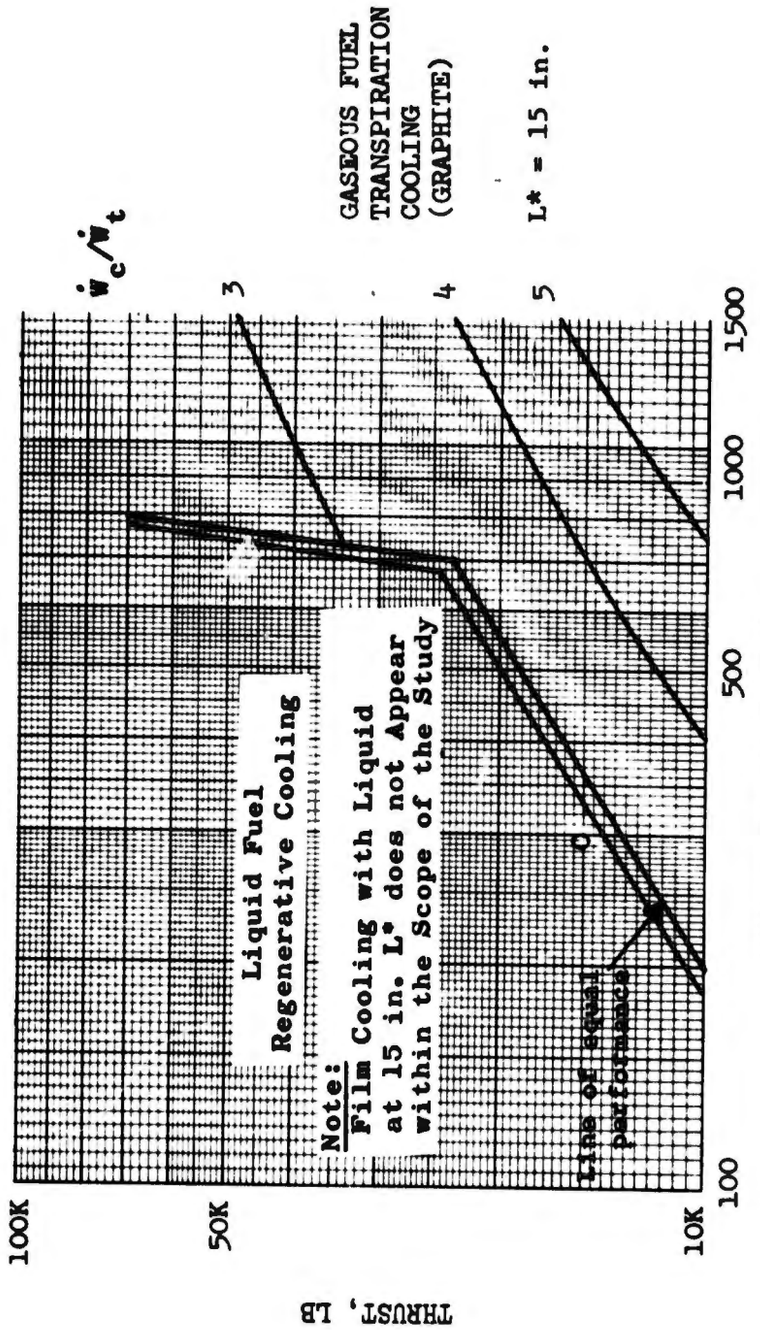

Figure 108. Operating Regimes of Various Cooling Methods, CLF_5/N_2H_4 (L* = 15 in.) (Gaseous Fuel)

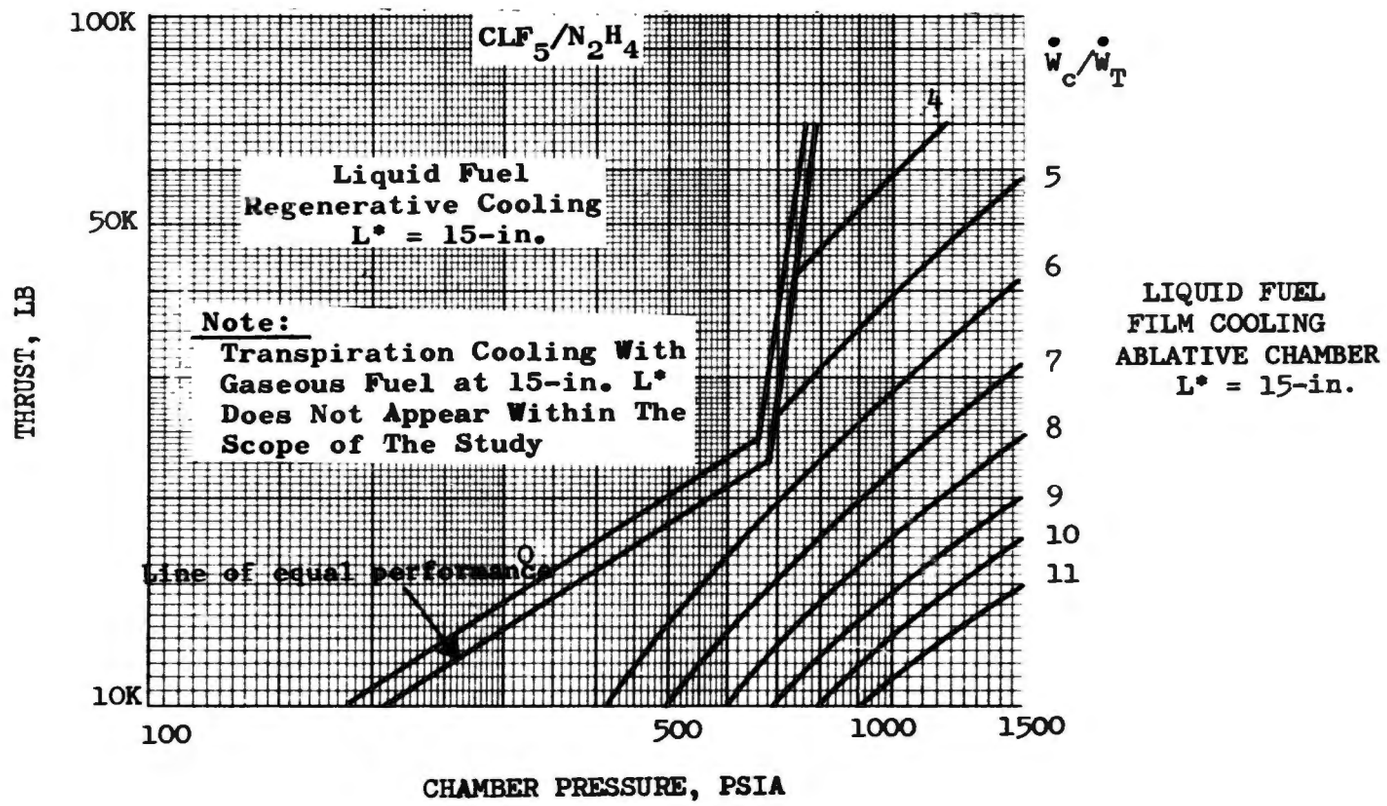

Figure 109. Operating Regimes of Regenerative, Film, and Transpiration Cooling Methods, CLF_5/N_2H_4 (L* = 15 in.) (Liquid Fuel) (Nickel Platelets)

A similar comparison is made between all fuel-cooled chambers in Figures No. 107 and No. 108. Again, the region for the regenerative chamber is practically unaffected by L* changes. However, the region of the ablative chamber shrinks considerably for a L* of 30-in. as can be seen on Figure No. 107 and disappears completely with a L* of 15-in. This clearly indicates a better performance for the gaseous fuel transpiration-cooled chambers over the oxidizer transpiration-cooled chambers.

In a third comparison, the effects of the chamber material upon the various regions was made by comparing Figure No. 108, which represents the fibrous graphite material, and Figure No. 109, the nickel material, for the gaseous fuel transpiration-cooled, 15-in. L* chamber. The results affect the transpiration-cooled and the ablative chamber only. They appear to indicate that the nickel material cannot compete with the ablative chamber upon the basis of a performance comparison. However, the ablative chamber is extremely burn duration limited at the higher chamber pressure, which extremely limits its mission applicability. Therefore, a performance penalty is incurred to obtain increased burn duration by applying the transpiration-cooled nickel platelets.

2. Staged-Combustion Cycles and Bleed Cycle Comparison

The cooling losses of the three cooling methods are compared; however, the staged-combustion cycle is used for the transpiration-cooled chamber to reduce the L* requirement. In this comparison, all transpiration-cooled chambers feature nickel platelets and all chamber cooling is achieved by the use of fuel.

The effect of L* is again demonstrated by comparing a L* of 10-in. (Figure No. 110) and a L* of 5-in. for the transpiration-cooled chamber (Figure No. 111) with both of the other cooling methods, each having a L* of 15-in. The results indicate that the region of the transpiration-cooled chambers increases drastically with a decreasing L* by reducing the cooling requirements for a given thrust and chamber pressure.

3. Effect of Selected Fuels Upon Cooling Region

Finally, the effect of the specified fuels upon the preferred cooling region is demonstrated by comparing a L* of 15-in. for the regenerative and ablative engines with a L* of 5-in. for the transpiration-cooled chambers, which represents the shortest L* obtainable for the bleed cycle and the staged-combustion cycle.

The results are presented on Figure No. 111 for N_2H_4, Figure No. 112 for MHF-5, and Figure No. 113 for MMH. They indicate a reduction of the regeneratively-cooled region by changing fuel from N_2H_4. In the case of MMH, only a very small region remains to be cooled regeneratively while the rest of the area is divided equally by the ablative and transpiration-cooled chamber.

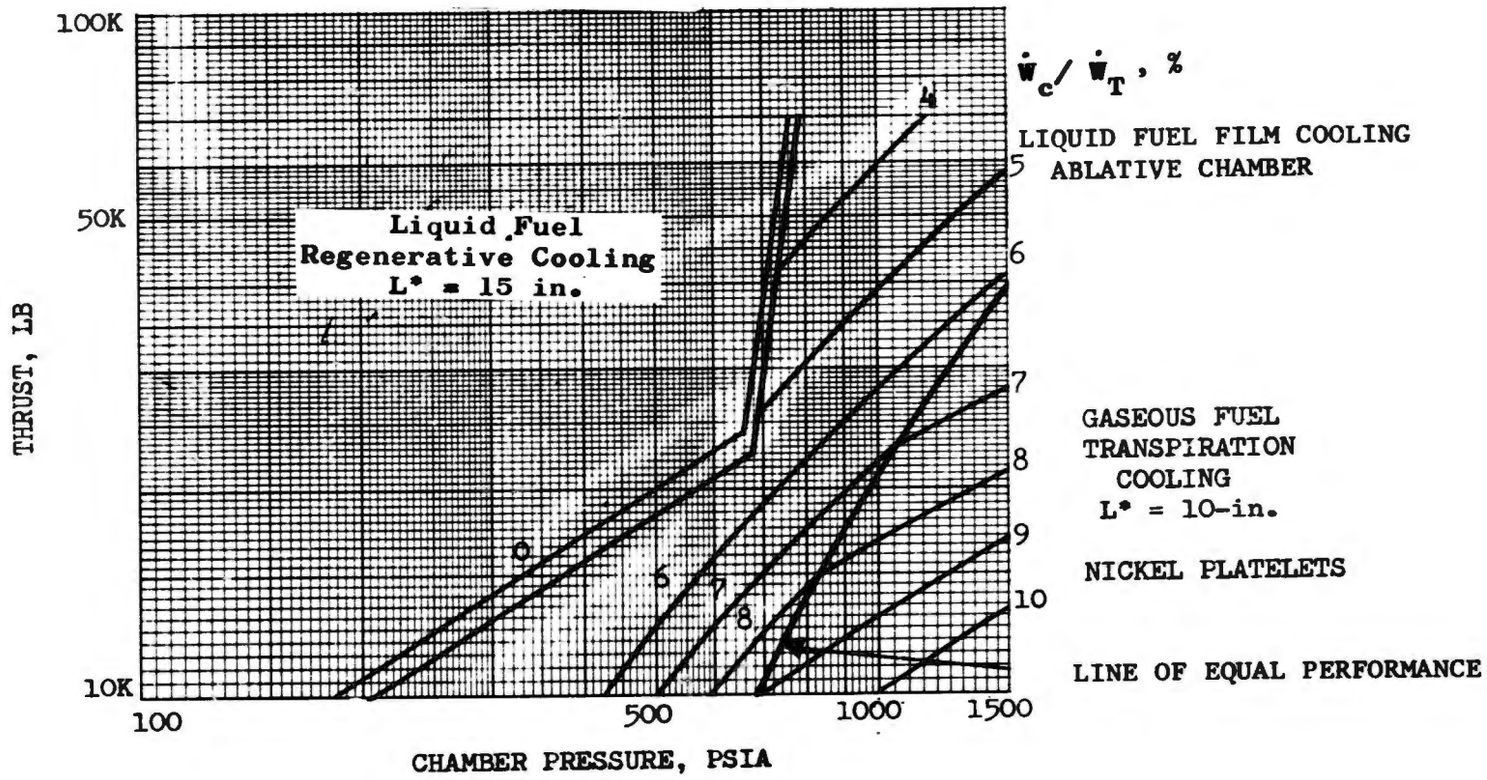

Figure 110. Operating Regimes of Various Cooling Methods, CLF_5/N_2H_4 (L* = 10 in.) (Gaseous Fuel) (Nickel Platelets)

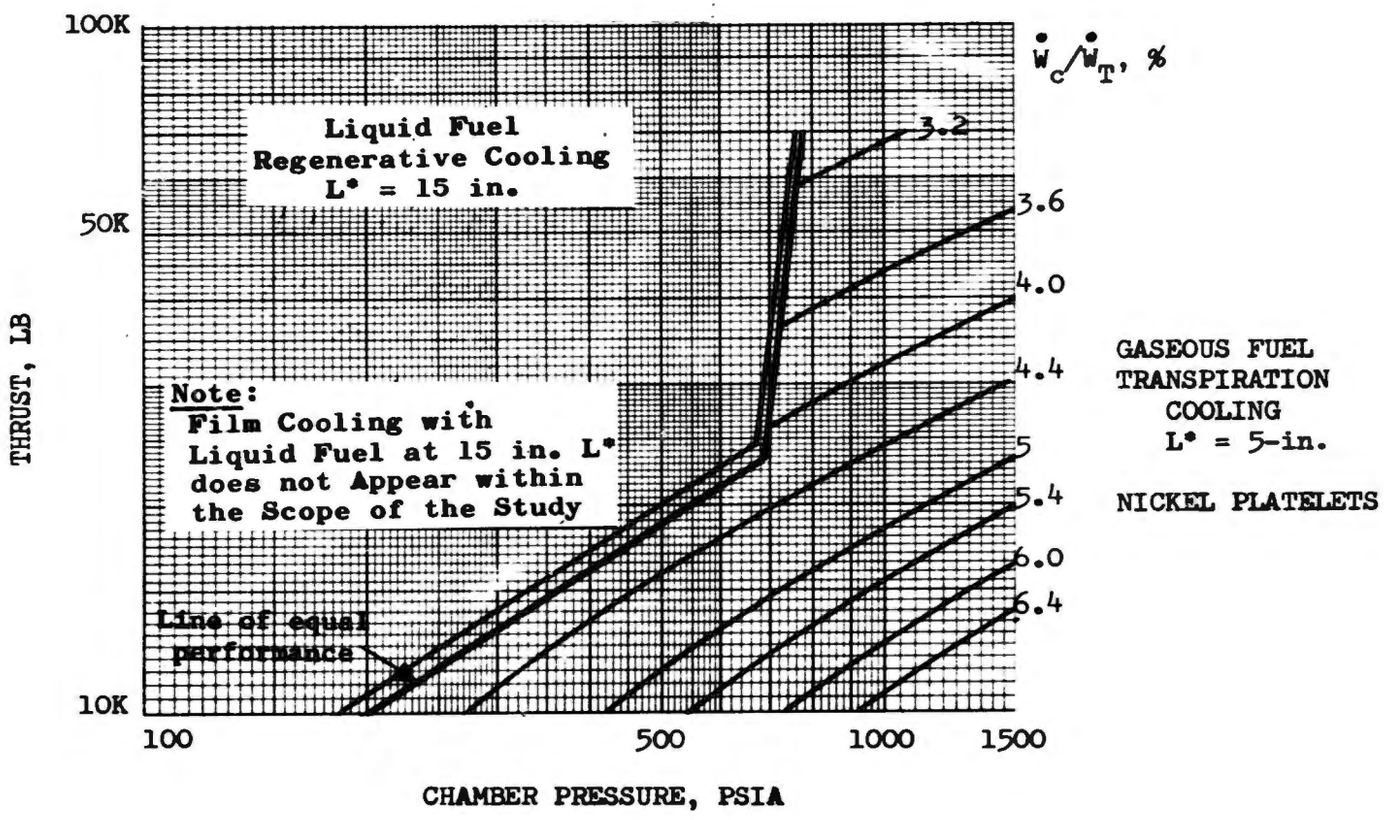

Figure 111. Operating Regimes of Various Cooling Methods, CLF_5/N_2H_4 (L* = 5 in.) (Gaseous Fuel) (Nickel Platelets)

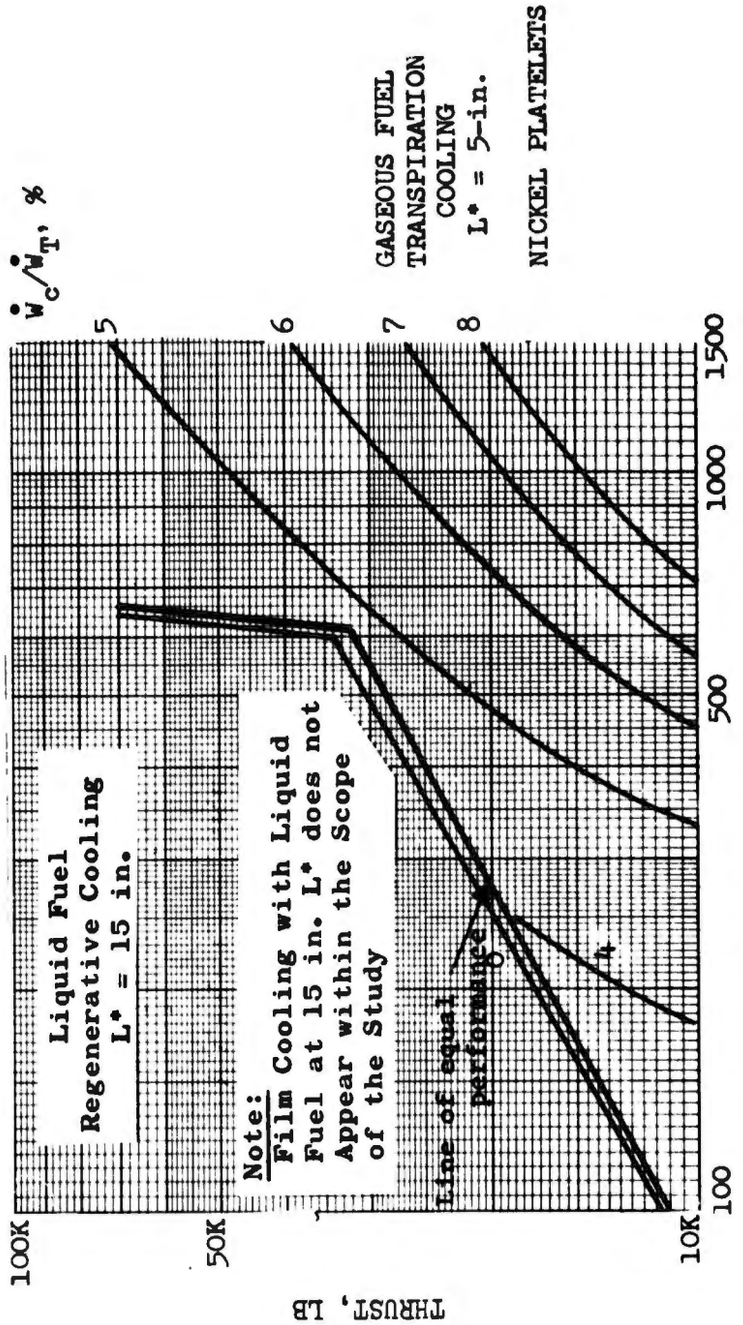

Figure 112. Operating Regimes of Various Cooling Methods, CLF_5/MHF-5

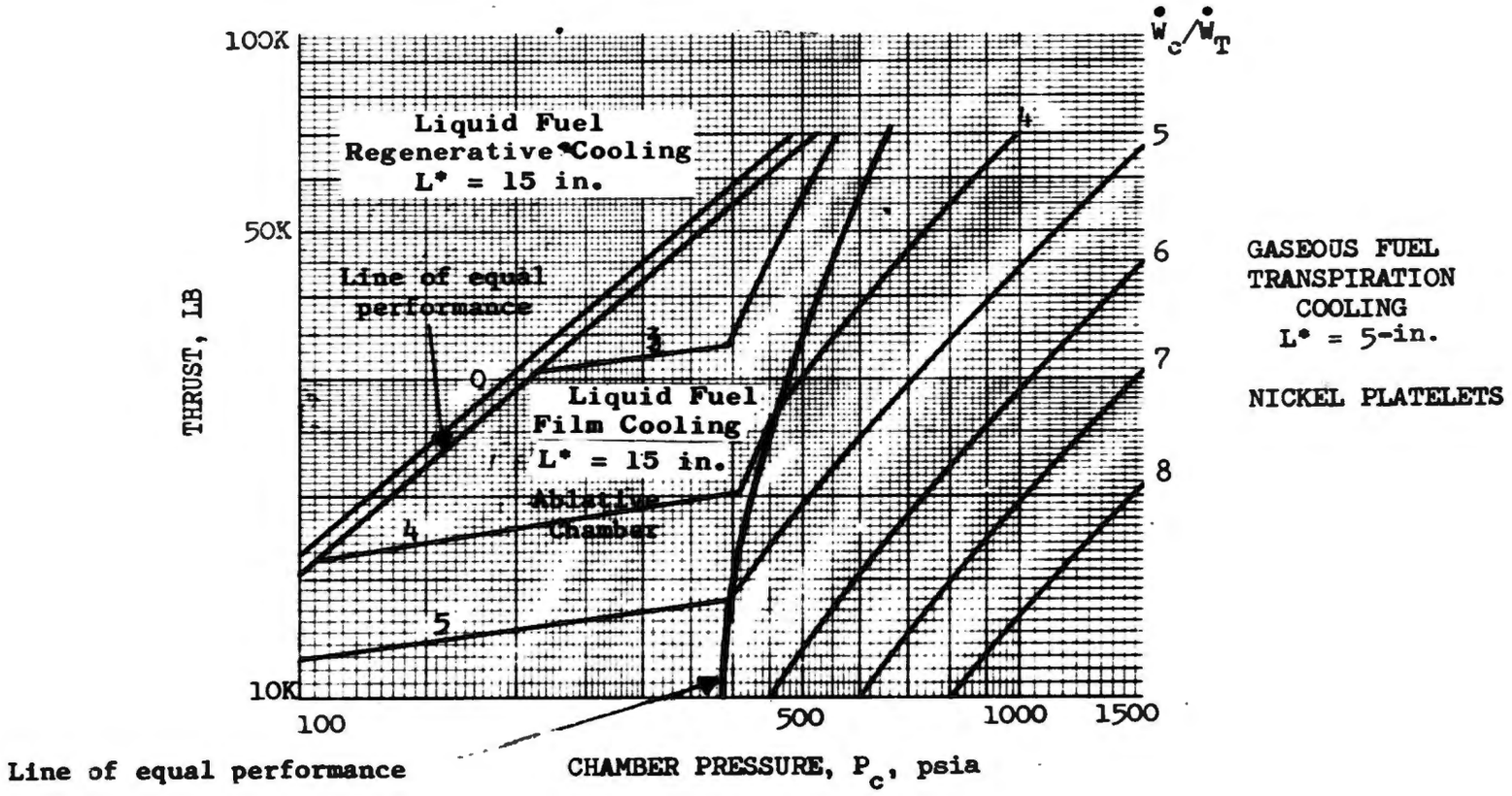

Figure 113. Operating Regimes of Various Cooling Methods, CLF_5/MMH

The results presented here pertain to cooling losses only. Where comparisons are made between different L*'s, which indicates different cycles or injector designs, the change in energy release losses (see Figure No. 105) and turbine drive losses must be considered to obtain a comparison of over-all engine performance.

VI. PARAMETRIC ENGINE CHARACTERISTICS

The point design engines discussed in Section IV.of this report were used to establish absolute engine weight, performance, length, and diameter values for a specific engine type, thrust, chamber pressure, and area ratio. However, this information is needed for a range of thrust, chamber pressure, and area ratio before the maximum payload or ideal velocity increment capability can be determined for a given mission. Therefore, parametric engine data was established for Point Design Engines No. I, No. IV, No. VII, and No. VIII as being representative of the four major engine cycles (pressure-fed, bleed, gas/liquid staged-combustion, and gas/gas staged-combustion). This same data also was generated for Point Design Engine No. V because it represents current technology for pump-fed engines and provides a reference point for comparing the more advanced engine types. The remaining point design engines (No. II, No. III, and No. IX) served to correlate the parametric data as well as to establish an engine variation capability (i.e., effect of different types of combustion chamber cooling methods).

The range of thrust and chamber pressure presented as part of this parametric data is restricted because the operation beyond this range is not practical. However, this range of thrust and chamber pressure is adequate to assure maximum results from mission analyses while providing greater accuracy because only minimal scaling of the point design engine was needed to establish the data. Table XXVI lists the range of variables for each parametric engine. As can be seen, the pressure-fed engines, which are represented by the parametric data for Engine No. I, have a chamber pressure range of 100 psia to 300 psia and a thrust range of 10K to 30K. The minimal chamber pressure and thrust values were established by the contract work statement. Transtage and Apollo experience indicated that the two maximum values were greater than those consistent with maximum mission capability.

Similarly, the bleed cycle engines, represented by Engine No. IV, were restricted to a chamber pressure range of 300 psia to 600 psia and a thrust of 25K to 70K. Mission analysis studies of in-space engines indicated that pump-fed, passively-cooled systems became optimum at chamber pressures within the indicated range and at thrust levels above 25K. The 70K maximum was established by the contract work statement.

The remaining pump-fed engines have a chamber pressure range of 300 psia to 1500 psia and a thrust range of 25K to 70K. The minimal values were established as previously discussed for Engine No. IV while the maximum values were dictated by the contract work statement.

The scaling equations used to obtain the parametric data for the selected design point engines are delineated in Appendices II and III of this report (Part II). The parametric data consists of:

TABLE XXVI

RANGE OF VARIABLES

Engine Feed System	Pressure Fed	Pump Fed
Cooling System	Passive	Passive & Active
Thrust (lb)	10K to 30K	25K to 70K
Chamber Pressure (psia)	100 to 300	300 to 1500
Throttling Range	1:1 to 10:1	1:1 to 10:1
Max Burn Duration (sec)	100 to 600	1500 to 3000*
Max Cont Burn (sec)	100 to 300	100 to 300
Number of Restarts	0 to 30	0 to 30
Minimum Coast Period (sec)	300	300

*Including refurbishment

- delivered specific impulse
- engine wet weight
- specific impulse at throttled thrust levels
- engine mixture ratio
- engine diameter for the range of chamber pressures, thrust levels, and area ratios indicated above

The parametric performance data for pressure-fed, pump-fed bleed cycle, pump-fed gas/liquid or liquid/gas staged-combustion, and pump-fed gas/gas staged-combustion engines are presented on Figures No. 114, No. 115, No. 116, and No. 117, respectively. Parametric engine data for Design Point Engine No. V, which is considered the baseline technology engine, is shown on Figure No. 118.

This performance data consists of deliverable engine specific impulse as a function of chamber pressure, thrust level, and nozzle area ratio. The range of thrust level and chamber pressure used is consistent with the previously indicated range restrictions.

Engine weight for pressure-fed, pump-fed bleed cycle, pump-fed gas/liquid or liquid/gas staged-combustion, and pump-fed gas/gas staged-combustion engines are shown on Figures No. 119, No. 120, No. 121, and No. 122, respectively. Again, similarly to performance, the parametric weight data for Engine No. V is provided (see Figure No. 123).

This weight information consists of engine thrust to weight ratio as a function of chamber pressure, thrust level, and nozzle area ratio.

Weight and performance data can be shown together as thrust to weight ratio versus specific impulse for various thrust levels and nozzle area ratios. This comparison for CLF_5/N_2H_4 propellants and an area ratio of 40:1 is shown on Figure No. 124 and for an area ratio of 150:1 is shown on Figure No. 125.

It can be noted on the indicated figures that each engine type appears as an operating envelope encompassed by constant thrust level and chamber pressure lines. Generally, the highest thrust to weight ratio and the highest performance within each envelope indicates the thrust level and chamber pressure consistent with maximum mission capability. In addition, relative mission capability between engines can be assessed by comparing the operating envelopes for the parametric engines. The dashed line in the parametric envelope for pressure-fed engines (Engine No. I) at the 150:1 area ratio (Figure No. 114) indicates the limitation imposed by the 10 ft exit diameter. The current technology engine (Engine No. V) is limited in chamber pressure to values over 600 psia because of the regenerative cooling limitations of the engine.

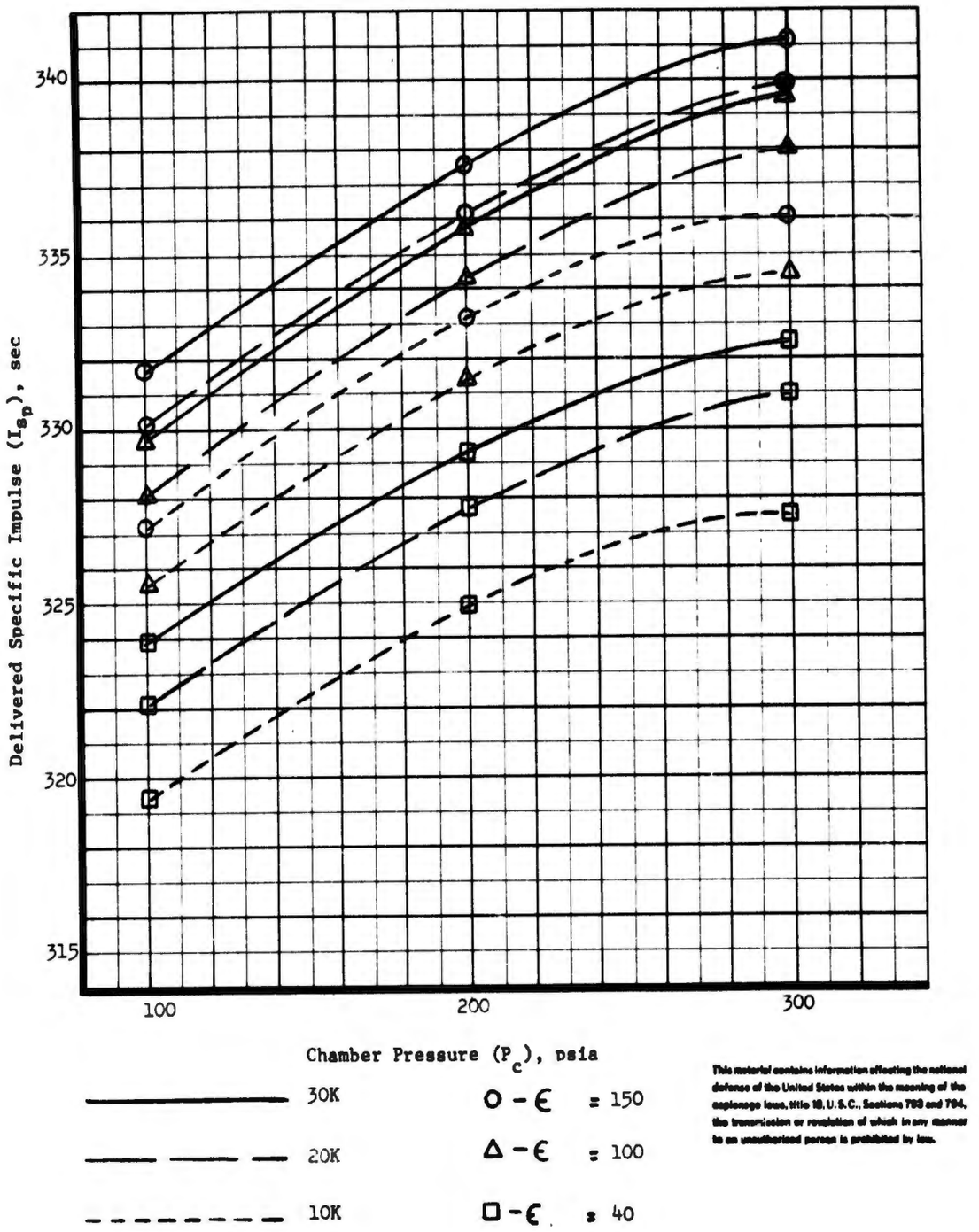

Figure 114. Parametric Performance Data, Engine No. I (u)

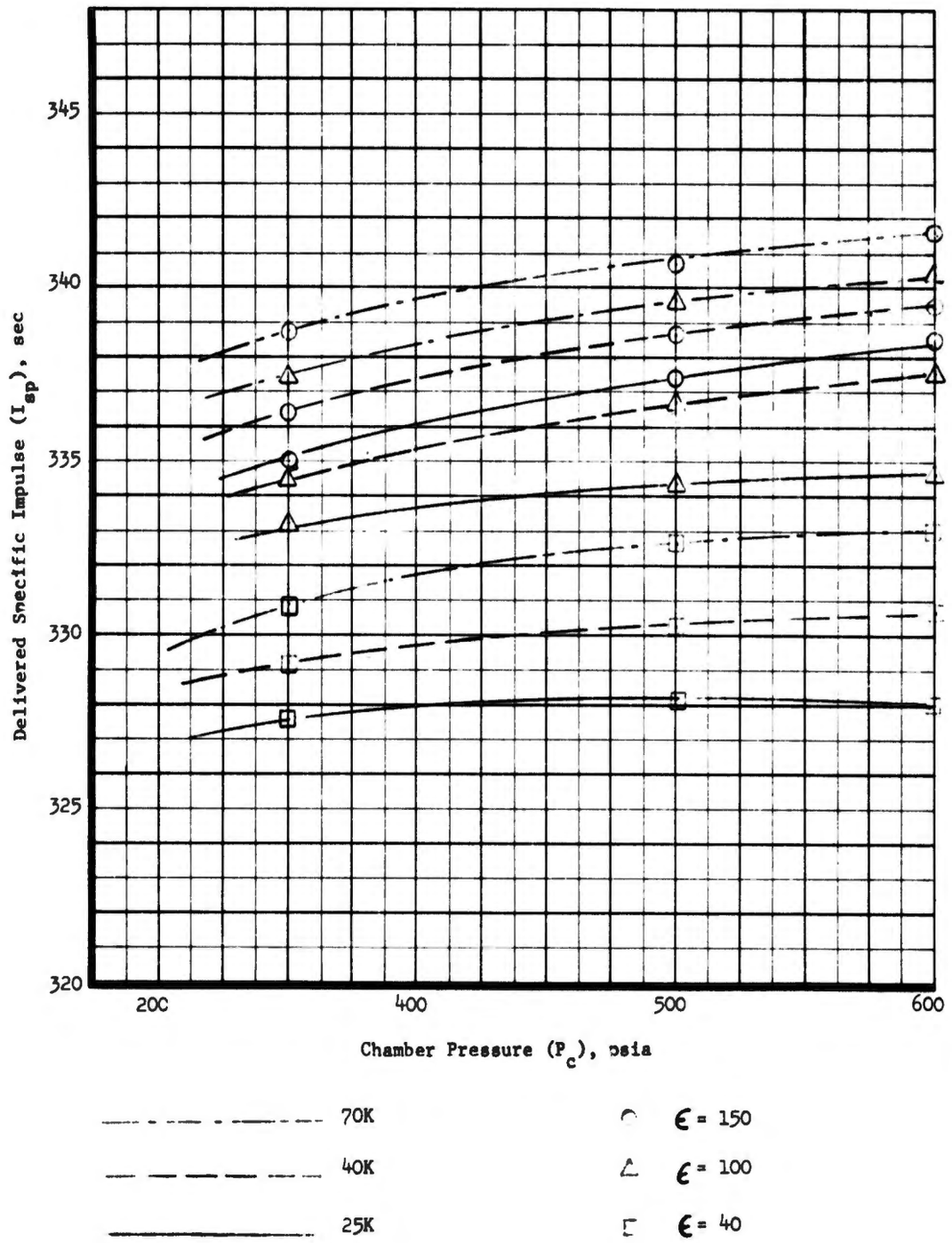

Figure 115. Parametric Performance Data, Engine No. IV (u)

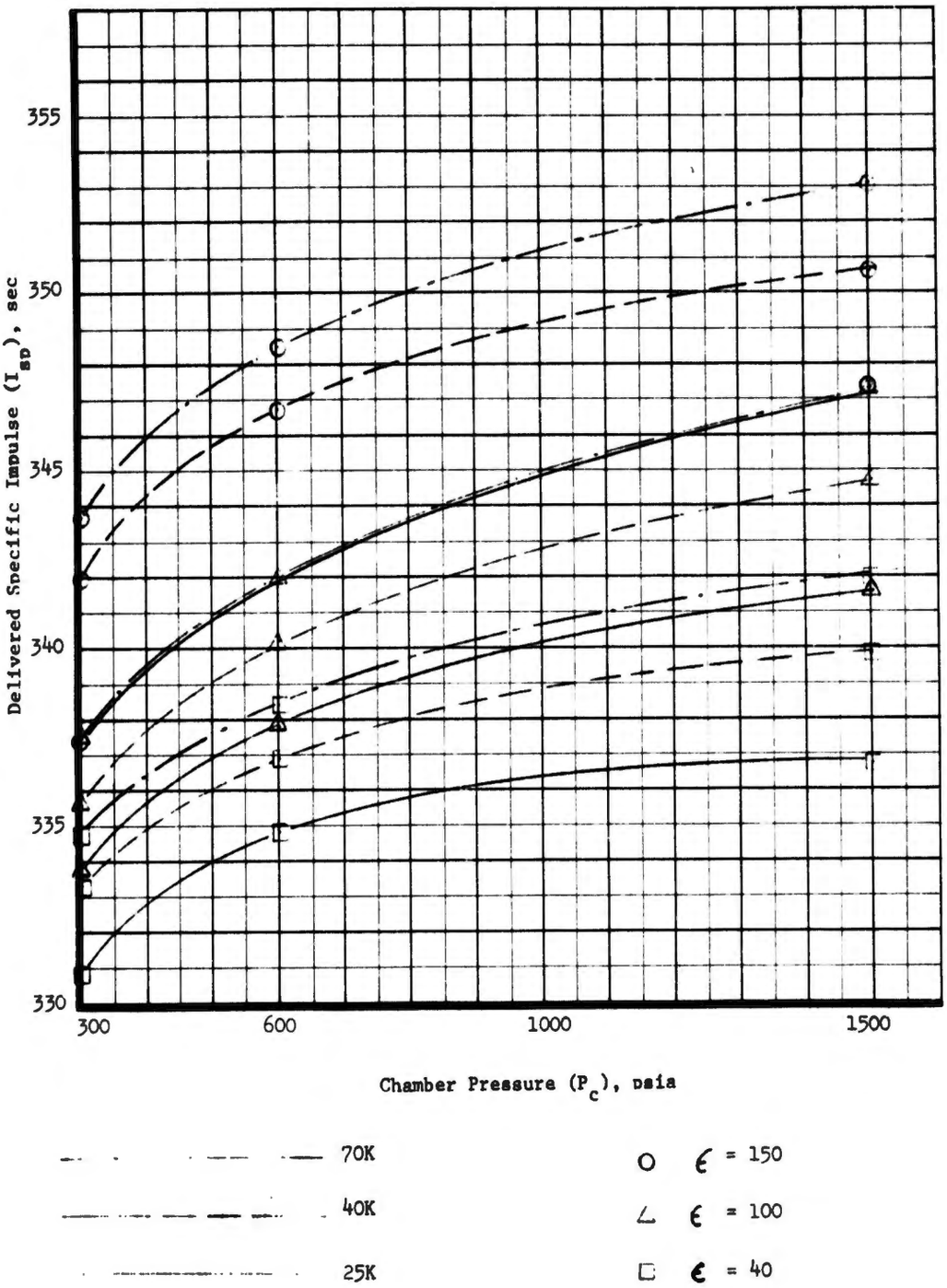

Figure 116. Parametric Performance Data, Engine No. VII (u)

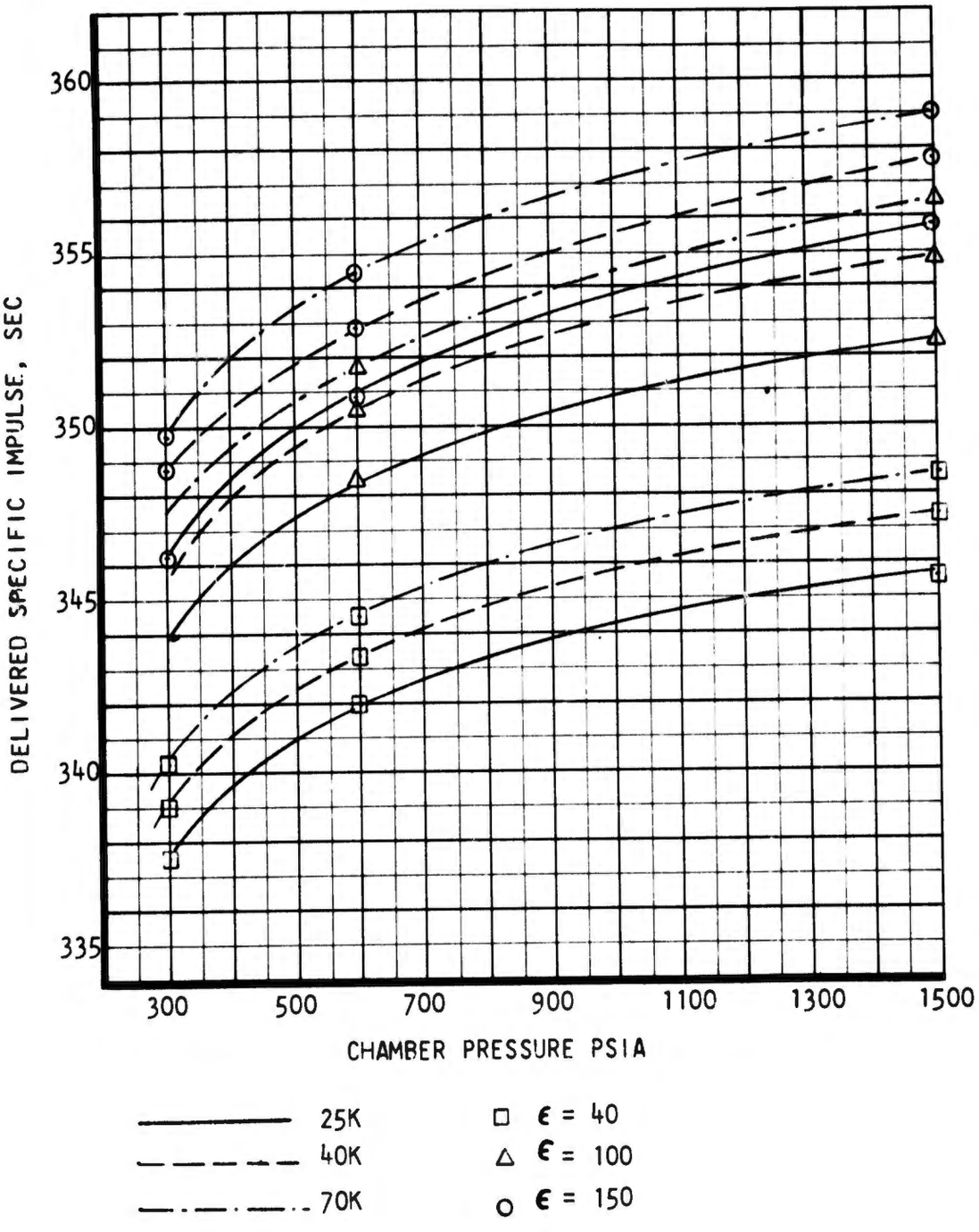

Figure 117. Engine No. VIII, Delivered I_s vs Chamber Pressure, Thrust and Expansion Ratio, ClF_5/N_2H_4, Gas/Gas, Gaseous Fuel Cooled (u)

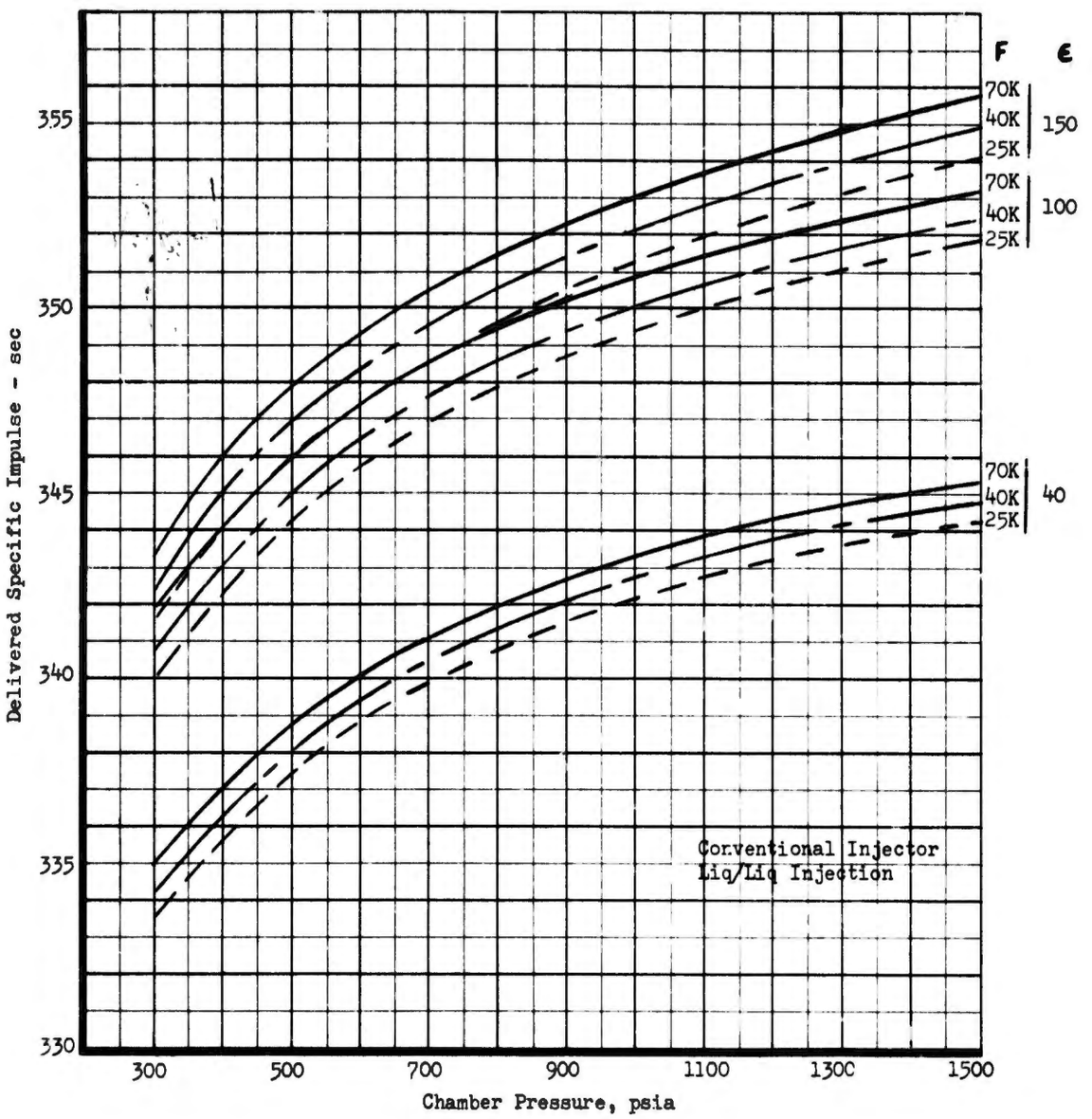

Figure 118. Engine No. V, Thrust Chamber Parametric Performance - Zero Coolant Flow (u)

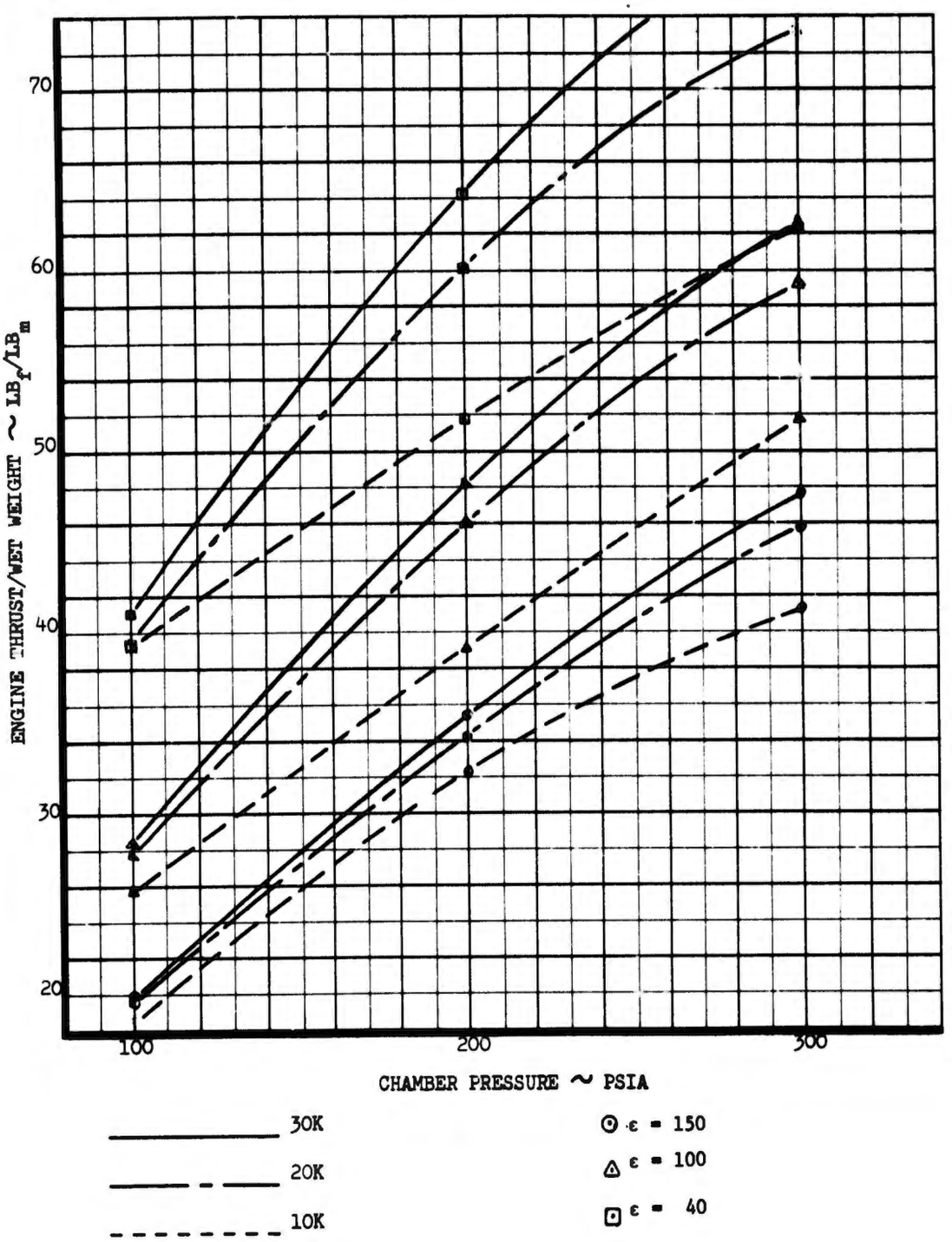

Figure 119. Engine No. I Parametric Weight

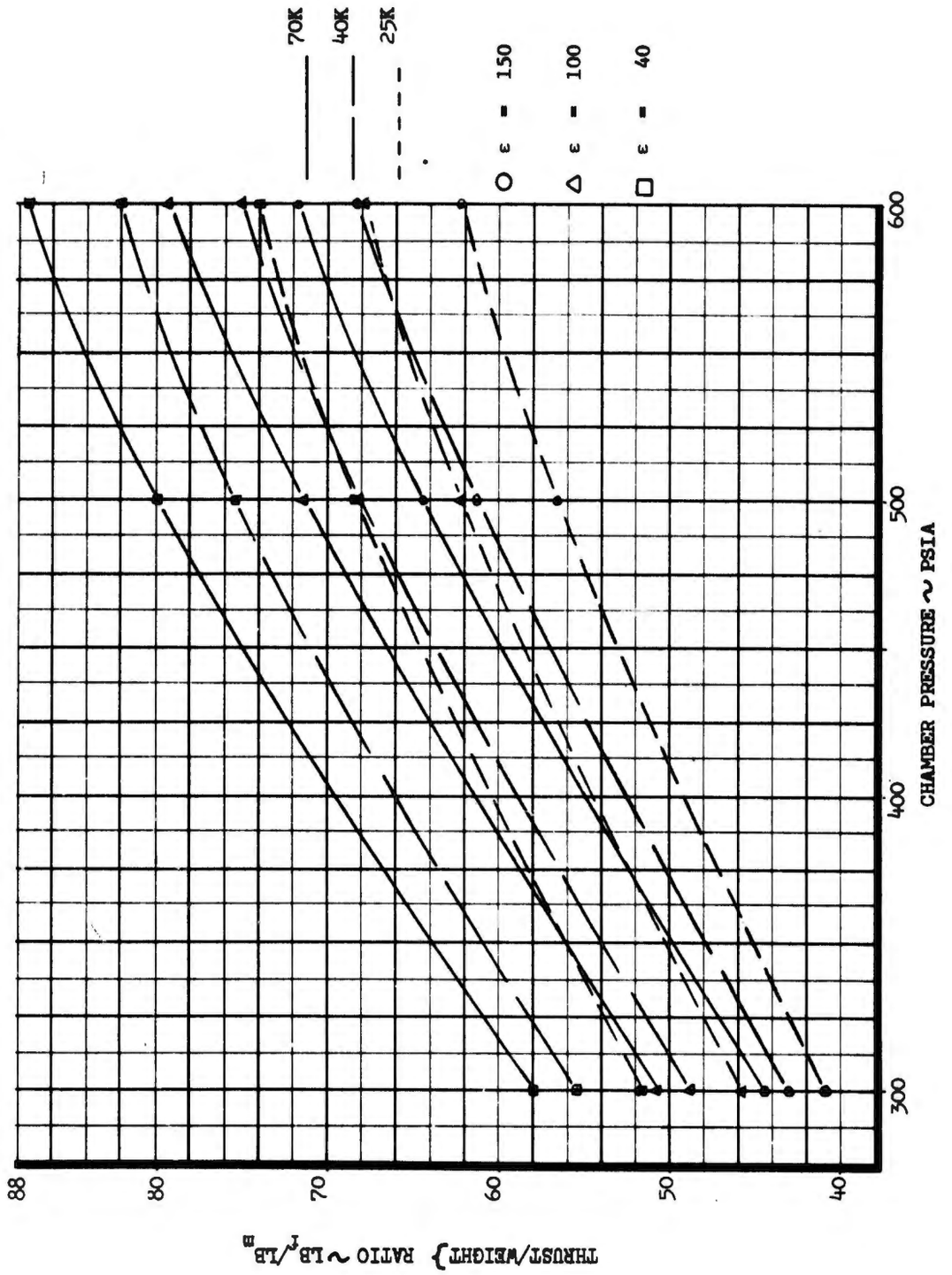

Figure 120. Engine No. IV, 600 sec, Ablative Thickness = 2.62-in.

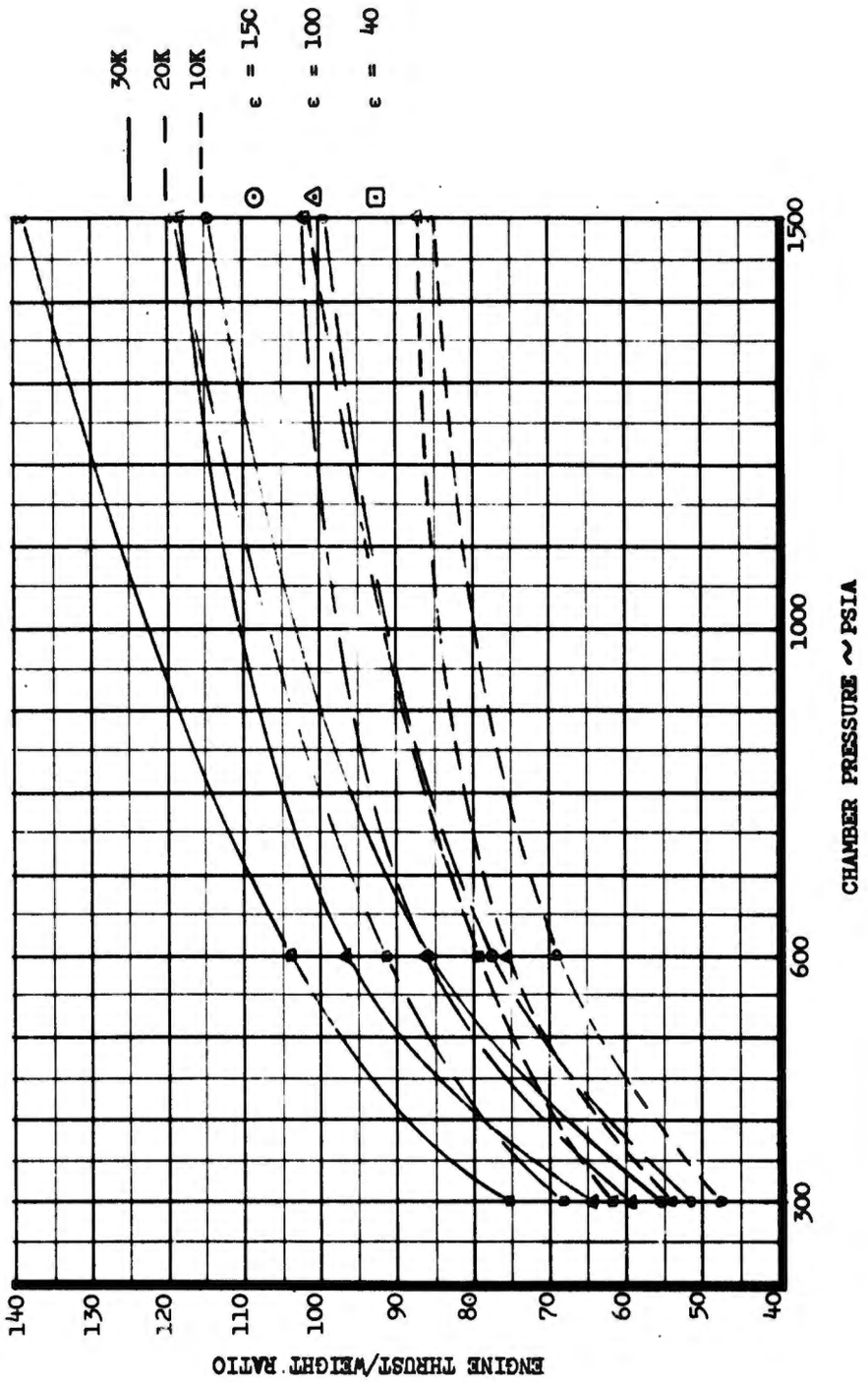

Figure 121. Engine No. VII Parametric Weight

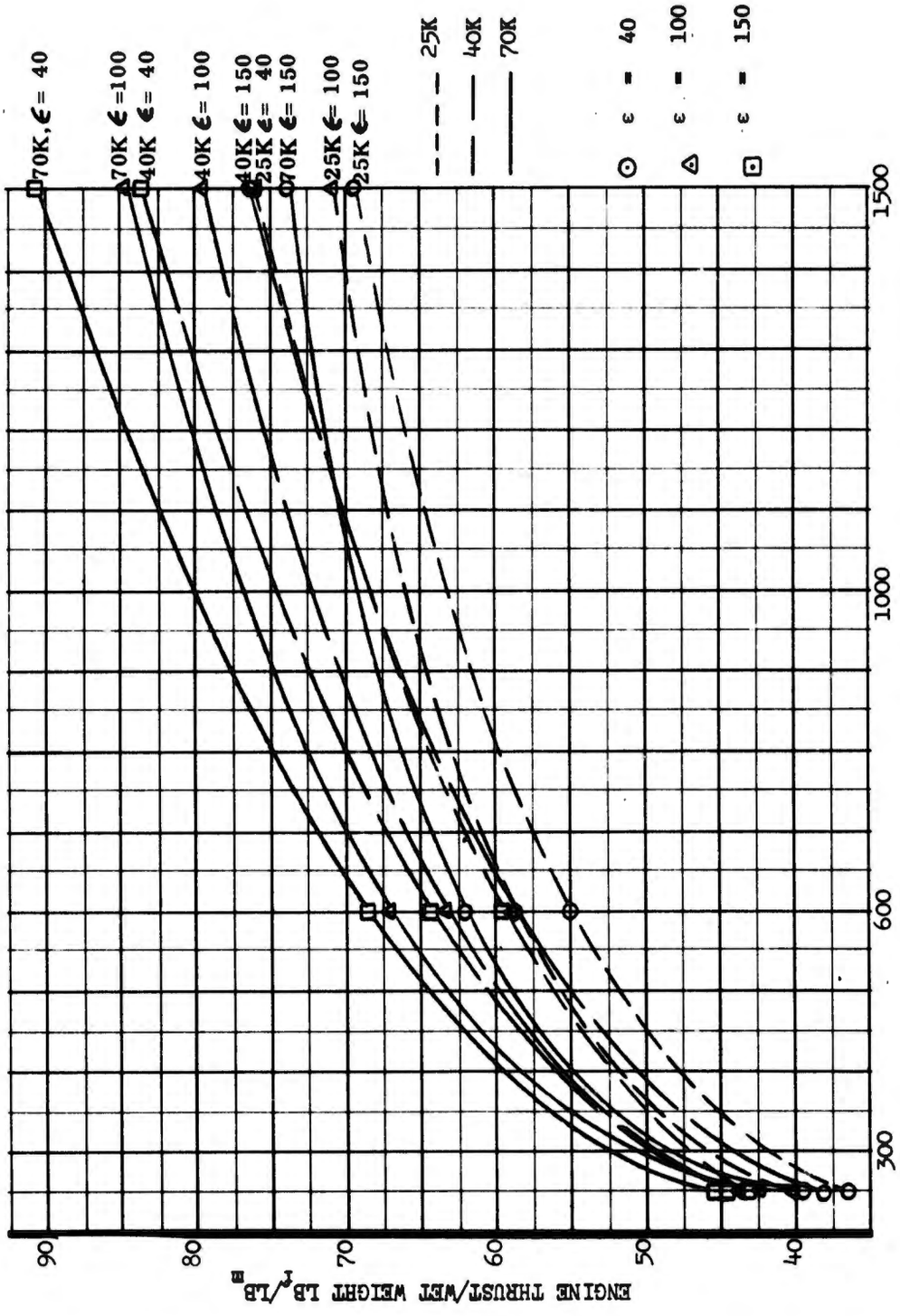

Figure 122. Engine No. VIII Parametric Weight

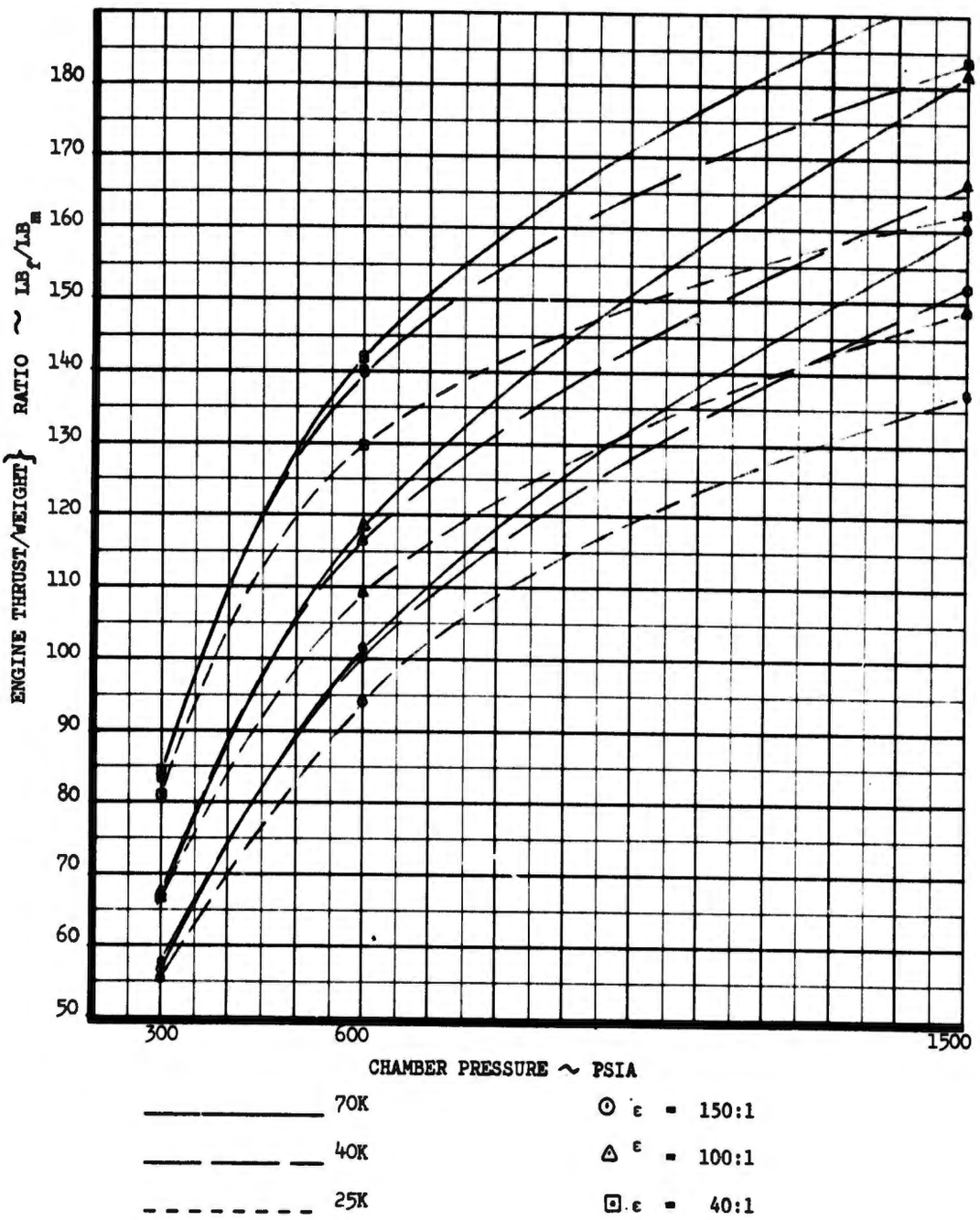

Figure 123. Engine No. V Parametric Weight

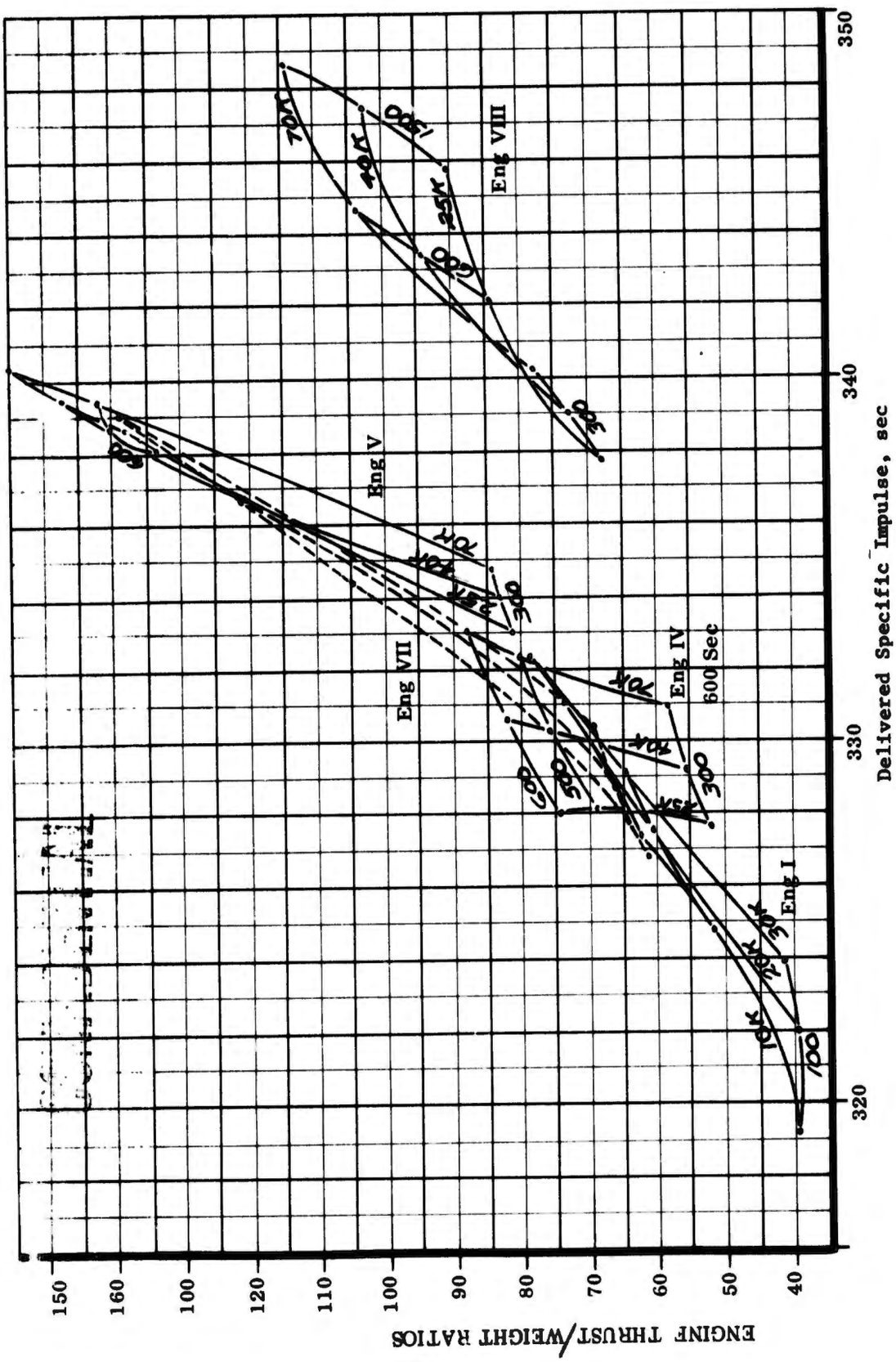

Figure 124. Delivered Specific Impulse Point Design Engine Thrust/Weight Ratio vs Specific Impulse, ε = 40:1 (u)

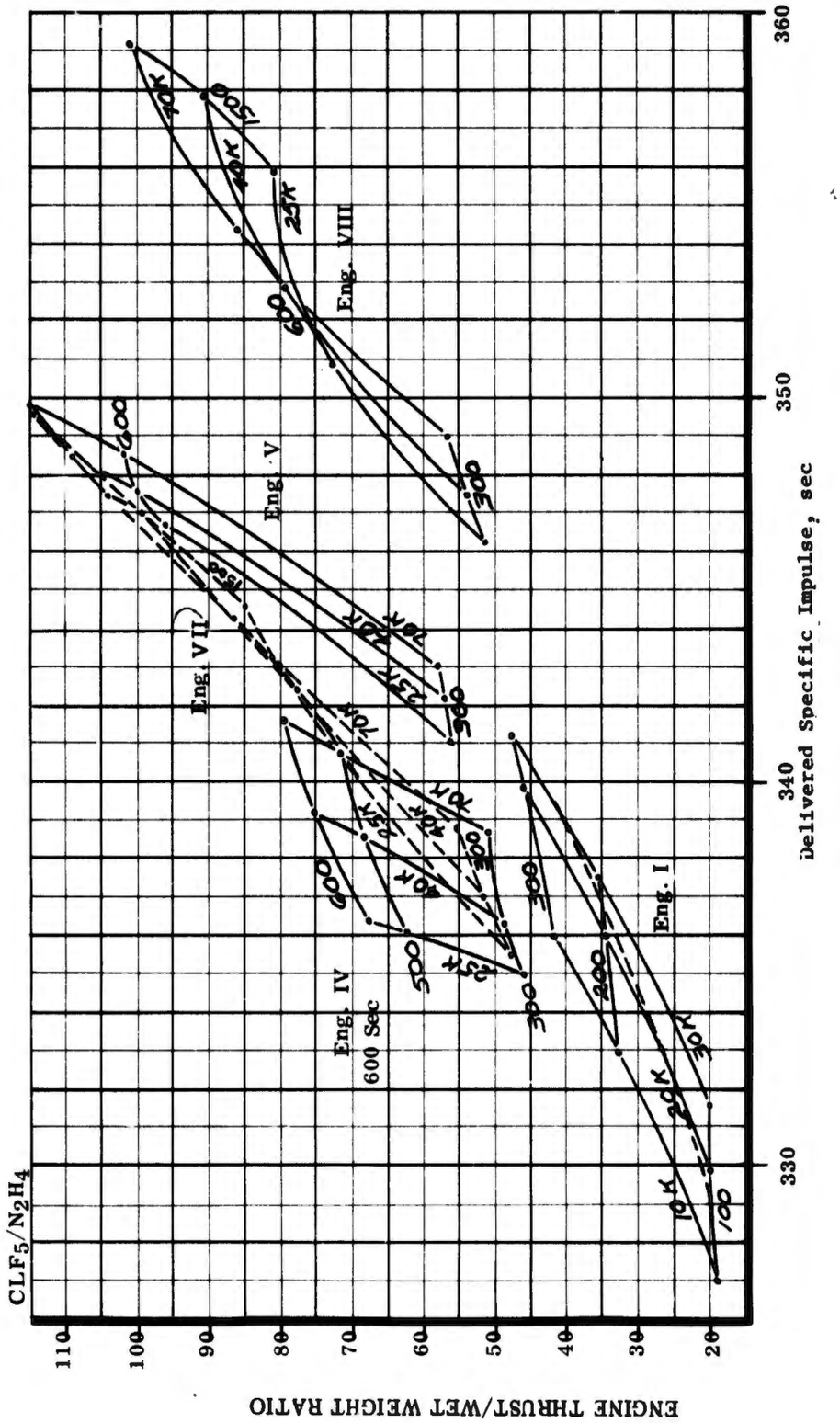

Figure 125. Delivered Specific Impulse Point Design Engine Thrust/Weight Ratio vs Specific Impulse, $\mathcal{E}$ = 150:1 (u)

Engine throttling performance in terms of the specific impulse degradation with the percentage of thrust is presented on Figures No. 126 and No. 127 for Engines No. I, No. IV, No. VII, and No. VIII as a function of the chamber pressure at full thrust. The influence of thrust level and area ratio has only secondary effects upon the results. Engine No. V is not shown because the regenerative cooling system is inconsistent with the required 10:1 throttling range.

The gas/gas staged-combustion engine (Engine No. VIII) results in the least performance degradation at the 10:1 throttling range as shown.

Engine mixture ratios consistent with the maximum delivered specific impulse is shown on Figure No. 128 as a function of chamber pressure and thrust level. Also included on this figure are the coolant flow rates as a percentage of the total engine flow rate. Note that the fuel-cooled engines (No. I, No. V, and No. VII) operate within a mixture ratio range from 1.9 to 2.3 while the oxidizer-cooled engines operate between 2.5 and 3.1. Although the oxidizer cooled engines (No. VII and No. IX) are lower in performance, the higher mixture ratio will result in an improved propellant bulk density for the vehicle.

Engine total length for the parametric engines is shown on Figures No. 129, No. 130, and No. 131 for nozzle area ratios of 40:1, 100:1, and 150:1, respectively. These lengths are presented as a function of chamber pressure and thrust level. The main difference in length between engines is associated with the combustion chamber characteristic lengths (L*'s) because the other major engine components are side-mounted to the thrust chamber. Therefore, the engine having the shortest L* requirement will result in the shortest engine length. As shown, Engine No. VIII which has only a 5-in. L* requirement, is the shortest engine.

Maximum engine diameter of the selected engines is shown parametrically on Figure No. 132. In all cases, this diameter is consistent with the exit diameter of the nozzle because, even at area ratios of 40:1, the other major engine components do not extent beyond the nozzle diameter. For plotting purposes, the engine diameter shown on Figure No. 132 is divided by the square root of the area ratio to reduce the number of variables. The diameter limit condition consistent with the 10 ft diameter limitation specified by the contract work statement also is shown.

The parametric data presented in this discussion is for one specific engine type within each major engine cycle category. Each engine is consistent with a given set of technology areas (i.e., injector type and cooling method). However, the selected technology areas for a specified mission may be different than the technology areas incorporated into the selected parametric engines. Therefore, the changes that occur in such considerations as weight and performance, when a technology area is altered within the engine, must be known before changes in technology can be evaluated in a mission analysis study.

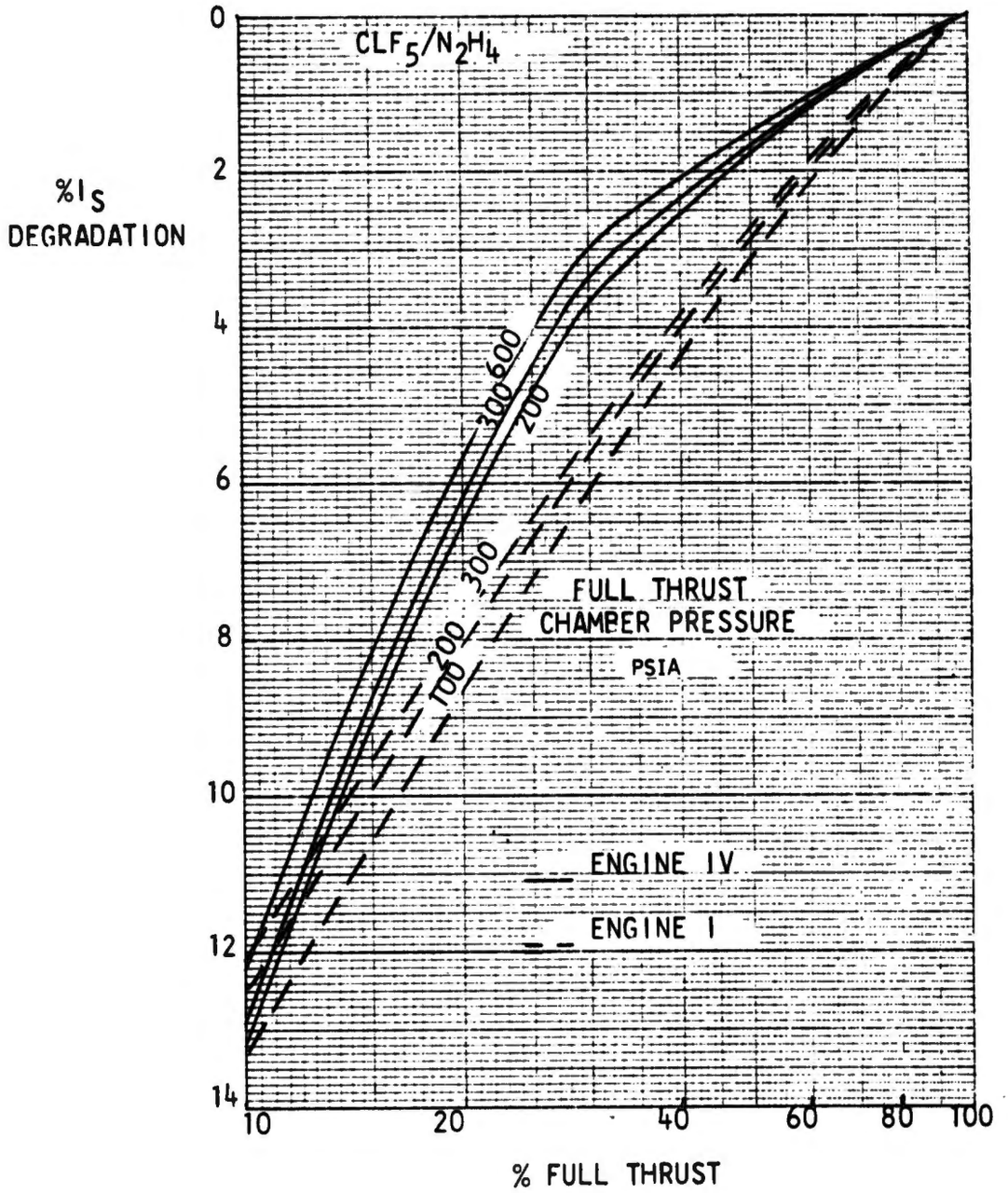

Figure 126. Specific Impulse Degradation with Throttling, Engines No. I and No. IV

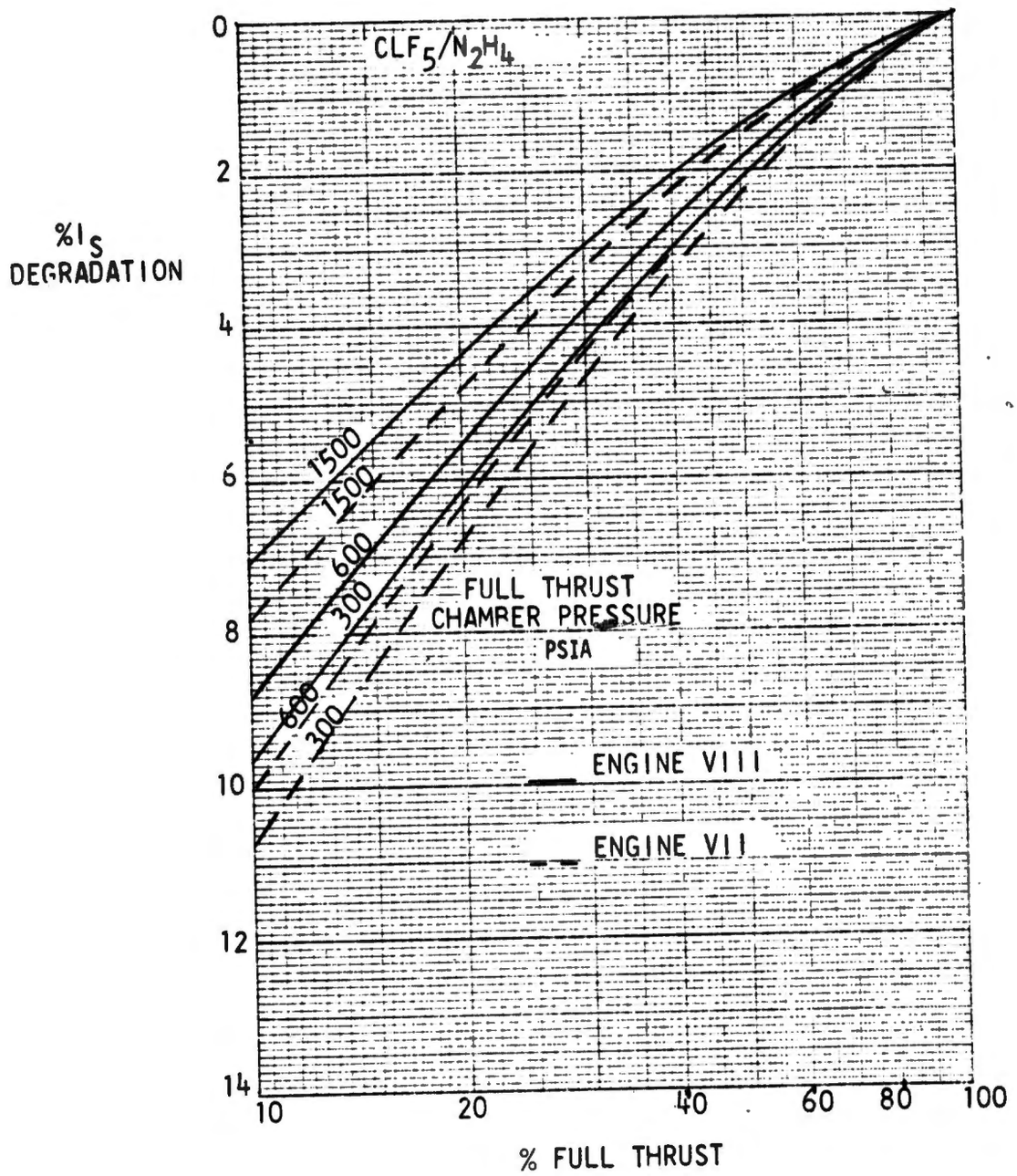

Figure 127. Specific Impulse Degradation with Throttling, Engines No. VII and No. VIII

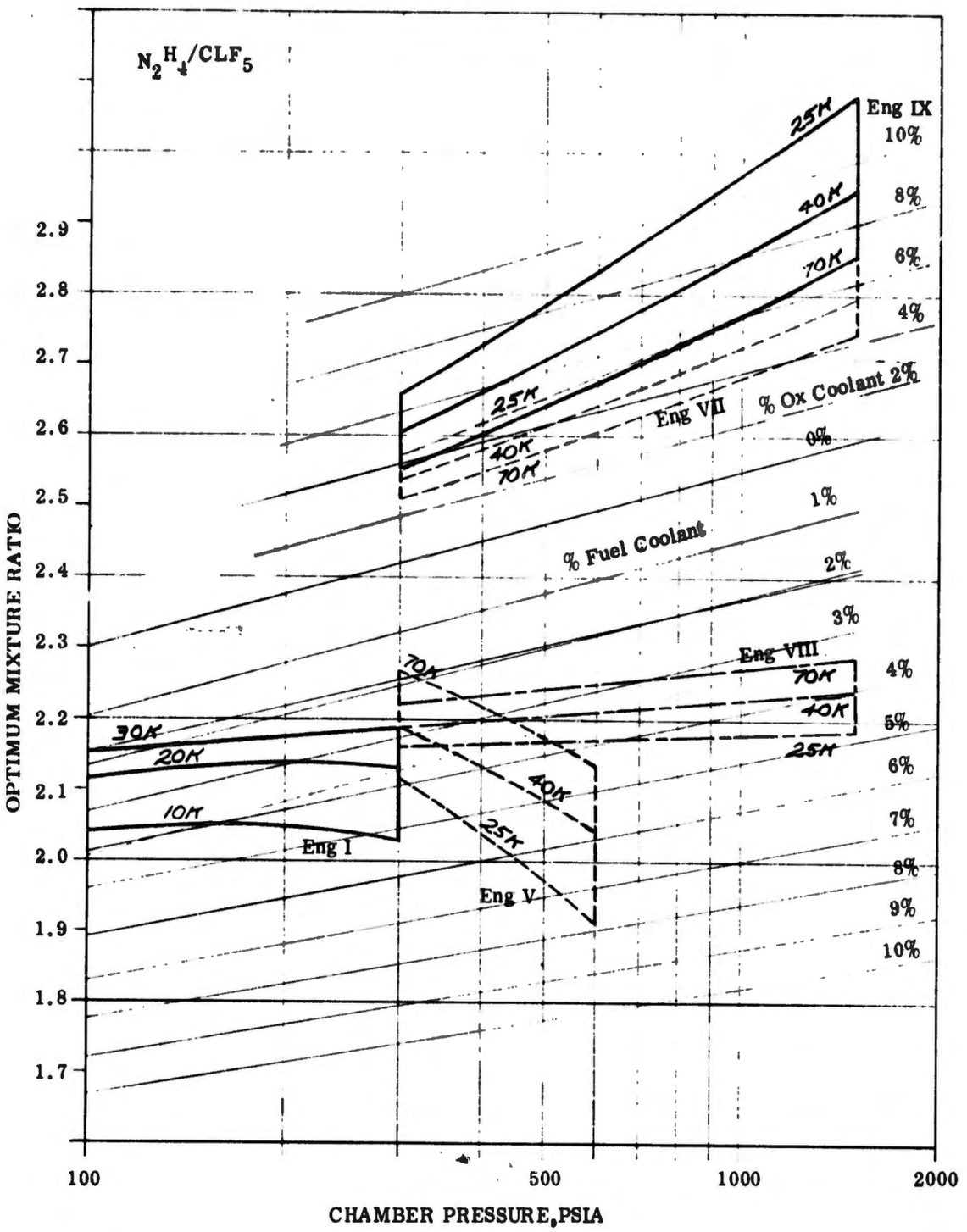

Figure 128. Optimum Mixture Ratio for Point Design Engines

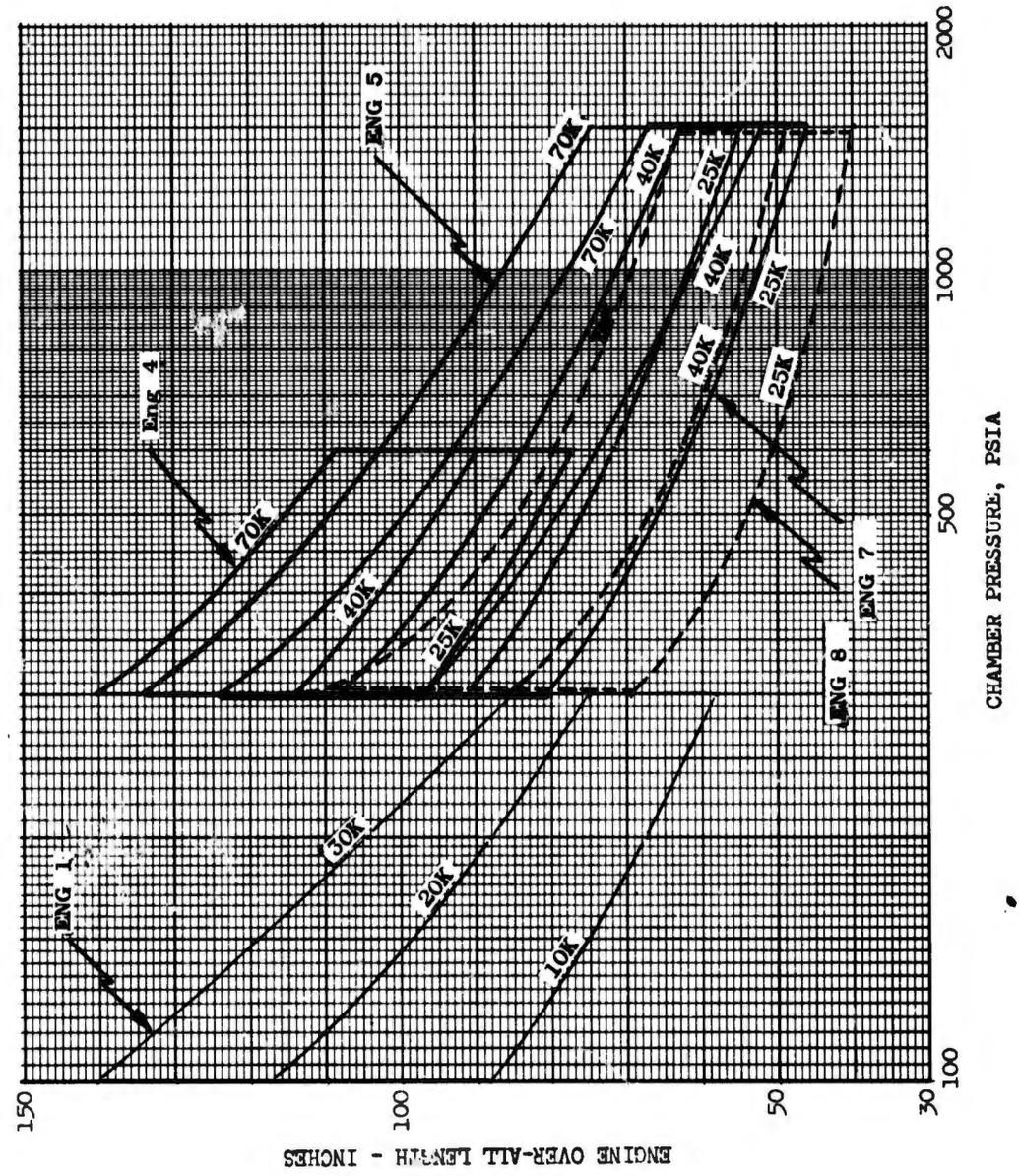

Figure 129. Point Design Engine Length, ϵ = 40:1

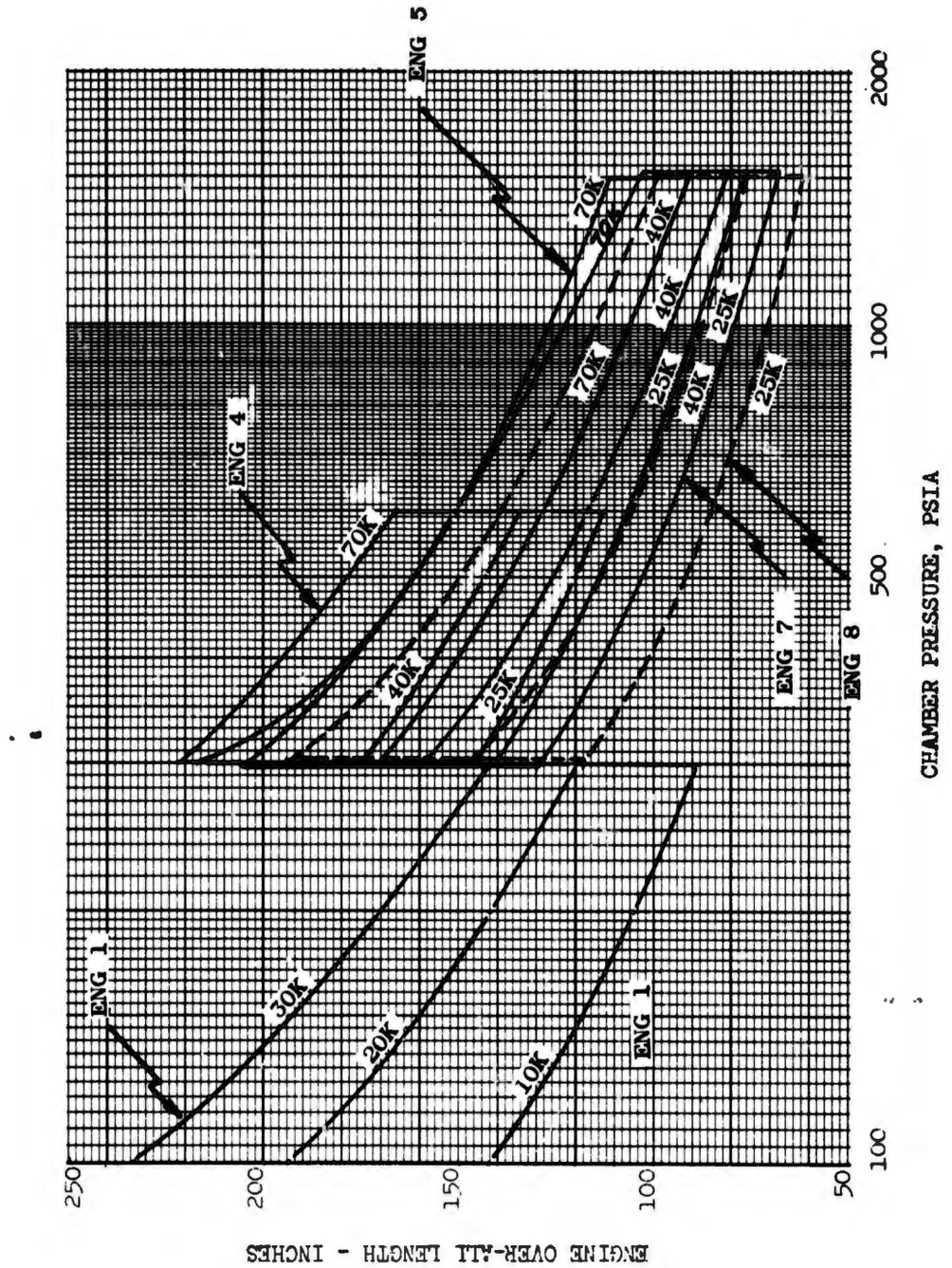

Figure 130. Point Design Engine Length, ϵ = 100:1

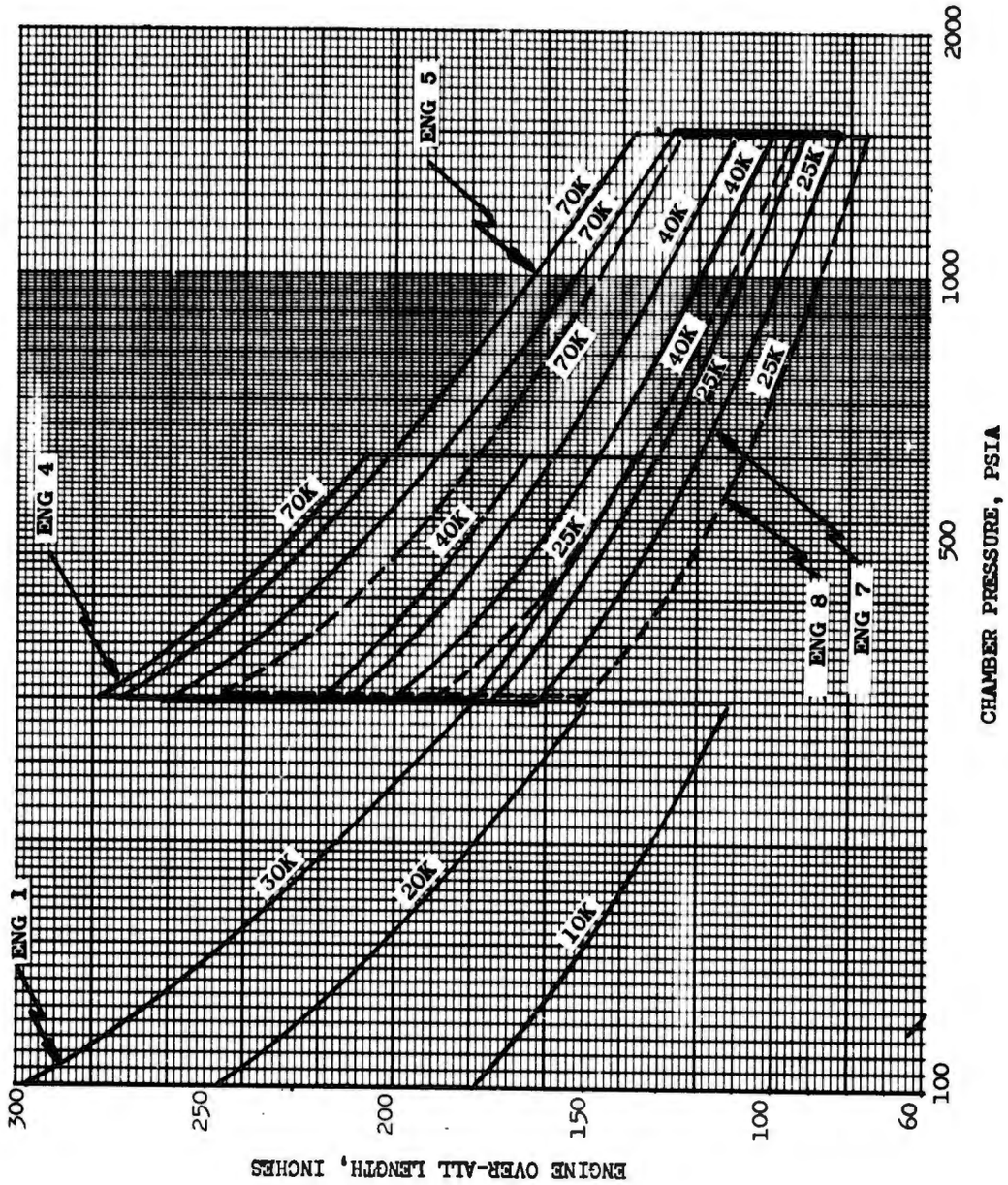

Figure 131. Point Design Engine Length, ϵ = 150:1

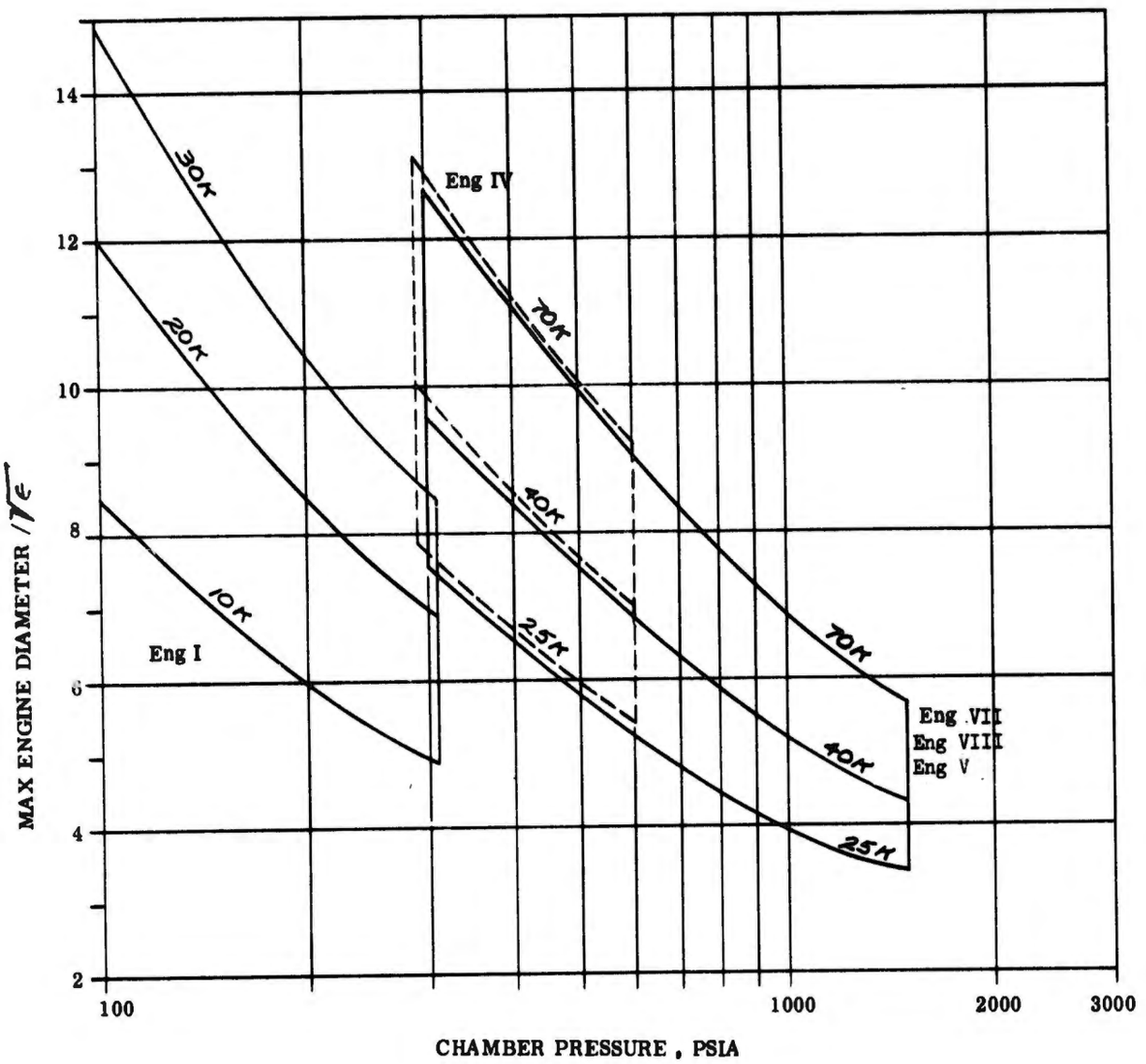

Figure 132. Engine Maximum Diameter vs Chamber Pressure and Thrust

The capability for calculating engine data for selected technological areas that are unlike those utilized for the parametric engine data as discussed above is accomplished through the use of the data utilization procedures which are presented in the subsequent section (VII) of this report. The data utilization procedure was used to compare selected technological areas during the course of this study upon the basis of weight and performance. Section VIII of this report is a discussion of these technology comparisons.

The basic parameter engine data as well as that for the technology comparison provide information for a number of different engines. Table XXVII presents a summary of all of the engine types possible within the scope of this study as well as an index to the location of specific engine information. Where data are not available, the data utilization procedure are used to obtain it.

TABLE XXVII

LOCATIONS FOR EXISTING ENGINE INFORMATION FOR MISSION ANALYSES WITH CLF_5/N_2H_4

Engine Type							*Mission Data Location					
Prop. Feed System	Cycle Type	Inj. Type	Throat Cool Method	Cool Type	Throat Mat.	Nozzle Ext. Cool.	Engine Wet Weight	Full Thrust Isp	Throttled Isp	Engine Mixture Ratio	Engine Length	Engine Dia.
Press.	Press.	Conv.	Rad.	Fuel	Graph	NA	187	187	124	126	127,128, 129	130
			Abl.	Fuel	Graph	NA						
		Mom. Exch.	Rad.	Fuel	Graph	NA	195	195				
			Abl.	Fuel	Graph	NA						
		Plate-let	Rad.	Fuel	Graph	NA	117	112				
			Abl.	Fuel	Graph	NA						
Pump	Liq/Liq Bleed	Conv.	Rad.	Fuel	Graph	NA	187	187				
			Abl.	Fuel	Graph	NA						
			Regen.	Fuel	Inconel	NA	121	116				
			Tran-spire	Ox. Gas Fuel	Ni Ni	NA Regen. Rad.						
			Tran-spire	Ox Gas Fuel	Graph Graph	NA Regen. Rad.						

*Note - 1. Numbers indicate figure locations.
2. DU indicates that data must be obtained from data utilization procedures.
3. NA indicates not applicable.

UNCLASSIFIED

TABLE XXVII (cont.)

Engine Type							*Mission Data Location					
Prop. Feed System	Cycle Type	Inj. Type	Throat Cool Method	Cool Type	Throat Mat.	Nozzle Ext. Cool.	Engine Wet Weight	Full Thrust Isp	Throttled Isp	Engine Mixture Ratio	Engine Length	Engine Dia.
		Mom. Exch.	Rad.	Fuel	Graph	NA	188	188				
			Abl.	Fuel	Graph	NA	118	113	124	126	127,128 129	130
			Regen.	Fuel	Inconel	NA						
			Tran-spire	Ox Gas Fuel	Ni Ni	NA Regen.						
			Tran-spire	Ox. Gas Fuel	Graph Graph	Rad. NA Regen.						
						Rad.						
Pump	Bleed	Plate-let	Rad.	Fuel	Graph	NA						
			Abl.	Fuel	Graph	NA						
			Regen.	Fuel	Inconel	NA						
			Tran-spire	Ox. Gas Fuel	Ni Ni	NA Regen.						
						Rad.	193,194	193,194				
			Tran-spire	Ox. Gas Fuel	Graph Graph	NA Regen.						
						Rad.						

UNCLASSIFIED

TABLE XXVII (cont.)

Engine Type							*Mission Data Location					
Prop. Feed System	Cycle Type	Inj. Type	Throat Cool Method	Cool Type	Throat Mat.	Nozzle Ext. Cool.	Engine Wet Weight	Full Thrust Isp	Throt-tled Isp	Engine Mixture Ratio	Engine Length	Engine Dia.
	Gas/ Liq S.C.	Conv.	Rad.	Fuel	Graph	NA						
			Abl.	Fuel	Graph	NA						
			Regen.	Fuel	Inconel	NA						
			Tran-	Ox.	Ni	NA						
			spire	Gas Fuel	Ni	Regen.						
						Rad.						
			Tran-	Ox.	Graph	NA						
			spire	Gas Fuel	Graph	Regen.						
						Rad.						
		Plate- let	Rad.	Fuel	Graph	NA						
			Abl.	Fuel	Graph	NA						
			Regen.	Fuel	Inconel	NA						
			Tran-	Ox.	Ni	NA	119	114	125	126	127,128 129	130
			spire	Gas Fuel	Ni	Regen.						
						Rad.	193,194 197,198	193,194 197,198				
			Tran-	Ox.	Graph	NA						
			spire	Gas Fuel	Graph	Regen.						
						Rad						

UNCLASSIFIED

TABLE XXVII (cont.)

Engine Type							*Mission Data Location					
Prop. Feed System	Cycle Type	Inj. Type	Throat Cool Method	Cool Type	Throat Mat.	Nozzle Ext. Cool.	Engine Wet Weight	Full Thrust Isp	Throttled Isp	Engine Mixture Ratio	Engine Length	Engine Dia.
Pump	Liq/Gas S.C.	Conv.	Rad.	Fuel	Graph	NA						
			Abl.	Fuel	Graph	NA						
			Regen.	Fuel	Inconel	NA						
			Transpire	Ox. Gas Fuel	Ni	NA						
					Ni	Regen. Rad.						
			Transpire	Ox. Gas Fuel	Graph	Regen. Rad.						
		Platelet	Rad.	Fuel	Graph	NA						
			Abl.	Fuel	Graph	NA						
			Regen.	Fuel	Inconel	NA						
			Transpire	Ox. Gas Fuel	Ni	NA						
					Ni	Regen. Rad.	193,194	193,194				
			Transpire	Ox. Gas Fuel	Graph	Regen. Rad.						

TABLE XXVII (cont.)

Engine Type							*Mission Data Location					
Prop. Feed System	Cycle Type	Inj. Type	Throat Cool Method	Cool Type	Throat Mat.	Nozzle Ext. Cool.	Engine Wet Weight	Full Thrust Isp	Throttled Isp	Engine Mixture Ratio	Engine Length	Engine Dia.
	Gas/ Gas S.C.	Tubelet or Platelet	Rad.	Fuel	Graph	NA						
			Abl.	Fuel	Graph	NA						
			Regen.	Fuel	Inconel	NA	190,191	190,191				
			Tran-spire	Ox. Gas Fuel	Ni Ni	NA Regen.	190,191 120	190,191 115	125	126	127,128 129	130
						Rad.	190,191	190,191				
			Tran-spire	Ox. Gas Fuel	Graph Graph	Regen. Rad.	199	199				

UNCLASSIFIED

VII. DATA UTILIZATION

All point design and parametric data generated for the baseline engines can be utilized in mission analyses to determine relative payloads or ideal velocity increments. However, many possible engine types exist within the scope of this program that are not the same as the selected baseline engines. Therefore, it is necessary to provide a capability for determining weight, specific impulse, mixture ratio, engine length, and engine diameter to be used in mission analysis studies for those other engine variations. This data utilization discussion presents detailed procedures that can be used to provide the necessary engine data. The procedures described were used to evolve the data subsequently discussed as part of the Technology Comparison section of this report.

A. ENGINE CHARACTERISTICS

The initial step in calculating engine data is to ascertain the over-all engine characteristics, which are dependent upon the type of mission being considered. These characteristics are as follows:

- Propellant supply system (i.e., pressure-fed or pump-fed)
- Type of engine cycle (i.e., bleed or staged-combustion) for pump-fed engines
- Injector type (i.e., platelet, momentum exchange, or conventional)
- Type of cooling (i.e., active or passive)
- Cooling method (i.e., radiation, ablative, regenerative, or vaporization)
- Material technology (i.e., graphite vs nickel for transpiration cooling)

Figure No. 133 shows an over-all "family tree" of engine characteristics that are within the scope of this study. These characteristics are broken down further in Figures No. 134 through No. 138 for the pressure-fed, pump-fed bleed cycle, and pump-fed staged-combustion systems. By tracing the "family tree" route from the box labeled "engine characteristics" to that of the material type provides a specific type of engine, the pertinent characteristics of which are summarized within each branch. In addition, the mission capability characteristics of each type is noted on the appropriate figure. For example, all engines incorporating current technology, which is a necessary characteristic for some missions, are indicated as such. Thus, when the

ENGINE CH

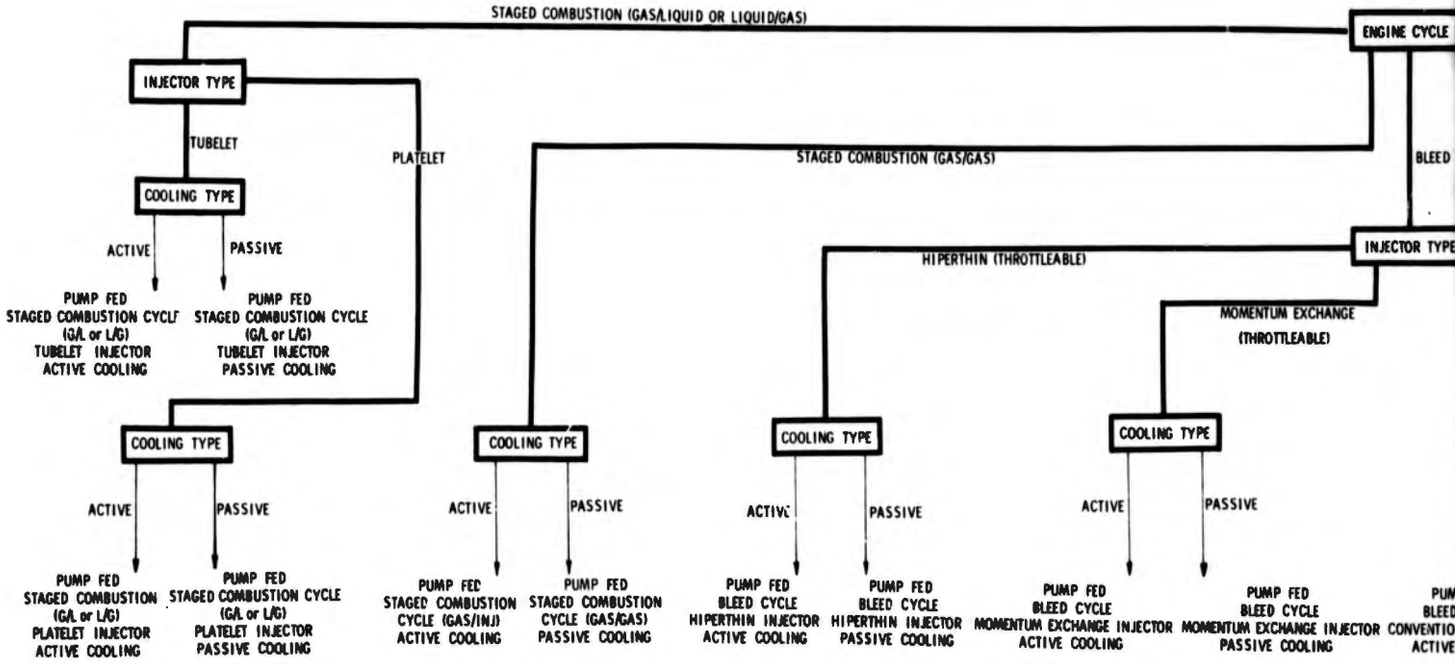
STAGED COMBUSTION (GAS/LIQUID OR LIQUID/GAS)
ENGINE CYCLE
INJECTOR TYPE
TUBELET
PLATELET
COOLING TYPE
ACTIVE
PASSIVE
PUMP FED STAGED COMBUSTION CYCLE (G/L or L/G) TUBELET INJECTOR ACTIVE COOLING
PUMP FED STAGED COMBUSTION CYCLE (G/L or L/G) TUBELET INJECTOR PASSIVE COOLING
COOLING TYPE
ACTIVE
PASSIVE
PUMP FED STAGED COMBUSTION (G/L or L/G) PLATELET INJECTOR ACTIVE COOLING
PUMP FED STAGED COMBUSTION CYCLE (G/L or L/G) PLATELET INJECTOR PASSIVE COOLING
STAGED COMBUSTION (GAS/GAS)
COOLING TYPE
ACTIVE
PASSIVE
PUMP FED STAGED COMBUSTION CYCLE (GAS/INJ) ACTIVE COOLING
PUMP FED STAGED COMBUSTION CYCLE (GAS/GAS) PASSIVE COOLING
BLEED
INJECTOR TYPE
HIPERTHIN (THROTTLEABLE)
COOLING TYPE
ACTIVE
PASSIVE
PUMP FED BLEED CYCLE HIPERTHIN INJECTOR ACTIVE COOLING
PUMP FED BLEED CYCLE HIPERTHIN INJECTOR PASSIVE COOLING
MOMENTUM EXCHANGE (THROTTLEABLE)
COOLING TYPE
ACTIVE
PASSIVE
PUMP FED BLEED CYCLE MOMENTUM EXCHANGE INJECTOR ACTIVE COOLING
PUMP FED BLEED CYCLE MOMENTUM EXCHANGE INJECTOR PASSIVE COOLING
PUM
BLEED
CONVENTIO
ACTIVE

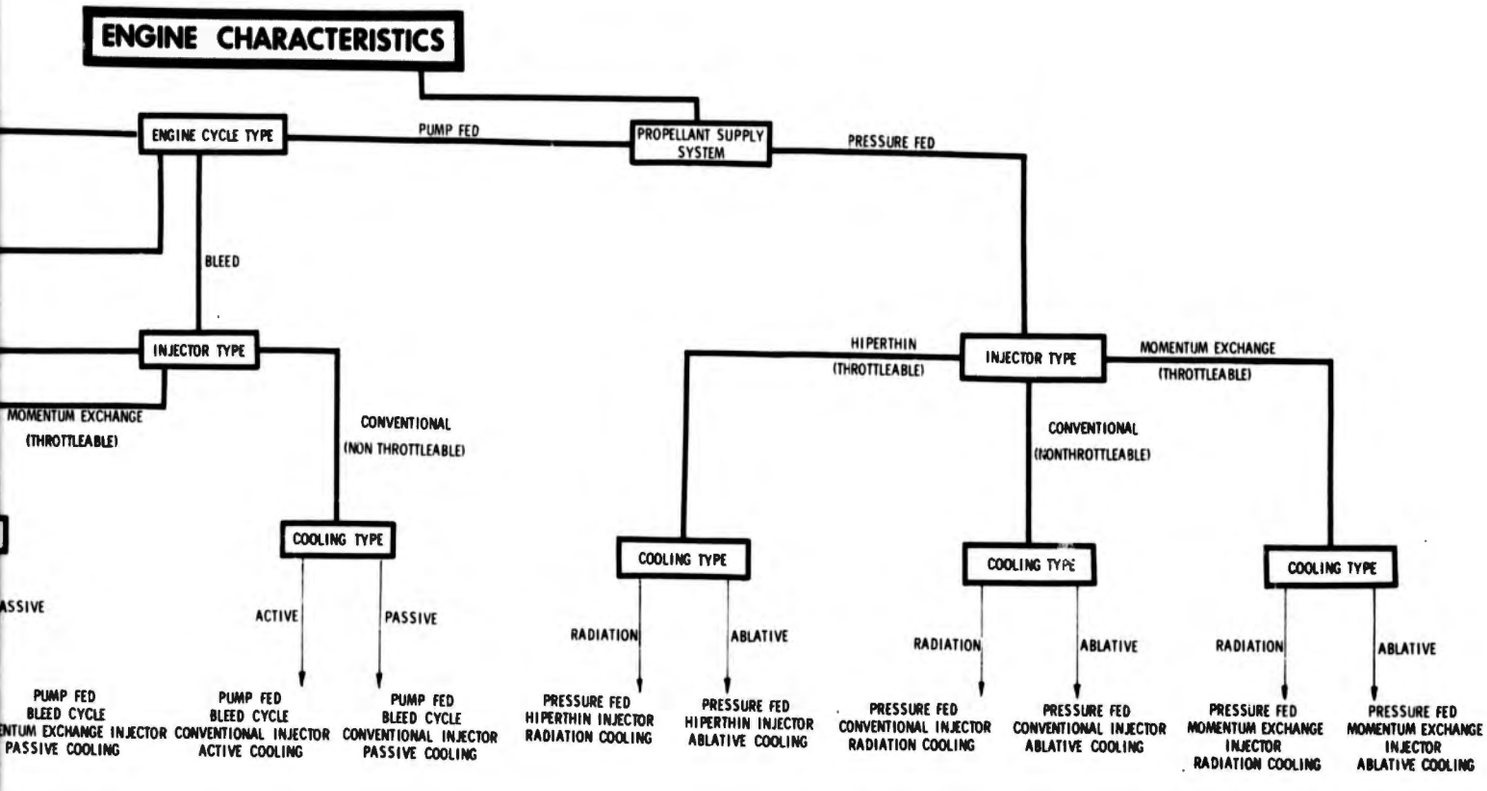

Figure 133. Over-All "Family Tree" of Engine Characteristics

NOTE: X indicates engine consistent with listed mission requirements

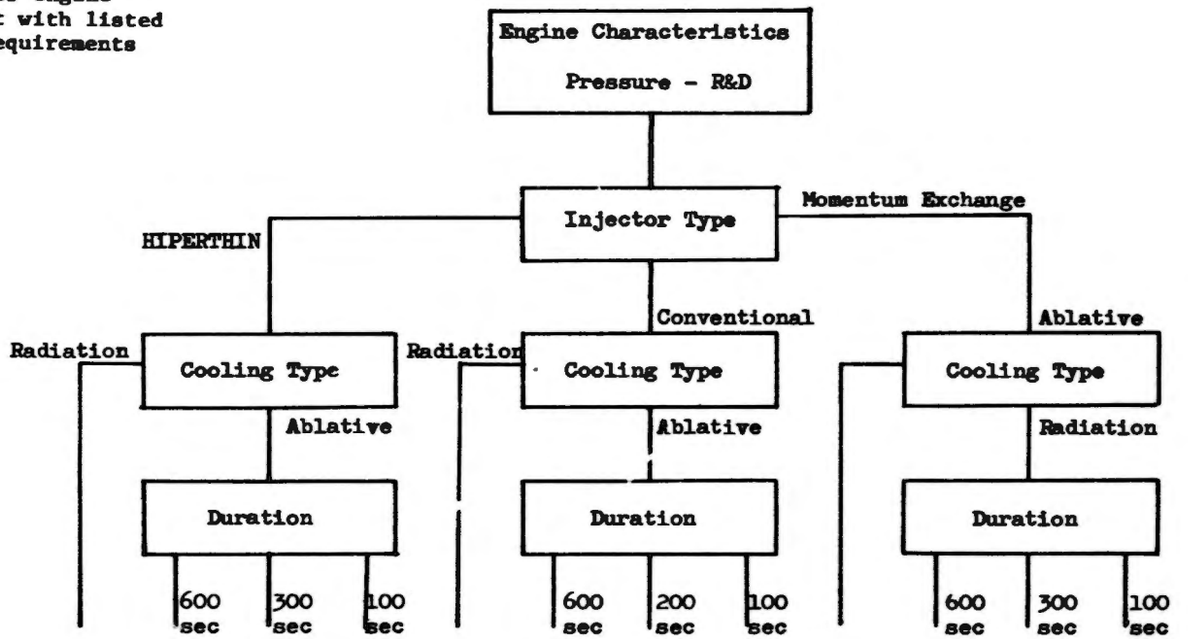

Mission Capability													
1. Current technology				X	X		X	X	X			X	X
2. 10:1 throttling													
3. Submerged installation			X	X	X		X	X	X		X	X	X
4. Minimum start impulse	X		X	X	X		X	X	X	X	X	X	X
5. 600 sec burn duration	X		X			X	X			X	X		
6. Accepts all specified propellants	X		X	X	X								
7. Restart flexibility	X					X				X			
8. Reuse													

Figure 134. Pressure-Fed Engine Characteristics

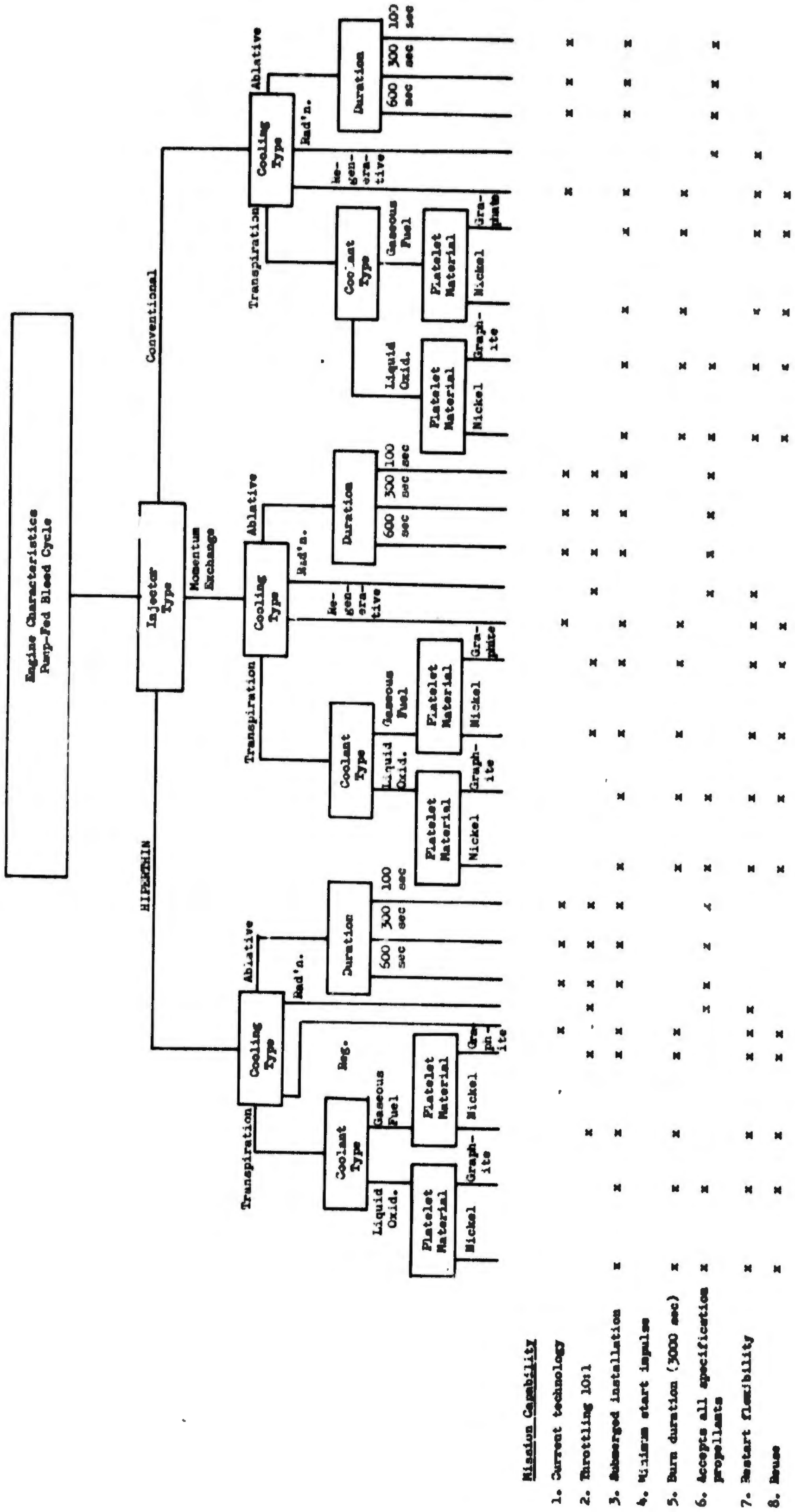

Figure 135. Pump-Fed Bleed Cycle Engine Characteristics

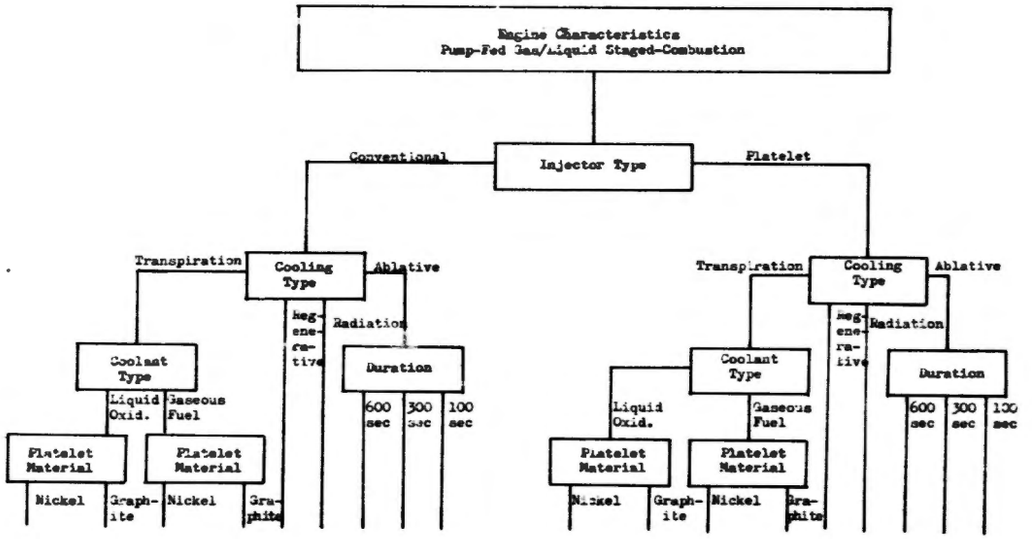

Mission Capability																			
1. Current technology																			
2. Throttling 10:1													x	x		x	x	x	x
3. Submerged installation	x		x	x	x	x	x	x		x	x	x	x	x		x	x	x	
4. Minimum start impulse																			
5. Burn duration (3000 sec)	x		x	x	x					x	x	x	x	x					
6. Accepts all specified propellants										x	x	x	x		x	x	x	x	
7. Restart flexibility	x		x	x	x					x	x	x	x	x	x				
8. Reuse	x		x	x	x					x	x	x	x	x					

Figure 136. Pump-Fed, Gas/Liquid, Staged-Combustion Engine Characteristics

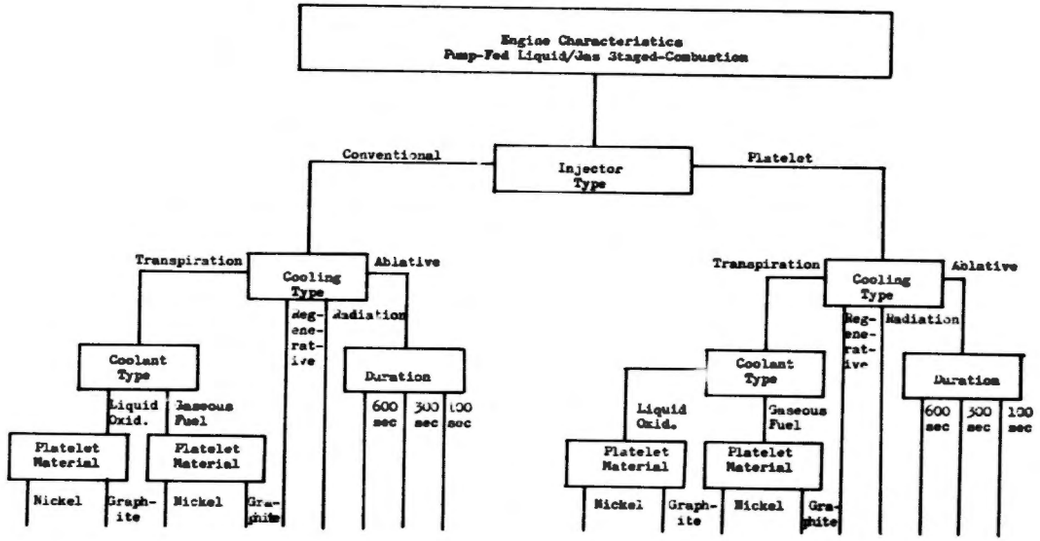

Mission Capability																		
1. Current technology																		
2. Throttling 10:1												x	x		x	x	x	x
3. Submerged installation	x	x	x	x	x	x	x	x	x	x	x	x	x	x		x	x	x
4. Minimum start impulse																		
5. Burn duration (3000 sec)	x	x	x	x	x					x	x	x	x	x				
6. Accepts all specified propellants																		
7. Restart feasibility																		
8. Reuse	x	x	x	x	x					x	x	x	x	x				

Figure 137. Pump-Fed, Liquid/Gas, Staged-Combustion Engine Characteristics

NOTE: x indicates engines consistent with listed mission requirements.

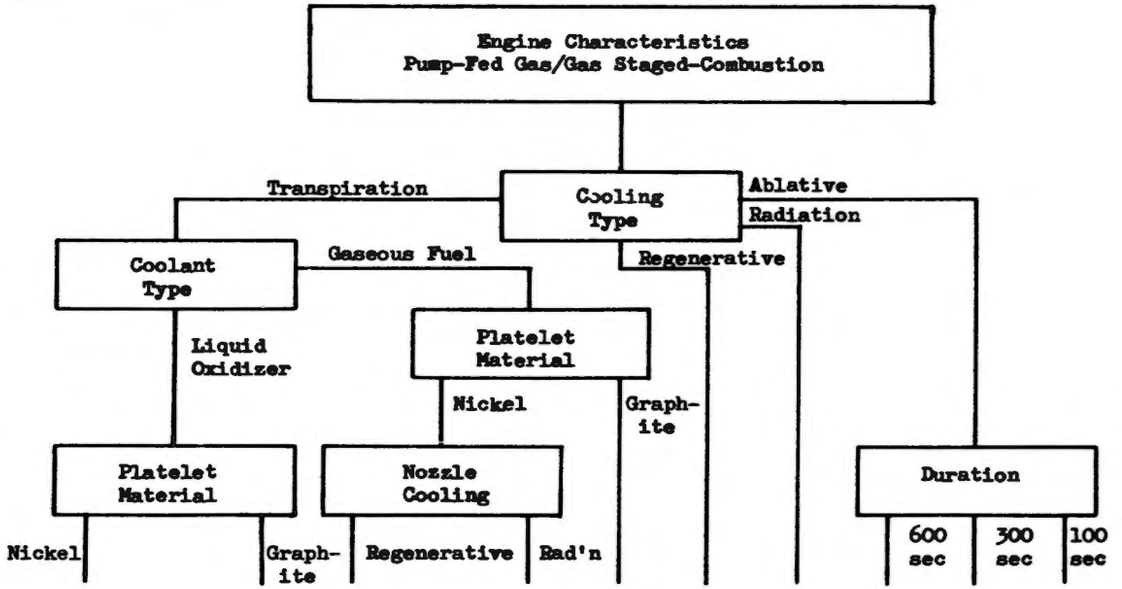

Mission Capability									
1. Current technology									
2. Throttling 10:1			x	x	x		x	x	x	x
3. Submerged installation	x	x	x	x	x	x		x	x	x
4. Minimum start impulse									
5. 3000 sec burn duration	x	x	x	x	x	x	x			
6. Accepts all specified propellants									
7. Restart flexibility	x	x	x	x	x	x	x	x	x	x
8. Reuse	x	x	x	x	x	x	x			

Figure 138. Pump-Fed, Gas/Gas, Staged-Combustion Engine Characteristics

required mission capability is specified, Figures No. 134 through No. 138 can be used to ascertain the engine characteristics that are consistent with the mission requirement. It is possible to obtain several types of engines that would satisfy specific mission requirements; therefore, all of them must be included in the mission analysis study.

The following mission requirements are included:

- Current technology
- Throttling to 10:1
- Submerged installation
- Minimum start impulse
- Infinite burn duration
- Propellant flexibility
- Restart
- Reusability

All of these requirements were discussed previously in the Technology Limits section (V).

B. PRIMARY ENGINE VARIABLES

Once the engine characteristics are established, the primary engine variables can be determined. These variables, which consist of thrust level (F), chamber pressure (Pc), nozzle area ratio (ϵ_A), and propellant type, must be determined before such parameters as weight or specific impulse can be established. The range of acceptable values for some of the primary engine variables is limited by the engine characteristics.

Table XXVI presented the acceptable range of the primary variables for a pressure-fed system. It is necessary to select several parametric values (i.e., thrust and chamber pressure) to accomplish a mission analysis optimization study. The engine diameter is the only limitation that must be examined after the thrusts, chamber pressures, and area ratios have been established because it may exceed the maximum allowable for the specific mission. This is accomplished by determining the engine diameter from Figure No. 132 for the selected primary engine variables.

The pump-fed system primary variables also are shown on Table XXVI for passively-cooled and actively-cooled engine systems. The thrust level and chamber pressure limits associated with regenerative cooling for each fuel type can be determined from the applicable values listed on Table XXVI. All pump-fed engines, for the range of primary variables shown, have an engine envelope diameter that is less than 10 ft, which is the limitation imposed by the contract work statement. However, if a smaller engine diameter is selected as the limit, the use of Table XXVI together with the primary variables that were selected will provide the actual engine diameter. A comparison of this result with the selected diameter limit will assure that the diameter limitation has not been exceeded.

C. DATA CALCULATION PROCEDURES

After the engine characteristics and primary engine variables have been established, the engine data necessary for mission analysis can be generated. The calculation procedures are separated into the following six categories:

- Engine wet weight
- Engine delivered specific impulse
- Throttling performance
- Engine mixture ratio
- Engine length
- Engine diameter

1. Engine Wet Weight

The calculation procedure for weight utilizes the parametric data previously discussed in Section VI of this report for the point design engines as a base point. Selected engine characteristics which differ from the base point engine are incorporated by correcting the base point parametric data.

The following weight procedure enables the base engine configurations to be modified for:

- Throat cooling method
- Type of injector
- Type of nozzle extension
- Throat cooling material
- Type of fuel

The previously selected engine characteristics will be used to establish the necessary modifications.

To effectively utilize the calculation procedure, it is essential that instructions be adhered to in the order indicated.

STEP 1: From selected values of F, P_c, and ε_A, obtain the baseline thrust to-weight ratio from the applicable parametric figures listed below. Also, note the base engine characteristics consistent with the parametric engine types.

Engine Type	Figure Location of Baseline Weight	Inj. Type	Base Engine Characteristics: Throat Cooling Method	Nozzle Cooling Method	Thrust, K	Chamber Pressure, psia	Throat Diameter, in.
a. Pressure Fed	FIG. NO. 139	Liq./Liq. HIPERTHIN	Radiation	N/A	10	100	8.49
b. Pump Fed (Bleed Cycle)	FIG. NO. 140	Liq./Liq. Momentum Exchange	Ablative	N/A	30	600	5.98
c. Pump Fed (Gas/Liquid or Liquid/ Gas Staged Combustion Cycle)	FIG. NO. 141	(Gas/Liq.) HIPERTHIN	Transpiration (Liq. Ox.)	Graphite	40	1500	4.31
d. Pump Fed (Gas/Gas Staged Combustion Cycle)	FIG. NO. 142	Gas/Gas	Transpiration (Gaseous Fuel)	Gas Fuel Regen.	40	1500	4.31

NOTE: The injector type is dictated by the types of propellant (i.e., liquid/liquid) injected in addition to the injector type (i.e., HIPERTHIN). The nozzle cooling method refers to the nozzle section downstream of the throat cooling and upstream of the columbium radiation-cooled skirt. Where this section does not exist, it is noted as being not applicable (N/A).

STEP 2: Obtain engine wet weight as follows:

$$W_{Eng} = \frac{F}{(F/W)_{base}}$$

= wet engine weight, lb

where

F = selected thrust level, lb

$(F/W)_{base}$ = base thrust-to-weight ratio obtained from the figures listed in Step 1.

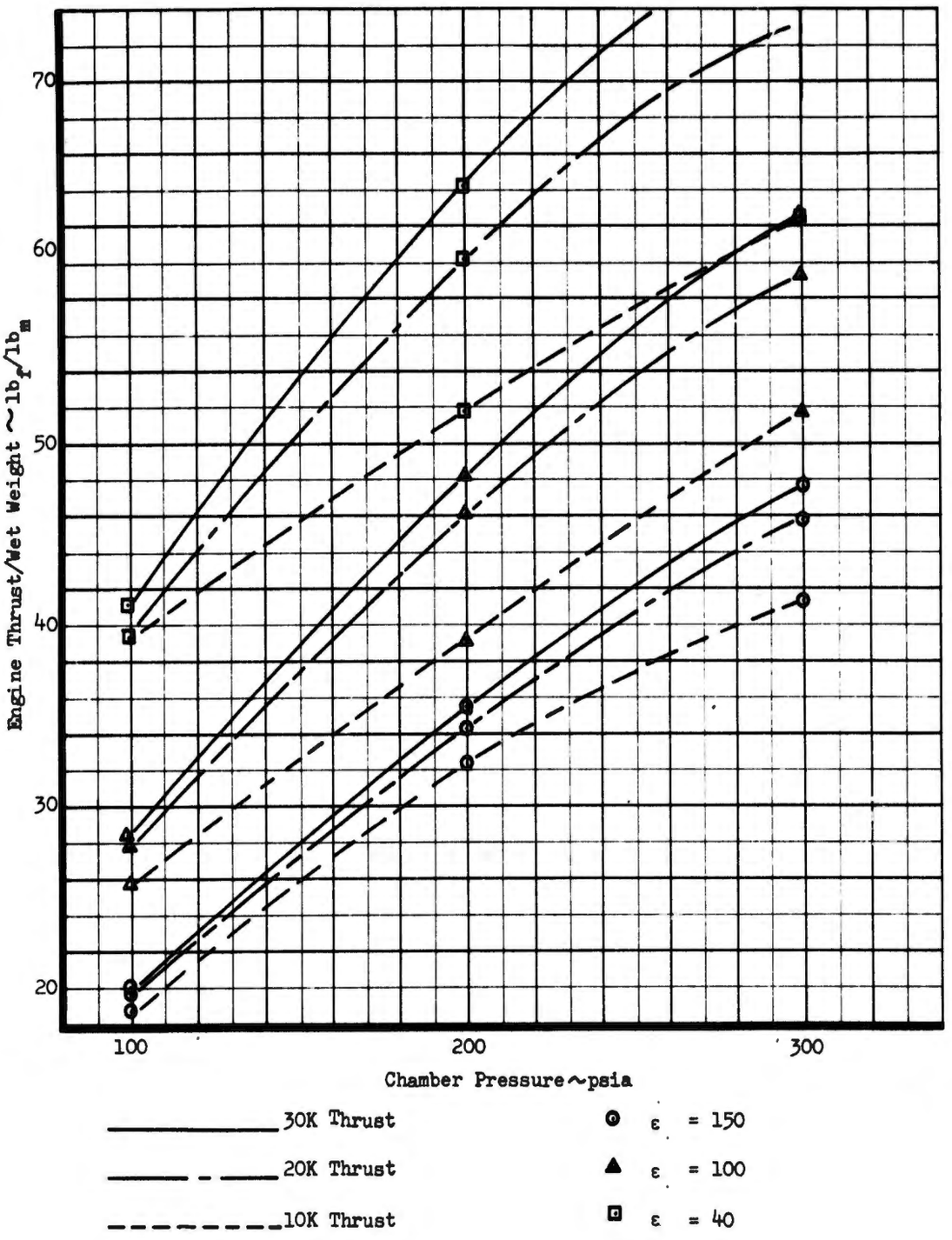

Figure 139. Pressure-Fed Parametric Weight

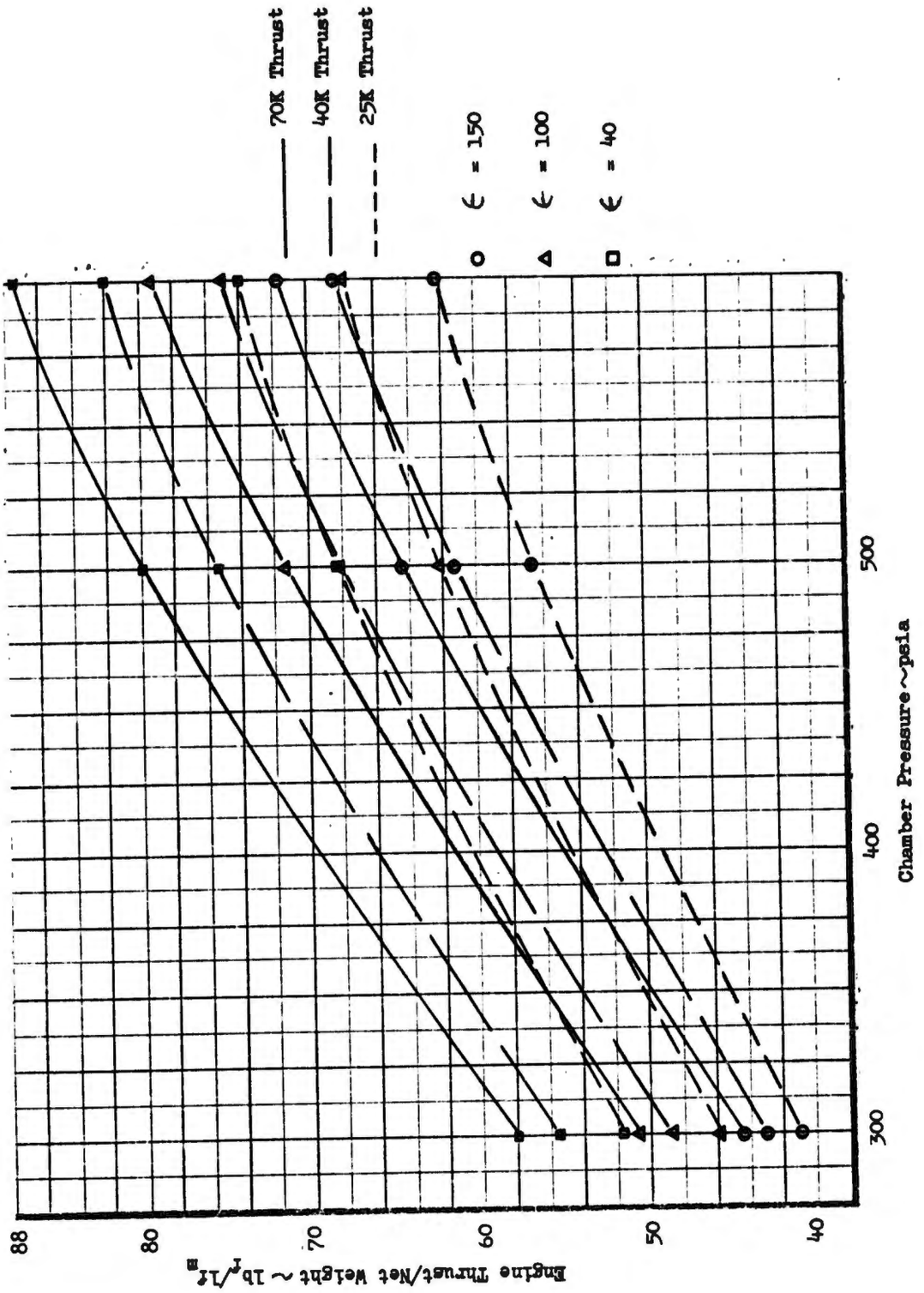

Figure 140. Pump-Fed (Bleed Cycle) Parametric Weight

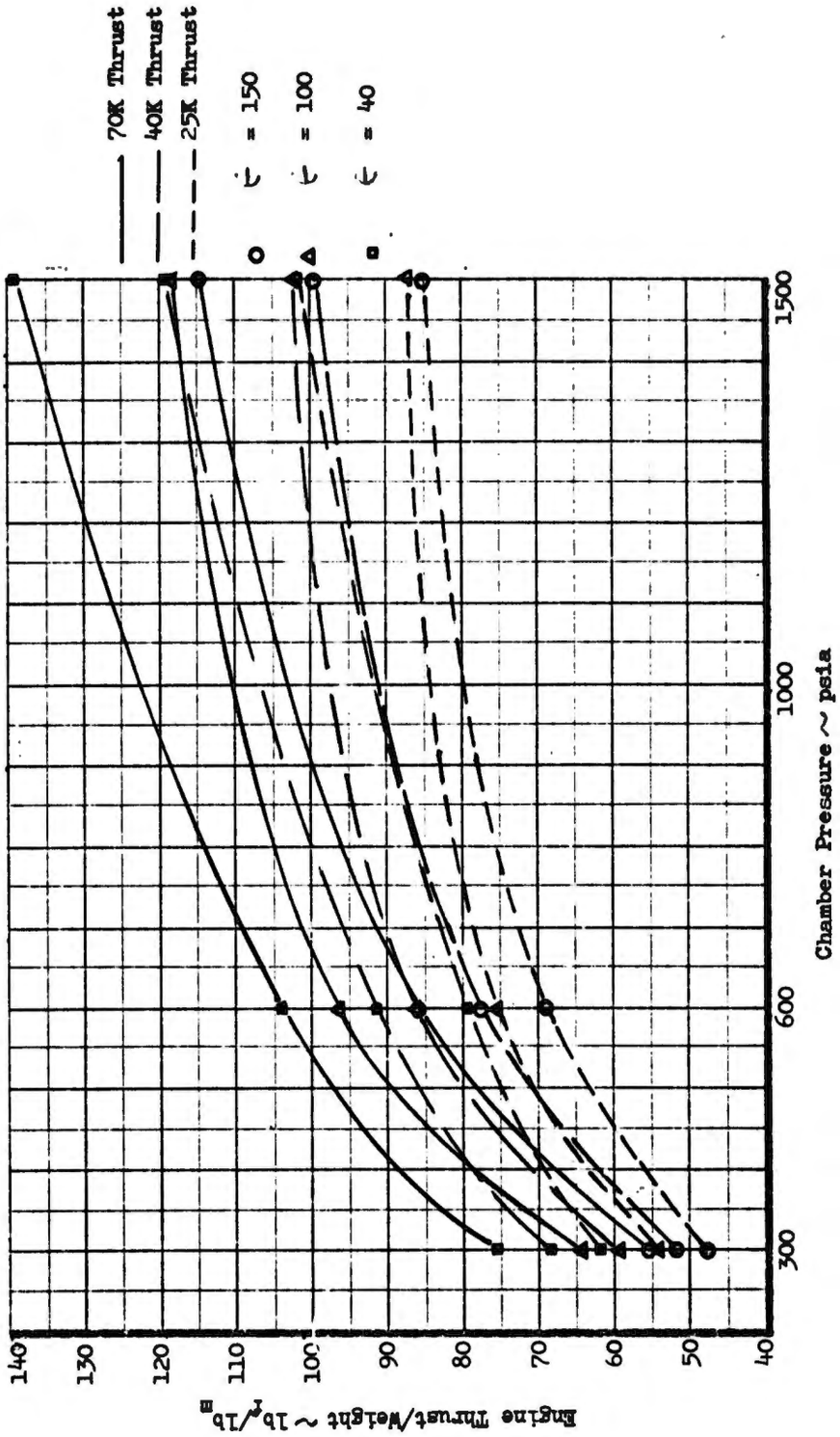

Figure 141. Pump-Fed (Gas/Liquid or Liquid/Gas Staged-Combustion) Parametric Weight

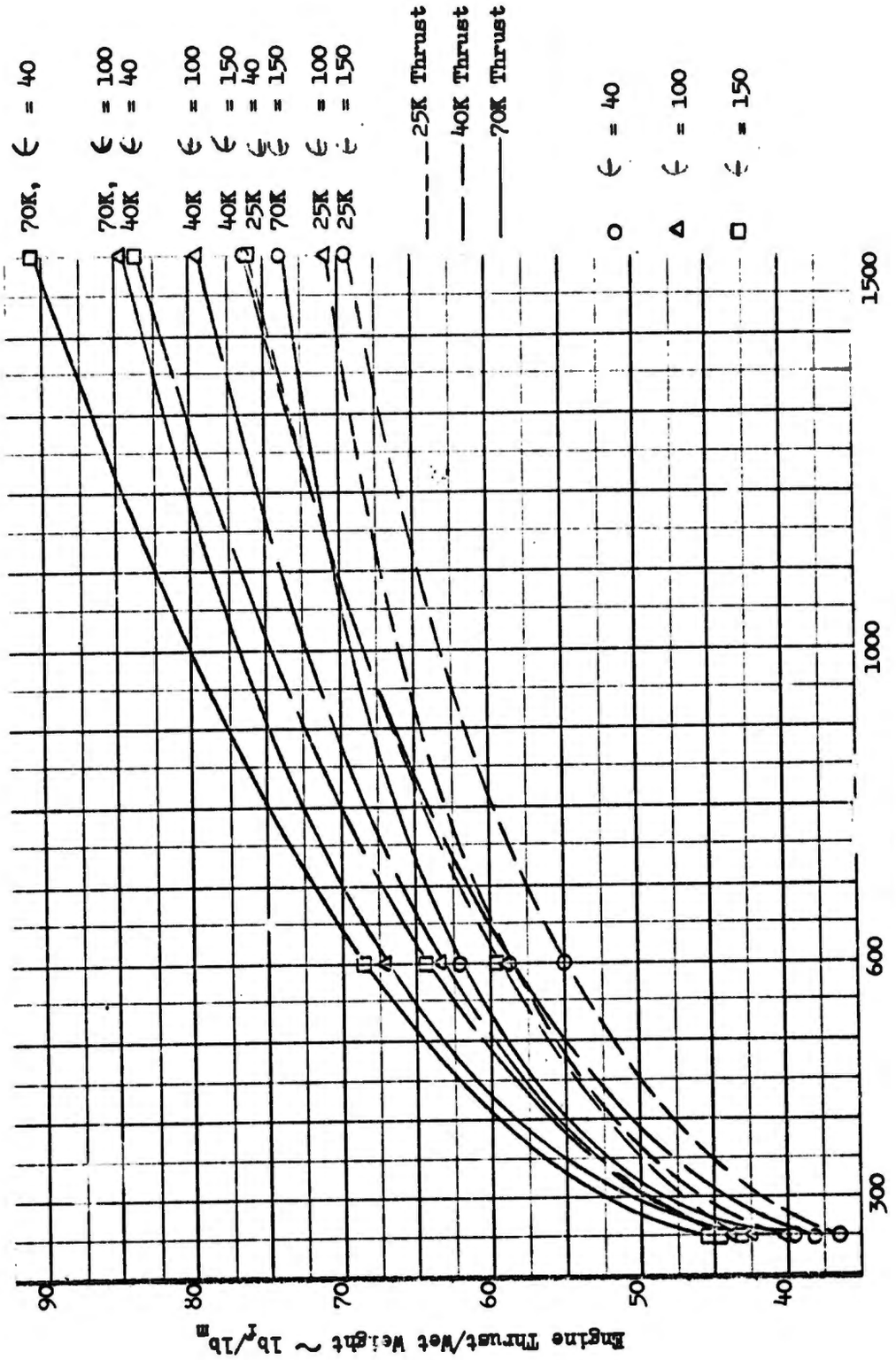

Figure 142. Pump-Fed (Gas/Gas Staged-Combustion) Parametric Weight

STEP 3: If the selected throat cooling method is different from the base engine characteristic, proceed with Step 4. If the selected throat cooling method is the same as the base engine characteristic, proceed to Step 17.

STEP 4: Establish the baseline engine transition ratio ($\varepsilon_{TR_{base}}$) between the throat cooling method and nozzle cooling from the applicable figures or values listed below:

Engine Type	Figure No. or Value
a. Pressure-Fed	Figure No. 143
b. Pump-Fed (Bleed Cycle)	6.0
c. Pump-Fed (Staged-Combustion Gas/Liquid or Liquid/Gas)	Figure No. 144
d. Pump-Fed (Gas/Gas Staged-Combustion)	5.0

STEP 5: Calculate the engine throat diameter from

$$D_E = D_b \sqrt{\frac{F}{F_b} \frac{P_{c_b}}{P_c}}$$

= Engine throat diameter, in.

where

F = selected thrust

F_b = base point thrust listed in Step 1

P_c = selected chamber pressure

P_{c_b} = base point chamber pressure listed in Step 1

D_b = base point chamber throat diameter listed in Step 1

STEP 6: Determine the total nozzle throat to exit surface area (A) from Figure No. 145.

STEP 7: Determine the fraction of total nozzle baseline engine surface area ($A_{F_{base}}$) associated with throat cooling from Figure No. 146 or by using the following relationship:

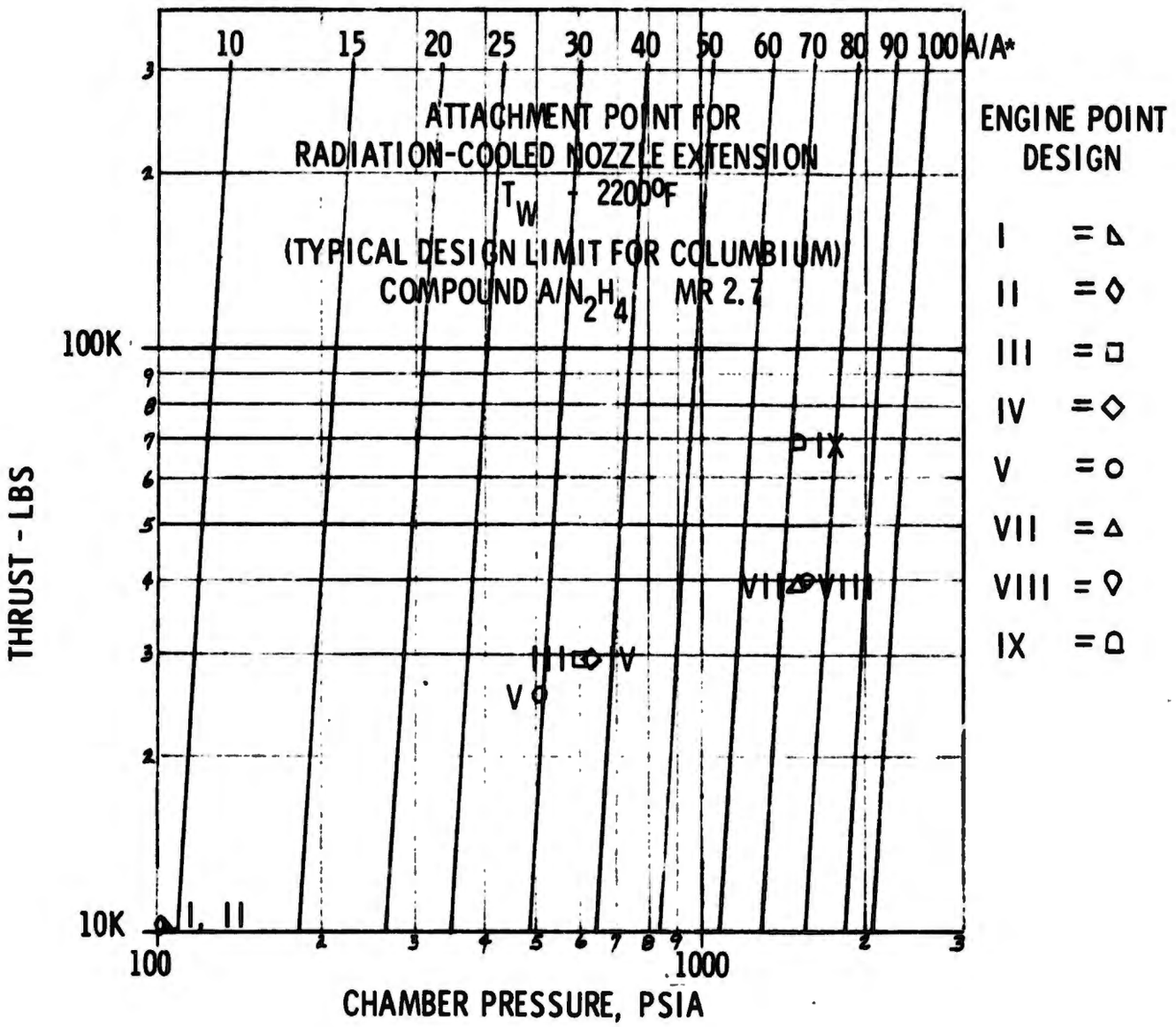

Figure 143. Attachment Point for Radiation-Cooled Nozzle Extension

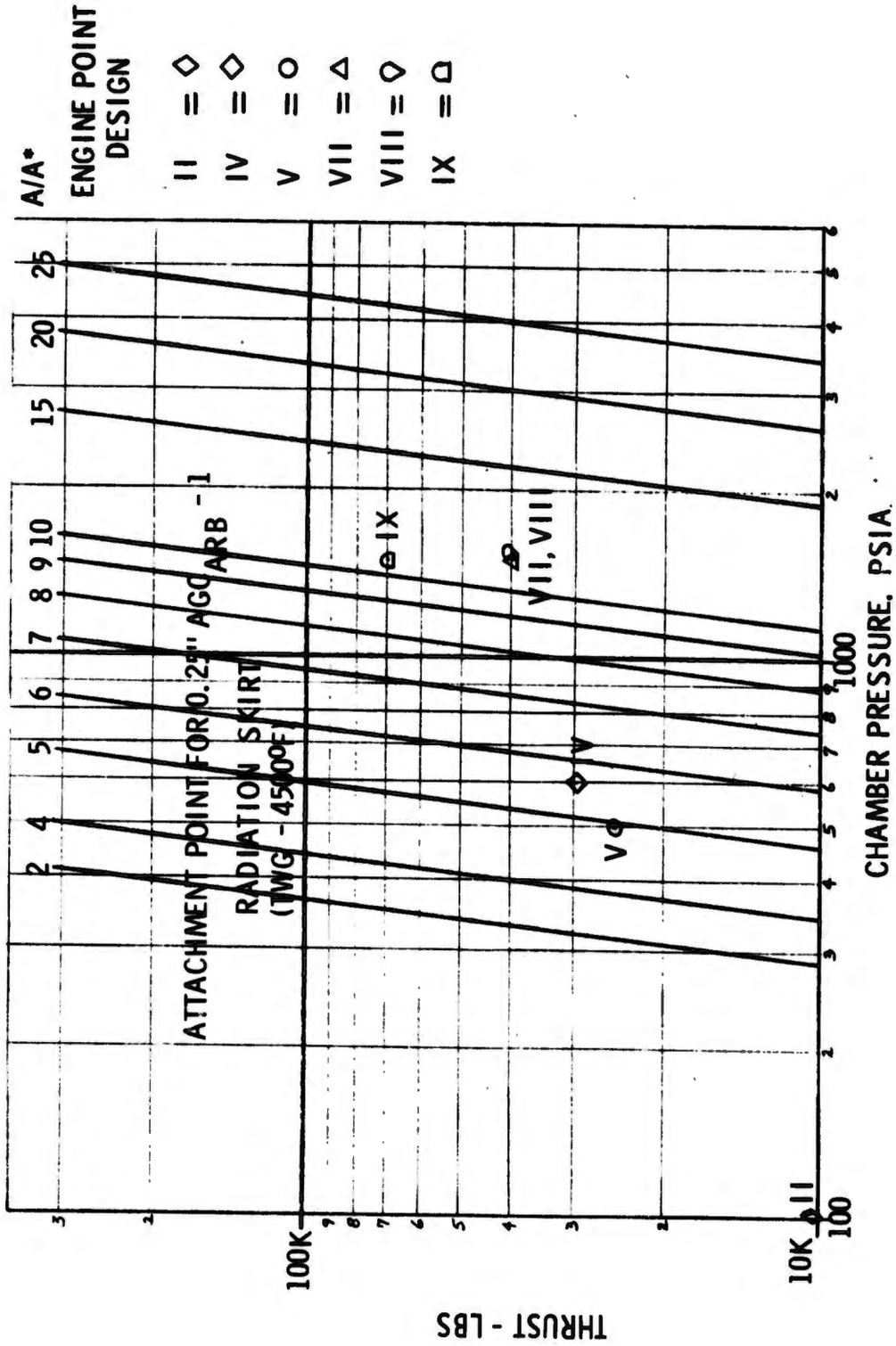

Figure 144. Attachment Point for 0.25-in. AGC Radiation Skirt

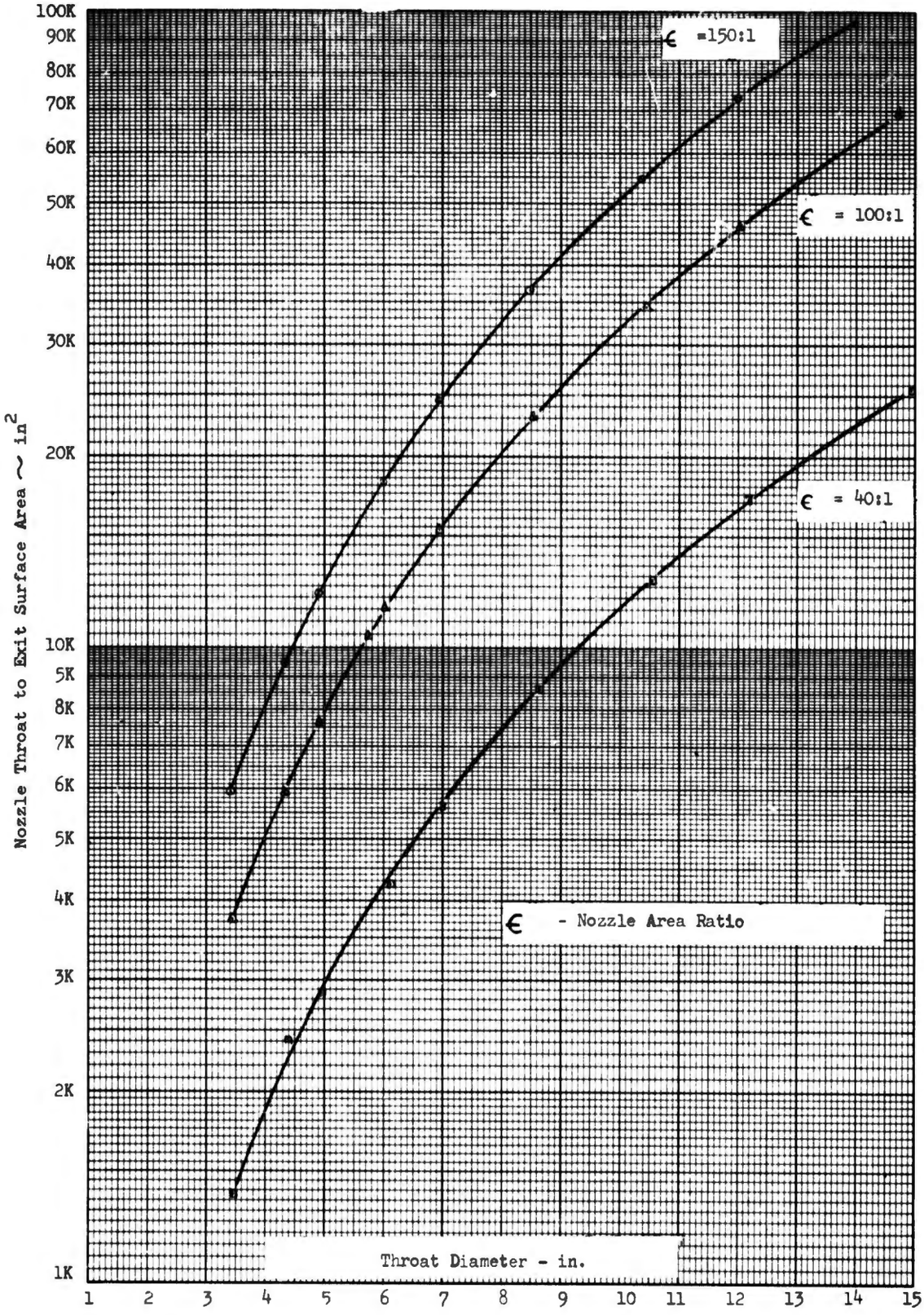

Figure 145. Nozzle Throat to Exit Surface Area vs Throat Diameter

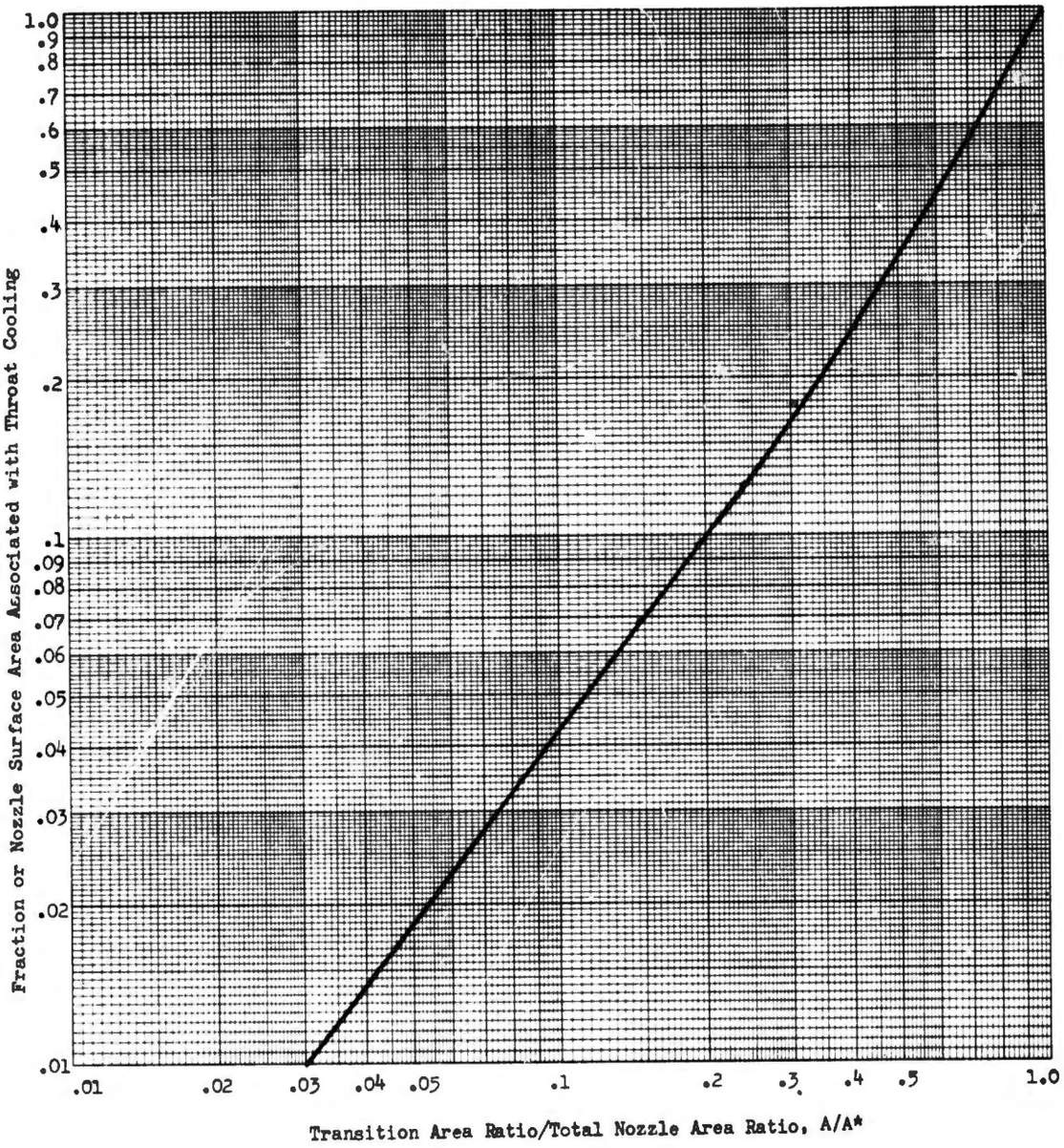

Figure 146. Surface Area vs Nozzle Area Ratio Comparison

For $\varepsilon_{TR}/\varepsilon_A$ from .03 to .45

$$A_F = .75\left(\frac{\varepsilon_{TR}}{\varepsilon_A}\right)^{1.232}$$

For $\varepsilon_{TR}/\varepsilon_A$ from .45 to 1.0

$$A_F = \left(\frac{\varepsilon_{TR}}{\varepsilon_A}\right)^{1.605}$$

where ε_{TR} = transition area ratio obtained from Step 4.

ε_A = Total selected area ratio

STEP 8: Calculate the baseline engine nozzle surface area (An_{base}) associated with throat cooling as follows:

$An_{base} = A\,A_{F_{base}}$

= Nozzle surface associated with throat cooling, $in.^2$

where

A = Total nozzle surface area obtained from Step 6, $in.^2$

A_F = Nozzle surface area associated with throat cooling method divided by total nozzle surface area as obtained from Step 7.

STEP 9: Determine the baseline engine combustion chamber surface area (Acc_{base}) from Figure No. 147, consistent with the baseline characistics presented in Step 1.

STEP 10: Establish transition area ratio: ($\varepsilon_{TR_{SK}}$) between nozzle cooling and columbium radiation cooled sheet from Figure No. 143. This area ratio is the same for both the baseline and selected engines.

STEP 11: Determine the fraction of total nozzle surface area (A_{F_N}) associated with the throat to columbium radiation-cooled throat section from Figure No. 146 or by utilizing the relationships presented in Step 7.

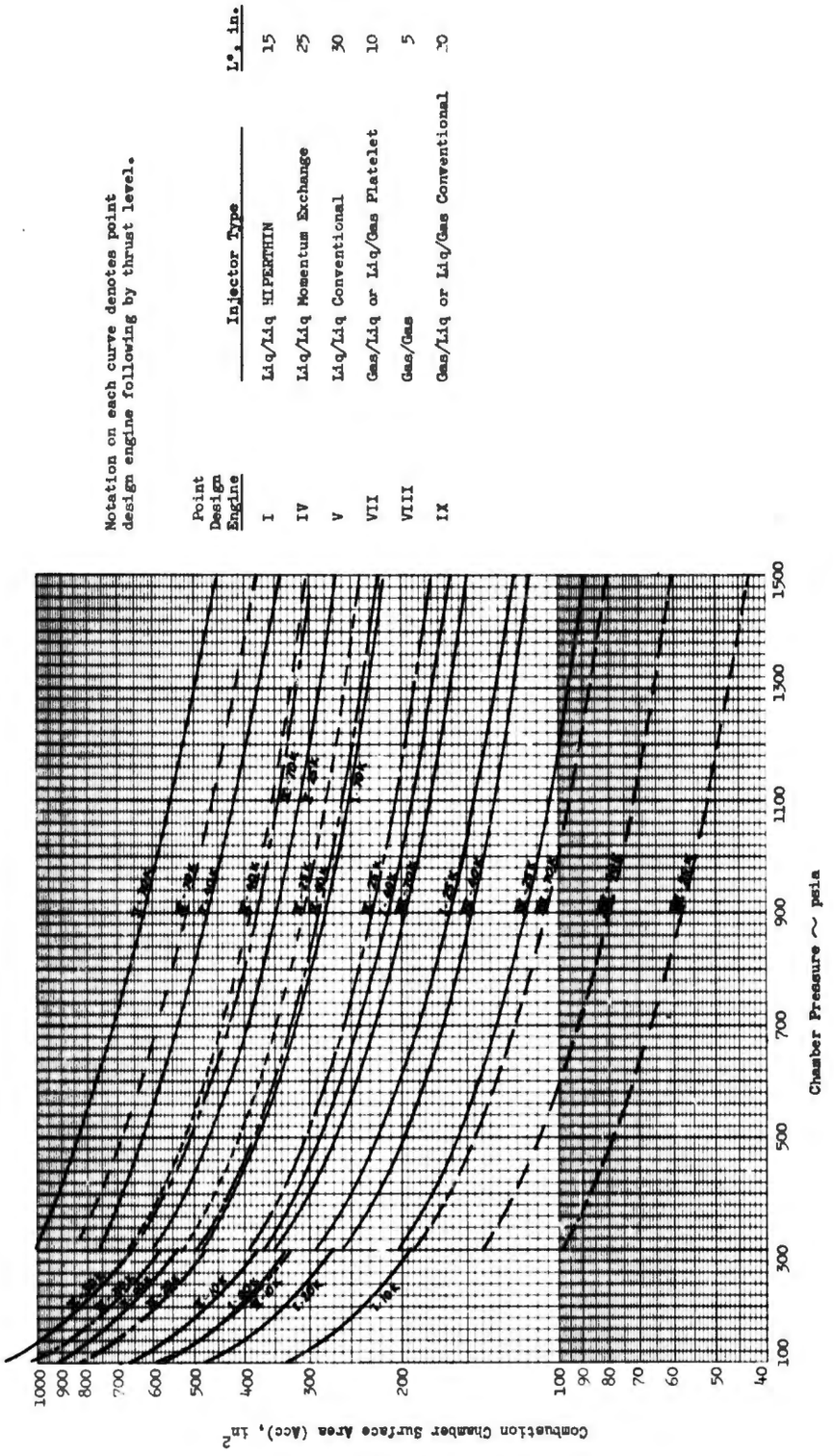

Figure 147. Chamber Convergent Section Surface Area vs Chamber Pressure

STEP 12: Calculate the combustion chamber and nozzle midsection weight ($W_{T_{ccn_{base}}}$) for the baseline engine as follows:

$$W_{T_{ccn_{base}}} = \rho_{TC_{base}} (Acc_{base} + An_{base}) + \rho_{NC_{base}} A (A_{F_N} - A_F)_{base\ base}$$

= combustion chamber and nozzle weight for baseline engine, lb

where Acc_{base} = combustion chamber surface area attained from Step 9, $in.^2$

An_{base} = nozzle surface area associated with throat cooling attained from Step 8, $in.^2$

A = total nozzle surface area attained from Step 6, $in.^2$

$A_{F_N}{}_{base}$ = nozzle surface area from throat to columbium skirt divided by total nozzle surface area as determined in Step 11.

$A_{F}{}_{base}$ = nozzle surface area associated with the throat cooling method divided by the total nozzle surface area as determined in Step 7.

$\rho_{TC_{base}}$ = effective surface density of throat cooling method for baseline engine, $lb/in.^2$

ρNC_{base} = effective surface density of nozzle cooling method for baseline engine, $lb/in.^2$

The effective surface densities for the baseline engine types are as follows:

	Baseline Engine Type	$\rho_{TC_{base}}$, $lb/in.^2$	ρNC_{base}, $lb/in.^2$
a.	Pressure-Rad	0.0202	0.0202
b.	Pump-Rad (Blood Cycle)	0.149	0.149
c.	Pump-Rad (G/L or L/G Staged-Combustion)	0.24	0.0202
d.	Pump-Rad (G/G Staged-combustion)	0.58	0.033

STEP 13: Determine the transition area ratio between throat cooling and nozzle cooling methods for the selected cooling technology from the following figures or values:

Selected Throat and Nozzle Cooling Method	Figure Location or Value of GTR	
	Bleed Cycles	Other Cycles
a. Radiation, Ablative, or Regenerative	6.0	Figure No. 143
b. Transpiration with Gaseous Fuel	6.0	5.0
c. Transpiration with Liquid Oxid.	6.0	Figure No. 144

STEP 14: Determine the fraction of total nozzle surface area (A_F) associated with the throat cooling method from Figure No. 146 or by using the relationship presented in Step 7.

STEP 15: Calculate the combustion chamber and nozzle midsection weight ($W_{T_{ccn}}$) for the selected engine as follows:

$$W_{T_{ccn}} = \rho_{TC} (Acc_{base} + A A_F) + \rho_{NC} A (A_{F_{N_{base}}} - A_F)$$

= combustion chamber and nozzle weight for selected engine, lb

where A_F = nozzle surface area fraction associated with the throat cooling method for the selected engine as determined in Step 14.

ρ_{TC} = effective surface density of selected throat cooling method, $lb/in.^2$

ρ_{NC} = effective surface density of selected nozzle cooling method, $lb/in.^2$

The effective surface densities for selected cooling technology is as follows:

Selected Throat Cooling Method	ρ_{TC}, $lb/in.^2$	Selected Nozzle Cooling Method	ρ_{NC}, $lb/in.^2$
a. Radiation	0.0202	Radiation	0.0202
b. Ablative (100 sec div.)	0.0643	Ablative (100 sec div.)	0.0643
c. Ablative (300 sec div.)	0.102	Ablative (300 sec div.)	0.102
d. Ablative (600 sec div.)	0.149	Ablative (600 sec div.)	0.149
e. Regenerative	0.033	Regenerative	0.033
f. Transpiration (Gas Fuel)	0.24	Graphite	0.0202
Transpiration (Gas Fuel)	0.58	Regenerative	0.033
g. Transpiration (Liquid Oxid)	0.24	Graphite	0.0202

STEP 16: Calculate the engine weight corrected for selected throat cooling type as follows:

$$Wt_{eng_{corr.}} = WT_{eng.} - (W_{T_{ccn_{base}}} + W_{T_{ccn}})$$

= Wet engine weight corrected for cooling type, lb

where

$W_{T_{ccn_{base}}}$ = Combustion chamber and nozzle midsection weight for baseline engine as obtained from Step 12.

$W_{T_{ccn}}$ = Combustion chamber and nozzle midsection weight for selected engine as obtained from Step 15.

STEP 17: If selected injector type is different from the baseline engine characteristics presented in Step 1, proceed with Step 12. If the selected injector type is the same as baseline engine characteristics, proceed to Step 23.

STEP 18: Determine the baseline engine injector assembly weight ($Wt_{inj_{base}}$) from Figure No. 148.

STEP 19: Determine the selected injector type assembly weight (Wt_{inj}) from Figure No. 148.

STEP 20: Determine the baseline engine combustion chamber surface area (A_{ccBase}) from Figure No. 147 or use the value obtained from Step 9.

STEP 21: Determine the combustion chamber surface area (A_{cc}) from Figure No. 147 for the selected injector type.

STEP 22: Calculate the engine weight corrected for selected injector type as follows:

$$Wt_{eng_{corr}} = Wt_{eng} - \rho\,(Acc_{base} - Acc) - Wt_{inj_{base}} + Wt_{inj}$$

= Engine wet weight corrected for injector type, lb

where

ρ = effective surface density for selected throat coolant type, lb/in.^{2} (same as used in Step 15)

Wt_{eng} = Engine wet weight from Step 10.

Acc_{base} = Baseline engine combustion chamber surface area as obtained from Step 20, in.^{2}

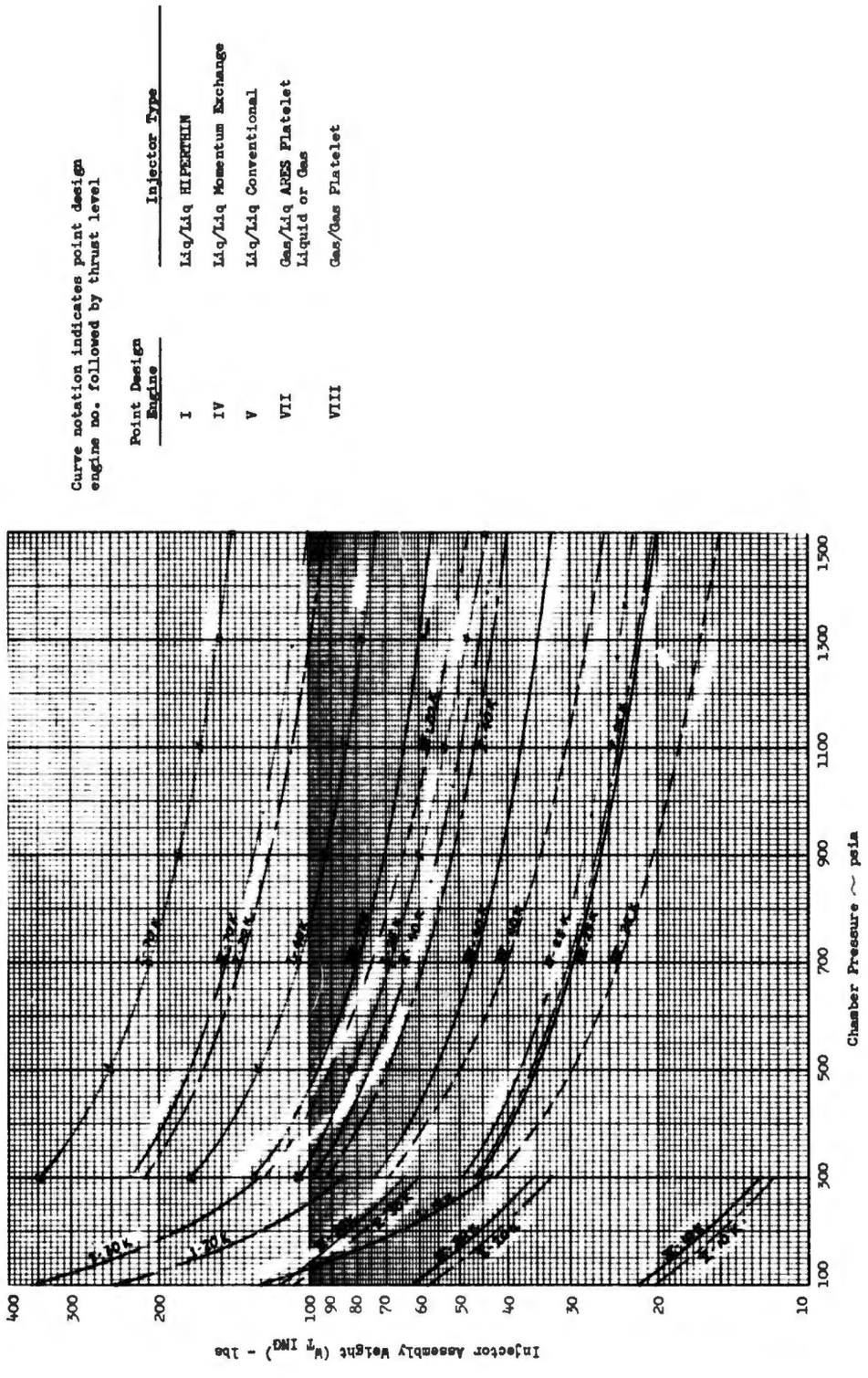

Figure 148. Injector Assembly Weights for Parametric Engines

Acc = selected engine combustion chamber surface area, as obtained from Step 21, $in.^2$

$Wt_{inj_{base}}$ = baseline injector assembly weight as obtained from Step 18, lb

Wt_{inj} = selected injector type assembly weight as obtained from Step 19, lb

STEP 23: If selected throat coolant type is transpiration cooling and the selected transpiration material is graphite, proceed to Step 24; otherwise, proceed to Step 29.

STEP 24: Calculate the combustion chamber (A_{cc}) and nozzle (A_n) surface areas associated with the selected throat cooling method as described in Step 21 and in the following relationship, respectively:

$$A_n = A\,A_F$$

= nozzle surface area associated with the throat cooling method, $in.^2$

where

A = total nozzle surface area as obtained from Step 6, $in.^2$

A_F = fraction of nozzle surface area associated with the selected throat cooling as determined in Step 14.

STEP 25: If the selected cooling media is gaseous fuel, proceed to Step 26; otherwise, proceed to Step 28.

STEP 26: Determine the baseline CAT-Pack assembly weight ($Wt_{cp_{base}}$) from Figure No. 149 for turbine gas temperature of 1400°F.

STEP 27: Determine the high temperature (turbine gas temperature of 1600°F) CAT-Pack assembly weight (Wt_{cp}) from Figure No. 149.

STEP 28: Calculate engine weight, corrected for graphite platelet transpiration cooling, as follows:

$$Wt_{eng} = Wt_{eng} - (A_{cc} + A_n)\,(\rho_{base} - \rho_{gp} - (Wt_{cp_{base}} - Wt_{cp})$$

= Wet engine weight corrected for graphite platelet transpiration cooling, lb

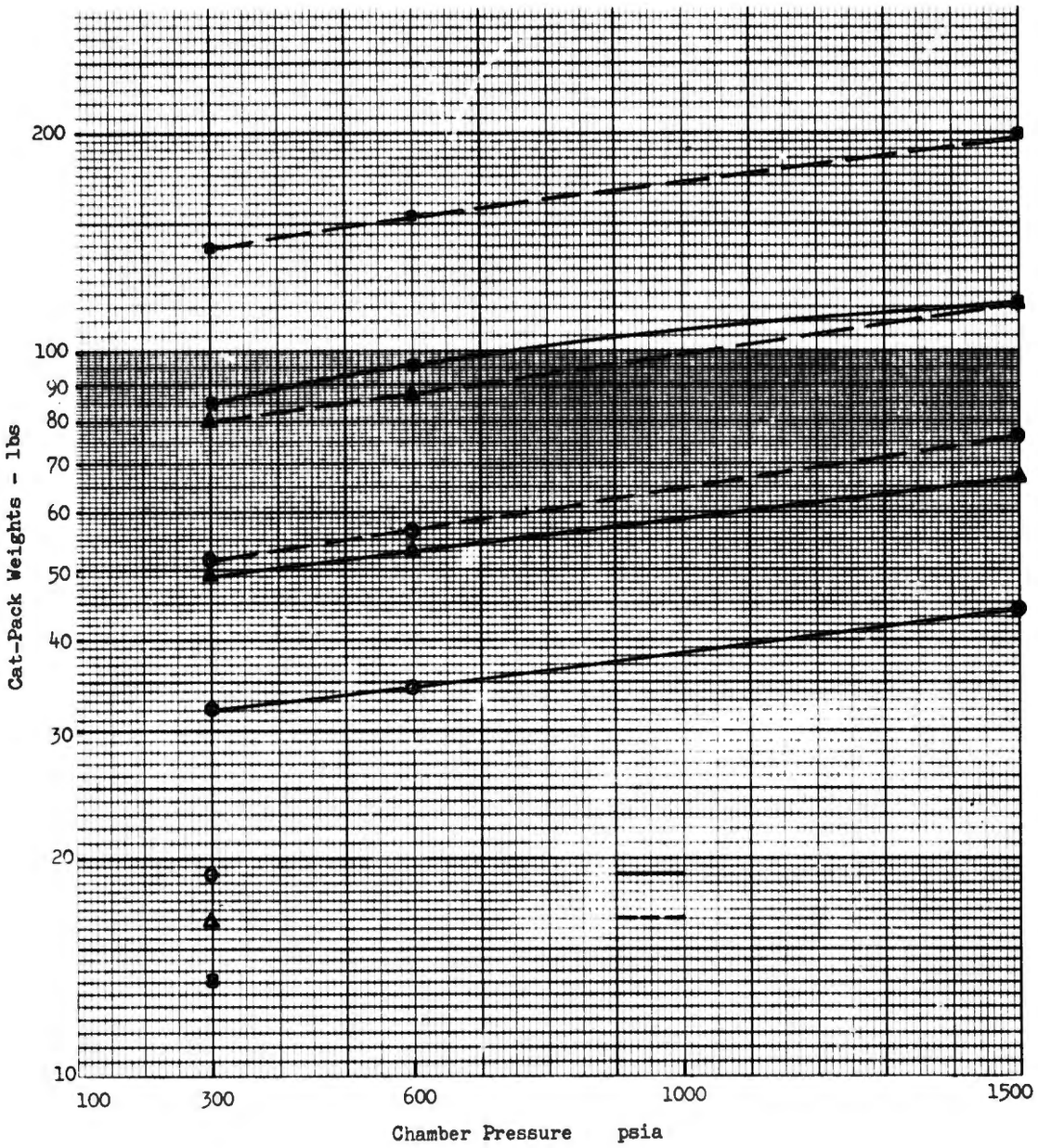

Figure 149. Staged-Combustion Cat-Pack Weights vs Chamber Pressure

where

Wt_{eng} = wet engine weight from Step 22, lb

ρ_{base} = effective surface density for nickel platelets, $lb/in.^2$

= .24, $lb/in.^2$

ρ_{gp} = effective surface density for graphite platelets, $lb/in.^2$

= .088 $lb/in.^2$

$Wt_{cp_{base}}$ = baseline CAT-Pack weight as obtained from Step 26, lb

Wt_{cp} = high temperature CAT-Pack weight as obtained from Step 27, lb

The selection of graphite platelets eliminates the use of regenerative cooling for the nozzle extension. Therefore, the nozzle cooling method selected in Step 15 should be graphite.

STEP 29: If selected fuel is N_2H_4, proceed to Step 31; otherwise proceed to Step 30.

STEP 30: Calculate engine weight corrected for fuel type as follows:

$Wt_{eng} = Wt_{eng} - (Wt_{cp} + Wt_{gg})$

= Wet engine weight corrected for fuel type, lb

where

Wt_{eng} = engine weight from Step 28, lb

Wt_{cp} = CAT-Pack weight consistent with the cooling material selection as determined in Steps 25 to 28.

Wt_{gg} = Gas generator assembly weight obtained from Figure No. 150.

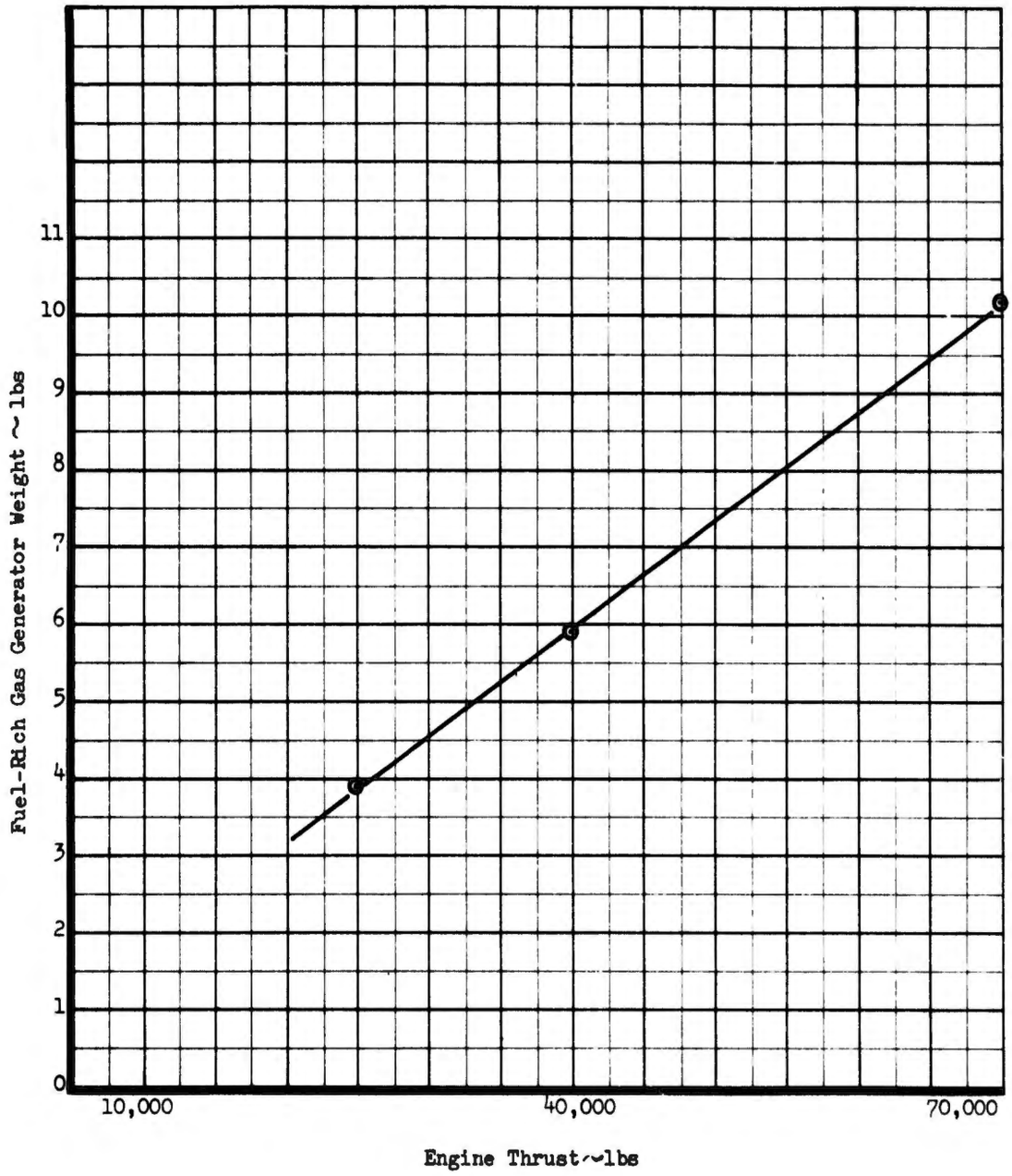

Figure 150. Fuel-Rich Gas Generator Weight as a Function of Engine Thrust

2. Engine Delivered Specific Impulse

Engine delivered specific impulse is obtained by utilizing the parametric performance data that has been generated for the base point engine. Selected engine characteristics which differ from the base point engines will be incorporated by modifying the base point performance.

The following detailed calculation procedure enables the base point engine data to be modified for:

- type of fuel
- cooling method
- type of injector
- throat cooling material

The previously selected engine characteristics establish which of these modifications is necessary.

Again, the following calculations should be performed in the order indicated.

STEP 1: Obtain baseline thrust chamber zero coolant specific impulse ($I_{sp_{base}}$) from the applicable figures listed below for selected values of F, P_c, and ε_A. Note that the baseline characteristics are also listed.

Engine Type	Base Perf. Location	Baseline Cool. Method	Baseline Cool. Mat'l	Baseline Injector Type
a. Pressure-Fed	Figure No. 151	Radiation	Graphite	Liq./Liq. Platelet
b. Pump-Fed (Bleed Cycle)	Figure No. 152	Ablative	Graphite Throat	Liq./Liq. Momentum Exchange
c. Pump-Fed (Gas/ Liquid or Liquid/ Gas Staged Combustion)	Figure No. 153	Liquid Ox. Transpira-tion	Nickel	Gas/Liq. Platelet
d. Pump-Fed (Gas/Gas Staged-Combustion)	Figure No. 154	Gas Fuel Transpiration	Nickel	Gas/Gas

STEP 2: If selected engine type is pump-fed (bleed cycle), proceed to Step 3; otherwise proceed to Step 5.

STEP 3: Obtain performance loss ($I_{sp_{TE}}$) caused by turbine exhaust from Figure No. 155.

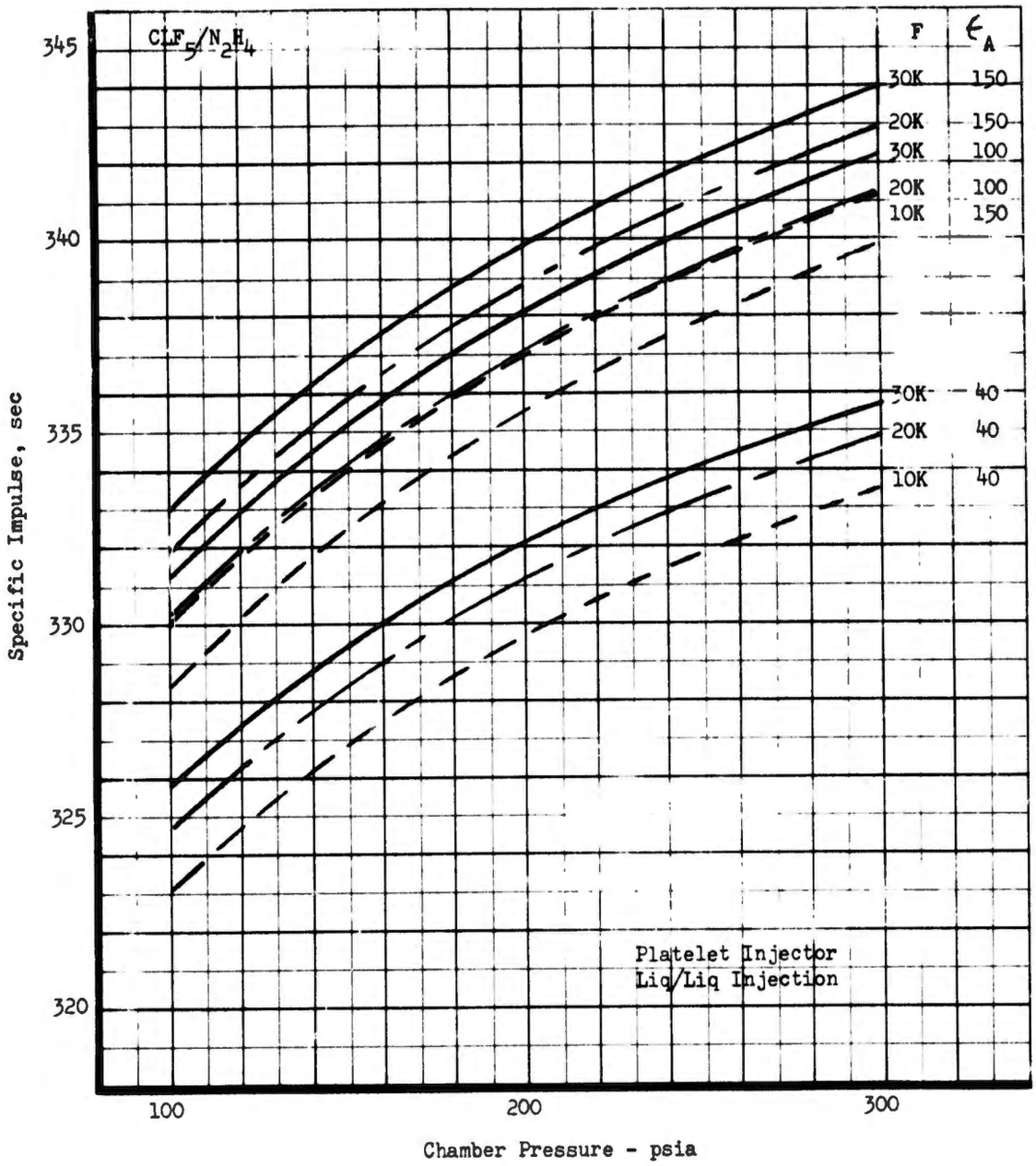

Figure 151. Pressure-Fed Parametric Performance for Zero Coolant Flow (u)

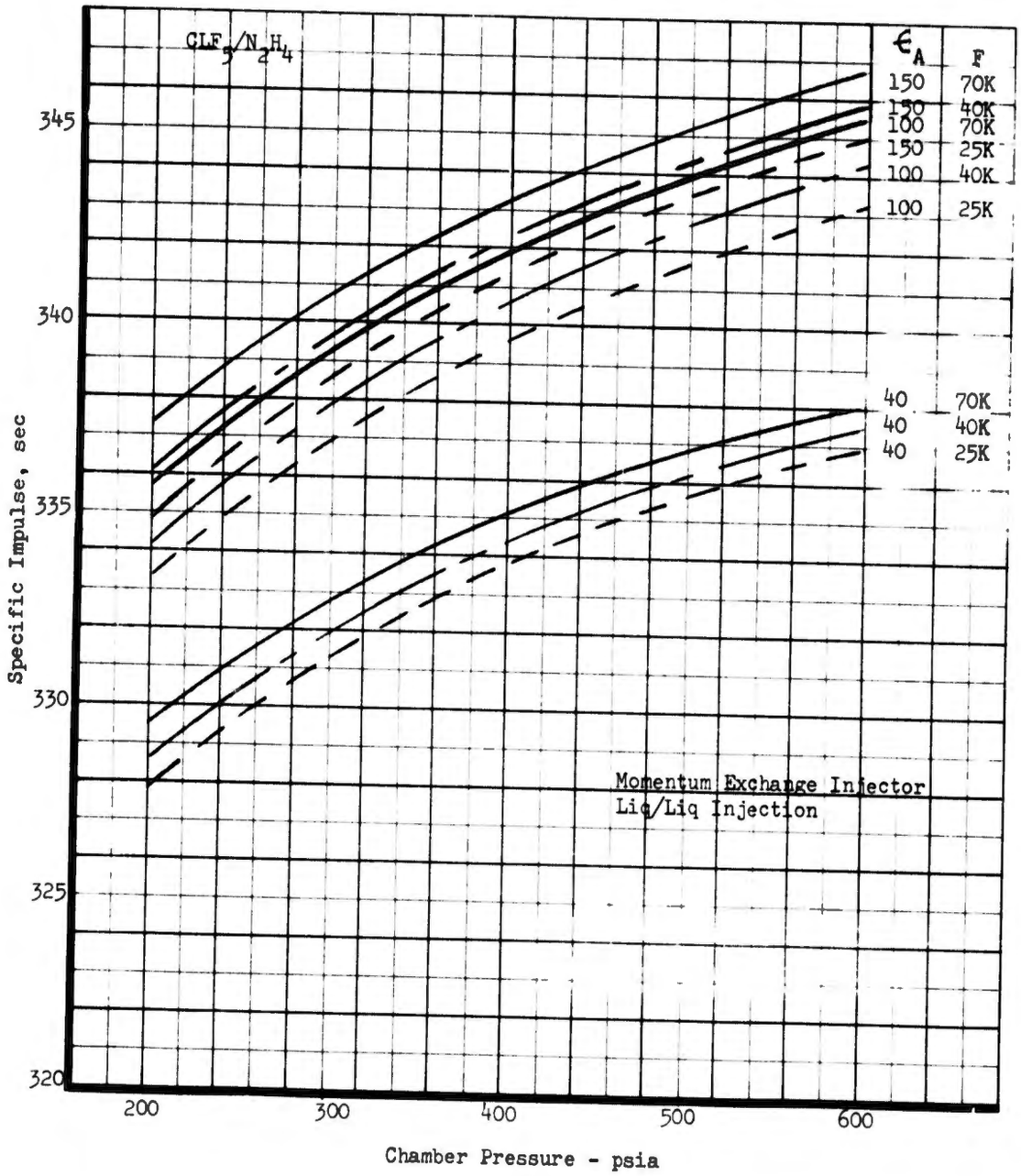

Figure 152. Pump-Fed (Bleed Cycle) Parametric Performance for Zero Coolant Flow (u)

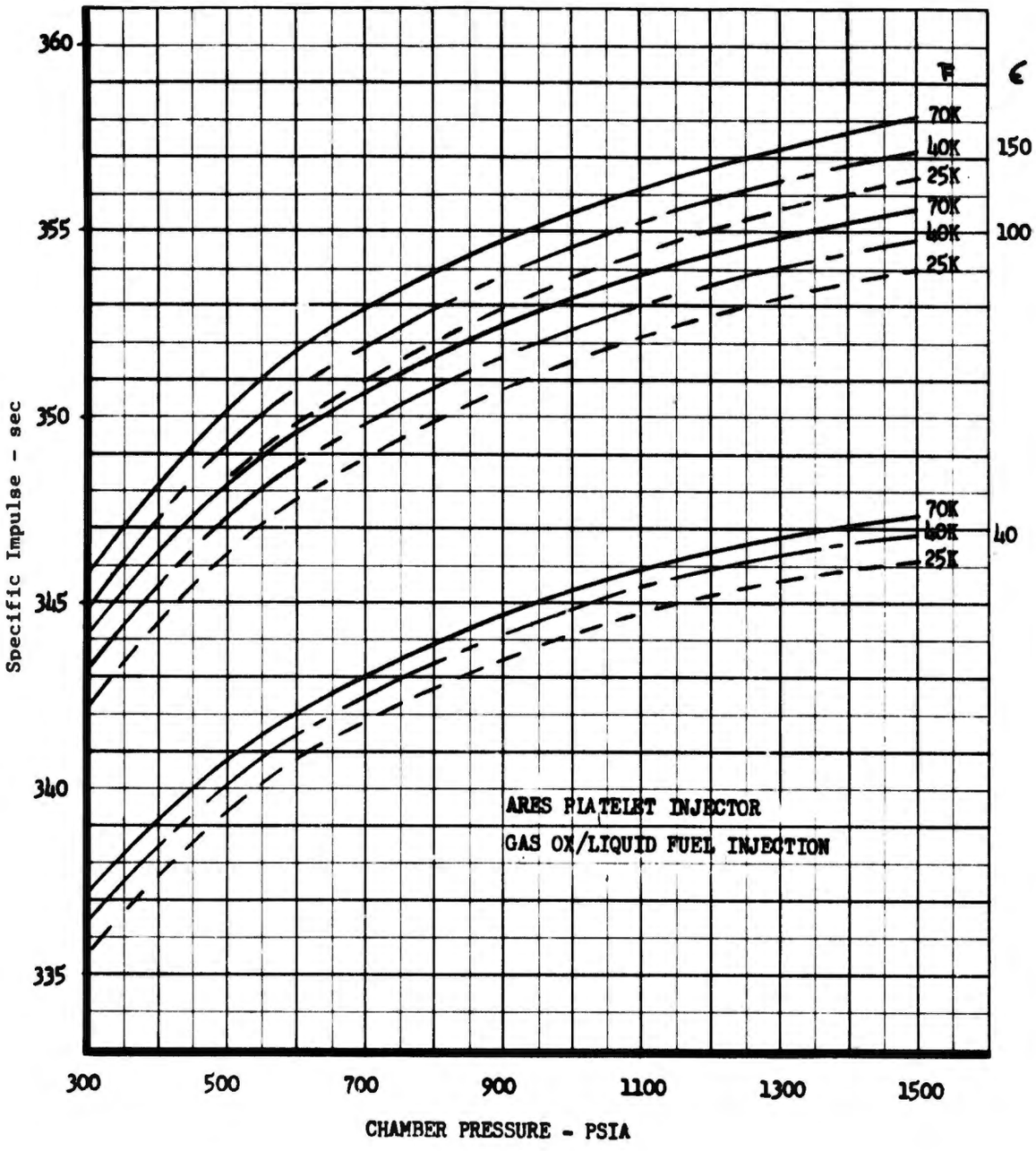

Figure 153. Pump-Fed (Gas/Liquid or Liquid/Gas Staged-Combustion) Parametric Performance for Zero Coolant Flow (u)

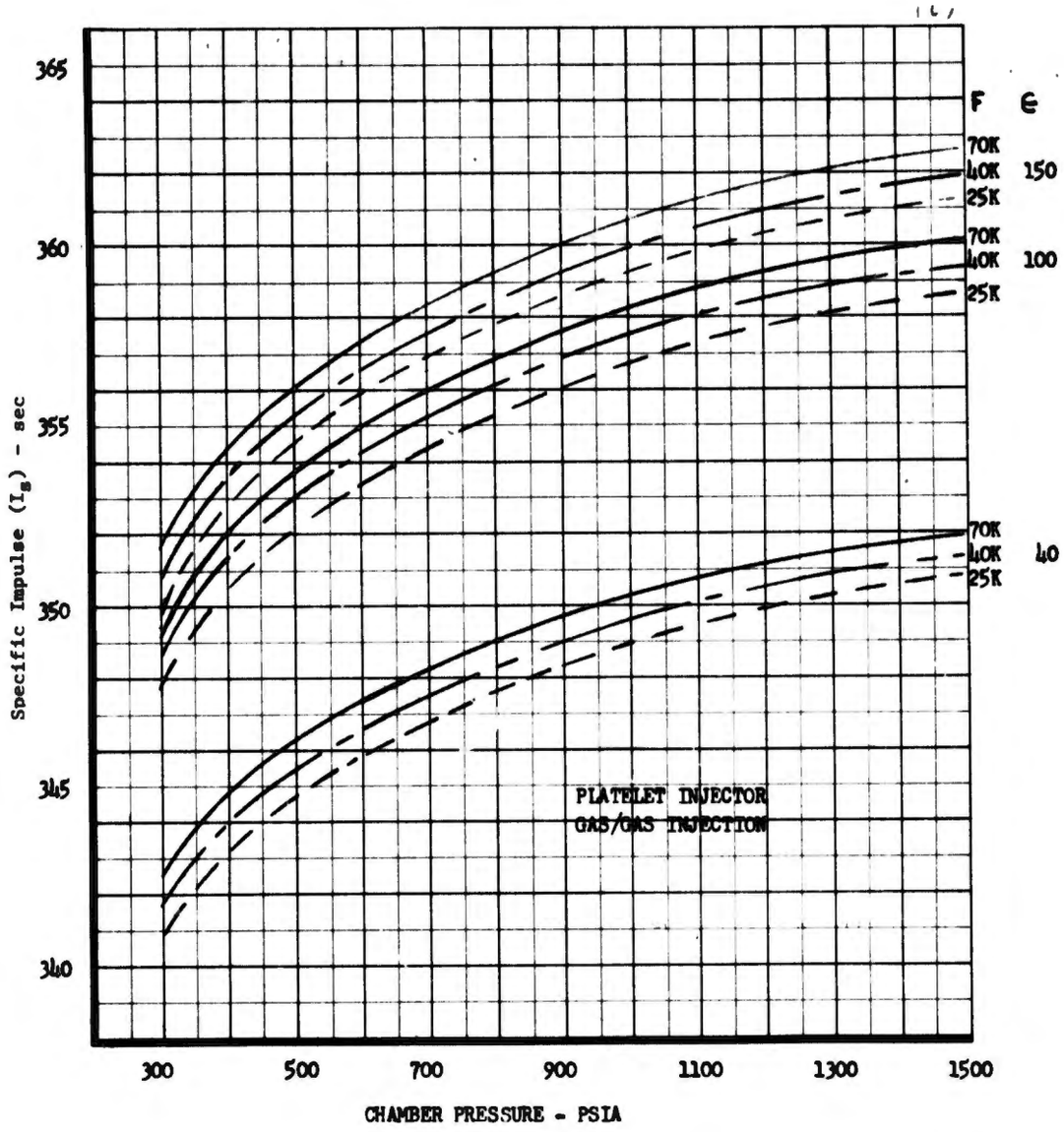

Figure 154. Pump-Fed (Gas/Gas Staged-Combustion) Parametric Performance for Zero Coolant Flow (u)

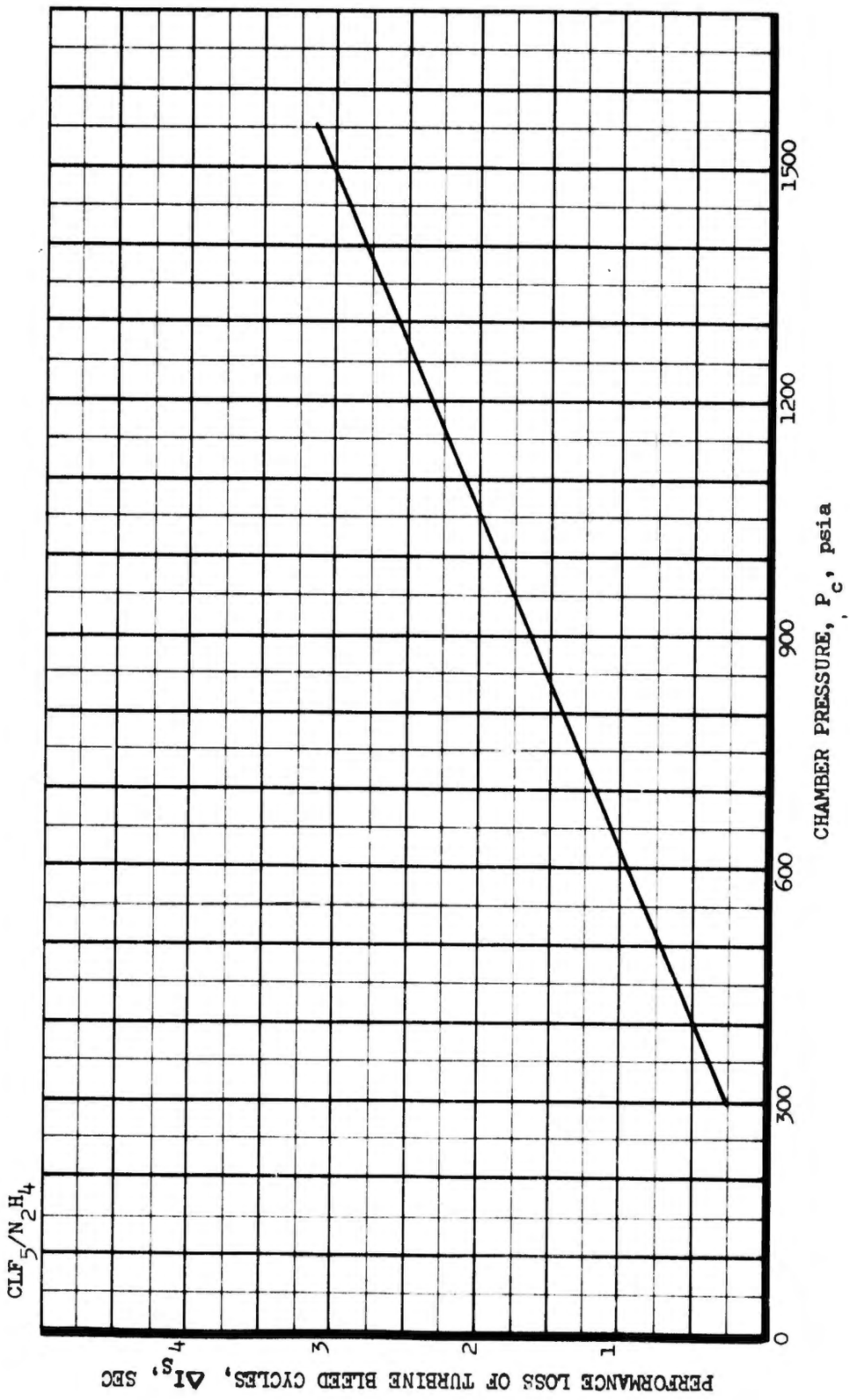

Figure 155. Performance Loss of Turbine Bleed Cycles vs Chamber Pressure

STEP 4: Calculate engine performance ($\Delta I_{sp_{eng_{sc}}}$) for zero coolant flow rate for pump-fed (bleed cycle) engine as follows:

$$I_{sp_{eng_{sc}}} = I_{sp_{base}} - \Delta I_{sp_{TE}}$$

where $I_{sp_{base}}$ is obtainted from Step 1, sec

$\Delta I_{sp_{TE}}$ is obtained from Step 3, sec

STEP 5: If selected fuel is N_2H_4, proceed to Step 9; otherwise, proceed to Step 6.

STEP 6: Obtain theoretical performance ($I_{sp_{theo}\ N_2H_4}$) of N_2H_4 from Figure No. 156.

STEP 7: Obtain theoretical performance ($I_{sp_{theo}}$) of selected fuel from Figure No. 156.

STEP 8: Correct the base engine performance for fuel type as follows:

$$I_{sp_{\substack{\text{corrected} \\ \text{for fuel} \\ \text{type}}}} = I_{sp_{base}} - I_{sp_{theo_{N_2H_4}}} + I_{sp_{theo}}$$

where

$I_{sp_{base}}$ = zero coolant specific impulse obtained from Steps 1 or 4.

$I_{sp_{theo_{N_2H_4}}}$ = theoretical specific impulse for N_2H_4; obtained from Step 6.

$I_{sp_{theo}}$ = theoretical specific impulse for selected fuel; obtained from Step 7.

STEP 9: Obtain the coolant flow rate for N_2H_4 from the applicable figures listed below:

Engine Type	Coolant Flow Rate Location Total Flow Rate
a. Pressure-Fed	Figure No. 157
b. Pump-Fed (Bleed Cycle)	Figure No. 158
c. Pump-Fed (Gas/Liquid or Liquid/Gas Staged-Combustion)	Figure No. 159
d. Pump-Fed (Gas/Gas Staged-Combustion)	Figure No. 160

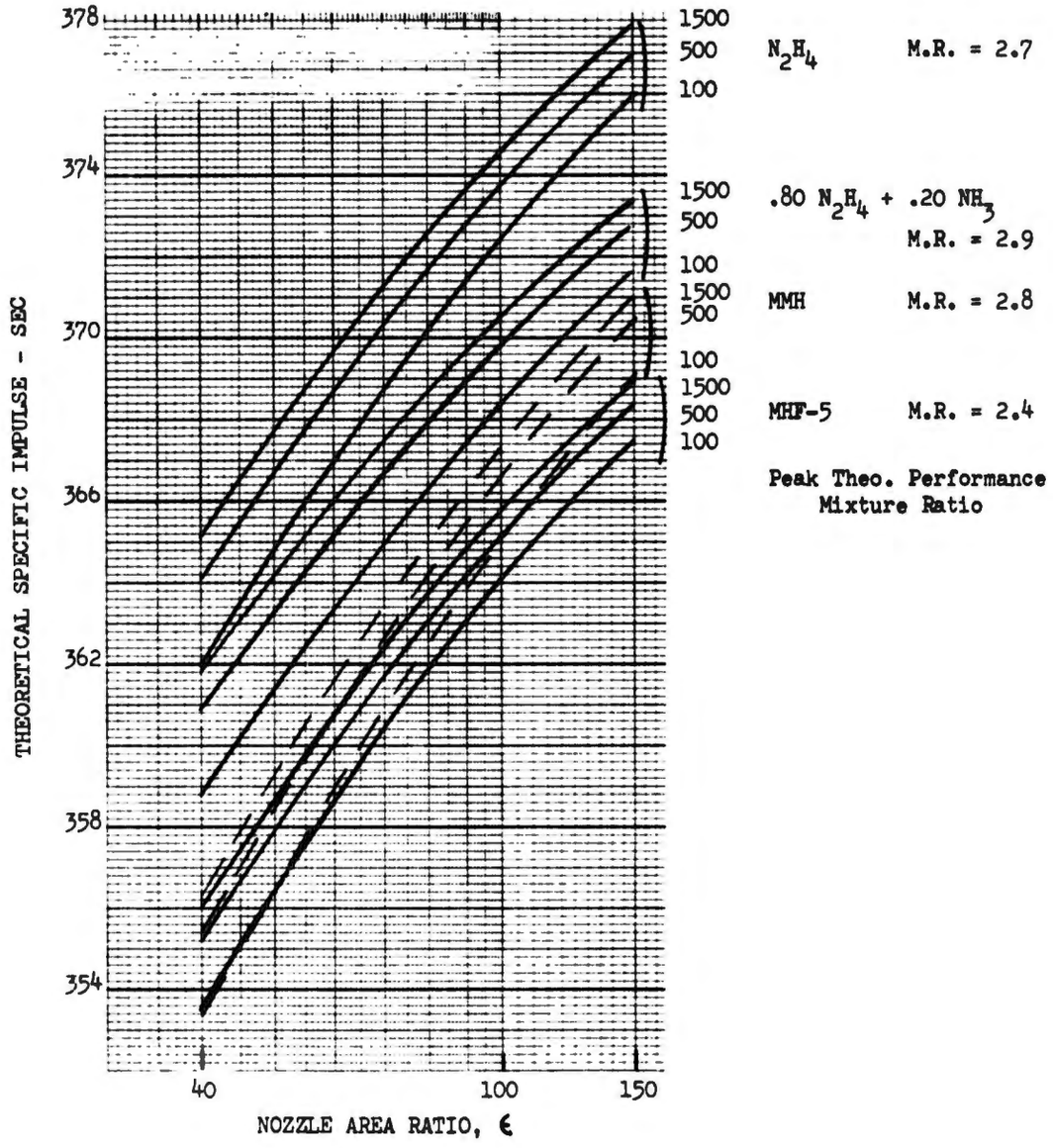

Figure 156. Theoretical Performance for Selected Propellant Combinations

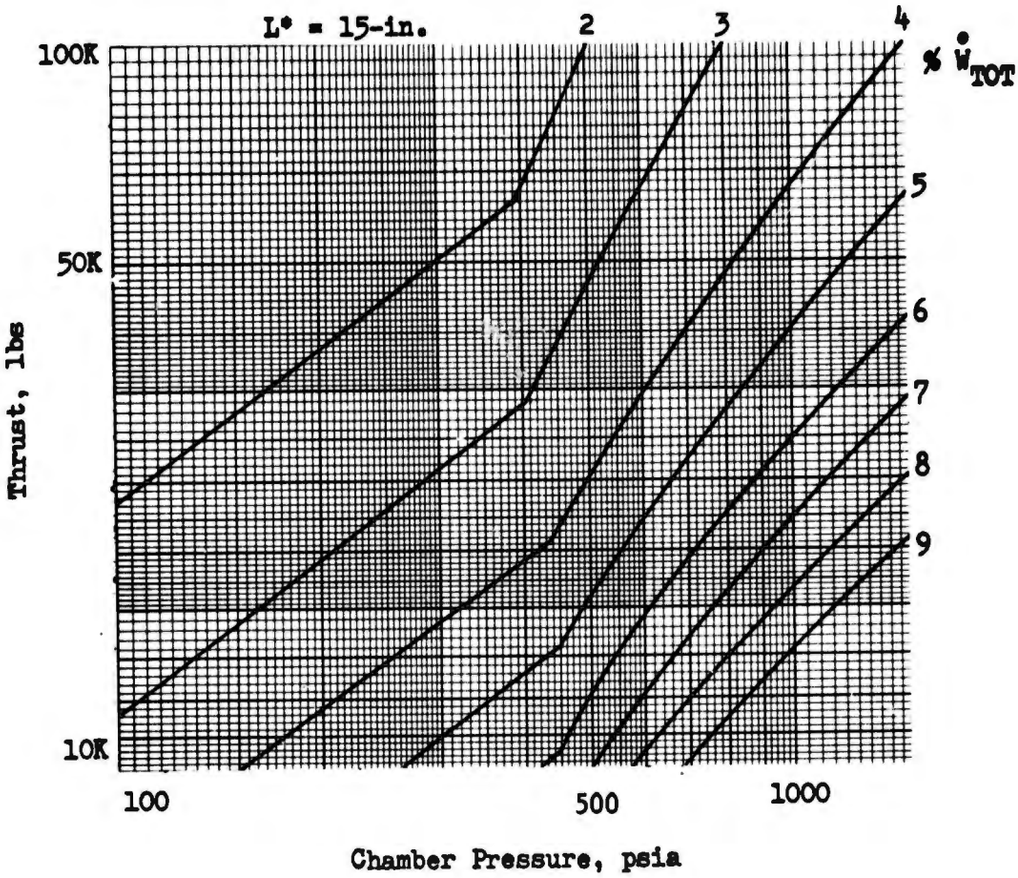

Figure 157. Pressure-Fed Cooling Requirements (Hiperthin Injector)

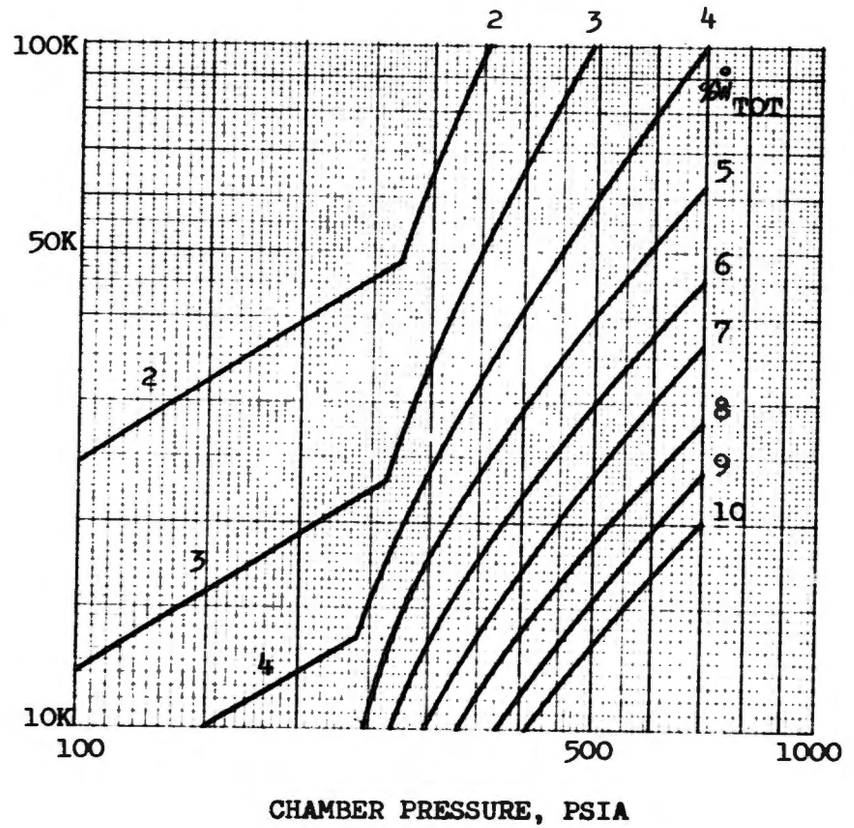

NOTE: OVER THE INDICATED F - P_C RANGE, THE THROAT COOLING REQUIREMENTS (SHOWN) EXCEED THE FLANGE COOLING REQUIREMENTS.

Figure 158. Pump-Fed Film Cooling Requirements (Momentum Exchange Injector)

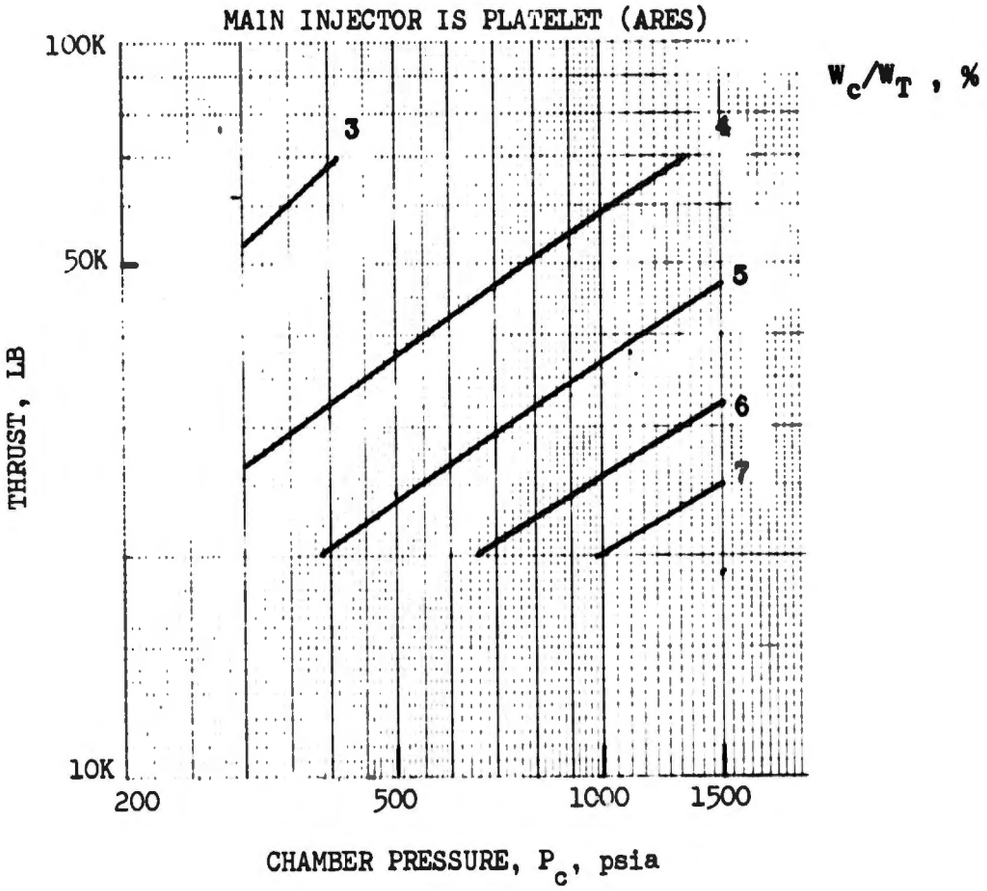

Figure 159. Transpiration Coolant Flow Rates for Gas/Liquid or Liquid/Gas Staged-Combustion with Liquid Oxidizer Cooling

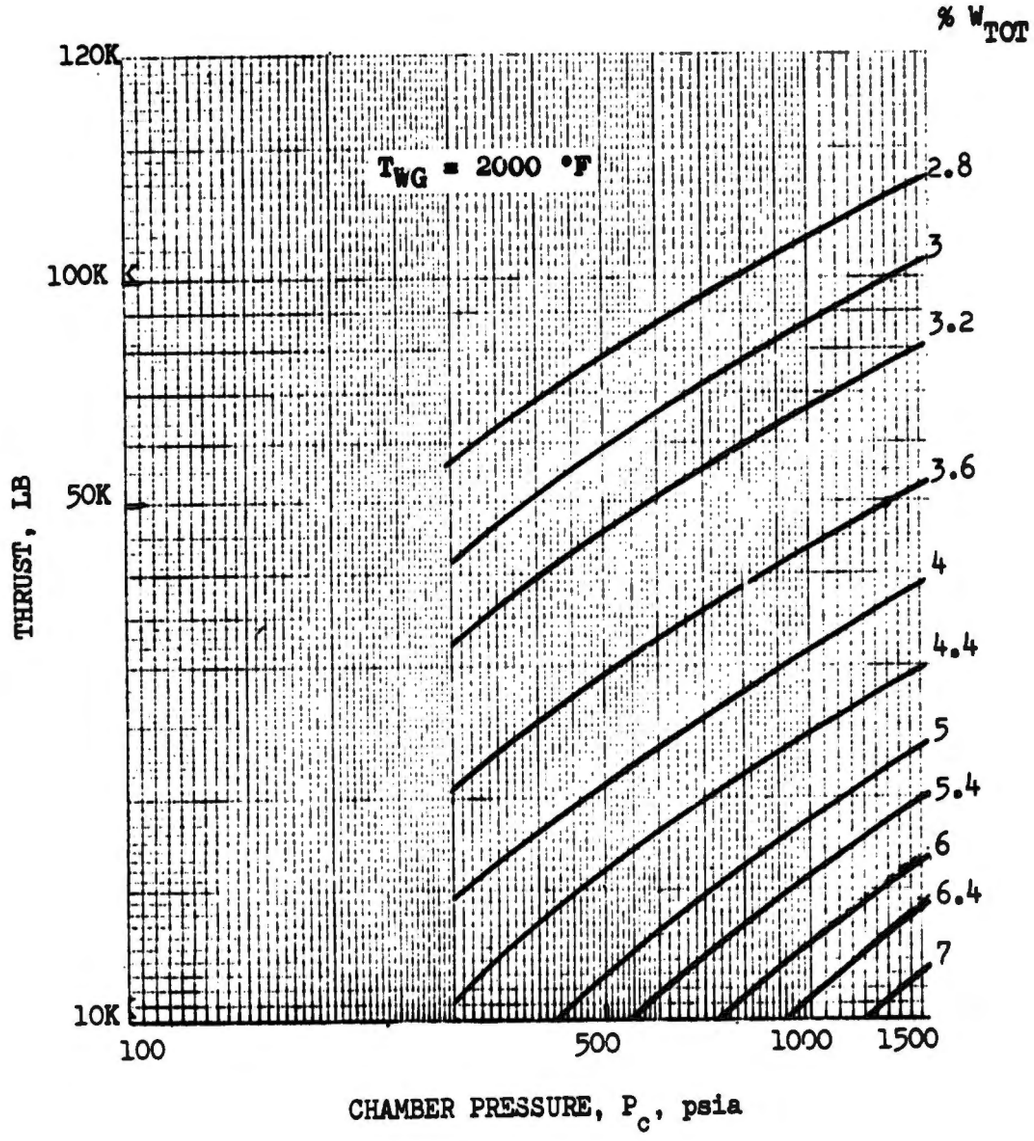

Figure 160. Gas-Gas Staged-Combustion Transpiration Coolant Requirements

STEP 10: If selected cooling method differs from the baseline methods presented in Step 1, proceed to Step 11; if the same, proceed to Step 12.

STEP 11: Calculate the coolant flow rate/total flow rate ratio $(\dot{W}_c/W_T)_{cm}$ for the selected engine as follows:

$$\left(\frac{\dot{W}_c}{\dot{W}_T}\right)_{cm} = \frac{\dot{W}_C}{\dot{W}_{T_{base}}} \quad K_{cm}$$

K_{cm} = coolant method constant

Values of the coolant method constant (K_{cm}) are listed below for the baseline and possible selected cooling methods.

Baseline Cooling Method	Selected Cooling Method	K_{cm}
a. Pressure-Fed - Radiation	Ablative	1.0
b. Pump-Fed (Bleed Cycle) - Ablative	Radiation	1.0
c. Pump-Fed (Gas/Liq or Liq/Gas Staged-Combustion) - Liquid Oxidizer Transpiration	Gas Fuel - Transpiration	1.12
	Regenerative	0
d. Pump-Fed (Gas/Gas Staged-Combustion) - Gaseous Fuel Transpiration	Liquid Oxygen - Transpiration	.89
	Regenerative	0
	Radiation or Ablative See Steps 16 and 17	

STEP 12: Determine rate of coolant flow rate to total flow rate $(\dot{W}_c/W_T)$ for selected engine from Figure No. 157.

STEP 13: Determine surface area of combustion chamber $(Acc_{10" L^*})$ for 10-in. L* from Figure No. 147.

STEP 14: Determine surface area of combustion chamber $(Acc_{15" L^*})$ consistent with a 15-in. L* from Figure No. 147.

STEP 15: Calculate coolant flow rate ratio $(W_c/W_T)_{cm}$ consistent with a 10-in. L* radiation or ablative cooled combustion chamber as follows:

$$\left(\frac{\dot{W}_c}{W_T}\right)_{cm} = \left(\frac{W_c}{W_T}\right) \left(\frac{Acc_{10" L*}}{Acc_{15" L*}}\right)$$

= Coolant flow rate ratio for radiation or ablative cooled gas/liquid or liquid/gas staged-combustion engine.

where $\frac{W_c}{W_T}$ = coolant flow rate ratio obtained from Step 12.

$Acc_{10" L*}$ = combustion chamber surface area consistent with 10-in. L* as obtained from Step 13.

$Acc_{15" L*}$ = combustion chamber surface area consistent with 15-in. L* as obtained from Step 14.

STEP 16: Determine surface area of combustion chamber ($Acc_{5" L*}$) associated with a 5-in. L* from Figure No. 147.

STEP 17: Calculate coolant flow rate ratio $(W_c/W_t)_{cm}$ consistent with a 5-in. L* radiation on ablative cooled combustion chamber as follows:

$$\left(\frac{W_c}{W_T}\right)_{cm} = \left(\frac{W_c}{W_T}\right) \left(\frac{Acc_{5" L*}}{Acc_{15" L*}}\right)$$

= Coolant flow rate ratio for radiation or ablative cooled gas/gas staged-combustion engine.

where

$Acc_{5" L*}$ = combustion chamber surface area consistent with 5-in. L* as obtained from Step 16.

STEP 18: If the selected injector type is the same as the baseline type presented in Step 1, proceed to Step 23; otherwise, proceed to Step 19.

STEP 19: Determine the combustion chamber surface area (Acc_{base}) of the baseline engine from Figure No. 147.

STEP 20: Determine the combustion chamber surface area (Acc) of the selected engine from Figure No. 147.

STEP 21: Calculate the coolant flow rate ratio $(W_c/W_t)_{inj}$ for the selected injector type as follows:

$$\left(\frac{W_c}{W_T}\right)_{inj} = \left(\frac{W_c}{W_T}\right)_{cm} \frac{Acc}{Acc_{base}}$$

where

$(W_c/W_T)_{cm}$ is obtained from Step 11

Acc_{base} is obtained from Step 19

Acc is obtained from Step 20

STEP 22: Determine the injector ERL loss (η_{ERL}) for the selected engine injector type from Figure No. 161.

STEP 23: Determine the baseline injector ERL loss ($\eta_{ERL_{base}}$) from Figure No. 161.

STEP 24: Obtain the coolant flow correction factor (K_{cfc}) from the applicable figures listed below for the selected fuel type.

Coolant Type	Coolant Flow Correction Factor
a. Radiation or Ablative	Figure No. 162
b. Liquid Oxidizer Transpiration Cooling	Figure No. 163
c. Gaseous Fuel Transpiration-Cooling	Figure No. 164

STEP 25: Calculate the coolant flow rate ratio $(W_c/W_T)_{SE}$ for the selected engine as follows:

$$(W_c/W_T)_{SE} = K_{cfc} \quad (W_c/W_T)_{inj}$$

where

K_{cfc} is obtained from Step 24

$(W_c/W_T)_{inj}$ is obtained from Step 21

STEP 26: If the selected throat cooling material is the same as the baseline type presented in Step 1, proceed to Step 29; otherwise proceed to Step 27.

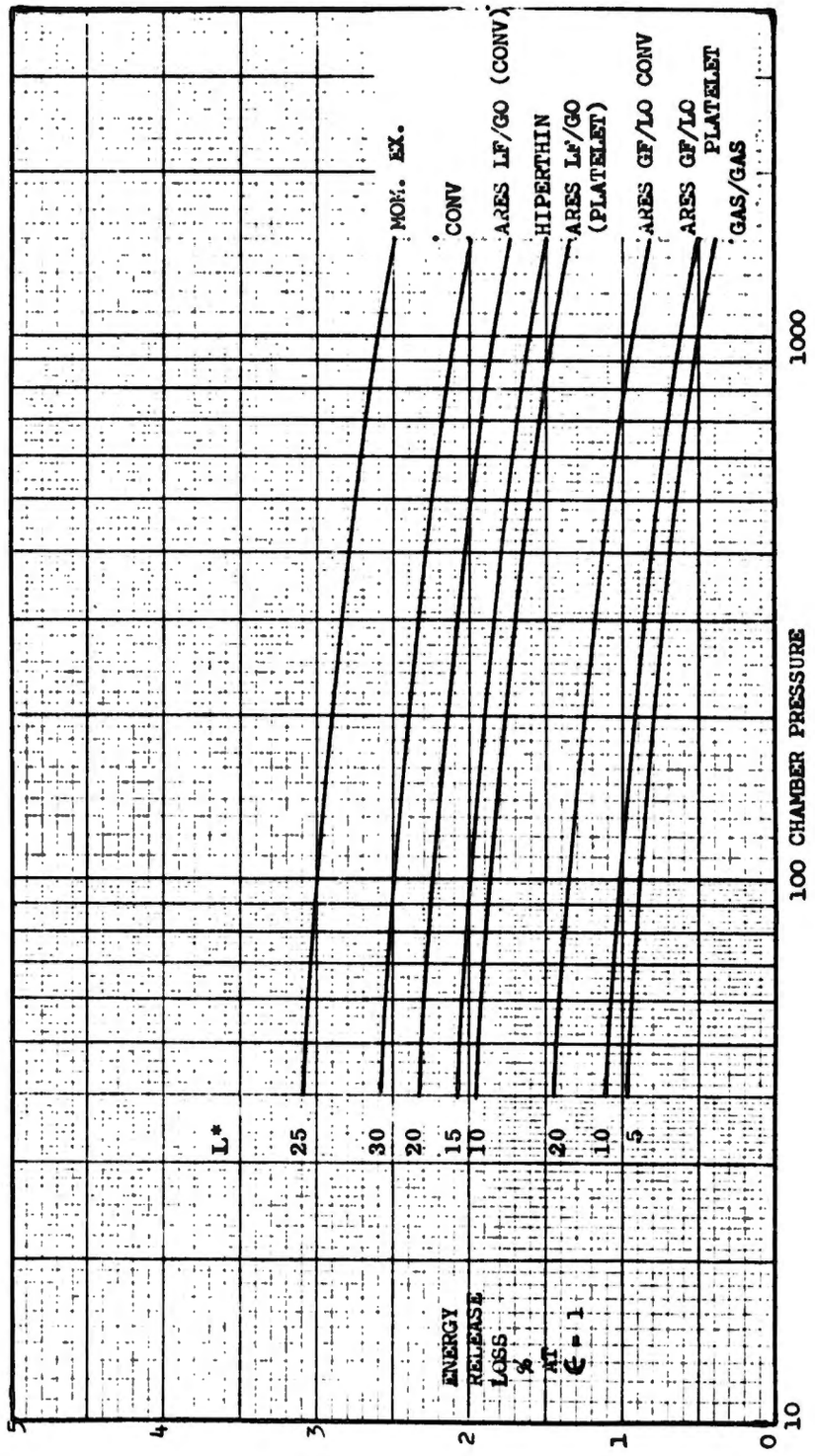

Figure 161. CLF_5/N_2H_4 Energy Release Loss-Injector Trade-Off

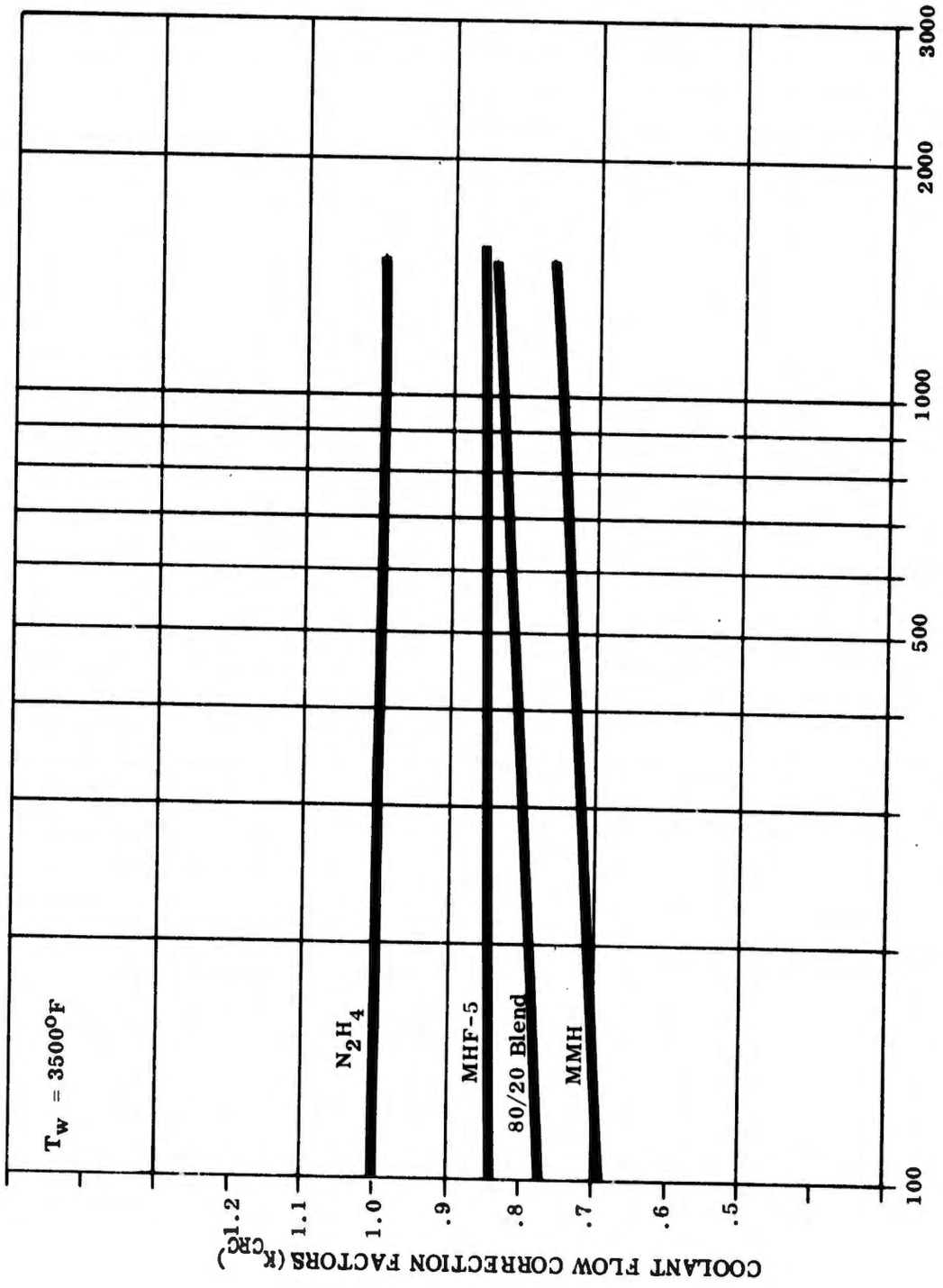

Figure 162. Coolant Flow Correction Factor for Fuel Film Cooling

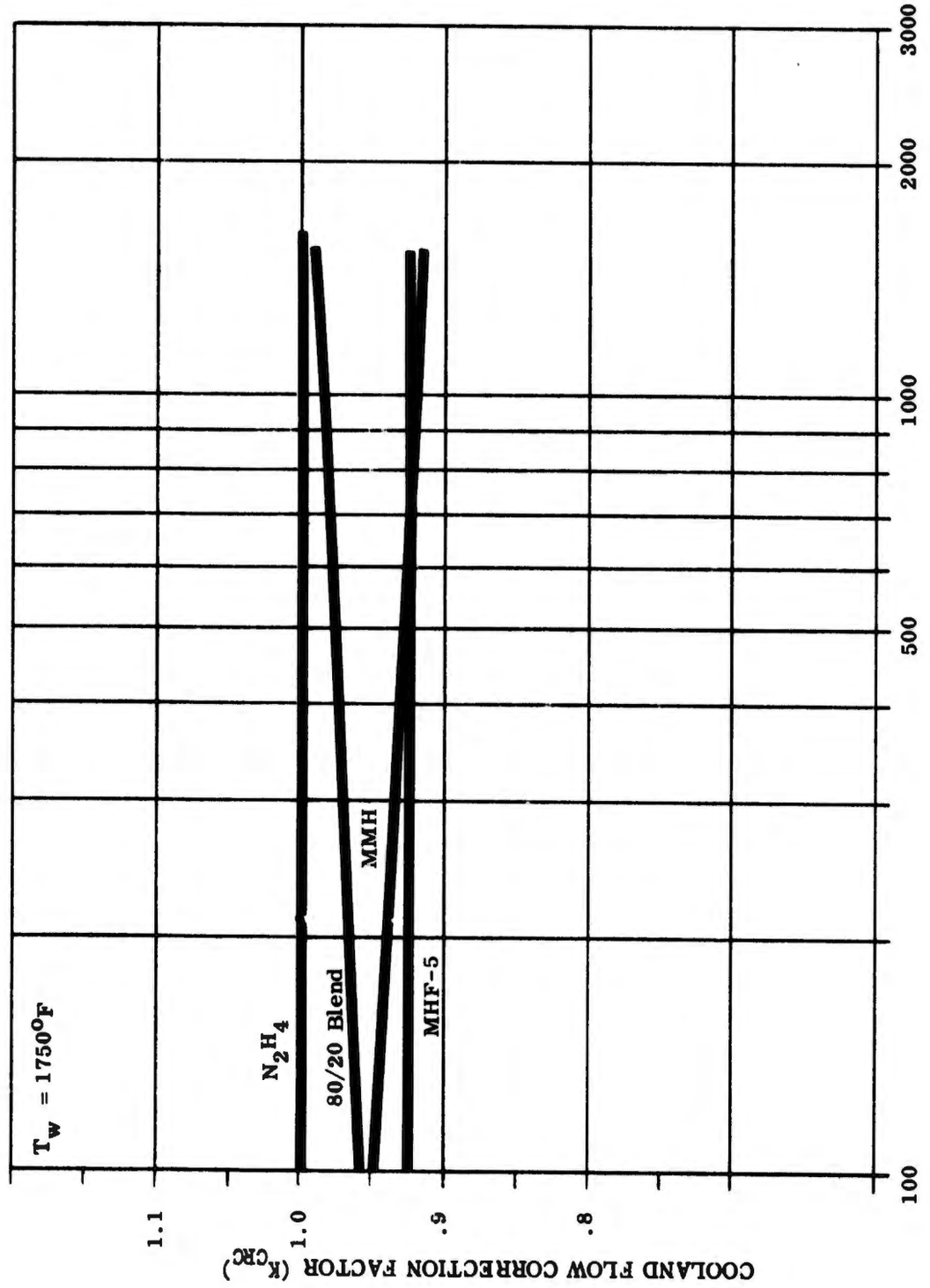

Figure 163. Coolant Flow Correction Factor for Liquid ClF_5 Transpiration Cooling

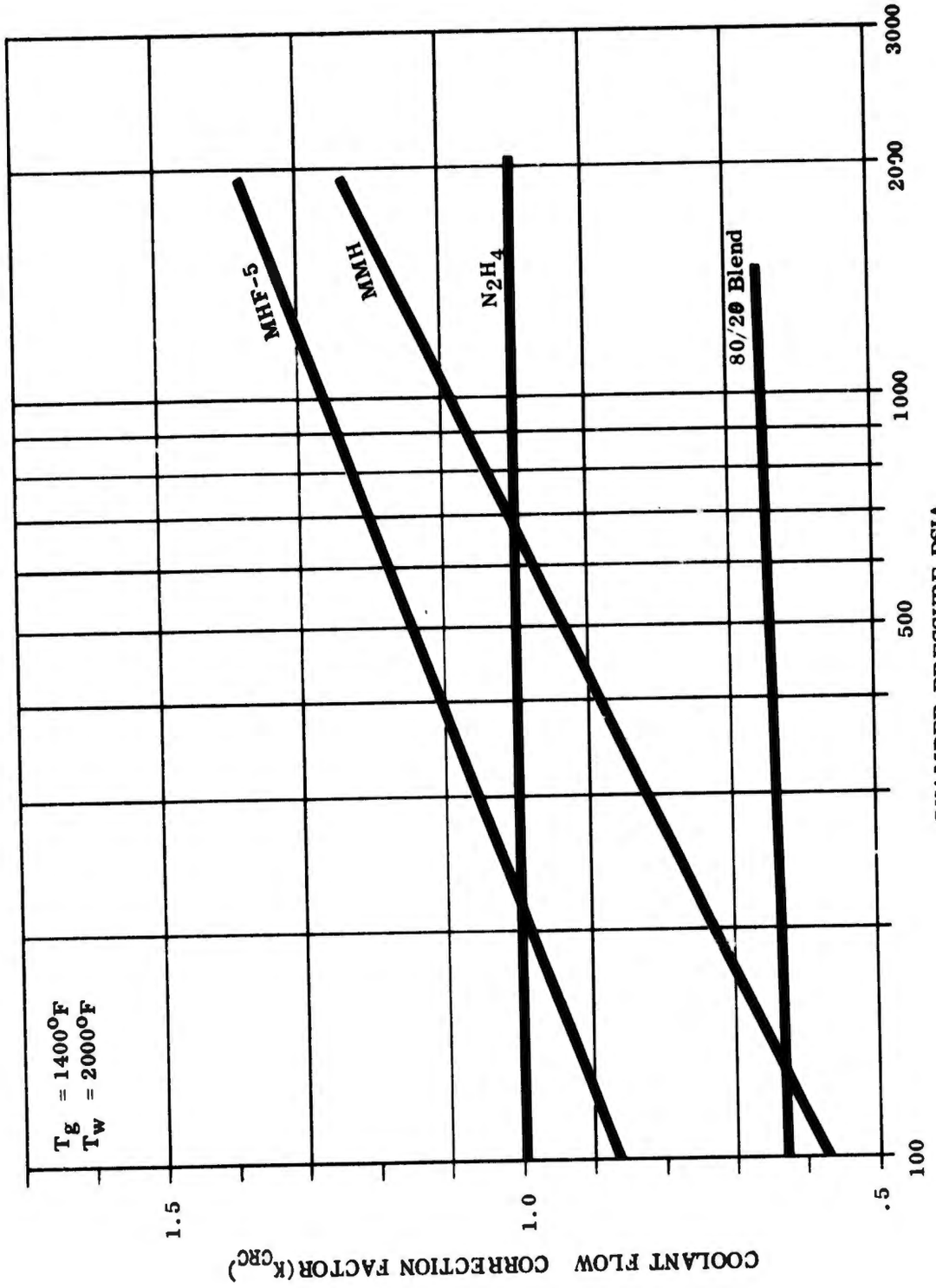

Figure 164. Coolant Flow Correction Factor for Gaseous Fuel Transpiration Cooling

STEP 27: Determine the coolant reduction factor (K_r) consistent with graphite material (allowable wall temperature of 4000°F) from Figure No. 165 for the MHF-5 or 80/20 blend and from Figure No. 166 for CLF_5, N_2H_4, or MMH.

STEP 28: Calculate the coolant flow rate $(W_c/W_t)_{seg}$ consistent with graphite throat cooling for the selected engine as follows:

$$\frac{(W_c)}{W_t}_{seg} = (W_c/W_t)_{SE} \quad K_F$$

where

$(W_c/W_t)_{SE}$ is obtained from Step 25

K_r is obtained from Step 27

STEP 29: Determine the performance loss factor (K_p) for the selected engine from Figure No. 167.

STEP 30: Calculate the delivered specific impulse for the selected engine as follows:

$$I_{sp} = I_{sp_{corr \text{ for fuel type}}} \frac{(1 - \eta_{ERL})}{(1 - \eta_{ERL_{base}})} - K_p \ (W_c/W_t)$$

where

$I_{sp_{corr. \text{ base fuel type}}}$ is obtained from Step 8

η_{ERL} is obtained from Step 22

$\eta_{ERL_{base}}$ is obtained from Step 23

K_p is obtained from Step 29

(W_c/W_t) is obtained from Step 28 or Step 25, as applicable.

3. Engine Throttling Performance

Throttling performance consists of the delivered engine specific impulse that can be achieved at thrust levels below full thrust capability. Therefore, this calculation procedure is applicable only to selected systems that are capable of throttling.

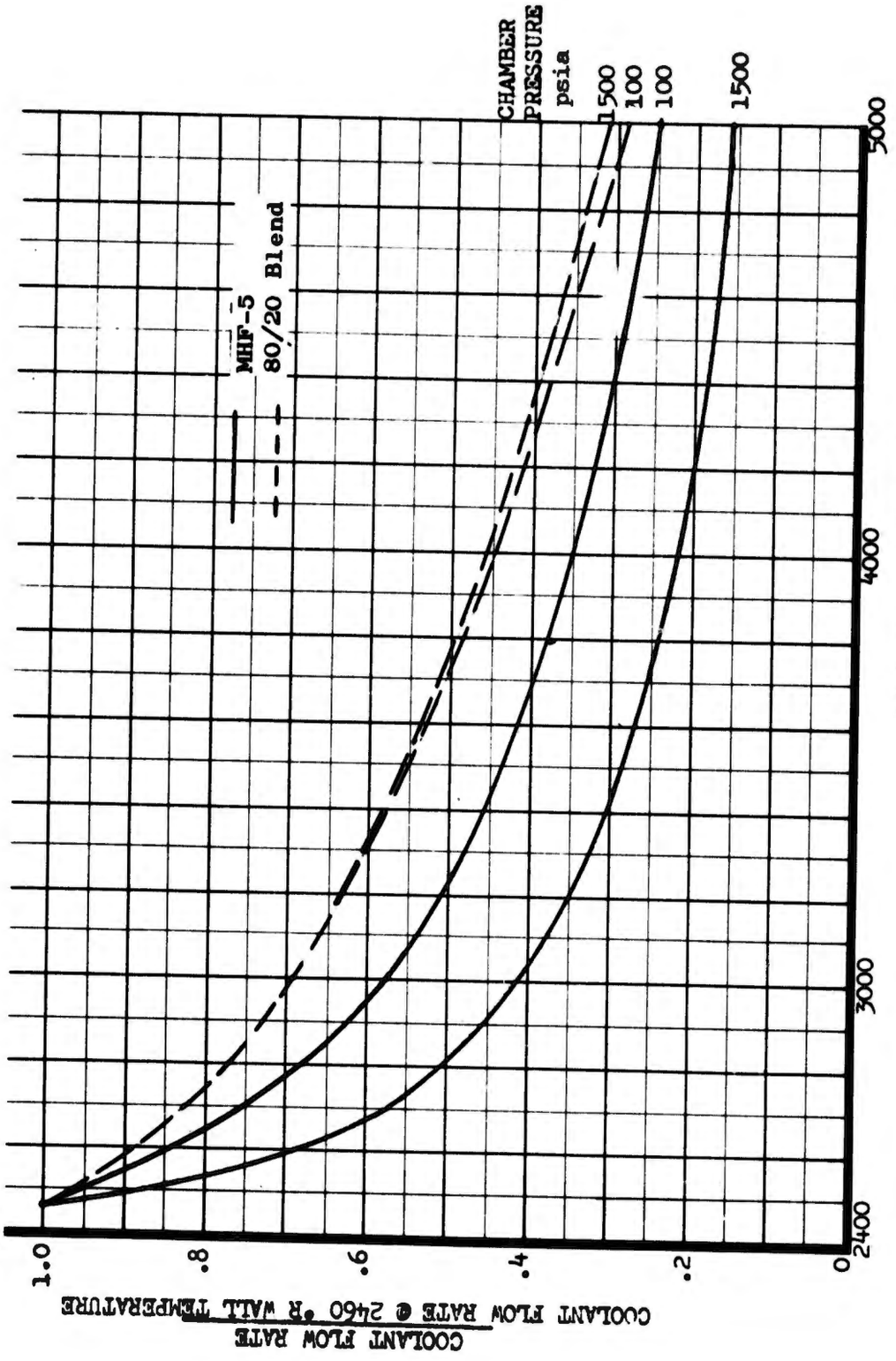

Figure 165. Coolant Flow Rate Reduction with Material Capability

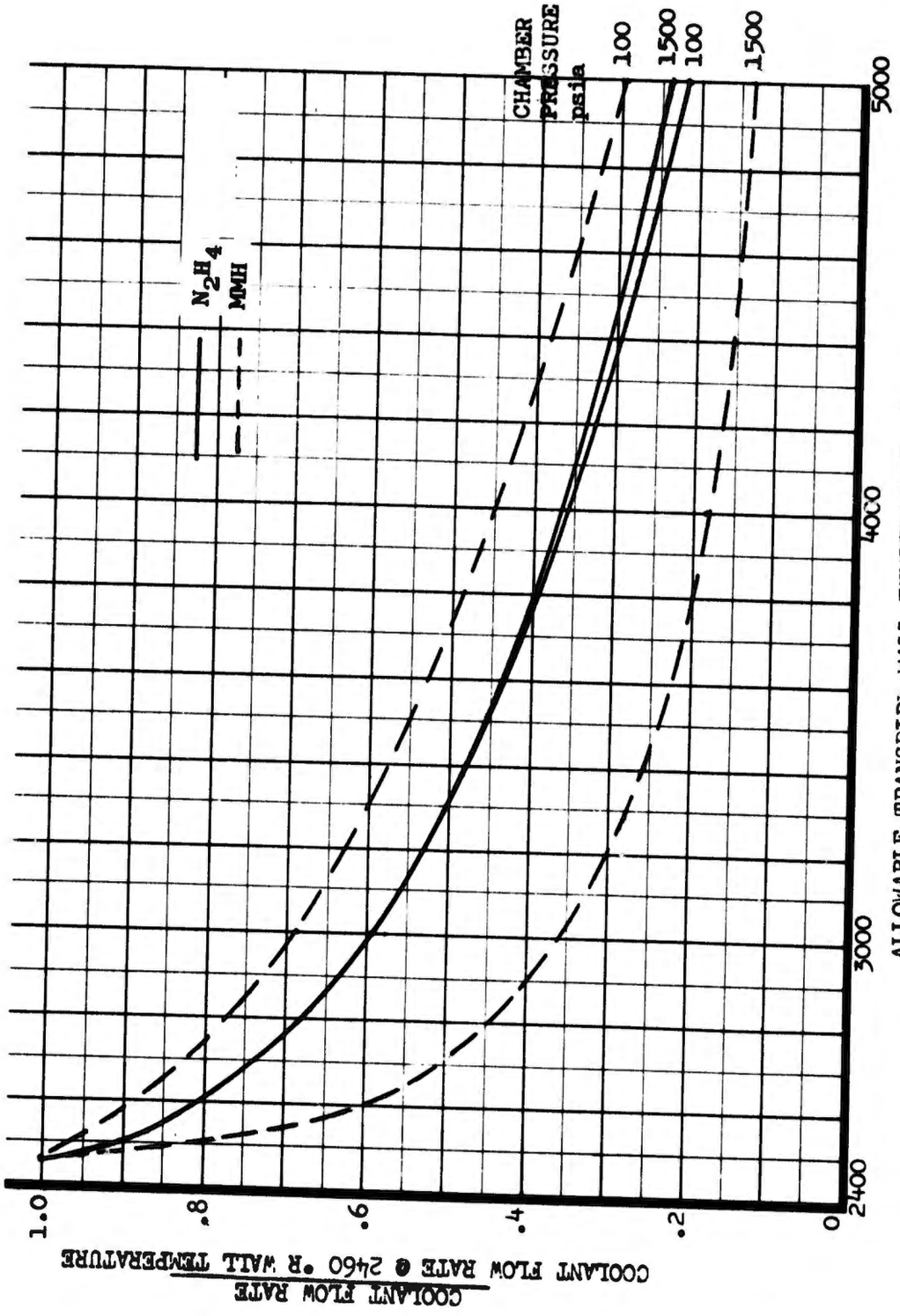

Figure 166. Coolant Flow Rate Reduction with Transpire Material Capability

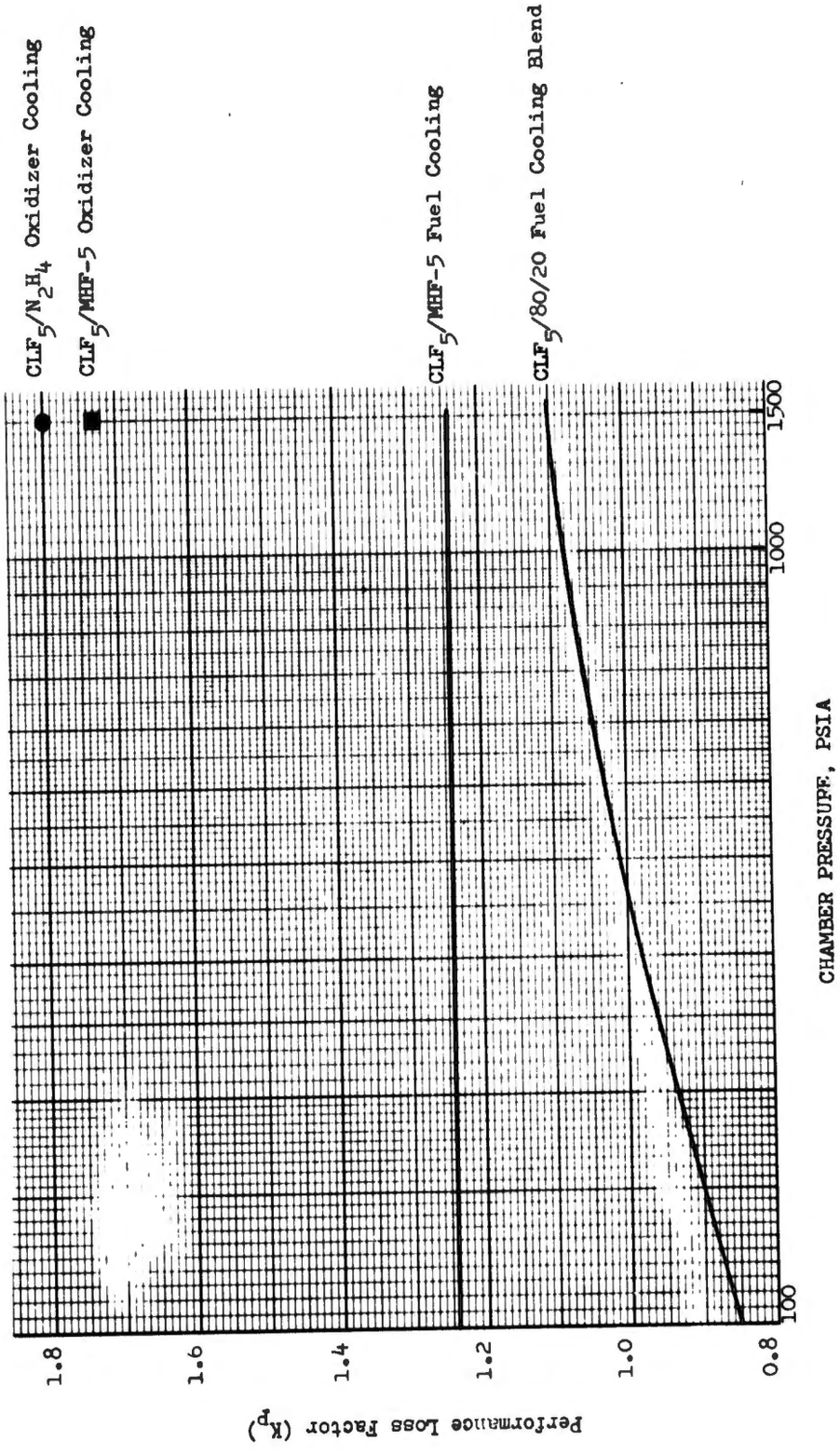

Figure 167. Performance-Coolant Flow Trade-Off Coefficients, $\mathcal{E} = 150$

STEP 1: Obtain delivered specific impulse (I_{sp}) for the selected engine, which was determined in the performance calculation procedure.

STEP 2: Determine specific impulse degradation ($\eta I_{sp_{TH}}$) with throttling for the selected engine from the applicable figures listed below:

Engine Type	Figure No.
a. Liquid/Liquid Platelet or Momentum Exchange	168
b. Gas/Liquid, Liquid/Gas, and Gas/Gas Platelet	169

STEP 3: Calculate specific impulse at the selected throttling level as follows:

$$I_{sp_{throttled}} = I_{sp} (1-\eta I_{sp_{TH}})$$

where

I_{sp} is obtained from Step 30 of the Performance Calculation Procedure

$\eta I_{sp_{TH}}$ is obtained from Step 2

4. Engine Mixture Ratio

A calculation procedure is provided to establish the engine mixture ratio consistent with the delivered specific impulse. Off-design mixture ratio operation and its associated influence upon engine specific impulse is discussed under Design Criteria Modifications.

STEP 1: Obtain the cooling flow rate ratio (W_c/W_t) value for the selected engine as determined from Steps 25 or 28 of the Performance Calculation Procedure.

STEP 2: Determine the optimum mixture ratio (MR_{opt}) for zero cooling flow for the selected engine propellant from Figure No. 170.

STEP 3: Calculate actual mixture ratio (MR) for the selected engine as follows:

a. Fuel Cooling

$$MR = \frac{MR_{opt} (1 - W_c/W_t)}{1 + MR_{opt} W_c/W_t}$$

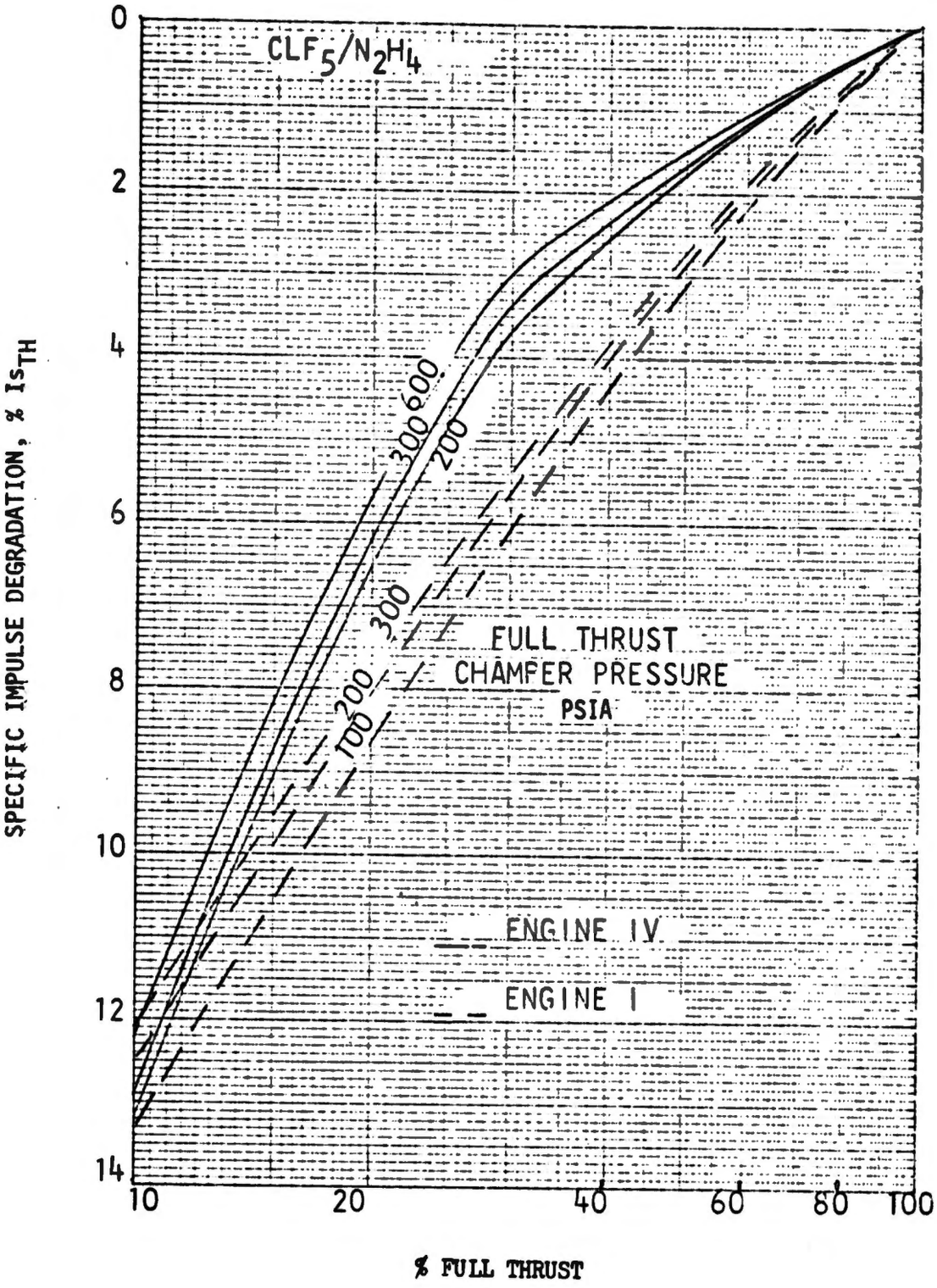

Figure 168. Specific Impulse Degradation with Throttling, Engines No. I and No. IV

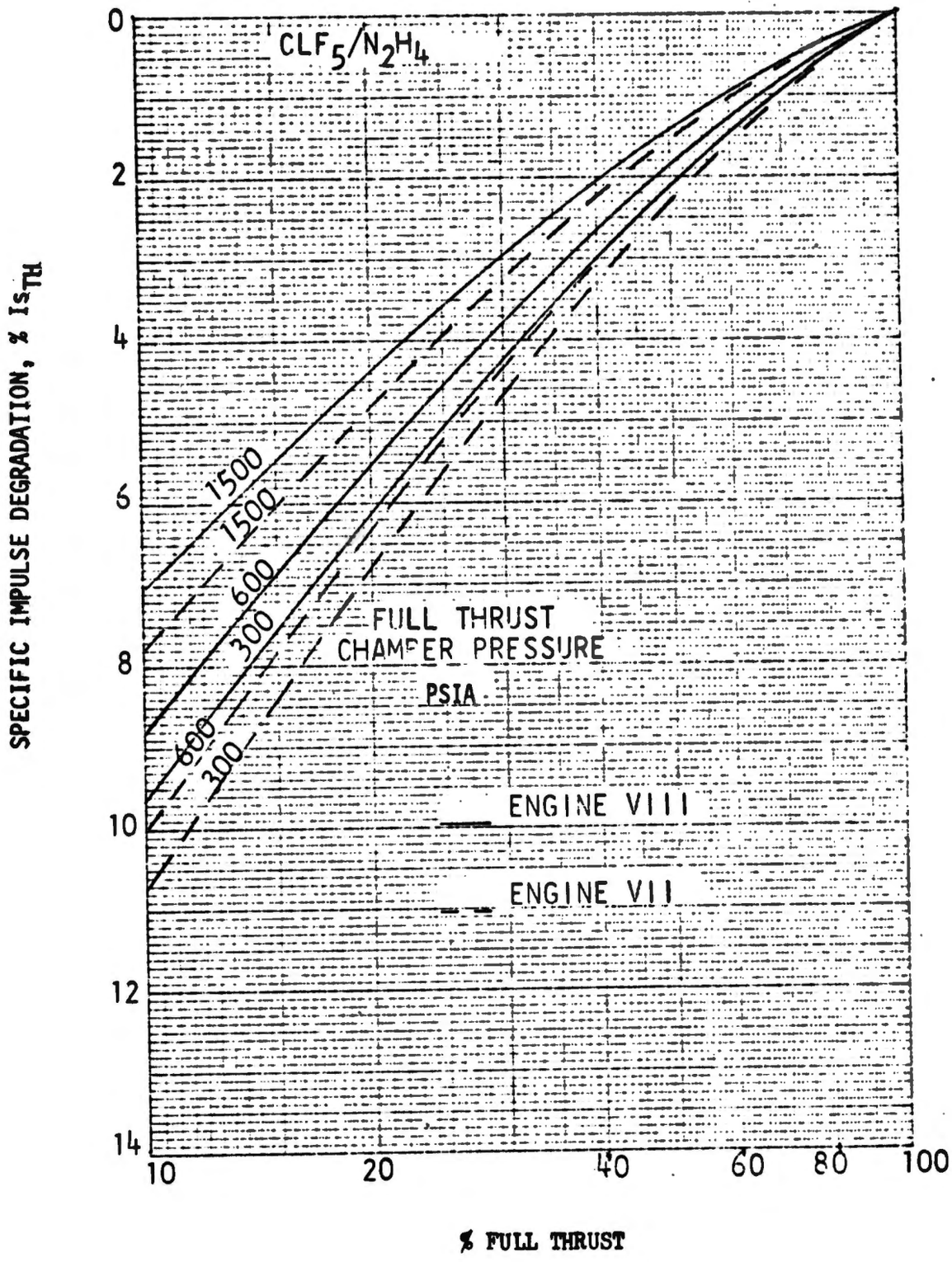

Figure 169. Specific Impulse Degradation with Throttling, Engines No. VII and No. VIII

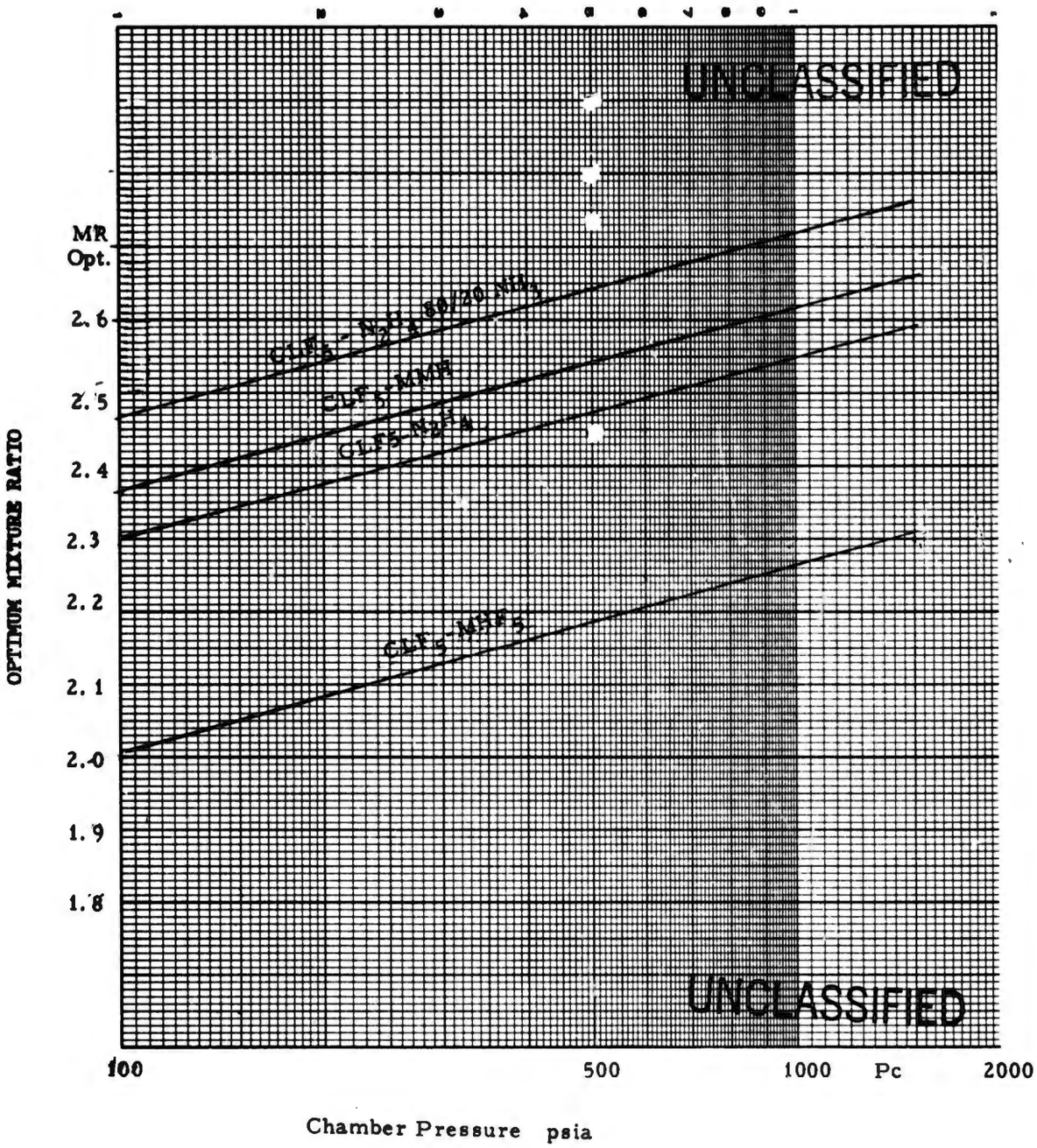

Figure 170. Optimum Mixture Ratio for Zero Coolant Flow vs Chamber Pressure

b. Oxidizer Cooling

$$MR = \frac{MR_{opt} + W_c/W_t}{1 - W_c/W_t}$$

where

MR_{opt} is obtained from Step 2

W_c/W_t is obtained from Performance Calculation Procedure (Steps 25 or 28)

5. Engine Diameter

The engine diameter provided by this calculation procedure is the maximum engine diameter for all area ratios between 40:1 and 150:1.

STEP 1: Obtain the diameter function ($D_E/\sqrt{\epsilon_A}$) from the applicable figures listed below.

Engine Type	Figure No.
a. Pressure-Fed	171
b. Pump-Fed (Bleed Cycle)	172
c. Pump-Fed (Staged-Combustion Cycle)	173

STEP 2: Calculate engine diameter (D_e) for the selected engine as follows:

$$D_E = \frac{D_e}{\sqrt{\epsilon_A}} \sqrt{\epsilon_A}$$

where

$\frac{D_E}{\sqrt{\epsilon_A}}$ is obtained from Step 1

ϵ_A is a selected engine parameter (total area ratio).

6. Engine Length

The engine length provided by this calculation procedure includes the distance from the nozzle exit to the gimbal plate and is the maximum length for the engine.

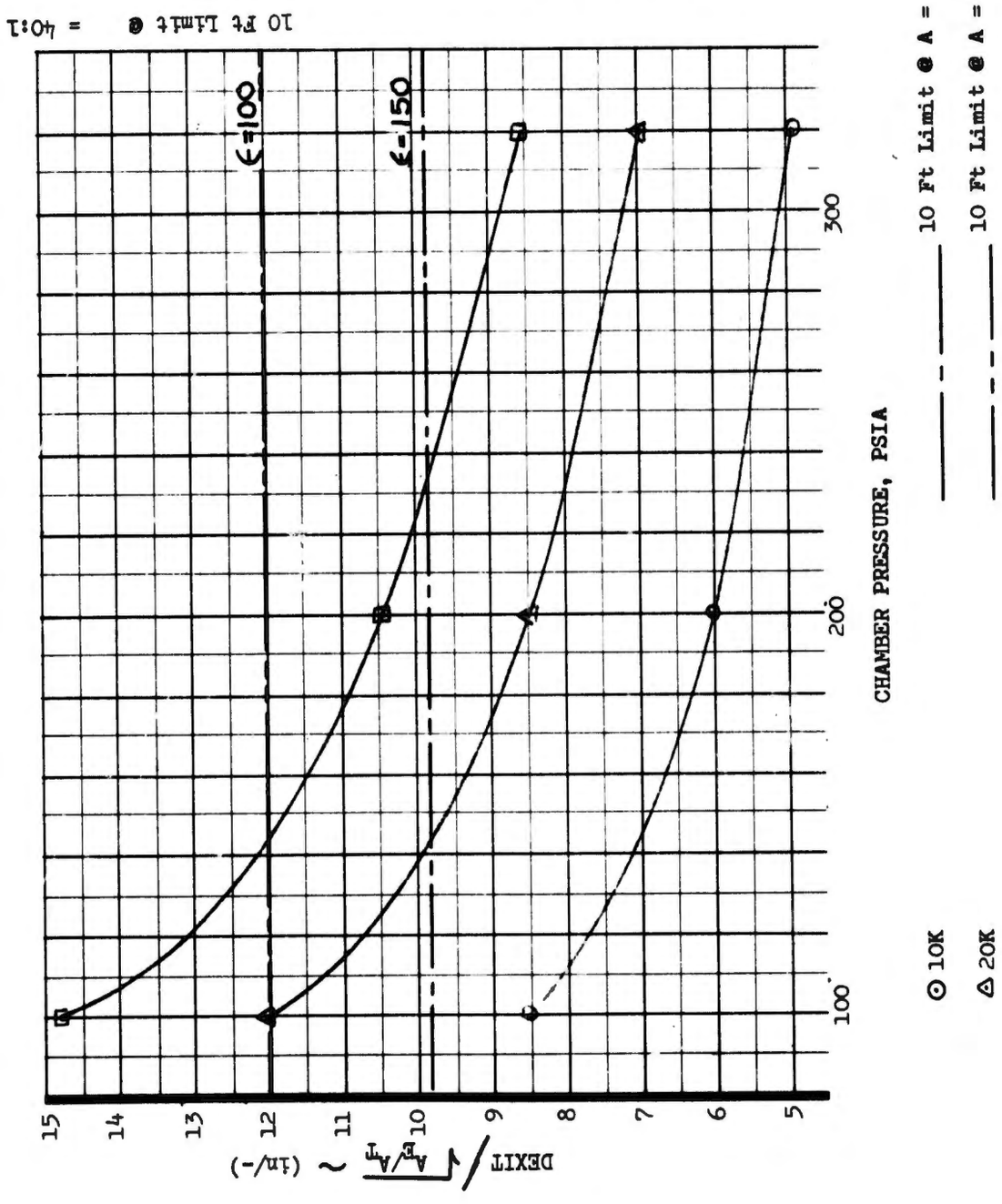

Figure 171. Diameter Function, Engine No. I

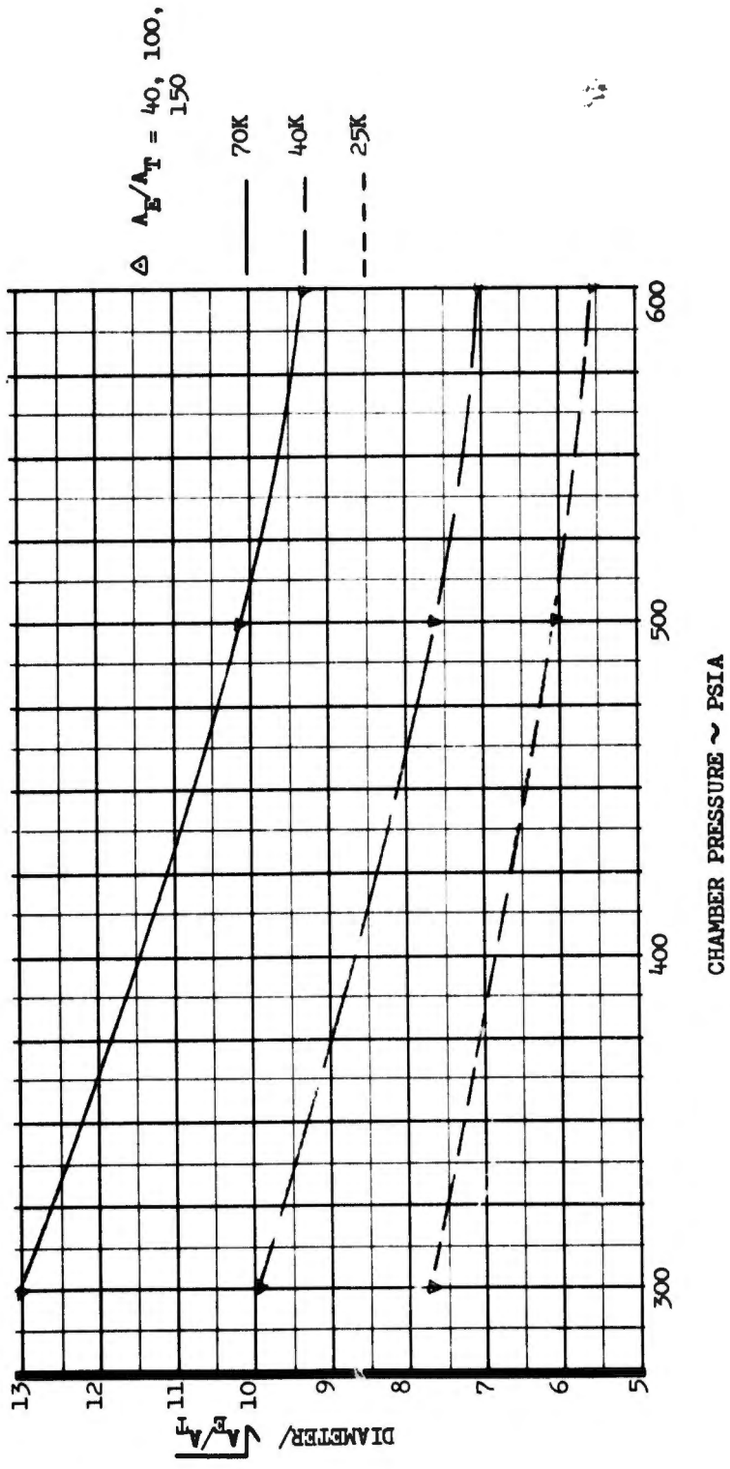

Figure 172. Diameter Function, Engine No. IV

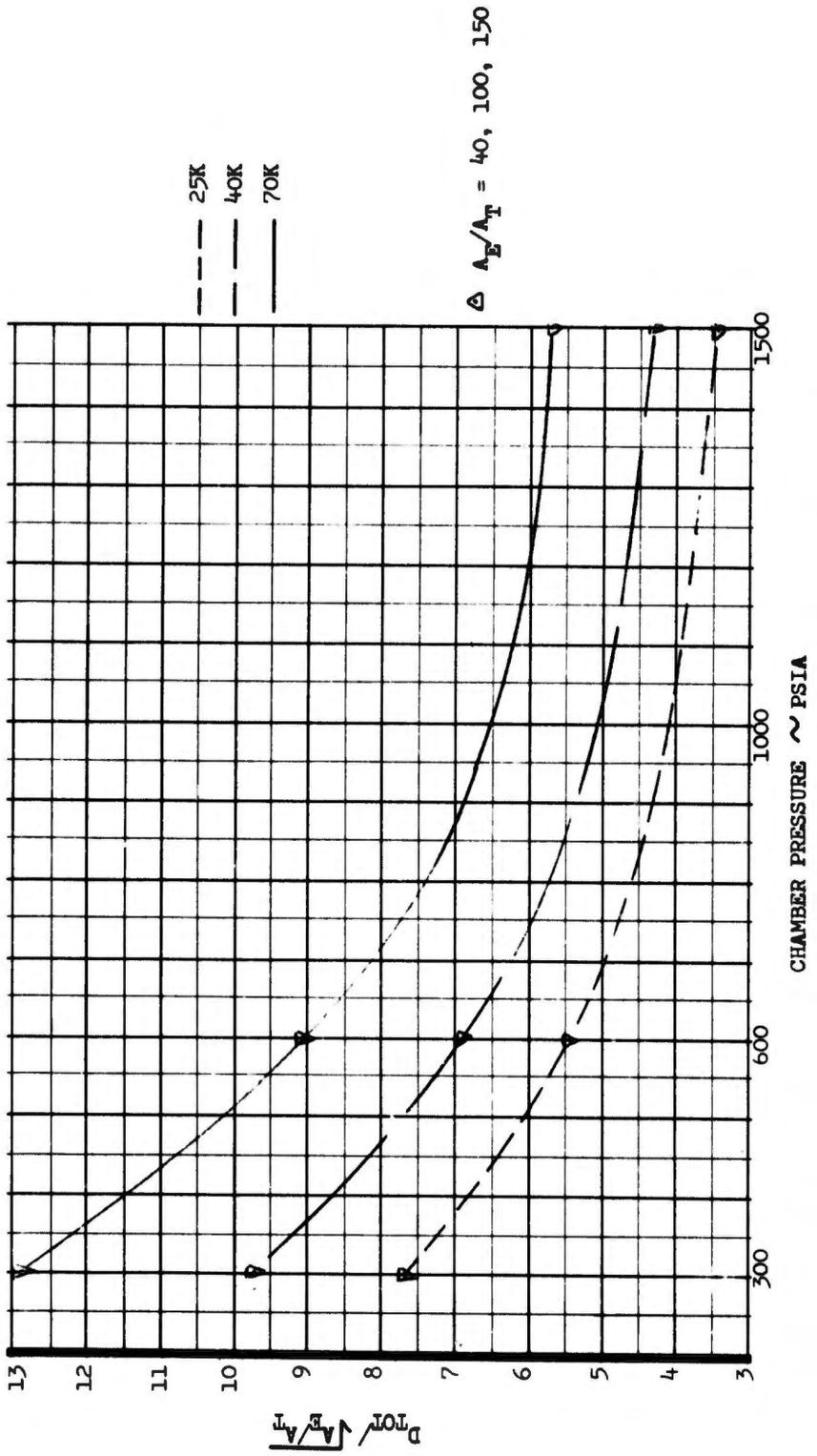

Figure 173. Diameter Function, Engine No. VIII

STEP 1: Determine the baseline engine length (L_{base}) from the applicable figures listed below:

Engine Type	Figure No.
a. Pressure-Fed	174
b. Pump-Fed (Bleed Cycle)	175
c. Pump-Fed (Gas/Liquid or Liquid/Gas Staged-Combustion)	176
d. Pump-Fed (Gas/Gas Staged-Combustion)	177, 178

STEP 2: If the selected injector type is the same as those listed below for the base engines, proceed to Step 6; otherwise, proceed to Step 3.

Base Engine Type	Injector Type
a. Pressure-Fed	Platelet - Liquid/Liquid
b. Pump-Fed (Bleed Cycle)	Momentum Exchange - Liquid/Liquid
c. Pump-Fed (Gas/Liquid or Liquid/Gas Staged-Combustion)	Platelet
d. Pump-Fed (Gas/Gas Staged-Combustion)	Platelet

STEP 3: Calculate the combustion chamber length ($L_{CH_{base}}$) for the baseline engine as follows:

$$L_{CH_{Base}} = \frac{3L^*_{base}}{1 + \varepsilon_{cr_{base}} + \sqrt{\varepsilon_{cr_{base}}}}$$

where values of characteristic length (L^*_{base}) and contraction area ratio ($\varepsilon_{cr_{base}}$) are obtained from the following:

Base Engine Type	L^*, in.$_{base}$	$\varepsilon_{cr_{base}}$
a. Pressure-Fed	15	2.0
b. Pump-Fed (Bleed Cycle)	25	2.0
c. Pump-Fed (Gas/Liquid or Liquid/Gas Staged-Combustion)	10	2.0
d. Pump-Fed (Gas/Gas Staged-Combustion)	5	2.8

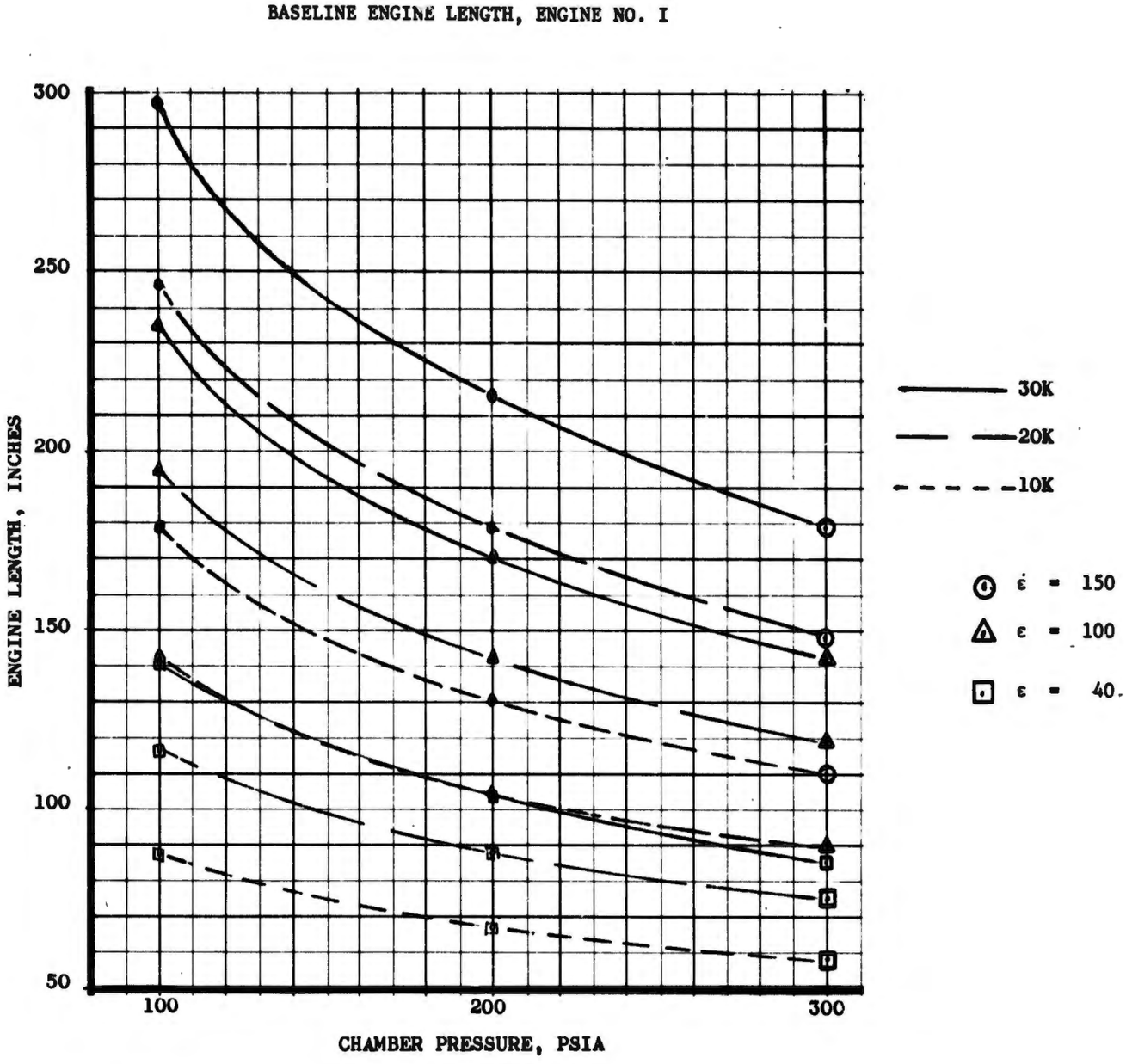

Figure 174. Baseline Engine Length, Engine No. I

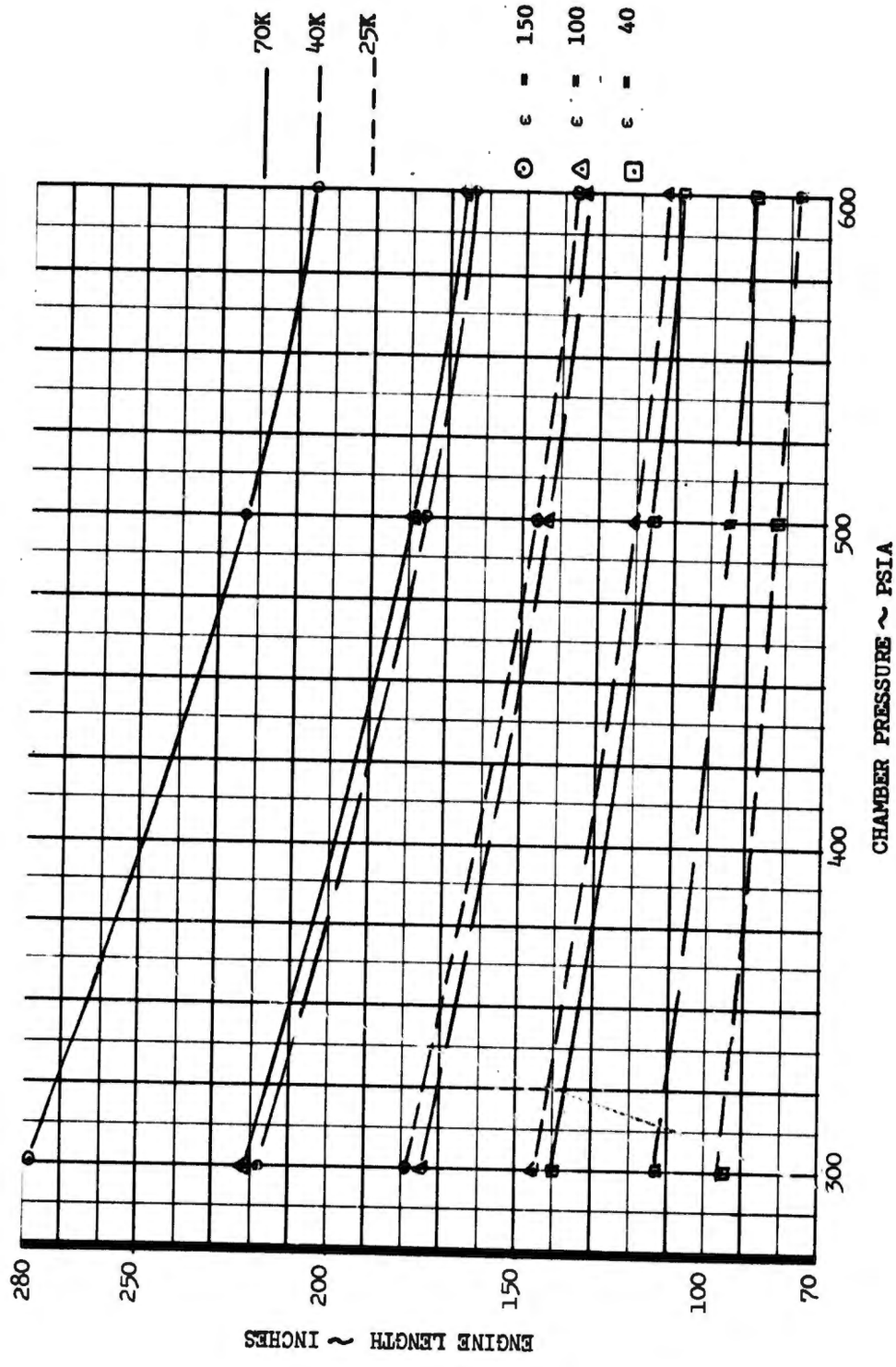

Figure 175. Baseline Engine Length, Engine No. IV

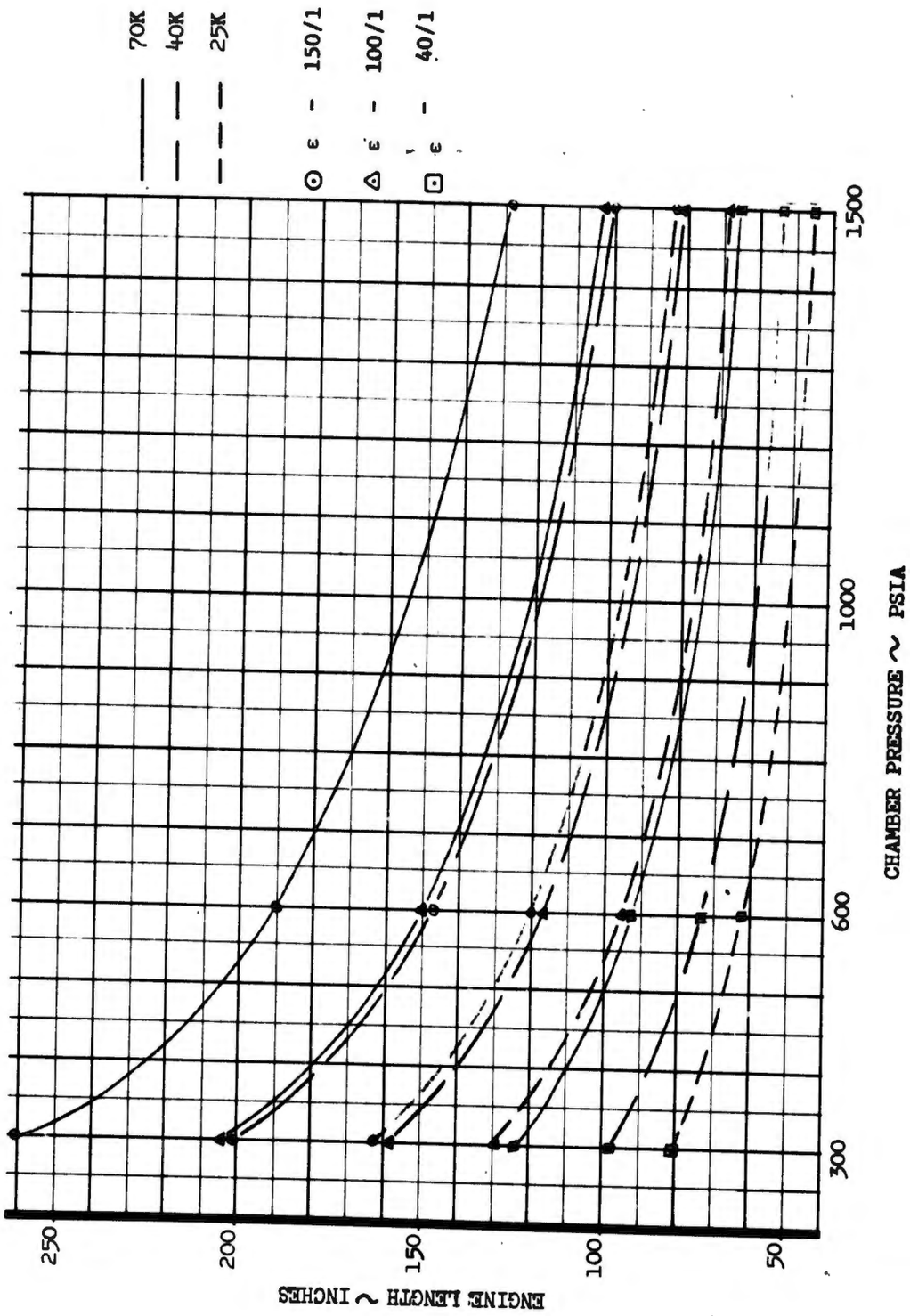

Figure 176. Baseline Engine Length, Engine No. VII

BASELINE ENGINE LENGTH, ENGINE NO. VIII (A_E/A_T = 40 AND A_E/A_T = 100)

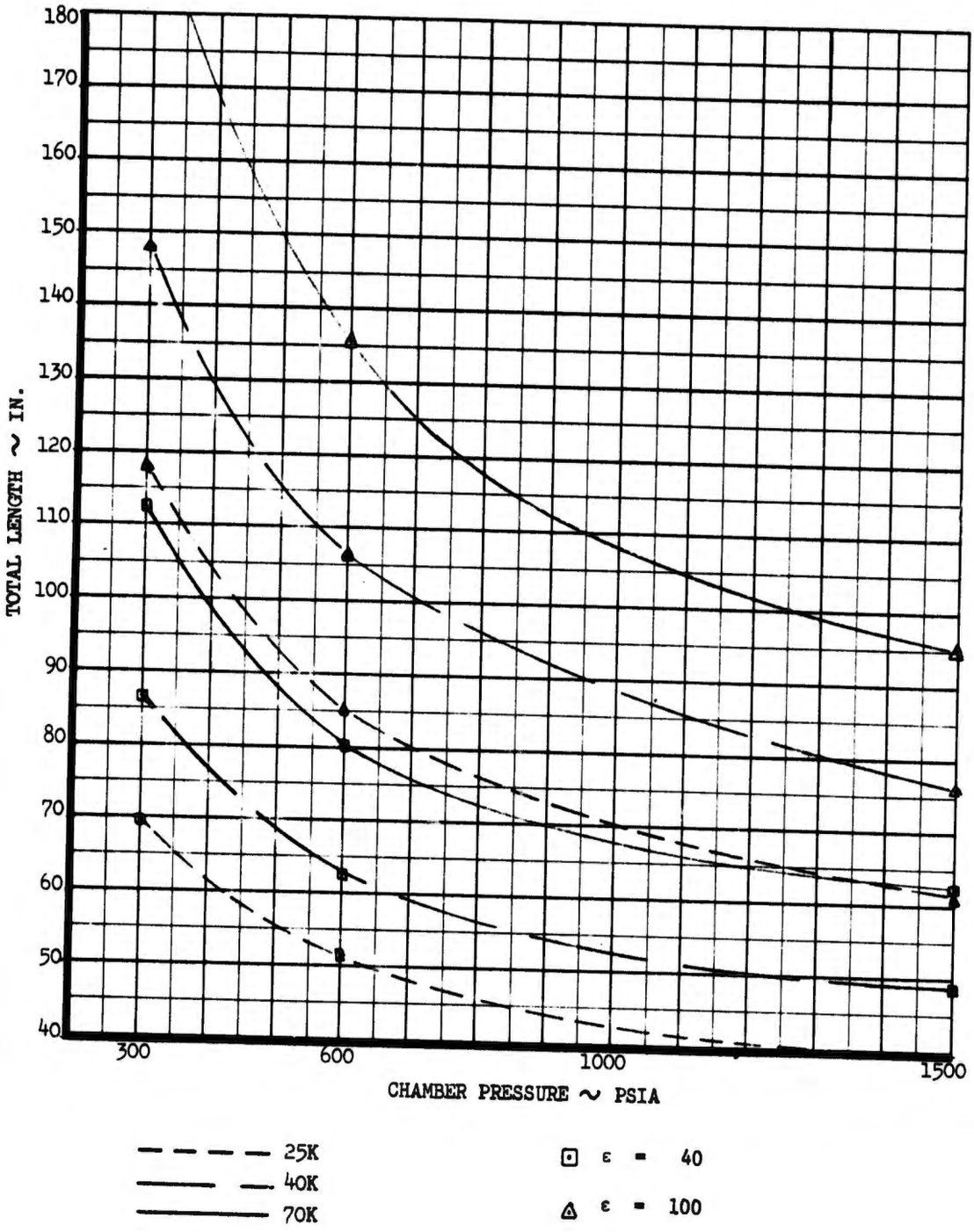

Figure 177. Baseline Engine Length, Engine No. VIII
(ϵ = 40 and ϵ = 100)

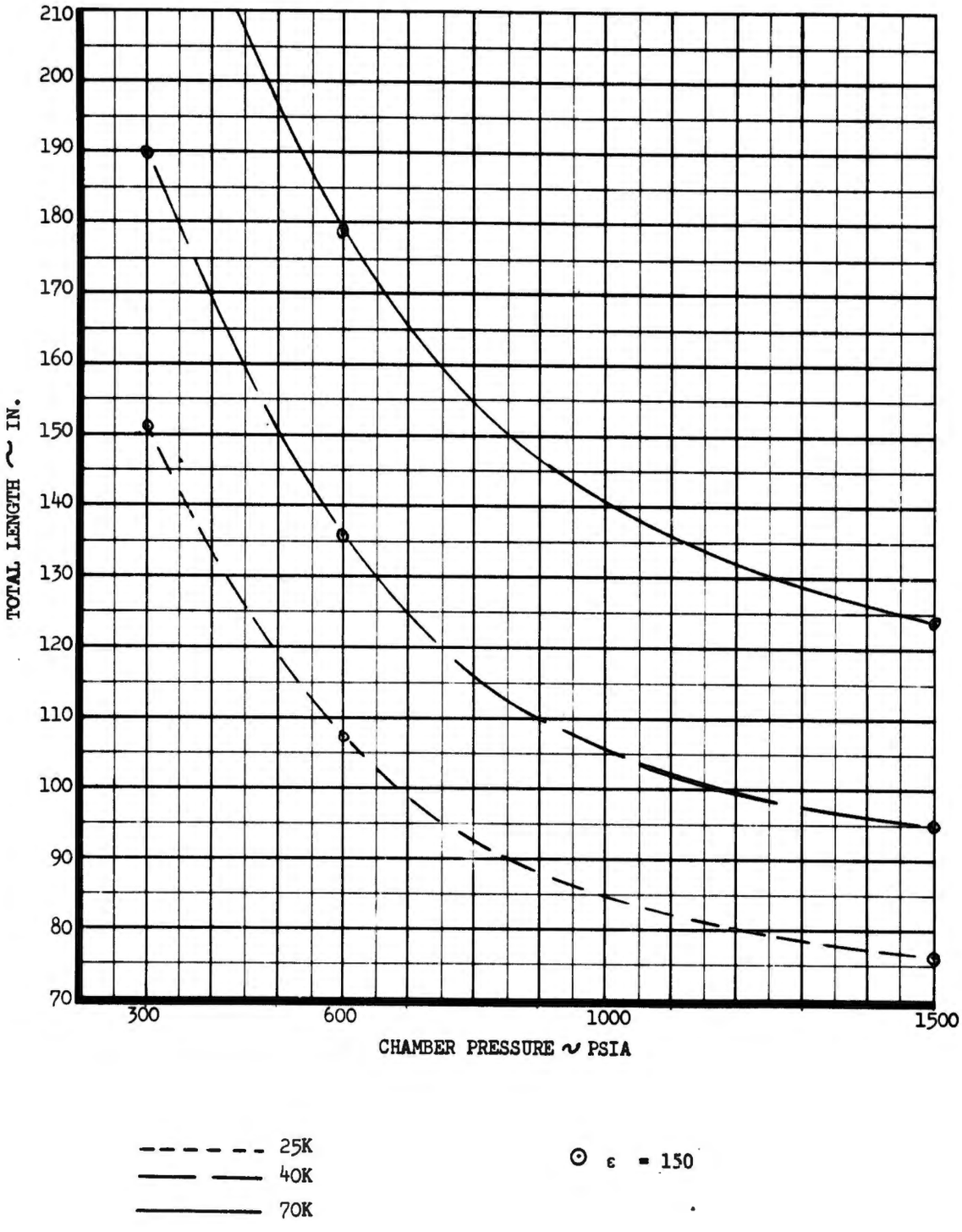

Figure 178. Baseline Engine Length, Engine No. VIII
(ε = 150)

STEP 4: Calculate the combustion chamber length (L_{CH}) for the selected engine as follows:

$$L_{CH} = \frac{3L^*}{1 + \varepsilon_{cr} + \sqrt{\varepsilon_{cr}}}$$

where the values of L^* and ε_{cr} are obtained from the following:

Injector Type	L^*, in.	ε_{cr}
Conventional - Liquid/Liquid	30	2.0
Momentum Exchange - Liquid/Liquid	25	2.0
Platelet - Liquid/Liquid	15	2.0
Conventional - Liquid/Gas - Gas/Liquid	20	2.0
Platelet - Liquid/Gas - Gas/Liquid	10	2.0
Platelet - Gas/Gas	5	2.8

STEP 5: Calculate the engine length (L_E) for the selected engine as follows:

$$L_E = L_{base} - L_{CH_{base}} + L_{CH}$$

where

L_{base} is obtained from Step 1

$L_{CH_{base}}$ is obtained from Step 3

L_{CH} is obtained from Step 4

VIII. DESIGN CRITERIA MODIFICATIONS

The parametric data generated for the point design engines (Section VI of this report) and the calculation procedures (Section VII) used to modify the point design engines provide engine data (i.e., weight and specific impulse) which are consistent with the design assumptions selected at the initiation of this study. Therefore, if new information becomes available which would justify changing one or more of the initial assumptions, the data provided by this study would become outdated. To minimize this possibility, a capability or consideration for adjusting the engine data is provided in the following areas:

- Combustion Chamber Characteristic Length (L*)
- Performance Loss
- Coolant Reaction
- Engine Mixture Ratio
- Combustion Chamber and Nozzle Wall Temperature
- Turbine Exhaust Cooling
- Stiffness Factor
- Turbopump Shaft Speed
- Pump Suction Pressure

A. COMBUSTION CHAMBER CHARACTERISTIC LENGTH

The selection of the combustion chamber characteristic length (L*) associated with each type of injector was based upon experience and engineering judgement as discussed under the Technology Applied (Section III). Modification of the L* values influence engine specific impulse, engine mixture ratio, engine weight, and engine length.

The injector types considered in this study include L* values ranging from 5-in. to 30-in. Therefore, a modification of L* for a particular injector type has the effect of changing the injector type. For instance, the gas/gas platelet injector has a 5-in. L* and modifying this value to 10-in. is tantamount to changing the injector type to a gas/liquid platelet. Therefore, the correct coolant flow rate and specific impulse can be obtained from the performance calculation procedure discussed in Section VII of this report by utilizing the injector type which corresponds to the L* selected. The calculated coolant flow rate in the engine mixture ratio calculation procedure (Section VII) will provide the modified engine mixture ratio which is consistent with the L* selected.

Any variation in L* for a given injector will alter the combustion chamber weight because of the change in chamber length. This weight change can be calculated by utilizing the engine weight calculations described in Section VII. In this procedure, combustion chamber weight is determined by multiplying the chamber surface area by the effective surface density for the selected cooling method. The combustion chamber surface area is a function of the L* selected; therefore, the corrected surface area can be achieved by picking an injector type which also is consistent with the L* selected. Applying this corrected surface area in the calculations procedure results in obtaining the corrected weight.

When a combustion chamber L* is modified, engine length can be determined from the engine length calculation procedure discussed in Section VII by utilizing an injector type which is consistent with the modified L*. Approximate engine length also can be determined from Figure No. 179. As shown, the length consists of two parts; the gimbal-block-to-the-throat and the nozzle-throat-to-the-exit. The gimbal-block-to-the-throat length can be determined from the curve on Figure No. 179 which is correlated to the point design engines. The distance from the nozzle-throat-to-the-exit can be determined by using the following relationship, which is shown on Figure No. 179.

$$L_2 = D_t \quad 1.565 \epsilon_A^{0.637}$$

where D_t = nozzle throat diameter, in.

ϵ_A = nozzle area ratio

The throat diameter can be determined as discussed in the weight calculation procedure of Section VII.

B. PERFORMANCE LOSS

The two types of losses, energy release and kinetic, used in the performance calculations are susceptible to modification as additional experimental data become available.

Energy release losses are a function of combustion chamber characteristic length (L*). Therefore, this loss must be considered in conjunction with any modification of L*. The energy release losses selected for this study as a function of the injector type were shown on Figure No. 5. The performance calculation procedure presented in Section VII uses these energy release losses to adjust for a change in injector type. However, this process can also be utilized to accommodate a modification in the energy release loss. For instance, at a chamber pressure of 100 psia, the energy release loss for a gas/gas injector is 0.9% and instead of using this value, a modified energy release loss can be substituted.

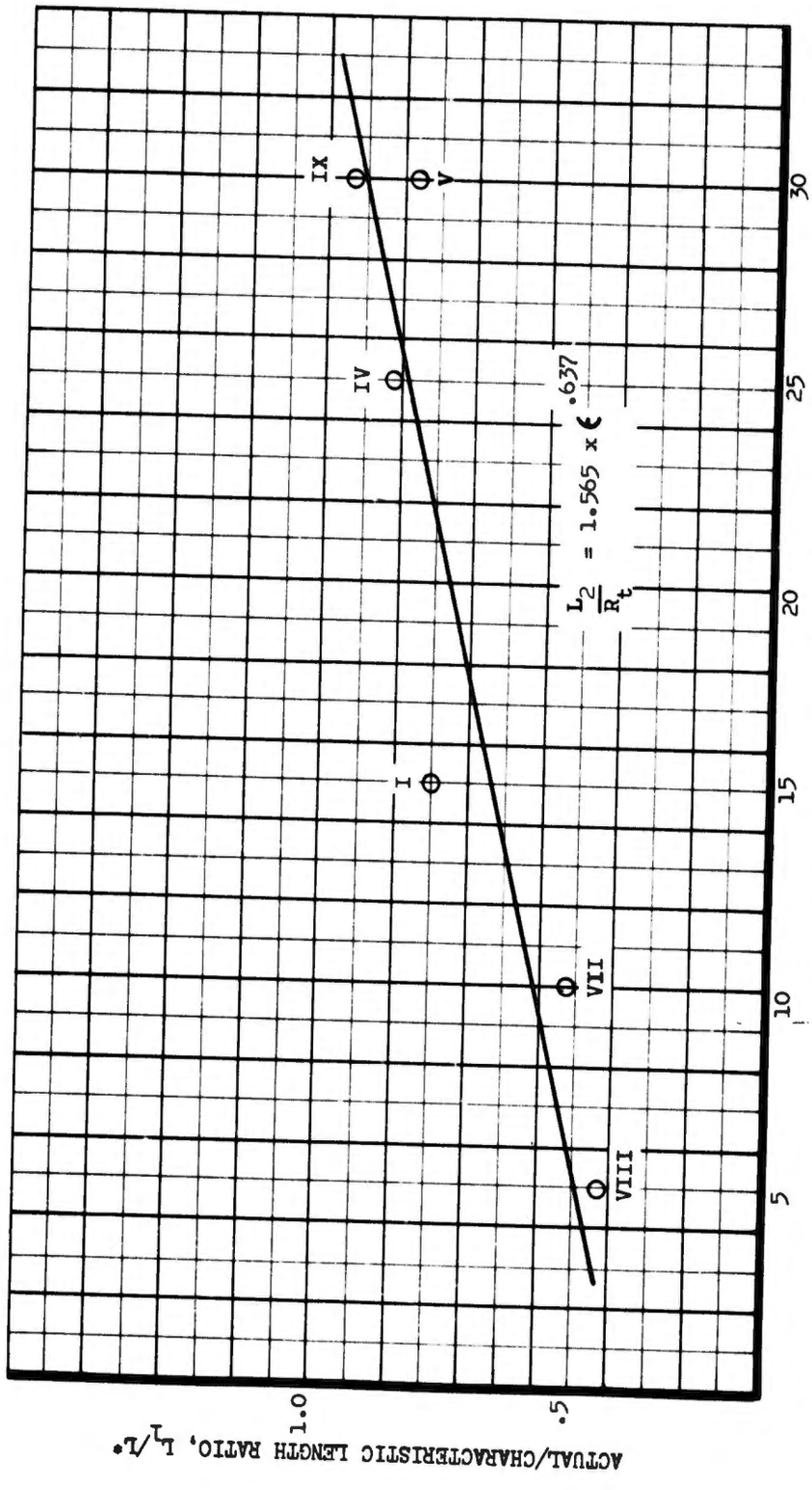

L_1 = Length from Gimbal Block to Throat
L_2 = Length from Throat to Exit

Figure 179. Actual Chamber Length Correlation vs L*, Gimbal-Block-to-Throat

Performance corrections for modifications in kinetic losses can be accomplished as follows:

$$\frac{\Delta I_{sp}}{I_{sp}} (100) = \eta_{kin} - \eta_{kin\ base}$$

where $\frac{\Delta I_{sp}}{I_{sp}} (100)$ = degradation in specific impulse, %

η_{kin} = kinetic performance loss for modified case, %

$\eta_{kin\ base}$ = kinetic performance loss for original case, %

The kinetic performance loss (η/kin base) for the base engine case can be determined from information provided in Appendix II (Part II of this report).

C. COOLANT REACTION

Some of the engine types utilize liquid oxidizer transpiration cooling in the main combustion chamber. However, the core flow of the engine is fuel-rich; therefore, some of the oxidizer mixes and burns with the core before exiting from the combustion chamber. This process increases the the engine performance as opposed to any instance where no reaction occurs. The performance values generated for this study assumed that 50% of the coolant flow rate will mix and burn with the main core.

Modification of the amount which reacts will result in a change of engine specific impulse. The change in specific impulse with the amount of reaction is shown on Figure No. 180. As shown, the loss in performance for each percentage of coolant flow rates is 1.8 sec for a 50% reaction. The performance correction can be accomplished as follows:

$$\Delta I_{sp} = \left(1.8 - \frac{\Delta I_{sp}}{\dot{W}_c/\dot{W}_t}\right) \left(\dot{W}_c/\dot{W}_T\right)$$

where $\frac{\Delta I_{sp}}{W_c/Wt}$ is obtained from Figure No. 180

$\dot{W}_c/\dot{W}_T$ is obtained from performance calculation procedure (Section VII)

D. ENGINE MIXTURE RATIO

The engine mixture ratios shown in previous discussions were consistent with the maximum delivered specific impulse. However, the influence of mixture ratio upon the vehicle tankage will result in a mixture ratio shift for maximum vehicle performance. Any change in engine mixture ratio will result in a degradation of delivered specific impulse. Figure No. 181 shows this specific impulse sensitivity as a function of the mixture ratio shift. Although this curve was generated for N_2H_4 at a 150:1 area ratio, the sensitivity is approximately the same for other area ratios and propellants. The specific impulse degradation can calculated as follows:

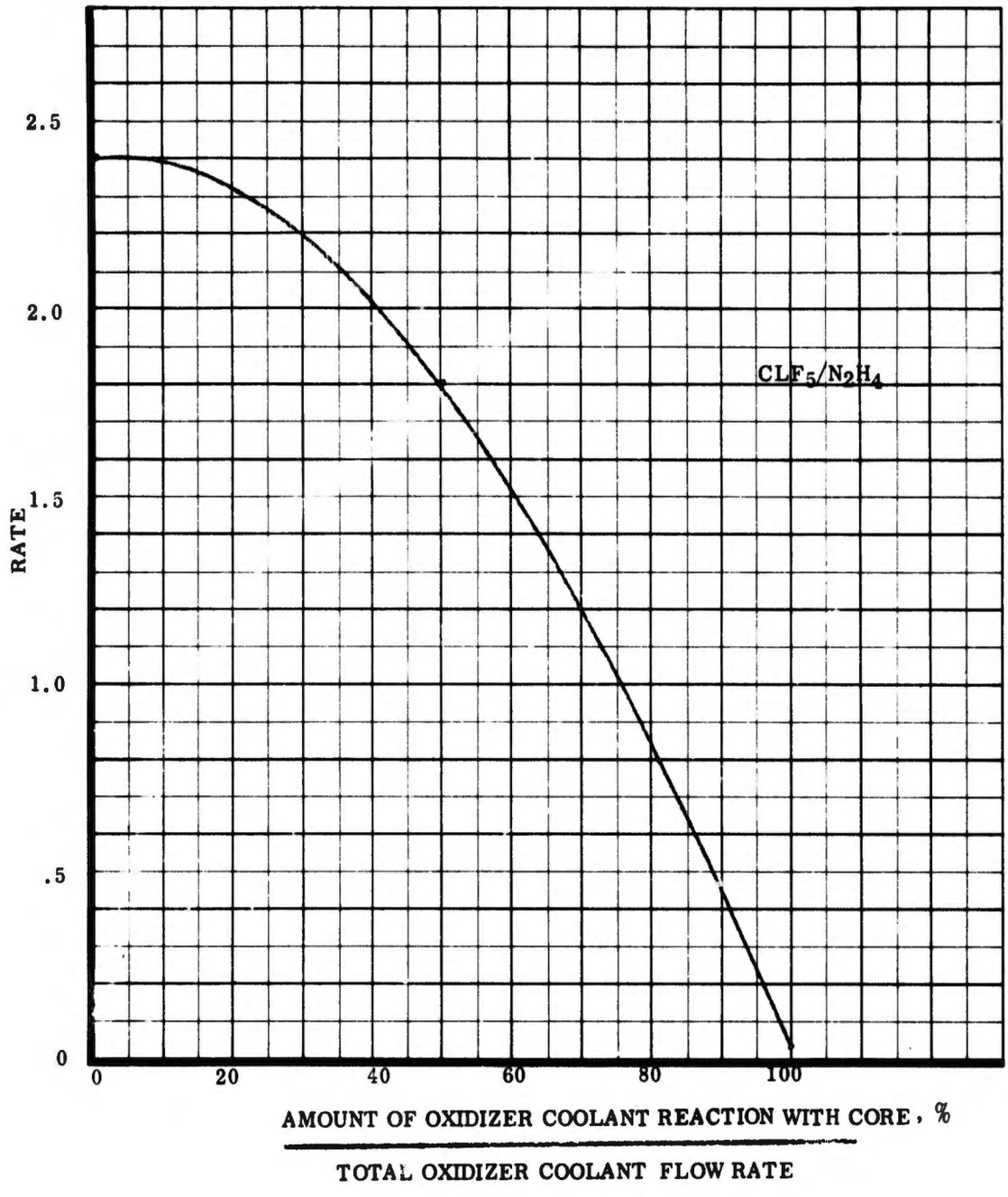

Figure 180. Performance Degradation with the Amount of Oxidizer Coolant Reaction with the Main Core

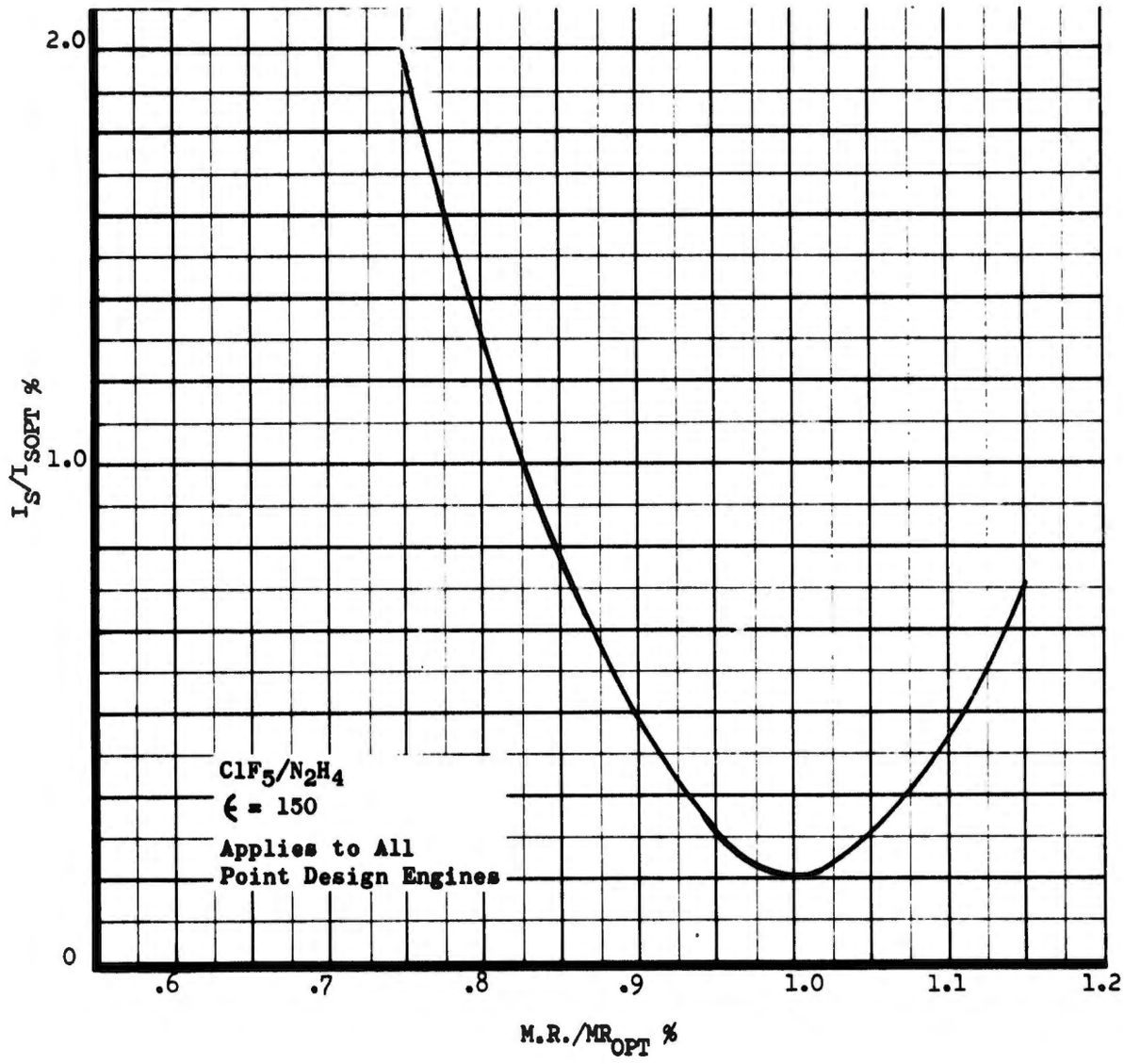

Figure 181. Specific Impulse Sensitivity to Mixture Ratio Shift (Zero Coolant Flow)

$$\Delta I_{sp} = I_{s\ opt} \left(1 - \frac{I_s}{I_{s\ opt}}\right)$$

= degradation in specific impulse, sec

Where $I_{s\ opt}$ = specific impulse consistent with zero coolant flow rate (obtained from performance calculation procedure of Section VII)

$\frac{I_s}{I_{s\ opt}}$ = specific impulse sensitivity (obtained from Figure No. 181 for a selected value of MR/MR opt)

MR = selected mixture ratio based upon vehicle considerations, etc.

MR opt = mixture ratio consistent with maximum specific impulse (obtained from the engine mixture ratio calculation procedure of Section VII)

E. COMBUSTION CHAMBER AND NOZZLE WALL TEMPERATURE

The selection of a permissible wall termperature has a strong influence upon the amount of film or transpiration cooling needed to maintain the structural integrity of the combustion chamber and nozzle walls. Cooling losses represent one of the major performance losses for the engine; therefore, the wall temperature selection is an important parameter and the wall temperature selected for this study may require changing as a result of subsequent research. Therefore, the cooling flow rates may require revision for these new engine conditions.

The performance calculation procedure presented in Section VII provides the capability for changing the transpire platelet material from nickel to graphite which is the equivalent of increasing the allowable wall temperature to 3500°F (selected value for graphite). The coolant flow rate correction factor was obtained from either Figure No. 165 or No. 166 depending upon the propellant type for a 3500°F wall temperature. However, this correction factor is presented as a function of allowable wall temperature. Therefore, instead of using the wall temperature selected in this study, the coolant flow corrective factor can be determined for a new permissible wall temperature. Utilizing this value in the performance calculation procedure will result in the corrected specific impulse and optimum engine mixture ratio.

Engine weight is also influenced by the permissible temperature selected for the material because this temperature is used in determining transition area ratios between cooling types (i.e., transpiration to radiation).

The transition area ratio is used in the weight calculation procedure (Section VII) to establish the surface areas associated with cooling of the throat and nozzle extension. This area ratio was established for the

baseline engines by utilizing Figure No.182 while the transition area ratio for a graphite nozzle extension (4500°F allowable wall temperature) was determined from Figure No. 183. Transition area ratios for a permissible wall temperature of 2500°F is shown on Figure No. 184.

A cross-plot of Figures No. 182, No. 183, and No. 184 will permit the transition area ratio to be established for any permissible wall temperature. This transition area ratio can then be used in the weight calculation procedures to provide the corrected weight.

F. TURBINE EXHAUST COOLING

In all of the pump-fed bleed cycle engines, the turbine exhaust is introduced in the nozzle downstream of the throat and acts as a film coolant before exiting from the nozzle. Heat transfer studies (see Appendix IV) indicated that the transition area ratio from throat cooling to nozzle extension cooling could be reduced because of the turbine exhaust cooling. This area ratio varied only slightly at various thrust levels and chamber pressures; therefore, a fixed value was selected (transition area ratio of 5.0). If the transition area ratio is changed, engine weight is significantly affected because the coolant flow rate required downstream of the throat is very small when compared with the coolant flow used in the main combustion chamber. The change in engine weight resulting from a change in the transition point associated with turbine exhaust cooling can be obtained by using the corrected transition area ratio in the engine weight calculation procedure of Section VII.

G. STIFFNESS FACTOR

The stiffness factor was discussed previously. It was used to ensure that the pressure schedule for the engine was consistent with low-frequency stability criteria. The value utilized for the stiffness factor has a direct effect upon the required pump discharge pressure and consequently, upon engine weight. For bleed cycle engines, the pump discharge pressure can be determined from the following relationship:

$$P_D = P_c \, SF$$

where P_c = combustion chamber pressure, psia

SF = stiffness factor.

Determining the pump discharge pressure for the staged-combustion engines is not as simple because the turbine pressure drop is in series with the pressure drop from pump discharge to chamber plenum. Therefore, a power balance of the system is necessary before the pump discharge pressure relationship with the stiffness criteria can be established. This capability was outside the scope of this study and is not available.

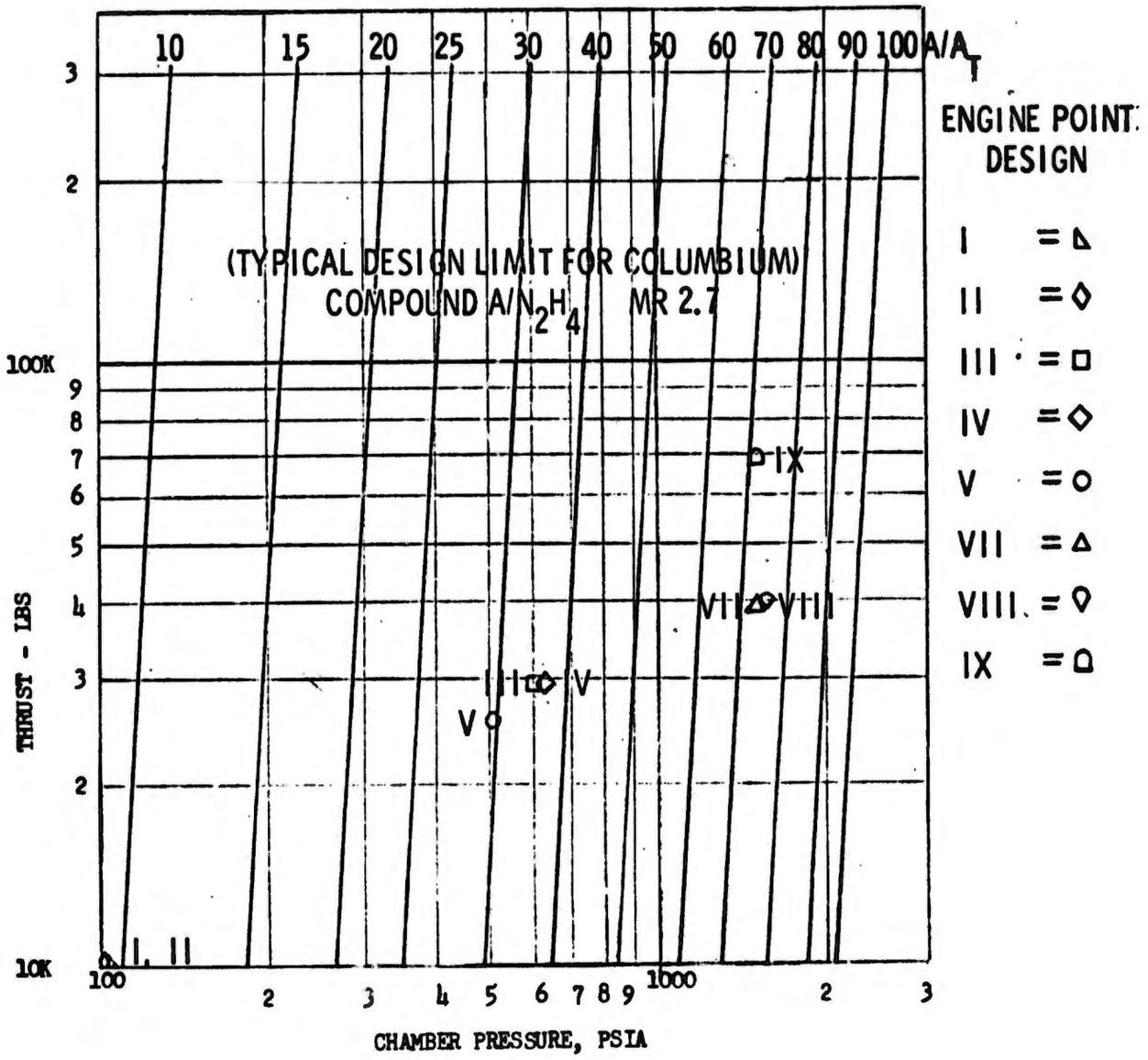

Figure 182. Attachment Point for Radiation-Cooled Nozzle Extension, T_w = 2200°F

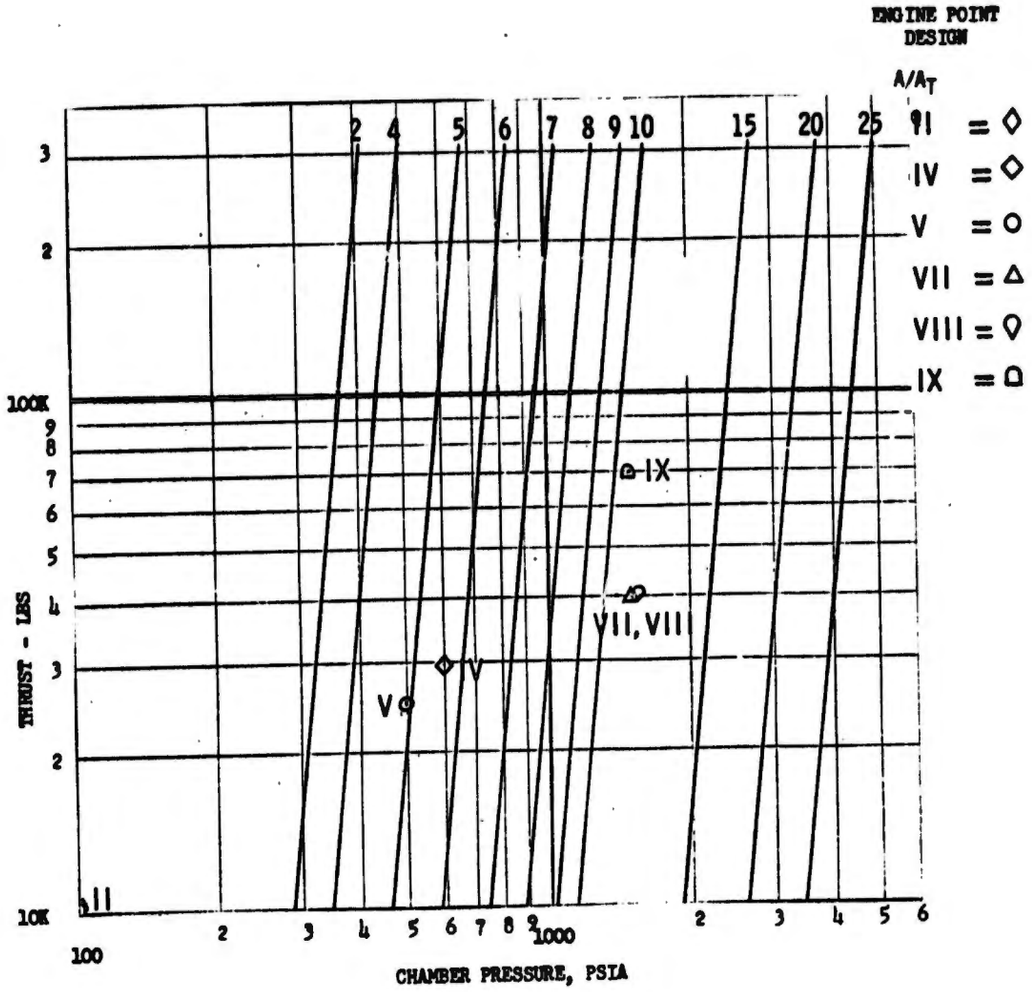

Figure 183. Attachment Point for 0.25-in. AGC Radiation Skirt, T_{WG} = 4500°F

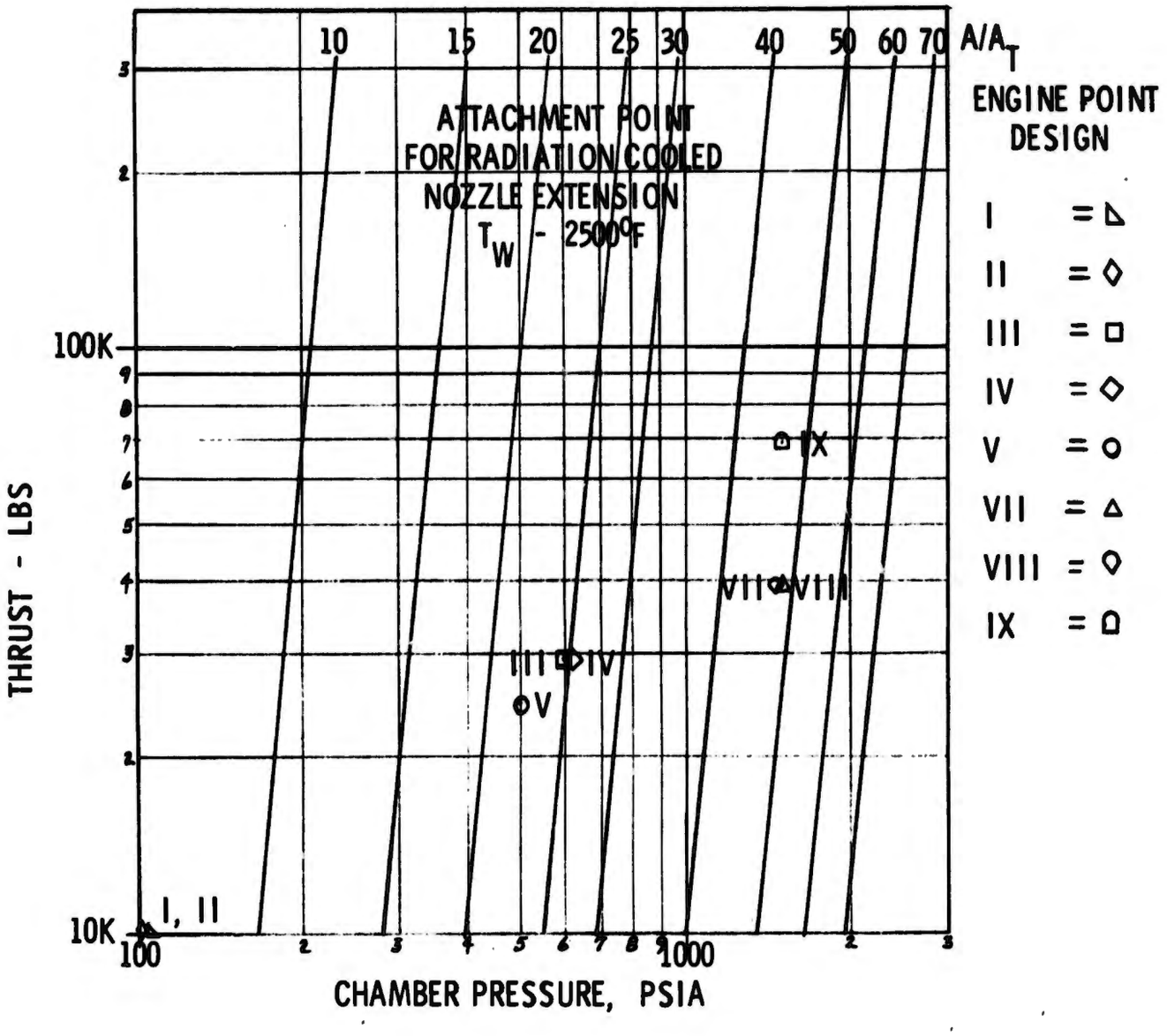

Figure 184. Attachment Point for Radiation-Cooled Nozzle Extension
T_W = 2500°F

The turbopump weight as a function of pump discharge pressure and oxidizer pump flow rate for bleed cycle engines is shown on Figure No. 185. The oxidizer flow rate can be determined from

$$\dot{W}_{ox} = \frac{MR_E}{1 + MR_E} \quad \frac{F}{I_{sp}}$$

where MR_E = engine mixture ratio

F = selected thrust level, lb

I_{sp} = delivered specific impulse, sec

The following procedure is to be used for correcting the engine weight as a result of a change in the stiffness factor:

Step 1: Calculate the base engine pump discharge pressure as discussed above for a stiffness factor of 1.35 for liquid/liquid system and 1.1 for gas/liquid, liquid/gas, or gas/gas system

Step 2: Calculate base engine oxidizer flow rate as discussed above.

Step 3: Determine the base turbopump weight ($W_{TPA_{base}}$) from Figure No. 185.

Step 4: Calculate the engine pump discharge pressure for the selected stiffness factor.

Step 5: Determine the turbopump weight (W_{TPA}) consistent with the selected stiffness factor from Figure No. 185. The oxidizer flow rate remains the same as that used for the base point.

Step 6: Calculate the engine weight corrected for the stiffness factor as follows:

$$W_{eng} = W_{eng_{base}} - W_{TPA_{base}} + W_{TPA}$$

where $W_{eng_{base}}$ = base engine weight obtained from the weight calculation procedure discussed in Section VII.

H. TURBOPUMP SHAFT SPEED

Turbopump speed is inversely proportional to the diameter; therefore, turbopump weight reduces as the speed is increased. The design parameters (i.e., specific speed, induced stress, and turbine pressure ratio) that were utilized in the study to determine turbopump speed are discussed in Appendix VI. The speed selection criteria are based upon technology status (i.e., bearing on limts) and component design criteria (i.e., propellant cooled bearings); therefore, the parameters currently limiting turbopump speed may change which would result in a turbopump weight change. As a result,

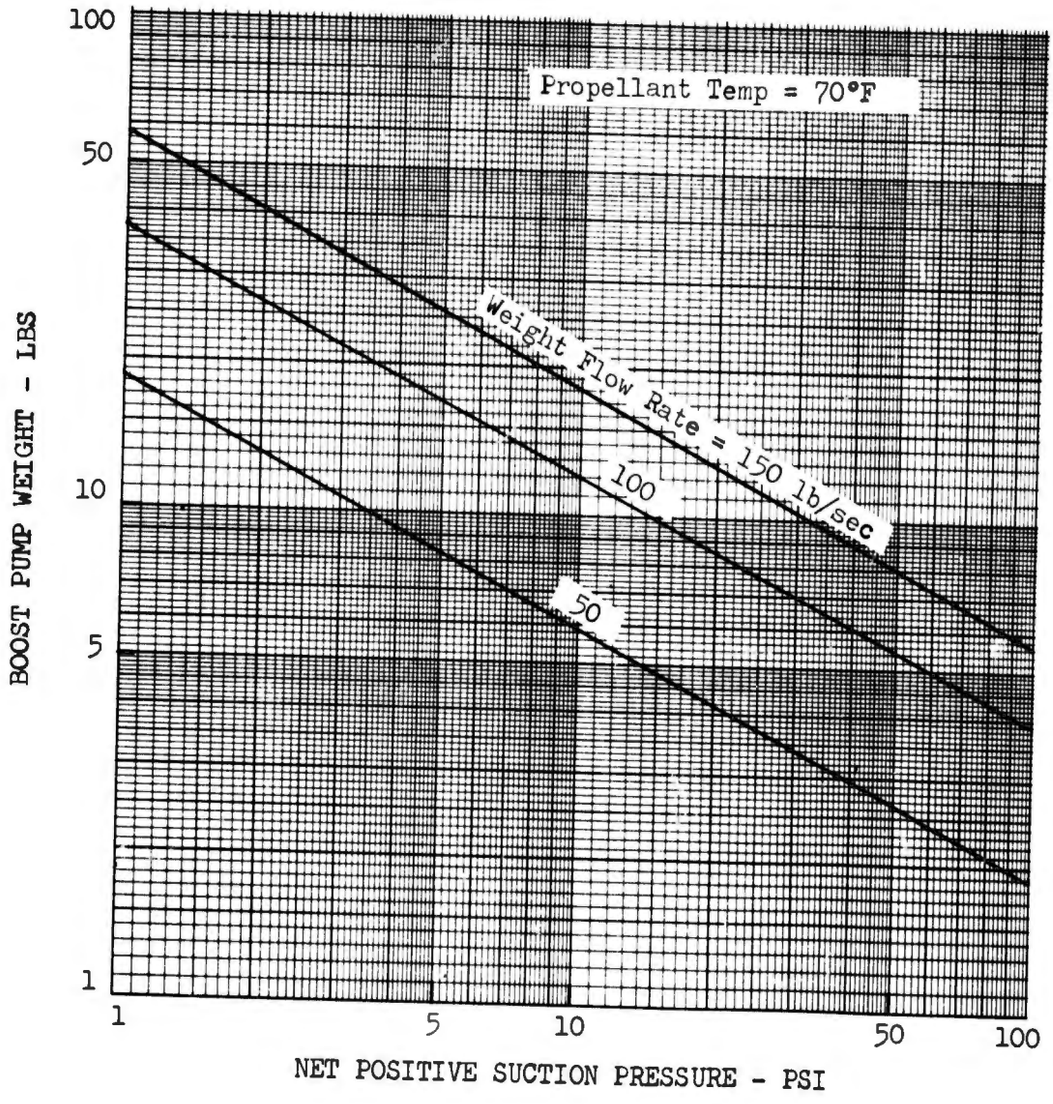

Figure 185. CPA Boost Pump Dry Weight vs Net Positive Suction Pressure

the capability for modifying turbopump weight with changes in pump speed would be desirable. The turbopump does not scale merely in relationship to speed because some of the components (i.e., bearings) do not change appreciably in size as the speed is altered. In addition, the pump scaling criteria are not the same as the turbine scaling criteria. Therefore. the fraction of turbopump weight associated with the pump and turbine must be known before scaling can be accomplished. This fraction changes with thrust and chamber pressure. A comprehensive discussion of the turbopump scaling criteria is presented in Appendix III. However, this area was not completed within the scope of this study and represents a capability that should be obtained through future investigation.

I. PUMP SUCTION PRESSURE

The engine weight previously presented does not include any boost pump weights. However, the requirement for boost pumps depends upon the vehicle trade-off between tank pressure and engine weights. The boost pump weights are small in comparison with total engine weight and as a result, boost pumps probably will offer the best compromise. This is especially true for CLF_5, which now requires a high pump suction pressure of 14 psia. Boost pump weights are shown on Figures No. 185 through No. 188 as a function of net positive suction pressure, propellant flow rate, and propellant types.

The propellant flow rate can be determined from the two relationships for fuel and oxidizer, respectively.

$$\dot{W}_F = \frac{1}{1 + MR_E} \quad \frac{F}{I_{sp}}$$

$$\dot{W}_o = \frac{MR_E}{1 + MR_E} \quad \frac{F}{I_{sp}}$$

where W_F = fuel flow rate, lb/sec

W_o = oxidizer flow rate, lb/sec

MR_E = engine mixture ratio

F = engine thrust level, lb

I_{sp} = engine delivered specific impulse, sec.

Net positive suction pressure can be obtained from the following relationship

$$P_{NPSP} = P_T - P_{VP}$$

where P_T = total propellant pressure at pump suction, psia

P_{VP} = propellant vapor pressure at pump suction, psia (see Appendix I)

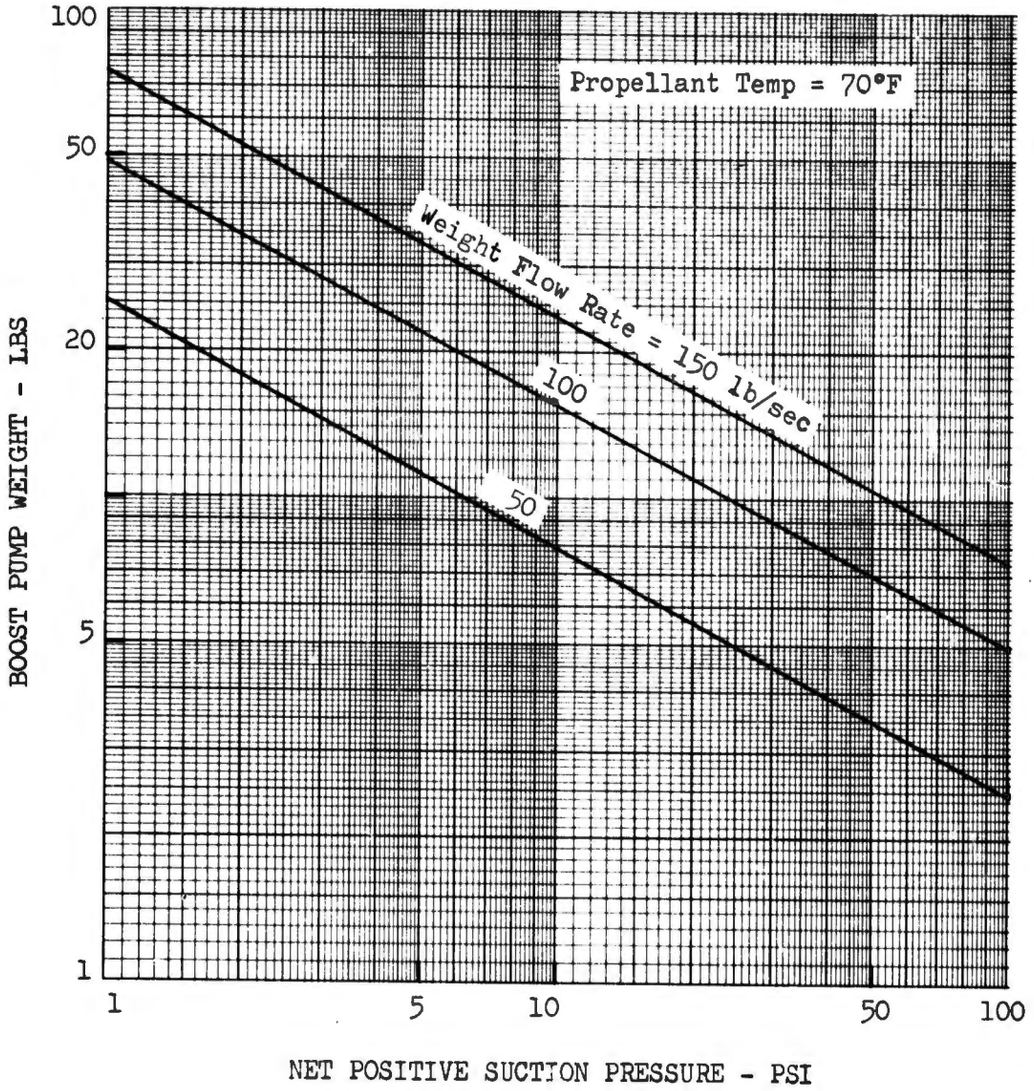

Figure 186. Hydrazine and MHF-5 Boost Pump Dry Weight vs Net Positive Suction Pressure

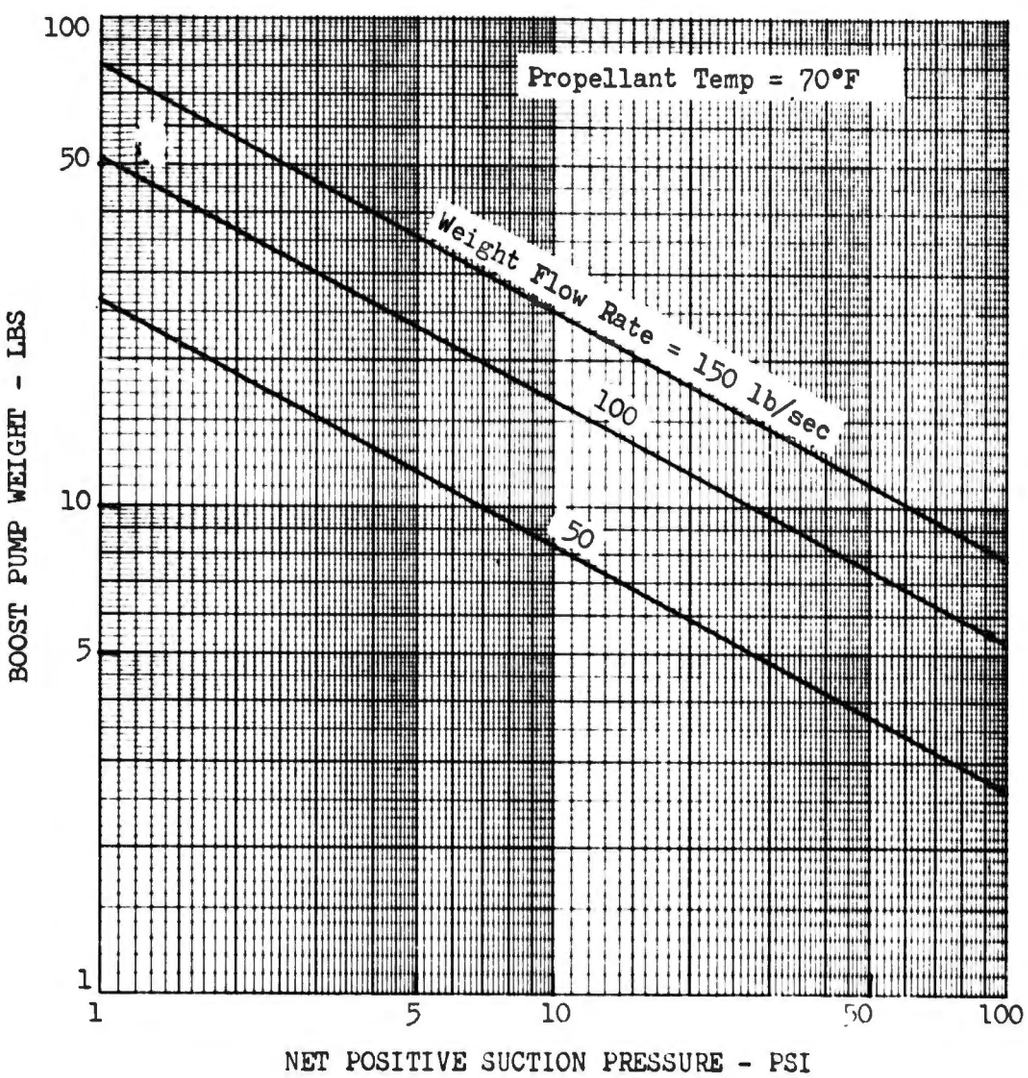

Figure 187. 80/20 Blend Boost Pump Dry Weight vs Net Positive Suction Pressure

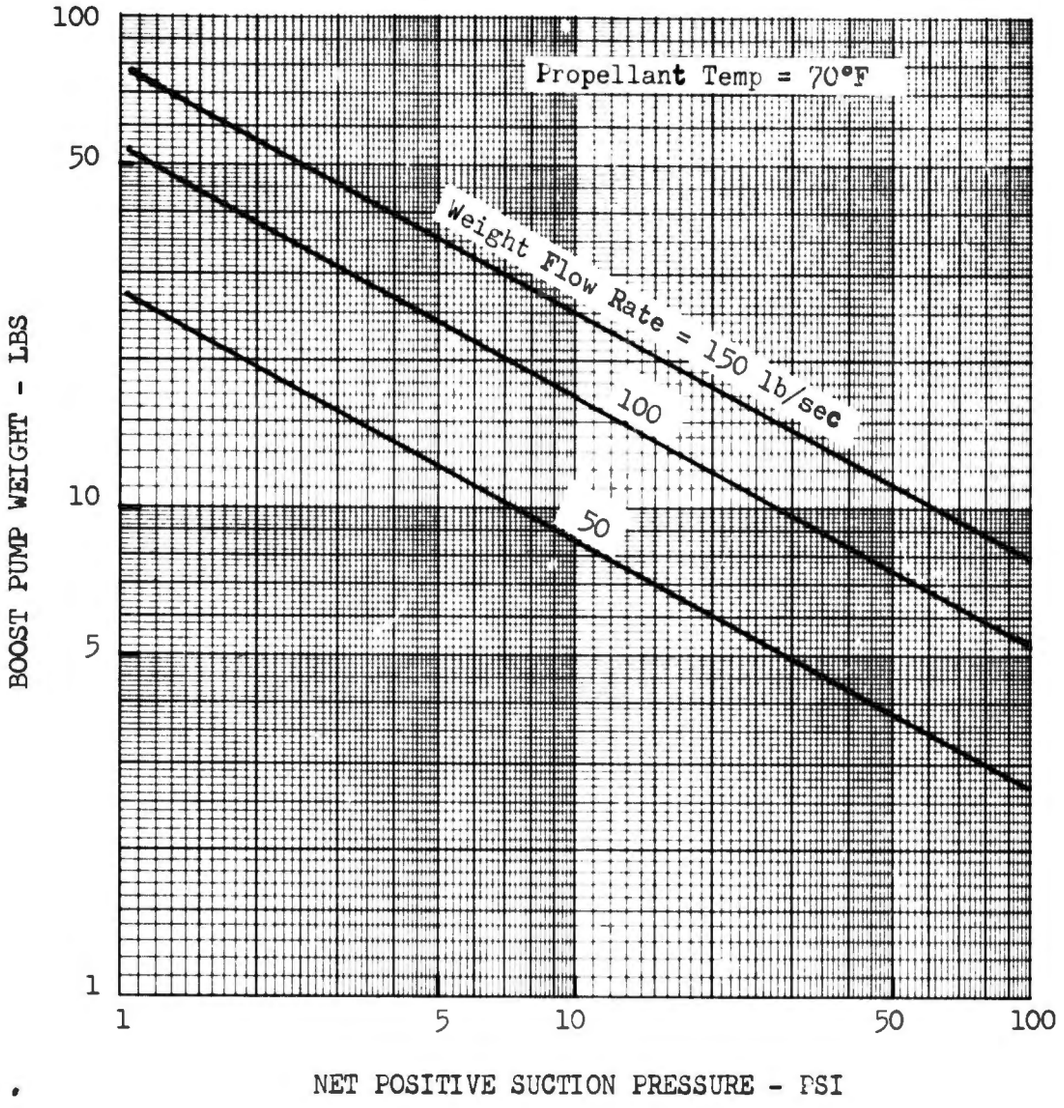

Figure 188. MMH Boost Pump Dry Weight vs Net Positive Suction Pressure

Once the boost pump weight has been determined for the selected engine pump suction pressure the weight must be added to the engine weight obtained from the weight calculation procedure of Section VII to obtain the total engine weight.

IX. TECHNOLOGY COMPARISON AND EVALUATION

In Section VI, the parametric weight and performance data were presented for each parametric engine in terms of thrust to weight ratio versus delivered specific impulse. It was presented in this manner because weight and specific impulse are the most sensitive parameters in any mission analysis study. Therefore, it is possible to determine which engine or technology area will be superior without necessarily conducting a mission analysis. The data presented in this report were used to establish technology comparisons, upon a weight and specific impulse basis, in the following areas:

- Propellant Feed Systems
- Cooling Methods
- Coolant Materials
- Propellant Injection Methods
- Throttling Methods

In addition to providing a basis for technology comparisons, the data presented herein serves to demonstrate the available capability for evaluating the relative merits utilizing varying states of technology.

A. PROPELLANT FEED SYSTEM

Two types of propellant feed systems were considered, pressure-fed and pump-fed. To assure validity in the comparison, both hypothetical engines used the same propellant (CLF_5/N_2H_4), the same injector type (conventional with liquid/liquid propellants), and the same cooling method (radiation cooling in conjunction with fuel film cooling). The results of this comparison are shown on Figure No. 189 as a function of chamber pressure, thrust level, and area ratio. The pump-fed engine is represented by one chamber pressure and thrust level for each area ratio, although an envelope can be generated. As shown, the pressure-fed systems have approximately the same performance as the pump fed systems but are approximately 20% heavier in weight. Therefore, upon a performance basis, the pump-fed engines will be superior for thrust levels down to 30K. However, tankage weights and pressurization weights are quite different and a comparison between the pressure-fed and pump-fed systems should be accomplished by means of mission analysis.

B. COOLING METHODS

The cooling method utilized for a specific engine represents an important area of technology because one of the major losses is that resulting from cooling performance. In addition, significant engine weight changes can result from the coolant method selected. Figure No. 190 shows a comparison between radiative and ablative cooling for a pump-fed engine utilizing CLF_5/N_2H_4 and a liquid/liquid momentum exchange injector. Both types of

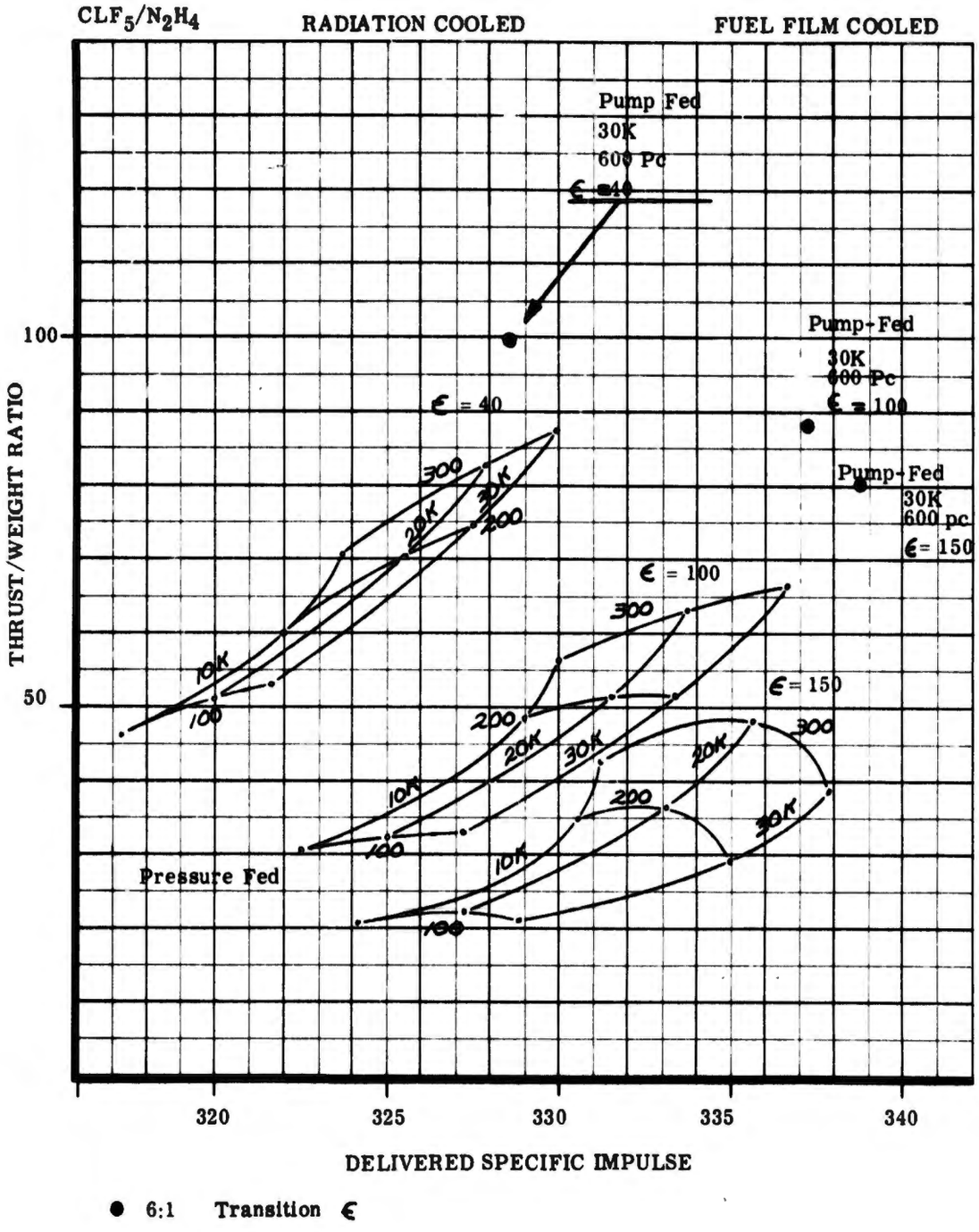

Figure 189. Comparison of Pump-Fed vs Pressure-Fed Engines, Conventional Liquid/Liquid Injector (u)

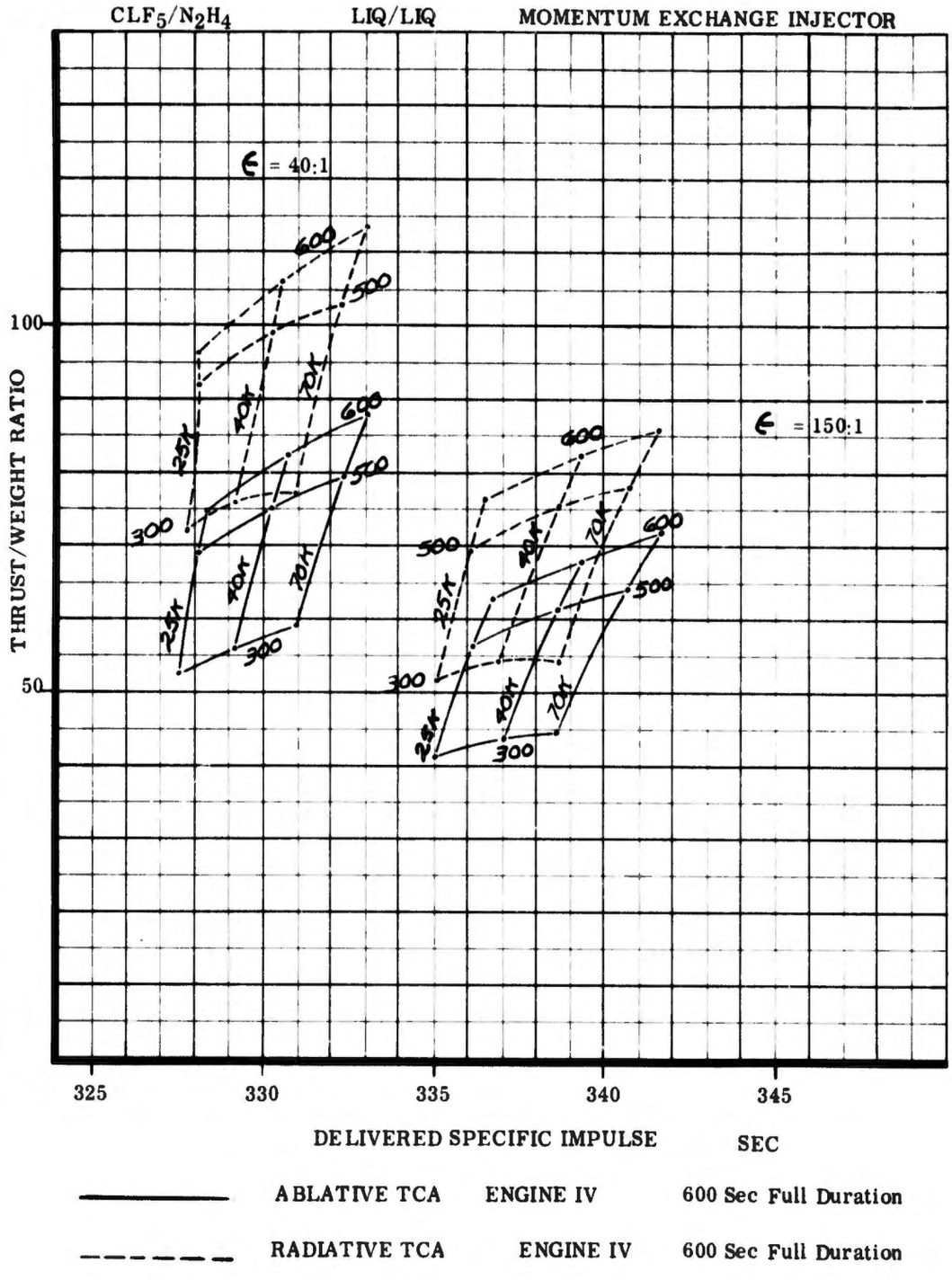

Figure 190. Pump-Fed Engine Comparison, Radiation-Cooled Chamber vs Ablative-Cooled Chamber (u)

cooling are capable of a 600 sec full duration firing. The operating envelopes shown for the two types of cooling are for area ratios of 40:1 and 150:1. Also, as shown, both cooling methods have approximately the same specific impulse. However, the radiation engine represents a significant reduction in engine weight (approximately 20%) as compared with the ablative-cooled engine. Therefore, if the vehicle installation permits the use of a radiative-cooled engine, this type of cooling will result in improved vehicle performance.

The above comparison was of an engine system using an ablative-cooled combustion chamber consistent with a 600 sec full thrust burn duration. The thickness of ablative material is a function of burn duration and decreases for missions requiring less total burn duration. A comparison between radiative and ablative cooling for a 100 sec duration burn time is shown on Figure No. 191. The weight improvement for a radiative-cooled engine has been reduced from 20% for a 600 sec burn duration to approximately 10% for a 100 sec duration. Therefore, engine availability requirements (technology status) and burn duration have a significant influence upon the selection of a cooling method for passively cooled engines.

Figures No. 192 and No. 193 present comparisons of active cooling methods for engines having area ratios of 40:1 and 150:1, respectively. All other engine parameters remain the same. They include gas/gas injection, CLF_5/N_2H_4 propellants, and nickel platelets for transpiration cooling. Three types of active cooling methods were considered; liquid fuel regenerative, liquid oxidizer transpiration, and gaseous fuel transpiration. The operating envelope shown for the regeneratively-cooled engine was limited by burnout heat flux considerations. The comparison indicates that regenerative cooling has nearly the same performance and is lighter in weight than the other cooling methods for both area ratios. Therefore, regenerative-cooling represents a high performing cooling system and is consistent with current technology. However, most in-space missions require throttling which is not consistent with regenerative cooling. Therefore, mission requirements are again a significant parameter in the selection of active cooling systems. Gaseous fuel transpiration cooling has only a 2 sec specific impulse advantage over liquid oxidizer transpiration cooling. In view of this, the selection of gaseous fuel or liquid oxidizer transpiration cooling will depend upon engine operating requirements (i.e., start transient and restart capability).

Gaseous fuel can be used as a regenerative coolant for a portion of the nozzle downstream of the throat without sacrificing throttling capability. This regenerative section attaches at an area ratio of approximately 6:1 and extends downstream to an area ratio consistent with the attachment of the radiation-cooled skirt. Another possible cooling method for this area is the use of radiation cooling with the fibrous graphite or any material capable of maintaining a 4500°F wall temperature. A comparison between radiation cooling and gaseous fuel regenerative cooling for the nozzle extension is shown on Figure No. 194 for area ratios of 40:1 and 150:1. Other engine variables for both types of cooling consisted of gas/gas propellant

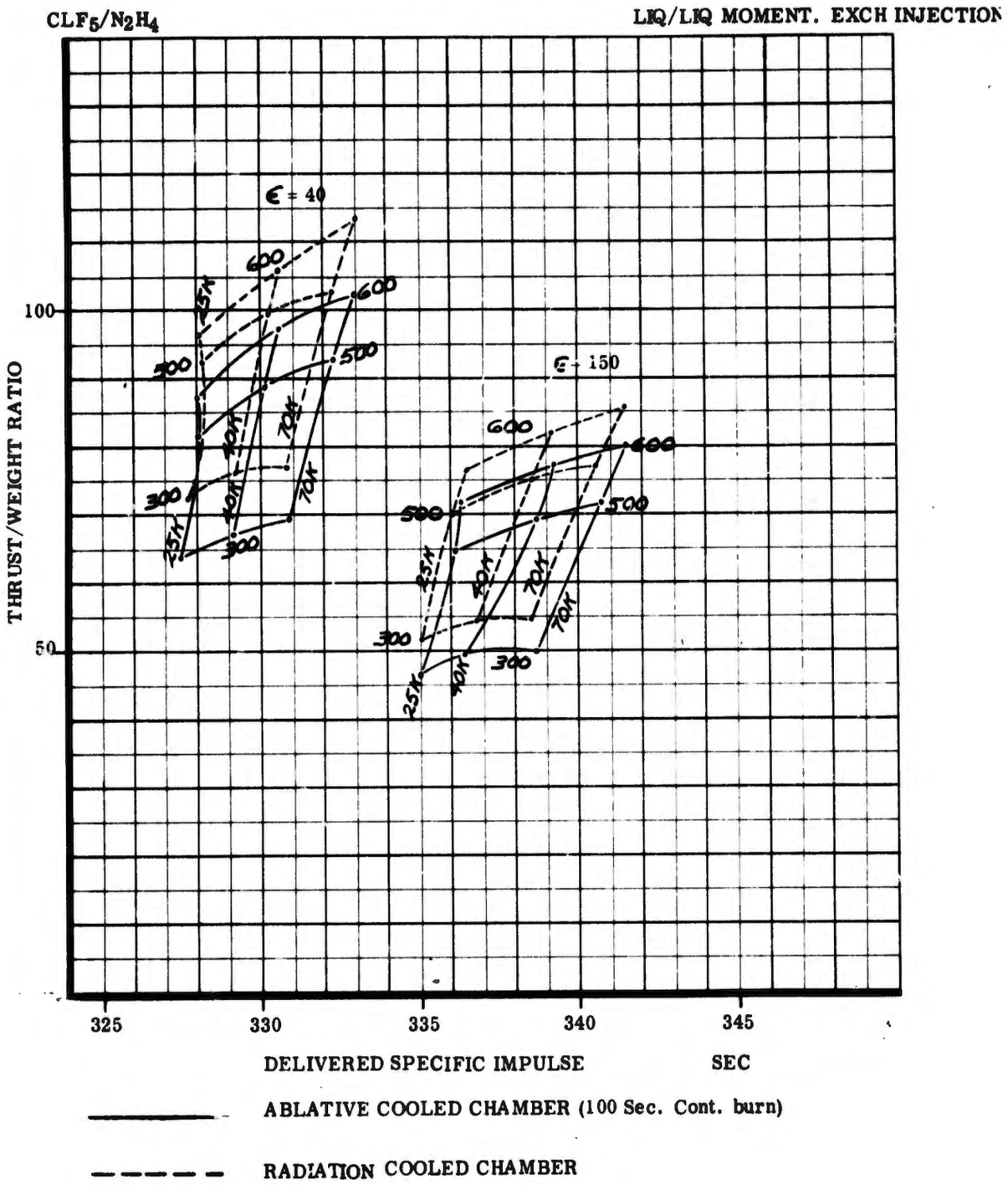

Figure 191. Comparison of Cooling Methods for Pump-Fed Engines, Ablative vs Radiation Cooling (u)

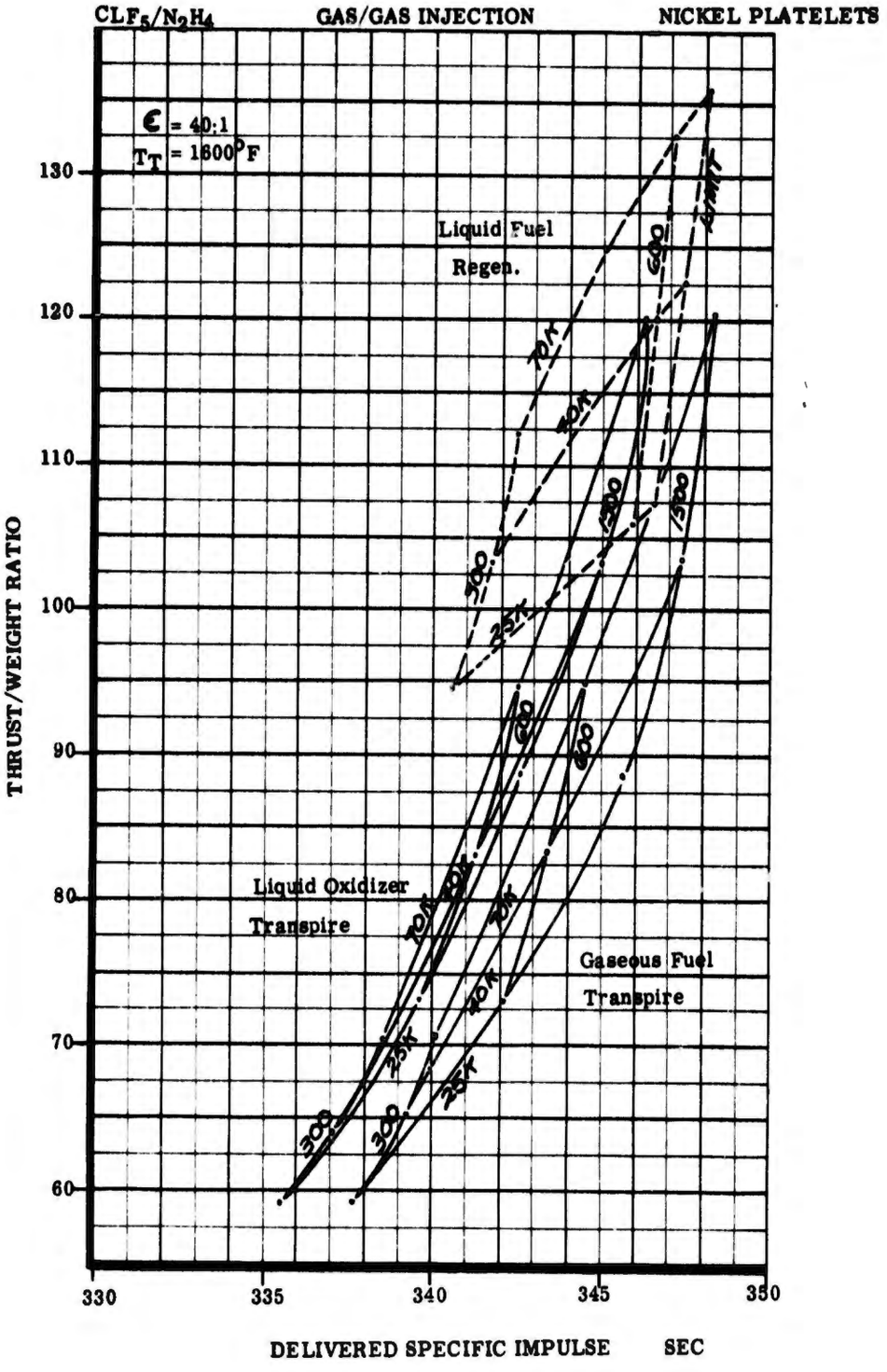

Figure 192. Comparison of Cooling Methods for Pump-Fed Engines (ϵ = 40:1) (u)

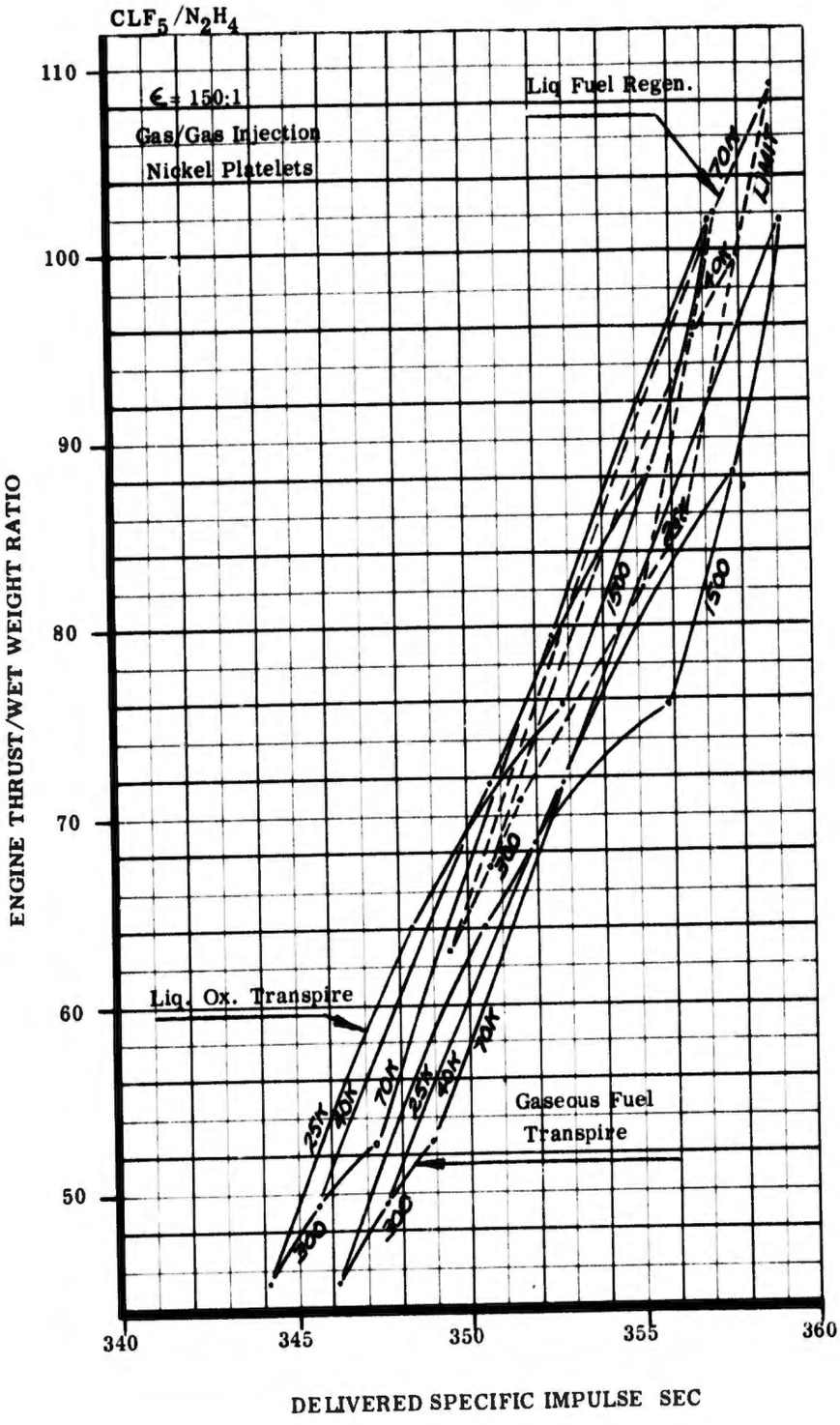

Figure 193. Comparison of Cooling Methods for Pump-Fed Engines (ϵ = 150:1) (u)

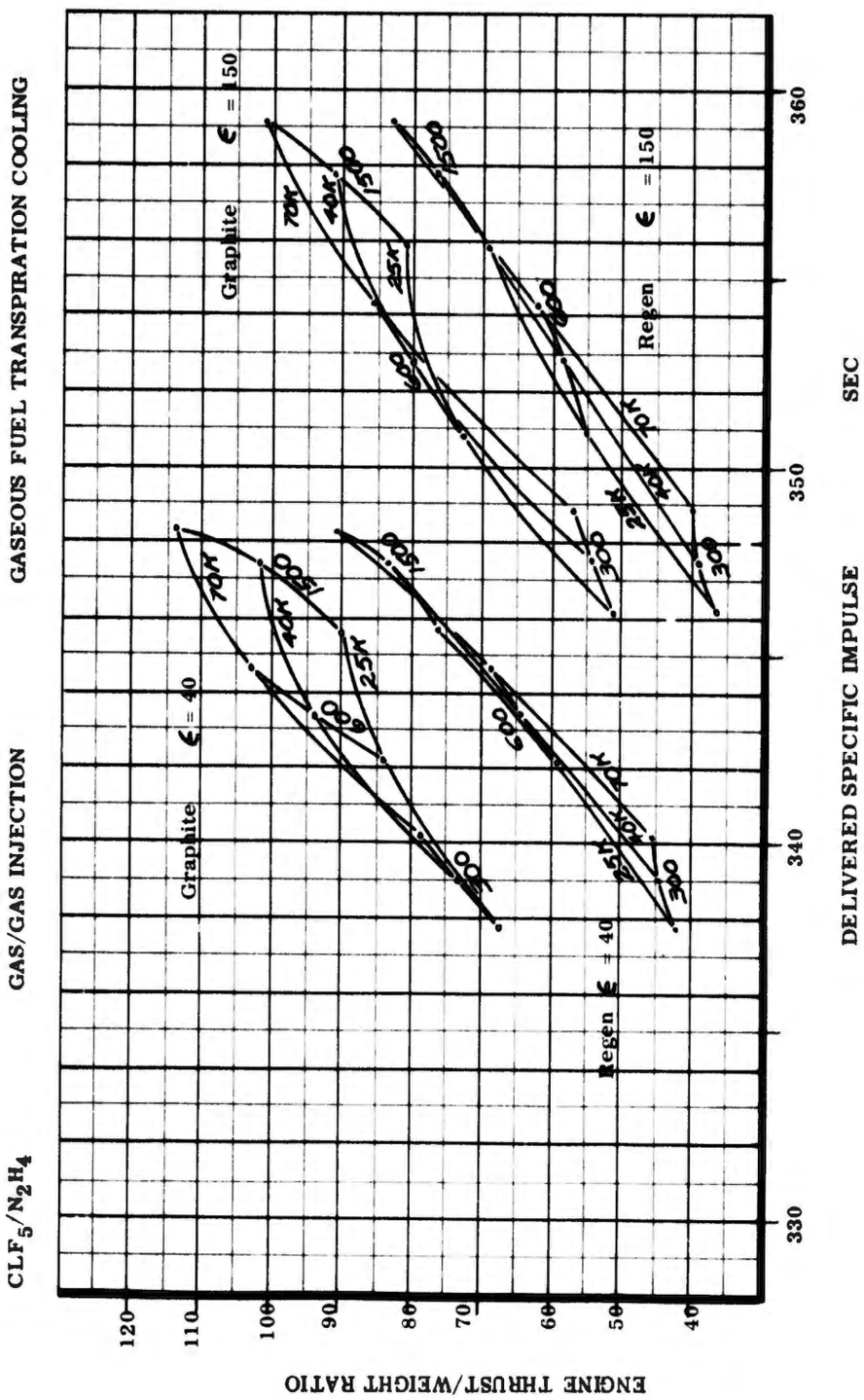

Figure 194. Nozzle Mid-Section Cooling Method Comparison (u)

injection with gaseous fuel transpiration throat cooling. As shown, engine performance is unchanged. However, engine weight is reduced by approximately 25% through the use of radiation cooling. This weight reduction occurs because the graphite is a lighter weight material than a regenerative tube bundle. Also, the transpiration throat cooling weight is less because no passages are required to duct the regenerative coolant flow. Again, graphite represents a higher level of technology, and provides a significant reduction in engine weight.

C. INJECTION METHODS

Another important technology area is associated with the type of main chamber injection system used. The type of injection influences the combustion chamber characteristic length, which has a direct influence upon the required amount of coolant flow rate as well as upon weight. A comparison of injection methods, including liquid/liquid platelets, gas/liquid platelets, liquid/gas platelets, and gas/gas is shown on Figures No. 195 and No. 196 for area ratios of 40:1 and 150:1, respectively. The other significant engine parameters that remained the same for all the methods are: gaseous fuel transpiration cooling; a turbine gas temperature of 1600°F; a gaseous fuel coolant temperature of 1400°F; nickel coolant platelets; and a graphite nozzle extension. As shown, gas/gas injection results in the highest performance with liquid/gas injection running a close second. Therefore, both of these injection methods will result in significant vehicle performance increases as opposed to the gas/liquid and liquid/liquid injection methods. This capability largely depends upon the energy release efficiency and combustion chamber characteristics length relationship that was established for each injection method in the Applied Technology discussion (III) and further expanded in Appendix B. The verification of this relationship is the subject of the Critical Technology discussion of Section X.

D. THROTTLING METHODS

Momentum exchange and laminar flow platelet were the two types of throttling methods considered for pressure-fed engines. A comparison between these two throttling methods is shown on Figure No. 197 for nozzle area ratios of 40:1 and 150:1. The engine parameters for the radiation-cooled chamber and the liquid/liquid injection remained fixed. As shown, the laminar flow platelet is slightly heavier, but offers approximately a 1% specific impulse advantage over the momentum exchange injection as a result of the reduced coolant flow requirement of the shorter L* chamber. Momentum exchange is relatively complex in terms of controls but laminar flow platelets represent a more advanced technology state. Therefore, other considerations may also influence the selection of the throttling method.

The same comparison for pump-fed engines is presented on Figure No. 198 for nozzle area ratios of 40:1 and 150:1. The engine parameters that remained constant are the ablative-cooled 600 sec duration chambers and the liquid/liquid injection. The operating envelope for laminar flow platelets is represented by a single point (25K and 600 psia) because insufficient time

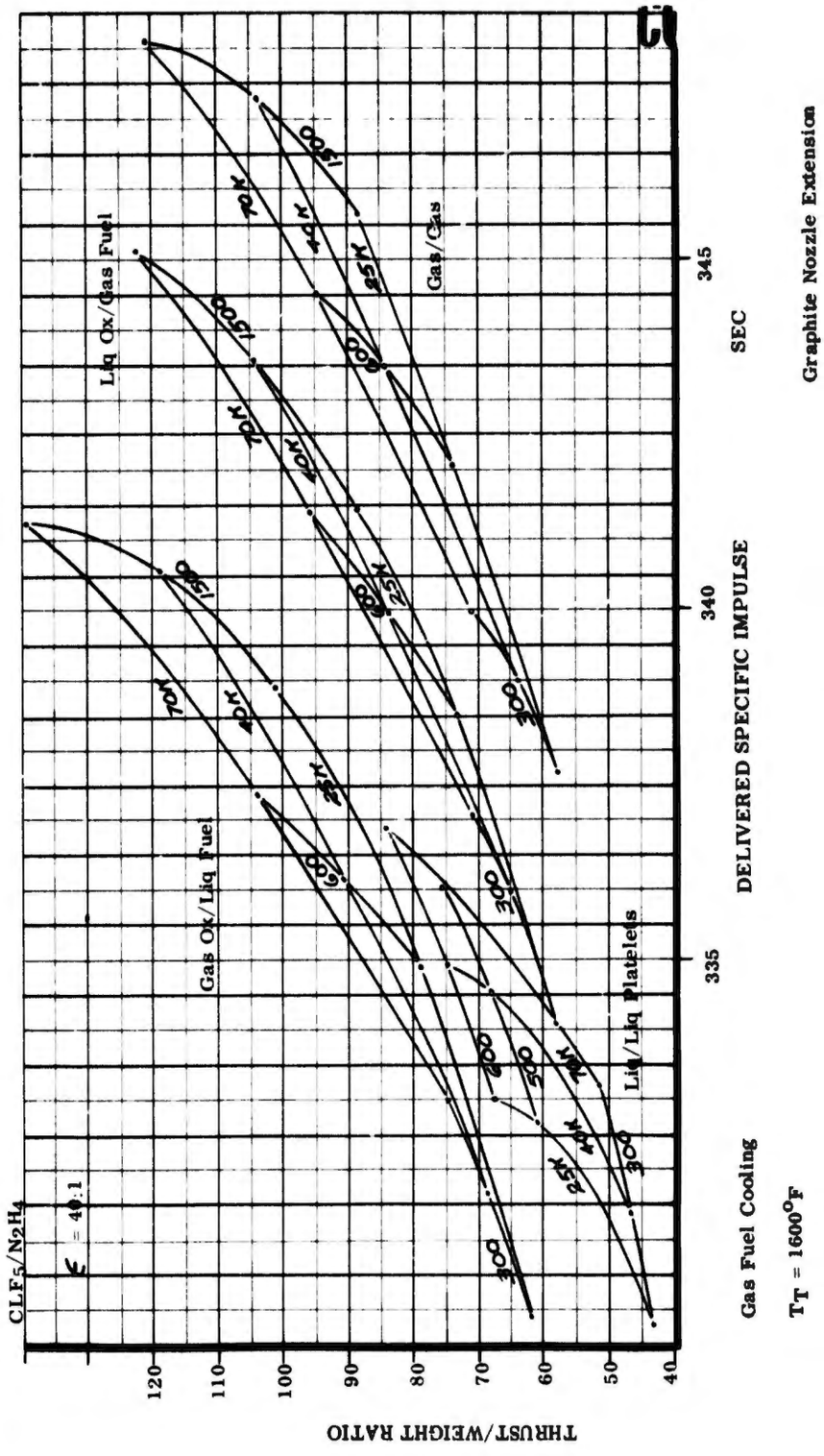

Figure 195. Comparison of Injection Methods for Pump-Fed Engines (ε = 40:1) (u)

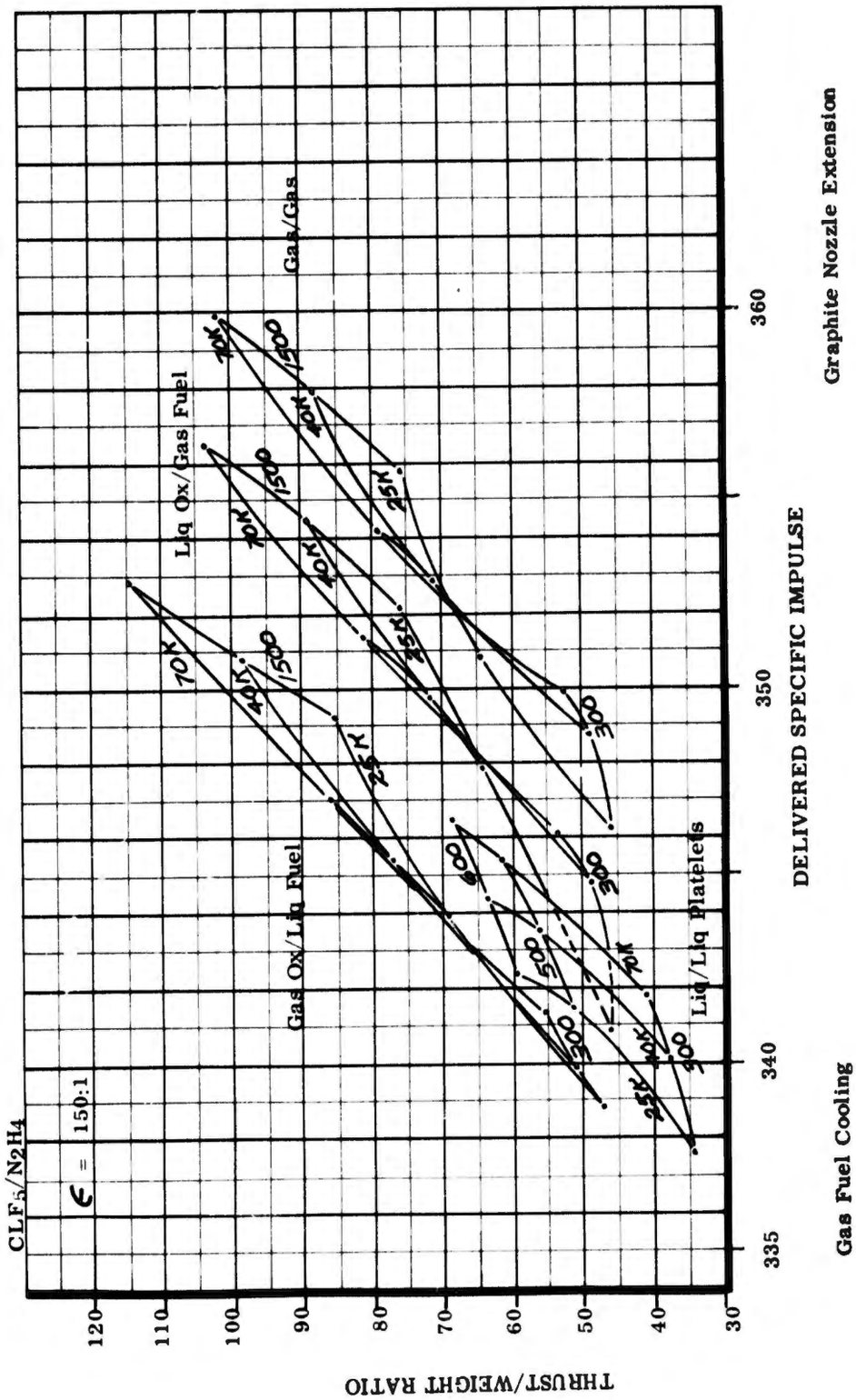

Figure 196. Comparison of Injection Methods for Pump-Fed Engines (ϵ = 150:1) (u)

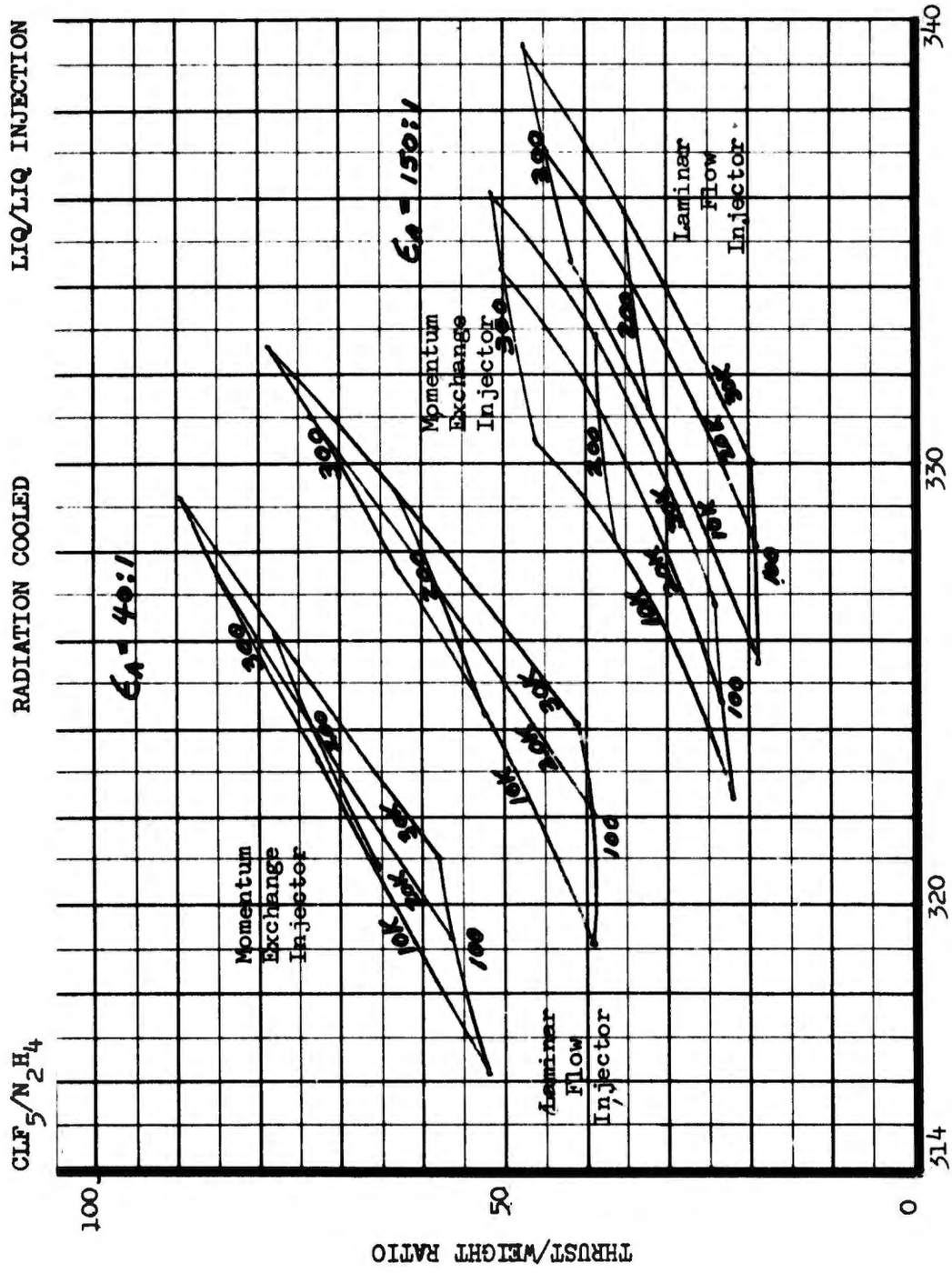

Figure 197. Comparison of Throttling Methods for Pressure-Fed Engines, Momentum Exchange vs Laminar Flow Platelet (u)

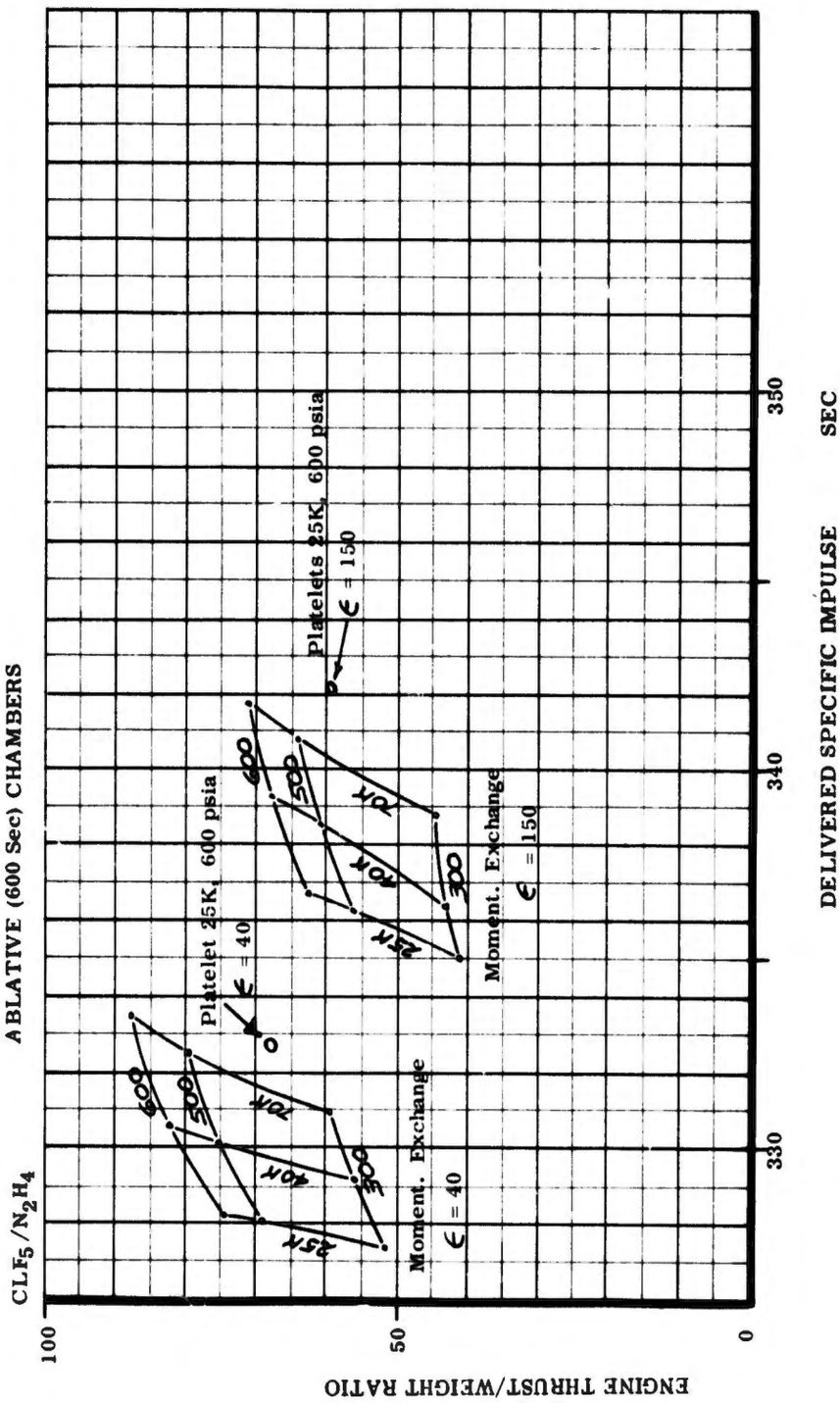

Figure 198. Comparison of Throttling Methods for Pump-Fed Engines, Momentum Exchange and Platelet Injectors (u)

was available to generate the envelope. A comparison of this point with the corresponding location in the momentum exchange envelope again indicated that the laminar flow platelets are slightly heavier although higher in specific impulse.

E. THRUST CHAMBER MATERIAL

One of the major results from this study is that the cooling performance loss represents a major loss in engine performance. This loss can be decreased by using cooling methods or materials that reduce the required amount of coolant flow rate. Cooling methods were discussed previously in Section III.

Engine comparisons presented previously utilized nickel platelets for the transpiration cooling which had an allowable wall temperature of 2000°F for gaseous fuel cooling and 1750°F for liquid oxidizer cooling. However, if graphite platelets can be utilized, the allowable wall temperature can be increased to 4500°F or higher. In addition to reducing the amount of coolant flow rate, the graphite is lighter in weight than nickel. A weight performance comparison between nickel and graphite platelets is shown on Figures No. 199 and No. 200 for nozzle area ratios of 40:1 and 150:1 respectively. The engine parameters remaining constant are: liquid oxidizer transpiration cooling; gas/liquid injection, and the 1200°F turbine gas temperature. As shown, the graphite platelets result in a significant improvement in both engine weight and performance. However, graphite platelets represent an advanced technology status.

The same comparison was accomplished for an engine having gaseous fuel transpiration cooling with gas/gas injection and is shown on Figure No. 201 for area ratios of 40:1 and 150:1. As shown, the graphite is again superior in both weight and performance. However, the amount of gain is less than that experienced for liquid oxidizer cooling because both gas/gas injection and gas fuel transpiration cooling have already minimized the required coolant flow rate.

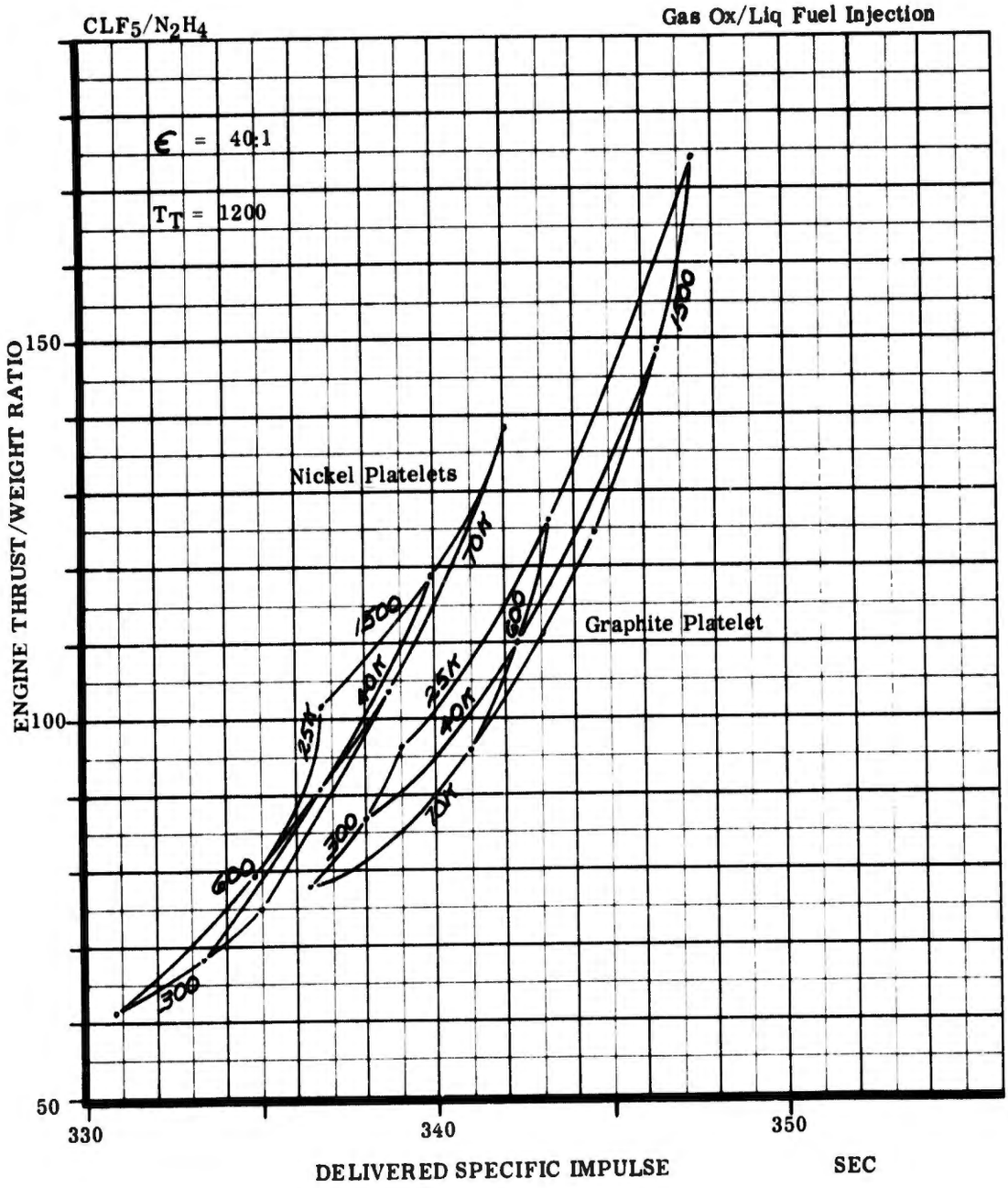

Figure 199. Comparison of Chamber Materials for Pump-Fed Engines, Liquid Oxidizer Cooled Transpiration Chamber (ϵ = 40:1) (u)

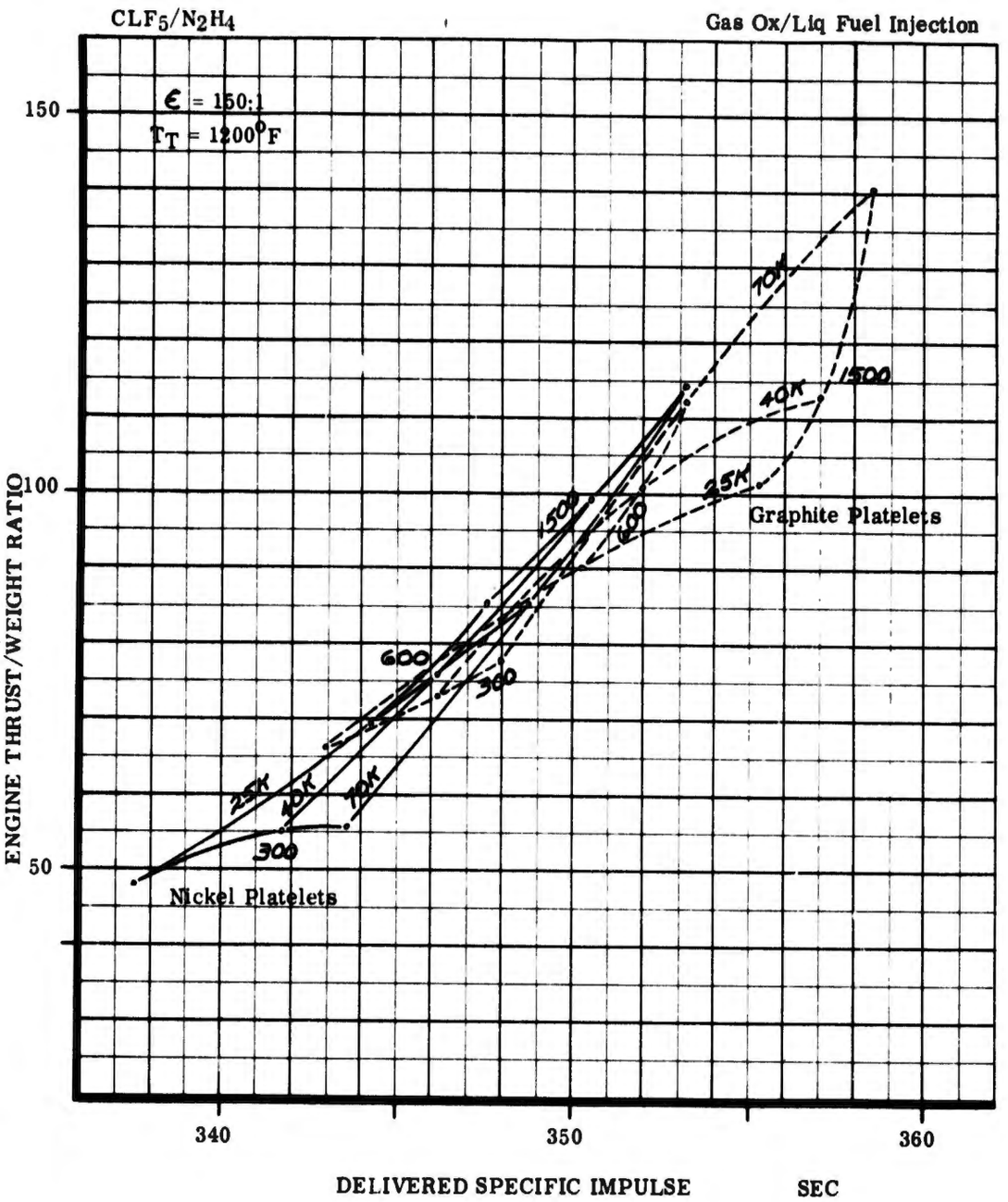

Figure 200. Comparison of Chamber Materials for Pump-Fed Engines, Liquid Oxidizer Cooled Transpiration Chamber (ϵ = 150:1) (u)

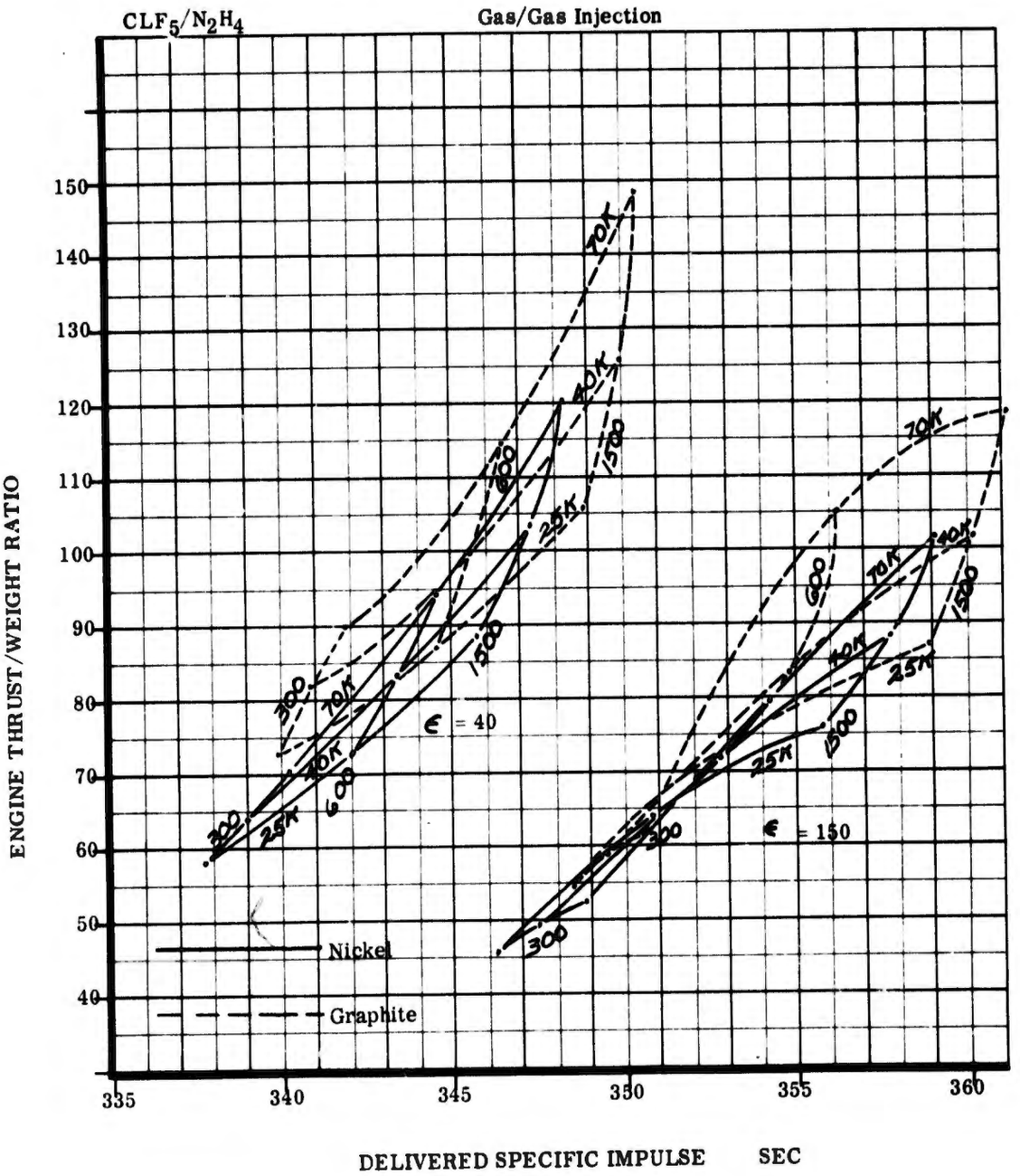

Figure 201. Comparison of Platelets Material for Gaseous Fuel Transpiration-Cooled Chambers on Pump-Fed Engines (u)

X. CRITICAL TECHNOLOGY

The critical technology for the improvement of the CLF_5/N_2H_4 engine mission capabilities are summarized in this discussion. Little experience exists regarding the application of these propellants; therefore, a large segment of the technology requirements listed are for the purpose of obtaining necessary design information or to establish the feasibility of new design concepts. The critical technologies are discussed in four major categories, which represent the end objectives of the recommended technology investigations. These categories are:

- Engine Performance
- Engine Mission Capability
- Engine Weight
- Engine Reliability

This critical technology discussion includes all of the technologies investigated. It is not restricted to those which resulted in the highest payload or ΔV capability for the missions investigated under this contract.

The primary and secondary technology requirements resulting from this study are summarized on Table XXVIII.

A. ENGINE PERFORMANCE

As previously indicated some of the basic information for the engine performance analysis is not available. This includes the energy release losses and minimum chamber length requirements as well as the actual level of the kinetic losses for the specified propellants and advanced injector concepts.

This information is considered essential because of its vital role in the validity of the technology pay-off mission study. It can be obtained by developing and testing advanced injection concepts, such as the HIPERTHIN injector for liquid/liquid injection and the platelet injector for the staged-combustion cycles using gas/gas or gas/liquid injection.

The definition of the minimum characteristic chamber length L* for the above injection methods and injector designs is highly significant because it has a directly proportional affect upon the chamber cooling requirements and coolant losses.

Also, the determination of the cooling capabilities of CLF_5 is most important for CLF_5/N_2H_4 engine concepts.

TABLE XXVIII

CLF_5/N_2H_4 ENGINE DESIGN STUDY CRITICAL TECHNOLOGY REQUIREMENTS

PRIMARY TECHNOLOGY REQUIREMENTS

1. Staged-Combustion Injector Technology (L* and ERL)
2. Throat Transpiration Cooling Utilizing Graphite Platelets
3. Oxidizer-Rich Gas Generator for 10:1 Throttle Capability
   Oxidizer-Rich Gas Generator Mixture Ratio Throttling Control
4. Turbine Inlet Temperature Compatibility for Fluorine-Rich Environment
5. CLF_5 Cooling Characteristics, Decomposition and Reaction Rate
6. Ammonia Blend CAT-Pack Propellant Development (N_2H_4 + (80/20 Wt) NH_3 and MMH + (90/10 Wt) NH_3
7. Monopropellant Gas Generator Development
8. Ring-Gate Valve Development (Back-up Technology)
9. Oxidizer-Rich Turbine Cooling Technology

SECONDARY TECHNOLOGY REQUIREMENTS

1. Thrust Chamber Assembly - Passive Cooling Systems

   Mechanical, Physical and Thermal Properties of Fibrous Graphite for Oxidizer-Rich and Fuel-Rich Exposure

   Char Depth Rate of Phenolic Graphite at Various P_c Levels

   Maximum Size of Fibrous Graphite Chambers and Nozzle Extensions

2. Thrust Chamber Assembly - Active Cooling Systems

   Ni Compatibility in CLF_5-Rich Environment at 500°F to 1750°F - Nickel Platelet Brazing Methods

   Thermal Anti-Oxidation Coatings for Columbium Skirts

   Composite Regeneratively-Cooled Graphite Wall Chamber

TABLE XXVIII (Cont.)

Secondary Technology Requirements (cont.)

3. Thrust Chamber Assembly - Injector

CLF_5 Two-Phase Flow Effects at Low P_c

Baffle Design for Low Pressure Stable Injector

Injector Heat-Sink Cooling Methods

Injector Face Thermal Barrier Coatings (Conventional and Momentum Exchange)

4. Gas Generators

N_2H_4 (CAT-Pack)

Layered Beds (To Lower Cost and Weight)

Staged CAT-Pack

Increased Pressure Drop Bed Designs

Operational and Performance Characteristics

N_2H_4 Blend CAT-Pack

Performance Characteristics

Design

Gas Properties Definition

Monopropellant (Thermal - Bed) MHF-5, MMH

Bed Design

Operational and Performance Characteristics

Gas Properties

Ignition System (Multiple)

TABLE XXVIII (Cont.)

Secondary Technology Requirements (cont.)

4. Gas Generators (Cont.)

Bipropellants Gas Generator

Fuel-Rich N_2H_4, N_2H_4-NH_3, MHF-5, MMH

Temperature Characteristics vs. Mixture Ratio and Pressure

Temperature Reduction Potential - Supplemental Beds

Gas Properties Definition

Stability, Material Compatibility Investigations

Throttling Effects on Response and Performance

Formation of Solids

Bipropellant Gas Generator

Oxidizer-Rich

Temperature Characteristics vs Mixture Ratio and Pressure

Gas Properties Definition

Stability, Material Compatibility

Throttling Effects on Performance

Mixture Ratio Control for Turbopump Assembly Throttling Requirements

5. Turbopump Assembly

Ring-Gate Valve Thrust and Mixture Ratio Control

Ring-Gate Valve Dynamic and Transient Characteristics

Ring-Gate Valve Zero Leakage Seat

TABLE XXVIII (Cont.)

Secondary Technology Requirements (cont.)

5. Turbopump Assembly (Cont.)

CLF_5/N_2H_4 Burn-Off Seal (Oxidizer and Fuel Rich)

Hydrostatic CLF_5 and Amine Lubricated Bearings (Full thrust and Throttling)

Allowable Turbine Temperature in Fluorine Containing Gases

Full-Flow Hydraulic Turbine-Driven Inducer

Lift-Off Seal and Static Seals

Oxidizer-Rich Turbine Cooling

6. Control

All Metal, Zero Leakage, Shut-Off Seals

It appears that thrust chamber cooling using CLF_5 is not desirable because of the stringent passivation requirements for most chamber materials as well as the danger of secondary hardware failure resulting in a complete engine malfunction. However, this consideration is offset when materials such as fibrous graphite, which does not require passivation, are used.

In this analysis, based upon existing data, CLF_5 was not considered to have any cooling benefit from the endothermic decomposition. However, these data only cover temperature levels experienced with regeneratively-cooled chambers. The transpiration-cooled chambers operate at considerable higher temperatures, particularly if fibrous graphite is used as the chamber material. At these temperatures, reaction may occur fast enough to result in some cooling enhancement.

To date, the use of fibrous graphite has been limited to radiation-cooled chambers exposed to combustion products. However, if used as platelet material for transpiration-cooled chambers, then the material is exposed to liquid and vaporous raw propellants and could possibly demonstrate different compatibility characteristics.

The compatibility of fibrous graphite with raw propellants is a very critical technology directly affecting engine performance as well as reliability.

B. ENGINE CAPABILITY

In this section, the critical technologies affecting engine mission capabilities are discussed. These capabilities include throttling, restart, and burn duration.

1. Throttling

The pressure-fed engine throttling limit is defined as the chamber pressure equalizing the CLF_5 vapor pressure because two-phase flow will exist in the injector orifice for chamber pressures lower than the vapor pressure. Also, performance prediction and injector face cooling analysis are complicated. Because the vapor pressure of CLF_5 is very high when compared to the other storable oxidizers, this assumption reduces the throttling range considerably. Therefore, it is recommended that the performance, cooling, and stability characteristics of throttling CLF_5/N_2H_4 engines be investigated for that area below the vapor pressure.

(C) Feed system throttling technologies have to be developed for pump-fed engines. Ring-gate valves are used to obtain throttling in the fuel-rich bleed turbine drives. This concept is only in the feasibility stage. It requires further development to determine the dynamic characteristics as well as a throttle and mixture ratio control concept.

(C) A different feed system throttling concept can be used for oxidizer-rich turbine drive. The opportunity exists to lower the turbine temperature by increasing the mixture ratio of the bipropellant gas generator. The critical technology of this throttling concept is the variable mixture ratio gas generator injector concept for obtaining adequate mixing at lower thrust levels.

(C) To date, no oxidizer-rich gas generator using fluorinated oxidizer has been satisfactorily demonstrated. It is a technology which has to be developed if the simple throttling concept of oxidizer bipropellant mixture ratio variation is to be used.

(C) For transpiration-cooled chamber using liquid CLF_5 as coolant, the minimum chamber pressure obtainable remains to be determined because throttling below vapor pressure at the throat is expected to result in rapidly decreasing throat cooling flow relative to the over-all coolant flow. The minimum chamber pressure is considered consistent regardless of the design chamber pressure. In a mission analysis, it must be considered as a design constraint.

(C) Within the assumptions of this investigation, the regeneratively cooled engine has a very limited throttling range depending upon which one of the specified fuels is used as the coolant. However, it is a very competitive cooling method because coolant losses are non-existent. Attempts should be made to increase its useful range by utilizing graphite laminated chambers and injection systems, which result in a very short L*. This shifts both the burn and heat flux limit as well as the gas side temperature limit.

(C) Gas generator injectors amenable to deep throttling (fuel-rich as well as oxidizer-rich, operating at constant mixture ratio) constitute another area of needed critical technology. The HIPERTHIN concept appears most promising for both the bleed and staged-combustion cycles. For the bleed cycle, gas injection into the gas generator injector may not necessarily incur an extensive weight penalty. Its application would permit greater use of the more conventional injectors for deep throttling of short duration.

2. Burn Duration

(C) The ablative chambers are known to be burn duration sensitive but real correlation of char rates and throat changes as a function of burn as well as operating condititons are not currently available for the graphite materials considered. Improved design criteria for various heat flux densities are needed and the constraints require definition.

(C) Only the gaseous fuel transpiration-cooled engine using MMH or MHF-5 is considered to be burn duration limited within the group of active cooling systems. To remove this constraint, it is recommended that either N_2H_4 or NH_3 additives be used to form CH_4 gas with the carbon. These propellant additives would result in a new fuel, free of carbon formation and should be investigated as to characteristics and properties.

3. Restart

(C) CLF_5/N_2H_4 yields the highest performance of all propellant combinations considered, but it has a very limited restart capability. The 80/20 blend fuel was introducted to overcome this shortcoming. It improves the restart capability and also results in very acceptable fuel-rich gas generator characteristic. However, its high vapor pressure and inadequate regenerative cooling capability do not permit the use of this propellant for all engine configurations.

(C) An improved restart capability for N_2H_4 can be provided by minimizing exposure of components to the liquid fuel and by protecting them from heat soak-back generated in the turbopump assembly and thrust chamber assembly. This can be accomplished by gassifying the fuel immediately at the pump discharge, which eliminates the danger of detonation in the injector during the restart transient. There is a good possibility that heat-sink compounds absorbing the heat soak-back is a technology which may improve the restart capabilities of engines using the monopropellant fuels considered. However, this technology has not progressed beyond the conceptual stage.

(U) For the most part, restart capability has to be designed into the engine by reducing heat conduction to the critical components and by providing for heat removal during the burning time by means of regenerative cooling. During the coast period, the feasibility for removing heat soak-back by radiation into space has to be provided.

(U) If restart requirements are severe, each engine concept must be evaluated as to which fuel propellant is best suited to meet the requirements for the least loss in payload or ΔV capability.

4. Reliability

(U) In this section, technologies are listed to provide information regarding the reliability of recommended concepts and materials.

(C) Nickel material has been successfully demonstrated in fluorinated oxidizers as injector material for conventional injectors. Based upon this experience, the material was selected as the prime candidate for the throat of transpiration-cooled chambers and platelet injectors. However, long duration operation of these materials, exposed to raw CLF_5, in temperatures up to 1750°F has not as yet been demonstrated. Also, brazing techniques for these materials are needed to fabricate nickel HIPERTHIN injectors on a low cost basis.

(C) Previously, fibrous graphite was discussed as a chamber material, but if this material is compatible with raw CLF_5, it also should be considered for oxidizer feed lines and oxidizer-rich gas generator liner material. Therefore, the mechanical, physical, and thermal properties of the fibrous graphite materials exposed to an oxidizer-rich and a fuel-rich environment should be defined.

(C) Fabrication methods for metering coolant flows in fibrous graphite platelets have not been established to date. It is recommended that the feasibility of brazing coated fibrous graphite to obtain an easy-to-machine lightweight element for fluorine compatible injector concepts be investigated.

(C) One of the assumptions of this investigation was that oxidizer-rich turbines can accept temperatures up to 1200°F, but no experience is available to date confirming this capability. A compatibility investigation is recommended because lower turbine temperatures will require higher pump discharge pressures and highly efficient turbopumps, which increases the weight of these components.

(U) As pointed out in the discussion of engine control methods, fluorinated oxidizer requires hard seat valve seats and seals. This technology is currently being established for low pressure and through-flow requirements. However, it should be extended to include electro-mechanical actuation systems and throttle control for high pressure and thrust requirements.

5. Weight and Cost Reduction

(C) Extensive use of CAT-Pack gas generators was made in this investigation because of the catalystic capability of the N_2H_4 fuel. Existing technology indicates that the weight of these CAT-Packs is large (approximately 2 lb) for each lb/sec of through flow. These weights are not significant where the turbine bleed cycles are of concern but they appear to be excessive

for the staged-combustion cycles where large flow rates must be accepted. To partially overcome this, the turbine temperatures selected were as high as possible and only the gases used for cooling were decomposed to lower temperatures, which resulted in a considerable weight savings.

(U) Lightweight design concepts for a CAT-Pack of increased bed loading have to be established to make them attractive for staged-combustion cycles.

(C) "Shell 405" was considered as the catalyst. It is very expensive and uses IRIDIUM, a strategic material. Therefore, layered packs should be considered which utilize less exotic catalysts (i.e., "Harshaw"). However, this is a technology which is not well established. Another approach would be the use of a small primary bipropellant gas generator as the initial heat source and decomposing the fuel in a thermal bed of low cost to acceptable temperature levels.

(C) The operational performance characteristics and response of these gas generators have not been defined and are considered an important technology to fully realize the potentialities of the CLF_5/N_2H_4 engine concepts.

XI. APPLICATION STUDIES

This effort had a two-fold objective. First, it was accomplished for the purpose of demonstrating the application of the engine parametric data generated within the scope of this study using evaluation techniques that would provide a reasonable and realistic estimate of the optimum engine design. Secondly, it served as the means for making recommendations of a specific engine design (based upon the quantitative performance results of the evaluation technique) and engine operating parameters for three specified missions while considering the interaction of the engine design with the entire propulsion system.

A. MISSIONS

Each of the specified missions[15] displays a somewhat different set of engine and propulsion system requirements. Mission I is typical of the type of vehicle which may be of interest to the Titan III SPO. Mission II is a representative application for the types of vehicles being studied under the S-5 program at Douglas and Martin under SAMSO-Aerospace Advanced Planning sponsorship. Mission III is typical of that class of vehicle being investigated by Lockheed and others for the Air Force Flight Dynamics Laboratory. The general mission considerations are summarized on Figure No. 202. A brief description of each mission, including system definition and performance evaluation objectives, follows.

1. Mission No. I

This mission is defined in terms of the propulsion system application, which concerns an orbital transfer with duty cycle and propulsion system similar in concept to the Transtage and Agena vehicles. The engine operating parameters, which provide maximum payload in synchronous orbit, are to be defined.

a. System Definition

This is an unmanned, expendable upper-stage for the T-III-M-7 segment, 120-in. SRM launch vehicle. The general stage configuration is shown on Figure No. 203. This stage consists of separate, oblate spherical, oxidizer and fuel tanks arranged in tandem and enclosed in an untapered, corrugated sandwich, outer shell structure. It is assumed that neither the

(15) Letter from Thomas A. McCreery, Lt. Col., USAF, Chief, Liquid Rocket Division, AFRPL, to Werner Luscher, Aerojet-General Corp., dated 9 August 1967, subject: "(U) Task II Application Studies, Contract F 04(611)-67-C-0092, Compound A/Hydrazine Engine Design Studies" (Confidential)

~ INDICATES VARIABLE

MISSION	I	II	III
GENERAL DESCRIPTION	UNMANNED UPPER-STAGE	TRAILER PROPULSION	HIGH L/D SPACECRAFT
	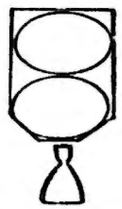		
EVALUATION CRITERIA	PAYLOAD IN SYNCH. ORBIT	VELOCITY WPL FIXED	PAYLOAD ΔV FIXED
PAYLOAD	~	15,000 & 5,000	~
VELOCITY	~	~ (80/20T)	10,000
GROSS WEIGHT	~	40,000 & 30,000	30,000
STAGE WEIGHT	~	25,000	~
THRUST MAX	~	40,000	30,000
THROTTLED		25,000	3,750
BOOSTER	TIII-M	N/A	N/A

EVALUATION OBJECTIVE	DEFINE	FOR
	WLO, F, PC, ε	WPL MAX
	PC, ε	ΔV MAX (15), ΔV (5)
	PC, ε	WPL MAX, ΔV (2), ΔV (80/20 F)

Figure 202. General Mission Considerations (u)

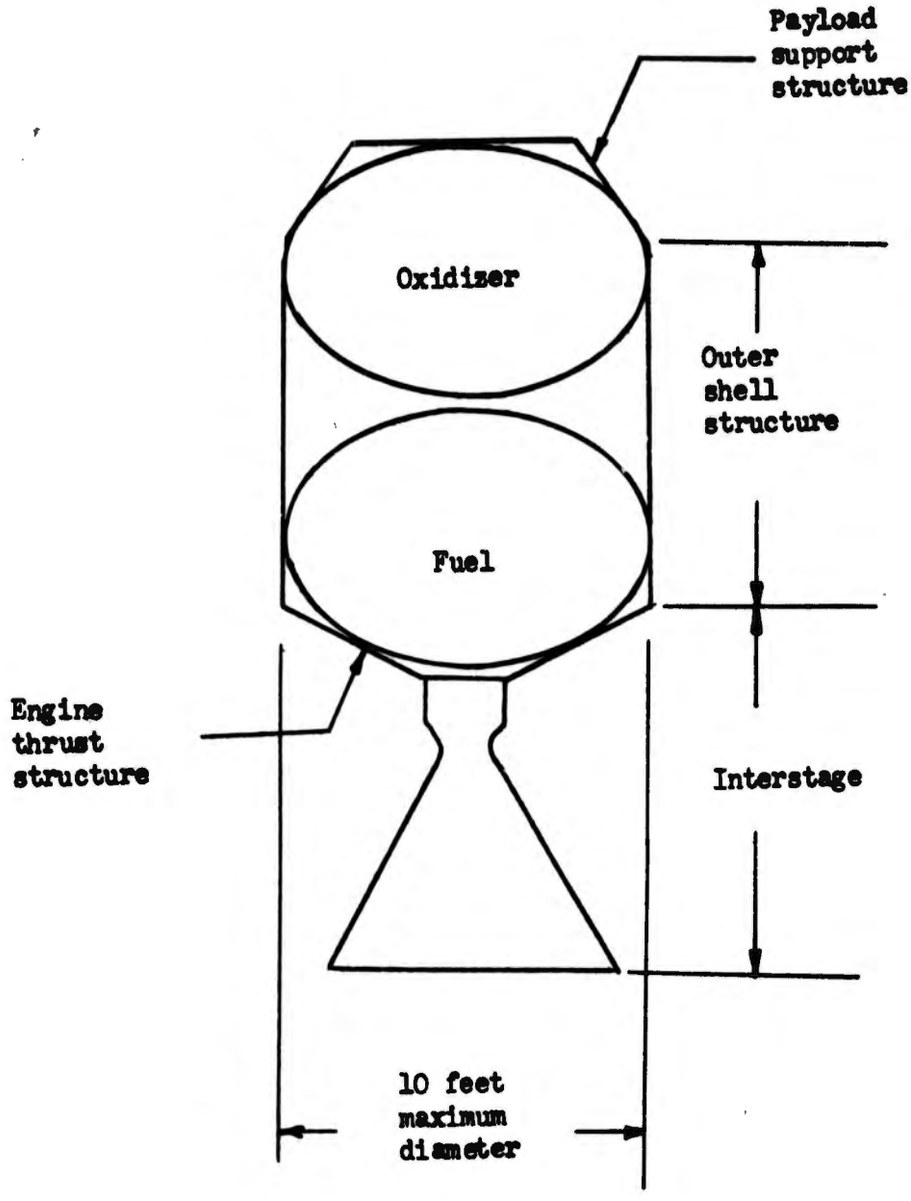

Figure 203. Typical Stage Configuration, Mission No. I

payload support nor the engine thrust structure are intimately attached to the tankage. Only single engine installation is considered. The basic configuration and weight scaling equations (Table XXIX) are based upon data presented in Report AFRPL-TR-65-252 (16).

(C) The stage diameter is 120-in. and interstage inert weight is estimated at 362 lb for a nominal engine length of 80-in. The weight is varied at 4.5 lb/in. of nozzle length in excess of 80-in. This interstage is jettisoned with the Titan III-M core second-stage at the time of upper-stage separation.

b. Objectives of Performance Evaluation

(U) The primary objective is to define the stage gross weight (including payload and interstage) and the engine operating parameters (thrust, chamber pressure, and nozzle expansion ratio) which result in a maximum payload delivered into synchronous orbit for each of the five sets of engine point design parametric data.

(U) When appropriate, a sub-orbital burn of the upper-stage is considered to maximize payload.

2. Mission No. II

(U) This mission entails defining a fixed stage weight (not including payload) that will provide a maximum in-space velocity increment capability when used as the trailer propulsion unit for manned or unmanned spacecraft.

a. System Definition

(C) This stage has a 25,000 lb gross weight (not including payload) of which 2000 lb is fixed inert weight. This fixed inert weight includes allowances for the following:

(1) Orientation controls
(2) Separation system
(3) Power supply
(4) Instrumentation
(5) Ordnance and umbilicals
(6) Unusable fluids
(7) Interstage structure to spacecraft
(8) Growth and contingency

(16) (U) Maneuvering Satellite Propulsion System Optimization Study, Technical Report AFRPL-TR-65-252, April 1966, Vol. II, Book 2, p. 48 (Confidential)

TABLE XXIX

JETTISON WEIGHTS - EQUATIONS AND ASSUMPTIONS

MISSION NO. I

Pump-fed	WJ = 2.025 VP + 2300 + WE
Pressure-fed	WJ = (9.0 + 0.0426 Pc) VP + WE
Interstage	WINT = 362 + 4.5 (LINT - 80)

MISSION NO. II

Pump-fed	WJ = 3.357VP + 2000 + WE
Pressure-fed	WJ = (1.80 + 0.0360 Pc) VP + 2000 + WE
Interstage	-2 FPS ΔV per in. > 80, WPL = 15,000
	-3 FPS ΔV per in. > 80, WPL = 5000

MISSION NO. III

Pump-fed PTOX = 75 PTF = 25

Pressure-fed PT = 1.5 Pc + 40

$$WJ = 10{,}000 - 0.313\,\Delta WP + 1.5\,\Delta WE + 0.7\,\Delta WO \times T + \Delta WFT + \Delta L$$

$\Delta WP = WP - 18{,}000$

$\Delta WE = WE - 558$

$$\Delta L = \left[\frac{1.5 + \frac{(CL - 11.6)}{10}}{1.5}\right] * WE - 558$$

$\Delta WOXT = WOXT - 127$ $\quad WOXT = 0.0713 * PT * (VOXT)^{2/3}$

$\Delta WFT = WFT - 80$ $\quad WFT = 0.165 * PT * (VFT)^{2/3}$

The remaining 23,000 lb is to be distributed between usable propellant and all other stage inert weights which include:

- Body structure
- Tanks
- Pressurization system
- Feed system
- Thrust vector control system
- Insulation (tanks and engine)
- Primary engine

(C) The general stage configuration is shown on Figure No. 204. This stage consists of an oblate spheroid oxidizer tank and four spherical fuel tanks supported by a space truss mounted to a cruciform beam, which is the thrust mount for the single engine installation with 40,000 lb thrust. The engine is throttleable to 25,000 lb. The general stage configuration and the weight scaling equations of Table XXIX are based upon data presented in NASA TMX-5127(17).

(C) Two payload configurations were considered: a 15,000 lb manned spacecraft and a smaller 5000 lb unmanned spacecraft. The manned application has a 40,000 lb gross weight with a ΔV penalty of 2 ft/sec per inch of variation in booster-trailer interstage length from a nominal length of 80-in. The unmanned application has a 30,000 lb gross weight and a ΔV penalty of 3 ft/sec per inch of variation in the interstage from an 80-in. nominal length.

b. Objectives of Performance Evaluation

(C) The primary objective is to define the engine chamber pressure and nozzle expansion ratio at the specified 40,000 lb full thrust for each of the five sets of engine point design parametric data, which provide the maximum in-space velocity increment capability for the manned spacecraft application. This velocity capability is based upon 80% of the available propellant being expended at full thrust and the remaining 20% being expended in the throttled 25,000 lb thrust mode. Gross weight for this application is 40,000 lb, fixed stage weight is 25,000 lb, and payload is 15,000 lb.

(C) For the unmanned spacecraft application, the 15,000 lb spacecraft is replaced with a 5000 lb spacecraft resulting in a 30,000 lb gross weight at ignition. The trailer and propulsion system characteristics defined in the larger manned spacecraft evaluation are used to calculate the in-space velocity increment exercising the velocity equation for the lighter gross weight.

(17) An Analysis of Chemical Upper Stages for NASA Scientific Mission, NASA TMX-52127, Advanced Development and Evaluation Division, NASA Lewis Research Center

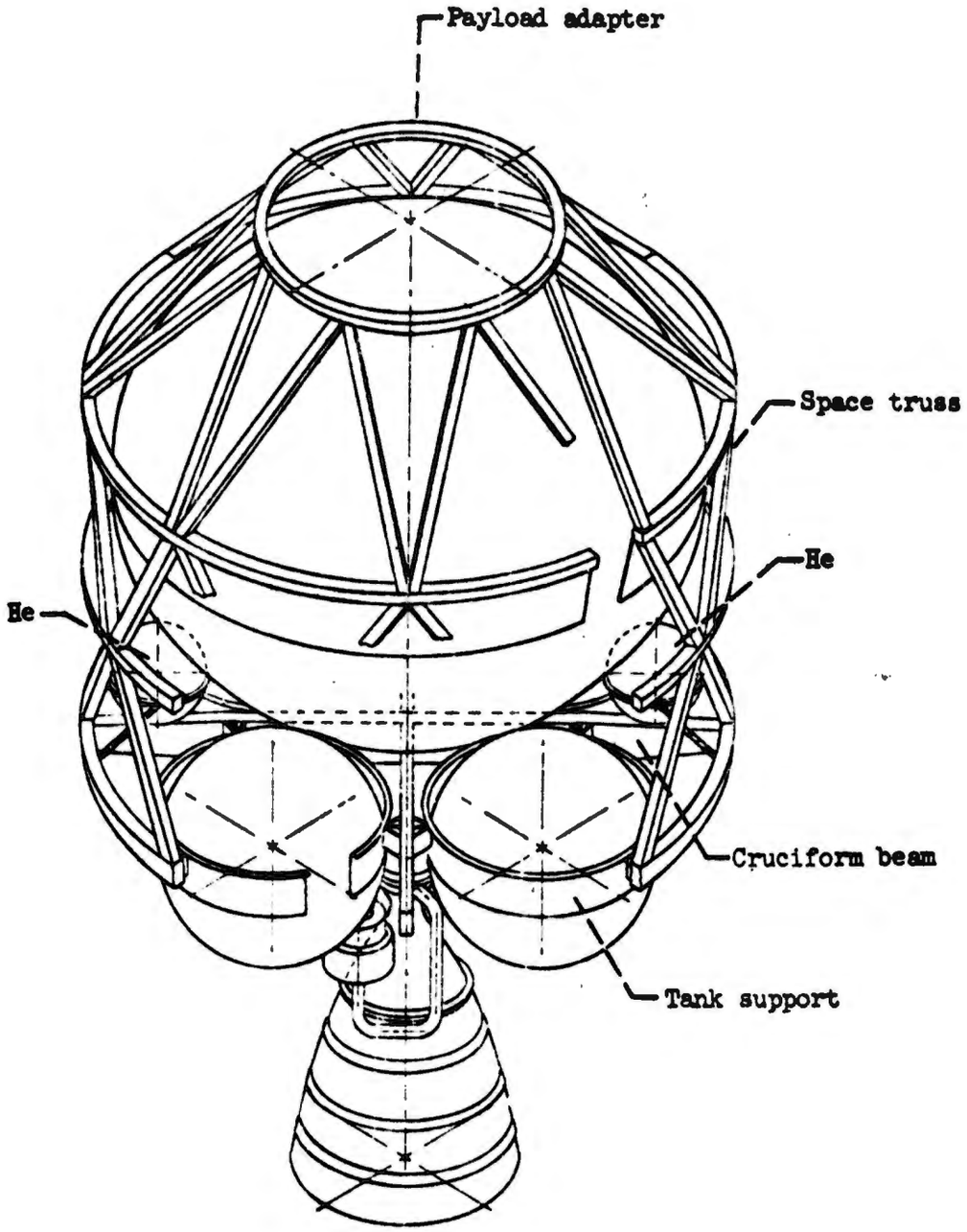

Figure 204. Typical Stage Configuration, Mission No. II

3. Mission No. III

(C) This mission requires the definition of an on-board propulsion system for a specified spacecraft configuration. This spacecraft is a manned, reusable, recoverable, high L/D vehicle with a full thrust velocity increment capability of 10,000 ft/sec and a 2000 lb payload.

a. System Definition

(C) The nominal vehicle defined[18] has the following characteristics.

(1)	Gross weight	30,000 lb
(2)	Velocity increment	10,000 ft/sec
(3)	Payload	2000 lb
(4)	Total vehicle volume	740 ft^3
(5)	Length	36 ft
(6)	Unloaded dry weight	10,000 lb
(7)	Propellant weight	18,000 lb
(8)	Engine full thrust	30,000 lb
(9)	Throttling capability	at least 8:1
(10)	Maximum nozzle exit diameter	42 in.
(11)	Payload density	20 lb/ft^3
(12)	Vehicle density	13.5 lb/ft^3

(U) In addition to the above characteristics, the engine location, propellant tank configuration, and exchange coefficients between system weights and payload were also specified[19].

(C) The nozzle throat (baseline configuration engine) is located at the plane of the vehicle aft end. This establishes the allowable engine combustion chamber compartment. Adjustments are made to the vehicle inert weight (ballast forward to maintain vehicle center-of-gravity) for varying thrust chamber lengths in accordance with the ΔL relationship specified on Table XXIX.

(U) Baseline vehicle tank weights, volume, and location within the vehicle also were specified. Tank weight adjustments, resulting from propellant volume changes and/or internal tank pressure changes, were made for each set of point design engine parametric data. It is assumed that an increase in propellant or payload volume adds directly to vehicle volume with a corresponding increase in vehicle unloaded dry weight and that gross weight remains constant. The equations for calculating oxidizer and fuel tank weights are presented on Table XXIX.

---

(18) Letter, McCreery to Luscher, 9 August 1967, op. cit.
(19) Ibid.

(C) The following exchange coefficients between spacecraft payload and system weight changes were specified[20].

System Weight Exchange (ΔX)	Exchange Coefficient $(\frac{\Delta Payload}{\Delta X})$
Propellant Weight	-0.687
Oxidizer Tank Weight	-0.70
Fuel Tank Weight	-1.0
Engine Weight	-1.5
Engine Location	$\frac{(1.5 + 0.1 \times L)}{1.5} \times W_E$

Where WE is engine weight and L is the distance from the nozzle throat to the vehicle aft plane and is positive in the aft direction.

(C) Additional baseline vehicle parameters that were established to evaluate changes in system weights resulting from changing engine design characteristics or engine operating parameters are:

- Engine weight 558 lb
- Oxidizer tank pressure 75 psia
- Fuel tank pressure 25 psia
- Oxidizer tank volume 115 ft^3
- Fuel tank volume 85 ft^3
- Oxidizer tank weight 127 lb
- Fuel tank weight 80 lb
- Engine mixture ratio 2.23
- Combustion chamber length 11.6 in.

b. Objectives of Performance Evaluation

(C) The effect upon payload and velocity increment was determined using the specified exchange coefficients for various engine design characteristics and various engine operating parameters (chamber pressure and nozzle expansion ratio) within the five sets of point design engine parametric data. The gain or loss in payload was determined at a velocity increment of 10,000 ft/sec at full thrust. Variations in velocity increment were determined with a fixed 2000 lb payload and a fixed 30,000 lb gross weight, also at full thrust.

(20) Ibid.

(C) In addition to the comparisons of payload and velocity at full thrust, adjusted velocity increments were calculated for each combination of engine operating parameters (chamber pressure and expansion ratio) based upon an assumption that 80% of the available propellant is expended in a fully-throttled (10:1) mode and the remaining 20% of the available propellant is expended at full thrust. Payload during this adjusted velocity increment evaluation is constant at 2000 lb and the gross weight is 30,000 lb.

B. PARAMETRIC ENGINE DATA

(U) The parametric engine data used in the application studies were generated during Task I of this study effort. A detailed description of the data was provided in the previous sections of this report. This discussion is limited to the propellant combination CPA/N_2H_4. It is primarily concerned with what parameters were considered and how these data were utilized in mission analysis to define the optimum engine operating parameters and to make a quantitative comparison between engine designs based upon over-all system performance.

(U) The basic data established in Task I, which are of initial importance in an engine performance evaluation, are:

- Engine length
- Engine diameter
- Engine weight
- Engine delivered vacuum specific impulse

Values for these four independent performance parameters are presented on Table XXX and were provided as a function of the following engine operating parameters.

- Engine vacuum thrust
- Engine chamber pressure
- Nozzle expansion ratio

(U) Five sets of these parametric data (based upon Point Design Engines No. I, No. IV, No. V, No. VII, and No. VIII defined during Task I) are considered.

(U) These "raw" data were processed by using a computer program to expand the matrix of 180 "raw" data points into a matrix of 256 data points (one matrix for each engine design) and to punch the input data cards containing the matrix data for use in the final mission analysis program. The resulting matrix (a 3 by 4 set in thrust, chamber pressure, and nozzle expansion ratio with four values, each equally-spaced within the limits of the "raw" data) provides 64 values each of engine length, engine diameter, engine weight, and engine delivered vacuum specific impulse. It is referred to as the "processed parametric data."

TABLE XXX

INDEPENDENT PERFORMANCE PARAMETERS (U)

Engine Design I

Fv	Pc	ε	Is	F/W	LE	DE
10,000	100	40	319.2	39.2	88	53.76
	200		324.8	51.8	67	37.95
	300		327.4	62.2	58	30.99
20,000	100		322.0	39.4	107	75.89
	200		327.6	60.2	88	53.76
	300		331.0	73.3	75	43.64
30,000	100		323.9	41.2	141	93.29
	200		329.1	64.3	104	66.09
	300		332.4	78.8	85	53.89
10,000	100	100	325.3	25.8	141	85.00
	200		331.2	41.0	105	60.00
	300		334.4	51.8	89	49.00
20,000	100		328.0	27.8	195	120.00
	200		334.2	46.5	142	85.00
	300		338.0	59.4	119	69.00
30,000	100		329.6	28.3	235	147.50
	200		335.7	48.1	170	104.50
	300		339.4	62.6	142	85.20
10,000	100	150	327.1	18.5	179	104.10
	200		333.0	32.3	130	73.48
	300		336.0	41.2	110	60.01
20,000	100		330.0	19.5	247	146.97
	200		336.0	34.1	179	104.10
	300		339.9	45.8	149	84.51
30,000	100		331.6	19.9	297	180.65
	200		337.5	35.3	216	127.99
	300		341.2	47.7	179	104.35

Chamber Length = 13.2
Engine Mixture Ratio = 2.16

Engine Design IV

Fv	Pc	c	Is	F/W @ 100 sec	LE	DE
25,000	300	40	327.6	63.4	95	48.70
	500		328.1	81.8	83	38.58
	600		328.0	87.5	78	35.10
40,000	300		329.2	67.0	112	62.93
	500		330.2	89.4	95	48.07
	600		330.6	96.4	89	44.59
70,000	300		330.9	69.0	140	82.22
	500		332.3	93.7	116	64.19
	600		333.0	101.5	109	58.82
25,000	300	100	333.5	53.4	145	77.00
	500		335.1	72.1	120	61.00
	600		335.6	78.3	113	55.50
40,000	300		335.3	56.9	175	99.50
	500		337.5	78.7	143	76.00
	600		338.5	85.7	134	70.50
70,000	300		337.8	58.3	221	130.00
	500		340.4	81.3	179	101.50
	600		341.4	90.0	167	93.00
25,000	300	150	335.0	46.8	179	94.31
	500		336.1	64.8	146	74.71
	600		338.5	70.9	137	67.97
40,000	300		336.3	49.2	218	121.86
	500		338.6	69.7	176	93.08
	600		339.2	77.0	164	86.34
70,000	300		338.7	50.3	278	159.22
	500		340.7	72.0	223	124.31
	600		341.6	80.2	206	113.90

Chamber Length = 20.2
Engine Mixture Ratio = 2.08

Engine Design V

Fv	Pc	c	Is	F/W	LE	DE
25,000	300	40	333.2	82.0	95	48.70
	600		338.5	133.0	78	38.58
	700		339.3	136.0	77	35.10
40,000	300		333.9	83.0	113	62.93
	600		338.6	140.0	89	48.07
	700		339.8	147.0	88	44.59
70,000	300		334.7	84.0	140	82.22
	600		339.3	142.0	109	64.19
	700		340.9	155.0	108	58.82
25,000	300	100	339.7	67.0	145	77.00
	600		345.4	111.0	113	61.00
	700		346.4	116.0	112	55.50
40,000	300		341.0	67.2	175	99.50
	600		345.7	117.0	134	76.00
	700		346.9	125.0	133	70.50
70,000	300		340.4	67.5	221	130.00
	600		346.6	119.0	167	101.50
	700		348.3	132.0	166	93.00
25,000	300	150	341.7	56.0	179	94.31
	600		347.0	96.0	137	74.71
	700		347.9	102.0	136	67.97
40,000	300		342.8	57.0	218	121.86
	600		347.5	100.0	164	93.08
	700		348.7	109.0	163	86.34
70,000	300		343.0	58.0	278	159.22
	600		348.4	102.0	206	124.31
	700		350.2	115.0	205	113.90

Chamber Length = 22.2
Engine Mixture Ratio = 2.47

TABLE XXX (cont.)

Engine Design VII							Engine Design VIII						
Fv	Pc	ε	Is	F/W	LE	DE	Fv	Pc	ε	Is	F/W	LE	DE
25,000	300	40	326.9	61.6	80	48.38	25,000	300	40	337.7	67.6	69	48.38
	600		331.1	79.4	62	34.15		600		342.1	84.0	52	34.15
	1500		334.2	101.6	46	21.63		1500		345.7	90.0	39	21.63
40,000	300		328.7	68.3	98	61.35	40,000	300		339.0	73.0	86	61.35
	600		333.0	91.0	74	43.64		600		343.4	94.0	62	43.64
	1500		336.7	119.2	54	27.20		1500		347.4	102.0	48	27.20
70,000	300		330.3	75.2	124	81.59	70,000	300		340.2	77.0	113	81.59
	600		334.4	104.2	93	57.55		600		344.6	103.0	80	57.55
	1500		339.0	139.0	67	36.05		1500		348.6	114.0	63	36.05
25,000	300	100	333.7	54.6	129	76.50	25,000	300	100	344.9	59.0	117	76.50
	600		338.1	75.8	96	54.00		600		349.3	81.0	85	54.00
	1500		342.0	87.2	68	34.20		1500		354.0	85.0	61	34.20
40,000	300		335.4	59.6	159	97.00	40,000	300		346.7	62.0	147	97.00
	600		340.2	86.2	117	69.00		600		350.8	89.0	106	69.00
	1500		344.6	102.0	81	43.00		1500		355.6	93.0	76	43.00
70,000	300		337.0	64.5	205	129.00	70,000	300		348.0	66.0	190	129.00
	600		342.0	96.9	150	91.00		600		352.9	96.0	135	91.00
	1500		347.0	118.5	103	57.00		1500		356.9	103.0	95	57.00
25,000	300	150	335.5	47.8	162	93.69	25,000	300	150	346.2	51.0	152	93.69
	600		340.2	69.2	120	66.14		600		350.8	73.0	107	66.14
	1500		344.5	85.0	83	41.89		1500		355.8	81.0	76	41.89
40,000	300		337.0	51.7	201	118.80	40,000	300		347.4	54.0	190	118.80
	600		342.4	77.5	147	84.51		600		352.8	80.0	136	84.51
	1500		347.0	99.2	100	52.66		1500		357.8	91.0	95	52.66
70,000	300		338.8	55.4	261	157.99	70,000	300		348.9	57.0	239	157.99
	600		344.2	86.2	190	111.45		600		354.3	86.0	178	111.45
	1500		349.6	114.8	128	69.81		1500		359.1	101.0	124	69.81

Chamber Length = 18.9
Engine Mixture Ratio = 2.82

Chamber Length = 11.6
Engine Mixture Ratio = 2.23

These data, by means of a parabolic curve fit and an interpolation scheme, are available as a subroutine to the main-line computer program. It provides specific values of length, diameter, weight, and impulse for any combination of thrust, chamber pressure, and expansion ratio for each of the five point designs. The first interpolation is for the argument thrust, providing 64 data points (values of LE, DE, WE, and Is in a 2 by 4 set in chamber pressure and expansion ratio) which are stored as the FINT, thrust interpolation, results. A second interpolation for the argument chamber pressure provides 16 data points (four values each of LE, LE, WE and Is at the four nozzle expansion ratio values) which also are stored as the PCINT results. A third interpolation for the argument nozzle expansion ratio, AEINT, provides the final four values (one each for LE, DE, WE and Is) at the specified thrust, chamber pressure, and expansion ratio. The values of these four parameters are used in each of the three missions to determine the over-all system performance (velocity and/or payload) for that specific set of engine operating parameters.

Subsequent interpolation in the processed data, for a variation in nozzle expansion ratio, is made for the 16 data points stored as a result of the PCINT interpolation. The performance is calculated for a step-wise increase in expansion ratio until a maximum performance value is obtained for each mission. At this time, if the chamber pressure also is to be made optimum, interpolation control is returned to the 64 values stored as a result of the FINT interpolation and a new set of 16 data points are obtained from PCINT. These values are used in AEINT to provide the specific LE, DE, WE, and Is values used in the mission analyses. The cycle is repeated until a maximum performance value is obtained as a function of chamber pressure. When thrust also is to be made optimum, interpolation control returns to FINT and the original 256 data points. The interpolation begins anew to establish a set of stored values in the FINT result and the cycle is repeated.

This technique of processed data storage and retrieval provides the four, first-order of importance parameters, LE, DE, WE, and Is necessary to perform application studies without any need for graphs or tabular interpolation. Adjustments to this processed reference data (i.e., Is degradation resulting from throttling and WE resulting from ablative liner thickness variations with burn time) are made within each mission as required. Further adjustments as a result of specific technology changes within a point design and/or a change in the fuel, can be incorporated with a minimum of program modification because either technology or fuel changes will have a minor affect upon engine envelope and will be reflected chiefly in terms of an adjustment to weight and specific impulse.

C. PROBLEM DEFINITION

The mission analysis task (II) requires a demonstration of how the engine parametric data from Task I can be applied to evaluation techniques for future application studies to:

- Define engine operating parameters resulting in optimum performance.

- Make quantitative performance comparisons between engine designs and missions.

Three typical missions, representing future application study requirements, were described earlier. The parametric data generated in Task I for the five point design engines also were described briefly. The diverse engine and propulsion system requirements dictated by the applications and the vast amount of parametric data previously described in detail suggest an application study approach that will minimize parametric data handling and interpolating. At the same time, it must provide consistent accuracy to define optimum performance and permit quantitative comparisons.

Prior to this study contract, Aerojet-General developed its own computer program to supply a standardized set of liquid propellant rocket engine performance parameters for application studies and performance comparisons. This program provides a tape storage and data retrieval system by means of curve fitting and interpolating for engine performance as a function of the propellant combination, engine thrust, chamber pressure, and nozzle expansion ratio. The program output can be printed or punched on cards in a standardized matrix form. This program also provides performance data, weights, and sizes of operational liquid propellant rocket engines as well as operational liquid propellant stage parameters such as size, weight, and tank volumes.

The curve fitting and interpolating portion of this program was used to process the "raw" parametric data generated in Task I. The processed data were then used in a computer program developed to incorporate the three specified applications of this study and an optimization scheme that would provide the engine operating parameters defining optimum performance. In this way, a reliable quantitative performance comparison between engine designs and missions is possible. The program can best be described by referring to the brief logic diagram shown on Figure No. 205. The following six major areas comprise the over-all program as it was used in this study:

- Input and control
- Stored parametric data
- Interpolation
- Missions
- Optimization
- Output

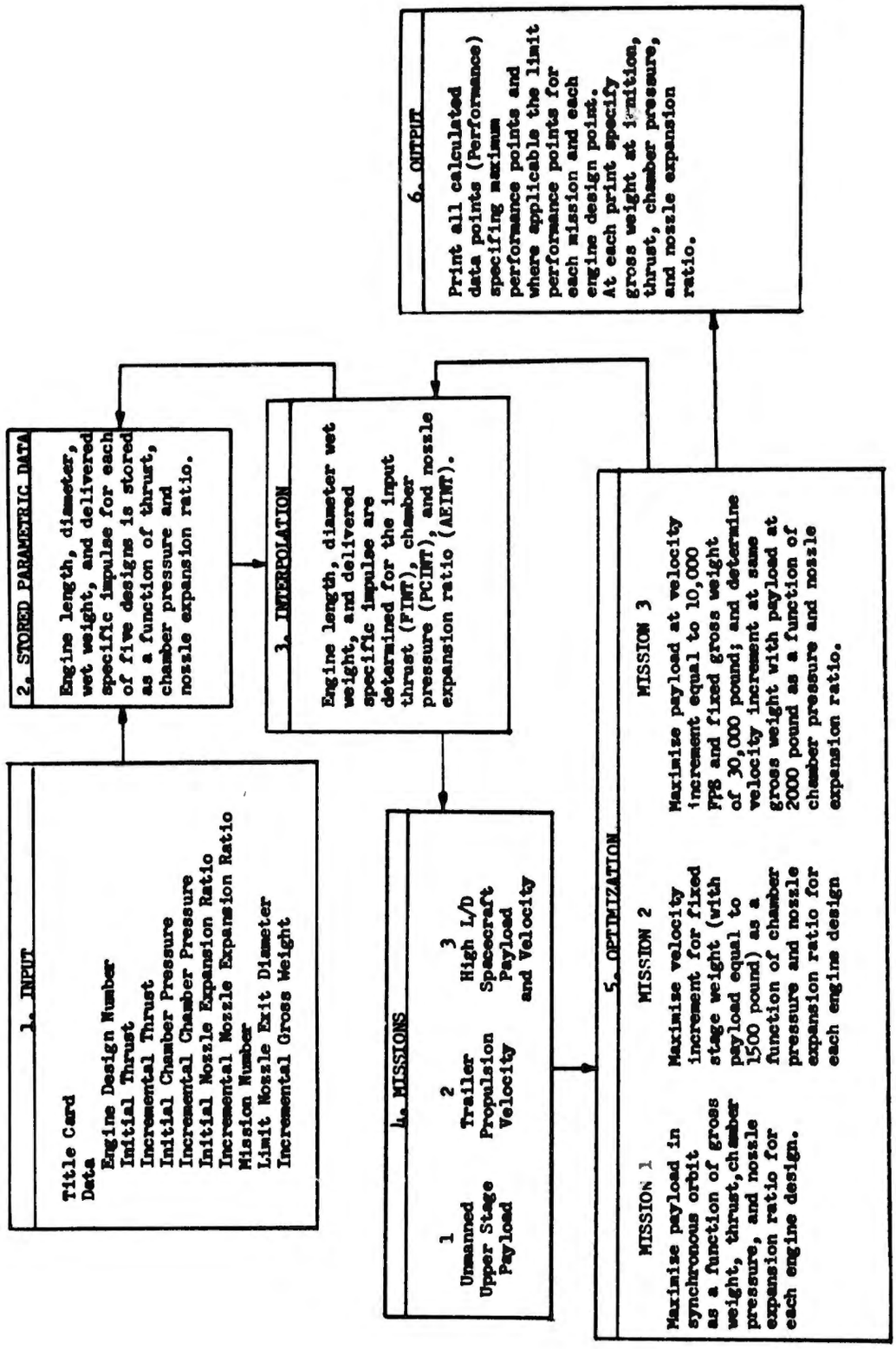

Figure 205. Computer Program Simplified Logic Diagram

1. Input and Control

Only two cards were required as input for each case. The first card contains the title and other identification for the specific case. The second card contains ten values which include the engine design number, the mission number, the initial engine operating parameters, the incremental values used to control the optimization and to vary the initial engine operating parameters, the increment to change initial gross weight (Mission No. I only), and the limit nozzle exit diameter.

2. Stored Parametric Data

Five arrays, each containing 256 parametric engine design points with values for engine length, nozzle exit diameter, engine weight and delivered vacuum specific impulse, are read in as part of the program deck and stored for reference during succeeding cases for the specified engine designs.

3. Interpolation

Specific values of engine length, diameter, weight, and specific impulse are obtained by parabolic interpolation of the stored array data for the input values of thrust, chamber pressure, and nozzle expansion ratio.

4. Missions

The three prescribed missions with specific assumptions pertaining to stage design and performance objectives are defined as subroutines and called into the mainline program by making reference to the input mission number. The output from each mission, either payload or velocity increment, is used as the controlling parameter during the optimization.

5. Optimization

A mission payload or velocity evaluation can be made for a specific set of engine operating conditions (thrust, chamber pressure, and nozzle expansion ratio) or these engine operating conditions can be incremented by input control to determine the optimum operating conditions, which result in maximum performance. The sequence of operation and control during this optimization has been previously described.

6. Output

All calculated data points for each set of engine operating conditions are printed. Specific output values are controlled by format within each mission to satisfy the specific mission performance requirements.

D. RESULTS

Performance evaluation results are summarized on Table XXXI for the three missions and the five engine designs. Payload and/or velocity increments specified are, where possible, the maximum values corresponding to optimum engine operating parameters. In addition to the quantitative performance comparison provided on Table XXXI, a series of plots (Figures No. 206 through No. 220) show variations in performance as a function of engine operating parameters for each mission and each engine design. All of these results are based upon using Compound A and Hydrazine as the propellant combination to demonstrate the application of Task I engine parametric data to evaluation techniques for future application studies.

Any realistic applications evaluation will rely upon other factors in addition to maximum performance to define optimum engine operating parameters. Generally, such an evaluation requires the establishment of constraints upon the engine operating parameters (Table XXXII) which, in this case, when considered with the previously described system definitions will:

1. Provide bounds for the allowable engine operating parameters.
2. Preclude the use of Hydrazine as a fuel in certain designs.
3. Restrict the application of some engine designs.

Perturbations in engine point design parametric data are provided in previous sections of this report. Included are effects such as performance changes with other fuels (80/20 blend, MMH, N_2H_4 + NH_3, and MHF-5) as well as weight and performance changes with advanced components and/or technologies (fibrous graphite transpire cooled throats and gaseous oxidizer and fuel injectants). As previously indicated, these technology change effects upon performance could be evaluated using the computer program to define new optimum engine operating parameters for each mission. However, such an evaluation is outside the scope of this study. As an alternative method of providing a realistic quantitative performance comparison, exchange coefficients (Figures No. 221 and No. 222) were established to evaluate changes in payload and/or velocity as a function of weight and specific impulse perturbations. The engine operating parameters (thrust, chamber pressure, and nozzle expansion ratio) established with CPA/N_2H_4 as the propellant were held constant and the performance values on Table XXXI adjusted to reflect changes in performance for different fuels and improved technology. These values are presented on Table XXXIII.

TABLE XXXI

EVALUATION SUMMARY (U)

Mission		I	II		III	
Engine Design	WLO F Pc ε	WPL max	Pc ε	ΔV max (15) ΔV (5)	Pc ε	WPL max ΔV (2) ΔV 80/20
I	*39,000 15,000 100 84	5,383	125 40	7,458 12,004		N/A
IV	61,558 55,000 1,000 92	8,301	881 93	8,472 13,940	73 53	2,175 10,234 N/A
V** (Burnout Heat Flux Limited)	62,486 35,000 **600 130	8,781	**600 96	8,620 14,220	**500 34	2,557 10,764 N/A
VII	62,287 40,188 1,411 153	8,757	1,412 135	8,725 14,364	1,322 124	2,546 10,748 10,122
VIII	63,548 21,838 1,452 133	9,399	1,360 131	8,998 14,803	1,246 119	2,933 11,314 10,712

*Lowest values considered not at true optimum.

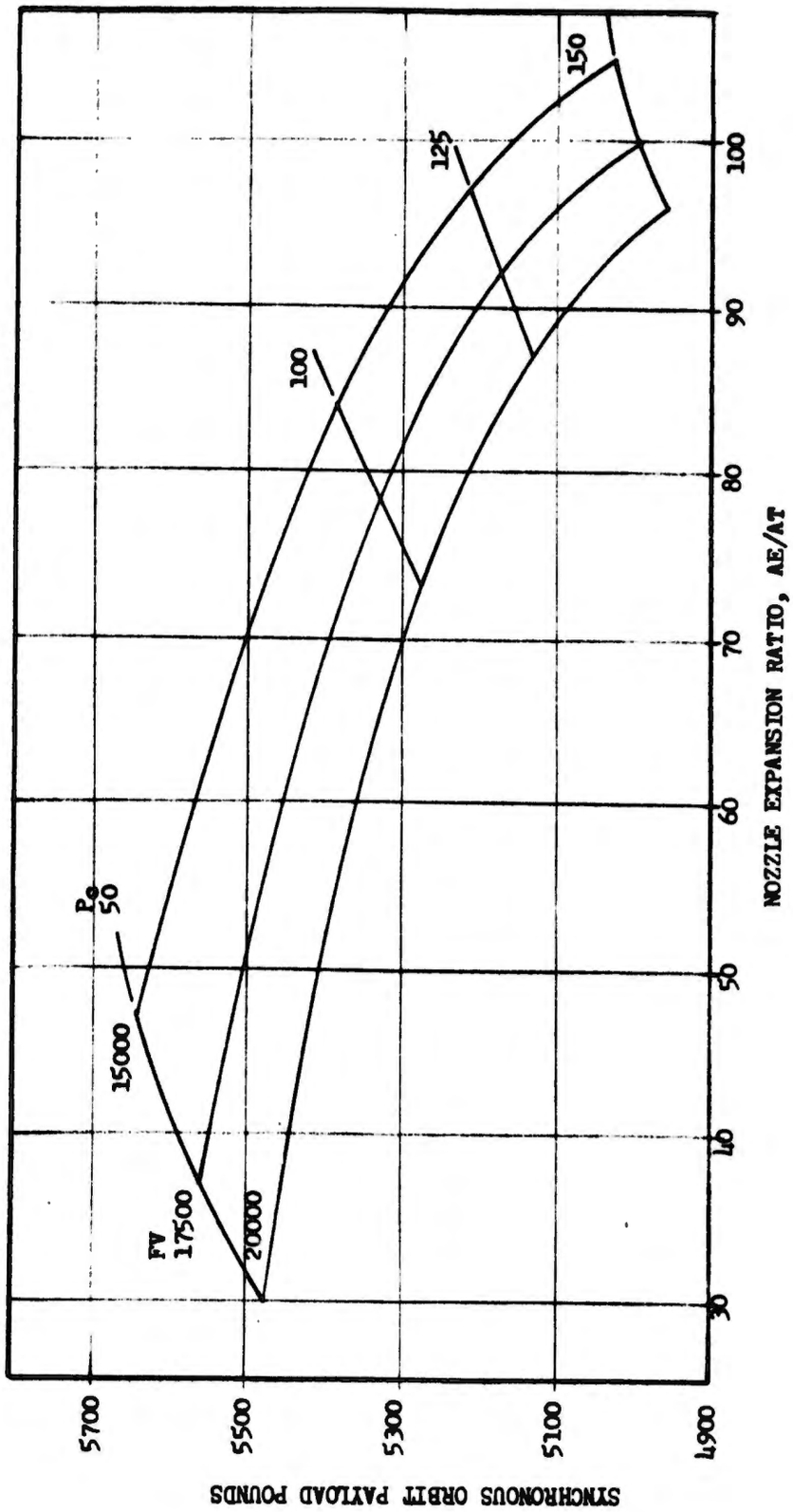

Figure 206. Mission No. I, Engine Design I (u)

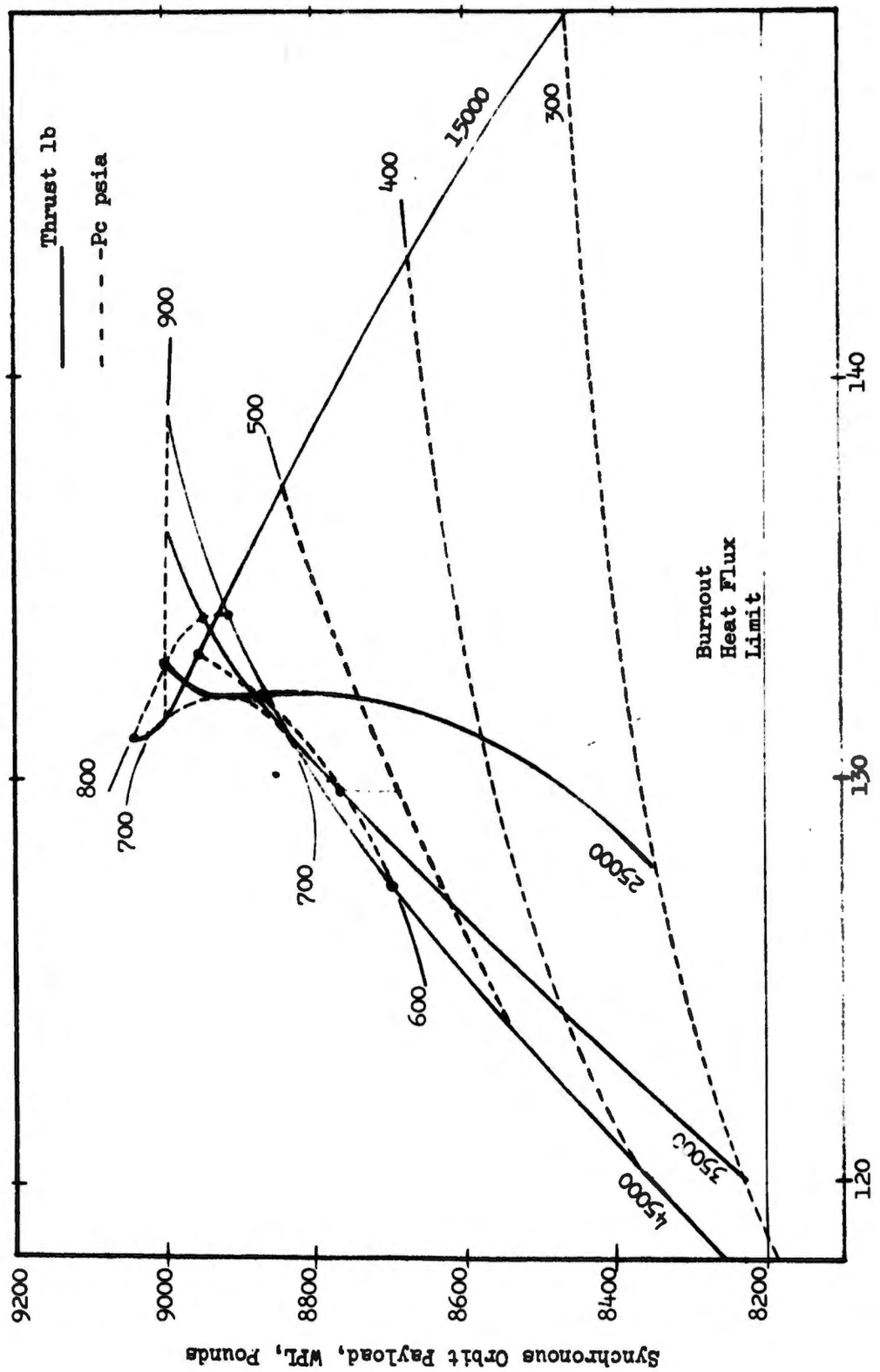

Figure 207. Mission No. I, Engine Design V (u)

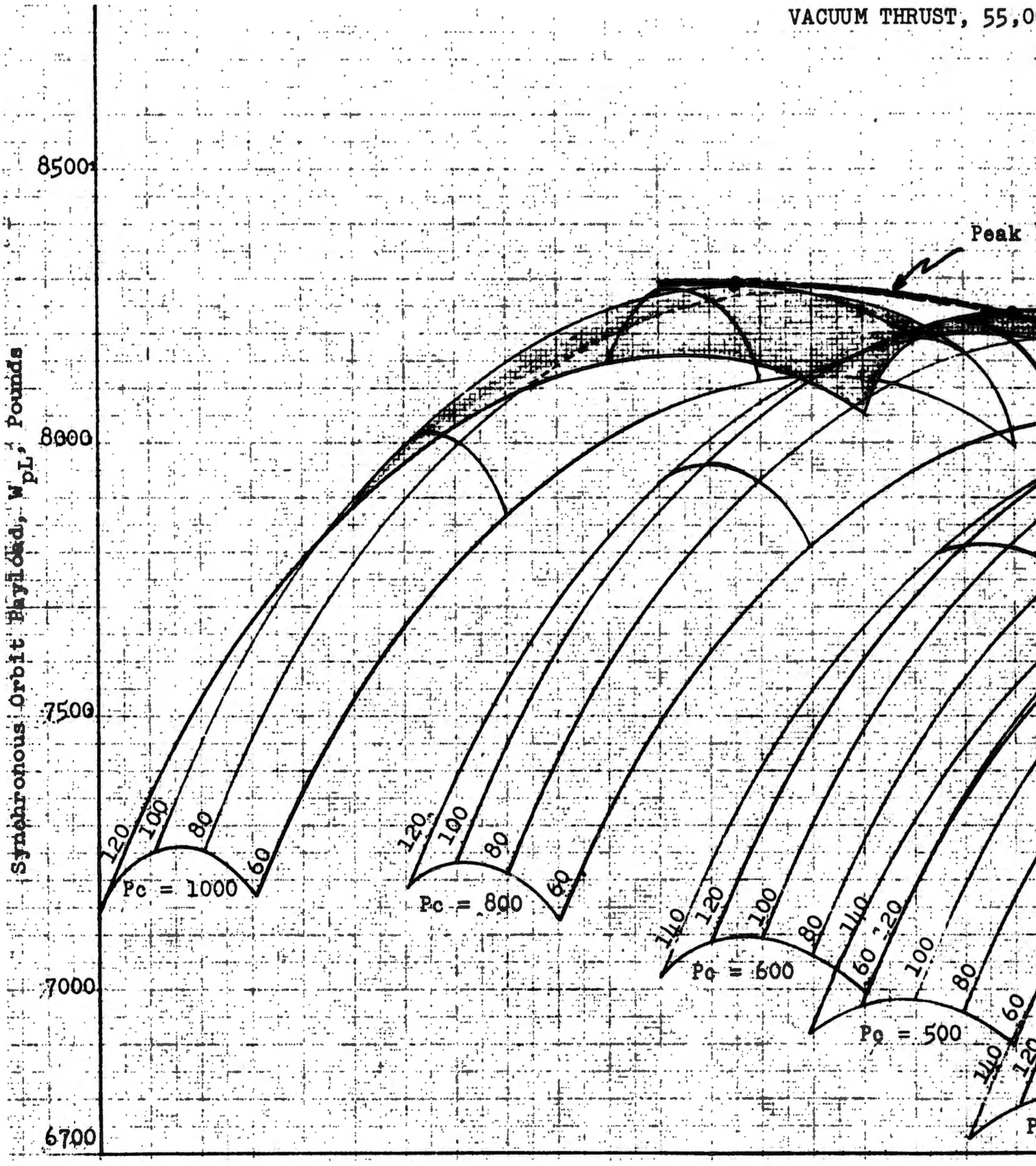
VACUUM THRUST, 55,0
Peak
8500
8000
7500
7000
6700
Synchronous Orbit Payload, W_{pL}, Pounds
120
100
80
60
Pc = 1000
120
100
80
60
Pc = 800
140
120
100
80
140
120
100
80
60
Pc = 600
100
80
60
140
120
Pc = 500

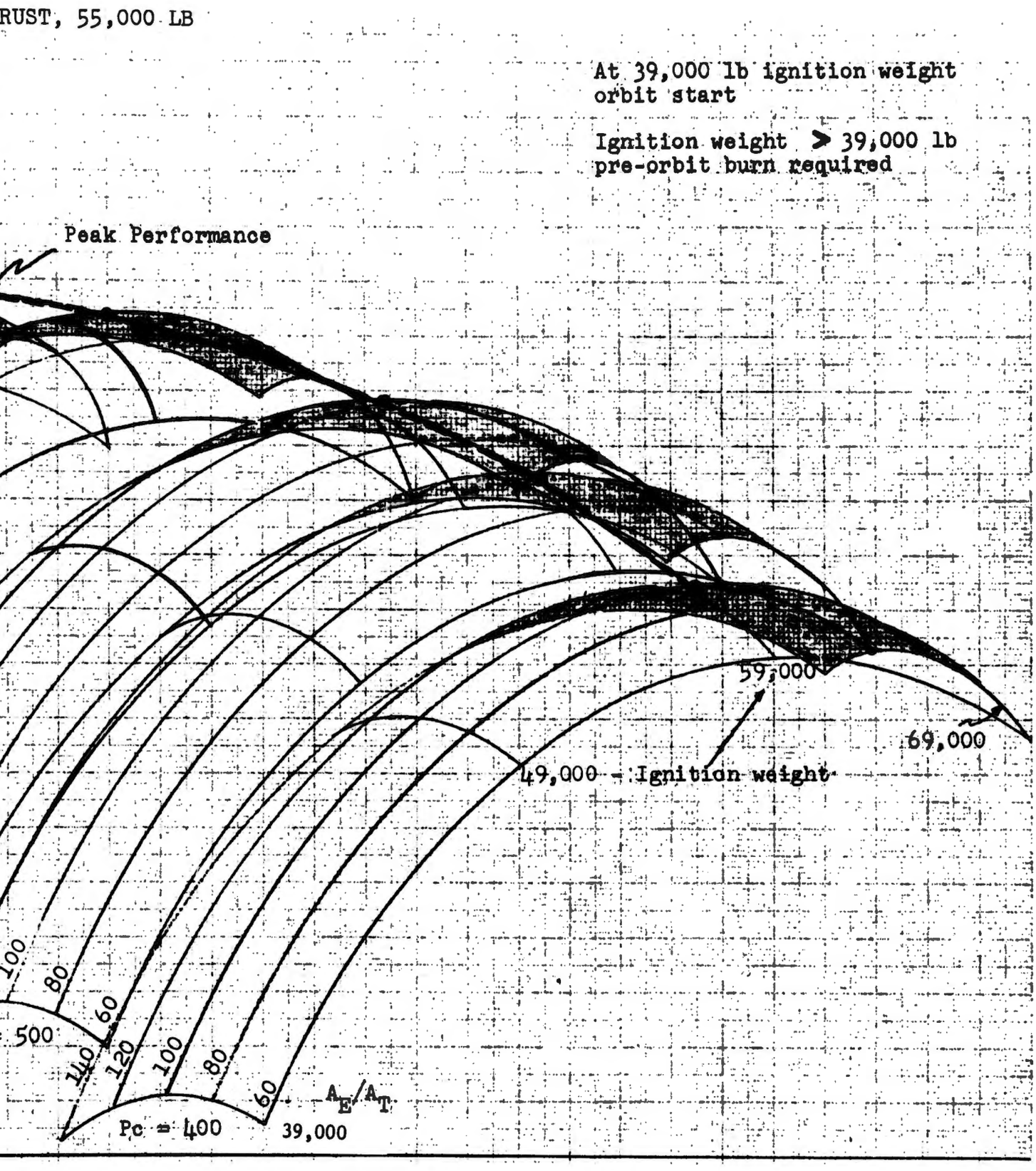

Figure 207. Mission No. I, Engine Design IV (u)

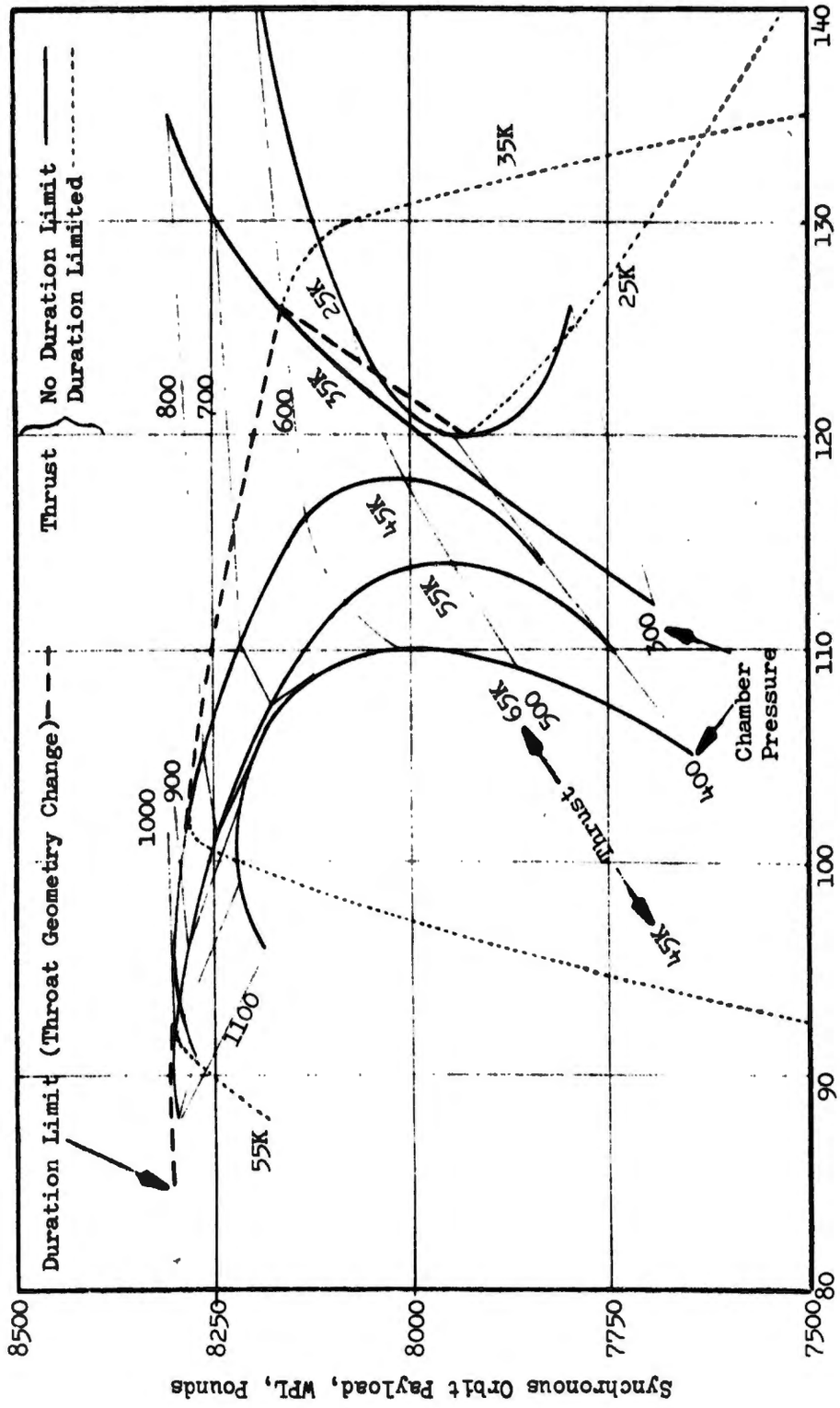

Figure 208. Mission No. I, Engine Design IV (u)
(Sheet 1 of 2)

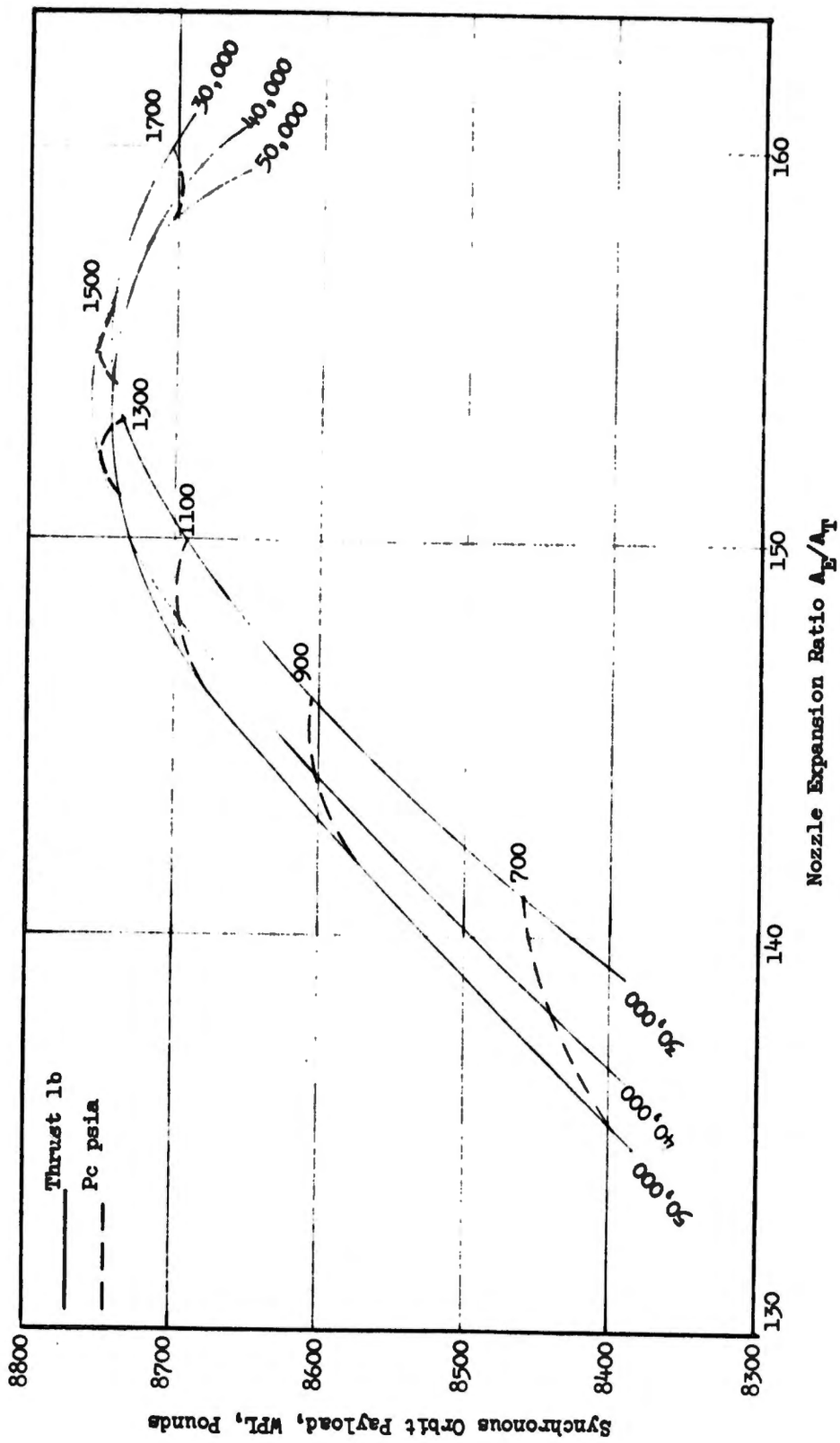

Figure 209. Mission No. I, Engine Design VII (u)

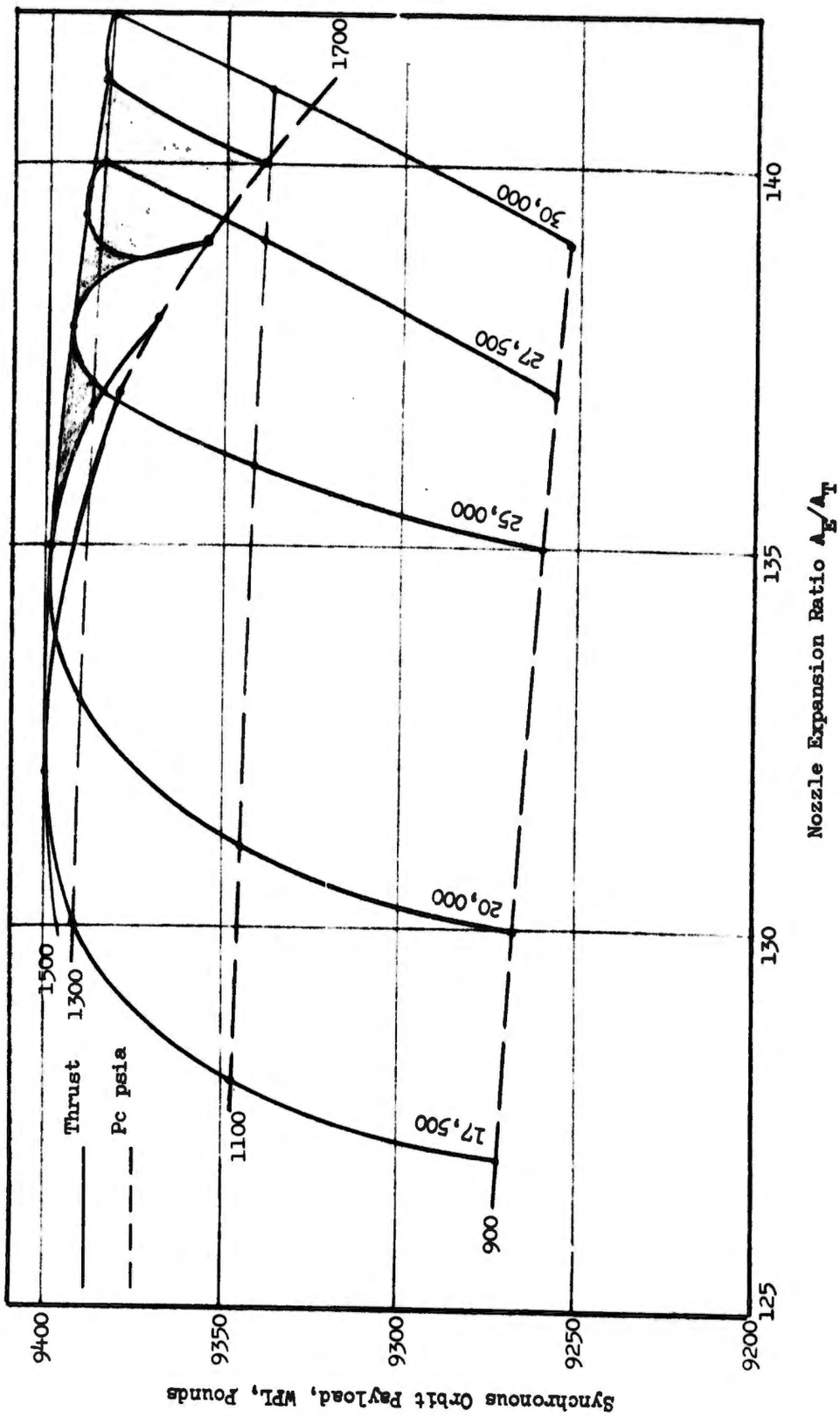

Figure 210. Mission No. I, Engine Design VIII (u)

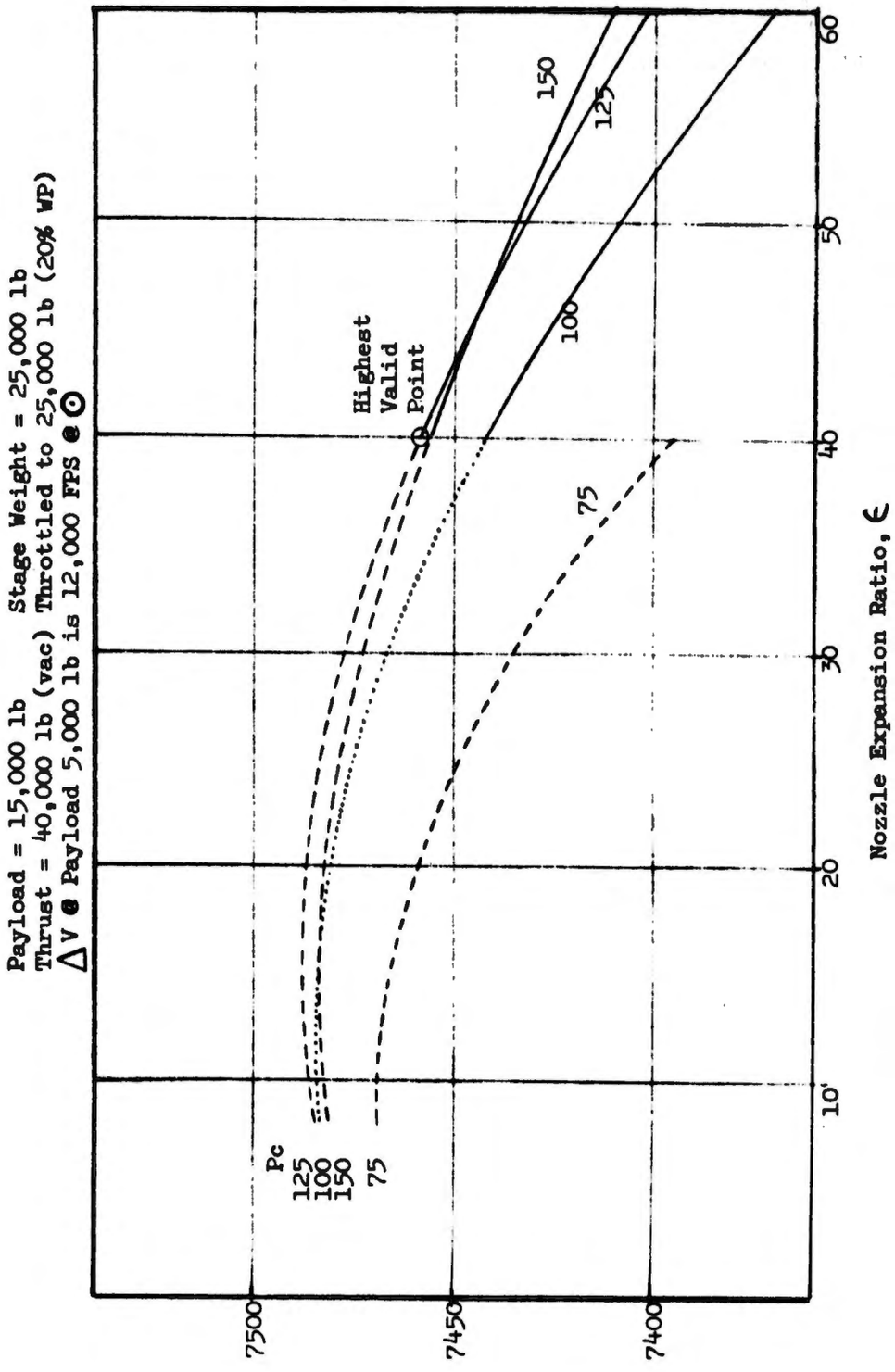

Figure 211. Mission No. II, Engine Design I (u)

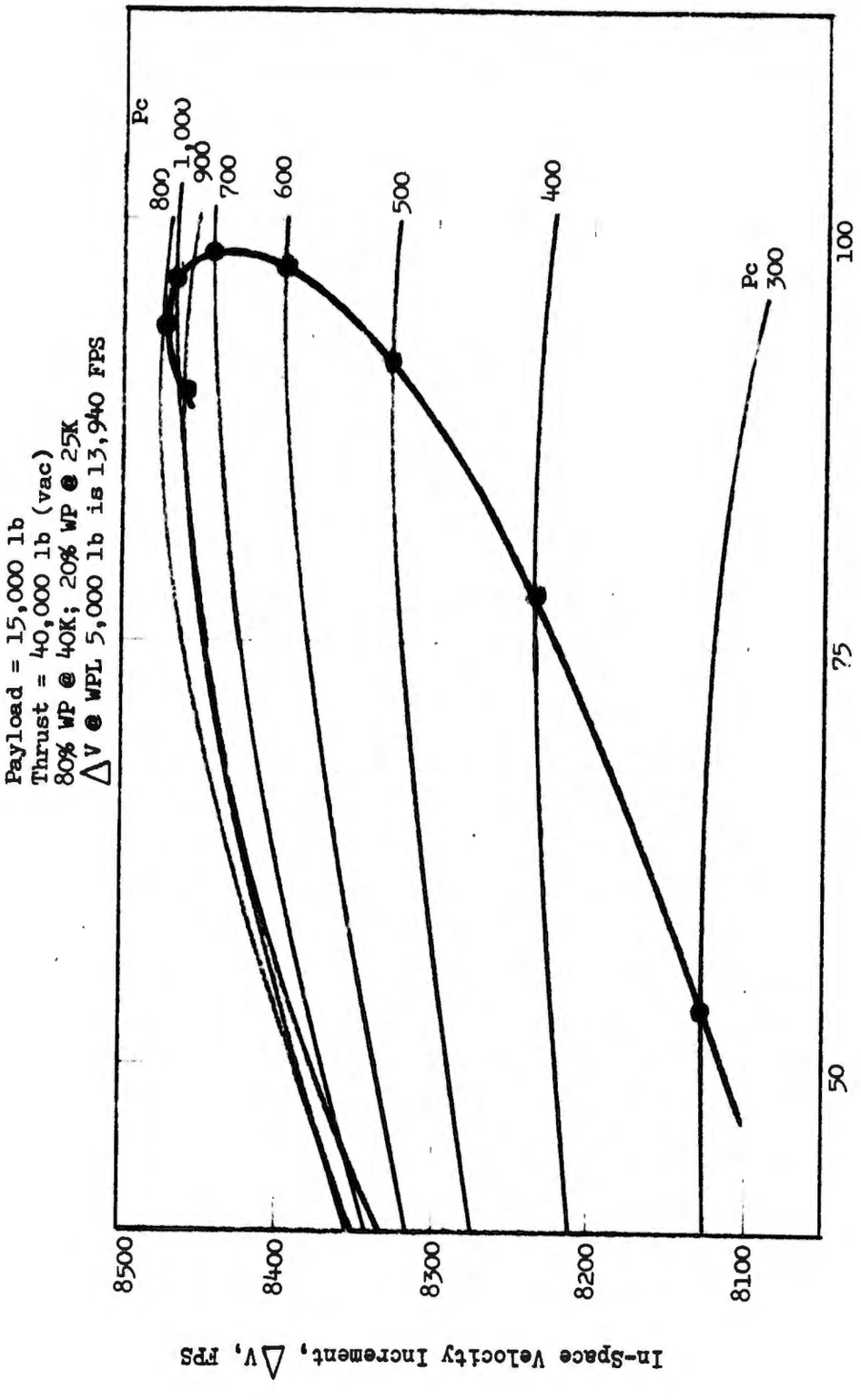

Figure 212. Mission No. II, Engine Design IV (u)

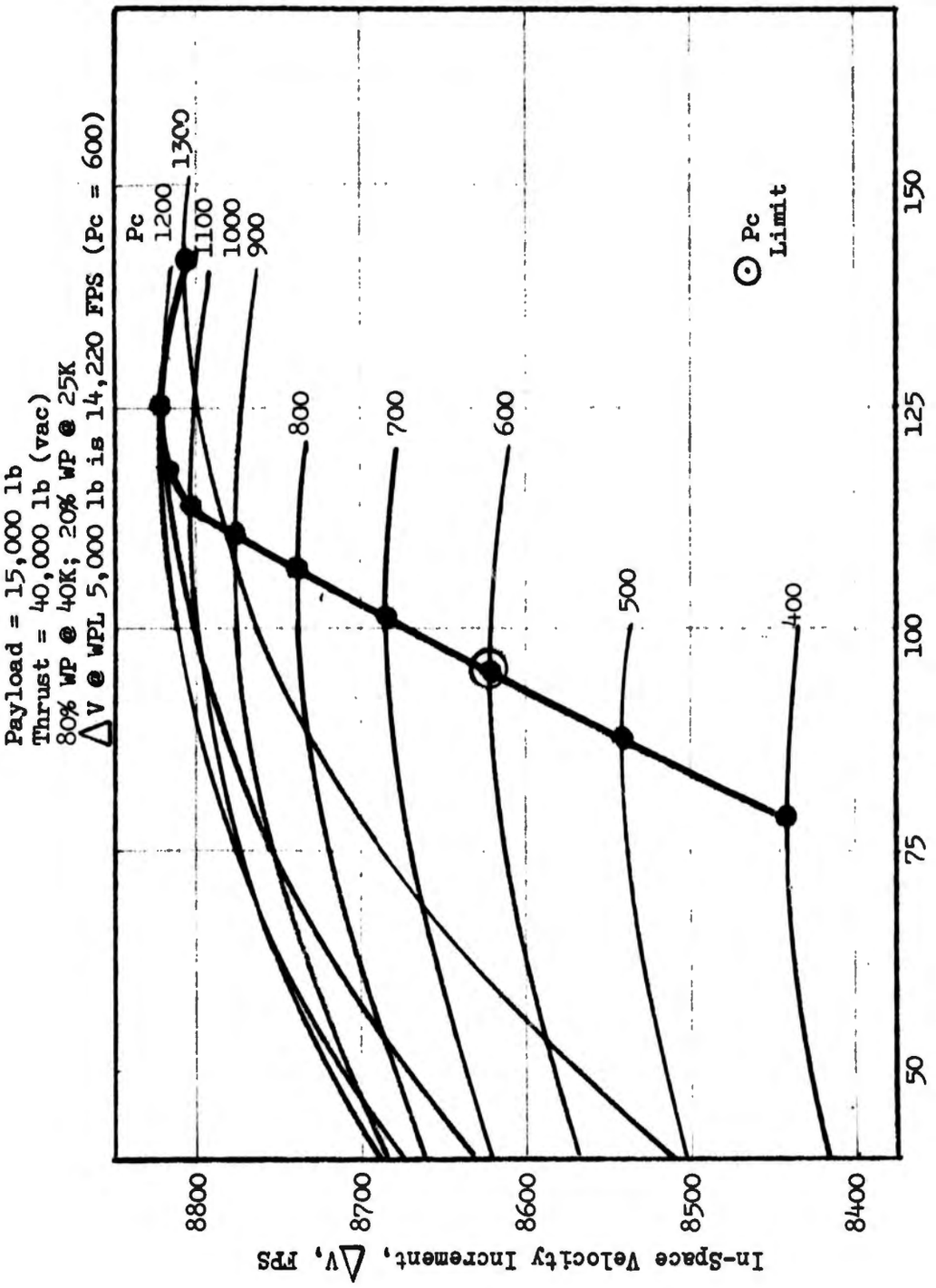

Figure 213. Mission No. II, Engine Design V (u)

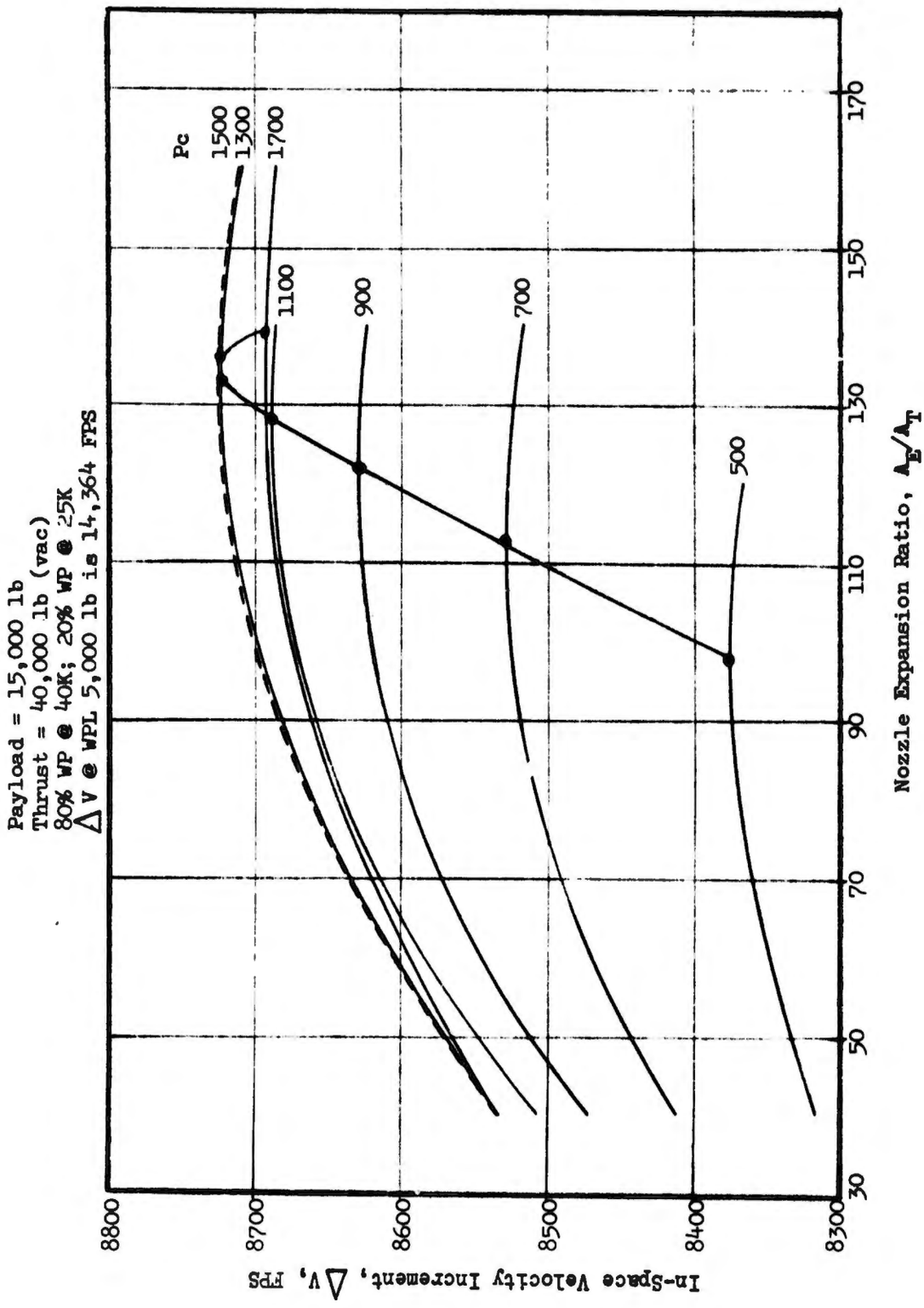

Figure 214. Mission No. II, Engine Design VII (u)

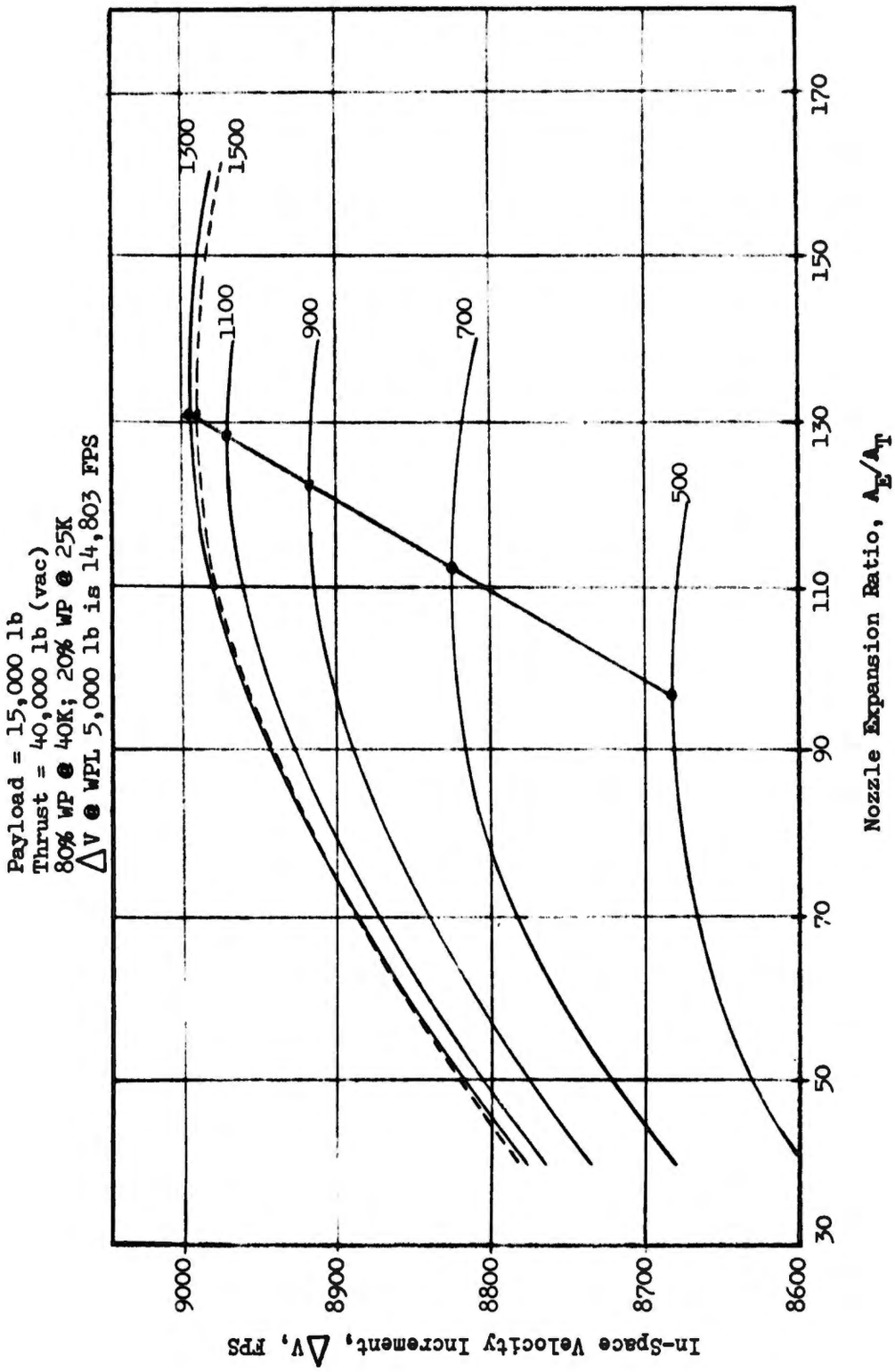

Figure 215. Mission No. II, Engine Design VIII (u)

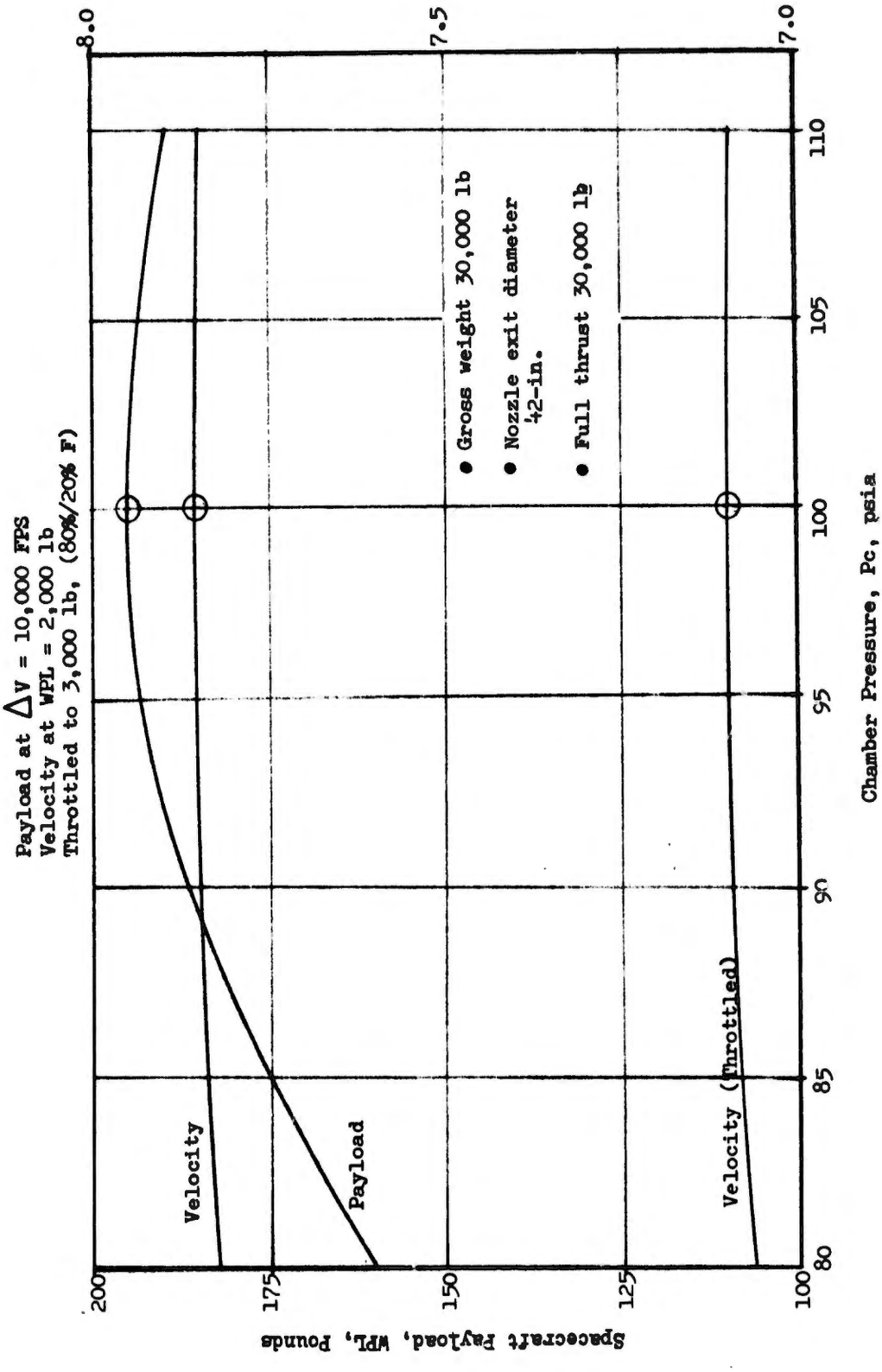

Figure 216. Mission No. III, Engine Design I (u)

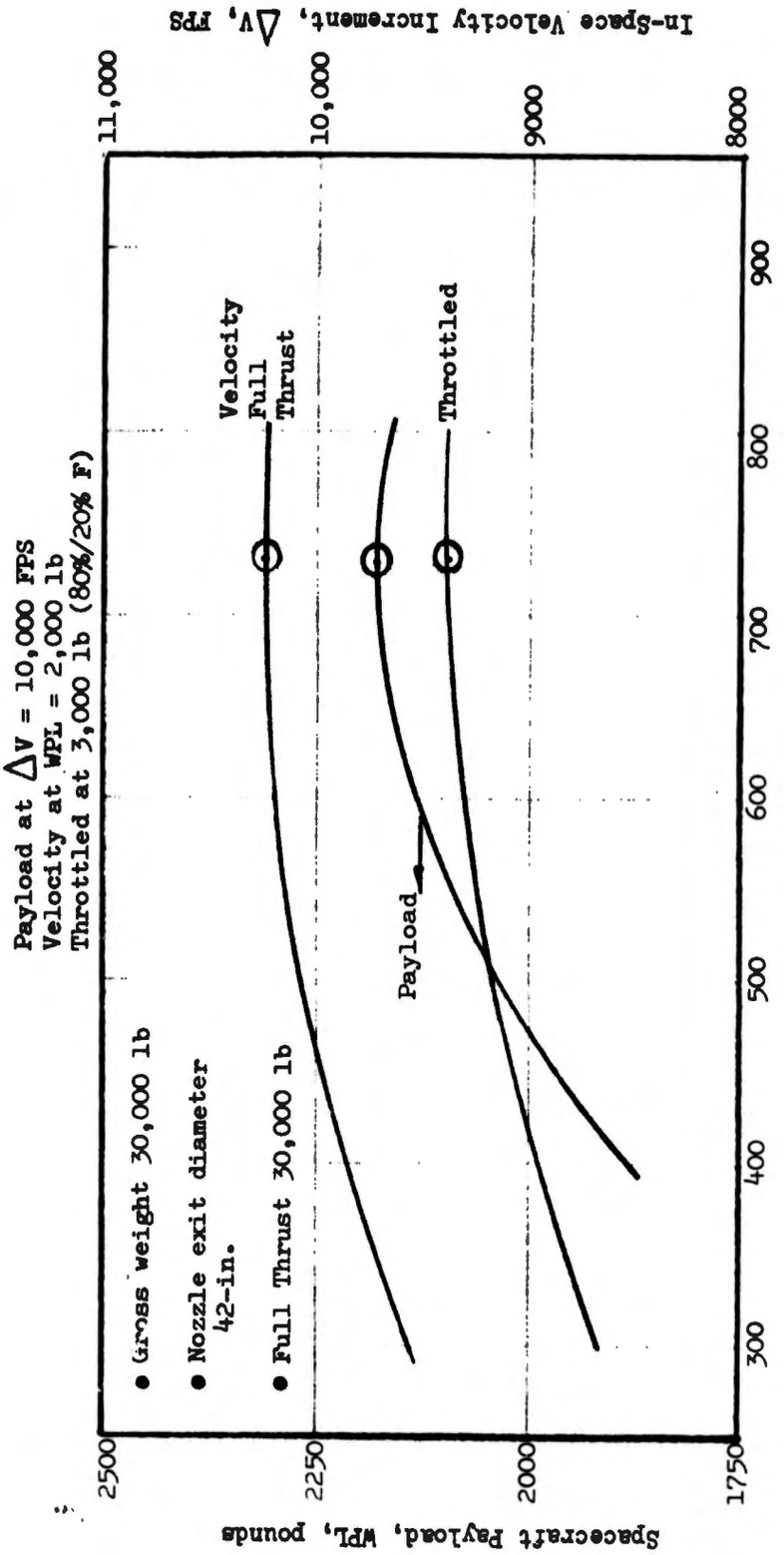

Figure 217. Mission No. III, Engine Design IV (u)

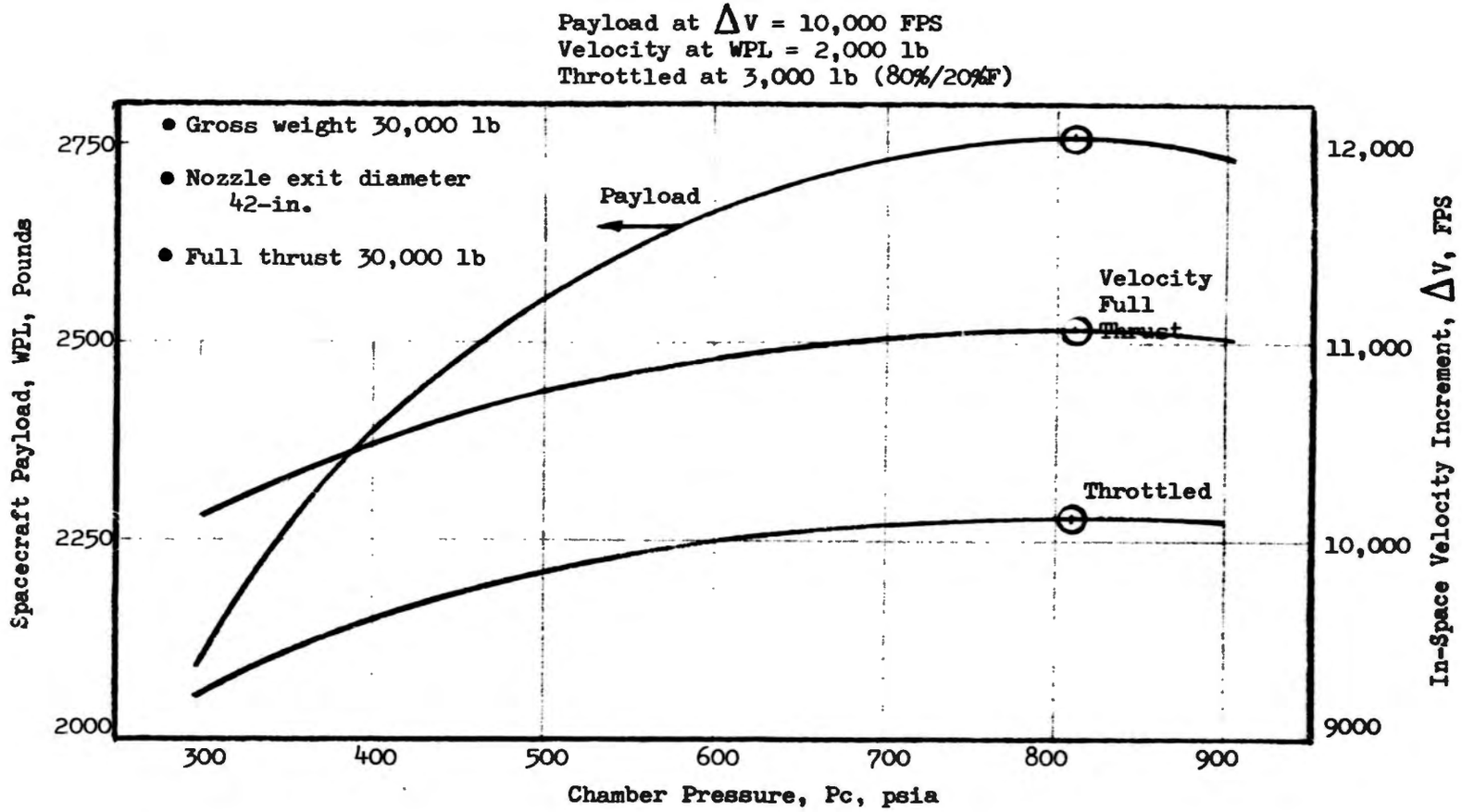

Figure 218. Mission No. III, Engine Design V (u)

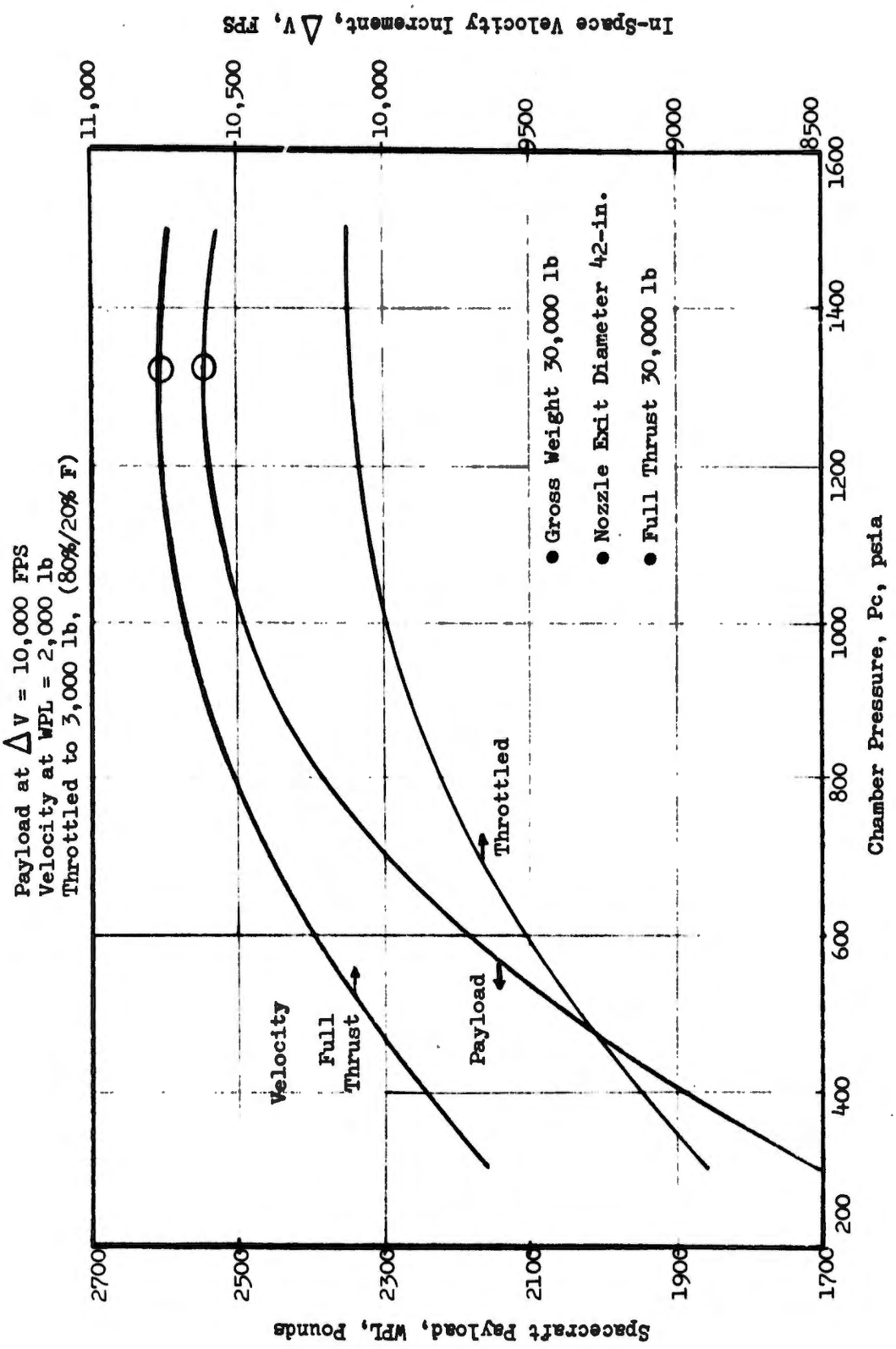

Figure 219. Mission No. III, Engine Design VII (u)

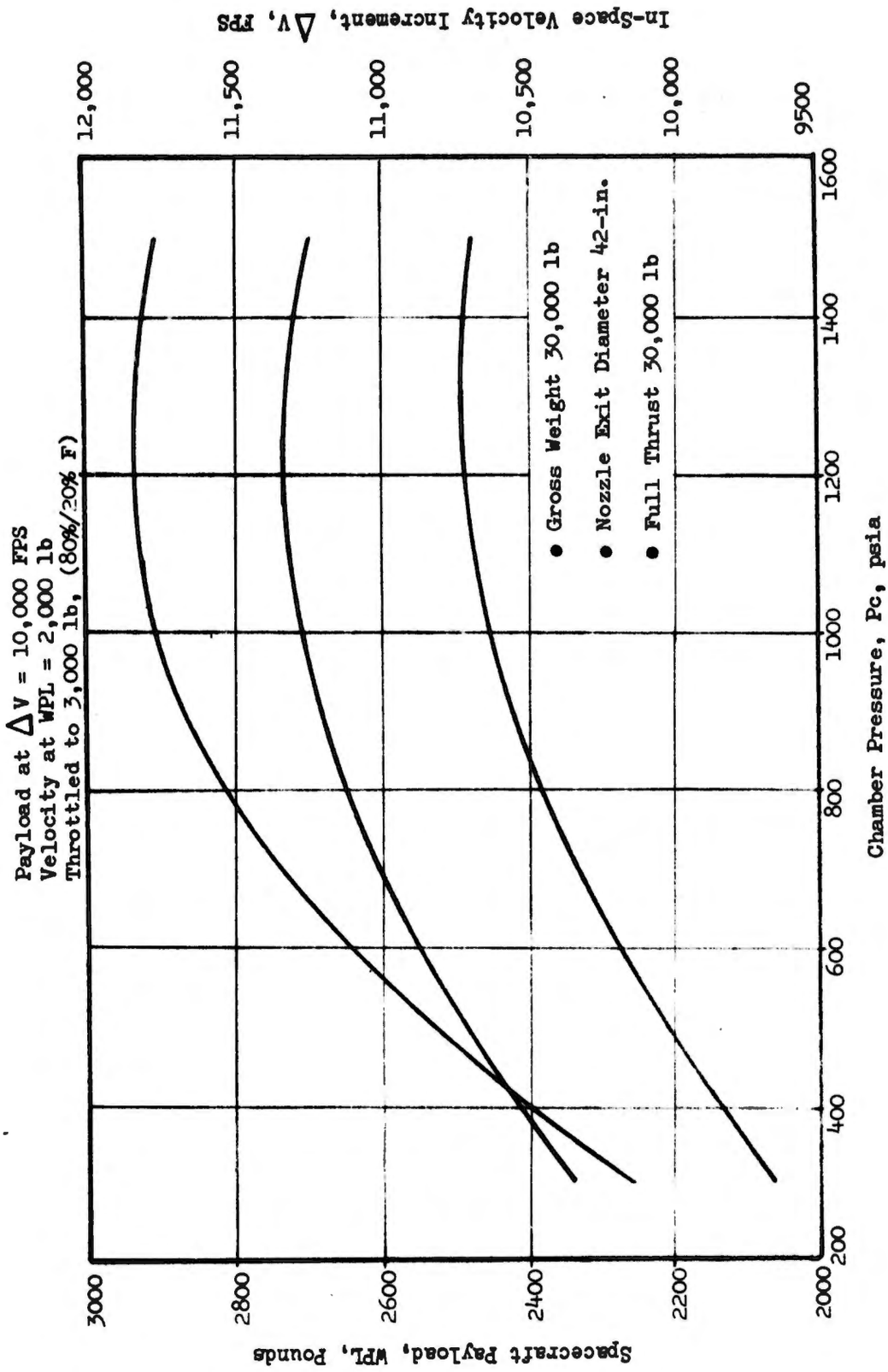

Figure 220. Mission No. III, Engine Design VIII (u)

TABLE XXXII

MISSION ANALYSIS - ENGINE DESIGN CONSTRAINTS (U)

Mission	Engine	Contraints	Reason
I	I	Pc > 100 psia	Combustion stability
II	I	Pc > 105 psia	Throttling requirement 35°F conditioned propellant
III	I	Pc > 800 psia	8:1 throttling requirement Radiation cooled chamber Not suitable for buried inst.
I	IV	Duration limited	Backside temperature Burn through
II	IV	Duration limited	Throat deposition
III	IV	Duration limited	Excessive wall thickness for throttling requirement
I	V	MHF-5 propellant only Pc_{max} = 600 psia, F > 35 K	Restart and shut down Tube wall temp limit Burnout heat flux
II	V	MHF-5 propellant only Pc_{max} = 350 psia, F = 25 K Pc_{max} = 600 psia, F = 40 K	
III	V	MHF-5 propellant only Pc_{max} = 500 psia, F = 30 K No throttling capability	

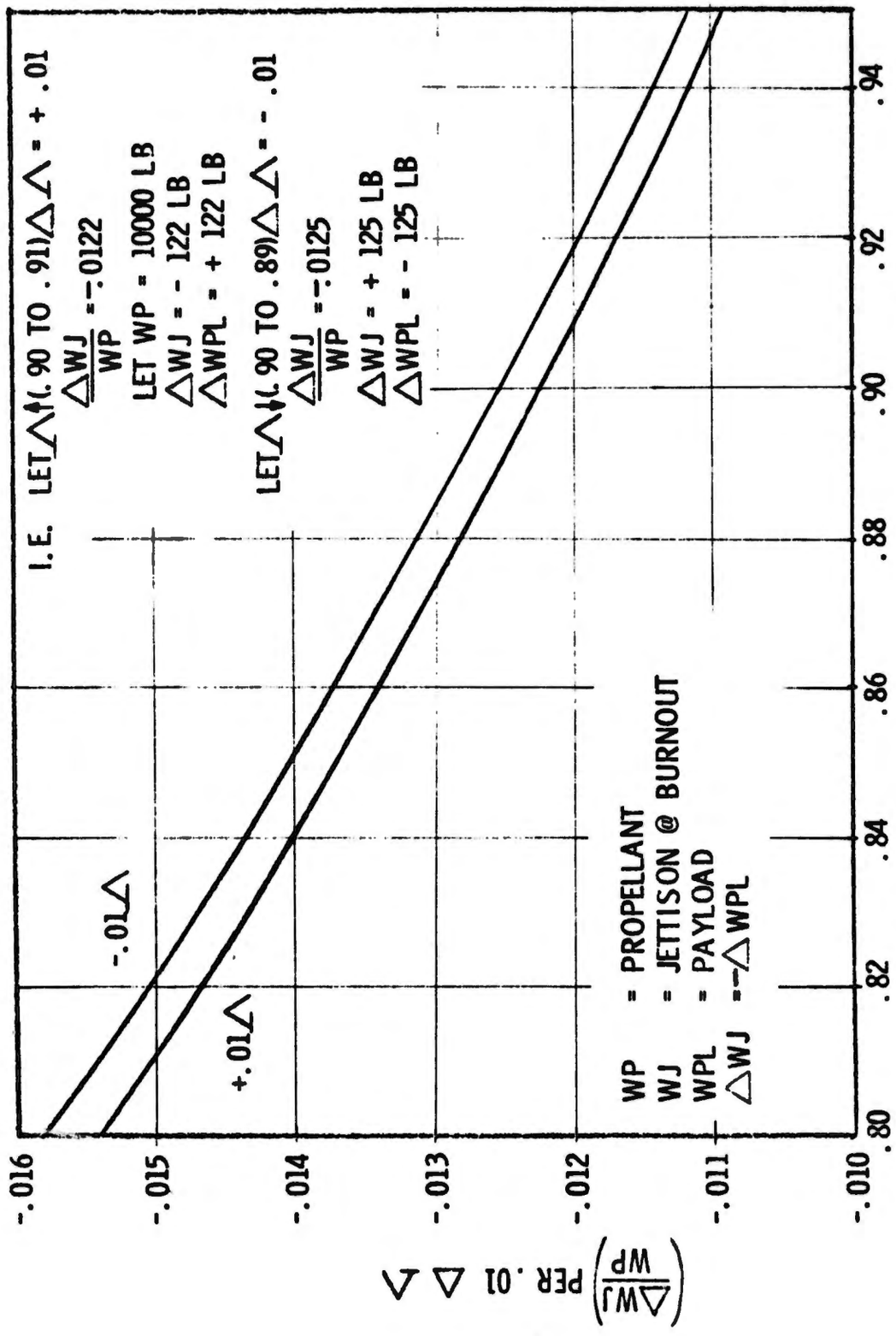

Figure 221. Jettison Weight (-Payload)/Mass Fraction Sensitivity (u)

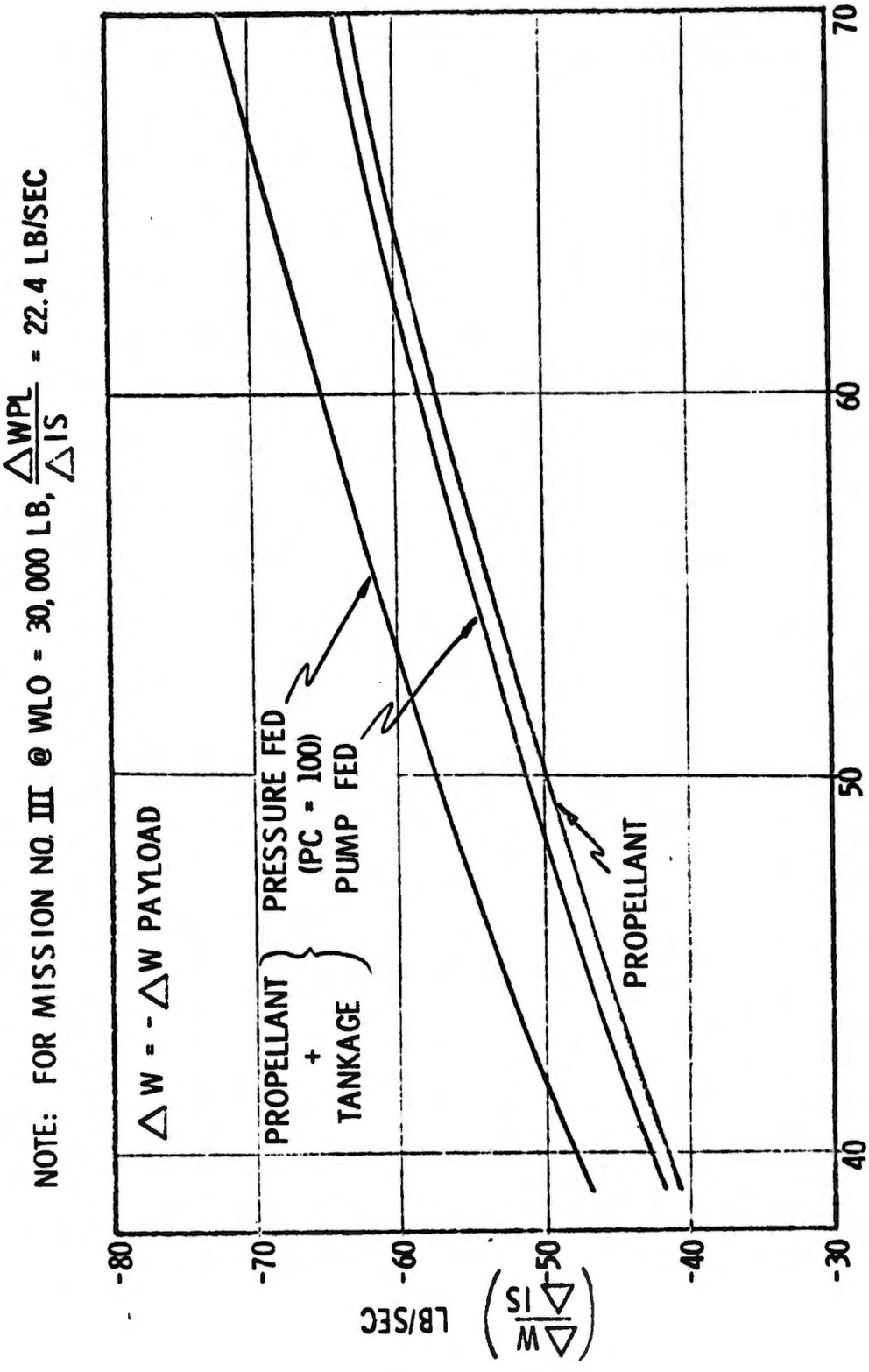

Figure 222. Weight Change/Specific Impulse Sensitivity, Mission No. I (u)

TABLE XXXIII

EVALUATION SUMMARY (ADJUSTED VALUES) (U)

Mission	I		II		III	
Engine Design	WLO F Pc ε	WPL max	Pc ε	ΔV max (15) V (5)	Pc ε	WPL max ΔV (2) ΔV 80/20
I	*39,000 15,000 100 84	5,383(N_2H_4)	125 40	7,458(N_2H_4) 12,004(N_2H_4)	N/A	
IV	61,558 55,000 1,000 92	8,124(80/20)	881 93	8,373(80/20) 13,784(80/20)	731 53	2,108(80/20) 10,144(80/20) N/A
V** (Burnout Heat Flux Limited)	62,486 35,000 **600 130	8,241(MHF-5)	600** 96	8,323(MHF-5) 13,752(MHF-5)	500 35	2,355(MHF-5) 10,494(MHF-5) N/A

*Lowest values considered not at true optimum.

TABLE XXXIII (cont.)

Mission		I	II		III	
Engine Design	WLO F Pc ε	WPL max	Pc ε	ΔV max (15) V (5)	Pc ε	WPL max ΔV (2) ΔV 80/20
VII	62,287 40,188 1,411 153	8,757(N_2H_4) 9,114(VIIA) 9,414(VII AA)	1,412 135	8,725(N_2H_4) 14,364(N_2H_4) 8,953(VIIA)(gas/gas) 14,723(VIIA) 9,083(VII AA)(gas/gas) 14,928(VII AA)(graphite)	1,322 124	2,546(N_2H_4) 10,748(N_2H_4) 10,122(N_2H_4) 2,701(VIIA) 10,955(VIIA)(gas/gas) 10,329(VIIA) 2,788(VII AA) 11,073(VII AA)(gas/gas) 10,447(VII AA)(graphite)
VIII	63,548 21,838 1,452 133	9,225(80/20)	1,360 131	8,902(80/20) 14,652(80/20)	1,246 119	2,868(80/20) 11,227(80/20) 10,625(80/20)